ABSTRACT BOOK

RCEM 2025

14th Symposium on River, Coastal and Estuarine Morphodynamics

Barcelona, 1-5 September

UNIVERSITAT POLITÈCNICA DE CATALUNYA
BARCELONATECH

CONTENT

WELCOME

This publication includes the detailed program and all the abstracts of the **14th Symposium on River, Coastal, and Estuarine Morphodynamics, RCEM2025**, organized by the Universitat Politècnica de Catalunya in **Barcelona, Spain, in 1-5 September 2025**.

RCEM provides a biennial forum focused on the morphodynamics of rivers, coasts and estuaries, in order to promote knowledge exchange and collaborations among the communities of hydraulic and coastal engineers, physicists, geologists, biologists, ecologists, computer scientists, applied mathematicians, and interested stakeholders. The conference is a must-attend event for scientists and professionals of all these disciplines who work on coastal and river processes at different scales and with divers methods.

The technical program includes morning sessions with three keynote lectures, plenary oral presentations and extensive poster discussion sessions, where we seek to encourage the exchanges between scientists of the three main topics. The afternoons consist of four parallel sessions of oral presentations organized to address the main RCEM environments: rivers, coasts and estuaries. The complementary activities are pre-conference courses, company exhibitions, many networking social events, and technical field trips or touristic tours. Due to sustainability considerations, the abstract book is not printed but a pdf copy is permanently available from the RCEM2025 website: https://esdeveniments.upc.edu/go/RCEM2025.html.

Francesca Ribas **Daniel Calvete**

Chairs of RCEM2025 conference

ORGANIZATION

LOCAL ORGANIZING COMMITTEE

CHAIRS

Daniel Calvete
Universitat Politècnica de Catalunya, Barcelona, Spain

Francesca Ribas
Universitat Politècnica de Catalunya, Barcelona, Spain

MEMBERS

Allen Bateman
Universitat Politècnica de Catalunya, Barcelona, Spain

Ivan Caceres
Universitat Politècnica de Catalunya, Barcelona, Spain

Antoni Calafat
Universitat de Barcelona, Barcelona, Spain

Nil Carrión
Universitat Politècnica de Catalunya, Barcelona, Spain

Giovanni Coco
University of Auckland, New Zealand

Maurizio D'Anna
Universitat Politècnica de Catalunya, Barcelona, Spain

Manuel Díez Minguito
Universidad de Granada, Granada, Spain

Ruth Duran
Institut de Ciències del Mar, Barcelona, Spain

Àngels Fernandez Mora
Sistema d'Observació i Predicció Costera de les Illes Balears, Mallorca, Spain

Carla García Lozano
Universitat de Girona, Girona, Spain

Candela Marco
Institut de Ciències del Mar, Barcelona, Spain

Josep Pintó
Universitat de Girona, Girona, Spain

Gonzalo Simarro
Institut de Ciències del Mar, Barcelona, Spain

Rafael O. Tinoco
University of Illinois at Urbana Champaign, USA

SCIENTIFIC COMMITTEE (RCEM BOARD)

CHAIR

Marcelo H. Garcia
University of Illinois, USA

SECRETARIAT

Astrid Blom
Delft University of Technology, the Netherlands

Guido Zolezzi
University di Trento, Italy

MEMBERS

Allen Bateman
Universitat Politècnica de Catalunya, Spain

Koen Blanckaert
Technical University Vienna, Austria

Karin Bryan
University of Auckland, New Zealand

Daniel Calvete
Universitat Politècnica de Catalunya, Spain

Giovanni Coco
University of Auckland, New Zealand

Nicholas Dodd
The University of Nottingham, UK

Cristian Escauriaza
Pontificia Universidad Catolica de Chile, Chile

Ton Hoitink Wageningen
University & Research, Netherlands

Stefano Lanzoni University di Padova, Italy

Edgardo M. Latrubesse Federal University of Goiás, Brasil

Nicoletta Leonardi
University of Liverpool, UK

Francois Metivier
Institut de Physique du Globe de Paris, France

Brad Murray Duke
University, USA

Yarko Nino
Universidad de Chile, Chile

Alejandra Ortiz
Colby College, USA

Paola Passalacqua
University of Texas at Austin, USA

Gerardo M. E. Perillo
Universidad Nacional del Sur, Argentina

Francesca Ribas Universitat Politècnica de Catalunya, Spain

Nicoletta Tambroni
Università degli Studi di Genova, Italy

Rafael O. Tinoco
University of Illinois at Urbana Champaign, USA

Greg Tucker
University of Colorado Boulder, USA

Enrica Viparelli
University of South Carolina, USA

Mengzhen Xu Tsinghua University China, China

Satomi Yamaguchi
Civil Engineering Research Institute for Cold Region, Japan

Miwa Yokokawa
Institute of Technology, Osaka, Japan

Zeng Zhou
Hohai University, China

PROGRAM AT A GLANCE

Sep. 1st	Sep. 2nd	Sep. 3rd	Sep. 4th	Sep. 5th
17:30 - 20:30 Registration	***8:30 - 18:00 Registration***	***8:30 - 18:00 Registration***	***8:30 - 18:00 Registration***	***Field trips***
9:00 - 17:00	***9:00 - 11:00***	***9:00 - 11:00***	***9:00 - 11:00***	***9:00 - 19:00***
Short courses: - Data science and climate for environmental engineers and scientists - Bathymetry estimation from drone videos	Communications Keynote Lecture I G.1: General Session I	Communications Keynote Lecture II G.3: General Session III	Communications Keynote Lecture III G.5: General Session V	9h-19h: - Costa Brava (9h-19h) - Susqueda Dam (9h-19h) 10h-18h: - Llobregat Delta (10h-18h) 10h-13:30h: - Barcelona City: BARCELONA 360° - Barcelona City: Rooftops Tour
	11:00 -12:30 Coffee-break	***11:00 -12:30 Coffee-break***	***11:00 -12:30 Coffee-break***	
	P.1: Poster Session I	P.2: Poster Session II	P.3: Poster Sesion III	
	12:30 - 13:30	***12:30 - 13:30***	***12:30 - 13:30***	
	G.2: General Session II	G.4: General Session IV	G.6: General Session VI	
	13:30 -15:00 Lunch	***13:30 -15:00 Lunch***	***13:30 -15:00 Lunch***	
	15:00 - 16:30	***15:00 - 16:30***	***15:00 - 16:30***	
	C.1: Shoreline Evolution E.1: Sediment Transport in Estuaries R.1: River Bars R.2: River Modelling	R.5: Human Interferences in Rivers E.3: Human Interferences in Estuaries C.3: Submerged Beach Processes C.4: Continental Shelf Processes	C.7: Nearshore Processes E.5: General Aspects in Estuaries I R.7: Lab experiments R.8: River Banks	
	16:30 - 17:00 Coffee-break	***16:30 - 17:00 Coffee-break***	***16:30 - 17:00 Coffee-break***	
	17:00 - 18:15	***17:00 - 18:15***	***17:00 - 18:15***	
	C.2: Tidal Systems E.2: Salt Marshes R.3: River Channels R.4: Bifurcations and Meanders I	R.6: General Aspecs in Rivers E.4: Estuarine Equilibrium C.5: Beach Morphodynamics C.6: Coastal Sediment Dynamics	C.8: Nearshore Sand Patterns E.6: General Aspects in Estuaries II R.9: Bifurcations and Meanders II R.10: Sediment Transport in Rivers	
18:00 - 19:00				
WICGE Round table				
19:00 - 21:00	***19:00- 21:00***	***19:00- 21:00***	***20:00 - 23:00***	
Wellcome - Ice breaker	WICGE evening	Young RCEM evening	RCEM Conference Dinner	

Tuesday, September 2nd · Morning

9:00	**Communications**	
	Keynote Lecture I	*Chair: Marcelo Garcia*
9:15 - 10:15	Climate-Based Met-Ocean Emulators for Compound Coastal Flooding and Long-term Morphodynamics	*Fernando Mendez*
	G.1: General Session I	*Chair: Suzanne Hulscher*
10:15	G.1-1: On the relationship between bedform morphology and meander dynamics	*Julia Cisneros*
10:30	G.1-2: Enigmatic lunate shaped bedforms in the Fehmarn Belt, Baltic Sea	*Winter Christian*
10:45	G.1-3: Designing ecosystems for climate change	*Johan van de Koppel*
11:00 - 12:30	**Poster Session / Coffee-break**	
P.1-01	Quantifying and monitoring the instream wood regime across multiple scales	*Virginia Ruiz-Villanueva*
P.1-02	Species-by-Species Pattern Analysis of Coastal Dune Vegetation	*Davide Demichele*
P.1-03	Measurement of Flow Velocity around a Developing Antidunes	*Yu Inami*
P.1-04	Observing Coastal Processes with X-Band Radar	*Laura Szczyrba*
P.1-05	Effects of canal excavation on the hydrodynamics of back-barrier lagoons	*Davide Tognin*
P.1-06	Spatial distributions of velocity and water level in an actual river channel including a bifurcation and a confluence	*Shun Kudo*
P.1-07	Comparing Morphology of Refurbished and Natural Coastal Dunes	*Cora Jones*
P.1-08	Linking morphodynamics of superimposed bedforms across environments	*Elpidio Guzman De La Cruz*
P.1-09	Evaluating Shoreline Dynamics with IH-SET: Case Studies in Varied Coastal Environments	*Camilo Jaramillo*
P.1-10	Morphological trends in a highly engineered estuary	*Pia Kolb*
P.1-11	Global Mapping of River Morphologies	*Daan Beelen*
P.1-12	Role of Wind-Induced Currents in Sediment Resuspension and Transport in a Micro-Tidal Bay	*Ho Kyung Ha*
P.1-13	Observations of Spatio-Temporal Variations in Groyne Field Bathymetry	*Eki Liptiay*
P.1-14	Comparison between shorelines derived from radar and multispectral satellite	*Riccardo Angelini*
P.1-15	Seasonal and interannual change of the extension of the Aiguillon Bay salt marsh.	*Loës Le Goff Le Gourrierec*
P.1-16	Sediment transport diffusion from a multi-scale perspective using DNS-DEM and stochastic models	*Christian González*
P.1-17	Analysis of Morphodynamics at the Mouth of Ebro River Delta	*Benjamí Calvillo*
P.1-18	Morphological changes before and after neck cutoffs in meandering rivers	*Kattia Rubi Arnez Ferrel*
P.1-19	Sediment Fluxes over Sand Deposits at Fire Island Shelf, New York	*Bilal Umut Ayhan*
P.1-20	The Natural Rhythm of Estuaries	*Marloes Bonenkamp*
P.1-21	Sediment transport modelling to inform river restoration design on a wandering gravel-bed river in Britain	*Samuel Watkiss*
P.1-22	Study of cliff ridge recession due to wind-induced waves in Port Foster (Deception Island, Antarctica)	*Óscar Aarón Caballero Martínez*
P.1-23	An experimental study of flow through spatially heterogeneous arrays of emergent cylinders: the case of Arundo Donax	*Arnau Prats*
P.1-24	Longshore Sediment Transport deduced from Accumulation at a Jetty Using Satellite Imagery	*Jacqueline Santos*
P.1-25	Dynamic Equilibrium in the Tisza River: A Long-Term Assessment of Post-Regulation Changes	*Gergely Török*
P.1-26	Fine sediment modelling at the catchment scale in Alpine streams	*Michele Combatti*
	G.2: General Session II	*Chair: Andrea D'Alpaltos*
12:30	G.2-1: Modelling interaction between free migrating bars and in-stream structures	*Marco Redolfi*
12:45	G.2-2: Inlet connectivity as new concept to understand the role of tidal divides in mesotidal barrier coast dynamics	*Pieter Roos*
13:00	G.2-3: Bed material or washload?	*Enrica Viparelli*
13:15	G.2-4: Flow and Sediment Distribution of a River Delta with a 1D Morphodynamic Model	*Michele Bolla Pittaluga*
13:30 - 15:00	***Lunch***	

Tuesday, September 2nd · Afternoon

	Auditori	Room LS.1	Room LS.11	Room LS.12
	C.1: Shoreline Evolution *Chair: Andrew Ashton*	**E.1: Sediment Transport in Estuaries** *Chair: Maitane Olabarrieta*	**R.1: River Bars** *Chair: Allen Bateman*	**R.2: River Modelling** *Chair: Yasuyuki Shimizu*
15:00	C.1-1: Monitoring of megacusp development events from satellite-derived shorelines: a case study of two Mediterranean microtidal beaches *Eduard Angelats Company*	E.1-1: A model-based reference state for suspended sediment concentration in the Wadden Sea *Jannek Gundlach*	R.1-1: Numerical modelling of bar formation in the Elbe river *Nils Reidar B. Olsen*	R.2-1: Numerical Calculation Method for Bed Height Variation of Two Grain-size Sediment based on the Avairable Porosity and Dynamic Rough Wall Law *Ryunosuke Mitani*
15:15	Predicting Short-term Satellite-Derived Shoreline Positions around New Zealand *Amirmahdi Gohari*	Sediment transport in the microtidal Misa River estuary *Agnese Baldoni*	Characterising alternate bars facilitating single beam fairway surveys *Till Branß*	Investigating flow-morphology interactions in a step-pool unit by combin-ing physical and numerical modeling *Chendi Zhang*
15:30	C.1-3: Non-Stationary Calibration of Equilibrium Shoreline Evolution Models via Cartesian Genetic Programming *Lucas de Freitas Pereira*	E.1-3: Flow Velocities on Fringing Intertidal Flats *Bram van Prooijen*	R.1-3: Free bars in straight channels: modulation and predictability through the Complex Ginzburg-Landau Equation *Francesco Weber*	R.2-3: Acceleration of the Sediment Transport Analysis for Braided Rivers Using the Average Component Acceleration Method *Yosei Kitayama*
15:45	C.1-4: Shoreline Evolution in a Natural Semi-Embayed Mediterranean Beach *Francisco Fabián Criado Sudau*	E.1-4: How does the spatial organization of roughness elements alter fine sediment erodibility and transport? *Maxime Laukens*	R.1-4: Numerical Modelling of Migrating and Steady Alternate Bar Dynamics during Floods in the Alpine Rhine River *David Vetsch*	R.2-4: Application of Multi Grid Model for Computing River Morphodynamics *Takeshi Sakai*
16:00	C.1-5: Coupling littoral and fluvial sediment transport for shoreline morphodynamics modelling: a sensitivity assessment *Marta Crivellaro*	E.1-5: Changes in estuarine SSC: long-term trends and variability *Van maren Bas*	R.1-5: Prediction of alternate bar characteristics using a neural network *Victor Chavarrias*	R.2-5: Modeling Boundary Shear Stress for River Width Prediction *Giada Artini*
16:15	C.1-6: Exploring Future Shoreline and Nearshore Evolution Under Sea-Level Rise Projections: Application of the LX-ST Model to Lacanau *Mohamad Traboulsi*	E.1-6: Transport pathways of microbial sediment aggregates with distinct fine-scale morphologies *Naiyu Zhang*	R.1-6: Experimental and analytical evidence of steady alternate bars forced by a localized asymmetric drag distribution *Mirko Musa*	R.2-6: Coupling a Slope Failure Model with Groundwater Effects and 2D Riverbed Deformation Model. *Yutaka Kasagi*

16:30 - 17:00	***Coffee-break***

	Auditori	Room LS.1	Room LS.11	Room LS.12
	C.2: Tidal Systems *Chair: Deborah Idier*	**E.2: Salt Marshes** *Chair: Nicoletta Tambroni*	**R.3: River Channels** *Chair: Douglas Edmonds*	**R.4: Bifurcations and Meanders I** *Chair: Brad Murray*
17:00	C.2-1: Breach development during successive hurricanes and impacts on the inner lagoon hydrodynamics *Ella Bear*	E.2-1: Identifying small-scale gradients in sediment stability as early indicators of saltmarsh cliff initiation *Victoria Mason*	R.3-1: Effects of an Arrested Avulsion on Long-Term River Channel Stability: Lower Mississippi River *Brandon McElroy*	R.4-1: Experimental observations on a tidal channel ifurcation *Ruffini Alessia*
17:15	C.2-2: The recent asymmetric morphological evolution of the Wadden Sea *Marvin Lorenz*	E.2-2: What controls the height of marsh edge cliffs? *Xiaotian Zhang*	R.3-2: River Avulsion Precursors Encoded in Alluvial Ridge Geometry *James Gearon*	R.4-2: Quantifying the evolution of channel-floodplain connectivity in a near-natural river widening via a Eulerian-Lagrangian numerical model *Francesco Caponi*
17:30	C.2-3: Effects of mud availability on suspended sediment concentrations in the Dutch Wadden Sea *Roy van Weerdenburg*	E.2-3: Storm Surge Impacts on Sediment Dynamics and Habitat Resilience in a Mangrove-Marsh Ecotone *Sanne M Vaassen*	R.3-3: Stochastic Dynamics of Morphological Units in Anabranching Rivers *Niccolo Ragno*	R.4-3: Detecting Compound Meanders Bends via Curvature Energy Spectrum *Sergio Lopez Dubon*
17:45	C.2-4: Balancing coastal urban flood protection with ecosystem resilience: in-sights from the Venice Lagoon, Italy *Andrea D'Alpaos*	E.2-4: Wave attenuation versus progressive damage during extreme storm condi-tions: a salt marsh vegetation trade-off *Pim Willemsen*	R.3-4: Numerical Testing of Channel Pattern Thresholds *Hannah Schwedhelm*	R.4-4: Geomorphic Evolution of Peatland Streams: Controls on Sinuosity and Channel Stability *Jeffrey Nittrouer*
18:00	C.2-5: Leveraging Vestigial Vegetation Imprints in Marsh LiDAR Geomorphometry *Tegan Blount*	E.2-5: A Reduced-Complexity Model for Morphodynamic Evolution and Equilibrium Creek Spacing in Salt Marsh Systems *Chia-Chu Chu*	R.3-5: 3D complex shapes of river dunes through nonlinear stability analysis *Costanza Carbonari*	R.4-5: Timescales of River Bifurcations *Gabriele Barile*

19:00 - 21:00	***WICGE evening***

Wednesday, September 3rd · Morning

9:00	**Communications**	
	Keynote Lecture II	*Chair: Astrid Blom*
9:15 - 10:15	Predicting Coastal Changes: The Role of Machine Learning in Morphodynamic Modeling	*Kristen Splinter*
	G.3: General Session III	*Chair: Albert Falques*
10:15	G.3-1: Salt marsh accretion with sea level rise is hindered by dense vegetation	*Stijn Temmerman*
10:30	G.3-2: Laboratory experiments of bedforms evolution during flood events	*Simona Francalanci*
10:45	G.3-3: DOZER: exploring morphodynamic intervention in coastal overwash	*Eli Lazarus*
11:00 - 12:30	**Poster Session / Coffee-break**	
P.2-01	Enhancing Biomorphodynamic Modeling by Incorporating Vegetation Friction Approaches	*Antonia Dallmeier*
P.2-02	The Influence of Tectonic Uplift on Shore Morphology, Wave Energy Delivery, and Coastal Erosion.	*Cesar Lopez*
P.2-03	Global river morphology atlas	*Niek Collot d'Escury*
P.2-04	Residual transport of sand across tidal divides in the Dutch Wadden Sea	*Thomas Veerman*
P.2-05	Mangrove vegetation density and channel density have trade-off effects on nature-based flood risk mitigation	*Ignace Pelckmans*
P.2-06	From large-scale meanders to human-induced floodplain deposition: history of the Congaree River valley (South Carolina, USA)	*Marcin Słowik*
P.2-07	Morphologic evolution of tidal flats in the Wadden Sea	*Marthe Wassink*
P.2-08	Future Delta Development at the Alpine Rhine River Mouth in Lake Constance	*Jana Schierjott*
P.2-09	Continuous-Wave Radar for Coastal Morphology	*Alejandro Orfila*
P.2-10	Oyster Reefs on Intertidal Morphological Evolution	*Daoxudong LIU*
P.2-11	Investigating the Impacts of Watershed Urbanization on Downstream Sedimentation and Geomorphology of a River	*Afrida Aranya*
P.2-12	Effects of initial topobathymetric variability on the modeling of washover deposits	*Nil Carrion-Bertran*
P.2-13	Morphological Effects of a Controlled Flood in Regulated Rivers: A Bathymetric Analysis in the Lower Ebro	*Cesar Mosso Aranda*
P.2-14	Blue Carbon in Salt Marshes of the North Adriatic Sea (Italy): Challenges and Opportunities for Wetland Restoration	*Alice Puppin*
P.2-15	Tidal-Driven Sediment Transport Across Oyster Reefs: Insights from Laboratory Experiments	*Javier Zumbado*
P.2-16	From Data to Decisions: Hydrotechnical Monitoring	*Blanca Marin-Esteve*
P.2-17	Repeated bathymetrical surveys reveal transient storage of sediment in the near-field region of the plunging Rhône River inflow into Lake Geneva	*Stan Thorez*
P.2-18	Interventions in a River Bifurcation Region: A Hybrid Modeling Strategy	*Marijn Wolf*
P.2-19	Field-Based Characterization of Hydro-Morphoydanmic Processes at Barrier Breaches Induced by Hurricanes Helene and Milton	*Sam Holberg*
P.2-20	Evolution of tides and water levels over 70 years in a macrotidal and highly urbanized estuary	*Pénicaud Juliette*
P.2-21	Erosion behaviour of cohesive riverine sediments: joint measurements with SETEG² and EROMES	*Hanna Haddad*
P.2-22	Impact of Steel Industry Waste Dumping on Shoreline Dynamics: A Remote Multi-Decadal Analysis in Sagunt, Valencia	*Carlos Cabezas*
P.2-23	Characterizing 10yr of Shoreline Dynamics of a Mediterranean Coast with Sentinel 2	*Raquel González-Fernádez*
P.2-24	Transverse finger bars at El Trabucador back-barrier beach	*Anna Mujal-Colilles*
P.2-25	Numerical Simulation of Dike Breaching Using a Generalized Curvilinear Coordinate System	*Shinichiro Onda*
P.2-26	Deciphering Sedimentary Activity in the Rivers of the Altiplano of the Atacama Desert over Recent Decades	*Hernan Alcayaga*
P.2-27	Morfo70: a multi-scale numerical model for shoreline and surf-zone morphodynamics	*Nabil Kakeh*
	G.4: General Session IV	*Chair: Giovanna Vittori*
12:30	G.4-1: Morphodynamic Evolution of the Venice Lagoon: Past, Present, and Future Perspectives	*Luca Carniello*
12:45	G.4-2: Multiscalar Response of an Experimental Fixed-Wall Meandering Channel to a Sediment Supply Increase	*Peter A. Nelson*
13:00	G.4-3: Satellite Evidence on Beach Width Cyclicity Along a Barrier Island	*Susana Costas*
13:15	G.4-4: Long-Term Channel Morphology Model Including the Evolution of Vegetation Applied to an Actual River	*Yasuyuki Shimizu*
13:30 - 15:00	***Lunch***	

Wednesday, September 3rd · Afternoon

	Auditori	Room LS.1	Room LS.11	Room LS.12
	R.5: Human Interferences in Rivers *Chair: Enrica Viparelli*	**E.3: Human Interferences in Estuaries** *Chair: Alvise Finotello*	**C.3: Submerged Beach Processes** *Chair: Angels Fernandez-Mora*	**C.4: Continental Shelf Processes** *Chair: Pieter Roos*
15:00	R.5-1: Evolution of mine tailings released in sand-bed rivers *Marcelo Garcia*	E.3-1: Morphodynamic feedbacks induced by water level regulation in the Venice Lagoon (Italy) *Alessandro Michielotto*	C.3-1: Machine learning implementation to capture morphological response on the Bay of Biscay *Manuel Viñes Recasens*	C.4-1: Effects of a sloping shelf on tidal sand wave formation: A linear stability analysis *Laura Portos-Amill*
15:15	Fundamental Study on Sand Storage Function of Sand Retarding Basins during Sediment and Flood Disaster *Mikako Ishikura*	Long-Term Impacts of Sediment Disposal Strategies in the Western Scheldt *Jeroen Stark*	Cohesive sediments alter coastal bar dynamics under waves and currents *Anne Baar*	The Role of Cohesive Sediment in Sand Wave Formation *Wout Ploeg*
15:30	R.5-3: Suppressed Morphodynamic Activity in Restored Gravel-Bed Rivers *Paul Demuth*	E.3-3: Lessons from the circular use of dredged sediment for tidal habitat resto-ration along the Access Channel to the Port of Rotterdam *Kees Sloff*	C.3-3: Numerical modelling of breaker bar morphodynamics and the role of longwave presence *Buckle Subbiah Elavazhagan*	C.4-3: Assessing Offshore Wind Farm Impacts on Marine Dune Migration: A Case Study in the Southern North Sea *Pablo Tassi*
15:45	R.5-4: Effect of engineered logjams on flow and local morphology *Simone Speltoni*	E.3-4: Morphodynamic evolution of estuarine intertidal flats under sea level rise and dredging strategies *Mick van der Wegen*	C.3-4: Integrating Physical and Numerical Models to Assess Wave Dissipation and Sediment Accumulation at Restored Oyster Reefs *Alberto Canestrelli*	C.4-4: Long-Term Interaction Between Offshore Sand Banks and the Active Beach *Dan Sebastian*
16:00	R.5-5: A disaster caused by overmining of sediment: case of Shi-ting River, China *Chenge An*	E.3-5: Nature-based mitigation of shoreline erosion risks in restored and created tidal marshes *Marte Stoorvogel*	C.3-5: Predicting Tombolo and Salient formations in complex coastal settings *Arnau Garcia Tort*	C.4-5: Modelling the Morphodynamic Response to Sand Extraction from Tidal Sandbanks in Sediment-Scarce Environments *Sem Geerts*
16:15	R.5-6: Sediment supply effects on fish habitat dynamics in a morphologically active river widening *Mahmoud O. M. Awadallah*	E.3-6: Biodiverse and spatially self-organized tidal marshes are most effective for nature-based shoreline protection *Ken Schoutens*	C.3-6: River sand inputs, headland bypassing, and the infilling of a pocket beach *Ruth Durán*	C.4-6: Predicting decadal evolution of coastal morphodynamics: A case study on the Belgian Continental Shelf *Yagiz Arda Cicek*
16:30 - 17:00	***Coffee-Break***			
	Auditori	**Room LS.1**	**Room LS.11**	**Room LS.12**
	R.6: General Aspecs in Rivers *Chair: Raffael Tinoco*	**E.4: Estuarine Equilibrium** *Chair: Zheng Bing Wang*	**C.5: Beach Morphodynamics** *Chair: Susana Costas*	**C.6: Coastal Sediment Dynamics** *Chair: Ana Vila-Concejo*
17:00	R.6-1: Cyclone-Driven Sediment Pulses and River Morphodynamic Response in Tairāwhiti, Aotearoa New Zealand *Jon Tunnicliffe*	E.4-1: Sensitivity of Morphodynamic Equilibria of Double-Inlet Systems to Basin Width *Henk Schuttelaars*	C.5-1: High-resolution morphodynamic evolution of a dune field in the macrotidal bay of Somme (France) *Tatiana Goulas*	C.6-1: On the role of ripple secondary crest on nearbed hydrodynamics *Chuang Jin*
17:15	R.6-2: Morphodynamics of hanging ice dams: interaction between flow, sediment, frazil ice and a solid ice roof *Gary Parker*	E.4-2: Using an equilibrium model to explore the influence of climate variations on estuarine evolution *Edouard Basquin*	C.5-2: The role of outwash on barrier evolution: how shoreface-dune couplings influence barrier recovery *Katherine Anarde*	C.6-2: Unraveling sediment transport by shallow waves over rippled beds: insights from particle-resolved Direct Numerical Simulation *Marco Mazzuoli*
17:30	R.6-3: Temporal evolution of water residence times throughout the growth of a river dominated delta *Matthew Hiatt*	E.4-3: Tidal inlet and estuary equilibrium relationships *Ian Townend*	C.5-3: Spit Responses to a Severe Storm *Drude Fritzboeger Christensen*	C.6-3: Biofilms as the "ecosystem engineers": the microbiological mediation of in-tertidal sediment behavior *Xindi Chen*
17:45	R.6-4: Certainty of floodplain flux source as a function of river discharge *Andrew Moodie*	E.4-4: The Role of Estuarine Processes in River Width Equilibrium *Lorenzo Durante*	C.5-4: Assessment of the intermittency of river mouths using cloud-enabled Earth observation analysis *Marcus Silva-Santana*	C.6-4: Sediment Dynamics in Coral Rubble Flats *Ana Vila-Concejo*
18:00	R.6-5: The impact of hydrograph shapes on riverbed evolution at a knickpoint *Soichi Tanabe*	E.4-5: Tidal influence over river width distribution, an analytical approach. *Enrico Moresco*	C.5-5: Assessing the impact of sand fences on foredune development in high urban beach: A four-year study of Calafell Beach (Costa Daurada, Spain) *Carla Garcia Lozano*	C.6-5: 3D evolution of the Millars River and shoreline changes on the surround-ing beaches. Case of study in Castelló (E Spain) *Josep Eliseu Pardo-.Pascual*
19:00 - 21:00	***Young RCEM evening***			

Thursday, September 4th · Morning

9:00	**Communications**	
	Keynote Lecture III	*Chair: Guido Zolezzi*
9:15 - 10:15	Biomorphodynamics of Tidal Wetlands: Processes, Feedback and Modelling	*Zeng Zhou*
	G.5: General Session V	*Chair: Gary Parker*
10:15	G.5-1: Coastal Vegetation Stochastic Dynamics	*Carlo Camporeale*
10:30	G.5-2: Empirical/Theoretical modeling the evolution of multi-species marshes	*Brad Murray*
10:45	G.5-3: Size sorting due to fine infiltration in coarse river beds	*Philippe Frey*
11:00 - 12:30	**Poster Session / Coffee-break**	
P.3-01	Extraction of patches and stripes in saltmarsh wetlands using deep neural networks	*Zichao Guo*
P.3-02	Turbulence Induced by River Bedforms in Supercritical Flows	*Sofi Farazande*
P.3-03	Dynamic Interactions Between Vegetation and Delta Morphology: Insights for Coastal Restoration	*Madoche Jean Louis*
P.3-04	Geomorphic Responses of a Partially Regulated River to Sequential Flood Events	*Maha Sheikh*
P.3-05	Acoustic inversion of high sediment concentrations	*Shiyu Bao*
P.3-06	Laboratory study of wave-driven alongshore velocity and bed shear stress on fixed smooth and rough planar beaches	*Schueller Alexandra*
P.3-07	Experiment on Geomorphological Changes in the Floodplain Caused by the Cohesive Levee Breach	*Yuzuno Kanbara*
P.3-08	Numerical experiments on wave-driven morphodynamics in the Wadden Sea	*Magdalena Uber*
P.3-09	Quantifying Bedform Morphology in Meandering Rivers	*Daniel Alvarez*
P.3-10	A Hybrid Approach for Morphodynamic Prediction in Estuaries	*Mirian Jiménez Tobío*
P.3-11	PIV measurements of periodic waves around emerged vertical cylinders	*Johann K Delgado*
P.3-12	One-dimensional morphodynamic effects of perpendicular logs as obstacles in rivers	*Manuel Faúndez*
P.3-13	From Physical to Numerical Model: Simulating Laboratory Experiments to Generate Synthetic Data of Shoreline Response to Sea-Level Rise	*Maurizio D'Anna*
P.3-14	Fundamental Hydraulic Experiments on Channel Alternation in a Gourd Shaped Channel	*Hirokazu Matsui*
P.3-15	Natural levees are hotspots for organic carbon sequestration in tidal marshes	*Mona Huyzentruyt*
P.3-16	Long-Term Numerical Modelling of Sediment Transport Impacts on Sand Nourishments Distribution	*Ana Margarida Ferreira*
P.3-17	Experimental study on the three-dimensional flow field in a river confluence	*Juan Pablo García Rivera*
P.3-18	Measuring overnight tidal beach overwash events at Cape Cod National Seashore, USA using thermal infrared imagery timestacks	*Evan T. Heberlein*
P.3-19	River Flow Variability as a Catalyst for Vegetation Growth and Carbon Pumping	*Luca Salerno*
P.3-20	Improving Flood Forecasting in Estuaries with Satellite-Derived Digital Elevation Models	*Ernesto Tonatiuh mendoza*
P.3-21	Morphodynamic Response of River Deltas to Unsteady Discharge and Sed-iment Supply	*Zhenwei Wu*
P.3-22	Research on mixed-grain sediment on bed rock channels	*Yekyun Song*
P.3-23	Influence of Vegetation-Induced Roughness on the Morphodynamics of River-Dominated Deltas	*Anderson Amaya-Saldarriaga*
P.3-24	Recirculation zones in meandering rivers: the Sabine River case study	*Riccardo Bonanomi*
P.3-25	Quantifying Morphological Changes Driven by Oyster Reef Breakwaters under Different Tidal and Wave Conditions	*Jacopo Composta*
P.3-26	Embayed Beach Morphodynamics Under Extreme Forcing and Sediment Delivery	*Candela Marco-Peretó*
	G.6: General Session VI	*Chair: Karin Bryan*
12:30	G.6-1: 3D morphodynamic modelling of tidal inlets	*Xavier Bertin*
12:45	G.6-2: Historical development of tidal dynamics and morphodynamics in the Dutch Wadden Sea	*Zheng Bing Wang*
13:00	G.6-3: Fully nonlinear evolution of free migrating river bars: domain length effects, wavenumber selection, and timescale dynamics	*Annunziato Siviglia*
13:15	G.6-4: Investigating the role of geotechnical sediment properties on storm-driven geomorphodynamics	*Nina Stark*
13:30 - 15:00	***Lunch***	

Thursday, September 4th · Afternoon

	Auditori	Room LS.1	Room LS.11	Room LS.12
	C.7: Nearshore Processes *Chair: Francesca Ribas*	**E.5: General Aspects in Estuaries I** *Chair: Ian Townend*	**R.7: Lab experiments** *Chair: Eli Lazarus*	**R.8: River Banks** *Chair: Simona Francalanci*
15:00	C.7-1: Transition to turbulence close to a rough sea bottom *Giovanna Vittori*	E.5-1: Interface with sedimentary grains favors biofilm retention and anti-erosion under shear stress *Guotao Tang*	R.7-1: Effects of Unsteady Flow on Bar Morphology and Dynamics in an Experimental Flume *Atsuko Mizoguchi*	R.8-1: Riverbed and banks coupled evolution *Ludovico Agostini*
15:15	Impacts of Extreme Storms on Urban Beaches: A Comprehensive Study of the Gloria Storm in Cala Millor, Balearic Islands *Angels Fernandez Mora*	Vegetation impacts on crevasse splay dynamics and channel-floodplain connectivity in a river delta *Sarah Brannum*	A simple laboratory test case for suspended load modelling *Benoit Camenen*	Hydro-Environmental Conditions Modulate the Temporal Variability of Streambank Erodibility Parameters *Celso Castro-Bolinaga*
15:30	C.7-3: Assessment of the risks of flooding in Andalusia (Spain) for the XXI century *Manuel Cobos*	E.5-3: A hydrological switch drives the transition from saltmarsh to reedland ecosystem *Archontoula Valsamidou*	R.7-3: Morphological and non-morphological bedload varying river confinement: a laboratory investigation *Enrico Pandrin*	R.8-3: Hydraulic or seepage erosion: What drives bank collapse in tidal environments? *Kun Zhao*
15:45	C.7-4: Automatic shoreline detection in time-exposure images by using bi-LSTM networks: Input channel selection for high accuracy *Miquel Caballeria Suriñach*	E.5-4: Stream Meandering in Tidal Wetlands: Unveiling Patterns, Drivers, and Ecomorphodynamic Impacts *Alvise Finotello*	R.7-4: Lab experiments on the permeability of a gravelly river bed *Anouk Boon*	R.8-4: Numerical Investigation of Alluvial Ridge Development in Meandering Rivers *JeongYeon Han*
16:00	C.7-5: Morphological evolution of a channel-shoal complex in the mouth of the Ems estuary (Dutch Wadden Sea) *Rinse de Swart*	E.5-5: Geometry and morphology of channels around estuarine islands *Maarten van der Vegt*	R.7-5: Using porosity and submergence ratio to assess particle transport past submersed in-stream structures *Rafael Tinoco*	R.8-5: Modeling of Natural Levee Formation in an Engineered Compound Channel of the Abira River, Japan *Kensuke Naito*
16:15	C.7-6: Investigating the stability of hoa channels bisecting reef islands *Andrew Ashton*	E.5-6: Dynamics, Mixing, and Sediment Transport in Freshwater Plumes *Cristian Escauriaza*	R.7-6: Laboratory Study on the Flocculation and Settling Behaviour of Sediment from the Three Gorges Reservoir *Dayu Wang*	R.8-6: Measuring the abundance and dimensions of natural river levees *Eric Barefoot*
16:30 - 17:00	***Coffee-Break***			
	Auditori	**Room LS.1**	**Room LS.11**	**Room LS.12**
	C.8: Nearshore Sand Patterns *Chair: Daniel Calvete*	**E.6: General Aspects in Estuaries II** *Chair: Bram van Prooijen*	**R.9: Bifurcations and Meanders II** *Chair: Niccolo Ragno*	**R.10: Sediment Transport in Rivers** *Chair: Stefano Lanzoni*
17:00	C.8-1: Numerical Modelling of Long Transverse Finger Bars at El Trabucador Beach, Spain *Nicholas Dodd*	E.6-1: Automated Characterisation of Tidal Course Morphology for Intertidal Mud-flat Study *Chitrachandika Bhoobun*	R.9-1: Using Gaussian mixture models and topo-bathymetric LiDAR to decipher morphology of large rivers *Andréault Alex*	R.10-1: Using passive acoustics to map bedload over migrating bars *Jules Le Guern*
17:15	C.8-2: History of km-scale shoreline sandwave research and perspectives *Deborah Idier*	E.6-2: Machine Learning for Nearshore Satellite-Derived Bathymetry in regions with different tidal regimes and high optical complexity. *Mario Luiz Mascagni*	R.9-2: Climate Change Impact on a River Bifurcation Region *Kifayath Chowdhury*	R.10-2: How to build a 3D probabilistic drainage network by hydraulic geometry *Li Zhang*
17:30	C.8-3: Effects of shelf sand ridges on decadal shoreline evolution under sea level rise: An idealized modelling approach *Abdel Nnafie*	E.6-3: On The Joint Action of Flood-Tidal and Wave-Driven Longshore Currents On an Erosion Hotspot Near the Sado River Mouth *Alphonse Nahon*	R.9-3: Measuring planimetric features of fluvial bifurcations *Pascal Pirlot*	R.10-3: Improving and extending a unified model for bedload and suspended sediment transport modes *Kim-Jehanne Lupinski*
17:45	C.8-4: Self-organized patterns in Coastal Morphodynamics *Albert Falqués*	E.6-4: Modeling salt-wedge dynamics and suspended sediment transport in the microtidal Rhône estuary *Kim Anh Do*	R.9-4: Processes of channel formation on meandering river floodplains revealed by repeat lidar *Doug Edmonds*	R.10-4: Large scale assessment of the clogging dynamics in gravel-bed river : experimental and numerical approaches. *Dorian Hernandez*
18:00	C.8-4: Self-organized patterns in Coastal Morphodynamics *Albert Falqués*	E.6-5: Bathymetric Evaluation by Remote Sensing Tools at an Energetic Estuary *M. Said Parlak*	R.9-5: Creation of Oxbow Lakes Depends on Bifurcation Dynamics *Ye Jing*	R.10-5: Effect of Suspended Sediment on Turbulent Flow Diffusion *Allen Batemen*
20:00 - 23:00	***RCEM Conference Dinner***			

KEYNOTE SPEAKERS

KEYNOTE SPEAKERS

KRISTEN SPLINTER

Associate Professor at UNSW Sydney, Australia

Keynote title: Predicting Coastal Changes: The Role of Machine Learning in Morphodynamic Modeling

Dr. Kristen Splinter is an Associate Professor and Managing Director at the Water Research Laboratory within the School of Civil and Environmental Engineering (UNSW Sydney, Australia). Her research covers broad topics including storm to inter-annual shoreline change monitoring and modelling; coastal erosion and beach recovery; dune erosion; and remote sensing of the coastal environment. She is currently leading a 4-year ARC Future Fellowship to develop regional scale forecasting of sandy coastal change around NSW. This involves the development of new shoreline models, including adaptive empirical approaches and machine learning techniques. Her goal is to not only develop skill models for our complex coastlines but also use these models to further learn about dynamic systems. As a female engineer, Kristen has a strong desire to support and encourage more women and diverse backgrounds into the discipline and enjoys working with young children to support interest in STEM. She is the co-founder of the international seminar series, Comomola: COastal MOrphodynamics and Machine LeArning: Building an Inclusive International Network of Scientists.

FERNANDO MENDEZ

Full Professor at University of Cantabria, Spain

Keynote title: Climate-Based Met-Ocean Emulators for Compound Coastal Flooding and Long-term Morphodynamics

Dr. Fernando Méndez is full professor of Coastal Engineering at University of Cantabria (Spain), where is the head of the research group on “Geomatics and Ocean Engineering”. His research lines are focused on building knowledge to incorporate climate characterization and data science in coastal engineering, including databases of marine variables, statistical models of extremes, data mining, statistical downscaling, climate variability, climate change, tropical cyclones, dynamical downscaling, flooding and coastal erosion. He is a leading expert in his discipline and has on-going collaborations within many research groups, in USA (Duke Univ., OSU, SCRIPPS, USGS, NOAA), Brazil (UFSC), New Zealand (NIWA, U. Auckland), Spain (UPC, Univ. Granada, AZTI, U. Coruña) and Australia (CSIRO, U. Sydney, UNSW).

ZENG ZHOU

Full professor at Hohai University, China

Keynote title: Biomorphodynamics of Tidal Wetlands: Processes, Feedback and Modelling

Dr. Zeng Zhou obtained his PhD on tidal network morphodynamics at University of Cantabria in 2015. Upon completion of the PhD, he worked as a researcher at Deltares and University of Auckland before he joined Hohai University (China) in 2016. In 2019, he was promoted to full professor on coastal (bio-)morphodynamics. He is leading a research team to study biophysical interactions of coastal wetlands and the associated morphodynamic feedbacks using various techniques (e.g., remote sensing, field and laboratory experiments, numerical modelling). He serves as the director for Jiangsu Provincial Key Laboratory of Coastal Ocean Resources Development and Environmental Security, the associate editor for Anthropocene Coasts journal, and is also a member of the international advisory board for the journal Earth Surface Processes and Landforms. During the last decade, he has been leading a number of Chinese national key research projects on coastal wetland management, sustainable development and nature-based solutions.

ABSTRACTS

On the relationship between bedform morphology and meander dynamics

Julia Cisneros[1], Anne Baar[2]
[1]Department of Geosciences, Virginia Tech, Blacksburg VA, USA
[2]Department of Water Management, Faculty of Civil Engineering and Geosciences, TU Delft, Delft, NL
Corresponding author: cisneros@vt.edu

Keywords: bedform morphology, river bends, transverse slope, sediment transport, flow dynamics

1 Introduction

Rivers experience dynamic flow and sediment transport within bends. Bedform morphodynamics leads to spatial heterogeneity of sediment flux through river bends, resulting in variable sedimentation and deposition [1]. On a larger scale, this variability enhances river bend migration and evolution. Meander rates link to erosion rates through sedimentary system transport zones, which supply sediment to vulnerable coastal environments [1].

In big rivers and flow models, bedform morphology is shown to influence flow dynamics differently than assumed by morphodynamics equations, with lower resistance and higher shear stresses occurring over low angle dunes compared to high angle dunes, which may lead to higher sediment fluxes [2,3]. Still, how different bedform scales and shapes interact and influence flow and contribute to sediment transport is unknown in river bends [4].

2 Methodology

We compare bedform morphology, transverse slope, and sediment transport parameter estimates in field and experimental datasets. Our field study area is the Kootenai River, ID, USA, covering 3 bends in a meandering section. Our experimental data is an extended analysis of bedforms formed in a rotating annular flume across grain sizes, sediment mobilities and bend radii [4].

Bedform morphology was measured via the Bedform Analysis Method for Bathymetric Information [2], from field and experimental scans. Bedform morphology was spatially averaged along river centerlines for field and averaged based on equilibrium conditions for lab. Transverse slopes were measured along river centerline for field and in each lab experiment. Sediment transport parameters were estimated via field flow depth relationships and lab ADV measurements.

3 Results

3.1 Field data

Bedform morphology in the Kootenai River displays spatial variability linked to river planform morphology. Bedform height and leeside angle abruptly increase with steepening transverse slope near the river bend apex. Heights range from 0.8 to 1.6 m and leeside angles are 15.5° to 33.5°. Along river, wavelength is variable and ranges between 42 – 181 m.

3.2 Experimental data

A positive relationship between leeside angle and transverse slope occurs. In coarser grains (>1 mm), this relationship is enhanced where leeside angles are greater with increasing grain size.

4 Implications

Based on these findings, we hypothesize bedforms influence how sediment is distributed across rivers and thus influence river dynamics. This mechanism is primarily rooted in the feedback between spatially variable bedform morphology and transverse slopes in a river bend. The abrupt increase in leeside angle within the bend increases local flow resistance, decreases near-bed shear stress, and decreases downslope sediment flux. The positive relationship with coarsening grain size suggests this process becomes more pronounced in coarse grained rivers. Overall, this morphodynamic feedback increases the adaptation length between flow perturbations and morphologic response of river meander dynamics.

Acknowledgments

We thank Taylor J. Dudunake for his support in securing water surface elevation maps from the raw, unpublished dataset from USGS survey data release (https://doi.org/10.5066/P9OC5QMH).

References

[1] Hickin, E.J., 1974. The development of meanders in natural river-channels. Am. J. Sci., 274, 414–442.
[2] Cisneros, J., Best, J., van Dijk, T., Almeida, R. P. D., Amsler, M., Boldt, J., ... & Zhang, Y. (2020). Dunes in the world's big rivers are characterized by low-angle lee-side slopes and a complex shape. Nature Geoscience, 13(2), 156-162.
[3] Lefebvre, A., & Cisneros, J. (2023). The influence of dune lee side shape on time-averaged velocities and turbulence. Earth Surface Dynamics, 11(4), 575-591.
[4] Baar, A. W., de Smit, J., Uijttewaal, W. S., & Kleinhans, M. G. (2018). Sediment transport of fine sand to fine gravel on transverse bed slopes in rotating annular flume experiments. Water Resources Research, 54(1), 19-45.
[5] Baar, A. W., Boechat Albernaz, M., Van Dijk, W. M., & Kleinhans, M. G. (2019). Critical dependence of morphodynamic models of fluvial and tidal systems on empirical downslope sediment transport. Nature communications, 10(1), 4903.

Enigmatic lunate shaped bedforms in the Fehmarn Belt, Baltic Sea

Christian Winter[1], Giuliana Diaz Mendoza[1], Knut Krämer[1], Anja Conventz[1], Marius Becker[1]
[1] Institute of Geosciences, CAU Kiel, Germany
Corresponding author: christian.winter@ifg.uni-kiel.de

Keywords: dunes, barchans, sand-silt waves, microtidal, ,

1 Abstract

In the microtidal Western Baltic Sea, a large field of lunate bedforms has been mapped and described by few earlier studies. None of them are conclusive on the formation mechanisms, internal structure, and dynamics. The bedforms are characterised by their isolated occurrence and crescentic or barchanoid shapes. The central part is of height O(1m) and often two tails of lengths in O(100 m) predominantly open towards the South-East, suggesting an active migration towards this direction. New data from a multibeam echo sounder survey, sediment cores and subbottom profiles reveal morphodynamics, sedimentology, and the internal bedding and challenge previous assumptions on the formation and dynamics of the bedforms.

2 Introduction

Coastal morphodynamics along the coasts and basins of the microtidal Western Baltic Sea are mainly driven by waves and wind induced currents, and by the effects of seiches which develop after higher wind conditions. Along with the typical dynamics of beaches and bars, here various kinds of bedforms are found on the seafloor, i.e. a large compound dune field in medium to coarse sands (Feldens et al. 2014, Krämer et al., 2023), or various other natural or human made features on the seafloor.

In this study we discuss a large field of crescentic bedforms in water depths exceeding 20 m covering a region of about 217 km^2 in the central Fehmarn Belt. The heights of individual bedforms is 0.5–1.0 m and the width about 50 m. The distance between individual features is in the order of a few hundred meters. The crescentic planform geometry resembles barchanoid dunes, often with two tails of lengths in O(100 m) opening towards the E or SE.

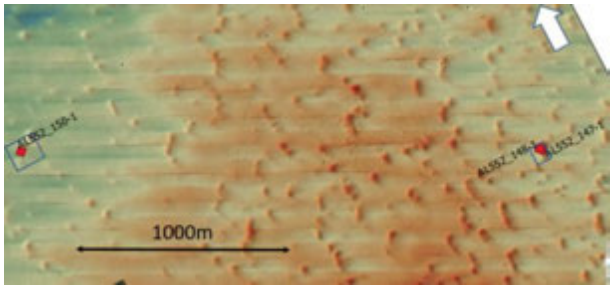

Figure 1: MBES bathymetry subset of the lunate bedform field in between different core locations NE of Fehmarn island

Despite the large extent of these features only few studies have approached their characterisation. Jensen et al. (2003) described them as *isolated sand-silt waves* because of their solitary occurrence in muddy to fine sediments. Based on a limited set of observations, they were first described as "NE-SW striking ridges of considerable length" without a clear asymmetry or preferred orientation.

In the framework of the environmental impact assessment for the large Fehmarn Belt tunnel construction the so called *lunate bedform field* was revealed by a large scale multibeam echo sounder (MBES) mapping (FEHY, 2013). Many similar bedforms of characteristic shape were identified as regularly spaced with distances between individual features of a few hundred meters, on an area of 217 km^2 (Fig. 1). The authors speculate on a high activity of the bedforms i.e., migrations in the order of several meters per annum towards the NE or SW based on their similarity of a calculation of local sediment transport potential.

Although the existence, distribution, and role as roughness elements on the local hydrodynamics has been described before, the discussion on the genesis, morphology, and dynamics of these bedforms are still not conclusive.

3 Methods

Different expeditions with the research vessel R/V ALKOR to the Fehmarn Belt were conducted in 2020, 2021, 2022, and 2023. During the expeditions, the bedform field was investigated by multibeam echo sounder mapping, parametric echo sounder profiles, gravity coring and bed surface sediment grab sampling. Grain size distributions were measured in the CAU Kiel, sedimentology laboratory.

4 Results

An area of about 6 km^2 was (re-)mapped with multibeam and parametric echo sounders. The processed high-resolution bathymetry confirms the existence of individual bedforms in heights in the order of one meter, which often feature a crescentic shape with a density of about 50 bedforms/km^2. Where present, the extremities ("horns") resemble the shape of barchanoid dunes, opened towards the SE. Successive surveys indicate little or no mobility of the bedforms.

In the high-resolution MBES data, sharp, angular features, predominately on the Western side of the bedforms, are present. Based on earlier and recent underwater camera observations, these are interpreted as

Designing ecosystems for climate change

Johan van de Koppel[1,2], Loreta Cornacchia[3], Roeland van de Vijsel[4], Brian Silliman[5]
[1] Royal Netherlands Institute of Sea Research, Yerseke, The Netherlands
[2] University of Groningen, The Netherlands
[3] Deltares, Delft, The Netherlands
[4] Wageningen University and Research, Wageningen, Netherlands
[5] Duke University Marine Lab, Beaufort, North Carolina, USA
Corresponding author: johan.van.de.koppel@nioz.nl

Keywords: wetlands, estuaries, salt marshes, self-organization, patterns

1 Introduction

Self-organization processes can play a key role in defining the adaptive response of ecosystems to climate change. Ecosystems can adjust spatial patterning, drainage creek or stream networks, or other spatial structures due to the interaction between sessile organisms such as plants of bivalves and physical processes such as water flow or infiltration rate, locally stimulating growth, but at the same time optimize growth conditions at the landscape scale. Modelling studies highlight that this process could play a crucial role in allowing ecosystems such as arid bushland, salt marshes and dunes to adjust to climate change.

2 Humans homogenise landscapes

Despite this adaptive potential, human activities severely constrain self-organisation processes. Agricultural practices have globally homogenised landscapes. Dykes and human buildings and infrastructure now constrain many coastal ecosystems, limiting the potential for ecosystems to adapt to the rising sea. In many estuaries, restoration efforts do not consider to optimise spatial organization of wetlands.

3 Creeks are crucial for restoration

Here, I discuss a series of publications in which we highlight that self-organisation is a crucial process defining the adaptive capacity of salt marsh ecosystems. Creek formation, shaped by a scale-dependent feedback between plant growth and sedimentation, is an important process defining how salt marshes can follow sea level rise. A follow-up study highlighted that the creek system formed during salt marsh development is even more important than plant characteristics for determining sediment accumulation, highlighting the need to conserve and restore natural patterns? in wetlands.

4 Designing Resilient Ecosystems

In many estuarine systems, wetlands are restored or even created to improve coastal safety in the face of sea level rise. When creating tidal wetlands, homogeneous agricultural fields are transitioned into tidal ecosystems by allowing in the tidal water, and roughly creating tidal creeks. Model analysis highlights that when these creeks closely mimic natural creek systems, these creeks create significant flow rates, allowing for quick sediment transport into the marsh. However, many constructed creeks were too wide, reducing sedimentation rate, lowering wetland resilience. Our study highlights that when designing new wetlands, adapting self-organisation principles may improve the resilience of ecosystems to sea level rise.

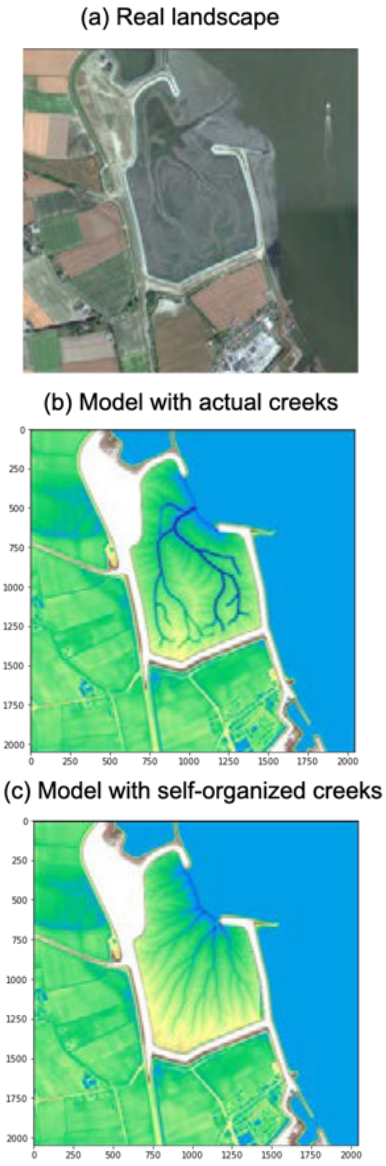

Figure 1. (a) Satellite image of the Perkpolder restoration site in 2023 (Google Earth). (b) Result of model simulation with the creek network in the shape of the real-world creek design and (c) bathymetry predicted by the model in the self-organized case (developed from a flat topography and no initial creek system).

Modelling interaction between free migrating bars and in-stream structures

Redolfi Marco[1], Victor Chavarrias[2], Marco Tubino [3]

[1]Dipartimento di Ingegneria "Enzo Ferrari", Università degli Studi di Modena e Reggio Emilia, Italy
[2]Department of River Dynamics and Inland Shipping, Deltares, The Netherlands
[3]Dipartimento di Ingegneria Civile, Ambientale e Meccanica, Università degli Studi di Trento, Italy

e-mail corresponding author: marco.redolfi@unimore.it

Keywords: *river morphodynamics, alternate bars, numerical modelling, nonlinear interactions*

1 Introduction

Bar migration in rivers is frequently disturbed and sometimes completely inhibited by geometrical discontinuities such as bends, bridges, jumps, and groynes. This phenomenon is expected to significantly influence the morphological and dynamical characteristics of the river. In this work we study numerically the interaction between migrating bars and a generic asymmetric obstacle, focusing on both the upstream and downstream effects.

2 Methods

Numerical simulations are performed using Delft3D. We considered a straight, 7000 m long and 35 m wide channel. Slope, discharge and grain size are varied according to uniform-flow relations in order to preserve Shields stress while varying channel width-to-depth ratio. A one-sided narrowing of the cross section is placed at half the channel length to locally reduce the width to 26.25 m. A periodic perturbation is then applied at the upstream boundary to trigger the development of migrating bars.

3 Results

Different evolutionary scenarios are found depending on channel width-to-depth ratio being smaller or larger than the resonant value.

Under sub-resonant conditions (Figure 1), the obstacle initially generates a train of alternate bars that tend to be conveyed downstream. The first two or three bars close to the obstacle rapidly slow down, eventually turning into longer, steady bedforms. However, as bars decelerate their height significantly reduces, leading to spatially damped steady bars that are consistent with predictions by linear models [2]. Meanwhile, migrating bars that continuously originate from the upstream boundary propagate through the narrowing, leading to a final regime configuration where they coexist with steady bars forced by the obstacle. Interestingly, as illustrated in Figure 1, simulations clearly show that morphodynamic information travels faster than bars themselves, revealing that the group speed of bed waves is systematically higher than their phase speed.

Under super-resonant conditions, migrating bars generated by the obstacle are again observed to slow down and elongate, but in this case their amplitude does not reduce, leading to a pattern of nearly periodic steady bars [1]. Migrating bars originating from the upstream boundary are again observed to pass through the obstacle. However, the regime configuration downstream of the obstacle is more affected by nonlinear interaction between steady and migrating bars. Additionally, bar migration in the upstream region also appears to be disturbed by the obstacle, suggesting a possible upstream influence [3]. Nonetheless, this effect is sensitive to the choice of numerical scheme and associated parameters, which motivates further investigation that is currently in progress.

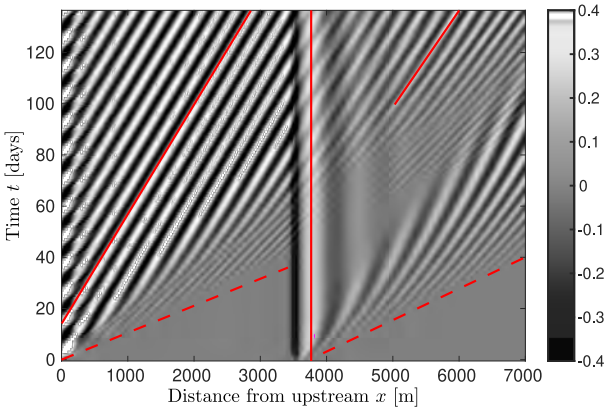

Figure 1: Space-time diagram showing the evolution of bed elevation as downstream-migrating bars pass through a one-sided narrowing located at $x = 3500$ m (sub-resonant conditions). Solid and dashed lines indicate the phase and group speed of bars in different regions of the diagram, with vertical lines representing zero speed (i.e. steady bars).

Overall, these results highlight the key role of the channel width-to-depth ratio in determining the impact of in-stream structures on bed morphodynamics.

References

[1] G. Seminara and M. Tubino. Weakly nonlinear theory of regular meanders. *J. Fluid Mech.*, 244: 257–288, 1992.

[2] N Struiksma, KW Olesen, C Flokstra, and HJ De Vriend. Bed deformation in curved alluvial channels. *J. Hydraul. Res.*, 23(1):57–79, 1985.

[3] G. Zolezzi and G. Seminara. Downstream and upstream influence in river meandering. part 1. general theory and application to overdeepening. *J. Fluid Mech.*, 438(13):183–211, 2001.

Inlet connectivity as new concept to understand the role of tidal divides in mesotidal barrier coast dynamics

Pieter C. Roos[1], Henk M. Schuttelaars[2]
[1]Water Engineering & Management, University of Twente, Enschede, The Netherlands
[2]Applied Mathematics, Delft University of Technology, Delft, The Netherlands
Corresponding author: p.c.roos@utwente.nl

Keywords: Barrier coasts, double inlet systems, cross-sectional stability, morphodynamic equilibria, tidal divides

1 Introduction

Whether and how the inlets in mesotidal barrier coasts (e.g., Long Island, Ria Formosa, Venice Lagoon, Wadden Sea) affect one another morphodynamically is not only theoretically, but also practically relevant. For example, dredging operations in one inlet may trigger sedimentation at another inlet. Based on Escoffier's [1] cross-sectional *inlet stability* principle, past studies explored the possible return to equilibrium after perturbing one or more inlets [2]. However, *inlet stability* neglects the degree to which inlets influence each other. This calls for a new concept, here referred to as *inlet connectivity*, that is likely to depend on various characteristics, such as back-barrier geometry, inlet spacing and tidal divides. Here we (i) introduce and quantify this new concept, and moreover (ii) implement and analyse it in an exploratory double inlet model, extended to include a tidal divide (Fig.1a).

2 Methods

Starting point is any stable equilibrium in a multiple inlet system. We consider the system's return to equilibrium after perturbing one of the inlets, while leaving the other(s) unaffected. We then define the *connectivity quotient* C_{jq} as the maximum cross-sectional change experienced by the (initially unperturbed) inlet j, divided by the initial perturbation of inlet q's cross-section (Fig.1b). Clearly, large $|C_{jq}|$-values imply strong connectivity, and $C_{jq}\approx 0$ means weak connectivity. We implement these ideas in a new double inlet model, extending earlier work [2] by including a tidal divide using a stepped topography (Fig.1a). A novelty herein is our derivation of eigenfunctions for the entire back-barrier basin, accounting for this stepped topography.

3 Results

Our model results show how increasing the tidal divide height or the inlet spacing either turns an unstable inlet system into a stable one, or reduces connectivity if it is already stable (Fig.1c). Moreover, all runs for this double inlet system reveal *negative* values of the connectivity quotient. This suggests that the system's return to equilibrium after perturbing one inlet's cross-section is always attended with an *opposite* response at the other inlet: an *increase* of 1 implies a (temporary) *decrease* at 2; as in Fig.1b. Further results as well as potential implications for the Western Wadden Sea (a triple inlet system consisting of Texel inlet, Vlie inlet and Eijerlandse Gat system) will be discussed.

References

[1] Escoffier, F. F. (1940). The stability of tidal inlets, *Shore and Beach*, 8, 114-115.
[2] Roos, P. C., H. M. Schuttelaars & R. L. Brouwer (2013). Observations of barrier island length explained using an exploratory morphodynamic model, *Geophys. Res. Lett.*, 40(16), 4338-4343.

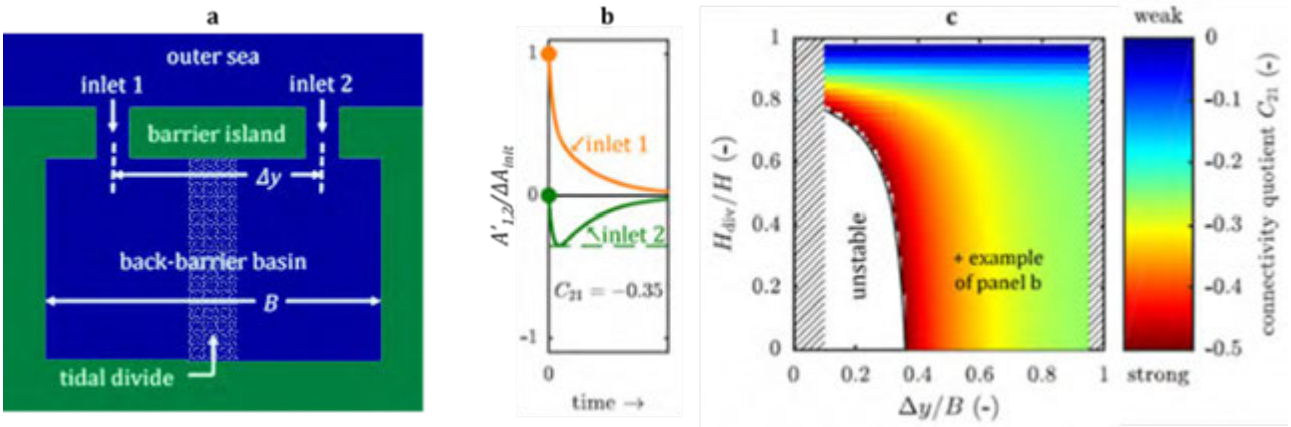

Figure 1: **a** Top view of model geometry showing double inlet system with stepwise tidal divide. **b** Example of system's return to equilibrium after perturbing inlet 1, corresponding to a connectivity quotient of C_{21}=-0.35. The plot shows the time evolution of the *perturbations* to the cross-sectional areas of inlet 1 (A'_1 in orange) and 2 (A'_2 in green), scaled with inlet 1's initial perturbation ΔA_{init}. **c** Sensitivity of connectivity quotient C_{21} to *inlet spacing* Δy and *tidal divide height* H_{div} (scaled with basin width B and depth H, resp.). Warmer colours indicate stronger connectivity, colder colours imply weaker connectivity. The example highlighted in panel b is denoted with +.

Bed material or washload?

Enrica Viparelli[1], Haiqing Xu[2], Astrid Blom[3], Raymond Torres[1], Matthew Czapiga[4], J. Wesley Lauer[5], Bidhan Sahu[1], Gary Parker[6]
[1]University of South Carolina at Columbia
[2]University of Texas Rio Grande Valley
[3]Delft University of Technology
[4]Tulane University
[5]Seattle University
[6]Univeristy of Illinois at Urbana-Champaign
Corresponding author: viparell@cec.sc.edu
Keywords: alluvial channels, equilibrium slope, equilibrium bed surface grain size

1 Introduction

In the study of alluvial rivers, sediment is broadly divided in two grain size classes, bed material and washload. Church [1] defines bed material as the sediment that is generally found on the bed and in the lower part of the banks and mostly controls channel morphology. Washload is sediment that is found in small quantities in the channel bed [1]. Large quantities of this material, however, may be found in floodplain deposits [1]. Identifying a threshold grain size between bed material and wash material, if it exists, remains a problem.

Einstein [2] reports that this threshold grain size is the D_{10} of the bed deposit, others consider 0.062 mm as the threshold between bed material and washload [2,3]. Paola [4] approaches the problem differently and defines wash material as *the component of the total load that does not directly affect the river slope*.

Here we use an analytical model to compute equilibrium bed slope and surface grain size distribution [5]. Input parameters are inspired by the Congaree River, South Carolina, where data is available to constrain channel slope and width, sediment supply and grain size distribution [6]. Simulations are performed with the same annual load, sum of bed material load and washload. The threshold grain size between bed material and washload T_S is arbitrarily increased from 0.015 mm to 0.425 mm. As T_S increases the supply of bed material decreases and the bed material coarsens.

2 Formulation

Bed material is modeled with N_d size classes. The channel cross section is assumed to be rectangular. At equilibrium the bed material load is equal to the annual supply to respect mass conservation. Thus, bed slope and grain size distribution of the bed surface sediment are computed with a Chezy formulation for flow resistance and a calibrated Naito-type [3] bulk load relation for bed material load calculations [5].

3 Results

Equilibrium results are presented in Figure 1 in terms of geometric mean size of the bed surface sediment and slope as functions of T_S.

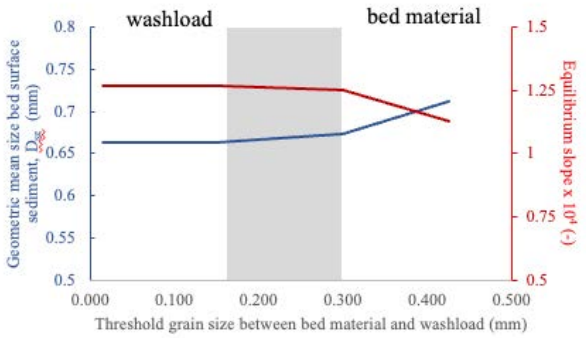

Figure 1: Equilibrium results.

Results indicate that sediment finer than 0.15 mm -0.3 mm does not seem to directly affect bed slope and surface grain size. Sediment exchange between channel and floodplain, however, should be consider to broaden the analysis and explore if and how the relative magnitude between the annual supply of bed material and washload, as well as the bed material grain size, control bankfull width and depth.

Acknowledgments

Support by NSF EAR 2501994 is acknowledged

References

[1] Church, M. (2006). Bed material transport and the morphology of alluvial river channels. *Ann Rev Earth Planet. Sci.* 34, 325–354

[2] Einstein, H.A. (1950) *The bed-load function for sediment transportation in open channel*. USDA Technical Bulletin 1026.

[3] Naito, K., Ma, H. et al. (2019). Extended Engelund–Hansen type sediment transport relation for mixtures based on the sandsilt-bed Lower Yellow River, China. J. Hydr. Res. *57*(6), 770–785.

[4] Paola, C. (2001). Modelling stream braiding over a range of scales. In *Gravel Bed Rivers V*

[5] Blom, A. et al. (2017), The equilibrium alluvial river under variable flow and its channel-forming discharge, J. Geopys. Res.: Earth Surf., 122, 1924–1948.

[6] Logan, W.N. (2023). Channel Morphology of a Leaky Coastal Plain River: The Congaree River, SC 1884-2022. MS Thesis, U. of South Carolina.

Flow and Sediment Distribution of a River Delta with a 1D Morphodynamic Model

Lorenzo Durante[1], Nicoletta Tambroni[1], Michele Bolla Pittaluga[1]

[1]University of Genoa, Genoa, Italy

e-mail corresponding author: michele.bollapittaluga@unige.it

Keywords: *river bifurcation; morphodynamic equilibrium; delta*

1 Introduction

The concept of morphodynamic equilibrium has been successfully applied worldwide to interpret field observations along river systems, with morphodynamic models offering the advantage of simultaneously predicting riverbed equilibrium, formative discharge, and associated sediment flux [1]. The application of one-dimensional (1D) morphodynamic models to multi-thread channels characteristic of river-dominated deltas requires the incorporation of nodal point conditions to accurately predict flow and sediment distribution throughout the river network.

Moreover, in natural river systems, channel width often varies significantly along the river due to both natural processes and anthropogenic factors. Consequently, the assumption of rectangular cylindrical channels, which is commonly employed in studies of morphodynamic equilibrium in river deltas, may be overly restrictive when comparing model predictions with field observations as it fails to fully capture the influence of these variations on flow dynamics and sediment transport, ultimately affecting flow depth, free surface elevation, and bed equilibrium configuration along the river branches.

In the present study we extend the novel delta model introduced by [2] incorporating physically based nodal point relations at bifurcations and accounting for width variability along the branches of the river delta network. As a result, the model significantly enhances the prediction of field data, providing a more accurate representation of the equilibrium configuration of river deltas.

2 Methods

We include width variations in the model proposed by [2] where water and sediment fluxes along the river network are determined by physically-based nodal point conditions. The model is here applied to the Po River Delta (Italy) to predict the configuration of morphodynamic equilibrium and the influence of width variations along the river branches.

3 Results and Conclusions

The updated model more accurately represents the free-surface slope in each Po Delta branch. The assumption of cylindrical channels in the original model by [2] allows for a rapid and reliable computation of flow distribution within the delta while maintaining a correct average bed slope for each branch. However, incorporating width variations into the model leads to a significant improvement of the representation of bed elevation at each cross-section.

Figure 1 illustrates the equilibrium bed and free-surface profiles of the Po Delta's main channel for an upstream flow discharge of 2700 m^3/s, corresponding to the formative discharge of the Po River at the delta apex.

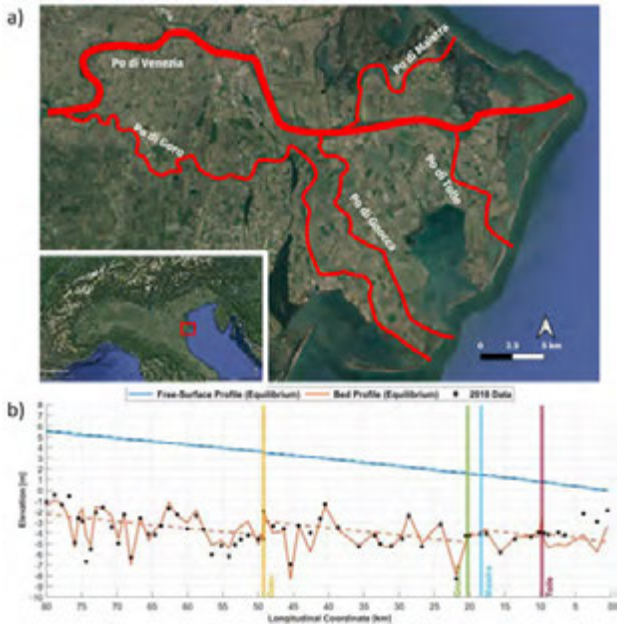

Figure 1: (a) The Po River Delta distributary network and (b) a comparison of modeled equilibrium bed and free-surface profiles with 2018 data along the main (Po di Venezia) channel.

By integrating the analysis of historical trends in the Po Delta with an accurate representation of recent field data, this study facilitates the estimation of a morphological equilibrium flow discharge for this region of high economical and environmental interest. The same modeling approach can be readily applied to predict the morphodynamic equilibrium configuration of other river deltas worldwide.

References

[1] M. Bolla Pittaluga, R. Luchi, and G. Seminara. On the equilibrium profile of river beds. *J. Geophy. Res.: Earth Surface*, 119(2):317–332, 2014.

[2] L. Durante, N. Tambroni, and M. Bolla Pittaluga. Multiple equilibrium configurations in river-dominated deltas. *EGUsphere*, 2024:1–25, 2024.

Salt marsh accretion with sea level rise is hindered by dense vegetation

S. Temmerman[1], O. Gourgue[2], J.P. Belliard[1,2], D.W. Wang[3], J.H. Bai[3], C. Gu[4], M.G. Kleinhans[5], Y.Y. Xu[6], S. Fagherazzi[6]
[1] ECOSPHERE Research Group, University of Antwerp, Antwerp, Belgium
[2] Operational Directorate Natural Environment, Royal Belgian Institute of Natural Sciences, Brussels, Belgium
[3] State Key Laboratory of Water Environment Simulation, Beijing Normal University, Beijing, China
[4] Environmental Research Center, Duke Kunshan University, Kunshan, China
[5] Department of Physical Geography, Utrecht University, Utrecht, The Netherlands
[6] Department of Earth and Environment, Boston University, Boston, Massachusetts, USA
Corresponding author: stijn.temmerman@uantwerpen.be

Keywords: Tidal wetlands, coastal marshes, sedimentation, sea level rise, bio-geomorphology

1 Introduction

Tidal marshes are characteristic landforms along muddy estuarine shorelines, which form and evolve through bio-geomorphic feedbacks between hydrodynamics, sediment and vegetation dynamics. A plethora of studies has focussed on understanding and predicting sediment accretion rates, as this is key for survival of tidal marshes under rising sea level. Their dense vegetation is generally thought to favour sediment accretion and hence marsh resilience to sea level rise. However, in contrast with this idea, we demonstrate that dense marsh vegetation can inhibit sediment accretion, hence reducing the ability of marshes to keep up with sea level rise.

2 Methods

We used a process-based bio-geomorphic modelling approach, simulating how mutual feedbacks between tidal hydrodynamics, sediment dynamics and vegetation dynamics govern the long-term (decades) formation and evolution of tidal marsh landscapes (~km^2), consisting of tidal channel networks intertwined by intertidal platforms. We simulated scenarios of marsh landscape evolution under (1) colonization by dense vegetation (*Spartina* type); (2) sparse vegetation (*Salicornia* or *Suaeda* type); (3) without vegetation [1]. Model outcomes are analysed and qualitatively compared to field observations of elevation profiles in invasive *Spartina* marshes versus native *Suaeda* marshes in China (Yellow River delta) [2].

3 Results and discussion

The model simulations showed that the dense vegetation scenario resulted in an overall (spatially-averaged) lower sediment accretion rate as compared to the sparse vegetation and no vegetation scenarios [1]. At first sight, this result may seem surprising, but analysing the model simulations allowed to identify two key mechanisms by which vegetation hinders sediment transport from tidal channels towards adjacent marsh platforms. First, vegetation presence on the platforms concentrates tidal flow and sediment transport inside the channels, hence reducing sediment supply from the channels to the platforms. Second, vegetation presence enhances sediment accretion rates in marsh zones fringing along channel banks, consequently limiting sediment supply and deposition in marsh interior zones farther away from channels. As a consequence, a levee-basin topography developed in the vegetated scenarios (with levees adjacent to channel edges, being ~0.3-0.4 m higher than basins > 40 m away from channels), while such levee-basin topography did not develop without vegetation [1].

Model simulations are qualitatively compared to observations from the Yellow River delta in China, where native *Suaeda salsa* marshes (a sparse, short-growing species) are invaded and replaced by non-native *Spartina alterniflora* (a tall, dense-growing species). The data show levee-basin topography is nearly absent in sparse *Suaeda* vegetations and prominently developed in dense *Spartina* marshes [2], suggesting the *Spartina* interior marsh zones are more vulnerable to sea level rise than the *Suaeda* interior marsh zones, in line with the model outcomes. Also other studies have identified negative effects of marsh vegetation on sediment accretion [3]. In conclusion, these findings indicate higher vulnerability of densely vegetated marshes to sea level rise than previously thought.

References

[1] Gourgue, O., Belliard, J.P., Xu, Y.Y., Kleinhans, M.G., Fagherazzi, S., Temmerman, S., 2024, Dense vegetation hinders sediment transport toward saltmarsh interiors: Limnology & Oceanography Letters, v. 9, no. 6, p. 764-775.
[2] Wang, D.W., Gu, C.H., Temmerman, S., Belliard, J.P., Gourgue, O., Xue, L.M., Bai, J.H., 2025, Coastal Marsh Vulnerability to Sea-Level Rise Is Exacerbated by Plant Species Invasion: Global Change Biology, v. 31, no. 2.
[3] Boechat Albernaz, M., Brückner, M.Z.M., van Maanen, B., van der Spek, A.J.F., & Kleinhans, M.G., 2023. Vegetation reconfigures barrier coasts and affects tidal basin infilling under sea level rise: Journal of Geophysical Research Earth Surface, 128, e2022JF006703.

Laboratory experiments of bedforms evolution during flood events

Simona Francalanci[1], Eduardo Banchelli[1], Nicola Marchiani[1]
[1]Department of Civile and Environmental Engineering, University of Florence
Corresponding author: simona.francalanci@unifi.it

Keywords: dune bed, flow resistance, flood events.

1 Introduction

The experimental analysis of bedforms and roughness evolution during floods has been investigated in recent works [1, 2]. Most of these studies have focused on understanding how bedforms and roughness change during flood events. Research has shown that bedforms, such as dunes, develop during floods, affecting roughness and flood levels. The development of dunes with floods has been observed to influence roughness and floodwater levels significantly [1, 3]. However, when subjected to high discharges, dunes may undergo a transitional phase before ultimately washing out to form an upper stage plane bed. This morphological transition tends to decrease flow resistance, subsequently diminishing water levels and mitigating the risk of flooding, thus enabling rivers to self-regulate [2].

Our experiments aim to characterize dune morphology in response to peak flow during unsteady hydrograph, to address a significant research gap on river morphodynamics during extreme events.

2 Experiments

The experiments were carried out in the River Hydraulics, Lagoon and Biofluidodynamic Laboratory: the recirculating flume was narrowed to 0.27 m for a length of 8 m, with adjustable slope and equipped with a feeding system for sediment (sand D_{50} = 0.43 mm). There were two lines for the water recirculating system, one of whom is equipped with an Electro-Hydraulic Actuator (EHA) valve for automatic adjustment of the flow during the experiments, creating an unsteady hydrograph.

During the experiments several measurements were collected: water levels via transducers sensors; bed level sensors for data collection in wet conditions; side-images of the migrating dunes through the glass wall; detailed bedform topography with photogrammetric image techniques (Structure from Motion) in dry conditions; sediment input and output.

We conducted two experimental series in steady conditions with flow discharge of 8 l/s and 12 l/s, respectively SA and SB. The equilibrium conditions were achieved when dune bedforms was fully developed, the bed slope was stable, the sediment input was equal to the sediment output.

Each steady experiment was repeated three times, and it was followed by three unsteady experiments: USA (peak discharge 14 l/s) and USB (peak discharge 18 l/s). The three unsteady hydrographs were assumed with triangular shape, and different durations: 30', 60' and 120'. Sediment input was maintained constant during the unsteady experiments: 1.5g/s for series A and 3g/s for series B.

3 Discussion of the results

The collected data were analysed in terms of dune bed characteristics (see Fig. 1): mean bed slope, dune height, dune length, celerity, total shear stress.

Dune lengths were in the range 45-53 cm for steady A and 55-70 cm for steady B; dune heights were in the range 1.2-1.35 cm for steady A and 1.5-1.7 cm for steady B. Mean dune celerity was in the order of 0.03 cm/s (SA) and 0.06-0.07 cm/s (SB). During the unsteady experiments dunes were observed to increase in length and height, remaining in the region of fully developed bedforms.

A third series of experiments is planned to investigate dune developments in wash out transitional regime.

Figure 1: Dune bedforms after USB3 run (120').

Acknowledgments

This work was funded within the framework project PRIN 2022 "The role of morphodynamics in river floods: assessment of relevant processes, advanced physics-based modelling, and real-time forecasting (MORFLOOD)".

References

[1] Bhattacharya, B., Shams, M. S., & Popescu, I. On the influence of bed forms on flood levels. *Environmental Engineering and Management Journal*, 12(5), 857–863 (2013).

[2] Naqshband, S., & Hoitink, A. J. F. Scale-Dependent Evanescence of River Dunes During Discharge Extremes. *Geophysical Research Letters*, 47(6), 1–8 (2020).

[3] Van Rijn, L. C. Sediment transport, part III: bed forms and alluvial roughness. *Journal of Hydraulic Engineering*, 110(12), 1733–1754 (1984).

DOZER: exploring morphodynamic intervention in coastal overwash

Eli D Lazarus[1]
[1]Environmental Dynamics Lab, School of Geography & Environmental Science, University of Southampton, UK
Corresponding author: E.D.Lazarus@soton.ac.uk

Keywords: overwash, washover, storm, anthropogenic, serious game

1 Is there a bulldozer in your model?

In low-lying coastal settings, sediment deposition by coastal storms can disrupt the function of critical infrastructure such as road networks. Much as snowplows are dispatched during snow storms, mechanised sandplowing crews (i.e., bulldozers, graders, front-end loaders) may be deployed during a coastal storm to keep roads passable for emergency services and to repair sections of fronting dune. However, morphodynamic models of coastal storm impacts do not include real-time mechanised human interventions in storm-driven geomorphic change [1].

Here I present DOZER (Fig. 1), an exploratory numerical model in which the morphodynamics of washover deposition are coupled to the contemporaneous actions of a bulldozer that clears the model domain of sand. Actions by the eponymous 'dozer – where it moves, when it plows, where it redistributes sand – are controlled by a human player.

Figure 1: *Start screen (left) and during play (right).*

DOZER can be described as a "serious game": a heuristic toy model in both a literal and formal sense, intended to serve as a dynamical thought-experiment in a sphere of morphodynamics that challenges prediction. DOZER can also be described as a deliberately simplified human-in-the-loop model of a complex adaptive system, in which the adaptive mechanics are handled by a participatory player. Ceding control of specific model mechanics to a player yields system dynamics that are neither deterministic nor stochastic.

2 Model dynamics

In the model, which operates on a gridded domain representing the back-barrier floodplain of a sandy barrier system, sediment transport occurs through two independent processes: overwash and plowing.

Overwash transports sand onto the back-barrier in pulses, through a series of throats in the fronting dune. Washover deposition is rule-based, distributed as a function of local slope and overwash flow depth. As washover morphology develops, flow and subsequent deposition is steered toward accommodation spaces. Despite being deliberately simplified, washover in the model reflects dynamic allometry and morphometry similar to that described in physical experiments [2].

Meanwhile, the model "player" controls the compass orientation of the bulldozer (rotation to the right or left) and its direction of travel (forward or reverse). The player also controls the plow blade (up or down). When moving forward with the blade down, DOZER plows ahead any sand it encounters, up to a maximum volume that is the blade capacity. When the player raises the blade, any sand on the plow is deposited.

The player operates DOZER however they choose in response to the evolving pattern of washover deposition. By plowing sand, DOZER rearranges the back-barrier topography, cumulatively steering pulses of overwash flow and washover deposition. If the player begins to plug one of the overwash throats, the forcing flow is diverted laterally to other throats in the dune. This "whack-a-mole" dynamic means that by addressing one washover site the player exacerbates another. The game ends when a throat incises through the dune to the base elevation of the back-barrier.

3 Analytical opportunities

During a game, a control version of the model – with the same initial conditions but no bulldozer – runs in the background. This enables quantitative comparison of observed versus expected post-storm morphology: the back-barrier terrain that DOZER reshapes versus the topography that would have evolved in the absence of any intervention. DOZER thus captures divergence between observed and predicted geomorphic change in this coupled system, and points to a departure from scaling relationships characteristic of natural washover. Analysis of collective player decisions may reveal emergent patterns of adaptive strategy.

Acknowledgments

E. Goldstein, A. Payson, and D. Page for fundamental discussions; M. Lazarus for beta testing. Supported by NE/X011496/1.

References

[1] E. D. Lazarus and E. B. Goldstein. Is there a bulldozer in your model? *Journal of Geophysical Research: Earth Surface*, 124(3):696–699, 2019.

[2] E. D. Lazarus, K. L. Davenport, and A. Matias. Dynamic allometry in coastal overwash morphology. *Earth Surface Dynamics*, 8(1):37–50, 2020.

MORPHODYNAMIC EVOLUTION OF THE VENICE LAGOON: PAST, PRESENT, AND FUTURE PERSPECTIVES

Carniello L.[1], D'Alpaos A.[2], Finotello A.[2], Marani M.[1], Pivato M.[1], Tognin D.[1], Viero D.P.[1]
[1]Università di Padova, Dept. ICEA, Padova, Italy
[2] Università di Padova, Dept. of Geosciences, Padova, Italy
Corresponding author: luca.carniello@unipd.it

Keywords: lagoons, sediment transport, morphodynamics, flood regulation

1 Introduction

Coastal lagoons are valuable environments providing a wide variety of ecosystem services. However, their future is threatened by climate-change induced sea level rise and increasing anthropogenic pressure The survival of these environments depends on their ability to maintain their inherent diversity, which includes a mix of intertidal and subtidal features. Focusing on the Venice Lagoon, a microtidal, sediment-starved coastal, back-barrier basin, we use numerical modeling to study sediment dynamics over yearly timescales. Our analyses include also the morphodynamic effect of flood regulation by the Mo.S.E. system, operational since October 2020 to prevent flooding in Venice.

2 Methods & Data

We used a numerical morphodynamic model [1, 2] to simulate hydrodynamic and sediment transport processes. Model performance was first tested against a set of field data, including salt-marsh accretion rates measured at three different stations and mean annual topographic changes of tidal flats derived from recent bathymetric surveys. We performed three, one-year long simulations representing three meteorologically distinct years from the past two decades (2005 – stormy; 2019 – calm; 2020 - typical wind conditions).

3 Results & Conclusions

Numerical results highlighted the critical role of storm events, which drive the morphological evolution of the lagoon by enhancing sediment resuspension from wind-wave exposed tidal-flat areas, resulting in a net loss of sediments from these areas. Resuspended sediment (see Fig. 1) is partially deposited over salt marshes, supporting their vertical accretion and ability to cope with sea-level rise. However, the majority of sediment remobilized from tidal flats is either discharged into the sea through the inlets, or deposited within channels, promoting their infilling. In either case, this sediment becomes unavailable for further remobilization by wind waves and is therefore lost in terms of contributing to the morphodynamic evolution of the lagoon.

Besides affecting the intensity of the sediment reworking, storm events in the Venice Lagoon, mainly driven by north-easterly Bora winds, induce a southward circulation that promotes greater sediment accumulation in the southern basin and affects sediment fluxes through the inlets. Indeed, while fair weather conditions result in higher seaward sediment flux through the Lido inlet, storm events drive the majority of sediment flow through the Malamocco and Chioggia inlets. We also investigated the impact of the Mo.S.E. system on sediment dynamics. Our findings indicate that while floodgate operations reduce the net volume of sediment flowing into the sea through the inlets, their contribution to morphological preservation is less significant than expected. Flood barrier closures limit water levels within the lagoon, reducing salt marsh inundation and consequently decreasing mineral sedimentation. Additionally, the closures contribute to increased channel infilling.

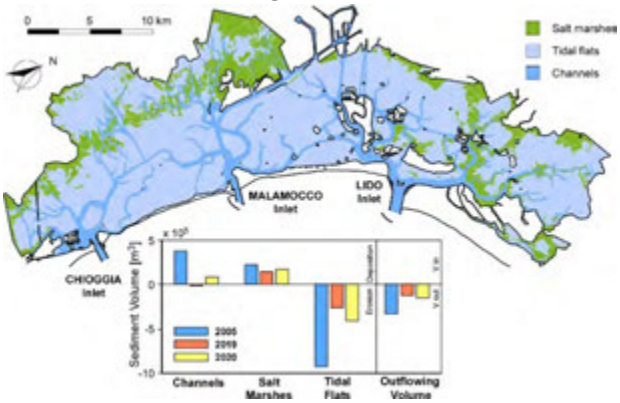

Figure 1: Computed sediment volume redistribution among the lagoon morphologies (i.e., channels, salt marshes, tidal flats) and sediment volume flowing out the lagoon for years 2005, 2019 and 2020.

Acknowledgments

Venezia2021 Res. Proj.; iNEST funded by the European Union NextGenerationEU (grant no. ECS00000043); PRIN project, "Prot&Cons" (grant no. 2022FZNH82).

References

[1] Carniello, L., A. D'Alpaos and A. Defina. Modeling wind waves and tidal flows in shallow microtidal basins, *Estuarine, Coastal and Shelf Science*, doi:10.1016/j.ecss.2011.01.001, 2011.

[2] Carniello, L., A. Defina and L. D'Alpaos. Modeling sand-mud transport induced by tidal currents and wind waves in shallow microtidal basins: Application to the Venice Lagoon (Italy), *Estuarine, Coastal and Shelf Science*, doi:10.1016/j.ecss.2012.03.016, 2012.

Multiscalar Response of an Experimental Fixed-Wall Meandering Channel to a Sediment Supply Increase

Peter A. Nelson[1], David J. Cortese[1]
[1]Colorado State University, Fort Collins, Colorado, USA
Corresponding author: peter.nelson@colostate.edu

Keywords: flume experiments, sediment supply, sorting, bedforms

1 Introduction

Disturbances to watersheds and river systems, such as land use change, wildfire, dam installation and removal, or catastrophic flooding, alter the amount of sediment and water supplied to channels, leading to morphologic changes that can have important ecologic or societal consequences. Rivers respond to changes in water discharge and sediment supply through adjustments to sorting patterns, cross-sectional shape, and reach-scale morphology, but what are the relative magnitudes of these changes, do they happen simultaneously or in sequence, and how do they depend on the channel width or planform?

2 Methods

We conducted flume experiments documenting the temporal progression of responses across scales of a fixed-wall meandering channel to a sediment supply increase. The experimental channel consisted of four meander bends following a sine-generated trace, with an initial bed slope of 0.005, width of 0.344 m, and wavelength of 2.75 m (Figure 1). The channel was provided constant flow of 2 L/s so that the width-to-depth ratio would be approximately 20. The sediment constituting the initial bed and sediment supply had a size range from 0.0125 to 2.8 mm with a median grain size of 0.62 mm. Sediment was initially fed at a constant rate of 20 g/min until quasi-equilibrium conditions were reached, after 80 hours of runtime. Subsequently, the sediment feed was doubled to 40 g/min and the experiment continued for another 150 hours.

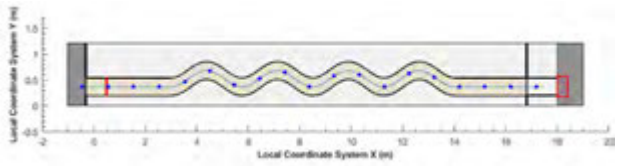

Figure 1. Diagram of the experimental channel.

Bed topography was periodically measured during dry-bed conditions using structure-from-motion (SfM) photogrammetry. High-resolution images were also used with SfM methods to characterize grain-scale roughness elements. Water surface elevations were collected during the experiment with ultrasonic sensors, bedload material was collected in the flume tailbox, and facies maps were drawn by hand during the experiment to visually characterize sorting patterns. Scales of topographic response were separated between bar-scale, dune-scale, and grain-scale by applying a spectral filter to the SfM topography data.

3 Results

The channel developed a characteristic bar-pool morphology and sorting patterns with superimposed, mobile, scaled gravel-dune bed forms during both phases of the experiment. After the sediment supply increase, dynamic adjustments occurring from smaller to larger scales took place. Initially, the dunes essentially disappeared, after which the relief of the bars decreased, however, ultimately the dunes and bar-pool morphology returned to their conditions at the beginning of the sediment supply increase. The long-term and largest-scale response to the supply increase was a 44% increase in bed slope.

4 Discussion and Conclusions

To explain these observations, we propose a conceptual model wherein the channel undergoes a temporal progression of responses from smaller to larger spatial scales, with the total response potential at each scale related to the conditions and constraints at that scale. Similar to Eaton et al.'s rational regime model [1], we consider the total system resistance to be a combination of resistance due to surface grain size, bed forms, bar-pool features, and sinuosity. Accommodation of higher sediment supply requires an overall reduction of total system resistance, which is accommodated by temporally changing adjustments to each constituent component of resistance. In our experiment, the smaller spatial scale responses in our system had less response potential to reduce system resistance resulting in slope increase as the dominant response.

Acknowledgments

Financial support for this work was provided by the National Science Foundation award EAR-1455259.

References

[1] Eaton, B. C., Church, M., & Millar, R. G. Rational regime model of alluvial channel morphology and response. *Earth Surface Processes and Landforms*, 29(4), 511–529, 2004

Satellite Evidence on Beach Width Cyclicity Along a Barrier Island

Susana Costas[1], Vincent Kümmerer[1], Valeria Fanti[1], Jacqueline Santos[1,3], Theocharis Plomaritis[2], Katerina Kombiadou[1], and Rui Taborda[3]
[1]University of Algarve, Center for Marine and Environmental Research, Faro, Portugal
[2]INMAR / Applied Physics, University of Cadiz, Cadiz, Spain
[3]IDL / FCUL, University of Lisbon, Lisbon, Portugal
Corresponding author: scotero@ualg.pt

Keywords: tidal inlet, ebb-delta, shoal attachment, longshore sediment transport

1 Introduction

Sandspits follow cyclic development patterns that are still not fully understood. Some studies attributed the onset of this cyclic behaviour to external forces, particularly variation in wave climate [*1*], while others found sandspit morphodynamics to be self-regulated with wave regime explaining only a small part of their evolution [*2*]. Here, we analyse the evolution of Culatra Island, a barrier island located in South Portugal, formed by a series of longitudinally attached sandspits that contributed to the elongation of the island. The growth of the island has been linked to the attachment of shoals from an adjacent ebb-delta, through a process of ebb-shoal collapse, driven by moderate to extreme storm events in a context of ebb-tidal current decay [*3*]. This work aims to explore the processes of sandspit formation and elongation through satellite imagery, and the key interactions with the adjacent ebb-deltas.

2 Approach

The present work applies the open-source Python-based CoastSat toolkit [*4*] for the detection of satellite-derived shorelines (SDS) from Landsat 5, 7, 8 and 9 imagery, covering 40 years (1984 to 2024). Beach area was estimated using the vegetation line as the landward beach limit. Wave regime was determined using buoy data and hindcast models.

3 Results

The updrift zone of the barrier island is characterised by low erosive trends (< 0.5 m/yr), driven by a pulsating response with stability intermittently disrupted by episodes of rapid retreat. This zone was artificially replenished in 2014 (Figure 1). The central part of the island experiences similar retreat, but follows a more complex trend with a more distinct cyclic pattern. Rapid beach growth events (~2 years) are followed by gradual retreat (~10 years) (Figure 1), resembling a typical response after artificial beach nourishment. While the cycle duration remains consistent, its magnitude appears to decrease over time. The downdrift end of the island exhibits highly variable growth rates, alternating between periods of very rapid growth (6.0 m/yr) and shoreline stability (0.2 m/yr).

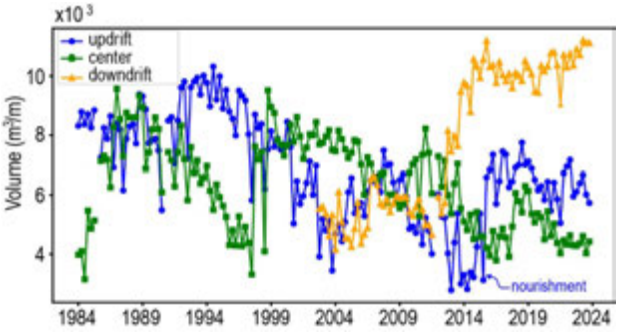

Figure 1: Changes in volume derived from SDS.

4 Discussion

High temporal resolution satellite imagery allowed the documentation of sand accumulation pulses in Culatra for the first time, helping to understand the mechanisms of barrier elongation and growth. These pulses do not appear linked to the local wave regime, reinforcing the self-regulation hypothesis, likely related to ebb shoal formation and attachment cycles. In fact, the pulses can be associated with the shoaling of bars within the swash platform and eventual attachment to the adjacent beach.

Acknowledgments

FCT projects: 2022.05392.PTDC, LA/P/0069/2020, UID/00350/2020, and contract 2021.04286.CEECIND.

References

[1] Allard, J., Bertin, X., Chaumillon, E., Pouget, F., Sand spit rhythmic development: A potential record of wave climate variations? Arçay Spit, western coast of France. Mar Geol 253, 107–131, 2008.

[2] Taveneau, A., Almar, R., Bergsma, E. W. J., On the cyclic behavior of wave-driven sandspits with implications for coastal zone management. Estuar Coast Shelf Sci, 303, 108798, 2024.

[3] Pacheco, A., Williams, J. J., Ferreira, Ó., Garel, E., Reynolds, S., Applicability of sediment transport models to evaluate medium term evolution of tidal inlet systems. Estuar Coast Shelf Sci, 95, 119–134, 2011.

[4] Vos, K., Splinter, K. D., Harley, M. D., Simmons, J. A., Turner, I. L., CoastSat: A Google Earth Engine-enabled Python toolkit to extract shorelines from publicly available satellite imagery. Environ Model Softw, 122, 104528, 2019.

Long-Term Channel Morphology Model Including the Evolution of Vegetation Applied to an Actual River

Y. Shimizu[1], T. Kyuka[2], S. Yamaguchi[3], J. Nelson[4] and K. Watanabe[5]

[1] Faculty of Engineering, Hokkai Gakuen University, Hokkaido, Japan
[2] Department of Civil Engineering, Toyama Prefectural University, Toyama, Japan
[3] River Hydraulics Laboratory, Civil Engineering Research Institute, Hokkaido, Japan
[4]River Mechanics Inc., Colorado, USA
[5]Nippon Koei Co., Ltd.
Corresponding author: shimizu-y@hgu.jp

Keywords: Sand bar, Bed evolution, Vegetation, Numerical Model.

1 Introduction

Vegetation plays a critical role in shaping river geomorphology, often as significant as the effects of flow and sediment transport. While numerous studies have focused on flow dynamics, sediment transport, and channel morphology (e.g., Schuurman et al. 2016), fewer have explored vegetation dynamics, including sprouting, growth, colonization, and disappearance in river channels (e.g., Gurnell 2013).

At the RCEM2023 symposium, we presented a riverbed evolution model that incorporates the influence of forested areas within river channels. Using an idealized river channel and flow conditions, we demonstrated the model's validity. This study extends that work by applying the model to a real river under actual flow conditions, enabling validation and further insights into these processes.

2 Improvement of the Computational Model and Application to a Real River

Previously, we introduced a two-dimensional numerical model that simulated river flows and bed evolution. The approach included the interrelation of tree growth dynamics, flow resistance, sediment transport, riverbed changes, and tree removal due to erosion. Using an idealized channel and flow history, we demonstrated the ability to reproduce key processes: sandbar formation, stabilization by tree, removal of sandbars and trees during floods, and subsequent regeneration under normal time-varying flows.

In this study, we enhanced the model by incorporating mechanical moments exerted on trees by flowing water, enabling the simulation of tree uprooting and removal. The improved model was applied to the Bisei River, a tributary of the Tokachi River system in Hokkaido, Japan. Using real discharge data from 2014–2023, which included diverse hydrological events (e.g., typhoon-induced floods, snowmelt, and summer low-flow periods), we performed numerical simulations over a long period of time. These results were validated against satellite imagery and drone aerial photographs captured at multiple intervals during the study.

To account for tree uprooting due to hydrodynamic forces, the model utilized resistance values derived from field tests using heavy machinery to measure root pull-out strength. The simulations reproduced the sandbar formation and tree growth processes in the Bisei River, as well as its riverbed and meandering morphology. These results matched observed flood event sequences in the discharge history, enabling discussions on the formation processes of riverbed morphology with coexisting sandbar evolution and tree growth.

References

[1] Gurnell, A. (2013). Plants as river system engineers. Earth Surf. Process. Landforms39, pp425, doi: 10.1002 /esp.3397

[2] Schuurman, F., Shimizu, Y.,Iwasaki, T. and M.G. Kleinhans, M.G.(2026). Dynamic meandering in response to upstream perturbations and floodplain formation. Geomorphology253, pp94-109, doi:10.1016/geomorph.2015.05.039

(a) 2016before Flood (Coexistence of sandbars and forested areas)

(b) 2016 after flood (Channel resetting due to the outflow of sandbars and forested areas)

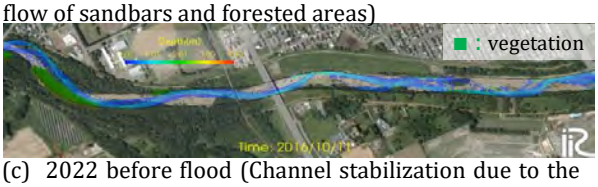

(c) 2022 before flood (Channel stabilization due to the fixation of forested areas)

(d) 2022 after flood (Partial removal of forested areas)

Figure 1: Simulated bed evolution and channel vegetations in the Bisei River

Coastal Vegetation Stochastic Dynamics

C. Camporeale[1], M. Latella[2]

[1]Department of Environment, Land and Infrastructure Engineering (DIATI), Politecnico di Torino, Italy
[2]CMCC Foundation – Euro-Mediterranean Center on Climate Change, Italy

e-mail corresponding author: carlo.camporeale@polito.it

Keywords: *coastal dunes; stochastic vegetation dynamics; wind variability; dune stability; ecosystem modeling*

Abstract

We present a physically-based modeling framework to capture the spatio-temporal dynamics of coastal dune vegetation under stochastic environmental disturbances. By treating wind speed as a compound Poisson process and wave runup as a random variable, the model evaluates vegetation cover along a cross-shore dimensionless framework. Dune topography is parameterized by slope, wavelength, and height, while disturbances affecting vegetation—wind-driven scour and wave-induced flooding—are assessed using threshold-based analysis.

The vegetation dynamics are modeled as a state-dependent dichotomic process, where growth and decay depend on external forcing and vegetation cover. Analytical solutions of the master equation reveal the impacts of wind variability, dune steepness, and roughness on vegetation patterns. A Suitability Index is introduced to assess dune stability based on topographic and environmental factors.

Validation against satellite imagery and high-resolution elevation data from U.S. coastlines confirms the model's robustness. The findings enhance understanding of coastal dune ecosystems and offer a predictive tool for coastal management and restoration strategies.

1 Introduction

Coastal dunes provide essential ecosystem services, including flood protection, sand storage, and carbon sequestration. However, rising sea levels, climate change, and urbanization threaten their stability. Vegetation plays a crucial role in dune formation and stabilization, yet its response to stochastic environmental forces remains poorly understood.

This study develops a threshold-guided stochastic model to analyze vegetation cover dynamics under random wind and wave disturbances. The model integrates boundary layer theory, wave mechanics, and sediment transport, offering a novel approach to predicting dune vegetation patterns. By leveraging global datasets, it provides a scalable framework for assessing dune resilience and informing nature-based coastal restoration efforts.

2 Methods

A one-dimensional cross-shore model describes the response of vegetation cover to stochastic wind speed and wave runup. Wind speed is modeled as a Gamma-distributed compound Poisson process, while wave runup follows empirical scaling laws. The model incorporates: i) A topographic framework representing dune profiles with swash zones and Gaussian crests; ii) A threshold-based vegetation response to wind-driven scour and wave-induced flooding; iii) A stochastic dichotomic growth-decay model governed by vegetation thresholds; iv) Analytical solutions for vegetation probability distributions and critical stability conditions.

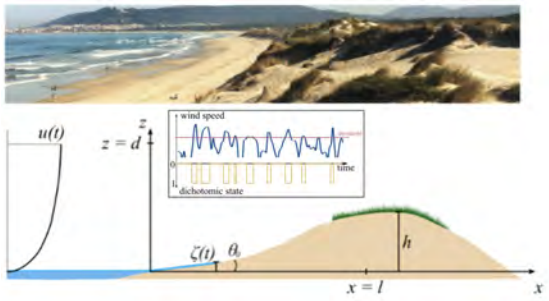

Figure 1: Modeling framework

3 Results and Conclusions

Sensitivity analysis identifies key drivers of dune vegetation stability, including wind variability, dune steepness, and roughness. Increased steepness promotes backshore vegetation while reducing shorefront cover. Wind fluctuations influence vegetation persistence, with higher variability supporting growth by increasing sub-threshold events.

A Suitability Index quantifies dune resilience, revealing optimal conditions for vegetation establishment. The model successfully reproduces real-world vegetation patterns, aligning with satellite observations from Sentinel-2 and PlanetScope. These findings highlight the importance of stochastic environmental factors in shaping coastal dune ecosystems.

The developed model provides a novel framework for predicting coastal dune vegetation dynamics under stochastic forcing. By integrating wind and wave disturbances within a threshold-based stochastic process, it offers new insights into dune stabilization and ecosystem resilience.

The model's validation against Earth Observation data underscores its applicability for coastal management. The Suitability Index serves as a practical tool for guiding dune restoration efforts, supporting sustainable adaptation strategies in response to climate change and anthropogenic pressures.

Empirical/Theoretical modeling of the evolution of multi-species marshes

Conner Lester[1], A. Brad Murray[1], Morgan Alexander[1], Nathaniel Blackford[1], Andrea D'Alpaos[2], Orencio Duran[3], Marco Marani[2], Tegan Blount[2], Daniella Rubio[1], Sonia Silvestri[4], Zhicheng Yang[1,5]

[1]Duke University, USA
[2] University of Padova, Italy
[3] Texas A&M University, USA
[4] University of Bologna, Italy
[5] University of Georgia, USA
Corresponding author: abmurray@duke.edu

Keywords: intertidal morphodynamics, tidal marshes, sea level rise, multiple species, forecasting evolution

1 Introduction

We have developed a simple, empirically and theoretically based approach to modeling how coastal marshes respond to changes in the rate of sea level rise (SLR) and sediment concentration. This approach produces plan view distributions of elevations and the densities of multiple marsh species and bare soil, for any combination of suspended sediment concentration in a channel network and SLR rate, for specific marshes.

2 Modeling Approach

The approach involves techniques to detect the spatial distributions of fractional cover and biomass densities of multiple marsh species from satellite observations. These techniques were developed using a combination of field observations and drone and airborne lidar and multispectral data from the East Coast of the United States and the Venice Lagoon, and can be applied to any coastal environment with similar mixes of vegetation types. Biomass density can be treated as a function of elevation, resulting in the realized niches of observed vegetation species, or mixtures of species.

The approach also involves results showing that, within marsh basins, tidal current velocities and rates of inorganic sediment deposition are essentially independent of biomass. Given this simplification, and the relationship between biomass density and elevation (realized niches), solving for equilibrium depths and biomass densities as a function of distance from the nearest channel becomes straightforward (Figure 1).

The rate of change of depth D (below high-water level) is given by:

$$\frac{\partial D}{\partial t} = R - A_{inorg} - A_{org} \qquad (1)$$

where R is the rate of SLR, A_{inorg} and A_{org} are the rates of accretion of inorganic and organic sediment, respectively. A_{inorg} is equal to DC, where C is sediment concentration. In Figure 1 equilibrium depths ($\frac{\partial D}{\partial t} = 0; R - A_{inorg} = A_{org}$) are graphically determined.

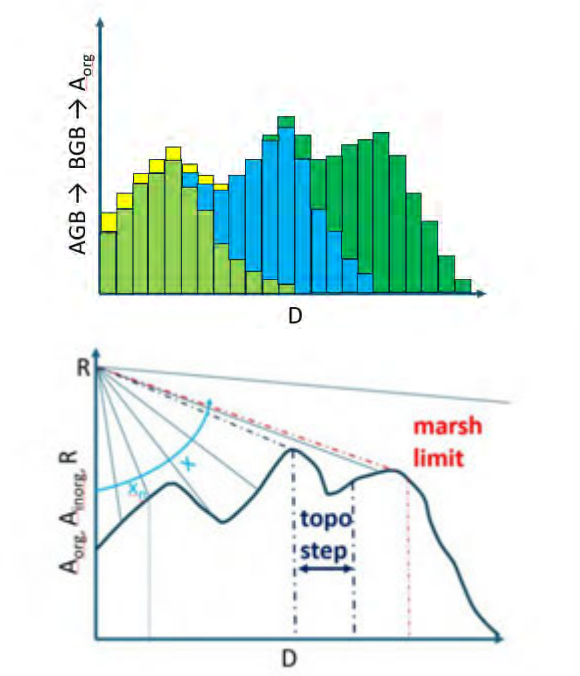

Figure 1: (Top) Hypothetical relationship between A_{org} (proportional to biomass density) and D for multiple species (different colors) and mixtures of species. (Bottom) Graphical representation of equilibria in Equation (1) for some future R. Slanting lines represent A_{inorg} at different nondimensional distances from a channel (with C decreasing with distance from a channel). Intersections between the slanting lines and the curve represent equilibrium depths at different distances from a channel. Sections of the curve that are not intersected by slanting lines represent topographic steps and abrupt vegetation zonation. (Equilibria are unstable when the local slope of the curve is more negative than the slope of the intersecting line.)

Acknowledgments

Supported by the US NSF Geomorphology and Land Use Dynamics program (2016068), and AD, MM, and SS were also supported by the RETURN Extended Partnership and received funding from the European Union Next-GenerationEU (National Recovery and Resilience Plan – NRRP, Mission 4, Component 2, Investment 1.3 – D.D. 1243 2/8/2022, PE0000005).

Size sorting due to fine infiltration in coarse river beds

P. Frey[1], C. Ducottet[2], A. Dudill[3]
[1]Univ. Grenoble Alpes, INRAE, IGE, Saint Martin d'Hères, France
[2]Univ. Lyon, UJM-Saint-Etienne, CNRS, IOGS, Laboratoire Hubert Curien UMR5516, Saint-Etienne, France
[3]University of British Columbia, Dept of Geography, Now at Northwest Hydraulic Consultants, Vancouver, Canada
Corresponding author: philippe.frey@inrae.fr

Keywords: sediment transport, bedload, size sorting, particle tracking

1 Introduction

Bedload transport has major consequences for public safety, water resources, and environmental sustainability. Size sorting also named segregation is largely responsible for our limited ability to predict sediment flux and river morphology, especially in mountains where steep slopes drive an intense transport of a wide range of grain sizes.

Specific experiments [1] were carried out in a tilted, narrow, glass-sided channel. The objective was to study the influence upon segregation of both the grain size ratio and the percentage of the fine feed rate.

In this contribution, we will analyze the depth profiles of particle streamwise velocity and concentration of the coarse beads for the new two-size equilibrium.

2 Experimental Facility and methods

All of the experiments were carried out at slope 10 % and width 10.3 mm, at University Grenoble Alpes, INRAE (ex Irstea), IGE, France, with a constant turbulent and supercritical flow rate in two stages. In the first stage, coarse spherical beads of diameter 5 mm were introduced at a constant feed rate to obtain a sediment bed in one-size-equilibrium. In the second stage, beads of different diameters (from 0.7 mm to 4mm) were introduced at different feed rates, the coarse feed rate remaining the same.

Each experiment was first analyzed at low temporal frequency, analyzing essentially the evolution of the slope from the one size to the two-size equilibrium [1]. Each experiment was also recorded at high temporal frequency using a high-speed camera. Image processing algorithms permitted us to detect the water free surface, the bed elevation and the coarse beads, and to calculate their trajectories. The particle tracking algorithm is currently being improved based on a continuous minimization energy method [2].

3 Results and discussion

Depending on the grain size ratio and the percentage of the fine feed rate in the total feed, the slope of the bed evolved eventually reaching a new two-size equilibrium value either larger (aggradation) or smaller (degradation) than the one-size slope [1]. A layer of fine grains, on top of which coarse grains moved, which varied in thickness, was observed (Fig.1).

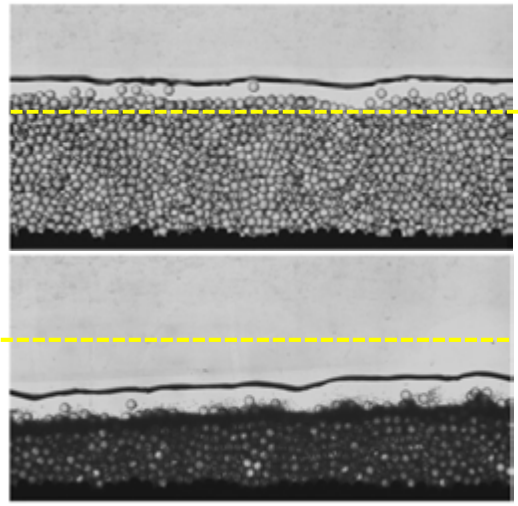

Figure 1. Flow from left to right. a) Initial one-size equilibrium with spherical beads of 5 mm. Bed slope 10% b) two-size equilibrium after introducing 23% of fine 0.7 mm material resulting in a lower slope 7.2%. Yellow dashed line is the mean one-size bedline reported on the two-size case.

Analysis and discussion will be on the depth profiles of particle streamwise velocity and concentration of the coarse beads for the two-size equilibrium [2].

4 Conclusion

Depending on the grain size ratio and the percentage of the finer feed rate in the total feed, aggradation or degradation occurred. Coarse grains moved either in concentrated low velocity clusters or individually at higher velocity (Fig.1).

Analysis of the depth profiles of particle streamwise velocity, concentration, and sediment transport rate of the coarse beads proved a valuable tool to investigate intergranular interactions.

Better understanding of bedload segregation should permit upscaling and improvement of sediment transport and river morphology modelling.

References

[1] Dudill A, Lafaye de Micheaux H, Frey P, Church M. 2018. Introducing finer grains into bedload: The transition to a new equilibrium. *Journal of Geophysical Research: Earth Surface* 123(10): 2602-2619.

[2] Frey, P., Ducottet, C., submitted. Particle Tracking with Continuous Energy Minimization for the Study of Segregation in Bedload Transport. *Experiments in Fluids.*

3D morphodynamic modelling of tidal inlets

Xavier Bertin[1] and Baptiste Mengual[2]
[1]UMR 7266 LIENSs, CNRS La Rochelle University, France
[2]Waeles Marine Consultants, Brest, France
Corresponding author: xbertin@univ-lr.fr

Keywords: Tidal Inlets, morphodynamics, 3D process-based modelling, SCHISM

1 Introduction

Tidal inlets connect the ocean to inner water bodies and experience fast morphological changes while they concentrate socio-economic and environmental challenges. Yet, the physical processes responsible for their dynamics remain only partly understood. To address these challenges, morphodynamic process-based models appear as promising tools. However, most applications employ 2DH approaches (e.g. Duong et al., 2016), which cannot represent the sheared flows that take place in bended channels or in surf zones. Over the last decades, major progresses were achieved regarding the representation of wave-current interactions in 3D (e.g. Bennis et al., 2010; Martins et al., 2022), auguring important advances in model predictive skills. Yet, 3D morpodynamic applications are scarce in the literature, suggesting that important challenges remain. This study presents recent developments in the 3D morphodynamic modelling system SCHISM (Zhang et al., 2016), which allow for a realistic representation of flows and sediment transport in bended channels and surfzones adjacent to tidal inlets.

2 The 3D morphodynamic model

The 3D modelling system SCHISM, fully couples a 3D circulation model with the spectral wave model WWMII and the sediment transport and bed update model SED3D (Zhang *et al.*, 2016). Waves and currents are fully coupled in 3D using a vortex force formalism, as described in Martins *et al.* (2022). Suspended sediment transport is computed solving an advection diffusion equation and bedload sediment transport is computed following Soulsby and Damgaard (2005). The Exner equation is solved using a Euler-WENO approach, which avoids using filters or artificial diffusion (Guérin *et al.*, 2016).

3 Results and perspectives

Our new 3D modelling system is applied to the idealized inlet-lagoon of Nahon et al. (2012), considering a monochromatic tide of amplitude 1.5 m and constant waves of H_s = 1.5 m breaking at about 10° with respect to shore. After 1 year of morphological evolution, the model is able to reproduce the development of realistic ebb- and flood deltas while the main channel migrates downdrift by about 200 m (Figure 1). At inlet adjacent beaches, a double sandbar system develops, with subtidal and intertidal transverse sandbars. Compared to classical 2DH approaches (e.g. Nahon et al., 2012), our new 3D model naturally allows to maintain realistic slopes at adjacent beaches, which is essential as it controls the magnitude of longshore transport.

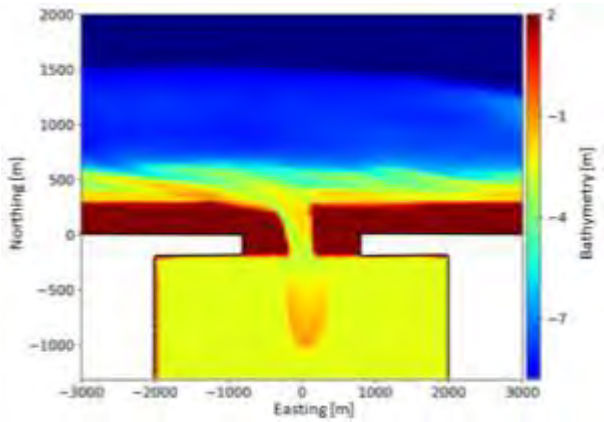

Figure 1. Bathymetry of the inlet-lagoon after one year of morphological evolution.

Meander dynamics is also better captured in the region of the flood delta. Applications to realistic tidal inlets is being carried out and suggest improved morphological predictions compared to classical 2DH approaches.

References

[1] Bennis, A.C., Ardhuin, F., Dumas, F., (2011). On the coupling of wave and three-dimensional circulation models. *Ocean Modelling* 40, 260–272.
[2] Duong, T.M., Ranasinghe, R., Walstra, D.J., Roelvink, J.A. (2016). Assessing climate change impacts on the stability of small tidal inlet systems: Why and how? *Earth-Science Reviews* 154, 369-380.
[3] Guérin, T., Bertin, X., Dodet, G. (2016). A numerical scheme to simulate coastal morphodynamics on unstructured grids. *Ocean Modelling* 104, 45-53.
[4] Martins K., Bertin X., Mengual B., Pezerat M., Lavaud L., Guérin T., Zhang Y.J., (2022). Wave-induced mean currents and setup over barred and steep sandy beaches. *Ocean Modelling*, 179, art. no. 102110.
[5] Nahon, A., Bertin, X., Fortunato, A.B. and Oliveira, A. (2012). Process-based 2DH morphodynamic modeling of tidal inlets: a comparison with empirical classifications and theories. *Marine Geology* 291–294, 1-11.
[6] Soulsby, R.L. and Damgaard, J.S. (2005). Bedload sediment transport in coastal waters. *Coastal Engineering*, 52 (8), 673-689.
[7] Zhang, Y.J., Ye, F., Stanev, E.V., Grashorn, S., 2016. Seamless cross-scale modeling with SCHISM. *Ocean Modelling*, 102, 64-81.

Historical development of tidal dynamics and morphodynamics in the Dutch Wadden Sea

Zheng Bing Wang[1,2], Nirubha Raghavi Thillaigovindarasu[1], Edwin P.L. Elias[1], Quirijn J. Lodder[2,3]
[1]Deltares, Delft, The Netherlands
[2]Delft University of Technology, Delft, The Netherlands
[3]Rijkswaterstaat, Utrecht, The Netherlands
Corresponding author: z.b.wang@tudelft.nl

Keywords: Tidal amplification, tidal asymmetry, morphodynamics, Wadden Sea

1 Introduction

The Wadden Sea, a unique coastal wetland containing the world largest uninterrupted stretch of tidal flats, is under pressure of climate change and specifically the associated acceleration in sea level rise. Sustainable Wadden Sea management to ensure safety against flooding of the hinterland, to protect the environmental value and to optimise the economic activities, requires predictions of the future morphological development.

Understanding the interaction between tidal dynamics and morphodynamics is important for predicting the future development of the Wadden Sea. In this study, we investigate the historical developments of morphodynamics and tidal dynamics in the Dutch part of the Wadden Sea using bathymetry data and water level measurements. The objectives of the study are to determine and to explain the historical changes of tidal dynamics in the Dutch Wadden Sea at various timescales.

2 Method

Morphodynamic development in the tidal basins of the Wadden Sea is analysed by determining their sediment budget and various morphological parameters using historical bathymetry data obtained between 1926 and 2024.

Tidal dynamics are investigated by analysing the development of tidal amplification and tidal deformation for each basin. For this purpose the water level timeseries measured in 10-minute intervals at stations in and around the Dutch Wadden Sea are collected. The time series is divided into periods of 24 hours and 50 minutes (~1 lunar day). For each period of about a lunar day a Fourier series is determined resulting in the quantities: the average water level a_0, the amplitudes and phases of the diurnal (a_1 and ϕ_1), semi-diurnal (a_2 and ϕ_2), quarter-diurnal (a_4 and ϕ_4), and six-times-daily (a_6 and ϕ_6), components of the tide. This method of analysing water level data has been applied earlier to the Guadalquivir estuary and to the Western Scheldt estuary [1,2]. Tidal amplification in a tidal basin is analysed by determining the amplification factor, i.e. the amplitude ratio of the semi-diurnal tide between a station in the basin and a station near the inlet. The tidal deformation is analysed by comparing the tidal asymmetry at the same two stations. As indicators for tidal asymmetry, the relative phase lag between quarter diurnal and semi-diurnal tides and the ratio between periods of rising and falling tides T_r/T_f are determined.

3 Main findings

The tidal amplification and deformation in the Dutch Wadden Sea show changes at three different timescales: long-term (decades) variations, seasonal variation and spring-neap variation.

The long-term variation is related to the morphological changes, mainly due to human interferences in the past. Like in the Western Scheldt [2], the observed changes of tidal dynamics can be well explained by the morphological changes, but not the other way around.

The spring-neap variation in tidal dynamics can be explained by the variation of the tidal amplitude itself. Tide is less amplified during spring tide because of more damping due to bottom friction which is non-linearly related to the flow velocity [1].

The seasonal variation in tidal dynamics is surprisingly strong in the Dutch Wadden Sea. This appears to be related to the variation in mean water level. The mean water level in the Dutch Wadden Sea is higher in winter than in summer and causes a significant difference of water depth up to 0.5 m. Interestingly, the seasonal variation of mean water level has opposite effects on tidal amplification in the large basins in western part than in the small basins in the eastern part of the Dutch Wadden Sea.

The findings from this study are relevant for modelling of long-term morphological development with process-based models as well as aggregated models.

References

[1] Z.B. Wang, J.C. Winterwerp, Q. He (2014). Interaction between suspended sediment and tidal amplification in the Guadalquivir Estuary. Ocean Dyn 64:1487–1498. https://doi.org/10.1007/-s10236-014-0758-x1487-1498.

[2] E.P.L. Elias, A.J.F. Van der Spek, Z.B. Wang, J. Cleveringa, C.J.L. Jeuken, M. Taal, and J.J. Van der Werf (2023). Large-scale morphological changes and sediment budget of the Western Scheldt estuary 1955–2020: the impact of largescale sediment management. *Netherlands Journal of Geosciences*, Volume 102, e12. https://doi.org/10.1017/-njg.2023.11.

Fully nonlinear evolution of free migrating river bars: domain length effects, wavenumber selection, and timescale dynamics

F. Weber [1], M.Toffolon[1], M. Colombini[2] and H.A. Dijkstra[1,3], A. Siviglia[1]

[1]Department of Civil Environmental and Mechanical Engineering, via Mesiano 77, Trento, Italy
[3]Institute for Marine and Atmospheric research Utrecht, Princetonplein 5, Utrecht, The Netherlands
[2]Department of Civil Chemical and Environmental Engineering, Via Montallegro, 1, 16145 Genova, Italy

e-mail corresponding author: annunziato.siviglia@unitn.it

Keywords: *river morphodynamics, free bars, spectral methods*

1 Introduction

The formation and growth of river bars (Fig. 1A) have been extensively studied using linear and weakly nonlinear (WNL) theories. Linear stability analysis quantifies the critical dimensionless width-to-depth ratio, β_c, and identifies the range of bar wavenumbers, k, that can grow under uniform flow conditions when $\beta > \beta_c$ (Fig. 1A). WNL approaches further describe the selection and development of bar patterns near β_c, yielding predictions for equilibrium amplitude and characteristic timescales. However, far from the instability threshold, nonlinear interactions significantly alter the background flow, necessitating numerical methods to capture the full dynamics of free bar evolution.

2 Methods

The 2D depth-averaged shallow water and Exner equations, valid under bedload sediment transport conditions, are solved using a fully nonlinear spectral method [1]. In our approach, the dimensionless morphodynamic variables are expressed as truncated Fourier series, yielding a system of ordinary differential equations for the modal amplitudes that are discretized in time via a semi-implicit scheme. Starting from a flat bed with a small random perturbation in the bottom topography, we study the formation and evolution of migrating bars as a function of the channel aspect ratio β and base flow transport intensity. We performed simulations using domains of varying lengths. Our reference solution is obtained from a simulation with a domain length equal to 24 times the wavelength of the bars at critical conditions (i.e., β_c). In each simulation, we measured the wavelength λ, propagation celerity ω, and bar amplitude A. For each simulation with a shorter domain, we computed the error as the percentage difference between the values of λ, ω, and A obtained in that simulation and those from the reference simulation.

3 Results

Our results demonstrate that fully nonlinear competition between unstable longitudinal modes selects a significantly shorter wavenumber than that predicted by linear theory (Fig. 1B). The domain length plays a crucial role in determining the equilibrium patterns and dynamics. Specifically, as the domain length increases, the error in the computed variables decreases, falling below 10% when the domain length is at least 8 times the critical wavelength (Fig. 1C). Finally, we identify three distinct timescales governing the evolution of migrating river bars. The first timescale corresponds to the initial instability phase characterized by linear growth. The second is associated with nonlinear saturation and the selection of dominant modes, as captured by weakly nonlinear (WNL) theory near criticality. The third timescale represents a long-term equilibration phase during which the bars transition to a steady or slowly modulated migratory state.

4 Conclusions

Our work extends the results of linear and weakly nonlinear theories by capturing bar formation and development far from criticality. The strong dependence on domain length underscores the importance of using sufficiently large computational domains to obtain reliable predictions and suggests that flume experiments must be designed with appropriately scaled domains.

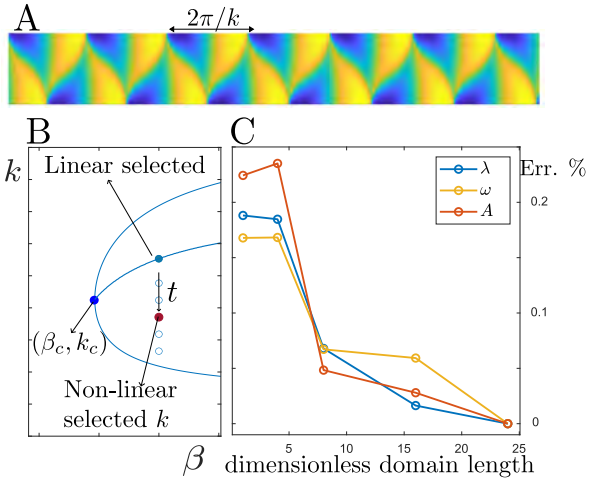

Figure 1: (A) Numerical results of a typical equilibrium topography of migrating free bars ($\Lambda/\Lambda_c = 16$ domain). (B) Stability diagram for free bars in the (k, β) plane. (C) Percentage error in the computed wavelength (λ), propagation celerity (ω), and bar amplitude (A) for various domain lengths.

References

[1] M Colombini and Marco Tubino. Finite amplitude free-bars: a fully nonlinear spectral solution. In *EUROMECH colloquium on sand transport in rivers, estuaries and the sea. 262*, pages 163–169, 1991.

Investigating the role of geotechnical sediment properties on storm-driven geomorphodynamics

Nina Stark[1], Michael H. Gardner[2]
[1]University of Florida, Engineering School of Sustainable Infrastructure and Environment, Gainesville, Florida, USA
[2]University of California, Davis, Department of Civil and Environmental Engineering, Davis, California, USA
Corresponding author: nina.stark@ufl.edu

Keywords: sediment strength, bulk density, wave-soil interaction, erodibility

1 Introduction

Hurricanes Helene and Milton made landfall just two weeks apart in Fall 2024 at central and northern Florida's west coast. The storms led to major damages to the built environment, erosion, and even barrier island breaches. The impacted coastal areas are characterized by a wide range of seabed and coastal sediment properties and conditions ranging from loose to dense sands to fine-grained extremely soft muds. While surface roughness and morphological features are often included in hydraulic models predicting storm surge and inundation, possible infiltration/exfiltration or almost impervious surfaces from fine-grained soils are typically not included. Similarly, erosion predictions typically consider just soil type as sands being erodible and muds being hardly erodible, or possibly considering a grain size value. However, this ignores many geomechanical processes and properties such as bulk density, plasticity, or sediment strength, pore pressure response to waves and rapid inundation, and others. However, there are limited data sets to-date which include geomechanical details as well as measurements of geomorphodynamics and hydrodynamics.

A large interdisciplinary team mobilized to collect data before, during and after Hurricanes Helene and Milton. The collected data includes a detailed soil characterization, water level and wave gages, as well as topographic and bathymetric data. The purpose of this conference contribution is to introduce the collected data set that is publicly available at [1] as well as to discuss initial observations regarding the relationship between observed geomorphological change and geomechanical properties in different areas impacted by Hurricanes Helene and Milton.

2 Data Collection

One day before landfall of Hurricane Helene, topographic data and aerial imagery was collected in the community of Cedar Key, Florida. Additionally, 17 wave gages and water level sensors were deployed as well as 4 pore pressure sensors which collected data throughout the storm. After the storm, a large interdisciplinary team collected multi-disciplinary data including current patterns, topography and bathymetry, and surficial and sub-surface soil conditions including sediment type as well as in-situ strength testing. Similar data products were collected during a second data collection phase at the locations of barrier island breaches during Hurricane Milton, namely Midnight Pass and Milton Pass.

3 Initial Results

Initial results suggest that even very soft and poorly consolidated fine-grained sediments exhibited significant resistance against erosion. This seemed to also apply if fines contents were less than 50% of the sediment sample. In sandy sediments, pore pressure response to wave action appeared to have contributed to increased or decreased erodibility reflected in severe or minor geomorphological change.

Acknowledgments

The authors acknowledge funding from the National Science Foundation through grants 1939275 (NEER), 1826118 (GEER), 2130997 (NHERI RAPID), and 2501467 (Stark). The authors also acknowledge all NEER/GEER team members including researchers, practitioners, federal agency representatives, professional staff from the UW NHERI RAPID facility and the UF CCS, and students who participated in person or remotely without whom this data collection effort would not have been possible. Most importantly, the authors would like to thank the community members and local authorities who have been supportive throughout the data collection efforts and provided access to the measurement locations.

References

[1] Stark, N., M. Gardner, M. Grilliot, A. Lyda, K. Dedinsky, J. Mueller, C. Pezoldt, J. Hubler, C. Castro-Bolinaga, A. Schueller, W. Zhan, M. Haefeli, S. Burghardt, M. Wondolowski, S. Holberg, M. Hassan, J. Parker, J. Laurel-Castillo, L. Eggensberger, E. Nichols, H. Herndon, P. Wang, M. Olabarrieta Lizaso, B. Raubenheimer, Y. Hashash, S. Adusei, and N. Jafari (2025). "NEER/GEER: Hurricanes Helene & Milton", in NEER/GEER: Hurricanes Helene and Milton. DesignSafe-CI. https://doi.org/10.17603/ds2-m8h3-5802

Quantifying and monitoring the instream wood regime across multiple scales

Virginia Ruiz-Villanueva[1,2,3], Janbert Aarnink[2], Gabriele Consoli[1,2], Bryce Finch[2], Javier Gibaja[2], Ivan Pascal[2], Maha Sheikh[1,3], Marceline Vuaridel[2]

[1]Institute of Geography, University of Bern, Hallerstrasse 12, 3012 Bern, Switzerland
[2]Institute of Earth Surface Dynamics, University of Lausanne, Geopolis, 1015 Lausanne, Switzerland
[3]Oeschger Centre for Climate Change Research, University of Bern, Bern, Switzerland

Corresponding author: virginia.ruiz@unibe.ch

Keywords: instream wood, fluvial ecosystem, river morphology, flood dynamics

Abstract

Traditionally, the study of rivers has focused on water and sediment as primary drivers of fluvial systems. However, this perspective is increasingly being expanded to incorporate vegetation and instream wood, elements that play a crucial role in shaping river morphology, sediment dynamics, and ecosystem functions [1]. Instream wood, including downed trees, trunks, root wads, and branches, significantly influences nutrient cycling, organic carbon fluxes, and the creation of physical habitats [2]. Therefore, the integrity of river systems depends on the natural interplay between water, sediment, and wood regimes [3].

Despite its ecological importance, the role of instream wood remains largely overlooked, and its removal has been common in managed river systems, often without considering the resulting ecological and morphological consequences.

While research on instream wood has grown in recent years, significant knowledge gaps persist. These include understanding the complex and variable recruitment processes that supply wood to rivers, challenges in tracing the origins of transported wood, and the lack of direct observational data on wood dynamics. Addressing these gaps is critical for advancing the scientific understanding of fluvial systems and improving their management. This was the aim of this work.

This scientific project, funded by the Swiss National Science Foundation between 2020 and 2025, aimed to enhance the understanding of fluvial ecosystem functioning by integrating the instream wood regime across multiple disciplines and spatial and temporal scales. Specifically, the project addressed the following objectives:

1. Advancement of wood supply and transfer modelling: for the first time, the concept of the wood cascade was described and developed as a model.
2. Development of methods to infer the origin of stored instream wood by combining dendrochemistry and fingerprinting techniques.
3. Establishment of a network of cameras and tracking devices to monitor wood transport in several alpine rivers, providing unprecedented insights into wood dynamics.
4. Monitoring and quantifying wood fluxes and storage by combining drone surveys and novel machine learning techniques.

The outcomes of this project significantly advanced the scientific understanding of river systems, particularly regarding the role of instream wood. These findings have profound implications for flood hazard assessment, as well as forest and river management strategies. Quantifying and monitoring the instream wood regime can enhance river restoration efforts, mitigate flood hazards, and improve the resilience of fluvial ecosystems to environmental changes.

Acknowledgements

This study has been supported by the Swiss National Science Foundation (PCEFP2_186963), the Universities of Lausanne and Bern (Switzerland).

References

[1] Gurnell, A. M., Bertoldi, W. 2024. Plants and river morphodynamics: The emergence of fluvial biogeomorphology. *River Research and Applications*, 40(6), 887–942. https://doi.org/10.1002/rra.4271

[2] Verdonschot, P.F.M., Verdonschot, R.C.M. 2024. Ecological Functions and Management of Large Wood in Fluvial Systems. *Curr. For. Rep.* 10, 39–55. https://doi.org/10.1007/s40725-023-00209-x

[3] Wohl, Kramer, Ruiz-Villanueva, N Scott, Comiti, M Gurnell, Piegay, B Lininger, L Jaeger, M Walters, D Fausch. 2019. The Natural Wood Regime in Rivers, *BioScience*, 69, Issue 4, 259–273, https://doi.org/10.1093/biosci/biz013

SPECIES-BY-SPECIES PATTERN ANALYSIS OF COASTAL DUNE VEGETATION

Davide Demichele[1], Elena Belcore[1], Marco Piras[1], Carlo Camporeale[1]
[1] DIATI, Department of Environment, Land and Infrastructure Engineering, Politechnic of Turin, Corso Duca degli Abruzzi, 24, 10129 Turin, Italy
Corresponding author: davide.demichele@polito.it
Keywords: Vegetaion Pattern, Coastal Eco-morphology, Geostatistics, Classification.

1 Introduction

Coastal dunes are ecotones hosting an extraordinary floristic and faunistic biodiversity. They play a crucial role in mitigating the impacts of climate change, acting as a natural barrier against coastal erosion and storm surges, and contributing to the coastline's overall sediment balance. Coastal dunes are shaped by the complex mutual interaction between terrain morphology, environmental forcings, such as wind and waves, and vegetation which triggers sand accumulation and stabilizes the terrain underneath with roots.

Despite their importance, coastal dunes are subjected to several threats, due to anthropic pressure (e.g., environmental degradation, sand extraction, etc.) and climate change-driven hazards (e.g., coastal erosion). Looking forward to achieving more effective and sustainable plans for conservation and restoration of coastal dunes, is crucial to understand and model the evolution of endemic vegetation.

The aim of this study is to provide a fine-scale species-by-species analysis of vegetation spatial patterns, representing a benchmark for tuning and validating coastal eco-morphodynamic models.

2 Material and Methods

Three study areas (about 500x400m each) within the San Rossore–Migliarino–Massacciuccoli Regional Park have been selected for this study. One of the areas (A1) is heavily impacted by anthropic presence, while the other two are undisturbed.

A comprehensive vegetation dataset has been generated using an Object-Based Image Analysis (OBIA) algorithm [1] applied to high-resolution ortho-images of the study areas. This dataset facilitated the detection and classification of plant individuals from 12 different species and the extraction of important morphometric features such as location, equivalent diameter (ED), local spatial density, and ground cover. A hi-resolution Digital Terrain Model (DTM) of the study area was created to characterize the dune morphology (e.g., beach slope, dune crest, etc.).

Geostatistical tools such as semi-variograms, nearest neighbor index (NNI), and modified Ripley's L-function have been used to characterize vegetation spatial arrangement.

Additionally, a wave runup analysis was conducted using Stockdon's method [3] to understand the interaction between vegetation and hydrodynamic forcings.

3 Key Results

Vegetation threshold distance from the coastline, L_{veg}, beyond which vegetation survival becomes viable [2] is superimposed by the reaching distance of wave runup during extreme events. Furthermore, the ratio between average L_{veg} and the average distance of the foredune crestline, x_{crest}, lies consistently around 0.6 in all three study areas, regardless of their different dune morphologies.

Foredune size is closely related to the abundance (i.e., the ratio between the number of elements of a single species and the total amount of plants present in an area) of dune-building species, like *Ammophila arenaria*, which also appears to be one of the most sensitive species to direct human disturbances.

Terrain morphology significantly affects vegetation zonation: on taller and undisturbed dunefields, species zonation is clearer and more defined, whereas on flatter and disturbed ones spatial distribution of vegetation is significantly sparser, leading to a fuzzier and indistinct zonation.

Abundance stands out as one of the most relevant eco-morphological parameters, as it also strongly affects the average spatial density of a species and its pattern type, with less abundant species showing a wider variability in local spatial density, leading to more tightly clustered spatial patterns. This result is corroborated by point pattern analysis, from which emerged a positive correlation between the abundance of a species and its NNI, denoting the degree of spatial clustering. Furthermore, modified Ripley's L-function revealed a multi-scale clustered pattern for most species under examination.

References

[1] Belcore, E., Latella, M., Piras, M., & Camporeale, C. (2024). Enhancing precision in coastal dunes vegetation mapping: Ultra-high resolution hierarchical classification at the individual plant level. Int. J. of Remote Sens., 45 (13), 4527–4552.

[2] Duràn, O., & Moore, L. J. (2013). Vegetation controls on the maximum size of coastal dunes. Proceedings of the National Academy of Sciences, 110 (43), 17217–17222.

[3] Stockdon, H. F., Holman, R. A., Howd, P. A., & Sallenger Jr, A. H. (2006). Empirical parameterization of setup, swash, and runup. Coastal engineering, 53 (7), 573–588.

Measurement of Flow Velocity around a Developing Antidunes

Yu Inami[1], Takuya Inoue[2], Shinichiro Onda[3]
[1]Civil Engineering Research Institute for Cold Region, Sapporo, Hokkaido
[2]Hiroshima University, Higashi-hiroshima, Japan, [3]Kyoto University, Kyoto, Japan
Corresponding author: inami-y@ceri.go.jp

Keywords: Formation Processes of Antidunes, Flume Experiment

1 Introduction

The formation processes of 3D bedforms remain largely unresolved (Best, 2005). Focusing on antidunes, their formation processes have been primarily studied with an emphasis on depositional structures (e.g., Cartigny et al., 2014). Recent studies have advanced our understanding of the relationship between 3D antidune formation processes and flow structures. For instance, Inoue et al. (2020) conducted the flume experiments to investigate the relationship between the formation conditions of 3D antidunes and the flow field. However, they did not investigate the formation processes of antidunes from a flat bed. This study aims to clarify the processes leading to the formation of antidunes from a flat bed. To achieve this, the flow structures around developing antidunes were measured in detail through flume experiments.

2 Flume Experiment

We used the straight channel with a width of 0.5 m, a length of 25 m, and a bed slope of 0.018. The experimental conditions included a flow discharge of 42.9 L/s, with a free outflow condition at the downstream end. First, we performed experiments to form 3D antidunes from a flat bed and used image analysis to measure the bed topography during and after their development. The bed material is well sorted 5 mm gravel. Then, we made a fixed bed simulating the shape of measured antidunes using mortar and covered with 5 mm gravel. The velocity distributions in the x–y plane were measured along the longitudinal section at the flume centerline. Measurements were taken at 0.057 m intervals in the x-direction and at 0.01 m intervals in the z-direction, from the bed to the water surface. For the y–z plane, velocity distributions were measured at each cross-section with a spatial resolution of 0.01 m in the y-direction and 0.01 m in the z-direction from the bed to the water surface.

3 Results and Conclusions

Initially, small irregularities formed on the flat bed, which gradually merged to create a 3D antidune in the central part of the flume. The antidune had a wavelength of approximately 0.2 m and a wave height of 0.04 m. In this section, we present an example of velocity measurement results obtained using the bedforms during the intermediate stage of antidune development. On the stoss side, upward flow increases with the rise of the water surface (Figure 1). Near the bed, lateral flow directed to avoid the crest region is observed. At the crest, upward flow becomes dominant, and lateral velocity components are nearly absent (Figure 2). In the trough, downward flow intensifies as the water surface lowers (Figure 3). Near the bed in the trough region, lateral flow directed toward the deepest part of the trough is observed.

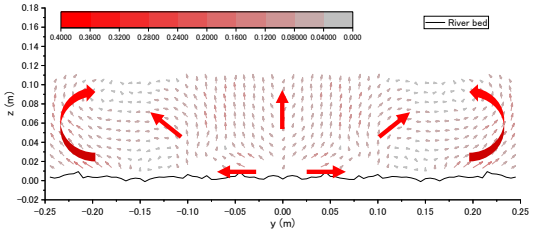

Figure 1: Y-Z Velocity (stoss side).

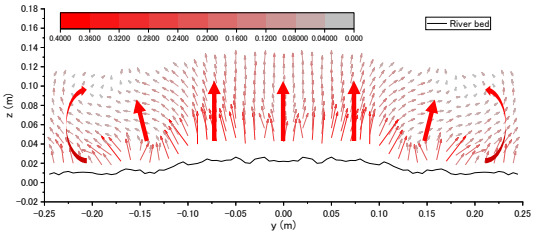

Figure 2: Y-Z Velocity (crest).

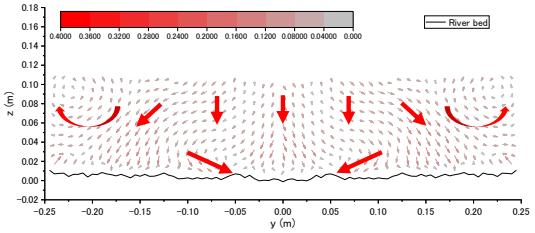

Figure 3: Y-Z Velocity (trough).

References

[1] J. L. Best. The fluid dynamics of river dunes: a review and some future research directions. *J. Geophys. Res. Earth Surf*, 110, F04S02, 2005.

[2] M. J. Cartigny, D. Ventra, G. Postma and J. H. van Den Berg. Morphodynamics and sedimentary structures of bedforms under supercritical - flow conditions: new insights from flume experiments. *Sedimentology*, 61(3), 712-748, 2014.

[3] T. Inoue, Y. Watanabe, T. Iwasaki and J. Otsuka. Three-dimensional antidunes coexisting with alternate bars. *Earth Surf. Process. Landforms*, 45: 2897–2911, 2020.

Observing Coastal Processes with X-Band Radar

Laura Szczyrba[1,2], Ryan Mulligan[2], Peir Pufahl[2], Josh Humberston[3], Jesse McNinch[4]
[1]BGC Engineering Inc., Kingston, Ontario, Canada
[2]Queen's University, Kingston, Ontario, Canada
[3]Coastal Measures, Seacoast Region County, New Hampshire, United States of America
[4]United States Army Corps of Engineers, Vicksburg, Massachusetts, United States of America
Corresponding author: lszczyrba@bgcengineering.ca

Keywords: remote sensing, refraction, rip currents, bathymetry

1 Introduction

Storms are difficult to study in detail, leading to a lack of observational data. Remote sensing technologies, such as optical video, radar, and lidar, are well-suited for these challenging conditions, offering high-quality, continuous data across broad scales. This research utilizes X-band radar (XBR) to observe coastal processes, including wave refraction, rip current activity, and bathymetric evolution. XBR systems emit electromagnetic frequencies and measure the backscatter of the signal, which intensifies as the ocean surface becomes rougher, particularly during storms. Unlike many traditional methods, radar excels in capturing data at night and during adverse weather conditions such as fog and rain, making it an invaluable tool for nearshore monitoring.

2 Methods

An XBR system was deployed at two sandy beaches in the Outer Banks of North Carolina (NC) in the United States: Duck and Kitty Hawk. XBR backscatter observations during several high-energy storm events in 2017 and 2019 were collected in 15-minute bursts across a spatial scale of 1 – 3 km at a resolution of 5 m x 5 m. Estimates of wave refraction and rip current activity were calculated and results were compared to in-situ sensors and nonhydrostatic modelling results. Finally, the cBathy algorithm [1] was applied to invert measured incoming wave speed to an estimate of depth.

3 Results

The XBR system performed best when local significant wave heights were greater than or equal to 1 m. Observations of wave refraction documented alongshore variability in wave refraction patterns in the nearshore and were accurate within ±5°. At a site with complex bathymetry, the XBR system observed two discrete zones where enhanced backscatter was consistently recorded outside of the surf zone during high-energy conditions (Figure 1). These observations were interpreted to be rip currents that produced local zones of enhanced sea surface roughness [2]. Rip currents regenerated at the apex of bends in the nearshore bathymetric contours.

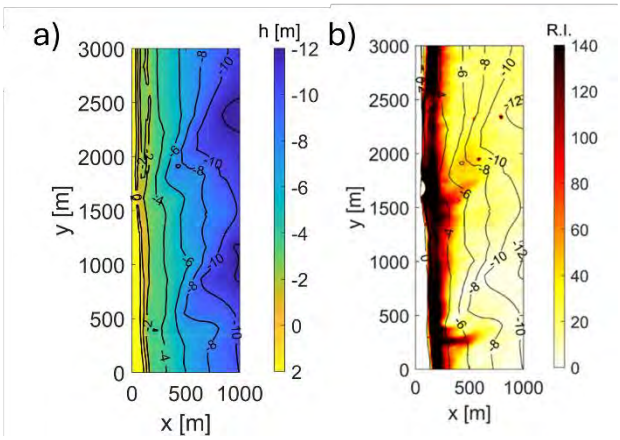

Figure 1: Water depth (h) (a) and XBR backscatter return intensity (R.I.) (b) at Kitty Hawk, NC. Depth contours are plotted and labelled in black.

Finally, XBR data provided adequate estimates of bathymetry that compared well with available seasonal survey data. The bathymetric estimates were most accurate between 4 and 7 m depth. Depth was overestimated shoreward of the 4 m depth and underestimated offshore of 7 m depth.

4 Conclusions

XBR is capable of continuously monitoring and accurately measuring a wide range of nearshore processes, including wave refraction, wave speed, wave breaking, and rip currents, and can also provide reliable bathymetric estimates. Its ability to operate effectively in adverse conditions makes it an excellent supplement to in-situ observations and a valuable tool where sensor or survey data are unavailable. However, further work is needed to refine the extraction of bathymetric information from radar observations.

References

[1] Holman, R., & Bergsma, E. W. Updates to and performance of the cbathy algorithm for estimating nearshore bathymetry from remote sensing imagery. *Remote Sensing*, 13(19), 3996, 2021.

[2] Szczyrba, L., Mulligan, R. P., Pufahl, P., Humberston, J., & McNinch, J. (2024). Nearshore flow dynamics over shore-oblique bathymetric features during storm wave conditions. Journal of Geophysical Research: Oceans, 129, e2023JC020630.

Effects of canal excavation on the hydrodynamics of back-barrier lagoons

Davide Tognin[1], Angelica Piazza[1], Luca Carniello[1]
[1]Università degli Studi di Padova, Padova, Italy
Corresponding author: davide.tognin@unipd.it

Keywords: dredging, excavation, channel, lagoon

1 Introduction

Historically, estuaries and lagoons have been pivotal to navigation, as they often hosted harbours, because of their sheltered locations. Over centuries, human interventions such as channel dredging and canal excavation have modified these environments to accommodate increasingly larger vessels and enhance harbour accessibility [1]. Although these modifications offered immediate benefits for navigation, they altered the delicate hydro-morphodynamic equilibrium of shallow tidal systems, potentially exacerbating erosion and vulnerability to sea level rise. Therefore, understanding the side effects and long-term consequences of dredging and excavation is crucial for developing informed management strategies for back-barrier lagoons.

2 Methods

Here we explored how canal excavation and dredging affected the hydrodynamics of two back-barrier lagoon systems in the northern Adriatic Sea: the Venice and the Marano-Grado Lagoons. In the Venice Lagoon, the Malamocco-Marghera canal was excavated in 1970 and is maintained at a minimum depth of -10 m along its 16-km path connecting the Marghera harbour to the open sea through the Malamocco inlet (Figure 1a). In the Marano-Grado Lagoon, a 6-m deep canal completed in 1969 connects the industrial harbours on the Corno and Ausa rivers to the Porto Buso inlet (Figure 1b).

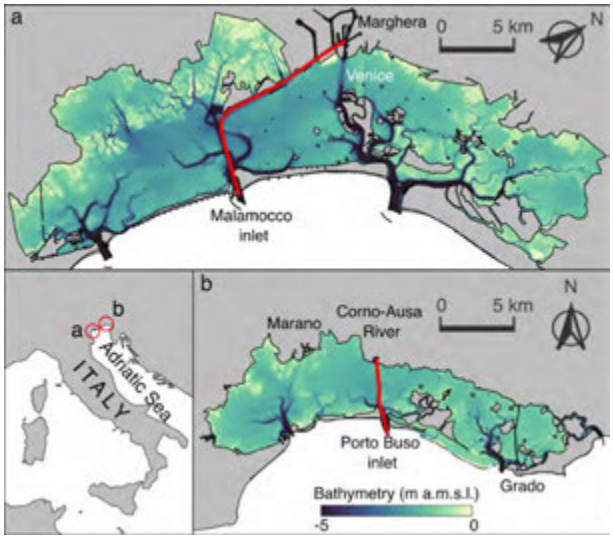

Figure 1: Venice Lagoon (a) and Marano-Grado Lagoon (b). Excavated canals are highlighted in red.

Using available bathymetric surveys, we constructed computational grids for the pre- and post-intervention scenarios, and for the present-day configurations. We applied a 2-D finite element hydrodynamic model [3] to simulate tidal flows in the considered configurations, setting as boundary conditions a sinusoidal tidal wave with a 0.50 m amplitude and a 12-hour period, representative of the tidal regime in the northern Adriatic Sea.

3 Results and Conclusions

Despite differences in morphology and intervention scale, similar trends can be observed between the effects on the hydrodynamics of the two lagoons. Comparisons between pre- and post-intervention scenarios reveal increased water discharge through the inlet connected to the excavated channel, which leads to a lagoon-wide redistribution of the sub-basin areas connected to each inlet. In particular, the ebb-phase discharge increase exceeds that of the flood phase, promoting a shift toward ebb-dominance. This shift has significant implications for water and sediment dynamics.

These findings reveal the potential long-term consequences of dredging and excavation in shallow tidal systems and highlight the need for management strategies that balance navigational demands with the preservation of the morphological integrity of back-barrier lagoons.

Acknowledgments

This work was funded by NextGenerationEU, within the iNEST Innovation Ecosystem (ECS00000043) and the PRIN2022 Prot&Cons project (Reconciling coastal flooding protection and morphological conservation of shallow coastal environments; 2022FZNH82).

References

[1] Bruun, P. (1994). Engineering projects in coastal lagoons, in *Coastal Lagoon Processes*, ed. B. Kjerfve.

[2] Cox, J. R., Lingbeek, J., Weisscher, S. A. H., & Kleinhans, M. G. (2022). Effects of sea-level rise on dredging and dredged estuary morphology. *Journal of Geophysical Research: Earth Surface*, 127.

[3] Carniello, L., D'Alpaos, A., & Defina, A. (2011). Modeling wind waves and tidal flows in shallow micro-tidal basins. *Estuarine, Coastal and Shelf Science*, 92(2), 263-276.

Spatial distributions of velocity and water level in an actual river channel including a bifurcation and a confluence

Shun Kudo[1], Atsuhiro Yorozuya[1]
[1]Flood and River Responce Monitoring Team, River Dynamics Management Group,
Public Works Research Institute, Tsukuba, Ibaraki, Japan
Corresponding author: kudou-s573cl@pwri.go.jp

Keywords: UAV, PIV analysis, LiDAR, two-dimensional unsteady flow simulation

1 Introduction

This study aims to clarify the spatial distribution of velocity and water level using both observational and simulation techniques. The target area of this study includes a river bifurcation and a confluence. Understanding the flow characteristics of such parts of river is crucial for both flood protection planning and water use planning (e.g., bifurcation flow rates, backwater at a confluence point, sediment deposition).

Traditionally, the flow structure of bifurcations and confluences has been investigated primarily through experimental channels and numerical simulations, with subsequent application to actual rivers.

In recent years, Unmanned Aerial Vehicle (UAV) technology has advanced significantly, and the authors have conducted research on its application to actual river measurements. In this study, we first conducted observations using a UAV equipped with a video camera and a Light Detection and Ranging (LiDAR) system. This system enables the measurement of velocity or water level over a large area in a single flight. Furthermore, we applied two-dimensional unsteady flow simulation and verified both the observed and simulated distributions of velocity and water level.

2 Observation

Velocity distribution was obtained using a video camera mounted on a UAV and Particle Image Velocimetry (PIV) technique. The target area is shown in Figure 1, which includes both bifurcation and confluence points. To conduct PIV, we employed a geometric translation method that does not require any ground control points (GCPs). Instead of GCPs, the method requires information on the camera's position and angle, the vertical distance from the camera to the water surface, and a camera parameter related to the focal length. This method enables PIV analysis of video images taken from any area, even if the image shows only the water surface. Figure 2 shows the result of PIV analysis at the confluence point.

Water level distribution was obtained using a LiDAR mounted on the UAV. In this study, we used a Zenmuse L2, whose accuracy (RMS 1 σ) is 2 cm at a height of 150 m.

3 Verification of the velocities and water levels

We conducted ground measurements using an Acoustic Doppler Current Profiler (ADCP) and an electromagnetic current meter in areas that were difficult to obtain data by the aerial measurement. Finally, a two-dimensional unsteady flow simulation was conducted to finalise the velocity and water level distributions, ensuring physical conformity (i.e., the hydraulic quantities satisfying the continuity and momentum equations).

Figure 1: Observation and simulation area. (Ortho image obtained by pictures taken by a camera on UAV and Structure from Motion (SfM) technique)

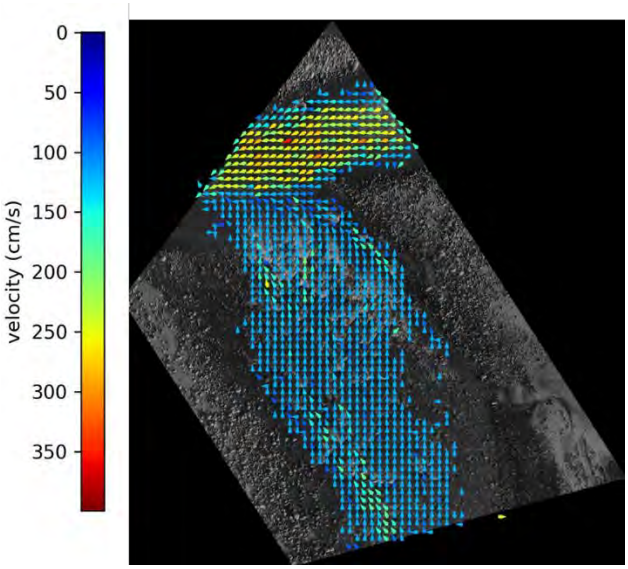

Figure 2: Water surface velocity and flow direction at confluence point by PIV analysis (surrounded by the red frame in Figure 1).

Comparing Morphology of Refurbished and Natural Coastal Dunes

Cora Jones[1], Julia Cisneros[1]
[1]Department of Geosciences, Virginia Tech, Blacksburg VA, USA
Corresponding author: coraj@vt.edu

Keywords: frontal dunes, refurbishment, erosion, dredging, revegetation

1 Introduction

Coastal frontal dunes are the first line of defence against storm surges [1]. Dunes can significantly mitigate damage to human infrastructure as well as natural ecosystems. As the climate continues to change, tropical cyclones have amplified in frequency and severity [2], leading to erosion of frontal dunes. Coastal conservation methods including sand-fencing, dredging, and re-vegetation have been studied to determine efficacy and optimization. Yet, the effects of these methods on dune morphology is understudied. In this study, I evaluate dune morphology of two beaches, one natural and one refurbished, along North Carolina's coast.

2 Study area

The two beaches included in this research are Fort Fisher and Oak Island, North Carolina. Fort Fisher is an east-facing beach. This beach is unpopulated, maintained by park staff, and is dominantly used as a recreation area. No significant refurbishment projects have been completed at Fort Fisher. Oak Island is a south-facing beach that is maintained by the local government. With a winter population of eight thousand and a summer population of nearly fifty thousand, the yearly influx of people to the beach has caused an increase in erosion. The increase in erosion can be traced to poorly vegetated dunes being disrupted by human actions, such as walking. The erosion of the dunes cost Oak Island over 29 million from 2021-2022 [3].

3 Methods

The morphology of dunes in Fort Fisher and Oak Island were first evaluated by downloading a-meter resolution DEM from North Carolina Spatial Download. We defined a research area of 1.4 km x 35 m on each beach. Profiles perpendicular to the dune crest were taken at the apex of each dune on Oak Island and every ~300 m on Fort Fisher. High spatial resolution DEMs were created over smaller regions in both study areas using a KAARTA Stencil 2 handheld Lidar unit. Pictures of the surface sediment were taken and analysed using image processing techniques to quantify grain size.

4 Results

On average, the Fort Fisher dunes reach a maximum height of 4.9 m, and the crestline of the dune extends across the entire research area (1.4 km long). On average, the Oak Island dunes reached a height of 3.9 m and have distinct human-made breaks every ~24.3 m. These breaks work as access points to the beach; foot traffic through these points leads to a large amount of sediment loss from the dune.

Stark differences are observed when comparing dune profiles across beaches. Fort Fisher's dunes have similar slopes on the stoss and lee side and a distinct crest. However, Oak Island dunes have a trapezoidal morphology with a flat crestal region and well defined stoss and lee sides similar to those described in [4].

Figure 1: Oak Island dune covered in sediment crust. Bottom left has been eroded, exposing finer sand.

Grain size and beach face measurements via Lidar survey suggest Fort Fisher's dunes have thick vegetation on the stoss and lee sides and are composed of well-sorted fine-medium quartz sand. Oak Island dunes are dominantly composed of fine-medium-sorted quartz sand but are capped by a 2-8 cm thick crust of shells, roots, and other miscellaneous sediments (Figure 1).

4 Conclusions

We conclude that these two geographically close beaches have drastically different dune characteristics. The morphological differences observed can be attributed to the extensive dredge and dump operations and revegetation efforts on Oak Island. At Oak Island, we hypothesize that sediment from previous dump operations does not function well with young rooting sea grass, leaving frontal dunes susceptible to high rates of erosion. These findings offer insight towards future management strategies to protect communities that depend on coastal resiliency.

Acknowledgments

We thank Dr. Sean Bemis for his support in operating and analysing data from the handheld lidar unit.

References

[1] Federal Emergency Management Agency [FEMA]. Primary Frontal Dunes Fact Sheet. (2021).

[2] O. Guzman, H. Jiang. Global increase in tropical cyclone rain rate. Nature Communications, (2021).

[3] D. Boraks. Rising Waters (Part II): Ocean towns face more frequent and costly beach rebuilding projects [WHQR], (2024).

[4] C. Kuang, X. Han, J. Zhang, Q. Zou, B. Dong. Morphodynamic Evolution of a Nourished Beach with Artificial Sandbars: Field Observations and Numerical Modeling, 4.1, (2021)

Linking morphodynamics of superimposed bedforms across environments

Elpidio Guzman De La Cruz [1], Julia Cisneros[1]
[1]Department of Geosciences, Virginia Tech, Blacksburg VA, USA
Corresponding author: elpidio@vt.edu

Keywords: Bedform, morphology, aeolian, fluvial

1 Introduction

The occurrence, formation and interactions between multiple scales of bedforms across a range of environments remains understudied. Superimposed dunes are bedforms that form and climb over existing primary dunes. These dunes can form in a range of environments, including aeolian and fluvial [1-5]. In rivers, the conditions of multiple scales of bedform formation have been linked to flow and sediment flux variability [2-4]. These studies have informed our understanding of these compound bedforms and the agents that shape them in fluvial regimes [3-4], thus offering a framework to investigate similar interactions in aeolian environments. First, we review the state of frameworks used to investigate bedform morphodynamics in both environments. Then, we present a morphologic analysis of aeolian bedforms using methods developed for fluvial bedforms to reveal the interactions between multiple scales of bedforms in the aeolian regime.

2 Study area

The Algodones Dune Field is a US National Natural Landmark located in California, near the US-Mexico Border. The area spans approximately 72.4 km long by 9.7 km wide. Its isolated geography constitutes this area as a favorable location for dune dynamics studies. The regions of interest in Algodones are an area with giant primary and superimposed dunes, and an area with primary dunes of a similar scale to the superimposed dunes.

3 Methods

We use repeat DEMs from Lidar and SfM to quantify bedform morphology, scale, and spatial variability over time. Sand traps and sediment surface samples acquired in the field are used to quantify grain size and sediment flux spatially. Four, vertically stacked wind sensors deployed in the field are used to plot wind profiles spatially. Finally, spatial sediment flux was calculated from both the sand traps and dune movement. We characterize dune celerity from temporal DEMs following methods in [5].

4 Results

The literature on fluvial morphodynamics appears more developed in topics regarding sediment transport models and the interactions between primary and secondary dunes [3, 4]. In contrast, a large gap remains in the occurrence, morphology and spatial variability of superimposed bedforms in aeolian environments.

We find that superimposed dunes are an order of magnitude smaller in height compared to the primary dune they climb over. Temporal DEMs show that the superimposed dunes possess uniform migration from the primary dune trough, over the stoss, and to the crest. The superimposed dunes are not found on the primary dune leeside. Alternatively, bedforms similar in scale to superimposed bedforms exist as primary bedforms ~1 km to the west. In this area, bedforms have a large spatial variability in their movement and do not move in one direction. This suggests the morphology of the primary dune plays a role in determining the migration direction of the superimposed dunes.

Sand fluxes measured from sediment traps increase from the trough toward the primary dune crest. Variability from in situ sand flux measurements are also related to the morphology of the superimposed dunes. Sediment flux inferred from dune celerity shows similar trends. Surface sediment grain size (D50) varies between .132 - .256 mm, but variability is seen across superimposed dunes, especially between crests and troughs. Wind measurements suggest variability in both wind speed and direction across the dune field at the time of survey, though longer temporal records support a dominant northerly wind direction.

5 Conclusions

The morphology, wind flow and sediment fluxes observed improve our understanding of how multiple scales of bedforms interact across environments. The tools used to investigate these trends support the use of frameworks developed in fluvial settings to inform the morphodynamics of other environments. Thus, we offer improvements in how dune morphology and superimposition in aeolian regimes are parametrized and characterized.

References

[1] Wright, L. D., & Thom, B. G. (1977). *Coastal depositional landforms*.

[2] Galeazzi, C. P., Almeida, R. P., Mazoca, C. E. M., Best, J. L., Freitas, B. T., Iannirubertо, M., Cisneros, J., & Tamura, L. N. (2018). The significance of superimposed dunes in the Amazon River: Implications for how large rivers are identified in the rock record. *Sedimentology*, *65*(7), 2388–2403.

[3] Venditti, J.G., Church, M. and Bennett, S.J. (2005) Morphodynamics of small-scale superimposed sand waves over migrating dune bed forms. Water Resources Res., 41, W10423.

[4] Zomer, J. Y., & Hoitink, A. J. F. (2024). Evidence of Secondary Bedform Controls on River Dune Migration. Geophysical Research Letters, 51(15), e2024GL109320.

[5] Gunn, A., Casasanta, G., Di Liberto, L., Falcini, F., Lancaster, N., & Jerolmack, D. J. (2022). What sets aeolian dune height? Nature Communications, 13(1), 2401.

Evaluating Shoreline Dynamics with IH-SET: Case Studies in Varied Coastal Environments

Camilo Jaramillo[1], Lucas de Freitas[1], Alejandro Martínez[1], Mario Mascagni[1], Mauricio González[1], and Raúl Medina[1]
[1]IHCantabria – Instituto de Hidráulica Ambiental de la Universidad de Cantabria, Santander, Spain.
Corresponding author: jaramilloc@unican.es

Keywords: Shoreline modeling, Coastal Morphodynamics, Cross-shore, Longshore.

1 Introduction

Coastal areas are highly dynamic systems influenced by natural forces and human activities. Accurate predictions of shoreline changes are essential for effective coastal management. However, existing models often have limitations in scope and mathematical or numerical schemes, focusing on specific processes such as cross-shore or longshore sediment transport, and lacking integration across different modeling approaches. This hinders their flexibility and accessibility. To address these challenges, the Coastal Management and Engineering Group at IHCantabria developed IH-SET (Shoreline Evolution Tools), an open-source, user-friendly software for simulating coastal dynamics.

IH-SET features a collection of advanced models, including: (1) static equilibrium models for beach profiles and beach planform, (2) equilibrium-based shoreline evolution models (EBSEM), (3) oneline models, and (4) hybrid approaches. Its modular design allows users to input site-specific data and select suitable models for predicting shoreline evolution in a variety of environmental scenarios, both natural and human-driven.

This study investigates the potential of IH-SET for analysing diverse coastal environments in Spain and France. These regions exhibit varied tidal regimes, wave climates, and beach morphologies with different sediment characteristics. By applying IH-SET across these varied settings, we aim to evaluate its versatility in modeling shoreline evolution under distinct hydrodynamic and morphological conditions.

2 Methods

IH-SET employs a modular structure incorporating various models to simulate shoreline evolution. These include:

1) **Static equilibrium models:** Assess the planform shape of embayed beaches and beach profiles.
2) **EBSEM:** Predict long-term shoreline changes based on equilibrium principles for cross-shore and rotational movements.
3) **Oneline models:** Simulate shoreline evolution based on longshore transport gradients.
4) **Hybrid models:** Combine different modeling approaches for integrating sediment transport processes.

The tool is implemented as open-source software with an intuitive and user-friendly graphical interface (GUI) to facilitate its applicability.

3 Study Sites

IH-SET has been tested in various locations along the coasts of Spain and France, each characterized by diverse morphological and hydrodynamic conditions. Examples of these locations include:

- **San Jorge Beach** (Galicia, Spain): A west-northwest facing embayed beach exposed to the Atlantic Ocean in a dominated mesotidal environment.
- **Fenals Beach** (Catalonia, Spain): A southeast-facing beach along the Mediterranean coast, influenced by a microtidal regime.
- **Porsmilin Beach** (Brittany, France): A small southwest-facing beach on the Atlantic coast with a low-tide terrace in a region dominated by macrotidal tides.

4 Results

The IH-SET application in various coastal environments demonstrates its versatility in integrating state-of-the-art shoreline evolution models for diverse scenarios. The tool allows users to calibrate models using different methods and assess the impact of structures. It aids in identifying the most suitable model or models' ensemble for supporting coastal management decisions, depending on local conditions and data quality.

5 Conclusions

H-SET represents a significant advancement in shoreline evolution modeling by integrating multiple modeling approaches into a single, versatile framework. The tool's application across different coastal environments highlights its adaptability to varying hydrodynamic and morphological conditions. Its open-source nature and modular design make it a powerful tool for researchers and coastal engineers.

Acknowledgments

The authors acknowledge the support of the ThinkInAzul programme, supported by MCIN/Ministerio de Ciencia e Innovación with funding from the European Union NextGeneration EU (PRTR-C17.I1) and by Comunidad de Cantabria.

Morphological trends in a highly engineered estuary

Pia Kolb[1], Edgar Botero Campabadal[1], Franziska Lauer[1], Frank Kösters[1]
[1]Federal Waterways Engineering and Research Institute (BAW), Hamburg, Germany
Corresponding author: pia.kolb@baw.de

Keywords: Weser estuary, morphological trends, sedimentation, sediment management, maintenance dredging

1 Introduction

In highly engineered estuaries, the morphology is shaped by past measures (e.g. deepening of the navigational channel), maintenance dredging, and natural developments. A key challenge in these estuaries is to ensure navigability while keeping environmental impacts as small as possible. In order to improve sediment management concepts e.g. with regard to maintenance dredging or sediment dumping, it is essential to understand the morphological development of the estuary. In this study, we have created a comprehensive data set to analyse current morphological trends and estimate future developments and dredging demands for the Weser estuary, Germany.

2 Methods

With means of bathymetric data [1], the morphological development of the Weser estuary and specifically the navigational channel was examined. In addition, dredging volumes and sediment composition were evaluated based on records from sediment dredging [2]. Sedimentation rates were calculated [3]. All data were analysed to examine the system behaviour and estimate morphological trends. In addition to a statistical analysis, neural networks were set up to find correlations in the data and to estimate the future development of bathymetry and dredging needs.

3 Results

In the Lower Weser estuary, sedimentation in the navigation channel is strongly influenced by the position of the estuarine turbidity maximum (ETM) which varies with tides and river discharge. In the ETM zone, suspended sediment concentration (SSC), sedimentation rates, and dredging demand increase. At the upstream end of the ETM, unusual prolonged periods of very low discharge have caused an increase in SSC due to an upstream shift of the ETM at the end of 2020, 2021 and 2022. As a consequence, increased sedimentation of cohesive material occurred in the otherwise sandy section (see Figure 1). As periods of prolonged low river discharge increase due to climate change, an increase in sedimentation can be expected in this section in the near future.

In the Outer Weser estuary, several areas of currently sufficient depth are expected to extend above the nautical depth in the next years due to ongoing sedimentation, causing an increase in dredging volumes.

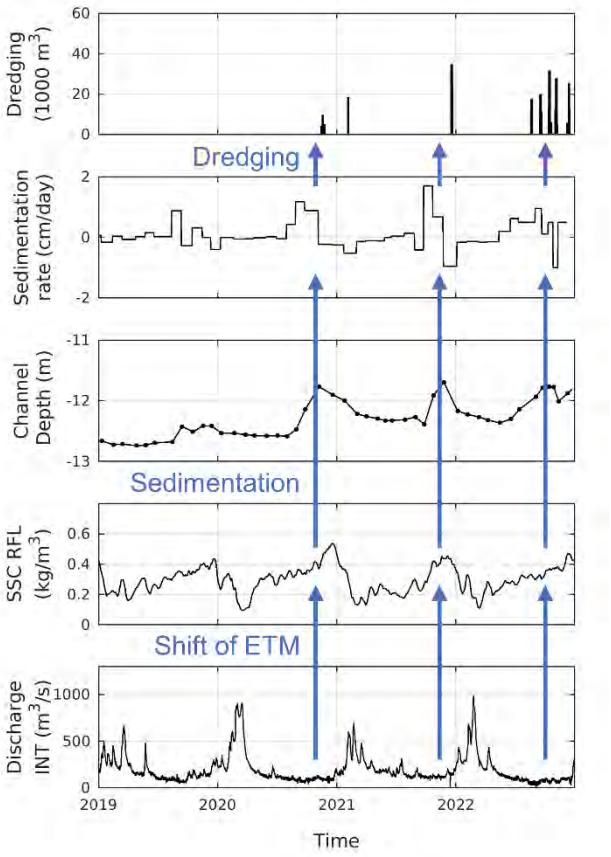

Figure 1: Effect of variations in discharge on SSC, sedimentation, and dredging at the upstream end of the ETM (Lower Weser estuary).

References

[1] Bathymetrical data, acquired from Funktionales Bodenmodell, BAW, methodology in [4].

[2] Maintenance dredging data of the Weser estuary, Federal Waterways and Shipping Administration (WSV) and Hahlbrock Marine Technology, acquired from the database MoNa.

[3] Sedimentation rates based on data from WSV, acquired from 3D-Datenarchiv, processed by the Federal Institute of Hydrology, BfG/M3.

[4] P. Milbradt, J. Valerius and M. Zeiler. Das Funktionale Bodenmodell: Aufbereitung einer konsistenten Datenbasis für die Morphologie und Sedimentologie. *Die Küste*, 83: 39–63, 2015. https://hdl.handle.net/20.500.11970/101736.

Global Mapping of River Confinement

Niek Collot D'Escury[1], Daan Beelen, Jaap Nienhuis[2,] Maarten Kleinhans[3] Esther Stouthamer[4]

[1]Utrecht University

Corresponding author: d.beelen@uu.nl

Keywords: River Confinement, Geographical Information Systems, River Morphology, Global mapping, Cluster analysis

Introduction

River confinement is a key factor in determining the river's morphology and its behavior, affecting flow properties, sediment transport, flood risk and floodplain development. Technological limitations have previously hindered global quantification of river confinement but advances in remote sensing and software now enable direct, automated measurements of river confinements [3].

Methods

In this study we present a new method that combines the state-of-the-art global river centerline dataset SWORD [1], with the elevation model FAB dem [2] to quantify river confinement across more than three million kilometer of rivers around the world. Our method measures the "entrenchment ratio", which is the ratio between the valley width and the channel width. Secondly we measure the "confinement slope", which is the gradient between the centerline and the surrounding topography.

Results

Our method enables us to identify five distinct classes. 1) Aggradational Rivers, with a negative confinement slope, due to sediment depositions raising the riverbed. 2) Flat Rivers, with no significant confinement slope. 3) Obstructed Rivers, partially confined by isolated topographic features. 4) Valley-confined Rivers, with a floodplain constrained by topography. 5) Entrenched Rivers, which have deeply incised V-shaped valleys. Our classification provides a globally consistent framework for quantifying river confinement, offering insights into river-landscape, flood risk, morphological change and fluvial infrastructure development.

Discussion

Our analysis demonstrates that the integration of SWORD and FAM DEM has enabled river confinement quantification globally. Our data-driven classification into five river types is robust and can help in informing future research on river morphology classification and control. For example, future research pursuits can involve testing whether the degree of river confinement determines the number of channels in a river system, if the degree of channel braiding correlates with river gradient, whether river morphologies are spatially correlated with climate zones, and whether lateral channel migration is correlated with confinement slope.

This improved understanding will allow us to make much better predictions on how human interventions into a river's natural course will change its shape, thereby enhancing our ability to manage water resources, mitigate flood risks, and preserve ecological habitats more effectively.

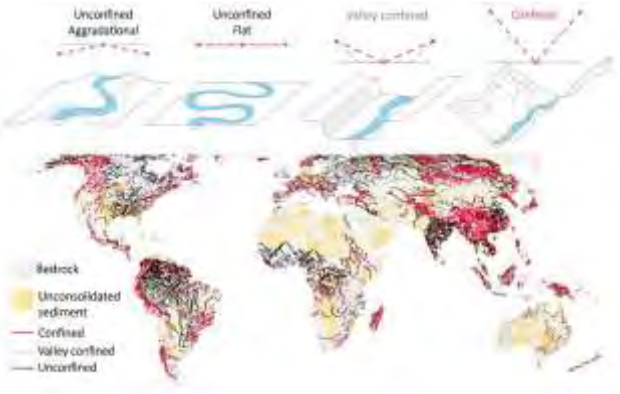

Figure 1: World map with mapped distribution of unconfined (black) valley confined (grey) and confined/entrenched (red).

References

[1] Altenau, E. H., Pavelsky, T. M., Durand, M. T., Yang, X., Frasson, R. P. D. M., & Bendezu, L. (2021). The Surface Water and Ocean Topography (SWOT) Mission River Database (SWORD): A global river network for satellite data products. Water Resources Research, 57(7), e2021WR030054.

[2] Hawker, L., & Neal, J. (2021). *FABDEM V1-0* [Data set]. doi:10.5523/BRIS.25WFY0F9UKOGE2GS7A5MQPQ2J7

[3] Fryirs, K. A., Wheaton, J. M., & Brierley, G. J. (2016). An approach for measuring confinement and assessing the influence of valley setting on river forms and processes. *Earth Surface Processes and Landforms*, *41*(5), 701–710. doi:10.1002/esp.3893

Role of Wind-Induced Currents in Sediment Resuspension and Transport in a Micro-Tidal Bay

Ho Kyung Ha[1], Chae Yeon Eun[2], Jun Young Seo[1,2], Sun Min Choi[1]
[1]Department of Ocean Sciences, Inha University, Incheon, Republic of Korea
[2]Department of Oceanography, Chonnam National University, Gwangju, Republic of Korea
Corresponding author: hahk@inha.ac.kr

Keywords: wind, residual current, sediment flux, resuspension, ADCP

1 Introduction

Coastal bays influence sediment dynamics by receiving and transporting sediments, organic matter, and contaminants from rivers. Their semi-enclosed nature can cause severe sedimentation, with resuspension driven by winds, currents, tides, and freshwater discharge. Wind significantly impacts hydrodynamics by altering current velocities, modifying vertical stratification, and driving alongshore currents and upwelling/downwelling. In micro-tidal environments, wind can dominate over tidal forces, reversing estuarine circulation and increasing landward sediment transport, which may carry contaminants. This study examines wind-induced sediment transport in Onsan Bay (Fig. 1), a heavily polluted "Special Management Coastal Zone," by analyzing residual currents and sediment fluxes.

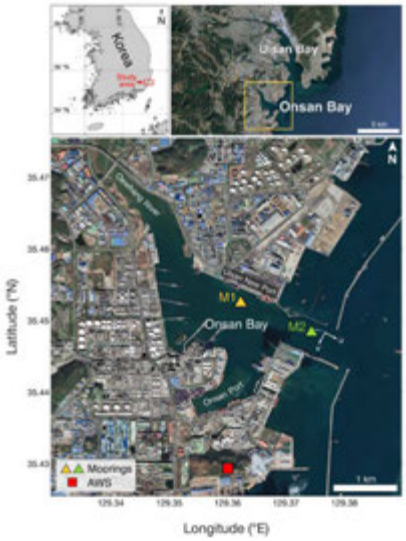

Figure 1: Map of the study area. The triangles indicate two ADCP mooring stations.

2 Materials and Methods

Two in-situ mooring systems (M1 and M2) were deployed on the eastern flank of the navigation channel, equipped with acoustic Doppler current profilers (ADCPs) to measure current velocities, water levels, temperature, and echo intensity at one-minute intervals. CTD and optical backscatter sensors were used to record temperature, salinity, turbidity, and suspended sediment concentration (SSC), with water samples collected and filtered to determine sediment mass. Wind and precipitation data were obtained from Onsan AWS, and wind stress was calculated using a standard equation, incorporating wind speed, air density, and drag coefficient. ADCP-derived SSC was estimated using sonar equations, with calibration coefficients determined via regression analysis, and SSC was decomposed into tidal and residual components to study sediment flux mechanisms. Suspended sediment fluxes and along-channel residual water transport were computed using tidal decomposition methods, with positive values indicating seaward transport and negative values representing landward transport.

3 Results

During the mooring period (four weeks in October–November 2022), the suspended sediments at both stations were transported seaward (landward) at the surface (bottom) layer mainly through the residual currents (mean-flow flux F_{mean}: > 70% of the total flux). Under northerly winds, the landward bottom residual currents at both stations strengthened, resulting in the “intensification” of landward F_{mean}. This suggests that the northerly winds might be a primary factor intensifying the landward sediment fluxes, potentially resulting in the increased sediment deposition into the bay. The findings provide insights into managing sedimentation in contaminated coastal bays and highlight the importance of wind effects on sediment transport in micro-tidal bays.

4 Conclusions

Residual currents in the bay followed classical estuarine circulation, driving suspended sediment transport mainly through residual currents (>70% of total flux). Wind forcing influenced current patterns, strengthening landward bottom flows under northerly winds and seaward surface flows under southerly winds. Northerly winds intensified landward sediment transport, increasing deposition of contaminated sediments in the bay.

Acknowledgments

This research was supported by Korea Institute of Marine Science and Technology Promotion (KIMST) and National Research Foundation of Korea (RS-2022-NR069113).

Observations of Spatio-Temporal Variations in Groyne Field Bathymetry

Eki Liptiay[1], Astrid Blom[1], Kees Sloff[1,2], Michiel Reneerkens[3], Wim Uijttewaal[1]

[1]Faculty of Civil Engineering and Geosciences, Delft University of Technology, Delft, The Netherlands
[2]Deltares, Delft, The Netherlands
[3]DG Rijkswaterstaat, Ministry of Infrastructure and Water Management, Utrecht, The Netherlands

e-mail corresponding author: e.j.a.liptiay@tudelft.nl

Keywords: *groyne fields; field observations; sediment fluxes*

1 Introduction

Groynes in rivers serve to protect their banks and to maintain sufficient navigable depth in the main channel. Between groynes, sediment deposition takes place, giving rise to groyne fields. Field experiments in the Waal River have shown that the morphological response between adjacent groyne fields can drastically differ: while one groyne field experiences aggradation, another can erode [1]. Furthermore, the changes in bed level within a groyne field vary considerably.

Little is known about such spatio-temporal variability within and between groyne fields. Knowledge about this variability is necessary to establish the reference dynamics of groyne field bathymetry, prior to interventions such as nourishments.

2 Methods

Our objective is to increase our understanding of the spatio-temporal variations of groyne field morphodynamics. To address the gaps in current research, a field campaign was launched that includes determination of the groyne field bathymetry for representative locations and conditions. We combine these new multibeam data with the existing data and analyse them, exploiting the high spatial resolution of the recent campaign.

3 Results and Discussion

As an example, we compare two subsequent periods of high discharge in which the groynes were submerged the entire time (Fig. 1a). Figs. 1b-c show field observations of the changes in groyne field bathymetry along a straight reach during respective periods A and B.

In both periods, bed level changes in the groyne field are smaller than in the main channel. However, we observe a substantial large variation in bed level changes within the groyne field. At the upstream groyne tip, sediment deposition is found followed by erosion further downstream and bed forms associated with the mixing layer during both periods. Small differences can be found when we compare the groyne field beaches, where we find erosion during period A and sedimentation during period B.

Further analyses of these observations of bathymetric data will enable us to gather a better understanding of the spatio-temporal variations also observed in earlier research.

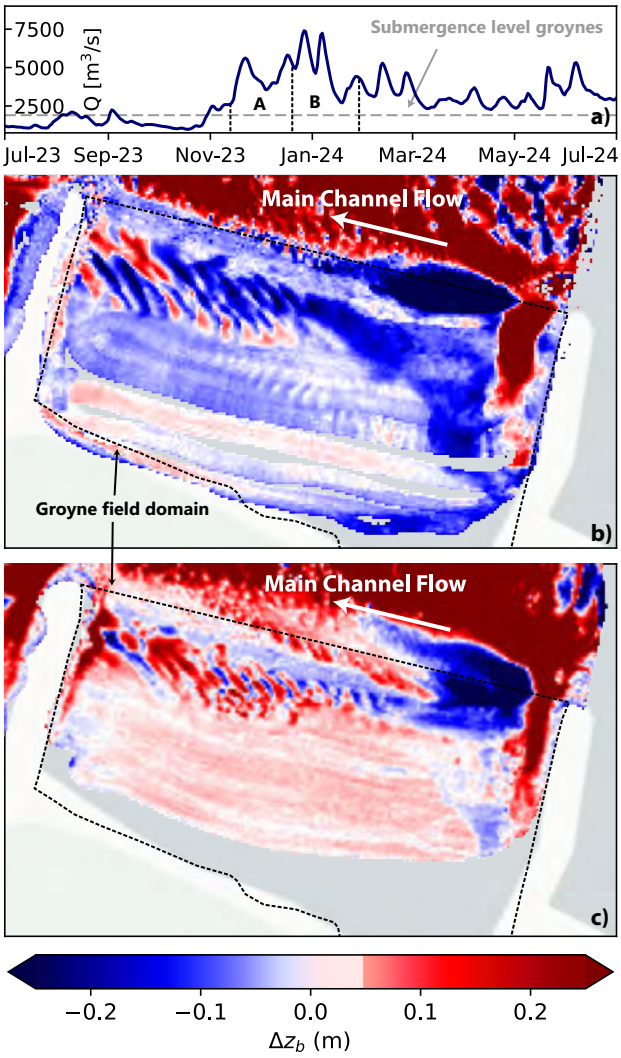

Figure 1: a) Hydrograph of the Rhine River at Lobith and observed bed level changes in the Waal branch between b) Nov-Dec 2023 (Period A) and c) Dec 2023-Jan 2024 (Period B). Changes are derived by subtracting the older bathymetry from the newer bathymetry.

References

[1] W. B. M. Ten Brinke. De sediment huishouding van kribvakken langs de Waal (in Dutch). Technical report, RIZA, Arnhem, 2003.

Comparison between shorelines derived from radar and multispectral satellite

Riccardo Angelini[1], Eduard Angelats[2], Fabiana di Ciaccio [1], Guido Luzi[2], Francesco Mugnai[1], Andrea Masiero [3], Francesca Ribas[4]

[1]University of Florence, Florence, Italy
[2]Centre Tecnològic de Telecomunicacions de Catalunya (CTTC/CERCA), Castelldefels, Spain
[3]University of Padua, Padua, Italy
[4]Universitat Politècnica de Catalunya, Barcelona, Spain

e-mail corresponding author: riccardo.angelini@unifi.it

Keywords: *shoreline extraction; remote sensing; radar; multispectral*

1 Introduction

Shoreline detection is crucial for coastal monitoring and management. Multispectral Satellite Imagery (MSI) has been widely used due to its high spatial resolution, but its dependence on atmospheric conditions limits its effectiveness. Synthetic Aperture Radar (SAR) imagery offers all-weather, day-and-night capabilities but suffers from noise and surface roughness effects. This study evaluates the accuracy of SAR- and MSI-derived shorelines from ESA satellite platforms (Sentinel-1 and Sentinel-2, 10 m pixel resolution) at two Mediterranean sandy beaches: Feniglia (FNG) (Italy) and the Southern Llobregat Delta (SLD) (Spain).

2 Dataset and Methodology

The dataset for SLD consisted of 8 S1 images and 7 S2 images, while for FNG Beach, the dataset included 2 S1 images and 3 S2 images. The shorelines used for validation were manually digitized from high-resolution orthomosaics (20 cm) provided by the respective regional authorities. The shoreline extraction methodology proposed in [1] for multispectral imagery was employed. The main steps involved image preprocessing (Figure 1a), the application of either fully automatic thresholding methods (Otsu) or clustering techniques (GMM and K-means) to separate water and land classes (Figure 1b), and the implementation of contour extraction algorithms (Figure 1c). Finally, validation was performed by computing the Mean Absolute Deviation (MAD) and Bias against the reference shorelines (Figure 1e). The core methodology remained the same for SAR images, but with two additional steps: denoising and outlier detection.

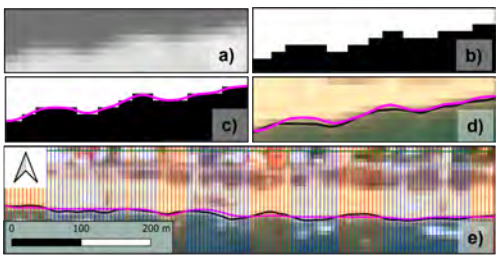

Figure 1: Main steps of shoreline extraction process.

3 Results

S1-derived shorelines at FNG achieved a MAD of about 4 m while S2-derived shorelines could reach even higher accuracies, up to 2 m (Table 1). At SLD, S1 accuracy varied from 6 m to 12 m. In this case, S2-derived shorelines clearly outperformed SAR methods, with a MAD of 4 m.

Ref Date	S1 date (days)	MAD S1 (m)	Bias S1 (m)	S2 date (days)	MAD (S2) (m)	Bias S2 (m)
19/07/19	1	3.9	-0.1	4	3.7	0.5
20/07/21	1	4.4	-0.4	2	2.1	0.9

Table 1: Best result in terms of MAD and Bias for S1 and S2 at FNG beach. Dates are given in days from the reference and errors in meters.

4 Conclusion

In this study, a very good level of accuracy was achieved for S2 imagery, up to subpixel error, comparable with benchmark studies, but being fully automatic. Obtained S1-derived shorelines had better accuracy than that in previous similar works [2], but worse than in the multispectral case. Future research will include expanding the available dataset and investigating the role of meteorological conditions on SAR images. Other satellites of higher resolution such as PlanetScope and TerraSAR-X are also being used. Combining data from both SAR and MSI platforms could optimize our shoreline extraction capabilities, ensuring both spatial accuracy with a better temporal resolution.

References

[1] R. Angelini, E. Angelats, G. Luzi, A. Masiero, G. Simarro, and F. Ribas. Development of methods for satellite shoreline detection and monitoring of megacusp undulations. *Remote Sens.*, 16 (23):4553, 2024.

[2] S. Zollini, D. Dominici, M. Alicandro, M. Cuevas-González, E. Angelats, F. Ribas, and G. Simarro. New methodology for shoreline extraction using optical and radar (SAR) satellite imagery. *J. Mar. Sci. Eng.*, 11(3):627, 2023.

Seasonal and interannual change of the extension of the Aiguillon Bay salt marsh.

Loës Le Goff Le Gourrierec[1,2], Xavier Bertin[1]
[1]LIENSs, La Rochelle, France
[2]CNES, Toulouse, France
Corresponding author: loes.le_goff_le_gourrierec@univ-lr.fr

Keywords: Remote sensing, Salt marsh, SCHISM

1 Introduction

Numerous studies have highlighted the multiple ecosystem services provided by salt marshes. Firstly, they act as a natural protection that mitigates the impact of coastal hazards [1]. Secondly, they play a significant role in capturing, sequestering, and storing greenhouse gases [2] and finally, they serve as essential habitats for a wide range of fauna. However, in the current context of global climate change and rising sea levels, studying their morphological evolution and adaptation potential is crucial. Nowadays, remote sensing tools allow us to study the evolution of these zones on different timescales (seasonal to multiannual) at high resolution.

2 Study site

The Aiguillon Bay, located on the French Atlantic Coast and crossed by the Sèvre Niortaise River, is bordered by a salt marsh (Figure 1a). This marsh expands laterally at an average rate of 8 m/year, leading to a surface area increase of 0.08 km^2/year from 1950 to 2020 [2]. This area is exposed to a semi-diurnal tidal regime with a maximum amplitude of 6.5 m. The sea state inside the bay is dominated by local wind-waves due to the shelter provided by the Ré Island. During winter, the site can experience energetic conditions during western storms.

3 Methods

To analyse the morphological evolution of this saltmarsh, we developed a semi-automated toolbox based on Sentinel-2 satellite imagery to monitor vegetated areas. In this study, we track the monthly evolution of the salt marsh since July 2017, analysing a total of 82 images. The method relies on NDWI processing to delineate the salt marsh/mudflat interface. Additionally, several airborne LiDAR surveys conducted by the Aiguillon Bay Nature Reserve, along with monthly drone-based photogrammetric surveys, were used to validate our detection method.

4 Results

Our results show an average annual increase of 0.094 km^2/year for the salt marsh between 2018 and 2025, which matches [2] and we also identify an accelerated growth in 2024 (Figure 1b). In addition to this upward trend, which probably corresponds to the spatial extension of persistent species (Obione, Spartina), we identify a seasonal variation around this trend. A spectral analysis of our time series reveals a peak period of 360 days (Figure 1c), which can be interpreted as the seasonal cycle of halophyte pioneer species (Salicornia).

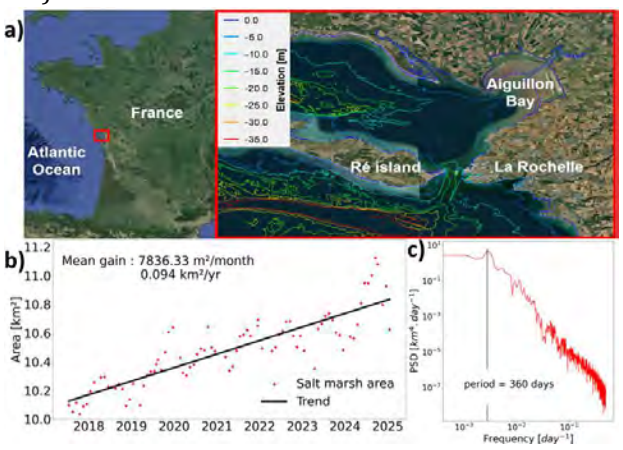

Figure 1: a) Aiguillon Bay on the French Atlantic coast. b) Salt marsh area evolution. c)PSD analysis.

5 Perspectives

In order to understand the origin of these patterns, we are implementing the coupled modelling system SCHISM, which fully couples a 3D circulation model, the spectral wave model WWMIII, the sediment transport model SED3D and the salt marsh model TMM as described by [3]. This modelling study will allow us to investigate the respective contribution of hydrodynamics, meteorology and sediment discharge for the surrounding rivers.

References

[1] Van Rooijen, A. A., McCall, R. T., Van Thiel de Vries, J. S. M., Van Dongeren, A. R., Reniers, A. J. H. M., & Roelvink, J. A. (2016). Modeling the effect of wave-vegetation interaction on wave setup. Journal of Geophysical Research: Oceans, 121(6), 4341-4359.

[2] Amann, B., Chaumillon, E., Schmidt, S., Olivier, L., Jupin, J., Perello, M. C., & Walsh, J. P. (2023). Multi-annual and multi-decadal evolution of sediment accretion in a saltmarsh of the French Atlantic coast: Implications for carbon sequestration. Estuarine, Coastal and Shelf Science, 293, 108467.

[3] Nunez, K., Zhang, Y. J., Bilkovic, D. M., & Hershner, C. (2021). Coastal setting determines tidal marsh sustainability with accelerating sea-level rise. *Ocean & Coastal Management*, *214*, 105898.

Sediment transport diffusion from a multi-scale perspective using DNS-DEM and stochastic models

Christian González[1], David Richter [2], Diogo Bolster [2], Joseph Calantoni[3], Cristián Escauriaza[4], Mark Schmeeckle[5]

[1]School of Civil Engineering, Universidad Diego Portales, Santiago, Chile
[2]Dept. of Civ. & Environ. Eng. & Earth Sci., University of Notre Dame, Notre Dame, IN, USA
[3]Naval Meteorology and Oceanography Command, Stennis Space Center, MS, USA
[4]Departamento de Ingeniería Hidráulica y Ambiental, Pontificia Universidad Católica de Chile, Santiago, Chile
[5]School of Geographical Sciences and Urban Planning, Arizona State University, Tempe, AZ, USA

e-mail corresponding author: christian.gonzalez@udp.cl

Keywords: *sediment transport; DNS-DEM simulations; Fickian/anomalous diffusion*

1 Introduction

Sediment transport in rivers and channels behaves as a diffusive process, with sediment particles dispersing downstream following Fickian or anomalous (superdiffusive/subdiffusive) dynamics. This behavior is governed by the temporal evolution of the variance σ^2 of the streamwise particle displacement $\mathfrak{X}$ (total distance traveled from a reference time):

$$\sigma^2_{\mathfrak{X}}(t) \propto t^{2\gamma} \tag{1}$$

where γ is a scaling exponent ($\gamma = 0.5$ for Fickian diffusion, $\gamma < 0.5$ for subdiffusion, $\gamma > 0.5$ for superdiffusion). Experimental studies reveal transitions between these diffusive regimes across different timescales (e.g. from superdiffusive to Fickian regime), aligning with the conceptual framework introduced by Nikora et al. [2]. Despite research efforts, the physical mechanisms behind diffusive regime transitions remain unclear. Understanding them is key to improving sediment transport modeling and predicting sediment dynamics.

2 Methodology

To investigate these mechanisms, we simulate sediment transport in a flat-bed channel using Direct Numerical Simulations (DNS) coupled with a Discrete Element Method (DEM) to model particle interactions (details in González et al. [1]). This two-way coupled approach accounts for particle collisions. From these simulations, we develop stochastic models calibrated with DNS-DEM results, incorporating advection-diffusion equations and autoregressive Markov models with Gaussian and non-Gaussian distributions. We analyze 8 cases spanning Shields numbers from 0.03 to 0.85, focusing on the temporal evolution of the mean, variance, skewness, and kurtosis of particle displacement $\mathfrak{X}$.

3 Results

Our findings indicate that sediment transport follows a ballistic regime at short timescales ($\gamma = 1$) and transitions toward a near-Fickian regime at larger timescales. Subdiffusion is also observed, particularly at low Shields numbers. However, the trends in variance, skewness, and kurtosis suggest an eventual convergence to Fickian behavior over extended timescales, with the rate of convergence dependent on the Shields number.

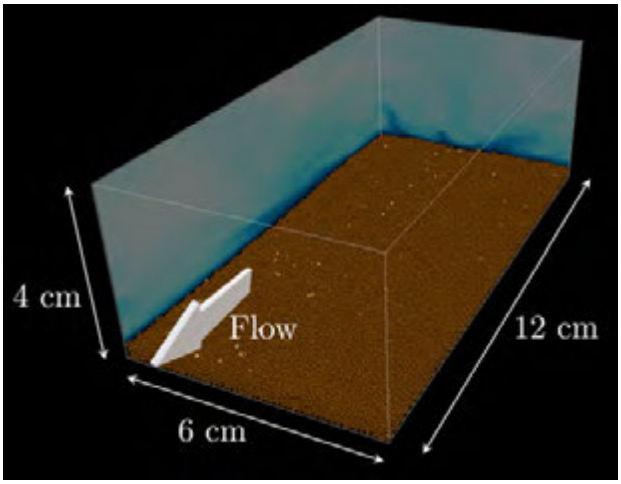

Figure 1: DNS-DEM simulation domain, whose results are used to calibrate stochastic models.

4 Conclusions

We identify particle inertia as the key factor governing the transition from ballistic to Fickian diffusion. This inertia is measured through particle motion correlation, enabling quantification of the relationship between regime transitions and the Shields number. Conversely, transitions to subdiffusive states cannot be attributed to particle inertia but are instead controlled by resting times.

Acknowledgements

CG acknowledges funding from FONDECYT-ANID grant No. 11251735

References

[1] C. González, D. Richter, D. Bolster, S. Bateman, J. Calantoni, and C. Escauriaza. Characterization of bedload intermittency near the threshold of motion using a lagrangian sediment transport model. *Environ. Fluid Mech.*, 17(1):111–137, 2017.

[2] V. Nikora, H. Habersack, T. Huber, and I. McEwan. On bed particle diffusion in gravel bed flows under weak bed load transport. *Water Resour. Res.*, 38(6):1081, 2002.

Analysis of Morphodynamics at the Mouth of Ebro River Delta

Calvillo, B.[1], Pavo-Fernández, E.[1], Puigdefabregas, J.[1], Grifoll, M.[1], Gracia, V.[1]
[1]Laboratori d'Enginyeria Marítima, Universitat Politècnica de Catalunya, Barcelona, Spain
Corresponding author: benjami.calvillo@upc.edu

Keywords: Morphology, Satellite-Derived Shoreline, Deltas, Estuaries

1 Introduction

Deltas stand out as one of the most vulnerable coastal environments to climate change and human pressure. The lack of sediment and the artificialization of discharge flow regimen due to the construction of dams along the river course, as well as the effects of climate change, make the monitoring of these deltaic environments essential. The Mediterranean deltas have suffered greatly from this lack of sediment contribution, which has increased erosion, as in the case of the Ebro River delta [1]. Recent studies show that the Ebro mouth is subject to erosion on its southern hemidelta and accretion on its northern side [2]. Since the end of 2022 until now, due to changes in the wave climate (i.e. decrease of waves from the E and increase of waves from the S) a salient has formed on the northern side of the Ebro's mouth, along with the emergence of a transversal bar. The objective of this study is to analyze the trend of the evolution of the coastline of the Ebro mouth, using high-resolution satellite images provided by Planet, using CoastSat.PlanetScope toolkit to extract the shoreline of the mouth and analyze the morphological changes of the Ebro mouth between 2016-2024, and characterize the correspondent hydrological and oceanographic conditions.

2 Materials and Methods

The coastline's evolution is analyzed using high-resolution satellite images supplied by Planet Labs from Planet satellites, which have a resolution of 3.5 m/pixel. One image per month has been selected, considering the best in terms of cloud coverage (<10%), from September 2016 to October 2024. The new open-source toolkit, CoastSat.PlanetScope was used for satellite-shoreline detection. To identify the coastline the toolkit applies the Weighted Peaks (WP) thresholding approach to the Near Infrared minus Blue (NmB) spectral index. This approach is the most accurate to extract the shoreline using PlanetScope images. For this study, hydromorphological data from the Ebro mouth (Figure 1) was also used, collected from field campaigns carried out between November 2023 and December 2024. The wave conditions were obtained from the Tarragona buoy, supported by Spanish Port Agency (*Puertos del Estado*).

3 Results

The results of the shoreline extraction of the study area are shown in Figure 1C. The trend in the Ebro mouth shows erosion on the southern side of the mouth and accretion on the northern side. In October 2022 a salient begins to form on the northern side and the mouth bar emerges in December 2022. Low flow conditions (i.e. 80 m3/s) occurred between July 2022 and November 2023, along with increases in the percentage of waves from the S and SW and decreases in the percentage of waves from the E and NE in 2023. The results of the Lagrangian buoy velocities indicated that the velocities in the eastwards shore of the river mouth are higher than northwards shore suggesting a shifting of the river flow eastwards.

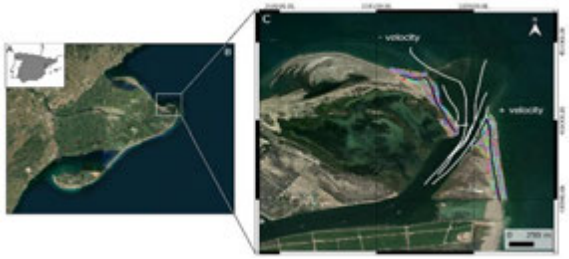

Figure 1. (A) Location of Ebro Delta in NW Mediterranean Sea. (B) Ebro Delta. (C) Shoreline evolution (2016-2024) with the black line indicating the current shoreline and white lines the Lagrangian buoy tracks.

4 Discussion and Conclusions

The analysis of the shorelines showed how the erosion of the southern side and the accretion of the northern side, align with the study of Aranda et al. (2015). The strong erosion of the Illa de Sant Antoni corresponds to the increase of sandy features in the Garxal. The erosion was accentuated from 2022 until 2024, which corresponds to the low discharge period of the Ebro River (2022-2023), as well as to a period of increasing S waves and decreasing E waves (2022 to 2024). These hydrological and oceanographic conditions allowed the formation of the salient and the emergence of the mouth bar. The results suggest how the main river channel discharge shifted from N to E, as velocities of Lagrangian buoys were higher at the E channel. The low discharge conditions of the Ebro River were not enough to keep the main river channel open, and the decrease of the E and NE waves contributed to the formation of sand forms in the Garxal.

Acknowledgments

This paper is funded by TED2021-129776B-C21 AEI/10.13039/501100011033/ Unión Europea NextGenerationEU/PRTR.

References

[1] J. A. Jiménez and A. Sánchez-Arcilla. Medium-term coastal response at the Ebro delta, Spain. *Marine Geology*, 114(1-2):105–118, 1993.

[2] M. Aranda García, F. J. Gracia Prieto, and I. Rodríguez-Santalla. Historical morphological changes (1956–2017) and future trends at the mouth of the Ebro River delta (NE Spain), 2022.

Morphological changes before and after neck cutoffs in meandering rivers

Kattia Rubi ARNEZ FERREL[1], Daisuke HARADA[2], Shinji EGASHIRA[2,3]
[1,2,3]International Centre for Water Hazard and Risk Management (ICHARM), Japan
Corresponding author: rubi@icharm.org

Keywords: neck cutoff, morphological changes, meanders, confluence

1 Introduction

Neck cutoffs significantly influence the morphology of meandering rivers by changing the channel slope, flow patterns, and erosion and deposition processes. Previous studies indicate that the effect of cutoffs extend downstream over distances proportional to the cutoff length with erosion rates increasing are increased by 25% post cutoffs [1]. In meandering channels with high sediment loads, the confluence location is influenced by meander neck cutoffs in the tributary channel [2]. This study investigates two cutoffs, each occurring in a different branch before a confluence in a meandering river. The first cutoff, located in the Sajta River, took place during the 2016-2017 rainy season, while the second, in the Ichilo River, is imminent (distance in the neck less than 10 m). The impacts of these two cutoffs on river morphology are particularly significant due to the proximity of a riverine community. The spatial distribution and extent of the effects of the future cutoff remain uncertain.

2 Methods

The Sajta River cutoff was investigated using satellite imagery by extracting the changes in the banklines pre and post cutoff through Google Earth Engine [3]. For the cutoff in the Ichilo River, we applied a 2D-depth-averaged numerical model to simulate bed elevation changes and bank evolution.

3 Preliminary results

Cutoff in the Sajta river (2016): Satellite imagery analysis of the Sajta River (Figure 1) reveals a gradual progression driven by bank erosion on both sides of the bank primarily occurring during the rainy season. The cutoff took place between the late 2016 and early 2017. A point bar formed downstream of the location of the neck cutoff, and new meander developed, gradually increasing in size. Vegetation was observed in the point bar, potentially promoting the stabilization of the bar. Over time, the bar migrated downstream, leading to the formation of a second point bar near the confluence. As the second point bar stabilized, erosion occurred along the left riverbank. The oxbow lake formed by the cutoff remained connected to the river and continued to flood during high discharge events, enhancing sedimentation within the oxbow lake. Planform changes following the cutoff resulted in a shift in the confluence angle from obtuse to acute. This change in the angle of the confluence may significantly influence confluence hydrodynamics.

Cutoff in the Ichilo river (ongoing) This ongoing cutoff has been closely monitored since 2019 [4] and is currently being investigated through numerical simulations to asses bed elevation changes and bank evolution, these simulations are still in progress and will provide further insights in the morphological adjustments expected after the cutoff occurs.

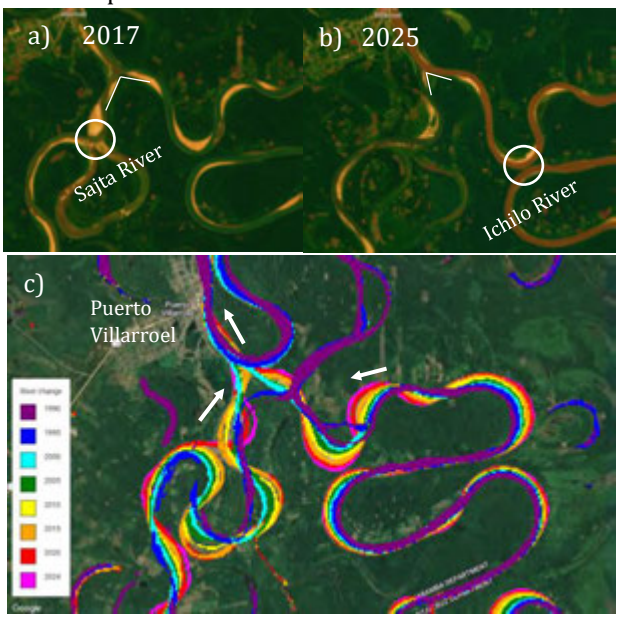

Figure 1. a, b) Change in the angle of the confluence after cutoff occurrence in the Sajta River, c) Planform evolution of the confluence between the Sajta and Ichilo Rivers in Puerto Villarroel, Bolivia (1990-2024) [3].

4 Conclusions

The preliminary results of this investigation provide insights into the morphological changes of the Ichilo River before and after the occurrence of cutoffs. Satellite imagery analysis revealed that the angle of the confluence changed from obtuse to acute following the cutoff occurred in the Sajta River in 2016.

References

[1] Jon Schwenk et al. Meander cutoffs nonlocally accelerate upstream and downstream migration and channel widening. *Geophysical Research Letters* Volume 43, Issue 24 p. 12,437-12,445, 2016.
[2] D.J. Simon et al. The planform mobility of river channel confluences: insights from analysis of remotely sensed imagery Earth *Sci. Rev.*, 176, pp. 1-18, 10.1016/j.earscirev.2017.09.009, 2018.
[3] Mapping River Change 1990 - 2020 with Earth Engine https://code.earthengine.google.com/d2c1197bbb9ab90af6b4f1a30d3fd527
[4] Arnez et al. Past, present and future of a meandering river in the Bolivian Amazon basin, *J. of Earth Surface Processes and Landforms*/ Volume 4. https://doi.org/10.1002/esp.5058, 2020.

Sediment Fluxes over Sand Deposits at Fire Island Shelf, New York

B. Umut Ayhan[1], M. Said Parlak[1], Tarandeep Kalra[2], Ilgar Safak[1]
[1]Istanbul Bilgi University, Türkiye
[2] Woods Hole Group, Woods Hole, MA, USA
Corresponding author: umut.ayhan@bilgi.edu.tr

Keywords: coastal morphodynamics, sand ridges, bedload fluxes, sediment transport, flow circulation

1 Introduction

Water exchange along and across the continental shelf and shoreline regulates sediment budget and morphodynamic evolution. In spite of extensive efforts to simulate these processes to forecast sediment exchange between the inner shelf and nearshore and resulting coastal morphodynamics, unknowns and uncertainties remain, especially in terms of the impacts of shelf bathymetry on cross-shore fluxes. Therefore, in this study, a comprehensive three-month-long field experiment and numerical modeling were conducted to investigate the complex hydrodynamics and morphodynamics off Fire Island, New York, USA. Fire Island Shelf is well-suited for this research due to its extensive and unique bathymetric features, particularly the shoreface-connected sand ridges (SFCR) off the western part of the Island.

2 Method

Following the in-depth analysis of the field data set, flow circulation, waves, and sediment processes were simulated using a numerical model that incorporates all relevant and realistic physics, forcings, and bathymetry. Addressing the gaps in the previous efforts [1, 2], the model is capable of accounting for also the impacts of skewed and asymmetric wave shapes that contribute to cross-shore bedload fluxes. Subsequently, the analysis of the data and model results included the evaluation of spatial and temporal variations of bedload fluxes under different forcing conditions and over the bathymetric features, i.e., SFCR.

3 Results

The hydrodynamic processes including the three-dimensional stratified flow field and the wave characteristics were satisfactorily reconstructed in the model [1]. The impacts of SFCR, particularly on the bedload fluxes, were further investigated to better understand the morphodynamic evolution mechanisms. In a preliminary analysis, accordingly, cross-shore bedload fluxes across two isobaths were extracted: 12-m-isobath where the SFCR is most apparent and 7-m-isobath which is relatively straight along the shoreline (Figure 1a). The preliminary results of time-integration of these fluxes over the experiment period suggest that SFCR may impact cross-shore fluxes at not only the SFCR locations but also the onshore region all the way to the shoreline. (Figure 1b).

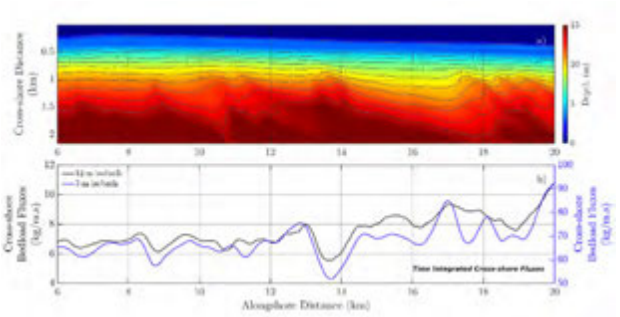

Figure 1: (a) The bathymetry of the nearshore and SFCR regions off Fire Island; (b) alongshore variations of time-integrated cross-shore bedload fluxes across the 7-m and 12-m isobaths.

4 Ongoing Work

The ongoing work is focusing on: i) the analysis of SONAR data to validate the model in terms of bedload fluxes; ii) long-term simulations to further assess the link between the SFCR and shoreline evolution.

Acknowledgments

Computing resources used in this work were provided by the National Center for High Performance Computing of Türkiye (UHeM) under grant number 1011242021.

References

[1] Parlak, M. S., Ayhan, B. U., Warner, J. C., Kalra, T. S., & Safak, I. (2023). Wave asymmetry impacts on sediment processes at the nearshore of Fire Island, New York. In *Coastal Sediments 2023: The Proceedings of the Coastal Sediments 2023* (pp. 1896-1901).

[2] Safak, I., List, J. H., Warner, J. C., & Schwab, W. C. (2017). Persistent shoreline shape induced from offshore geologic framework: Effects of shoreface connected ridges. *Journal of Geophysical Research: Oceans*, *122*(11), 8721-8738.

The Natural Rhythm of Estuaries

Marloes Bonenkamp[1], Anne Baar[1], Joep Storms[1], Jaap Nienhuis[2]
[1]Delft University of Technology, Delft, The Netherlands
[2]Utrecht University, Utrecht, The Netherlands
Corresponding author: m.bonenkamp@tudelft.nl

Keywords: estuaries, morphodynamics, global, Delft3D, remote sensing

1 Background

Estuaries are highly dynamic landscapes shaped by processes that are impacted by natural and anthropogenic factors. Changes in tidal prism, river discharge and sediment supply, will impact sediment dynamics, channel dimensions and water levels, ultimately influencing the long-term morphodynamic evolution. Estuaries across the globe will respond differently to these changes, due to the unique combination between environmental drivers and internal processes, such as basin geometry, sediment characteristics, and ecology.

In this research we will investigate the effect of river discharge variability and intermittency on estuarine morphology. While constant discharge conditions are often used in models [4], the effect of extreme events on long-term morphology remains poorly understood. Numerical morphodynamic models such as Delft3D are a useful tool simulate discharge variability and its effect on morphodynamic feedbacks over decadal to centennial timescales [1]. However, simulation outcomes are hard to validate. Recent global datasets of estuaries [2, 3] offer this opportunity. By expanding observations, the influence of local conditions can be reduced and general estuary behaviour can be further explained with numerical models.

2 Methods

This study integrates idealised Delft3D morphodynamic model simulations [1] with global datasets to investigate how discharge peaks and intermittency influence estuarine morphology. Using an idealised Delft3D estuary model setup, we study: (1) What role do extreme discharge events play in shaping estuarine morphology compared to average conditions? (2) How do estuaries with varying size respond differently to discharge peaks and intermittency? To this end, we developed model scenarios that systematically vary peak discharge relative to the mean annual discharge, return intervals, and estuary dimensions. The simulations will then be compared with observational data, to disentangle the effects of extreme events from long-term trends.

3 Expected outcomes / Future research

Our Delft3D simulation results are expected to reveal critical thresholds in discharge peak and intermittency that trigger feedback mechanisms, altering the rate and direction of estuarine morphodynamics. These thresholds, likely varying with estuary size, will provide insights into estuarine adaptation rates to natural variability and future changes in river discharge, improving understanding of estuarine resilience.

The next phase of the research will focus on conducting a data analysis of estuaries worldwide. This aims to classify estuaries into distinct categories based on their characteristics (e.g. fluvial discharge, tidal range, sediment type) and observed morphological changes, (e.g. slope and width). By systematically grouping estuaries, real-world changes can be linked to results of idealised Delft3D model scenarios, attributing specific morphological changes to the underlying processes and drivers. Integrating global data with numerical modelling capabilities will enhance understanding of estuarine dynamics and improve predictions of how these critical ecosystems adapt to environmental changes.

References

[1] A. W. Baar, L. Braat, and D. R. Parsons. Control of river discharge on large-scale estuary morphology. *Earth Surface Processes and Landforms*, 48(3):489–503, 2023.

[2] J.H. Nienhuis, A.J.F. Hoitink, and T.E. Törnqvist. Future change to tide-influenced deltas. *Geophysical Research Letters*, 45(8):3499-3507, 2018.

[3] J.H. Nienhuis, A.D. Ashton, and D.A. Edmonds. Global-scale human impact on delta morphology has led to net land area gain. *Nature* 577:514–518, 2020.

[4] J.R. Leuven, H. J. Pierik, M. V. D. Vegt, T. J. Bouma, and M.G. Kleinhans. Sea-level-rise-induced threats depend on the size of tide-influenced estuaries worldwide. *Nature Climate Change*, 9(12):986-992, 2019.

Sediment transport modelling to inform river restoration design on a wandering gravel-bed river in Britain

Samuel Watkiss[1], Kate Bradbrook[1] [1]JBA Consulting, North Yorkshire
Corresponding author: samuel.watkiss@jbaconsulting.com
Keywords: sediment transport modelling, fluvial geomorphology, river restoration, HEC-RAS

1 Introduction

Commercial gravel extraction during the 1900's on a dynamic, wandering gravel bed river, has caused up to 9m of channel incision, degrading the fluvial geomorphological character of the river along significant lengths to be a single thread, confined system, dominated by transportational processes [1]. This study focuses upon a large concrete ford with an up to downstream head difference of 3m and associated check weirs on the river, acting to control further channel incision upstream. An ambitious river restoration design project aims to remove the ford and weirs and re-establish the wandering morphological character of the river on the single thread 300m approach to the ford. Further upstream, the river retains much of its wandering character – the ford and weirs act to control further incision. A 2D HEC-RAS sediment transport model has been developed to assess the ability of the restoration design to achieve this aim and critically, to identify design risks, such as further channel incision. Model development highlighted significant sensitivity to selected sediment transport parameters. Appropriate testing and selection of model parameters has enabled the production of an effective tool which represents observed existing patterns of erosion and deposition. This has supported confidence in restoration design scenario modelling results, enabling the establishment of a design that supports dynamic patterns of erosion and deposition, even during extreme modelled events.

2 River Restoration design aims

The aim of this large-scale river restoration project is ultimately to re-establish the rivers dynamic, wandering morphological character on the 300m approach to the ford.

The designs which have been developed include ford and check weir removal, regrading the longitudinal bed profile, excavating a major inset floodplain and constructing a network of initial braided channels and gravel islands. The designs must achieve the restoration aims, whilst mitigating risks of the channel returning to an incised channel. The Water Framework Directive drives the scheme, aiming to improve the waterbody's ecological and hydromorphological classification.

3 Sediment transport model approach

A 2D HEC-RAS sediment transport model has been developed to assess the design's ability to re-establish dynamic, wandering gravel bed river forms and processes and to identify key design risks. Aims of modelling are not to provide precise predictions of channel evolution, but to indicate the risk of channel incision, or development of long-term dynamic wandering.

Model bed sediment gradation data utilises sampled surface bed sediment. The 2D terrain model utilises 0.3m drone surveyed LiDAR data within the channel, merged into wider 1m LiDAR data. Sediment transport parameters have been selected using HEC-RAS guidance and tested to represent observed patterns of erosion and deposition. Parameter testing has identified that erosion and deposition results present significant sensitivity to selected parameters, such as the sediment transport function and dynamic roughness.

4 Results and current project stage

Early design stage modelling indicated risk of channel incision occurring following construction, with flow eroding a preferential channel and uniform over-bank flow. This necessitated increasing the excavated floodplain width to reduce confinement, and kick-starting wandering forms and processes with the construction of a braided channel network and island features.

Bed erosion and deposition results following a 0.5% Annual Event Probability (AEP) for the current design scenario are presented within Figure 1. Sinuous patterns of erosion across the re-connected floodplain provide evidence that wandering channels with depositional bars and islands develop – these forms are indicative of existing wandering reaches modelled further upstream, aiding model validation. Results give confidence in the dynamic stability of the design during extreme events, enabling the design to be progressed and further investigated.

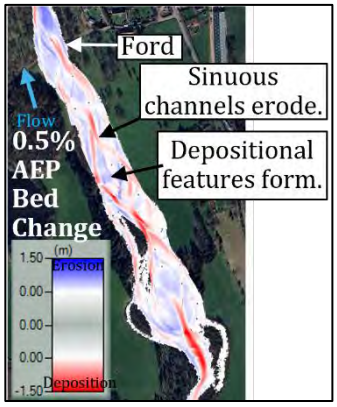

Figure 1: Restoration design, bed change, 0.5% AEP

References

[1] D. A. Sear and D. R. Archer. Effects of gravel extraction on stability of gravel-bed rivers: the Wooler Water, Northumberland, UK. In *Gravel-bed rivers in the Environment*; Klingeman, P.C., Beschta, R.L., Komar, P.D., Bradley, J.B., Eds.; Water Resources Publication: Highlands Ranch, CO, USA, 1998; pp. 415–432.

Study of cliff ridge recession due to wind-induced waves in Port Foster (Deception Island, Antarctica)

Óscar A. Caballero-Martínez[1,2], Carlos Paredes[3], Alejandro Román[4], Gabriel Navarro[4], Manuel Díez-Minguito[1,2]

[1]Environmental Fluid Dynamics Group. Andalusian Institute for Earth System Research, Granada, Spain
[2]Department of Structural Mechanics and Hydraulics Engineering, University of Granada, Spain
[3]Department of Geological and Mining Engineering, Technical University of Madrid, Spain
[4]Department of Ecology and Coastal Management, Institute of Marine Sciences of Andalusia (ICMAN), Spanish National Research Council (CSIC), Calle República Saharaui, 4, Puerto Real, Spain

e-mail corresponding author: oacm0001@ugr.es

Keywords: *Sediment transport, Wind-waves, Satellite and UAV Imagery, Antarctica, Port Foster*

1 Introduction

Deception Island (DI), part of the South Shetland Islands, is a 14 km wide volcanic island with a horseshoe shape, forming the semi-enclosed Port Foster (PF). It hosts two scientific bases: the Spanish "Gabriel de Castilla" and Argentinean "Decepción".

Recent years have seen coastal erosion along various stretches, influenced by ice sheet changes, waves, permafrost degradation, and sea level variations [2]. Affected areas include the coast near the base of Gabriel de Castilla, where mitigation measures such as gabion walls have been implemented.

2 Objectives

The main objective of this work is to analyze the effect of erosion on a cliff ridge between the two scientific bases due to wind-driven waves in both normal and extreme wave regimes. Changes in coastline are analyzed using a combined approach of telemetry imagery and sediment transport along the coast, and correlated with the recession rates and velocities that have been registered on the cliff ridge from 1956.

3 Methodology

In order to address this study, the significant wave height was calculated through 1.4 km of coastline each 25 m using wind data from the AEMET weather station. The wind that affects the study area has been studied according to its direction of origin in sectors of 15°. A comparison was made between significant calculated waves and measurements from a buoy from the DICHOSO project located in front of the Spanish base, considering the wind direction from east (0°) to north-west (135°), in order to know if there is a good correlation of the data. The directional wave climate was then propagated to the coast, considering the effects of shoaling, reflection, refraction, and diffraction. Once the significant wave height is propagated, the long-shore sediment transport can be calculated with the CERC equation [1]. Finally, a study of the historical erosion of the cliff ridge was performed using telemetry and satellite imagery of the study area.

4 Results and conclusions

Wind-induced waves are generally low, staying below 30 cm under normal $5\,\mathrm{m}\cdot\mathrm{s}^{-1}$ winds, while gusts of $12\,\mathrm{m}\cdot\mathrm{s}^{-1}$ can generate waves over 70 cm. Wave heights remain limited due to the basin's geometry restricting fetch. The small beach slope minimizes refraction and diffraction effects. Predominant winds from southwest to northeast do not affect the study area. Calculated and measured wave data show good correlation in both directions and magnitudes.

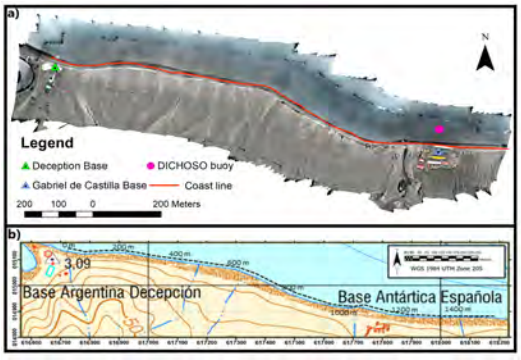

Figure 1: Location of the study area. Panel a shows the orthomosaic of the cliff between the two scientific bases and the buoy in front of the Spanish base, while Panel b shows a map of the same place from the National Geographic Institute (IGN)

Potential longshore sediment transport near the base ranges from $5,\mathrm{m}^3\cdot\mathrm{yr}^{-1}$ to $1000,\mathrm{m}^3\cdot\mathrm{yr}^{-1}$, depending on wave heights (0.11–$0.32,\mathrm{m}\cdot\mathrm{s}^{-1}$) and fetch distances ($4.5$–$6.3,\mathrm{km}$). Variations in coastal inclination drive differences in transport, affecting erosion and sediment deposition.

References

[1] U.S. Army Corps of Engineers. *Shore Protection Manual*, volume 1 and 2. Coastal Engineering Research Center (CERC), Waterways Experiment Station, Vicksburg, MS, 1984.

[2] Carlos Paredes, Javier Gonzalez-Posada, Rogelio De la Vega-Panizo, and Miguel Ropero. Spatiotemporal dynamic complexity of gully erosion in an antarctic periglacial shore environment: Foster bay, deception island (south shetlands). *SSRN Electronic Journal*, 01 2022. doi: 10.2139/ssrn.4064812.

An experimental study of flow through spatially heterogeneous arrays of emergent cylinders: the case of Arundo Donax

LOC-RCEM2025[1], A. Prats[2], C. Ferrer Boix[2], J.P. Martín-Vide[2]
[1]Universitat Politècnica de Catalunya, Barcelona, Spain
[2]Department of Civil and Enviromental Engineering, Technical University of Catalonia, Barcelona, Spain
Corresponding author: arnau.prats@upc.edu

Keywords: Vegetation, Drag, Momentum equation, Nonuniform distribution of stems, Double Averaged Method

1 Introduction

Arundo Donax (common name giant reed) is an invasive plant that provokes many negative effects in Mediterranean climate regions. Over there, the plant colonizes riparian areas of multiple streams, and the high obstruction of the stands leads to a flow resistance and flood risk increase.

The main objective of this study is to obtain the drag coefficient of Arundo Donax's stands. This coefficient is necessary to calculate the drag force of obstacles and also flow resistance coefficients. Due to the large size of the plant (6 m tall), this scientific research was conducted in a laboratory flume where a physical model was installed.

2 Methods

3.1 Field work

A harvest of an Arundo Donax stand was carried out along the Llobregat river channel (close to Barcelona) to obtain the characteristics of the reeds. The average diameter of the stems is 2.7 cm and the spatial density is 23 stems/m^2. However, the most interesting aspect is that the stems are distributed in a very heterogeneous pattern: there is a maximum of 78 stems/m^2 and a minimum of 4.

3.2 Experimental campaign

Laboratory experiments were performed in a 31 m long, 0.58 m wide flume. It was decided to study the situation of emergent vegetation (water depth is lower than plants height). Two reasons make flow through emergent vegetation easier to study than through submerged vegetation in a flume: there is no need to reproduce the bending of the stems, and the only obstacle to the flow is the cylindrical stem (the leaves appear only in the upper part). The stems were represented using steel cylinders of diameter 3.4 mm, resulting in a model scale of 8.

To determine the effect that an heterogeneous distribution of obstacles has on a flow, two models were built: one with obstacles distributed in a staggered array (homogeneous model), and another with obstacles distributed using the pattern measured in the field (heterogeneous model). Both models have the same number of obstacles and the flume width is totally vegetated. For each model, four different tests were conducted changing the water level at the flume outlet, always maintaining the same discharge, thus varying the velocity. The free surface longitudinal profile was measured using a rule, and velocity profiles using an ADV device. Measurements with ADV were taken in two measuring gaps covering the full section, separated 1 m in the longitudinal direction in order to obtain longitudinal gradients.

The Double-Averaged Method [1] was applied to analyse the flow. This method involves temporal and spatial decomposition of the variables. For the spatial decomposition, five velocity profiles were measured, spaced 0.5 cm apart in the transverse direction. In the homogeneous model, the profiles were measured at the central part of the measuring gaps. However, in the heterogeneous model measurements were also taken in two additional areas to calculate the transverse gradients. Reynolds and dispersive stresses were computed using temporal and spatial velocity fluctuations, respectively. The momentum balance was computed using the Double-Average Navier-Stokes equation.

3 Results

No significant differences are observed in the Reynolds stress values between the two models. However, the dispersive stresses are higher in the heterogeneous model, ranging from 1.5 to 7 times greater than in the homogeneous model. Nevertheless, the dispersive stresses are an order of magnitude lower than the Reynolds stresses.

The mean drag coefficient is 1.34 for the homogeneous model and 1.06 for the heterogeneous model. These values fall within the range established in the state of the art for the considered spatial density and flow velocity. The lower value in the heterogeneous model suggests that Arundo Donax's stems experience a smaller drag force compared to if they were arranged homogeneously.

Acknowledgments

We would like to thank the Urban River Lab for allowing us to use their canal for this experimental research.

References

[1] V. Nikora et.al. Double-Averaging concepts for rough-bed open channel and overlanf flows: Theoreticak background. Journal ofHydraulic Engineering 133(8): 873-883, 2007

Longshore Sediment Transport deduced from Accumulation at a Jetty Using Satellite Imagery

Jacqueline Santos[1,2,3], Susana Costas[1], Rui Taborda[2]
[1]Center for Marine and Environemental Research, University of Algarve, Faro, Portugal
[2] Instituto Dom Luiz, Faculty of Sciences, University of Lisbon, Lisbon, Portugal
[3]Portuguese Institute for Sea and Atmosphere, Tavira, Portugal
Corresponding author: jacsantos@ualg.pt

Keywords: satellite derived shorelines, Landsat, jetties, sediment accumulation

1 Introduction

Sediment accumulation around coastal structures like jetties provides insights into local sediment dynamics. Traditional studies frequently lack sufficient temporal resolution due to constraints in data availability, but satellite remote sensing now enables long-term shoreline monitoring at high spatial and temporal resolutions [1]. This study analyses 40 years of satellite-derived shoreline (SDS) data to assess sediment accumulation around the updrift Tavira Jetty and determine longshore sediment transport.

2 Methods

The CoastSat Python toolkit [2] was used to derive satellite-based shorelines (SDS) and estimate annual coastal changes in Tavira Barrier Island, Portugal, using Landsat imagery (1984-2024). Shoreline trends were assessed using 33 transects at 100-meter intervals near the updrift Tavira jetty. Sediment accumulation was estimated by analysing changes in beach width (vegetation line to shoreline). Sediment volume was estimated considering a closure depth of 6.0 m below mean sea-level [3] and a berm crest height of 2.0 m above mean sea-level.

3 Results and Discussion

This study shows significant sediment accumulation near Tavira Jetty, particularly until 2000, following its construction in 1977 (Figure 1). By 2000, the area near the jetty reached sediment saturation threshold causing expansion of the accumulation zone in the updrift direction, a trend that persisted through 2010. In the 2011-2024 period, erosion was observed near the jetty, likely influenced by wave interference with the structure, impacting the adjacent shoreline.

Sediment volume estimates align with those reported in the literature for the area [4], demonstrating the effectiveness of SDS in estimating sediment volume, providing a high-frequency, long-term perspective on coastal dynamics. By capturing shoreline changes over decades, this approach offers valuable insights for coastal management and future monitoring efforts.

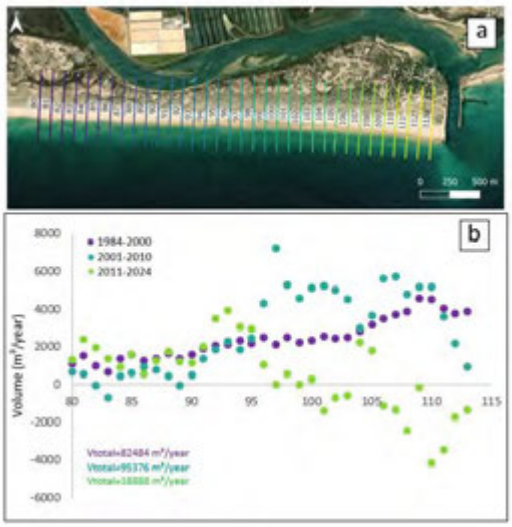

Figure 1: (a) Transects location. (b)Volume accumulation across the profiles 80 to 113 across three periods.

Acknowledgments

This work was funded by FCT, Ref. 2023.03101, and is a contribution of Coastal Resilience Remote Sensing Monitoring Project funded by FCT - Portuguese Foundation for Science and Technology Reference 2022.05392.PTDC, doi: https://doi.org/10.54499/2022.05392.PTDC.

References

[1] Vitousek, S., Buscombe, D., Vos, K., Barnard, P. L., Ritchie, A. C., & Warrick, J. A. (2023). The future of coastal monitoring through satellite remote sensing. *Cambridge Prisms: Coastal Futures*, 1, e10.

[2] Vos, K., Splinter, K. D., Harley, M. D., Simmons, J. A., & Turner, I. L. (2019). CoastSat: A Google Earth Engine-enabled Python toolkit to extract shorelines from publicly available satellite imagery. *Environmental Modelling & Software*, 122, 104528.

[3] López-Dóriga, U., & Ferreira, Ó. (2017). Longshore and cross-shore morphological variability of a berm–bar system under low to moderate wave energy. *Journal of Coastal Research*, *33*(5), 1161-1171.

[4] Santos, F. D., Lopes, A. M., Moniz, G., Ramos, L., & Taborda, R. (2014). Gestão da Zona Costeira. O desafio da mudança. Relatório do Grupo de Trabalho do Litoral. Lisbon, Portugal.

Dynamic Equilibrium in the Tisza River: A Long-Term Assessment of Post-Regulation Changes

Gergely T. Török[1], Sándor Baranya[1], György Sipos[2], Tímea Kiss[3]
[1]Department of Hydraulic and Water Resources Engineering, Budapest University of Technology and Economics, Budapest, Hungary
[2]Department of Physical and Environmental Geography, University of Szeged
[3]Independent researcher
Corresponding author: torok.gergely@emk.bme.hu

Keywords: dynamic equilibrium, bankfull Shields number, post-regulation assessment

1 Introduction

The Tisza River was originally a meandering, sandy-bed river in Central Europe. Extensive mid-19th-century regulations cut off 112 meanders, including 25 in the studied reach, shortening the river by 37% (studied reach: by 40%) and nearly doubling its slope (Figure 1). Between 1930 and 1960, accelerated channel migration threatened artificial levees, leading to widespread revetment construction. Today, over half of the banks are stabilized, but 58% of the revetments have begun to collapse, causing renewed bank erosion [1].

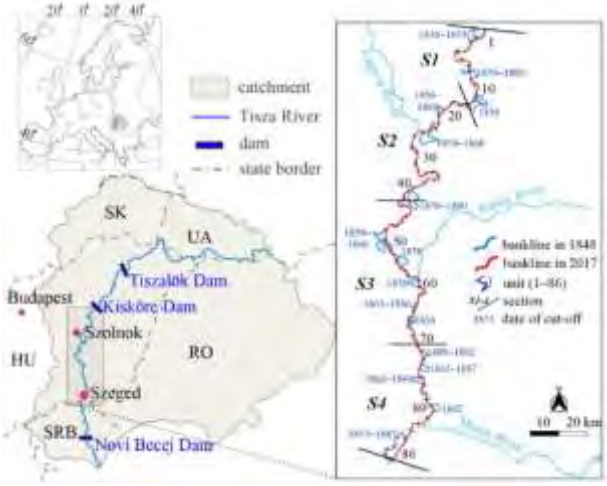

Figure 1: The studied section of the Tisza River, and the location and year of artificial cut-offs [1]

2 Goals and methods

The study aimed to evaluate the equilibrium state of the river. The question is whether the morphological processes induced by human interventions have stabilized the system, resulting in a new dynamic equilibrium, or further significant channel changes could be expected. We have analysed the changes in riverbed and bank elevation, channel depth and width, and slope (S) using cross-sectional data from 1890 (post-regulation), 1930, 1976, and 2017. The bankfull Shields number (τ_{bf}^*) was calculated. To assess the establishment of equilibrium conditions, the relationship proposed by Li et al. [2] was applied:

$$\frac{\tau_{bf}^*}{S^{0.53}} = 1220(D^*)^{-1} \qquad (1)$$

where D^* is the dimensionless grain size.

Supposing that the bed material (D^*) remained essentially the same [1], the values given by the left side of Equation 1 should remain nearly constant in the presence of dynamic equilibrium.

3 Conclusions

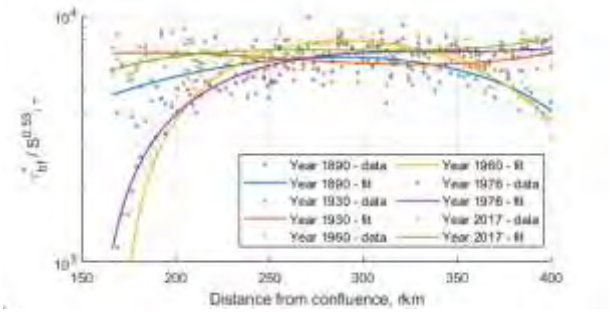

Figure 2: The ratio of $\tau_{bf}^*/S^{0.53}$ along the studied reach for different years. Continuous lines represent curves fitted to the data points.

Based on the results (Figure 2), the river did not exhibit equilibrium conditions immediately after the artificial cutoffs (blue line). By 1930 (orange line), a near-equilibrium state had developed. However, subsequent river engineering works between 1930 and 1960 disrupted this stability, leading to significant instability in 1960 (yellow line) and 1976 (purple line). Recently (2017: green line), the river has approached a near-equilibrium state once again.

References

[1] Kiss, T., Tóth, M., Török, G. T., & Sipos, G. (2024). Reconstruction of a Long-Term, Reach-Scale Sediment Budget Using Lateral Channel Movement Data as a Proxy: A Case Study on the Lowland Section of the Tisza River, Hungary. *Hydrology*, *11*(5), 67

[2] Li, C.; Czapiga, M. J.; Eke, E. C.; Viparelli, E.; Parker, G. (2014): Variable Shields number model for river bankfull geometry: bankfull shear velocity is viscosity-dependent but grain size-independent. *Journal of Hydraulic Research 53 (1),* 36-48.

Fine sediment modelling at the catchment scale in Alpine streams

Michele Combatti[1], Walter Bertoldi[1], Guido Zolezzi[1], Marco Tubino[1]

[1]Department of Civil, Environmental and Mechanical Engineering, University of Trento, Italy

e-mail corresponding author: michele.combatti@unitn.it

Keywords: *sediment transport; suspended load; Alpine rivers; basin-scale model*

1 Introduction

Various socio-economic and environmental implications are associated with the transport of fine-sediment in river networks, spanning from the loss of water storage capacity due to sedimentation in reservoirs to the impact of sediment laden flow on river ecosystems. In general, fluvial fine-material is mobilized and transferred downstream as suspended load or washload, depending on sediment grain size and flow intensity. A common approach is to assume that the bed material load, either bedload or suspended load, depends on local flow characteristics, which is not the case of fine-sediment load, particularly in mountain streams [1]. Most of the fine-sediment mass originates from upper bare areas of the catchment and is delivered downstream with a minimal exchange with the bed, except where the flow speed undergoes rapid variations, which in high-gradient reaches are frequently associated with natural (geomorphic) or artificial (man-made) discontinuities. This study aims to propose a basin-scale model for evaluating both bedload and fine-sediment load, accounting for the mass exchanges of the fine-fraction between the flow and the riverbed.

2 Methods

The proposed model adopts a structure similar to that presented by Schmitt et al. (2016)[2], where the river is treated as a simplified network of connected reaches. These reaches are described by a set of homogeneous parameters for channel geometry (width, slope) and hydraulics (flow discharge, water depth, sediment grain size). The variability of the hydrological forcing is expressed through the probability density function of the flow rate. The bed material consists of a sediment mixture, and the bedload rate is computed using a multi-size transport formula. Fine sediment is modelled as a solid flux transferred downstream, while exchanging mass with the bedload layer. The criterion to discriminate which sediment fractions are transported in suspension and which as bedload is based on the ratio between the settling velocity and the local shear velocity. By defining a maximum concentration at the interface between fine-sediment and bedload layers, the exchanged solid fluxes depend on the local channel conditions. Fine-sediment load is considered to be produced by bare-soil areas of the catchment through an empirical relation that is a function of the discharge and the ratio of sediment-contributing areas to basin area.

3 Results and conclusions

We applied the proposed model to the river network of the Leno Creek (S-E of Trentino, Italy, Figure 1), a small Alpine watercourse with a basin area of 42 km^2, subject to intense water exploitation for hydropower production. A fixed monitoring station was installed in a downstream reach of the creek to collect data on discharge, water depth, and turbidity, with the purpose of calibrating the sediment-production function of the catchment. Further information on sediment production was also available thanks to detailed bathymetric surveys of the volume of sediments accumulated in two artificial reservoirs. The main outcome is the estimation of the mean annual bedload and fine-sediment load in every reach of the network, through the integration of the resulting fine-sediment production function at the basin scale with a novel model of the mass-exchange processes between bedload and fine-sediment load at the reach scale.

Figure 1: River network of the Leno Creek and fine-sediment sources (bare soil areas) in the catchment.

Acknowledgements

We acknowledge the support of: MUR PNRR project INEST; PNRR M4C2 PRIN 2022 (funded by the NextGenerationEU); APRIE of the Trento Province.

References

[1] C. Fabre, M. Fressard, S. Bizzi, F. Branger, and H. Piegay. Combining hillslope erosion and river connectivity models to assess large scale fine sediment transfers: Application over the Rhône River (France). *E.S.P.L.*, 49:3027–3045, 2024.

[2] R.J.P. Schmitt, S. Bizzi, and A. Castelletti. Tracking multiple sediment cascades at the river network scale identifies controls and emerging patterns of sediment connectivity. *W.R.R.*, 52:3941–3965, 2016.

Enhancing Biomorphodynamic Modeling by Incorporating Vegetation Friction Approaches

Antonia Dallmeier[1], Rebekka Kopmann[2], Roser Casas Mulet[1], Hannah Schwedhelm[1], Felix Endres[1], Nils Rüther[1]
[1]Chair of Hydraulic Engineering, Technical University of Munich (TUM), Germany
[2]Dept. of Hydraulic Engineering, Federal Waterways Engineering and Research Institute (BAW), Germany
Corresponding author: antonia.dallmeier@tum.de

Keywords: bedload transport, numerical modeling, vegetation, hydromorphology, openTELEMAC

1 Introduction

Vegetation plays a crucial role in influencing the interactions among flow, sediment transport, and the morphological evolution of alluvial river systems. To study these complex hydromorphological processes, numerical modeling has become a powerful tool. The numerical modeling software openTELEMAC incorporates a biomorphodynamic model (in this study, named ex-BMDM), which quantifies the effect of vegetation on hydrodynamics as well as morphodynamics [1]. Hereby, the hydraulic resistance of vegetation is considered as a drag force of rigid cylinders while the sediment transport is adjusted using the equations of [2]. While the ex-BMDM incorporates only a single approach to account for the hydraulic resistance of rigid vegetation, [3] implemented and validated several vegetation friction approaches in openTELEMAC to calculate the hydraulic resistance of vegetation in various flow conditions and for multiple plant morphologies. To address the limitations of the ex-BMDM, we enhanced the ex-BMDM by incorporating vegetation friction approaches, transforming it into a modular structure, hence providing a basis for further development and testing of this updated biomorphodynamic model (up-BMDM) in different flow conditions.

2 Methods

To enhance the formulation of hydraulic resistance due to vegetation and to improve the calculation of vegetation drag, we enabled the application of multiple vegetation friction approaches available in openTELEMAC in the up-BMDM. The up-BMDM employing the vegetation friction approach of [4] was numerically tested against the ex-BMDM by simulating the laboratory experiments of [5], which investigated bedload transport through emergent rigid vegetation. Additionally, we conducted an analytical investigation of the behavior of different vegetation friction approaches for bedload transport through rigid vegetation under submerged flow conditions, utilizing the laboratory experiments of [2].

3 Results and Discussion

The numerical simulations of bedload transport through emergent rigid vegetation using the up-BMDM yield results identical to those obtained with the ex-BMDM. In contrast, the analytical investigation reveals distinct variations in total bed shear stress and the Shields parameter, depending on the submergence ratio and on the vegetation friction approach used.
These findings demonstrate that the up-BMDM performs equivalently to the ex-BMDM under emergent flow conditions while providing significant advantages under submerged flow conditions. Furthermore, the up-BMDM enhances user-friendliness by allowing an easy selection of different vegetation approaches and provides, therefore, a wide range of applications.

4 Outlook

This study lays the foundation for advancing biomorphodynamic modeling within openTELEMAC. Specifically, we aim to enhance the up-BMDM by incorporating additional vegetation friction approaches and methods for adjusting sediment transport in vegetated flows. To address the need for further validation, we will perform numerical simulations with the up-BMDM, focusing on scenarios of bedload transport through rigid vegetation under submerged flow conditions. Future investigations will extend to scenarios involving bedload transport through flexible, leafy vegetation under near-submerged flow conditions.

References

[1] J. Li, N. Claude, P. Tassi, F. Cordier, A. Vargas-Luna, A. Crosato and S. Rodrigues. Effects of Vegetation Patch Patterns on Channel Morphology: A Numerical Study. *Journal of Geophysical Research: Earth Surface*, 127(5), 2022.
[2] J. A. Bonilla-Porras, A. Armanini & A. Crosato. Extended Einstein's parameters to include vegetation in existing bedload predictors. *Advances in Water Resources*, 152, 103928, 2021.
[3] F. Folke, R. Kopmann, G. Dalledonne & M. Attieh. Comparison of different vegetation models using TELEMAC-2D. *XXVIth TELEMAC-MASCARET User Conference, 15th to 17th October 2019, Toulouse,* 2019.
[4] M. J. Baptist, V. Babovic, J. Rodríguez Uthurburu, M. Keijzer, R. E. Uittenbogaard, A. Mynett & A. Verwey. On inducing equations for vegetation resistance. *Journal of Hydraulic Research*, 45(4), 435–450, 2007.
[5] A. Armanini & V. Cavedon. Bed-load through emergent vegetation. *Advances in Water Resources*, 129, 250–259, 2019.

The Influence of Tectonic Uplift on Shore Morphology, Wave Energy Delivery, and Coastal Erosion.

Cesar G. Lopez, Claire C. Masteller
Washington University in St. Louis, St. Louis, MO, United States
Corresponding author: c.g.lopez@wustl.edu

Keywords: Erosion, Tectonics, Waves, Shore Platform

Introduction

Ocean waves are key drivers of coastal erosion, removing material from the shore[1] and driving cliff retreat[2]. While coastal erosion rates have been shown to scale with wave power and offshore wave climate[3], differing relationships have also been found[4]. This indicates that other nearshore and coastal factors influence coastal erosion rates across scales. The processes that modify nearshore and shore platform morphology are particularly important because of their role in wave energy transformations and dissipation[5, 6], which effects the availability of energy to erode the coast. While the role of wave action[2], wave climate[3], rock strength[4], and tidal range[6] in driving near shore morphology and coastal erosion rates have all been previously studied, the role of tectonic uplift has been noticeably absent. On millennial timescales, the interplay between changes in sea level and tectonic uplift results in the formation of marine terraces[7]. However, the role of tectonic uplift in controlling shore morphology and driving coastal erosion on decadal and centennial time scales remains largely unknown. Here, we characterize and constrain the influence of coastal processes on shore morphology and coastal retreat rates spanning the West Coast of the United States.

Methods

We characterize offshore, deepwater wave conditions by utilizing virtual buoys from hindcast wave models spanning Southern California through Northern Oregon. Nearshore morphology, specifically shore platform slope and width, is determined by extracting 2km wide swath profiles from bathymetric data. Shallow water wave transformations are computed along the dominant wave direction from the buoy to the shore for 111 sites to constrain wave energy availability at the shore. Along with the offshore wave climate and bathymetric data, we also incorporate shoreline change, tidal, lithologic, fault slip, and tectonic uplift datasets. We then utilize multivariate data analysis to interrogate and better constrain the relationships between these different processes.

Results and Discussion

We find that nearshore morphology is primarily controlled by rock strength and tectonic uplift, with the slope of the nearshore having a positive and significant correlation with rock strength. Shore platform width features a negative correlation with tectonic uplift corresponding to the millennial timescale, and a positive correlation with tectonic uplift corresponding to the decadal timescale. Additionally, we also find that erosion rates scale with nearshore morphology. As the shore platform becomes steeper and narrower, erosion rates increase due to better translation of offshore wave climate, enhanced wave energy delivery, and reduced dissipation in the nearshore. We also find that rock strength has a strong positive correlation with erosion rates, indicating that the enhanced energy delivery to the shore that occurs on steeper and narrower coasts exerts a greater control on erosion rates than the material property. These results demonstrate that tectonic uplift and rock strength exert important controls on coastal erosion rates by steepening and narrowing the nearshore and shore platform, thereby enhancing offshore wave climate translation and wave energy delivery to the shore, and driving greater coastal retreat.

References

[1] Ruggiero, P., Komar, P. D., McDougal, W. G., Marra, J. J, and Beach, R. A., 2001, Wave Runup, Extreme Water Levels and the Erosion of Properties Backing Beaches: Journal of Coastal Research, v. 17(2), p. 407–419.

[2] Adams, P.N., Storlazzi, C.D., and Anderson, R.S., 2005, Nearshore wave-induced cyclical flexing of sea cliffs: Journal of Geophysical Research, v. 110.

[3] Huppert, K. L., Perron, J. T., and Ashton, A. D., 2020, The influence of wave power on bedrock sea-cliff erosion in the Hawaiian Islands: Geology, v. 48, p. 499–503.

[4] Benumof, B.T., Storlazzi, C.D., Seymour, R.J., and Griggs, G.B., 2000, The relationship between incident wave energy and seacliff erosion rates: San Diego County, California: Journal of Coastal Research, v. 16, p. 1162–1178.

[5] Marshall, R. J. E., and Stephenson, W. J., 2011, The morphodynamics of shore platforms in a microtidal setting: Interactions between waves and morphology: Marine Geology, v. 288, p. 18–31.

[6] Trenhaile, A. S., 2000, Modeling the development of wave-cut shore platforms: Marine Geology, v. 166, p. 163-178.

[7] Anderson, R.S., Densmore, A.L., and Ellis, M.A., 1999, The generation and degradation of marine terraces: Basin Research, v. 11, p. 7–19.

Global river morphology atlas

Niek Collot d'Escury[1], Daan Beelen[1], Jaap Nienhuis[1], Maarten Kleinhans[1], Esther Stouthamer[1]

[1]Utrecht University, Utrecht, Netherlands

e-mail corresponding author: n.n.p.collotdescury@uu.nl

Keywords: *River morphology, global, remote sensing, SWORD*

1 Background

River morphologies are an important part of the hydrological cycle yet despite extensive study, the link between river form and its controlling factors remains partially enigmatic [5, 6, 2]. Rivers are typically classified into three or four classes which are: meandering, wandering, braiding and anastomosing [4]. This classification is traditionally based on sinuosity, degree of anabranching and a braiding index [5]. However, this classification has never been quantified globally. Previous studies have either focused on local or regional scale or lack a robust quantitative framework.

Therefore, the goal of this study is to create a global atlas of river morphologies defined by a consistent set of quantified morphological variables, enabling a concrete distribution of different river morphologies across the world.

2 Data

The Surface Water and Ocean Topography (SWOT) Mission River Database (SWORD) version 17 is the main data input for this study [3]. SWORD was created as a static precursor to the SWOT mission, enabling satellite observations to be linked to river reaches. SWORD is the result of a combination of various global datasets, but its foundation is the Global River Width Dataset (GRWL), [1] the first global dataset to depict seasonally averaged river planforms, based on Landsat imagery. The rivers included in SWORD are limited to at least 30 meters wide, which includes 248,647 rivers on Earth totalling over 2.2 million kilometers. Each of these mapped rivers has an accurately georeferenced centerline, channel width, flow accumulation, and downstream distance to the nearest river outlet.

3 Methods

The reach definition used by SWORD includes reaches that are too short to obtain a meaningful morphology classification so we combined reaches to increase the length to a minimum of 48 times the width. Thereafter, relevant fluvio-morphological parameters (FMPs) that define rivier morphologies are calculated. We focus on sinuosity, bend curvature and braiding index. Machine learning algorithms like k-means clustering are then applied to our global FMP dataset to statistically bin river reaches into morphology classes. Using this technique, the number of river morphology classes will be determined statistically rather than holistically and various sensitivity analyses can be used to test the reliability of our classification.

4 Expected outcome / Discussion

Given the absence of clear boundaries between fluvio-morphological parameters across the four classes, we expect to identify more than the traditional four river classes, including transitional or intermediate classes where parameters overlap. These transitional classes will likely reflect the complexity and diversity of river planforms, capturing subtle variations that were previously unaccounted for in conventional classifications.

References

[1] George H. Allen and Tamlin M. Pavelsky. Global river widths from landsat (grwl) database, 2018. URL https://zenodo.org/doi/10.5281/zenodo.1297434.

[2] John M. Buffington and David R. Montgomery. *Geomorphic Classification of Rivers: An Updated Review*, page 1143–1190. Elsevier, 2022. ISBN 9780128182352. doi: 10.1016/b978-0-12-818234-5.00077-8. URL http://dx.doi.org/10.1016/B978-0-12-818234-5.00077-8.

[3] Michael T. Durand Xiao Yang Renato P. d. M. Frasson Liam Bendezu Elizabeth H. Altenau, Tamlin M. Pavelsky. Swot river database (sword) (version v17).

[4] Maarten G. Kleinhans, William J. McMahon, and Neil S. Davies. What even is a meandering river? a philosophy-enhanced synthesis of multilevel causes and systemic interactions contributing to river meandering. *Geological Society, London, Special Publications*, 540(1):43–74, July 2023. ISSN 2041-4927. doi: 10.1144/sp540-2022-138. URL http://dx.doi.org/10.1144/sp540-2022-138.

[5] S. A. Schumm. Patterns of alluvial rivers. *Annual Review of Earth and Planetary Sciences*, 13(1):5–27, May 1985. ISSN 1545-4495. doi: 10.1146/annurev.ea.13.050185.000253. URL http://dx.doi.org/10.1146/annurev.ea.13.050185.000253.

[6] Marc Tadaki, Gary Brierley, and Carola Cullum. River classification: theory, practice, politics. *WIREs Water*, 1(4):349–367, April 2014. ISSN 2049-1948. doi: 10.1002/wat2.1026. URL http://dx.doi.org/10.1002/wat2.1026.

Residual transport of sand across tidal divides in the Dutch Wadden Sea

Thomas Veerman[1], Maarten van der Vegt[1], Theo Gerkema[2]

[1]Utrecht University, Utrecht, the Netherlands
[2]Royal Dutch Institute for Sea Research (NIOZ), Yerseke, the Netherlands

e-mail corresponding author: t.h.veerman@uu.nl

Keywords: *residual sediment transport, tidal divide, Wadden Sea*

1 Introduction

Studies (e.g. [1]) of water circulation in the Dutch Wadden Sea (DWS) indicate that long-term residual volume transport across the tidal divides is of similar magnitude as those through the inlets. At the divides, residual volume transport is driven by wind, as the tidal velocity amplitude is (near) zero, while at the inlets both wind and tide can be important [1]. If cross-divide sediment transport is similarly significant at a basin scale, models aimed at long-term morphological evolution and sediment budgets need to account for this. Here, we first focus on sand transport by local conditions, including wind-driven currents and waves, as mud requires a full-domain approach.

2 Methods

Depth-averaged flow velocity and water levels were extracted from a GETM model hindcast of the DWS, spanning 2005-2015 [1]. The model had a horizontal resolution of 200 m, and included tidal and meteorological forcing and freshwater discharge. Velocity and water level were extracted along transects for each inlet and tidal divide. Sand transport was computed using the Engelund-Hansen (EH) predictor. A uniform d_{50} of 250 μm was chosen as a reasonable estimate for both inlets and tidal divides. Residual rates were computed from the orthogonal component of sand transport vectors at each transect segment by spatially integrating and then averaging over all timesteps. Present results still omit wave effects. Work is ongoing to apply the Van Rijn transport model to include wave effects.

3 Results

The direction and magnitude of residual sand transport are indicated in Figure 1 and Table 1, respectively. Across the divides, residual sand transport is directed North and East, except Schiermonnikoog (G). All inlets except Pinkegat (5) are importing sand. The long-term residual sediment transport through the inlets is O10-O1000 greater than across adjacent tidal divides.

4 Discussion and conclusions

The magnitudes in Table 1 suggest that either cross-divide sand transport is irrelevant at basin scale, or that waves play a crucial but presently omitted role. We expect that results obtained with the Van Rijn transport predictor including the effect of waves will show a decreased disparity between inlets and divides. First, because waves will have a much stronger effect on the shallow divides than on the deeper inlets. Secondly, EH-transport scales with U^5, which favors the inlets, as strong currents occur regularly with the tide, while at divides they only occur during wind events. Third, EH-transport does not include a threshold of motion. The long-term residual is the balance of common and extreme conditions, and is often small compared to gross transport. For most of the tidal divides, computed sand transport during calm weather was directed opposite to the long-term residual, as was also observed for water by [1]. A threshold of motion will reduce calm weather transport and thereby increase long-term residual transport at the divides. The relative contribution of waves, wind-driven currents, and surges to cross-divide transport will be the topic of further analysis.

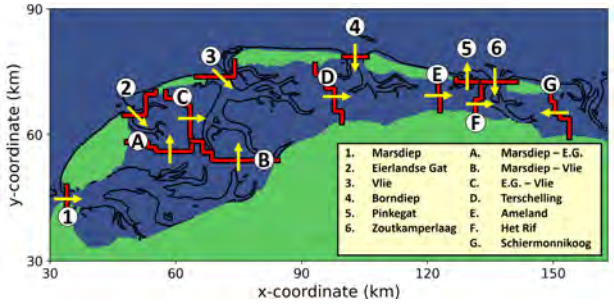

Figure 1: Map of the DWS in model coordinates. Arrows indicate the direction of residual sand transport.

Inlet	1	2	3	4	5	6
Q_{sand}	$1.01{\cdot}10^3$	5.13	176	194	56.4	17.1

Divide	A	B	C	D	E	F	G
Q_{sand}	1.27	11.0	1.53	1.70	0.04	0.06	1.81

Table 1: Residual fluxes of sand in kg/s. The numerical (alphabetical) list corresponds to the inlets (divides) as indicated in Figure 1.

Acknowledgements

We thank Aditi Mitra and Matias Duran-Matute of TU Eindhoven for making the GETM data available.

References

[1] Carmine Donatelli, Matias Duran-Matute, Ulf Gräwe, and Theo Gerkema. Residual circulation and freshwater retention within an event-driven system of intertidal basins. *Journal of Sea Research*, 186:102242, 2022.

Mangrove vegetation density and channel density have trade-off effects on nature-based flood risk mitigation

Ignace Pelckmans[1], Jean-Philippe Belliard[1,2], Olivier Gourgue[2], Luis E. Dominguez-Granda[3], Stijn Temmerman [1]
[1]Department of Biology, ECOSPHERE, University of Antwerp, Antwerp, Belgium.
[2]OD Nature, Royal Belgian Institute of Natural Sciences, Brussels, Belgium.
[3]Centro del Agua y Desarrollo Sostenible, Escuela Superior Politecnica del Litoral (ESPOL), Faculdad de Ciencias Naturales y Matematicas, Guayaquil, Ecuador
Corresponding author: ignace.pelckmans@uantwerpen.be

Keywords: mangroves, hydrodynamic modelling, flood protection, channel density, vegetation density

1 Introduction

Mangroves can mitigate coastal flood risks. Their conservation and restoration are therefore being increasingly recognized as cost-effective and sustainable nature-based strategies in addition to traditional engineered coastal protection measures such as dikes and sea barriers [1]. When surges or tidal waves propagate through dense, continuous mangrove forests, peak water levels are lowered because of the friction between the water flow and the mangroves' stilt roots and stems [2]. This process is referred to as within-wetland attenuation of high-water levels. When surges or tidal waves propagate through estuarine channels fringed by mangroves, water laterally floods the mangroves, which may cause the reduction of upstream peak water levels [3,4]. This process is referred to as along-channel attenuation.

2 Methods

We present a hydrodynamic model of a 20 km long tropical estuary (Guayas delta, Ecuador), which is calibrated and validated against field observations and accurately simulates within-wetland and along-channel attenuation. Through scenarios analyses, we simulate the effect of vegetation and channel density on both within-wetland and along-channel attenuation.

3 Results & Conclusions

We show that with a denser network of secondary sub-channels and sparser vegetation, larger water volumes can flow into the surrounding mangroves, resulting into higher along-channel attenuation. However, with the presence of secondary subchannels or sparser vegetation, within-wetland attenuation rate decreases. Hence, vegetation and channel density control a trade-off between within-wetland and along-channel attenuation. Future conservation and restoration efforts should therefore account for the trade-off between within-wetland and along-channel attenuation to ensure that nature-based flood protection effectively safeguards both human settlements behind unchanneled wetlands and those located along deltaic channels bordered by mangroves.

4 References

[1] Temmerman, S., Horstman, E. M., Krauss, K. W., Mullarney, J. C., Pelckmans, I., & Schoutens, K. Marshes and Mangroves as Nature-Based Coastal Storm Buffers. *Annual Review of Marine Science*, 15(1): 95–118. 2023.

[2] Montgomery, J., Bryan, K., Horstman, E., & Mullarney, J. Attenuation of Tides and Surges by Mangroves: Contrasting Case Studies from New Zealand. *Water*, 10: 1119. 2018.

[3] Pelckmans, I., Belliard, J.-P., Dominguez-Granda, L. E., Slobbe, C., Temmerman, S., & Gourgue, O. Mangrove ecosystem properties regulate high water levels in a river delta. *Natural Hazards and Earth System Sciences*, *23*(9): 3169–3183. 2023

[4] Pelckmans, I., Belliard, J.-P., Gourgue, O., Dominguez-Granda, L. E., & Temmerman, S. Mangroves as nature-based mitigation for ENSO-driven compound flood risks in a large river delta. *Hydrology and Earth System Sciences*, *28*(6): 1463–1476. 2024.

From large-scale meanders to human-induced floodplain deposition: history of the Congaree River valley (South Carolina, USA)

Marcin Słowik[1,2], Przemysław Niedzielski[3], Aleksandra Proch[3], George Starega[2]
[1] Adam Mickiewicz University, Institute of Geology, Geohazards Research Unit, Poznań, Poland
[2] University of South Carolina, School of the Earth Ocean and Environment, Columbia, SC, USA
[3]Adam Mickiewicz University, Faculty of Chemistry, Department of Analytical Chemistry, Poznań, Poland
Corresponding author: Marcin Słowik, slowikgeo@poczta.onet.pl

Keywords: human impact on rivers; river planform changes; floodplain geochemistry; floodplain sedimentation

1 Introduction

The Atlantic Coastal Plain was formed by rivers. The evolution of these rivers, including human impact, is understudied. We aimed to identify controls on channel planform changes in rivers of the Atlantic Coastal Plain (USA) using the example of the Congaree River Valley, South Carolina. We focused on the period of the last 200 years, characterized by intensive floodplain deposition caused by deforestation of upstream parts of the catchment. The main research tasks included: i) study the sedimentary architecture of the valley floor, ii) determine the main phases of fluvial activity, iii) the influence of floodplain sedimentation in the settlement period (the last over 200 years) on changes in the chemical composition of the Congaree floodplain deposits.

The Congaree River floodplain was selected for detailed research because it preserves a complex system of palaeochannels and abandoned meander belts. Floodplain channels and blackwater streams rework part of the ancient channels, and distribute floodwaters from the modern Congaree River throughout the floodplain [1].

2 Research methods

We used the following research methods:

- geological surveys to study the lithological variability of the floodplain
- geophysical surveys (ground-penetrating radar) to image the floodplain sedimentary structures
- radiocarbon dating to determine the age of the former channel and floodplain deposits
- chemical analyses of 165 floodplain sediment samples using inductively coupled plasma mass spectrometry with Integrated Collision Reaction Cell (ICP(iCRC)MS) to determine concentrations of chemical elements at various depths and types of deposits. Contents of Fe, Mn, Cu, Zn, Pb, Cr, As, Al, Si, Rb, Ba, Ca, Na, K, Mg, and REE (Rare Earth Elements) were analysed. Additionally, the Fe (III) and Fe (II) content was determined using a hyphenated technique of high-performance liquid chromatography with detection by inductively spectrometry coupled plasma high-resolution optical emission spectrometry (HPLC-ICP hrOES)
- statistical methods (cluster and one-way ANOVA analyses) to identify geochemical groups of sediments.

3 Results and conclusions

We found that large-scale meanders shaped the Congaree floodplain between 16,000 and 12,000 cal. BP. The large bends were replaced by meandering channel bends, active between 12,000 and 3,000 cal. BP. The river planform change was caused by an increase in climate humidity, resulting in frequent flooding phases [2]. The timing of the large bends' cutoffs corresponds to the inundation of south-eastern coast of North America, when the ocean level rose from -80 m to -60 m [3]. Compound meanders evolving by neck cutoffs were active since 3000 cal. BP in relatively drier climate conditions. The traces of the identified channel planforms can also be found in other river valleys of the Atlantic Coastal Plain.

The Congaree floodplain was subjected to an intensive deposition of fines resulting from deforestation and creation of agricultural areas in the Atlantic Coastal Plain during the last >200 years. We found that the chemical composition of the top 0.7 m of the floodplain, built of silts and clays, differs from the geochemical pattern of point bar deposits formed prior to the settlement period. The legacy deposits are characterized by increased contents of Mn, Zn, Cr, Pb, Ni, Rb, Co, K. P, Na, Fe (III) and REE. High concentrations of these elements resulted from increased deposition from suspension and accumulation of oxides in the floodplain fines. High contents of REE may be the trace of monazite placers mining in the Piedmont.

Acknowledgments

This study is the result of Fulbright scholarship awarded to Marcin Słowik, funded by Polish-American Fulbright Commission.

References

[1] H. Xu et al., Geomorphology of the Congaree River floodplain: implications for the inundation continuum. *Water Resources Research*, 57: e2020WR029456, DOI:10.1029/2020WR029456, 2021.

[2] R. Lombardi et al., Fluvial activity in major river basins of the eastern United States during the Holocene. *The Holocene*, 30: 1279-1295, 2020.

[3] W. de Lange, R.M. Carter, 2013, Observations: the hydrosphere and oceans. In: *Climate change reconsidered II*, C.D. Idso, R.M. Carter, S.F. Singer (Eds). Chicago, IL, The Heartland Institute, 729-824, 2013.

Morphologic evolution of tidal flats in the Wadden Sea

Marthe Wassink[1], Bas van Maren[1,2], Ymkje Huismans[1,2], Zheng Bing Wang[1,2]

[1]Delft University of Technology, Faculty of Civil Engineering and Geosciences, the Netherlands
[2]Deltares Research Institute, Delft, the Netherlands

e-mail corresponding author: m.wassink-2@tudelft.nl

Keywords: *morphodynamics, Wadden Sea, tidal basins, human interference, sea level rise*

1 Introduction

Tidal systems, including tidal flats and channels, are threatened by accelerating sea level rise (SLR). Without sufficient sediment accretion, intertidal areas will decline, negatively influencing the ecosystem and coastal safety. This study focuses on the Wadden Sea, the world's largest intertidal system, along the coastlines of the Netherlands, Germany and Denmark (Figure 1). Model studies [3] suggest that tidal flats in the Dutch Wadden Sea can only partially adapt to SLR, while at the same time observed present-day accretion rates in the German Wadden Sea are much higher than SLR [1]. The morphological changes on tidal flats are strongly influenced by sand-mud segregation [2], but to date this aspect is not yet accounted for in studies analysing long-term response of the tidal flats. Surprisingly, a uniform overview of sedimentation and erosion rates on tidal flats throughout the whole Wadden Sea does not appear to exist. Therefore, this study aims to investigate patterns of accretion and erosion of sand and mud on intertidal areas in the entire Wadden Sea.

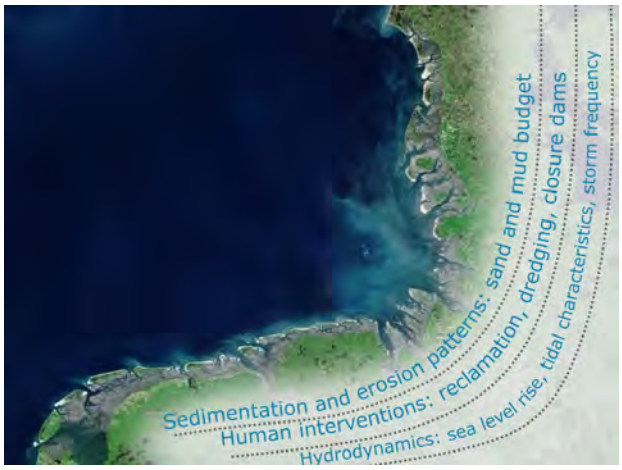

Figure 1: Satellite image of the trilateral Wadden Sea, from *www.waddensea-secretariat.org*, adapted to visualize research objectives

2 Methodology

In the first part of this study bathymetry and sediment composition data is used to analyse morphological development in the entire Wadden Sea. Characteristics such as intertidal-to-subtidal ratios, hypsometry and sediment composition are examined, providing insight into the spatial and temporal patterns of sediment accretion across the Wadden Sea.

Subsequently, these trends are related to their main drivers, focusing on human interventions such as basin closures [2], land reclamation [4] and dredging as well as large-scale hydrodynamic spatial and time variations in e.g. tidal range and storm surges. Furthermore, both the direct effect of SLR and its indirect impact on tidal characteristics are investigated. Relevant feedback loops and processes are analysed with numerical models to quantify the contribution of potential drivers.

3 Objectives

This research aims to find and explain trends in sedimentation and erosion of tidal flats in the Wadden Sea and identify the dominant drivers behind these changes. We hypothesize that both direct human impact–such as reclamation, dredging, and the construction of closure dams–as well as indirect effects of climate change, including sea level rise and its influence on tidal dynamics and storm activity, play important roles. By combining bathymetry and sediment data with numerical modeling, this research quantifies the impact of these drivers, contributing to our understanding of morphological evolution of tidal flats.

References

[1] M. Benninghoff and C. Winter. Recent morphologic evolution of the German Wadden Sea. *Scientific Reports*, 9(1):9293, 2019. doi: 10.1038/s41598-019-45683-1.

[2] A. Colina Alonso, D. S. van Maren, E. P. L. Elias, S. J. Holthuijsen, and Z. B. Wang. The contribution of sand and mud to infilling of tidal basins in response to a closure dam. *Marine Geology*, 439: 106544, 2021. doi: 10.1016/j.margeo.2021.106544.

[3] Y. Huismans, A. van der Spek, Q. Lodder, R. Zijlstra, E. Elias, and Z.B. Wang. Development of intertidal flats in the Dutch Wadden Sea in response to a rising sea level. *Ocean & Coastal Management*, 216:105969, 2022. doi: 10.1016/j.ocecoaman.2021.105969.

[4] R. A. Schrijvershof, D. S. van Maren, M. Van der Wegen, and A. J. F. Hoitink. Land Reclamation Controls on Multi-Centennial Estuarine Evolution. *Earth's Future*, 12(11):e2024EF005080, 2024.

Future Delta Development at the Alpine Rhine River Mouth in Lake Constance

Jana C. Schierjott [1], David F. Vetsch [1]

[1]Eidgenössische Technische Hochschule Zürich, Zürich, Switzerland

e-mail corresponding author: schierjott@vaw.baug.ethz.ch

Keywords: *lacustrine delta, underwater canyon, Alpine Rhine, hyperpycnal flows, homopycnal flows*

1 Introduction

The Alpine Rhine drains about 6120 km^2 and is responsible for a daily mean discharge into Lake Constance of 230 m^3/s. The current 300-year flood for the Lustenau site is given as 4300 m^3/s. Due to its alpine location, the discharge regime of the Alpine Rhine is characterized by snowmelt and has discharge peaks in spring.

According to [1], the natural Alpine Rhine delta by Altenrhein at the Rheinspitz used to be much steeper than it is nowadays in Fussach Bay. At the old delta, it was observed that the sediment-laden water from the river abruptly plunged and traveled far into the lake as an underwater current between stratified layers of lake water. High-density currents traveling along the bed are also thought to have existed, as several underwater canyons can be seen in the bathymetric data.

In order to mitigate and control flooding around Altenrhein, the river mouth was anthropogenically relocated 12 km to the east into Fussach Bay in 1900. To avoid and better mitigate upstream flooding due to backward sediment deposition, the mouth of the Alpine River has artificially been extended into the lake by a 4.8 km long channel ("Vorstreckung"), built on its own former delta deposits. To reduce aggradation, the gravel fraction of the bedload is removed from the river just before the "Vorstreckung" begins. Some sand is removed for industrial use inside the "Vorstreckung" also, but not much compared to the input. In recent years, a mouth bar has formed which may be reworked or eroded under higher discharge (figure 1). The channel was purposefully built with a bed slope of 0.3 m/km. At the relocated and extended river mouth, a mixture of homo- and hyperpycnal flows is observed, but no underwater canyon has developed so far.

2 Methods

We use a numerical approach to model the evolution of the new Alpine Rhine delta, focusing on potential underwater canyon formation. We use pyDeltaRCM [2], a computationally efficient, open source software specifically designed for delta simulations. The initial setup is a box of 2500 m width and 2500 m length. The width of the channel inlet is set to 180 m to mimic the width of the "Vorstreckung". The seafloor elevation follows the bathymetric data and drops from -1 m at the inlet to -50 m at the end of the modeling domain. The resolution as well as different initial geometries will be tested during the study. We run several sets of simulations, varying the bedload fraction, suspended sediment, peak discharge (>1000 m^3/s), lake level, and possibly adding flooding events during the simulation. The simulation time of the models will range from 10 to 100 years or more.

Figure 1: Looking upstream from the Alpine Rhine river mouth (source: International Rhine Regulation, situation on 24.08.2018, lake level 395.27 m a.s.l.)

3 Conclusions

We aim to understand the future development of the currently forming Alpine Rhine delta at the artificially extended river mouth, particularly whether new underwater canyons at the lake bottom are going to form and how the delta morphology will evolve over the course of 10 to 100 years and more. We investigate how different parameters such as suspended sediment load versus bedload, and delta slope affect the shape and advancement of the delta. This study will help maintaining the delta in order to mitigate floods, slow down sediment accumulation in Fussach bay and create a habitat for plants, animals and a recreational area for the inhabitants of Fussach and surroundings.

References

[1] Steven YJ Lai and Hervé Capart. Two-diffusion description of hyperpycnal deltas. *Journal of Geophysical Research: Earth Surface*, 112(F3), 2007.

[2] Andrew J Moodie, Jayaram Hariharan, Eric Barefoot, and Paola Passalacqua. pyDeltaRCM: a flexible numerical delta model. *Journal of Open Source Software*, 6(64):3398, 2021.

Continuous-Wave Radar for Coastal Morphology

Pau Luque[1], Johann K. Delgado[2], Albert Aguasca [3], Marta Marcos[1], Edwin A. Cowen[2], Alejandro Orfila[1,2]

[1]IMEDEA(CSIC-UIB). Esporles, Balearic Islands, Spain
[2]DeFrees Hydraulics Laboratory, Cornell University. Ithaca, NY, USA
[3]CommSensLab, UPC BarcelonaTech. Barcelona, Spain

e-mail corresponding author: alejandro.orfila@csic.es

Keywords: *coastal monitoring, remote sensing, wave radar, X-band radar, continuous-wave radar*

1 Introduction

Sandy beaches are dynamical systems with complex morphological evolution primarily induced by hydrodynamic forcing. Their study requires extensive data on both this forcing and the beach state, traditionally measured *in situ*, which due to the harsh characteristics of the marine environment results in datasets with limited resolution and coverage. In comparison, land-based instruments can cover bigger areas with higher sampling frequency *via* remote sensing. Pulsed X-band radar is one of the most popular techniques for this purpose, although a few studies demonstrated the capability of continuous-wave radar to measure wave fields, even in the nearshore [4]. This study adapted the frequency-modulated continuous-wave system of [1] to be used on sandy beaches, obtaining spatially-distributed wave height and beach depths, while identifying the breaker zone and shoreline positions.

2 Radar acquisition and processing

The radar system consists of two identical vertically-polarized antennae, with a horizontal and vertical beamwidths of 5.5 °and 22 °. One emits a continuous chirp signal in X-band, while the other samples a group of contiguous upchirps (a burst) twice a second until a 10 min time series is obtained. The measurement processing starts by computing the power spectral density (PSD) associated with each distance-chirp-burst tuple, which are cleaned *via* chirp binning and interference rejection. Second, radar cross-section (RCS) is estimated from the cleaned PSD and transformed to sea surface slopes relative to the radar azimuth, following [3] but incorporating a linear extrapolation between the time-averaged logarithm of RCS and the observation angle, which prevents limiting the wave height estimation while identifying the region suitable to be analyzed, the shoreline, and the breaker zone. Third, sea surface slopes are divided into overlapping zones based on distance, and the two-dimensional PSD along distance and time (2DPSD) is computed for each zone. Fourth, the dispersion relationship of ocean waves is estimated from each slope 2DPSD following [4]; this also retrieves the average depth and surface current at each zone. Fifth, free-surface elevation (FSE) 2DPSD is obtained from the slope 2DPSD *via* integration in the spectral domain, and bandpass-filtered around the dispersion curve. Finally, the filtered FSE 2DPSD is integrated along the spatial dimension to produce an estimate of non-directional amplitude wave spectra for each zone.

3 Results

Beach refracts wave trains to become almost normal to the shore, thus allowing non-moving antennae to measure sea surface echoes over a cross-shore transect when the local wind blows perpendicularly to the shore, which occurs during sea breeze events. Thus, the described system and algorithm were able to measure wave spectra, breaker zone position, and bathymetry in the Muro beach (north of Mallorca, western Mediterranean), which were validates using an AWAC located 3 km offshore, georectified images from a videomonitoring station, and depths from a multibeam echosounder [2]. Figure 1 shows the depth validation, revealing a bias and a root mean square error of -43 cm and 76 cm, which reduce to -8 cm and 15 cm when considering only the region where more than 75 % of radar measurements retreived depth.

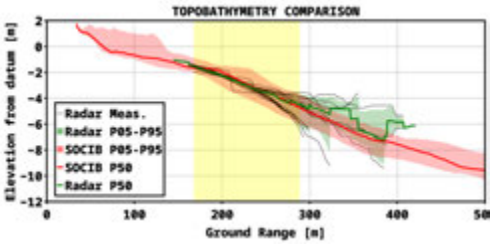

Figure 1: Comparison between the radar-derived bathymetry (green) and the in situ measurements (red), as percentiles of each ensemble. Black lines indicate individual radar measurements. Yellow area indicates the region where at least 75 % of radar measurements reported data.

References

[1] A. Aguasca, A. Broquetas, J.J. Mallorqui, and X. Fabregas. A solid state L to X-band flexible ground-based SAR system for continuous monitoring applications. In *IGARSS 2004. 2004 IEEE International Geoscience and Remote Sensing Symposium*, volume 2, page 757–760, sep 2004. doi: 10.1109/IGARSS.2004.1368512.

[2] F. Cardona, M. Marcos, À. Fernàndez-Mora, A. Orfila, E. Harms, V. Galvan, M. Blanco, J. Lacalle, , and M. Morikawa. Hotel Observatories to analyze beach dynamics in a global change context. In *40th Association of Marine Laboratories of the Caribbean Scientific Meeting*, Basseterre, Saint Kitts and Nevis, may 2023.

[3] H. Dankert and W. Rosenthal. Ocean surface determination from X-band radar-image sequences. *Journal of Geophysical Research: Oceans*, 109(C4):2003JC002130, April 2004. ISSN 0148-0227. doi: 10.1029/2003JC002130.

[4] Giovanni Ludeno, Matteo Antuono, Francesco Soldovieri, and Gianluca Gennarelli. A Feasibility Study of Nearshore Bathymetry Estimation via Short-Range K-Band MIMO Radar. *Remote Sensing*, 16(2):261, jan 2024. ISSN 2072-4292. doi: 10.3390/rs16020261.

Oyster Reefs on Intertidal Morphological Evolution

LIU Daoxudong[1], THOMAS Marine[2], LEUNG Felix[3], STOCCHINO Alessandro[1]

[1]The Hong Kong Polytechnic University
[3]The Nature Conservancy Hong Kong Foundation Limited
[3]Jockey Club Museum of Climate Change, The Chinese University of Hong Kong

e-mail corresponding author: daoliu@polyu.edu.hk

Keywords: *oyster reefs; morphodynamics; modeling; SCHISM*

1 General Information

Oyster reefs have critical effect in modifying the morphology and sediment dynamics of local shoals [1]. Positioned along shorelines, these reefs can act as natural breakwaters, influencing both hydrodynamics and sediment transport. This study examines how various configurations of oyster reefs—differing in length, width, and spatial distribution—affect morphodynamic evolution of intertidal environments under different tidal conditions. Understanding these relationships is crucial for optimizing oyster reefs restoration practices and mitigating shoreline erosion, as oyster reefs not only protect vulnerable coastlines but also contribute to sediment stabilization and habitat formation [2].

2 Numerical modeling

The morphological evolution is investigated using the numerical suite SCHISM, based on a semi-implicit finite-element/finite-volume scheme. For sediment transport simulations, a morphological factor is employed to accelerate morphological evolution of the system.

3 Results

Overall, the shoreline is extended offshore by over 200 meters around the reef formations. By comparing cases with varying tidal forcings under the same configuration and sediment classes, as well as cases with different sediment classes under the same configuration and tidal forcing, it is observed that tidal forcing plays a major role in altering the cross-sectional bathymetry. Larger tidal amplitudes generally lead to increased flow velocities, which in turn result in greater bed shear stress, thereby intensifying sediment transport and enhancing water-sediment exchange. Specifically, when a harmonic M2 tide with a 1-meter amplitude is applied, the shoreline extends further by more than 40 meters.

The river input is also analyzed as their existence and placement are simulated in two case placed at the upstream of oyster reefs directly discharging sediment mixed water into the basin and at the upstream of oyster reefs with deviation of 150 meters. The water input induces a channel as a results of erosion while sediments accumulates on the intertidal fronts and extends the coastline further offshore by over 100 meters.

4 Conclusion

Through numerical simulations in an idealized intertidal basin geometry, we explore the complex interactions between shallow water and sediment transport processes. The results suggest that the presence of reefs alters sediment distribution patterns, contributing to localized erosion and deposition both around the reefs and in adjacent offshore areas. The reefs serve as blocks and corridors for water flow during flood and ebb tides which, in turn, change the hydrodynamics and redistribute sediments [3]. Over time, estuarine morphology reaches an equilibrium, which varies based on the specific reef configurations. Our findings indicate that different reef structures can lead to distinct patterns of morphological evolution, emphasizing the importance of reef design in coastal management and habitat creation.

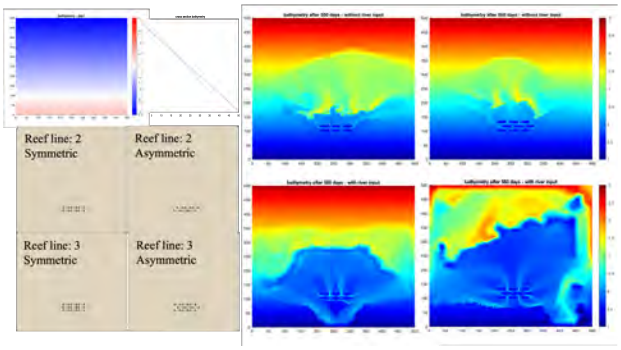

Figure 1: Left: The base configuration, different oyster reefs arrangement. Right: four bed elevation maps at equilibrium

References

[1] Allison M Colden, Kelsey A Fall, Grace M Cartwright, and Carl T Friedrichs. Sediment suspension and deposition across restored oyster reefs of varying orientation to flow: implications for restoration. *Estuaries and Coasts*, 39:1435–1448, 2016.

[2] Steven B Scyphers, Sean P Powers, Kenneth L Heck Jr, and Dorothy Byron. Oyster reefs as natural breakwaters mitigate shoreline loss and facilitate fisheries. *PloS one*, 6(8):e22396, 2011.

[3] Brenda Walles, João Salvador de Paiva, Bram C van Prooijen, Tom Ysebaert, and Aad C Smaal. The ecosystem engineer crassostrea gigas affects tidal flat morphology beyond the boundary of their reef structures. *Estuaries and Coasts*, 38(3): 941–950, 2015.

Investigating the Impacts of Watershed Urbanization on Downstream Sedimentation and Geomorphology of a River

Afrida Aranya[1], Julia Cisneros[1]
[1]Department of Geosciences, Virginia Tech, Blacksburg, VA, USA
Corresponding author: afrida@vt.edu

Keywords: sediment transport, sediment composition, sand-bedded rivers, urbanization

1 Introduction

Urbanization continues to alter natural landscapes by increasing impermeable surfaces, runoff, and erosion rates [1, 2]. These changes significantly impact the sediment dynamics of fluvial systems, often leading to heightened sediment loads, unnatural sediment composition, shifts in grain size distributions, and notable geomorphic changes [3, 4]. Although studies on gravel-bedded rivers provide a solid foundation for understanding fluvial responses to urbanization [3], the findings may not directly translate to other environments, such as sand-bedded rivers [4]. The impact of urbanization on the sediment dynamics of sand-bedded rivers is thus a critical knowledge gap [1, 4]. This study aims to address this gap by examining the effects of urbanization on sediment composition, distribution, and geomorphic adjustments in sand-bedded watersheds. Specifically, we 1) quantify changes in sediment composition in a sand-bedded river system affected by urbanization; 2) assess geomorphic responses, including channel morphology, bank erosion, and floodplain dynamics; and lastly, 3) correlate urban expansion with erosional and depositional changes.

2 Study Area

Our study area is Lake Austin, TX, a sand-bedded river system impacted by vast urban development. Due to documented urban expansion and observed hydrological modifications over the past decades, Lake Austin and its surrounding creeks provide a suitable case study. We focus on Lake Austin and two of its associated creeks, including Bulls Creek, which is one of the prominent contributors of flow and sediment supply into Lake Austin.

3 Methodology

We employ a range of field-based and GIS-based analysis methods to quantify the sediment dynamics and morphological changes of an urban river system. At the lake watershed scale, GIS and remote sensing techniques were employed to analyze land cover changes, urban expansion, and hydrological modifications using historical satellite imagery and elevation models. At the creek scale, detailed fieldwork was conducted to examine local sedimentary and hydrodynamic variations. Sediment samples were acquired from various locations to quantify grain size distribution and composition via sieve analysis in shallow creek watersheds. Channel morphology, including downstream and cross-section profiles, was acquired using remote sensing and geospatial tools like hand-held LiDAR, laser range finder/total station, and Jacob's staff. Decadal, urban expansion and historical land use changes were mapped and quantified using land cover data and city development maps. Finally, sedimentary and morphological characteristics were correlated to urban expansion maps via spatial correlation.

4 Results

We see a correlation between altered grain size distributions and enhanced urbanization. Furthermore, decadal maps reveal morphological changes in both channel width and floodplain size. The changes vary spatially, both within the lake watershed and between smaller creek watersheds that feed the lake.

5 Conclusions

The study integrates field data with geospatial analyses to address the knowledge gap in sand-bedded river responses to urban pressure. We provide an in-depth understanding of how urbanization affects sediment transport, composition, and channel morphology in sand-bedded environments. These findings may thus guide sustainable watershed management practices tailored to sand-bedded systems facing urban expansion.

References

[1] Chin, A. (2006). Urban transformation of river landscapes in a global context. Geomorphology, 79(3–4), 460–487.

[2] Konrad, Christopher & Booth, Derek. (2005). Hydrologic Changes in Urban Streams and Their Ecological Significance. American Fisheries Society Symposium. 47. 157-177

[3] Pizzuto, J. E., Hession, W. C., & McBride, M. (2000). Comparing gravel-bed rivers in paired urban and catchments of southeastern Pennsylvania. Geology, 28(1), 79.

[4] Wolman, M. G., & Schick, A. P. (1967). Effects of Construction on Fluvial Sediment, Urban and Suburban Areas of Maryland. Water Resources Research, 3(2), 451–464. https://doi.org/10.1029/WR003i002p00451.

Effects of initial topobathymetric variability on the modeling of washover deposits

Nil Carrion-Bertran[1], Daniel Calvete Manrique[1], Francesca Ribas Prats[1]
[1]Universitat Politècnica de Catalunya, Barcelona, Spain
Corresponding author: nil.carrion@upc.edu

Keywords: washover deposits, modeling, XBeach, storm.

1 Introduction

Low-lying beaches are highly dynamic coastal environments and particularly susceptible to flooding and storm impacts [1]. During these extreme events, sediment deposits can be observed in the emerged part of the beach, the washover deposits, which can modify the beach morphology contributing to its maintenance or affecting its protective capacity to future incoming storms. Numerical models are essential tools to understand the mechanisms that drive these processes and to develop strategies for coastal management. Therefore, the main goal of this study is to analyse how the initial topobathymetric variability can affect the modelling of the washover deposit formation during extreme events.

2 Methods

In this study, the process-based 2DH XBeach numerical model [2] was employed to simulate a 5-day storm event. As for the topobathymetric initial conditions, a Principal Component Analysis (PCA) and a cluster analysis were performed to 15 topobathymetries from Castelldefels beach (NW Mediterranean) to obtain 5 representative profiles that describe the real variability of the beach. These profiles were then replicated alongshore to obtain alongshore uniform (AU) initial topobathymetries and periodical morphological patterns as mega cusps (MC), rhythmic dunes (RD) and crescentic bars (CB) were included along the beach domain with several wavelengths (λ). To consider the wave group chronology effect, nine realizations of each scenario were simulated.

3 Results

The evaluation of the results was based in the quantification of the sediment deposited in the emerged beach after the storm simulation. The mean and standard deviation of the volumes deposited of each scenario were computed to be able to analyse and compare the outcomes for each case tested.

The results showed similar trends across most of the AU scenarios. In contrast, placing morphological patterns modified the deposited volumes. For the MC scenarios, bigger deposition rates were observed specially when large wavelengths were simulated (Figure 1). In CB and RD tests, these accumulations were significantly lower than in MC.

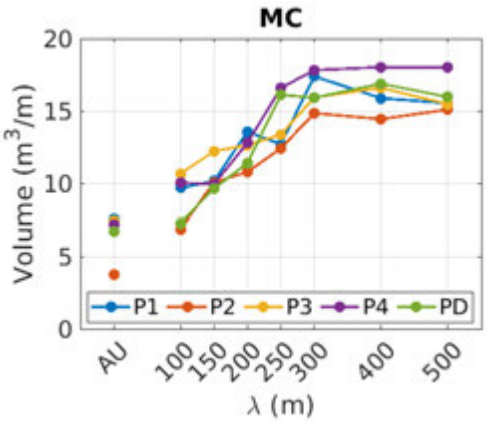

Figure 1: Volumes in AU and MC scenarios for each initial profile and wavelength (λ).

Currently, an extended morphological analysis of the beach evolution is being performed including the assessment of the hydrodynamics at different time steps of the simulation.

4 Conclusions

The results highlight the importance of considering the variability of the initial topobathymetric conditions when modelling the washover deposit formations. Also, these results could also have implications to develop strategies to perform nourishments, as specific scenarios such as MC of certain wavelengths could enhance sediment deposition in the emerged beach.

Acknowledgments

This study was supported by grants PID2021-124272OB-C22 and TED2021-130321B-I00, funded by MCIN/AEI/10.13039/501100011033/ of the Spanish government and by "ERDF A way of making Europe".

References

[1] Cohnn, N. and Ruggiero, P.: The influence of seasonal to interannual nearshore profile variability on extreme water levels, *Coastal Engineering*, col 115, pp. 79-92 (2016).

[2] Roelvink, D., Reniers, A., van Dongeren, A., de Vries, J. V. T., Mc-Call, R., and Lescinski, J.: Modelling storm impacts on beaches, dunes and barrier islands, *Coastal Engineering*., 53, 1133–1152 (2009).

Morphological Effects of a Controlled Flood in Regulated Rivers: A Bathymetric Analysis in the Lower Ebro

Mösso, C.[1,2], Calvillo, B.[1], Astudillo-Gutierrez, C.[1], Gracia, V.[1,2], Sospedra, Q.[1,2], García Vera, M.A.[3], López Gómez, D.[3], Sánchez-Arcilla, A.[1,2]
[1]Laboratori d'Enginyeria Marítima, Universitat Politècnica de Catalunya, Barcelona, Spain
[2]Centre Internacional d'Investigació dels Recursos Costaners (CIIRC), Barcelona, Spain
[3]Confederación Hidrográfica del Ebro (CHE), Zaragoza, Spain
Corresponding author: cesar.mosso@upc.edu

Keywords: Morphology changes, Sediment transport, Controlled flooding.

1 Introduction

Reservoirs provide essential benefits such as water supply, flood protection, electricity, and recreation. However, they disrupt fluvial environments, altering flow dynamics and sediment transport, causing erosion and sedimentation imbalances [1]. Since the mid-20th century, reservoir policies have significantly changed river sedimentation patterns [2]. The Ebro Basin (NE Spain) exemplifies this transformation, with morphological changes and sediment shortages affecting the Ebro Delta [3]. This study examines the morphological effects of a controlled flood in the lower Ebro, between the Mequinenza and Riba-roja reservoirs, to evaluate sediment deposition patterns.

2 Methodology

To assess the effects of an eight-hour controlled flood event at the Mequinenza and Riba-roja Reservoirs on 21/10/2024, two field campaigns were conducted: one before the event (15/10/2024), and another after (18/12/2024). Bathymetric data were acquired using a multibeam GPS-referenced echosounder for high spatial accuracy. Two study areas were selected: the upper Mequinenza Reservoir, where the Ebro and Segre rivers meet, and the downstream section, upstream of the Riba-roja Reservoir (Figure 1a). These sites were strategically chosen to analyse sediment redistribution and bottom evolution due to the flood event. A comparative analysis of pre- and post-flood bathymetric datasets was performed to assess geomorphological and sedimentological changes resulting from the hydrological disturbance.

3 Results and discussions

Figures 1b and 1c illustrate bathymetric variations in the Mequinenza and Riba-roja reservoirs, with bed elevation changes ranging from -3.5 m to 4.5 m. Although the controlled flood altered the bottom, no clear sediment mobilization patterns emerged. Mequinenza showed more pronounced erosion and accretion than Riba-roja, where changes were less significant. Near the Mequinenza dam spillway, a distinct erosion zone formed due to the discharged flow's power. Additionally, significant erosion along the riverbanks contributed to the development of a mid-channel bar. This process led to sediment accumulation in the central area of the Mequinenza Bridge but caused substantial erosion at its extremities, potentially threatening its foundation. In the area closest to the Riba-roja Reservoir, a distinct erosion zone was observed, consistent with processes triggered by the reservoir's opening.

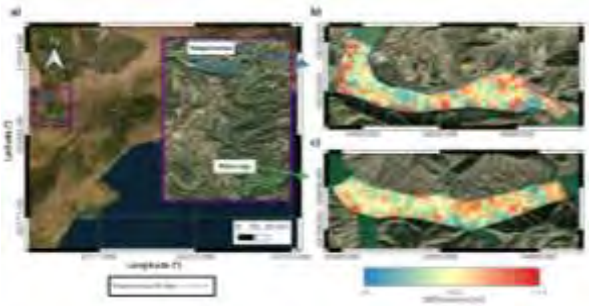

Figure 1. Location map of the study area (a) and the bathymetric differences of the Maquinenza (b) and Riba-roja (c) areas.

4 Conclusions

The controlled flood caused significant morphological changes, with more pronounced erosion and sediment redistribution in Mequinenza than in Riba-roja. Erosion was most intense near the Mequinenza spillway and along the riverbanks, contributing to mid-channel bar formation and the development of an accretion zone near the Mequinenza Bridge. In Riba-roja, erosion was primarily linked to reservoir discharge. While the controlled flood altered the morphology of the reservoir bottoms, it did not produce clear patterns of sediment mobilization.

Acknowledgements

The experiments described in this work were funded by REST-COAST project, (European Union's Horizon 2020 Research and Innovation action No. 101037097).

References

[1] G. E. Petts. Impounded rivers: perspectives for ecological management. Wiley, 1984.
[2] S. Gorostiza, et al. Where have all the sediments gone? Reservoir silting and sedimentary justice in the lower Ebro River. Political Geography 107, 102975, 2023.
[3] D. Vericat, and R. J. Batalla. "Sediment transport in a large impounded river: The lower Ebro, NE Iberian Peninsula." Geomorphology 79.1-2, 72-92. 2006.

Blue Carbon in Salt Marshes of the North Adriatic Sea (Italy): Challenges and Opportunities for Wetland Restoration

Puppin A.[1,2], Blount T.[2], Ghinassi M.[2], Finotello A.[2], D'Alpaos A.[2]
[1]Department of Land, Environment, Agriculture and Forestry, University of Padova, Padova, Italy
[2]Department of Geosciences, University of Padova, Padova, Italy
Corresponding author: alice.puppin@unipd.it

Keywords: Blue Carbon, salt marshes, restoration, wetlands

1 Introduction

Coastal areas, vital to human development and economic activity, provide essential ecological functions and diverse ecosystem services that enhance human well-being (Barbier et al., 2011). However, these ecosystems are increasingly threatened by anthropogenic pressures and climate change impacts. As a result, the protection and restoration of coastal ecosystems have gained attention as effective Nature-based Solutions (NbS). Vegetated coastal ecosystems, such as mangroves, tidal marshes, and seagrass meadows, are particularly valued for their blue carbon (BC) sequestration and storage potential (Macreadie et al., 2019).

The growing interest of the financial sector in natural climate solutions as tools for achieving corporate net-zero emissions targets underscores the importance of blue carbon projects as engines for coastal wetland conservation and restoration, which offer numerous co-benefits. However, significant uncertainties remain in estimating carbon stocks and sequestration rates in vegetated coastal environments, partly due to high variability at local scales (Puppin et al., 2024).

2 Aim and methods

To better understand variations in BC distribution in salt marsh soils and the physical and biological factors driving BC dynamics, we analysed soil organic content across diverse salt marshes in the wetland areas of the Northern Adriatic Sea (Italy).

The Northern Adriatic Sea basin is the shallowest and northernmost region of the Mediterranean, and its coastal wetlands are critical for biodiversity conservation at both national and international levels. Characterized by lagoon-river delta systems, moderate wave exposure, and a semi-diurnal microtidal regime, the region has experienced significant sediment supply reductions due to development pressures, leading to accelerated erosion and unprecedented loss of salt marshes (Lo et al., 2017).

In this study, we collected over 70 sediment cores, up to 1 m deep, from the Venice Lagoon and the Caorle Lagoon, with plans to expand sampling locations (e.g. Po Delta). Loss-on-Ignition (LOI) analysis was conducted to measure organic matter (OM) and organic carbon (OC) content in sediment samples. These analyses allowed us to link BC patterns to soil, geomorphic, and environmental variables, providing valuable insights to evaluate restoration approaches.

3 Preliminary results and conclusions

Our preliminary results show that the studied marshes store 171 ± 57 tons C km^{-2} in the Venice Lagoon and 115 ± 36 tons C km^{-2} in the Caorle Lagoon within the top 1 m of soil. We identified relationships between BC stock and factors such as autochthonous and allochthonous organic inputs, sediment properties, relative sea level rise, fluvial inputs, and wave action. Our findings emphasize the significant carbon storage potential of intertidal marshes and provide a conceptual framework for understanding BC dynamics and their drivers. These insights provide valuable guidance for improving coastal management and marsh restoration strategies, optimizing their effectiveness as Nature-based Solutions.

Acknowledgments

This study was funded within the RETURN Extended Partnership and received funding from the European Union Next-GenerationEU (National Recovery and Resilience Plan – NRRP, Mission 4, Component 2, Investment 1.3 – D.D. 1243 2/8/2022, PE0000005). This study was carried out within the PRIN 2022 project "Eco-geomorphic CArbon Pumping from rivers To blUe caRbon Ecosystems" (e-CAPTURE).

References

[1] E. B. Barbier, et al., The value of estuarine and coastal ecosystem services. *Ecological Monographs,* 81, 169–193, 2011.

[2] V. B. Lo, T. J. Bouma, J. van Belzen, C. Van Colen, L. Airoldi, Interactive effects of vegetation and sediment properties on erosion of salt marshes in the Northern Adriatic Sea. *Marine Environmental Research,* 131, 32–42, 2017.

[3] P. I. Macreadie, et al., The future of Blue Carbon science. *Nature Communi*cations, 10, 1–13, 2019.

[4] A. Puppin, et al., Blue Carbon Assessment in the Salt Marshes of the Venice Lagoon: Dimensions, Variability and Influence of Storm-Surge Regulation. *Earth's Futur*e, 12, 1–14, 2024.

Tidal-Driven Sediment Transport Across Oyster Reefs: Insights from Laboratory Experiments

Javier Zumbado-Gonzalez [1], Jorge San Juan [1]

[1]Department of Civil and Environmental Engineering, North Carolina State University, Raleigh, USA

e-mail corresponding author: jzumbad@ncsu.edu

Keywords: *hydrodynamics, sediment transport, turbulence, oyster reefs, currents, nature base solutions*

1 Introduction

Oyster reefs are ecosystem engineer species that significantly influence local hydrodynamics through their rough surfaces and structural complexity [2], and provide many ecosystem services such as water filtration, habitat provision, carbon sequestrations, oyster and fish production, among others [3].

Understanding the hydrodynamic and sediment transport processes over oyster reefs is essential for determining their impact on shoreline evolution while advancing ecological restoration and enhancing coastal resilience [1]. However, the effects of reef morphology, density, and porosity on sediment resuspension, deposition, and transport remain poorly understood, limiting the ability to improve reef restoration for sediment stabilization. This study investigates the sediment transport capacity of flow over a flume-scale oyster reef under controlled hydrodynamic conditions.

2 Methods

A physical model of the oyster reef will be fabricated from 3D scans of real oyster clusters and cast into flume-scale models. The oyster clusters will be designed with specific geometric parameters (e.g., cluster-to-cluster spacing, reef height and length, frontal area, and solid volume fraction) to assess the impact of reef complexity on suspended sediment transport. Experiments will be conducted in a 10-meter-long, 1-meter-wide, and 0.5-meter-deep recirculating flume at NC State University. Flow and turbulence parameters will be measured using an Acoustic Doppler Velocimeter (ADV) and a Particle Image Velocimetry (PIV) system. Suspended sediment concentrations will be determined using Optical Backscatter Sensors (OBS) and direct water sampling.

3 Results

Our findings will provide insights into the relationship between suspended sediment concentration—both near the bed and throughout the water column—and key flow parameters, including turbulent kinetic energy (TKE), hydraulic roughness, bed shear stress, and oyster canopy geometric characteristics. For instance, Figure 1 presents a TKE profile obtained in the laboratory, comparing sparse and dense oyster densities. The profiles diverge within the oyster canopy, which may have significant implications for sediment resuspension and deposition.

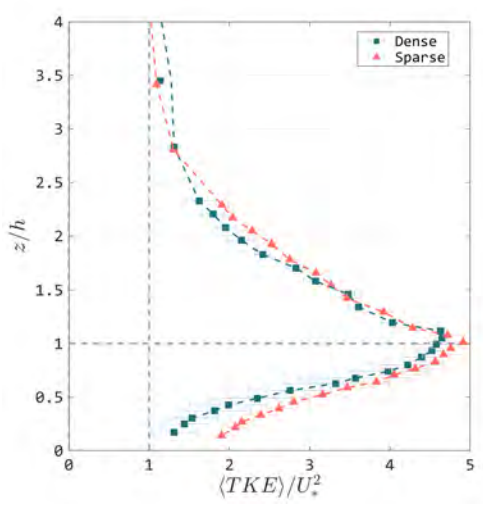

Figure 1: Turbulent kinetic energy profile along the water depth. h is the oyster height and U_* is the shear velocity.

These results will contribute to understanding the role of oyster reefs in the landscape evolution of wetlands and estuaries and their potential application as natural coastal protection to mitigate erosion and enhance resilience to climate change.

References

[1] Bas W. Borsje, Bregje K. Van Wesenbeeck, Frank Dekker, Peter Paalvast, Tjeerd J. Bouma, Marieke M. Van Katwijk, and Mindert B. De Vries. How ecological engineering can serve in coastal protection. *Ecological Engineering*, 37(2):113–122, February 2011. ISSN 09258574. doi: 10.1016/j.ecoleng.2010.11.027. URL https://linkinghub.elsevier.com/retrieve/pii/S0925857410003216.

[2] David J. Cannon, Kelly M. Kibler, Jyotismita Taye, and Stephen C. Medeiros. Characterizing canopy complexity of natural and restored intertidal oyster reefs (Crassostrea virginica) with a novel laser-scanning method. *Restoration Ecology*, 31(7):e13973, September 2023. ISSN 1061-2971, 1526-100X. doi: 10.1111/rec.13973. URL https://onlinelibrary.wiley.com/doi/10.1111/rec.13973.

[3] Jonathan H. Grabowski and Charles H. Peterson. Restoring oyster reefs to recover ecosystem services. In *Theoretical Ecology Series*, volume 4, pages 281–298. Elsevier, 2007. ISBN 978-0-12-373857-8. doi: 10.1016/S1875-306X(07)80017-7. URL https://linkinghub.elsevier.com/retrieve/pii/S1875306X07800177.

From Data to Decisions: Hydrotechnical Monitoring

Blanca Marin-Esteve[1], Sarah Davidson[1], Sarah Newton[2]
[1]BGC Engineering, Vancouver, Canada [2]Cambio Earth Systems, Calgary, Canada
Corresponding author: bmesteve@bgcengineering.ca

Keywords: real-time monitoring, geohazards, pipelines, linear infrastructure, infrastructure resilience

1 Introduction

In recent decades, hydrotechnical hazard management in linear infrastructure, such as pipelines and transportation corridors, relied on periodic inspections and Geographic Information System (GIS)-based mapping. These programs relied on static reports summarizing hazards without real-time spatial analysis, linking GIS points to report descriptions instead of interactive models, which limited dynamic risk assessment and made it difficult to track evolving conditions and respond efficiently.

With more real-time and near-real-time data, combined with advancements in artificial intelligence (AI) and geospatial analytics, infrastructure operators can better monitor and assess hydrotechnical and geohazard risks. This improves hazard identification, enables proactive decision-making, and enhances infrastructure resilience. However, managing the growing volume and variety of data presents challenges in processing and analysis, requiring advanced tools to extract meaningful insights efficiently [1].

2 Cambio™: A Comprehensive Geohazard Management Solution

Cambio™ produced by Cambio Earth Systems is a next-generation geohazard management software that centralizes and processes vast amounts of real-time and near-real-time data [2]. It acts as a single source of truth for project teams—including owners, contractors, and consultants—facilitating collaboration and data-driven decision-making.

Cambio™ integrates multiple data sources, including real-time hydrometric, alongside remote sensing technologies like LiDAR and InSAR. Additionally, it incorporates geotechnical instrumentation such as Inline Inspections (ILI), tool strain data, and LiDAR change detection (LCD). These capabilities enable continuous monitoring, early warning systems, and risk assessment for infrastructure vulnerable to geohazards.

AI is a crucial component of modern geohazard management, automating data processing, improving pattern recognition, and enhancing predictive modelling. Cambio Earth Systems and BGC Engineering continue to expand AI capabilities with tools such as InSAR time-series analysis and Morphological Change Detection. These advancements improve hazard detection, refine predictions, and enable real-time trend analysis for early warnings and proactive mitigation, streamlining risk assessments and decision-making.

3 Extreme Event Monitoring

Extreme event monitoring is one of the features of the Cambio™ platform, strengthened by its integration with inspection and assessment data. By leveraging snowpack, rainfall, and stream gauge information, Cambio™ provides real-time insights into high-risk hydrotechnical areas. When gauge data is unavailable or distant, the system interpolates and prorates values to the infrastructure location, ensuring accurate hazard assessment and timely response.

Cambio™'s digital stream network processes real-time data from thousands of gauges. The system delivers early warnings, enabling proactive responses and continuous monitoring throughout an event. This capability is used by to monitoring floods for 30 infrastructure operators spanning 560,000 km of pipelines, railways, and highways. Operators use Cambio™ to support emergency actions like mitigation measures, site closures, or pipeline shut-ins, followed by detailed post-event assessments to ensure infrastructure safety.

4 Future Directions

The next phase of development focuses on expanding AI-driven methodologies to further improve risk detection and mitigation. InSAR time-series analysis, Flood Forecasting, and Morphological Change Detection will enhance predictive capabilities, allowing operators to anticipate and respond to threats such as bank erosion and channel migration at the infrastructure location before threats escalate.

4 Conclusions

The rise of real-time data has transformed hydrotechnical hazard management, enabling risk-informed decisions and predictive modelling. Cambio™ integrates diverse datasets to identify key hazards like flooding and scour, providing operators with real-time and historical insights.

References

[1] C. Johnson, S. Schmidt, J. Taylor, and J. de La Chapelle. Geospatial Database Development: Supporting Geohazard Risk Assessments Through Real-Time Data and Geospatial Analytics. *ASME 2022 13th International Pipeline Conference,* 2022.

[2] A. Baumgard and K. Burkell. The Use of Advanced Geohazard Management Software to Incorporate Real-Time and Near-Time Data into Decision Making. *2024 Pipeline Technology Conference*, 2024.

Repeated bathymetrical surveys reveal transient storage of sediment in the near-field region of the plunging Rhône River inflow into Lake Geneva

Stan Thorez[1], Ulrich Lemmin[2], D. Andrew Barry[2], Koen Blanckaert[1]
[1] TU Wien, Vienna, Austria
[2]Ecole Polytechnique Fédérale de Lausanne (EPFL), Lausanne, Switzerland
Corresponding author: stan.thorez@tuwien.ac.at

Keywords: hyperpycnal inflows, plunging, erosion, transient sediment storage

1 Introduction

Negatively buoyant (hyperpycnal) river inflows plunge upon entering lakes or reservoirs, feeding gravity-driven underflows that propagate along the bed [1, 2]. When these underflows encounter a layer of equal density within the water column, they detach from the bed and transition into an interflow. In this light, the hydro-sedimentary processes related to plunging set the upstream boundary conditions for under- and interflows. The interaction of a plunging flow with the local lake bed is understudied as of yet. Using ADCP velocity and backscatter data, Thorez et al. (2024) [3] hypothesized that the plunging Rhône River inflow into Lake Geneva locally eroded the bed near the river mouth during high discharge and high suspended sediment conditions on June 26, 2019, yet they did not prove this using repeated bathymetrical survey data. The aim of the present contribution is to test and demonstrate this hypothesis.

2 Methods

Boat-towed ADCP measurements were used to elucidate the near-field bathymetry of the plunging Rhône River plume in Lake Geneva along longitudinal (away-from-mouth) transects. These measurements were performed on June 23, June 26 and July 11, 2019.

3 Results and discussion

Figure 1 reveals that between June 23 and June 26, 2019, the lake bed within the plunging region aggraded by an amount in the order of 1 m and up to a maximum of 2 m, indicating that the hydro-sedimentary processes related to plunging were nett depositional in nature. No significant changes in the bed height were measured further downstream. Between June 26 and July 11, 2019, the lake bed eroded by up to 10 m in the plunging region and in the order of 5 m further downstream. This is in accordance with the findings of Thorez et al. (2024) [3] that state that the conditions on June 26, 2019, most likely led to erosion. The consecutive periods of deposition and erosion comply with their hypothesis of transient storage of sediment within the plunging region.

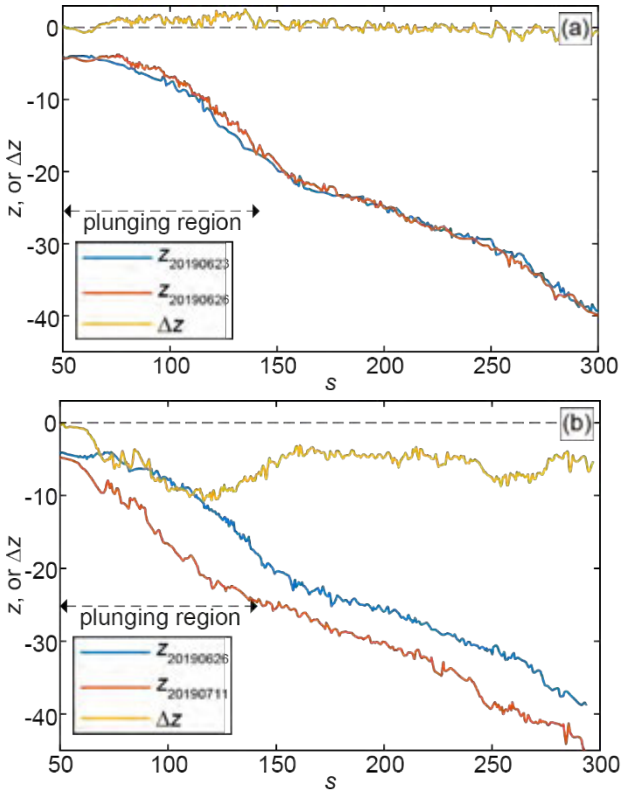

Figure 1: Longitudinal bathymetrical profiles on and differences between (a) June 23 and June 26, and (b) June 26 and July 11. Positive bathymetrical differences indicate deposition, negative values indicate erosion. A double arrow indicates the plunging region. The longitudinal distance from the river mouth is indicated by *s*, the local depth by *z* and the difference in depth by Δ*z*.

Acknowledgments

This work is supported by the Austrian Science Fund (FWF) (Grant number I 6180).

References

[1] F. A. Forel. Les ravins sous-lacustres des fleuves glaciaires. *C. R. Acad. Sci.*, 101: 725–728, 1885.

[2] H. B. Fischer, E. J. List, R. C. Y. Koh, J. Imberger and N. H. Brooks. *Mixing in inland and coastal waters*. Academic Press, San Diego, 1979.

[3] S. Thorez, U. Lemmin, D. A. Barry and K. Blanckaert. Hydro-Sedimentary Processes of a Plunging Hyperpycnal River Plume Revealed by Synchronized Remote Imagery and Gridded Current Measurements, *Water Resour. Res.*, 60, 2024.

Interventions in a River Bifurcation Region: A Hybrid Modeling Strategy

Marijn Wolf[1], Astrid Blom[1], Ralph Schielen[1,2]

[1]Delft University of Technology, Netherlands
[2]Ministry of Infrastructure and Water Management-Rijkswaterstaat, Netherlands

e-mail corresponding author: marijnwolf@gmail.com

Keywords: *river bifurcation, interventions, river response, numerical modelling*

1 Introduction

The Rhine River system has been subject to human interventions for centuries and represents one of the most heavily engineered river systems in Europe. Challenges such as continuing channel bed incision and hydrograph alterations due to climate change [3] are expected to have profound future implications on river functions like flood safety, freshwater availability, and inland shipping. Over the past decades, extensive projects including "Room for the River", the implementation of longitudinal training walls, and sediment nourishments have assured the Rhine to maintain its functions.

The Pannerdense Kop bifurcation, where the Dutch upper Rhine partitions flow and sediment among the Waal, and Pannerden Canal, shows a gradual change in flow division between the branches [2]. This shift seems to be linked to a series of peak flow events in the 1990s, which deposited sediment in one of the bifurcates, triggering a gradual change in flow partitioning since then. More recently, Blom et al. [1] suggested that the 1990s peak flows may have induced system tipping and the approach of an alternative equilibrium state.

Maintaining the desired flow partitioning is critical not only for ensuring water availability and navigability during low-flow conditions but also for managing flood risk during peak events.

2 Objective and Method

This study aims to assess a range of interventions designed to sustain the desired flow partitioning and reduce channel bed erosion over long time scales (50–150 years). Previous studies have assessed interventions like floodplain lowering and sediment nourishment outside the context of a bifurcation, or have modelled the bifurcation without interventions. This study, in contrast, focuses on interventions and climate change adaptation within the Pannerdense Kop bifurcation.

We explore two approaches to assess the effectiveness of combinations of conventional engineering measures and nature-based solutions: (1) a one-dimensional modelling approach, and (2) a hybrid one/two-dimensional modelling approach. The boundary conditions for the two-dimensional domain of the bifurcation are dynamically linked to the one-dimensional model sections of the river branches. We assess whether this dynamic coupling can capture lateral flow exchanges between the main channel and floodplain, sediment transport, and bed evolution processes within the bifurcation region, while retaining the computational efficiency characteristic of one-dimensional models.

3 Early results

Early results from a one-dimensional approach indicate that interventions covering several tenths of kilometres are less effective at reducing channel bed erosion than interventions covering multiple short sections. We expect that the effectiveness of interventions is significantly different in the presence of a bifurcation compared to single-channel conditions, with the specific design and location of interventions playing a crucial role. This analysis will provide insights into the relative effectiveness of a range of intervention strategies under various climate change scenarios, informing the development of adaptive management plans that enhance the long-term resilience of the Rhine River system.

References

[1] A. Blom, C. Ylla Arbós, M.K. Chowdhury, A. Doelman, M. Rietkerk, and R.M.J. Schielen. Indications of ongoing noise-tipping of a bifurcating river system. *Geophysical Research Letters*, 51 (22), 2024. doi: 10.1029/2024GL111846.

[2] M.K. Chowdhury, A. Blom, C. Ylla Arbós, M.C. Verbeek, M.H.I. Schropp, and R.M.J. Schielen. Semicentennial response of a bifurcation region in an engineered river to peak flows and human interventions. *Water Resources Research*, 59(4), 2023. doi: 10.1029/2022WR032741.

[3] C. Ylla Arbós, A. Blom, C.J. Sloff, and R.M.J. Schielen. Centennial channel response to climate change in an engineered river. *Geophysical Research Letters*, 50(8), 2023. doi: 10.1029/2023GL103000.

Field-Based Characterization of Hydro-Morphodynamic Processes at Barrier Breaches Induced by Hurricanes Helene and Milton

Sam Holberg[1], Celso Castro-Bolinaga[1], Nina Stark[2], Jonathan Hubler[3], Michael Gardner[4], Alexandra Schueller[5]
[1]Department of Biological and Agricultural Engineering, North Carolina State University; [2]Department of Civil and Coastal Engineering, University of Florida; [3]Department of Civil and Environmental Engineering, Villanova University; [4]Department of Civil and Environmental Engineering, University of California, Davis; [5]Department of Civil, Construction, and Environmental Engineering, University of Delaware

Keywords: hydraulics, sediment, barrier breach, hurricanes.

1 Introduction

A joint team from the Nearshore Extreme Events Reconnaissance (NEER) Association and from the Geotechnical Extreme Events Reconnaissance (GEER) Association, supported by the National Science Foundation, was mobilized in October and November of 2024 to investigate the impacts of storm surge and waves and resulting sediment erosion and deposition from Hurricanes Helene and Milton. As part of this investigation, the team conducted a comprehensive set of field measurements to characterize channel bathymetry, water flow regime, sediment transport conditions, as well as channel-bed sediment geotechnical characterization, erodibility, and composition at barrier breaches that occurred on the western coast of Florida, USA. This poster presentation will focus on the findings of the multifaceted set of field measurements, providing insights into the hydro-morphodynamic processes that modulate the onset of barrier breaches induced by severe storms.

2 Study Area

This poster presentation will specifically focus on two barrier breaches that occurred following Hurricanes Helene and Milton on the western coast of Florida, south of the City of Sarasota, USA. Both sites experienced extreme wind storm surges upwards of 1.5 m twice within a two-week period, causing the creation of Milton Pass and the reopening of the mechanically closed Midnight Pass (Fig. 1). Therefore, both sites are unique because they experienced the impact of consecutive severe storms within a short period of time.

3 Measurements and Results Outlook

The data collected at and around each of the barrier breaches included: channel bathymetry, flow velocities, and discharge data using a Teledyne RiverPro Acoustic Doppler Current Profiler (ADCP) (Fig. 1); shear strength, friction angle, and relative density of superficial channel-bed sediments using a portable free-fall penetrometer (PFFP) *blueDrop* [1]; cone resistance and layering of sands using an instrumented dynamic cone penetrometer (DCP) [2]; erodibility parameters of channel-bed sediment via Jet Erosion Testing [1]; and channel-bed sediment grain size distribution and composition from volumetric samples [1].

This poster presentation will provide an analysis of the collected data, specifically looking at the relationship between applied forces (as characterized via ADCP measurements) and resistive forces (as characterized via PFFP, DCP, and JET measurements), ultimately providing an improved understanding of hydraulic, sediment transport, and geotechnical characteristics at and around newly formed breaches. These data, together with the larger dataset collected by the NEER-GEER Team [3], aims to contribute towards improving risk assessment and impact prediction from severe storms on coastal communities.

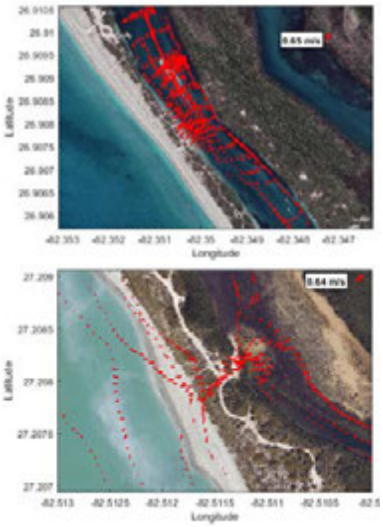

Figure 1: Milton Pass (Top) and Midnight Pass (Bottom) formed following Hurricanes Helene and Milton in November 2024. Red arrows illustrate the ADCP-measured depth-averaged velocities, indicating magnitude and direction. Underlying imagery shows barrier islands before breaching.

4 References

[1] Brilli, N. C., Stark, N., & Castro-Bolinaga, C. (2024). Relating Geotechnical Sediment Properties and Erodibility at a Sandy Beach. *J. Waterway, Port, Coastal, and Ocean Eng.*, https://doi.org/10.1061/JWPED5.WWENG-2016.

[2] Hubler, J. F., Mayer, T., Stark, N., Hummel, E., Zhang, J., & Hsu, T.-J. (2025). Measurement of Changes in Beach Sand Soil Stiffness due to Fluctuating Tides. *J. Waterway, Port, Coastal, and Ocean En.*, https://doi.org/10.1061/JWPED5.WWENG-2139.

[3] Stark, N., Gardner, M., Grilliot, M., Lyda, A., Dedinsky, K., Mueller, J., Pezoldt, C., Hubler, J., Castro-Bolinaga, C., Schueller, A., Zhan, W., Haefeli, M., Burghardt, S., Wondolowski, M., Holberg, S., Hassan, M., Parker, J., Laurel-Castillo, J., Eggensberger, L., Nichols, E., Herndon, H., Wang, P., Olabarrieta Lizaso, M., Raubenheimer, B., Hashash, Y., ADUSEI, S., Jafari, N., (2025). NEER/GEER: Hurricanes Helene & Milton Dataset, in *Multidisciplinary Pre, During and Post Storm Data Collection*. DesignSafe-CI. https://doi.org/10.17603/ds2-m8h3-5802

Acknowledgements

The authors acknowledge funding from the National Science Foundation through grants 1939275 (NEER), 1826118 (GEER), 2130997 (NHERI RAPID), and 2501467 (Stark). The authors also acknowledge all NEER/GEER team members, including researchers, practitioners, federal agency representatives, professional staff from the UW NHERI RAPID facility and the UF CCS, and students who participated in person or remotely, without whom this data collection effort would not have been possible. Most importantly, the authors would like to thank the community members and local authorities who have been supportive throughout the data collection efforts and provided access to the measurement locations.

Evolution of tides and water levels over 70 years in a macrotidal and highly urbanized estuary

Juliette Pénicaud[1], Aldo Sottolichio[1], Isabel Jalón-Rojas[1]
[1]Université de Bordeaux, France

Corresponding author: juliette.penicaud@hotmail.com

Keywords: extreme water level, tide, morphodynamics, Gironde estuary

1.Introduction

Coastal flooding is a major hazard, related to extreme level water levels dues to storm surges. In the context of increasing human pressure, accurate water level predictions are necessary to ensure the safety of local human society. In tidal estuaries, water level depends on several parameters including tidal range, mean water level, wind and waves. These parameters are subject to short and long term evolution under global and local effects. On one hand, mean water level has changed over last century due to the relative sea level rise. On an other hand, local morphological changes in estuaries, including anthropogenic engineering of channels and cross-section can modify tides and tidal propagation [1] [2] and therefore water levels. In this context, it is crucial to better understand the past evolution of water levels jointly with morphology, especially in documented, intensively developed areas.

2. Study area

The Gironde estuary is a highly-turbid, macrotidal convergent estuary, the largest in western Europe. After intense land reclamation the XIX century, it was less developed in the XX century. Compared to other macrotidal European estuaries, the Gironde estuary is therefore known to has a moderate natural morphology [3]. Under climate change and present-day conditions, more extreme water levels are expected to increase the risk of flooding and be very damaging to this densely populated and industrialised estuary.

Recent studies have focused on the tidal Garonne river upstream of the Gironde estuary. They revealed the impact of hydrological changes on the evolution of tidal distortion in the tidal river [4]. The reduction of river flow and the sand mining caused tidal range amplification and increase asymmetry, leading to more mud trappIng. However, the evolution of the lower portion of the estuary (downstream the confluence of the Garonne and Dordogne river) is less known.

The general objective of this work is to understand the evolution of tides and high water levels and to evaluate the impact of morphological changes.

3. Methodology and results

This study uses water level time series at four stations in the estuary downstream the confluence (Figure 1). The data are manually digitized for years 1945, 1953, 1962, 1971, and more recent data are added until 2020. The studies also exploites historical data of local bathymetry for the same periods. The study reveals that despite weak development in the Gironde estuary, morphological changes due to mud sedimentation and dynamics of the turbidity maximum promoted tidal amplification and increase of tidal asymmetry in a simiar way than the tidal rivers.

Figure 1 : General view of the Gironde estuary

References

1 Talke, S. A., & Jay, D. A. (2020). Changing tides: The role of natural and anthropogenic factors. *Annual review of marine science*, *12*(1), 121-151.

2 Moore, R. D., Wolf, J., Souza, A. J., & Flint, S. S. (2009). Morphological evolution of the Dee Estuary, Eastern Irish Sea, UK: A tidal asymmetry approach. *Geomorphology*, *103*(4), 588-596.

3 Sottolichio, A., Hanquiez, V., Périnotto, H., Sabouraud, L., & Weber, O. (2013). Evaluation of the recent morphological evolution of the Gironde estuary through the use of some preliminary synthetic indicators. *Journal of Coastal Research*, (65), 1224-1229.

4 Jalón-Rojas, I., Sottolichio, A., Hanquiez, V., Fort, A., & Schmidt, S. (2018). To what extent multidecadal changes in morphology and fluvial discharge impact tide in a convergent (turbid) tidal river. *Journal of Geophysical Research: Oceans*, *123*(5), 3241-3258.

Erosion behaviour of cohesive riverine sediments: joint measurements with SETEG² and EROMES

H. HADDAD[1], N. PELLERIN[2], H. DURY[3], M. JODEAU[4], E. VALETTE[5], M. DARBOT[1], T. FRETAUD[1], C. LEGOUT[6]
[1]CNR, Lyon, France
[2]INRAE, Lyon, France
[3]Suez consulting, Lyon, France
[4]LNHE, EDF R&D - LHSV, Chatou, France
[5]EDF Hydro, CIH, La Motte Servolex, France
[6]Univ. Grenoble Alpes, CNRS, IRD, Grenoble INP, IGE, Grenoble, France
Corresponding author: h.haddad@cnr.tm.fr

Keywords: Cohesive sediment, Rivers, Reservoirs, Erodibility, Laboratory tests

1 Introduction

Sedimentation of reservoirs has become critical in the last decades and constitutes a major challenge for operators and owners of hydraulic structures. To optimize and plan operations such as dredging or flushing operations, it is crucial to evaluate the erosion resistance of cohesive sediments deposited in rivers and reservoirs. These characteristics are implemented in numerical models to simulate reservoir flushing events and downstream deposits evolutions.

Various devices measure the resistance of cohesive sediment exist (e.g., jet erosion devices, annular flumes, etc.). However, there is no reference device among them and little inter-comparisons between devices was done, particularly for sediments from rivers and reservoirs.

Therefore, the aims of this study were to (i) create an erodibility measurements database of riverine sediments and (ii) compare the measurements of two instruments.

2 Methods

Sediment was sampled in four French reservoirs (Cheylas, St-Egreve, Vaugris, Genisssiat) located on the Isère or Rhône rivers. 27 cores were eroded in the CNR-CESAME laboratory with two distinct devices.

The SETEG² erodimeter [1] is a laboratory longitudinal erosion channel designed at CNR in partnership with the University of Stuttgart. It generates a longitudinal flow with shear stresses up to 15 Pa on a sediment test section. Cumulated eroded volume during a test is evaluated by an optical measurement with the Photosed system. The EROMES device [2] is a portable device. It generates a rotating flow using a propeller in a chamber (10cm diameter) with shear stresses up to 10-15 Pa. Turbidity is monitored and allows to evaluate the erosion rate during a test.

Two variables of the Partheniades law were derived from the measurements, a critical shear stress τ_c and an erosion rate M.

3 Results

Critical stresses were between 0.2 and 6 Pa for the EROMES while they ranged between 0.2 and 2.6 Pa for the SETEG² (Figure 1). There was no obvious relationship between the two instruments, but there was consistency. The measurements performed at various depths on sediment cores showed an increase in stress with depth (and therefore sediment consolidation) with differences between reservoirs. The Partheniades coefficient varied between 0.5 and 11 $g.m^{-2}.s^{-1}$ (EROMES) and between 0.5 and 18 $g.m^{-2}.s^{-1}$ (SETEG²).

The relevance of other erosion laws from the literature was also assessed: the Partheniades equation was suitable for both devices.

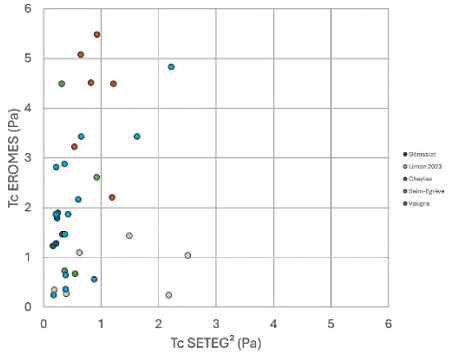

Figure 1: Comparison of critical shear stress measured by the two devices.

4 Perspectives

These measurements on riverine sediments question the measurement protocols. They need to be adapted to evaluate the measurement uncertainty. This work also highlights the different types of erosion (surface/mass) encountered in the laboratory and in situ.

References

[1] Noack, M., Schmid, G., Beckers, F., Haun, S., Wieprecht, S., 2018. PHOTOSED—PHOTOgrammetric Sediment Erosion Detection. Geosciences 8, 243.

[2] Andersen, T. J. (2001). Seasonal Variation in Erodibility of Two Temperate, Microtidal Mudflats. Estuarine, Coastal and Shelf Science, 53(1), 1–12.

Impact of Steel Industry Waste Dumping on Shoreline Dynamics: A Remote Multi-Decadal Analysis in Sagunt, Valencia

Josep E. Pardo-Pascual[1], Carlos Cabezas-Rabadán[2,3], Jesús Palomar-Vázquez[2]
[1]CGAT research group, Dept. Cartographic Eng., Universitat Politècnica de València, Spain
[2]Univ. Bordeaux, CNRS, Bordeaux INP, EPOC, UMR 5805, F-33600 Pessac, France
Corresponding author: carcara4@upv.es

Keywords: coastal erosion, shoreline monitoring, satellite-derived waterlines, SHOREX, Western Mediterranean.

1 Introduction

From 1923 to 1984, the iron and steel industry located next to the Port of Sagunt dumped into thecoast the waste from the transformation of iron ore. This led to the lithification of the coastal materials (sands and gravels) and transformed more than 4 km of beaches south of the port into a rocky coast, forming micro-cliffs. In this coast the wave regime (mainly from the ENE) combined with the coastline orientation, induces strong dowdrift toward the south. In this scenario, the Port of Sagunt (from the start of the 20th century) acted as a sediment trap, leading to northern sand accumulation without, however, causing significant shoreline retreat at its south [1]. This stability may be attributed to the lithification of materials induced by the cementitious components in slag deposits accumulated over decades. The port underwent a major expansion from April 2002 with the construction of a new southern breakwater. Here a remote approach for the multi-decadal characterisation of the shoreline position is presented describing the evolution from the time when the dumping ceased until the present day and analysing the changes in relation with the human action.

2 Materials and methods

From all cloud-free images acquired by Landsat 5, 7, 8 and 9 and Sentinel 2 satellites between 1/06/1984 and 5/02/2023, 1105 satellite-derived waterlines (SDWs) were extracted with an accuracy of about 3.5 m - 4 m RMSE using the tool SHOREX [3]. Spatial-temporal models (STMs) were derived [4] quantifying the mean annual shoreline changes.

3 Results and discussion

Shoreline position changes appear quantified with respect to the average position in 1984 (Figure 1). The blue (red) range of colours indicates accretion (erosion).

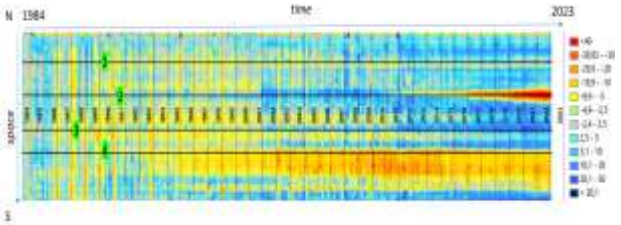

Figure 1: STM of the shoreline changes including the location of the analysed profiles (P1-P4).

Figure 2: Annual mean shoreline position changes.

Profiles 2 and 4 showed most important differences in shoreline behaviour (Figure 2). P2 was stable until 2009, when sharp erosion appeared. The waves managed to dismantle the cliff enabling the erosion on disaggregated materials (gravel and sand). Although the dyke built in 2002 provides shelter from the stronger ENE waves, it also impedes the arrival of new sediment from the north, probably leading to the progressive emptying of the submerged profile and facilitating the cliff breakage. The erosion appears linked to the main storms and may be related to the swell direction of each of these storms. The southernmost sector (P4) has experienced erosion from 1984, probably because lithification was reduced further away from the cementing source.

Acknowledgments

SIMONPLA project of the Thinkinazul programme supported by the MCIN with funds from the European Union Next GenerationEU (PRTR-C17.I1) and Generalitat Valenciana (GVA), and the contract CIAPOS/2023/394 funded by the GVA and the European Social Fund Plus.

References

[1] Pardo-Pascual. La erosión antrópica en el litoral valenciano. Conselleria d'Obres Públiques, Urbanisme i Transports, 1991.

[2] Cabezas-Rabadán, C., Pardo-Pascual, J.E., Palomar-Vázquez, J. Characterizing the relationship between the sediment grain size and the shoreline variability defined from sentinel-2 derived shorelines. *Remote Sensing*, 13(14), 2829, 2021

[3] Cabezas-Rabadán, C., Pardo-Pascual, J. E., Palomar-Vazquez, J., and Cooper, A. A remote monitoring approach for coastal engineering projects. *Scientific Reports*, 15(1), 2955, 2025.

Characterizing 10 years of shoreline dynamics of a Mediterranean coast with Sentinel 2

Raquel González-Fernández[1], Eduard Angelats[2], Francesca Ribas[3], Riccardo Angelini[4]
[1]Faculty of Geosciences, Utrecht University, The Netherlands
[2]Geomatics Research Unit, Centre Tecnologic de Telecomunicacions de Catalunya (CTTC/CERCA), Spain
[3]Physics Department, Universitat Politecnica de Catalunya, Spain
[4]Department of Civil and Environmental Engineering, University of Florence, Italy
Corresponding author: r.gonzalezfernandez@students.uu.nl

Keywords: coastal morphodynamics, megacusps, km-scale shoreline sand waves, shoreline, multispectral imagery

1 Introduction

Sandy beaches are dynamic, three-dimensional systems shaped by morphodynamic patterns that affect sediment transport in both cross-shore and alongshore directions. Factors such as Mean Sea Level Rise (MSLR) and shoreline undulations can reshape beach morphology and sediment dynamics, making shoreline monitoring essential for understanding coastal systems and improving coastal management. Despite their importance, many of these processes remain poorly understood [1] due to historical limitations in data availability. However, recent advances in open-access multispectral satellite imagery have played a key role in bridging this gap by providing medium- to high-resolution, high-frequency imagery with global coverage, transforming coastal studies into a data-rich field.

2 Materials and Methods

MegaShore, a tool for shoreline extraction and megacusp characterization from multispectral satellite imagery [2], was applied along a 12 km stretch of sandy coast in the South Llobregat Delta (SLD), in the western Mediterranean. Using Sentinel-2 satellite imagery, shoreline positions were extracted and analysed between 2015 and 2025. Three different water indices in combination with two binarization methods were tested to identify the most effective approach for shoreline extraction. Both cross-shore and alongshore shoreline variability were subsequently analysed. The alongshore-averaged cross-shore distance between the shoreline position and the backshore limit was calculated and a Linear Regression Rate was determined for the entire area as well as for individual sectors. Shoreline undulations, including megacusps and km-scale shoreline sand waves (KSSWs), were also identified and characterised using shoreline sinuosity (s) standard deviation (σ_s) mean amplitude (a) and mean wavelength (λ).

3 Results and conclusions

A total of 304 valid shorelines were extracted from 353 images using the Water Index (WI) and K-means binarization, which proved the most accurate results. The shoreline showed an overall mean retreat trend of 1.35 m/yr. However, the central sector exhibited an accretional trend of 1.50 m/yr, likely influenced by the High-Angle Wave Instability (HAWI) mechanism. Both megacusps (10–20 m amplitude, 200–400 m wavelength) and KSSWs (Figure 1, 20–40 m amplitude, 500–2000 m wavelength) were identified, showing significant spatial and temporal variability. The megacusp charactersitics were coherent with previous observations in SLD [1]. The potential KSSWs were identified for the first time in this site. Preliminary analysis showed no consistent link between wave parameters and the formation of undulations but a more in-depth research is needed. The successful application of the MegaShore for shoreline extraction and undulation characterization highlights the effectiveness of this tool for long-term, medium- high-resolution shoreline monitoring and provides an important framework for future coastal morphodynamic studies.

Figure 1: Shoreline position extracted from Sentinel-2 satellite image on 1 January 2019 showing potential KSSW undulations, with the corresponding image.

References

[1] R.L. de Swart, R.L., F. Ribas, F, D., Calvete, G., Simarro. J. Guillen. Observations of megacusp dynamics and their coupling with crescentic bars at an open, fetch-limited beach. Earth Surf. Process. Landf. 2022, 47, 3180–3198.

[2] R. Angelini, E. Angelats, G. Luzi, A. Masiero, g., Simarro, G., F. Ribas. Development of Methods for Satellite Shoreline Detection and Monitoring of Megacusp Undulations. Remote Sens. 2024, 16, 4553.

Transverse finger bars at El Trabucador back-barrier beach

A. Mujal-Colilles, A. Falqués, C. Puig-Polo, F. Ribas, M. Grifoll[1]

[1]Universitat Politècnica de Catalunya, Barcelona, Spain

e-mail corresponding author: Anna.Mujal@upc.edu

Keywords: *Transverse finger bars, back-barrier beaches, morphodynamic self-organization*

1 Observations

The SW margin of the Ebro Delta (NE Iberian Peninsula) features a long narrow spit (6 Km) called El Trabucador. The back-barrier beach is a very shallow terrace and its morphology has been monitored through aereal photos and field observations since 1946 [2]. Despite it is a low energy beach the morphology is very dynamic with an intricate bathymetry. Thin and elongated sandbars which are oriented nearly perpendicular to the shoreline are the most striking features (Transverse bars, TB). The cross-bar shape is sometimes symmetric, sometimes assymetric. They can be small, about $5-10$ m in length and $0.1-0.4$ m in relief. They are often grouped in alongshore rhythmic patches with a spacing of $10-20$ m (see Fig. 1). However, some of them can be much longer with a large spacing up to about 60 m. This is clearly observed in some of the aereal photos [2] (see Fig. 1). The number and sizes of the bars are variable. In some photos (see, e.g., Fig 1 taken in 2012), there are up to 90 bars and the most frequent alongshore spacing is in the range $15-25$ m.

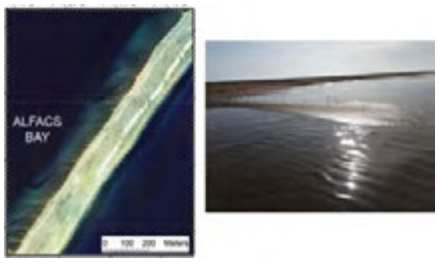

Figure 1: Left: aereal photo of El Trabucador spit, showing the TB at the back-barrier beach. Right: picture of a TB

2 Modelling studies

The origin of TB has been investigated with the morfo55 2DH model [2] and it is found that TB can emerge out of the feedback between morphology and the meandering longshore current. Figure 2 shows a numerical experiment where TB grow with an idealized wave forcing ($Hs = 0.28$ m, $Tp = 2.5s, \theta = 30^o$) during 37 h. The bars have an oblique orientation againts the longshore current, the alongshore spacing is about 30 m and there is a clear cross-bar assymmetry with steeper slope at the lee.

The waves approaching the bars undergo bathymetric refraction thereby turning their crests towards the bars and focusing their energy over them. Earlier studies indicated that this process together with a very gentle beach slope ([1]) were essential to TB formation while morfo55 modelling was insensitive to it. Therefore, Falqués et al. [1] proposed a totally different mechanism based on a beach profile being shallower than the equilibrium one. Figure 2 displays a numerical experiment with the reduced-complexity Q2Dmorfo model for an idealized situation. It is seen how TB can emerge after 20 days of an idealized constant shore-normal wave forcing with $Hs = 0.28$ m and $Tp = 2$ s. The alongshore spacing is about 26 m.

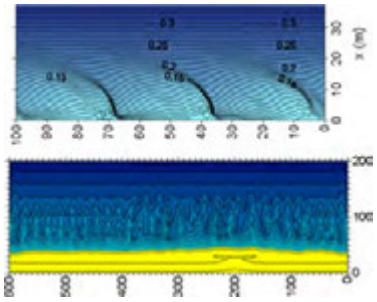

Figure 2: Numerical TB modelling. Top: oblique wave incidence, morfo55 . Down: normal wave incidence, Q2Dmorfo (depth contours spaced by 0.1 m.)

3 Discussion and conclusions

There are at least two different morphodynamic feedback mechanisms that could cause the formation of TB, one driven by the longshore current [2], the other driven by cross-shore transport [1]. The cross-bar shape is asymmetric for the former and symmetric for the latter, and both types have been observed. This suggest that both mechanisms can act depending on the environmental conditions. Nevertheless, the enigma of the origin of such bars is still far from being fully unraveled. In particular, there is a need for detailed field observations and measurements that should be conducted in the future.

Acknowledgements

This research has been funded by the Spanish Government and the EU under grant number PID2021-124272OB-C22 (MOLLY-MOD).

References

[1] A. Falqués, F. Ribas, A. Mujal-Colilles, and C. Puig-Polo. *Geophys. Res. Letters*, 2021. doi: doi.org/10.1029/2020GL091722.

[2] A. Mujal-Colilles, M. Grifoll, and A. Falqués. *Geomorphology*, 2019. doi: doi.org/10.1016/j.geomorph.2019.02.037.

Numerical Simulation of Dike Breaching Using a Generalized Curvilinear Coordinate System

Shinichiro Onda[1], Ichiro Kimura[2], Hidekazu Shirai[3]
[1]Kyoto University, Kyoto, Japan
[2]University of Toyama, Toyama, Japan
[3]Kitami Institute of Technology, Hokkaido, Japan
Corresponding author: onda.shinichiro.2e@kyoto-u.ac.jp

Keywords: 3D numerical simulation, dike breaching, generalized curvilinear coordinate system

1 Introduction

The dike breaching due to overtopping flows recently occurs during floods. To predict dike breaching process, numerical models are proposed using a depth averaged flow model [e.g. 1] and 3D flow model [2] in the Cartesian coordinate system. However, the depth averaged flow model cannot simulate flows behind the crest and around the dike toe more accurately, and the Cartesian coordinate system in the 3D model has disadvantages in fitting smoothly bed surface and simulating shallow water flows along the dike surface. Therefore, in this study, numerical model using a 3D flow model in a generalized curvilinear coordinate system and an equilibrium sediment transport model is developed. Comparing with the experiment, the performance of numerical model is evaluated.

2 Numerical Model

In this study, to simulate water surface variations and the filtration through the embankment, a density function method and a porous media approach are applied for the 3D flow model in a generalized curvilinear coordinate system. The Darcy's law is used for the drag force within the porous region.

As a sediment transport model, both bed load and suspended load are considered. The Mayer-Peter and Müller type and Hasegawa equations are utilised to calculate bed load fluxes in the streamwise and transversal directions, respectively. Moreover, to simulate suspended sediment, the advection discussion equation is solved, where the upward suspended rate from a bed and the settling velocity are evaluated by Itakura and Kishi equation and Rubey's formula, respectively. The temporal change of bed level is calculated by a continuity equation of bed materials.

3 Application and Discussions

The numerical model is applied to the hydraulic experiment. The dike model is implemented in the straight rectangular channel and the crest height, length and slope gradient are 0.3 m 0.1 m and 1:2, respectively. The non-cohesive sands are used for dike materials and the average sand diameter is 0.26 mm. The inlet discharge is 3.3 l/s.

Figure 1 shows the flow fields at t = 20 s, and the contour presents the density function Φ multiplied by the water volume fraction $(1-c)$ to observe clearly the dike surface. The overtopping flows with shallow water depth along the back side of dike can be simulated well and the seepage flows gradually propagate to the dike body. Figure 2 represents the comparison of bed level at t = 20 s. Although the erosion behind the crest is simulated well, the erosion downstream from the back side is consistently underestimated. This is because it is easier for bed load to deposit at the toe due to the change of bed height downstream from the slope and the suspended rate at the toe is underestimated.

Acknowledgments

This work was supported by JSPS KAKENHI Grant Number 24K00990.

References

[1] F.N. Cantero-Chinchilla, O. Castro-Orgaz, and S. Dey. Prediction of overtopping dike failure: sediment transport and dynamic granular bed deformation model. *Journal of Hydraulic Engineering*, 145(6): 04019021, 2019.

[2] S. Onda, T. Hosoda, N. M. Jaćimović and I. Kimura. Numerical modelling of simultaneous overtopping and seepage flows with application to dike breaching. *Journal of Hydraulic Research*, 57(1): 13-25, 2019.

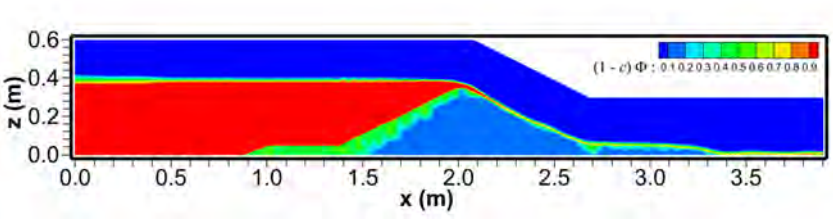

Figure 1: Flow fields at t = 20 s

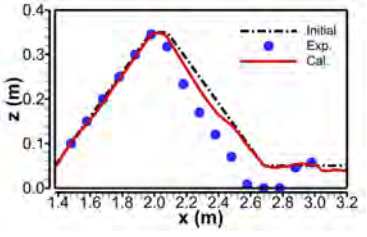

Figure 2: bed level at t = 20 s

Deciphering Sedimentary Activity in the Rivers of the Altiplano of the Atacama Desert over Recent Decades

Alcayaga H.[1], Caamaño D.[2], Soto-Álvarez M.[3], Larrone J.[4], Urrutia R.[5], and Valenzuela[1]
[1]Universidad Diego Portales, Santiago, Chile
[2]Universidad Católica de la Santísima Concepción, Concepción, Chile
[3]Universidad de Los Lagos, Puerto Montt, Chile
[4]Ben-Gurion University of the Negev, Beer Sheva, Israel
[5]Universidad de Concepción, Concepción Chile
Corresponding author: hernan.alcayaga@udp.cl

Keywords: Arid rivers, sedimentary activity, Atacama desert, flash floods

1 Introduction

The rivers of the Atacama Altiplano, mostly ephemeral and located in remote areas, are crucial hydrological systems that are poorly understood. In this extreme environment, sporadic storms trigger intense runoff that mobilizes large volumes of sediment, deposited in beaches, salt flats, lagoons, and reservoirs, significantly altering landscapes and affecting ecosystems. Climatic phenomena like El Niño (ENSO), the Pacific Decadal Oscillation (PDO), and climate change can intensify this sedimentary process. The limited research on these processes restricts our understanding of their behavior and role in morphodynamics. Recent studies (Alcayaga et al., 2022) emphasize the need for advanced techniques to study the interactions of storms, runoff, and sediment transport. This study aims to fill these knowledge gaps, improving our understanding of these processes in the Atacama Altiplano.

2 Methodology

2.1. Study site

The Atacama Desert, located in northern Chile and bordered by Peru and Bolivia, is the driest nonpolar desert on Earth (Bozkurt et al., 2016), with elevations ranging from sea level to 6,500 masl. The study site, Caritaya Reservoir, situated in the Altiplano, sees annual precipitation from 50 to 220 mm. Created by a dam in 1935, the basin spans 453 km2 with a maximum water depth of 31 m. The reservoir is notable for its high trap efficiency (>95%) and lack of hydraulic works to evacuate upstream incoming sediments, making it an endorheic basin in terms of sediment retention.

2.2. Methods

During 2023, topographic and photogrammetric surveys were conducted at the Caritaya Reservoir using GPS-RTK and drones with the SFM method in the delta's dry areas. In submerged zones, a bathymetric survey was performed using an echo sounder and GPS-RTK. Five sediment cores were extracted via Vibrocoring, and their analyses included granulometry with a Mastersizer 3000, dating with ^{137}Cs, and elemental identification using XRF scanner.

3 Results

The results of the element analyses (Fig. 1) in the top 70 cm and the dating in the top 30 cm show an increase in sedimentary activity over the past two decades (2003–2023), not necessarily linked to intense storms or El Niño events. This underscores the importance of local precipitation-runoff processes, characteristic of the Atacama region.

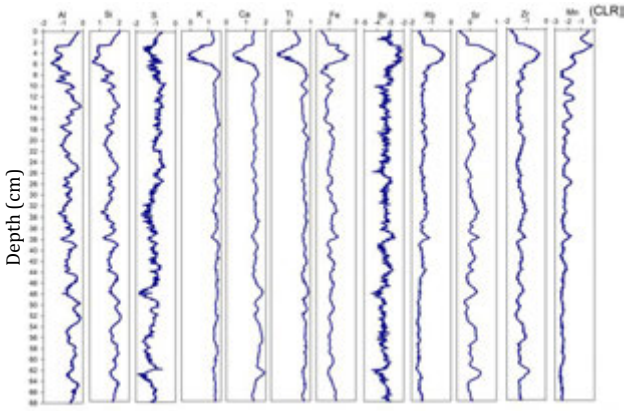

Figure 1. Results for elements with XRF analysis

4 Conclusions

The sedimentary records from the cores reveal intense runoff and sediment transport events whose occurrence intervals have shortened in recent decades, indicating an increase in the frequency of these episodes. The deposited sediments do not directly correlate with precipitation magnitude, highlighting the influence of sediment availability and connectivity, and suggesting that local records do not fully capture regional climate variability.

References

[1] Alcayaga H., et al. 2022. Runoff volume and sediment yield from an endorheic watershed generated by rare rainfall events in the Atacama Desert, Geomorphology 400. DOI: 10.1016/j.geomorph.2021.108107.

[2] Bozkurt D., et al. 2016. Impact of Warmer Eastern Tropical Pacific SST on the March 2015 Atacama Floods. Mon Wea Rev 144, 4441–4460.

Morfo70: a multi-scale numerical model for shoreline and surf-zone morphodynamics

Nabil Kakeh[1], Daniel Calvete[1], Albert Falqués[1]

[1]Department of Physics, Universitat Politècnica de Catalunya, Barcelona, Spain

e-mail corresponding author: nabil.kakeh@upc.edu

Keywords: *numerical modeling; morphodynamics; long-term evolution; surf zone; coastal processes*

1 Introduction

Understanding and predicting the evolution of sandy coasts over medium to long timescales remains a significant scientific challenge [1]. Process-based numerical models are essential tools, but are often limited by computational cost or numerical stability. This work introduces Morfo70, a new 2DH morphodynamic model designed for the efficient and robust simulation of coastal evolution across different spatial and temporal scales, from the emergence of nearshore and shoreline patterns to the multi-year response of large-scale engineering projects.

2 Model Description and Core Features

Morfo70 computes bathymetric evolution by coupling modules for wave transformation (including surface rollers), wave-averaged hydrodynamics (shallow water equations), and sediment transport. The model's efficiency stems from its core numerical innovations:

- **Semi-implicit parallel hydrodynamic solver** using an alternating-direction implicit (ADI) scheme. This robust method allows for hydrodynamic time steps up to 50 times larger than classic explicit schemes. For instance, a five-year simulation of a ten kilometers domain was completed in approximately 60 hours on a standard desktop computer.
- A stable **wet-dry algorithm** for accurately tracking shoreline migration.
- **Semi-implicit treatment of bed evolution**, which enhances stability at the shoreline where slope-driven transport processes are dominant and allows large Morphological Acelerator Factors [2]

The source code is openly available on GitHub to encourage its use and further development by the community.

3 Multi-Scale Applications

The capabilities of Morfo70 are demonstrated through two distinct application examples that highlight its multi-scale nature.

- **Medium-Scale Pattern Formation**: The model simulates the self-organized formation of crescentic sandbars and rip channels from an initially uniform bathymetry. This application shows the model's ability to capture the complex, non-linear feedbacks between hydrodynamics and topography that lead to the emergence of rhythmic nearshore patterns (Fig. 1a).
- **Large-Scale, Long-Term Evolution:** Morfo70 is applied to simulate the multi-year evolution of the ZandMotor mega-nourishment in The Netherlands. The model successfully reproduces the large-scale diffusion and alongshore redistribution of sediment over a three-year period, demonstrating its capability to tackle real-world, large-scale coastal engineering problems (Fig. 1b).

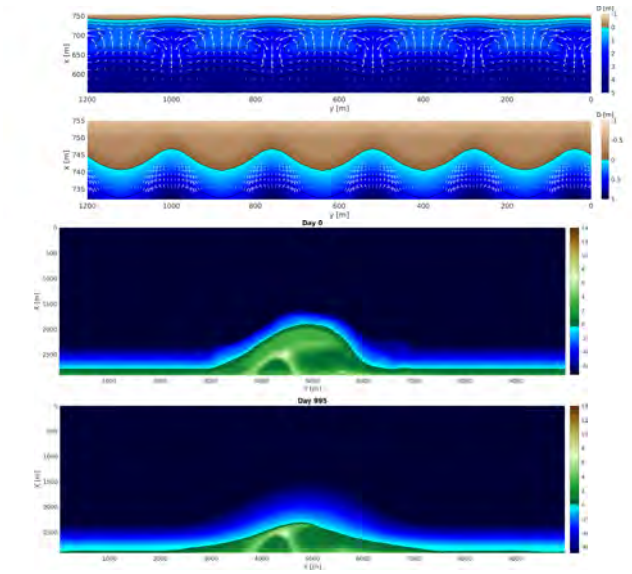

Figure 1: Morfo70's multi-scale capabilities: (a) Self-organized surf-zone morphologic patterns (rip channels and shoreline cusps) developed after 45 days of simulation. (b) Modeled initial and final state of the ZandMotor mega-nourishment after a 3-year simulation.

References

[1] H. J. de Vriend, M. Capobianco, T. Chesher, H. E. de Swart, B. Latteux, and M. J. F. Stive. Approaches to long-term modelling of coastal morphology: a review. *Coastal Engineering*, 21(1-3): 225–269, 1993.

[2] J.A. Roelvink. Coastal morphodynamic evolution techniques. *Coastal Engineering*, 53(2-3):277–287, feb 2006. doi: 10.1016/j.coastaleng.2005.10.015.

Extraction of patches and stripes in saltmarsh wetlands using deep neural networks

Zichao Guo[1], Zeng Zhou[1], Fan Xu[2] ,Yanyan Kang[1],Fernando Mendez[3]
[1]Hohai University, Nanjing 210024, China
[2]East China Normal University, Shanghai 200062, China
[3]Dpto Ciencias y Tecnicas del Agua y del Medio Ambiente, Universidad de Cantabria, Santander, Spain
Corresponding author: guozichao@hhu.edu.cn

Keywords: Deep learning,Neural networks,Saltmarsh wetlands,Debris stripes

1 Abstract

Saltmarsh are vital coastal ecosystems that protect shorelines, provide habitat, and support biodiversity, playing a crucial role in coastal resilience and carbon sequestration. This study aims to accurately extract patches from Saltmarsh tidal flats using an enhanced U-Net architecture with Focal Loss, CBAM attention, ASPP, and ResNet. These enhancements improve the model's ability to capture complex features and address class imbalance issues commonly found in ecological datasets. Our model significantly outperforms traditional methods, particularly in boundary delineation and small-scale feature extraction, contributing to more effective ecological mapping and better management of these important and dynamic coastal environments, thereby aiding long-term conservation efforts.

2 Introduction

This study enhances saltmarsh patch extraction using a modified U-Net , significantly improving feature extraction and segmentation accuracy for better ecological monitoring and management.

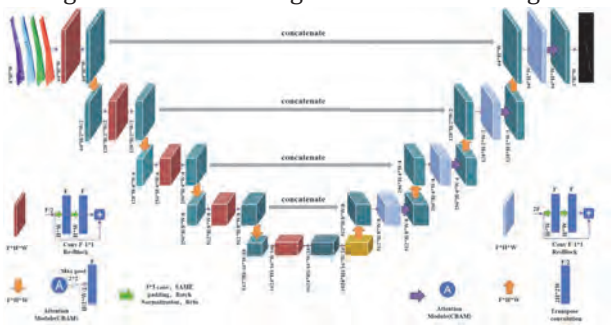

Figure 1: Improved U-net model structure[1]

3 Materials and Methods

The satellite imagery used in this study was obtained from Planet 4-band imagery, which includes red, green, blue, and near-infrared bands.Focal loss formula：

$$FL(P_t) = -(1-P_t)^{\gamma}\log P_t$$

$$P_t = \begin{cases} p & (\text{if } y = 1) \\ 1-p & (\text{otherwise}) \end{cases}$$

Focal Loss helps address class imbalance by focusing on hard-to-classify samples, which is particularly advantageous for accurately extracting small saltmarsh patches.

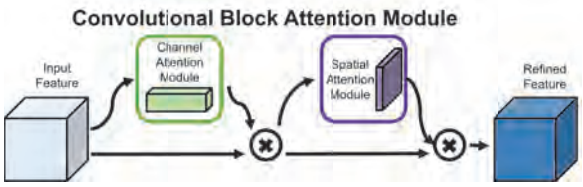

CBAM enhances patch extraction by helping the model focus on key features, improving segmentation of small and complex saltmarsh structures.

4 Results

It can recognize similar terrain effectively and has strong generalization and adaptability to different terrain types.

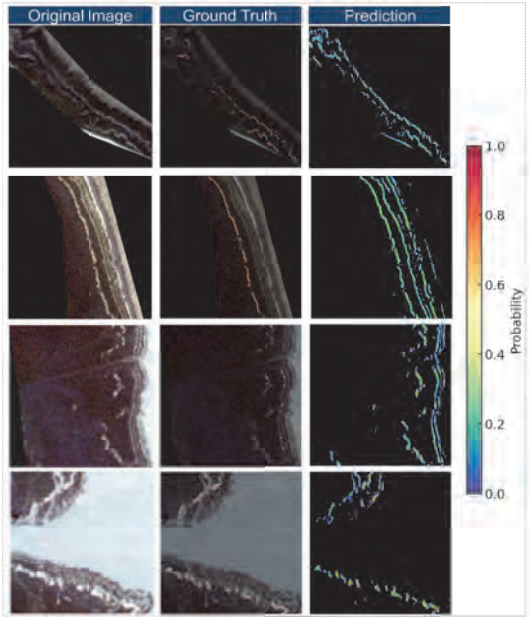

Figure 2: Model prediction result

Acknowledgments

This study is supported by the National Key R&D Program of China(2024YFE0103100), and the National Natural Science Foundation of China (42361144873, 42376161).

References

[1] Ronneberger, O., Fischer, P., & Brox, T. (2015). U-Net: Convolutional Networks for Biomedical Image Segmentation (No. arXiv:1505.04597). arXiv. https://doi.org/10.48550/arXiv.1505.04597

Turbulence Induced by River Bedforms in Supercritical Flows

Sofi Farazande[1], Christophe Ancey[1]

[1]École Polytechnique Fédérale de Lausanne, Switzerland

e-mail corresponding author: sofi.farazande@epfl.ch

Keywords: *antidunes; turbulence; supercritical flows; velocimetry*

1 Introduction

River bedforms such as dunes, antidunes, steps and pools arise from flow instabilities, and their features are determined by both flow conditions and bed characteristics [1]. In most cases, dunes are observed under subcritical flow conditions, while antidunes appear under supercritical conditions [3]. The interaction between these bedforms and the flow field, especially in supercritical regimes, is not yet fully understood. Models based on the shallow-water equations include skin friction (i.e., turbulent dissipation caused by bed roughness), but usually ignore the extra stress created by the bedforms. In light of these complexities, the present study conducts experimental investigations to better understand how antidunes affect the flow field.

2 Methodology

We conducted laboratory experiments in a flume of length 5.8 m and width 4 cm with a bed composed of well-sorted gravel of mean size 2.5 mm. To measure the flow field, we sieved polyamide particles (original $d_{50} = 100\,\mu m$) using an 80 µm mesh to retain particles larger than 80 µm, which were then injected as tracers into the water flow. Accurate tracking of the tracers required the absence of bedload transport concurrently. Therefore, we forced the flow to reach a state referred to as *stationary antidunes* [2] before injecting tracers. We performed experiments with various slope and water discharge combinations while keeping other parameters constant. A high-resolution, high-speed camera was positioned along the side of the flume to capture a window encompassing a couple of antidunes. The video footage was analyzed using Particle Image Velocimetry (PIV) and Particle Tracking Velocimetry (PTV) techniques to calculate the flow field.

3 Results and Conclusions

We compared turbulence parameters calculated from the velocimetry data against theoretical values suggested by the shallow-water equations. This comparison makes the case for a better evaluation of bed friction when bedforms significantly impact turbulence. Our preliminary results indicate that in the presence of antidunes, empirical values of turbulent kinetic energy are approximately 50% higher than the theoretical predictions. As a next step, we intend to propose an empirical parametrization of form drag for antidunes and supercritical flows and include it in a numerical model.

References

[1] A. Caruso, R. Vesipa, C. Camporeale, L. Ridolfi, and P. J. Schmid. River bedform inception by flow unsteadiness: A modal and nonmodal analysis. *Pjysical Review E*, 93(053110), 2016.

[2] F. Núñez-González and J.P. Martín-Vide. Analysis of antidune migration direction. *Journal of Geophysical Research-Earth Surface*, 116, 2011.

[3] I. Pascal, C. Ancey, and P. Bohorquez. The variability of antidune morphodynamics on steep slopes. *Earth Surface Processes and Landforms*, 46:1750–1765, 2021.

Dynamic Interactions Between Vegetation and Delta Morphology: Insights for Coastal Restoration

Madoche Jean Louis[1], Jasper Dijkstra[2], Tracy Quirk[1], Andre Rovai[3], Pim Willemsen[2,4], Matthew Hiatt[1]
[1] Dept. of Oceanography & Coastal Sciences, Louisiana State University, Baton Rouge, USA
[2] Dept. of Ecosystem and Sediment Dynamics, Deltares, Delft, The Netherlands
[3] Smithsonian Environmental Research Center, Edgewater, USA
[4] Dept. of Environmental Sciences, Wageningen University & Research, Wageningen, The Netherlands
Corresponding author: mjeanl1@lsu.edu

Keywords: Delta Morphodynamics, Vegetation Dynamics, Biogeomorphic Feedback, Coastal Restoration

1 Introduction

Understanding the feedback mechanisms between water, sediment, and seasonal vegetation dynamics in deltaic systems is critical for addressing land loss through marsh creation and sediment diversion, especially as rising sea levels threaten river deltas. This study examines how the co-evolution of delta growth and vegetation seasonal dynamics—along with their interactions and feedback—shapes delta morphology over time at network scales. It explores how these geomorphological processes influence deltaic evolution and its implications for ecosystem services.

2 Methods

Feedback between vegetation and hydromorphodynamics was simulated using Delft3D Flexible Mesh (DFM) coupled with a dynamic vegetation model (NBS) [1]. DFM solves the depth-averaged Navier-Stokes equations to model hydrodynamics and sediment transport. NBS dynamically integrates vegetation colonization, growth, mortality, and seasonal dynamics, adjusting hydraulic roughness based on density, height, and distribution. A decade of delta evolution was modeled, incorporating four dominant functional vegetation groups representative of hydrogeomorphic zones in the Wax Lake Delta (WLD), Louisiana, USA. Simulations included four scenarios: constant discharge without vegetation (Q0-No Veg) and with vegetation (Q0-NBS), and triangular flood hydrographs without vegetation (Q1-No Veg) and with vegetation (Q1-NBS), capturing vegetation dynamics under varying flow conditions similar to WLD.

3 Results

We present network-scale statistics of the final morphologies in Figure 1. Delta morphology and channel networks substantially differ between vegetated and non-vegetated scenarios. Vegetated scenarios produce larger, less fragmented islands (Figure 1a), shorter mean unchanneled path length (mUPL) (Figure 1b), and higher geometric efficiency (how well a channel network serves a marsh platform) (Figure 1c). Non-vegetated scenarios favor smaller islands (Figure 1b) and steeper exponential decay in island size distribution. All scenarios maintain consistent nearest-edge distance (Figure 1d) patterns, suggesting self-organization behavior independent of the presence or absence of vegetation.

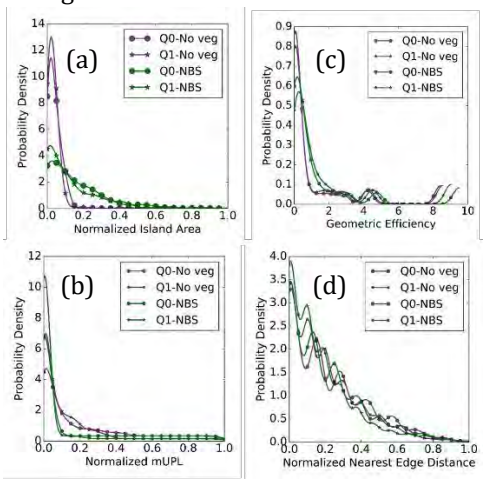

Figure 1. Probability distribution of network-scale metrics. (a) Island area, (b) Mean unchanneled path Length, (c) Geometric efficiency, (d) Nearest-edge distance.

4 Conclusion

This study highlights the critical role of vegetation in shaping and stabilizing deltaic landscapes through biogeomorphic feedback mechanisms. Vegetation enhances sediment cohesion, channel stabilization, and reduced sediment flux to islands, promoting elongated and efficient delta network with lower mUPL. In contrast, non-vegetated deltas exhibit fragmented islands, enhanced sediment flux to islands, and lower network efficiency. These findings emphasize integrating seasonal vegetation and biogeomorphological dynamics into modeling efforts to aid restoration and coastal ecosystem designs.

References

[1] Dzimballa, S., Willemsen, P., Kitsikoudis, V., Borsje, B., & Augustijn, D. (2025). Numerical modeling of biogeomorphological processes in salt marsh development: Do short-term vegetation dynamics influence long-term development? Geomorphology, 471, 109534.

Geomorphic Responses of a Partially Regulated River to Sequential Flood Events

Maha Sheikh[1, 2], Virginia Ruiz -Villanueva1[1,2]
[1] Geomorphology, Natural Hazards and Risks Research Unit, Institute of Geography, University of Bern
[2] Oeschger Centre for Climate Change Research, University of Bern, Bern, Switzerland
Corresponding author: maha.sheikh@unibe.ch

Keywords: Sequential floods, morphological changes, rivers, Geomorphic change detection

1 Introduction and Goals

Floods drastically alter river landscapes by driving processes like channel migration, riverbank erosion, and widening [1], changing conveyance capacity and redistributing sediment [2]. These natural changes, which may last long after floodwaters subside, create new habitats and renew river ecosystems, [3] but may also influence subsequent flood hazards. For instance, channel migration and bank erosion can endanger human life and result in the destruction of infrastructure and agricultural land [4] Global flood events have shown that morphological changes are crucial in determining the behaviour of floods and their effects. [4] These changes are still mostly ignored in flood hazard evaluations, despite their importance. Current flood risk frameworks place a lot of emphasis on hydraulic and hydrological parameters, but they frequently ignore the dynamic interactions between floodwaters and river morphology, including channel migration, erosion, and sediment deposition. [7] Additionally, a large portion of the existing literature focuses on individual floods or rivers, providing a limited understanding of the combined impacts of sequential floods [8] Research on the morphological effects of repeated flood events on partially managed rivers is noticeably lacking. By examining the morphological alterations of a partially regulated river after consecutive floods, this work seeks to bridge this knowledge gap and advance our understanding of these processes and their consequences for flood risk management.

2 Study Area and Methods

The geomorphological changes in the Spöl River, an alpine river that is partially controlled by the Punt dal Gall and Ova Spin dams, were examined in this study. The study site is in the lower Spöl River, which is subject to dynamic geomorphological processes due to the increased flow and sediment input from an unregulated tributary. Every year, as part of a restoration program, experimental floods are released from the Ova Spin dam, making the River Spöl a natural laboratory for researching and evaluating changes in river morphology following floods [5]. To evaluate the geomorphic changes during a succession of floods in terms of sediment erosion and deposition, we used high-resolution digital surface models (DSMs) generated from structure from motion based on drone-acquired data using the Geomorphic Change Detection 7.5.0 standalone software [6].

3 Results

The Spöl River underwent significant morphological changes that had an impact on its volume and area. About 24% and 18% of the entire region saw a positive elevation shift (deposition) while 16% and 35% experienced a negative elevation change (erosion), according to the 2023 and 2021 data respectively. Areal and volumetric changes indicated that sedimentation was more significant than erosion in the area of interest. The upstream part of the reach displayed considerable erosion, whereas the downstream area displayed a general pattern of deposition.

Future research will emphasize prediction models, while this study stresses achieving a balance between restoration objectives and infrastructure protection and flood resilience.

Acknowledgements

This study has been partially supported by the Swiss National Science Foundation (PCEFP2_186963), the Universities of Lausanne and Bern (Switzerland) and the Research Commission of the Swiss National Park (SNP) of the Swiss Academy of Sciences (SCNAT).

References

[1] Ruiz-Villanueva V, et al. (2023) *Sci Total Environ 903:166103*
[2] Rusnák M et al. (2014) *Geomorphology* 58:251–266
[3] T. Robinson Christopher et al. (2023) *Sci Total Environment*
[4] Environmental Agency. (2018). www.gov.uk/environment-agency
[5] Consoli G., Haller et al. (2022). *Journal of Environmental Management*
[6] James LA et al. (2012) *Geomorphology 137:181–198*
[7] Mingfu Guan et al. (2016) *Journal of Hydrology*
[8] Steinritz Vanessa et al. (2024) *Environmental Sciences Europe*

Acoustic observation of SSC in the hyperturbid Ems Estuary

Shiyu Bao[1] Henk Jongbloed[1] Reinier Schrijvershof[1] Lei Xu[2] Ton Hoitink[1]
[1]Departement of Environmental Sciences, Hydrology and Environmental Hydraulics, Wageningen University and Research, Wageningen, The Netherlands
[2]State Key Laboratory of Hydrology-Water Resources and Hydraulic Engineering, Hohai University, Nanjing, China
Corresponding author: shiyu.bao@wur.nl

Keywords: Field work, ADCP, Acoustic inversion

1 Introduction

Measuring sediment flux is crucial for managing estuaries, tidal rivers, and coastal regions. Estimating sediment flux primarily depends on observations of suspended sediment concentration (SSC), particularly in hyperturbid environments. Acoustic measurements using an Acoustic Doppler Current Profiler (ADCP) provide a non-intrusive method for simultaneously obtaining velocity and concentration data. This technique has been applied to various river systems [1, 2] and laboratory experiments [3]. However, its effectiveness in extremely high concentrations, where acoustic signals experience significant attenuation, remains uncertain. This study presents acoustic observations conducted in the Ems Estuary, where SSC can reach several hundred g/L.

2 Research area and method

Data were collected in the Emder Fahrwasser, a section of the Ems Estuary located along the Dutch-German border, where a highly concentrated benthic suspension is more likely to develop in the water column close to the bed. Boat surveys were conducted using a framed ADCP system (Fig. 1). The frame was equipped with a downward-looking ADCP, four Verder-flex pumps, and plastic tubes. During measurements, the boats remained anchored while the frame was gradually lowered toward the bed. It hovered approximately 2 meters above the bottom for several minutes, allowing for velocity and backscatter measurements within the near-bed layer.

Based on the Sonar equation, the method developed in this study is adapted for high concentrations by accounting for variable sediment acoustic properties within the ensonified volume. The relationship between sediment concentration and backscatter is calibrated using linear regression.

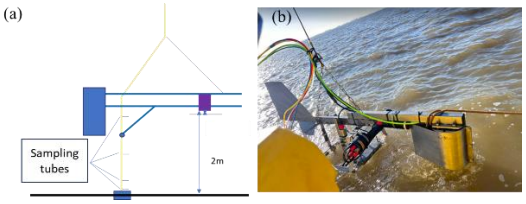

Figure 1: Conceptual structure and picture in fieldwork of the framed ADCP.

3 Results and conclusions

One of the measured backscatter profiles and the inverted results using existing algorithms—single-parameter (power law), double-parameter[1,2], and the multi-parameter method in this study, are shown in Fig. 2. Backscatter was strongly attenuated near the bed. In high-concentration conditions, estimations using the single-parameter method deviated significantly from measurements. The double-parameter method improved accuracy above the strongly attenuated region but still failed near the bed. Only the multi-parameter method provided a good fit, even in the near-bed region where concentrations exceeded 20 g/L.

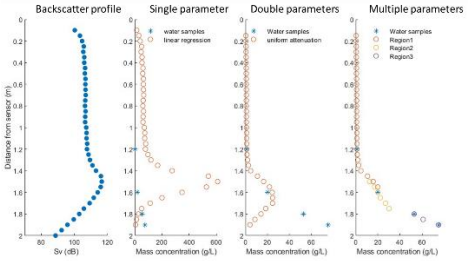

Figure 2: Backscatter profile and SSC estimations using different methods.

Acknowledgments

This work was funded by the Netherlands Organisation for Scientific Research (NOW) (Grant NWO-TTW 17062).

References

[1] Sassi, M.G., Hoitink, A.J.F. and Vermeulen, B., 2012. Impact of sound attenuation by suspended sediment on ADCP backscatter calibrations. Water Resources Research, 48(9).

[2] Haught, D., Venditti, J.G. and Wright, S.A., 2017. Calculation of in situ acoustic sediment attenuation using off-the-shelf horizontal A DCPs in low concentration settings. Water Resources Research, 53(6), pp.5017-5037.

[3] Guerrero, M. and Di Federico, V., 2018. Suspended sediment assessment by combining sound attenuation and backscatter measurements–analytical method and experimental validation. *Advances in water resources*, *113*, pp.167-179.

Laboratory study of wave-driven alongshore velocity and bed shear stress on fixed smooth and rough planar beaches

Alexandra Schueller[1], Kelsey Fall[1], Thomas Pendergast[2], Hyungyu Sung[3], Ben Davidson[3], Dawson Ethier[2], Jason Olsthoorn[2], Ryan Mulligan[2], Nimish Pujara[3], Jack Puleo[1]
[1]University of Delaware, Newark, DE, United States
[2]Queen's University, Kingston, ON, Canada
[3]University of Wisconsin-Madison, Madison, WI, United States
Corresponding author: schuelle@udel.edu

Keywords: swash, hydrodynamics, bed shear stress, wave basin

1 General Information

Beaches are coastal features that offer economic benefits, ecosystem services, and natural barriers against flooding. Sustainable management of beaches requires a firm understanding of hydrodynamics and sediment transport processes. The inner surf and swash zones are narrow and dynamic regions of the nearshore where breaking waves drive rapid, shallow, and intermittent flow conditions that can mobilize large volumes of sediment. Incident-band waves commonly approach beaches at oblique angles and drive flow and sediment transport in these regions in the cross-shore and alongshore directions. Most previous experimental studies on inner surf and swash zone flows have focused on cross-shore dynamics.

2 Methods

In this study, controlled laboratory experiments were conducted in a 26.0 m long, 20.6 m wide, and 1.0 m deep wave basin to investigate nearshore alongshore processes driven by obliquely incident waves. The beach consisted of fixed, smooth concrete with a 1:10 slope. After smooth bed tests, the surface was roughened through sandblasting, and subsequent measurements were collected for the rough surface. Sensors were deployed at various cross-shore and alongshore locations to collect detailed measurements of depth and velocity. The experiments included a range of wave forcing conditions (wave height and period) at different offshore incidence angles (0, 10, 20 degrees).

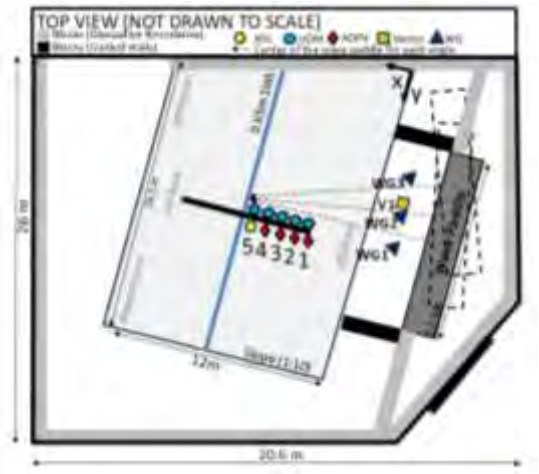

Figure 1: Experimental setup

3 Results Outlook

This study presents ongoing research based on new data collected in 2024, expanding on findings from our 2023 pilot study on a smooth bottom. The 2023 results demonstrated distinct cross-shore and alongshore flow characteristics, with cross-shore velocities reaching up to 0.5 m/s and bed shear stress peaking at 18 N/m^2. Alongshore flows exhibited non-monotonic variations with wave angle, influencing sediment and solute transport [1]. In 2024, we continue this investigation, applying a triple decomposition method to analyze time-averaged flow, wave-driven flow, and turbulence under varied wave conditions. An overview of the collaborative experiment and preliminary results on the relative importance of the alongshore component of near-bed velocity and bed shear stress will be presented, providing further insights into coastal hydro- and morphodynamics.

Acknowledgments

Funding for this project called "SWQUEENS" was provided by the National Science Foundation (Grant Nos. 508 OCE-2219845; OCE-2219846). Support for the collaborative lab effort was provided by Queen's University, the University of Wisconsin-Madison, and the University of Delaware. The authors acknowledge the lab assistance of Richard Foley, and Josh Coghlan. We thank two anonymous reviewers for detailed suggestions on manuscript 512 improvements.

References

[1] Schueller, A., Fall, K., Sung, H., Mulligan, R., Olsthoorn, J., Chardon-Maldonado, P., Oyelakin, R., Pujara, N., Puleo, J. (under review): 'Surf and swash zone hydrodynamics forced by oblique, monochromatic waves in a wave basin with a smooth, impermeable beach', submitted to the *Journal of Applied Ocean Research*.

Experiment on Geomorphological Changes in the Floodplain Caused by the Cohesive Levee Breach

Yuzuno Kanbara[1], Tomonori Shimada[1], Satomi Kawamura[1], Shunichi Maeda[1], Nobuyuki Hotta[1], Tsuyoshi Miura[2], Hisashi Kamei[3]
[1] Civil Engineering Research Institute for Cold Region, Hokkaido, Japan
[2]Hokkaido Regional Development Bureau, Hokkaido, Japan
[3]Obihiro Development and Construction Department, Hokkaido Regional Development Bureau, Hokkaido, Japan

Keywords: levee breach, floodplain, crevasse splay

1 Introduction

A levee breach causes not only floodplain inundation but also erosion and sedimentation, the damage spreads. However, few quantitative studies have analyzed geomorphological changes in floodplains compared to river channels. Thus, to clarify these phenomena, we investigated them through a full-scale cohesive levee breach experiment.

2 Methods

The experiment was conducted at the Chiyoda Experimental Channel in Hokkaido, Japan [1]. Figure 1 shows the test site. The levee was 2.5 m-high, 2 m-wide, and 30 m-long, while the floodplain was 70 m-long and 30 m-wide. Figure 2 shows the water depths on the floodplain. The flow was initially constant and was paused for measurements (Fig. 2A). Then, the flow rate was increased, and the levee breached after 6 hours (Fig. 2B). The levee material was cohesive soil containing 40% silt and clay (d_{50} = 0.12 mm), and the riverbed material was sand and gravel (d_{50} = 9.8 mm). We measured water levels, flow velocity, and elevation and recorded the flow regime on video.

3 Results

3.1 Geomorphological changes in the floodplain

Figure 3 shows elevation change and flow velocity. At the time of Fig. 2A, the erosion at the levee's back slope and toe was a few tens of cm, and sedimentation on the floodplain was a few cm. At the time of Fig. 2B, a 15 m-wide levee breach formed a 25 m-long, 2.3 m-deep crevasse channel. Sand and gravel were deposited around it, creating a tongue-shaped crevasse splay, 50 m in major axis and 0.65 m high. Behind it, fine soil accumulated, and soil clods, up to 1 m long, were scattered. These results suggest sediment sorting due to flow velocity differences.

3.2 Transport of Soil clods

The levee material was cohesive; therefore, little surface soil was transported by water. Similar to the lateral erosion of cohesive levees [2], sand and gravel in the foundation eroded first, followed by the collapse of the levee by 1 to 2 m in major axis, widening the breach. These clods were initially washed away as a single mass and gradually broke down into smaller pieces. While cohesive soil increased resistance to erosion; however, once the levee breached, the clods were transported farther than sand and gravel. This suggests that the drag force on soil clods exceeded resistance, as their wet density (1.50 g/cm³) was much lower than that of soil particles (2.65 g/cm³).

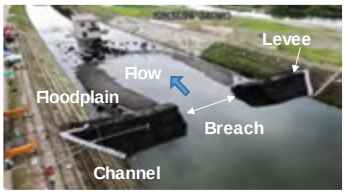

Figure 1: Test Site

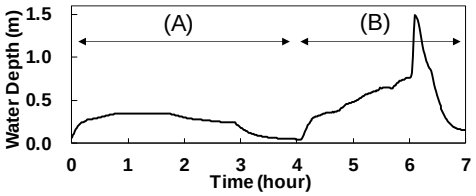

Figure2: Water Depth on the Floodplain

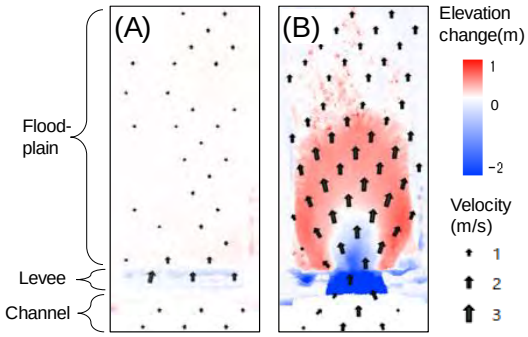

Figure 3: Elevation Change and Flow Velocity

4 Conclusions

In this study, we observed geomorphological changes in the floodplain, including sediment sorting. Our observations showed cohesive soil clods were transported farther, likely due to differences in wet density, but further study is needed. Next, we will compare the results with actual flood events for disaster prevention.

Acknowledgments

This research was supported by the Chiyoda Experimental Channel Advisory Committee and the Experimental Re view Committee.

References

[1] Experiment on a Levee Breach from Overtopping at the World's Largest Experimental Channel, https://www.ceri.go.jp/news/2024GEWEX_Shimada.pdf (See 2025-02-06)

[2] K. Zhang, Z. Gong, K. Zhao, K. Wang, S. Pan, G. Coco, Experimental and numerical modeling of overhanging riverbank stability, Journal of Geophysical Research-Earth Surface 126(10),2021.

Numerical experiments on wave-driven morphodynamics in the Wadden Sea

Magdalena Uber[1], Rita Seiffert[1], Robert Lepper[1], Benjamin Fricke[1], Nils Schade[2], Ingo Hache[3], Jessica Kelln[1]
[1]Federal Waterways Engineering and Research Institute, Hamburg, Germany
[2]Federal Maritime and Hydrographic Agency, Hamburg, Germany
[3]Waterways and Shipping Administration Elbe-North Sea, Hamburg, Germany
Corresponding author: Magdalena.Uber@baw.de

Keywords: Wadden Sea, waves, climate change, tidal flats, erosion

1 Introduction

The morphology of the Wadden Sea, the worlds largest coherent intertidal flat coastline stretching along the North Sea coast of the Netherlands, Germany and Denmark, is shaped by tide- and wave-driven morphodynamics. It is a fragile ecosystem with a rich biodiversity, irreplaceable in coastal protection and includes important shipping routes such as the access to the port of Hamburg. Due to shallow bed slopes and quick submergence, the Wadden Sea is threatened by climate change, notably sea level rise. The capacity of the Wadden Sea to cope with sea level rise depends on sediment availability, erosion, transport and deposition patterns. In shallow shelf seas, these processes are a result of the interplay of tides, wind and waves. Thus, sea state is an important driver of morphodynamics in the outer shoals of the Wadden Sea. Here, we assess the impact of contrasting meteorological forcing, notably calm vs. stormy years, on the evolution of the morphology in the Wadden Sea. To this end, we conduct a numerical experiment using a model of the North Sea [1] to estimate the bandwidth of morphologic evolution related to wind and waves.

2 Methods

2.1 Numerical modelling

We use a 3D hydrodynamic numerical model of the North Sea set up in the modelling framework UnTRIM²-SEDIMORPH and validated over a total of 20 years in previous work [1]. The model domain extends from Scotland to the English Channel and to the western Baltic Sea (Fig. 1). Sea state was modelled with the unstructured k-model (UnK) in the framework of the EasyGSH-DB project. UnK is a two-way coupled spectral wave model. Its simulated wave parameters were validated using five measurement stations. Plausibility checks of the representation of morphodynamic processes in the model compare modelled accumulation rates with Colina Alonso et al. [2]. To obtain a bandwidth of sea state, we use meteorological forcing of two extreme years based on the storminess, i.e. the number of gale days and the gale strength on gale days. Both indicators were provided by the Federal Maritime and Hydrographic Agency for the period 1995-2019 [3].

3 Preliminary results

The number of annual gale days in 1995-2019 varies strongly between 19 in 2009/2010 (July-June) and 54 in 2006/2007. Thus, the two years were chosen to represent the extremes and their meteorological conditions are used as input for the UnTRIM²-SEDIMORPH model. The UnK model was able to reproduce the temporal dynamics of significant wave heights even though absolute values were underestimated. For a total of 58 annual time series, the average mean error was 0.4 m. Using the simulations in UnTRIM²-SEDIMORPH, we analyse how contrasting sea state impacts accumulation rates and sediment transport in the Wadden Sea using what-if comparisons.

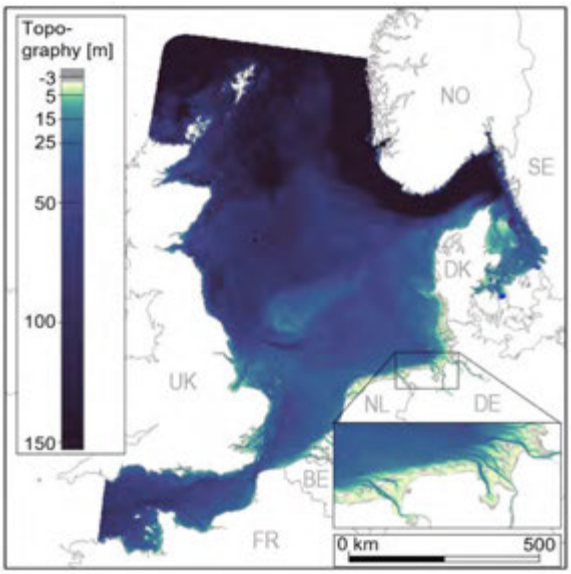

Figure 1: Model domain and topography.

References

[1] R. Hagen, A. Plüß, R. Ihde et al. An integrated marine data collection for the German Bight – Part 2: Tides, salinity, and waves (1996–2015). *Earth Syst. Sci. Data*, 13, 2573–2594, 2021.

[2] A. Colina Alonso, D. van Maren, A. Oost et al. A mud budget of the Wadden Sea and its implications for sediment management. *Commun. Earth Environ.*, 5, 153, 2024.

[3] N. Schade, C. Jensen, L. Schaffer and T. Kruschke. Large Scale Atmospheric Conditions favoring Storm Surges in the North and Baltic Seas and possible Future Changes. *In preparation.*

Quantifying Bedform Morphology in Meandering Rivers

Daniel Alvarez[1], Julia Cisneros[1]
[1]Department of Geosciences, Virginia Tech, Blacksburg, VA, USA
Corresponding author: dalvar17@vt.edu

Keywords: meandering rivers, geomorphology, river bends, bedforms

1 Motivation

Within sand-bedded alluvial rivers, bedforms exist as complex bathymetric features that contribute to bedload transport and bed roughness [1]. Depending on flow and sediment transport rates, bedforms can exist in a range of sizes and scales in rivers, resulting in spatial variability of bedform morphology [1]. In river bends, where complex hydrodynamics and sediment fluxes occur, the spatial variability of bedform morphology is unknown. Here, we quantify the spatial variability of bedform morphology in a river bend. We use these findings to predict how flow and bedload transport may be modulated within riverbends. Thus, we aim to predict how bedform dynamics influence meandering mechanisms.

2 Study Area

We analyse bathymetry (1.79 km^2) from the Sheepnose Bend, located in the Lower Missouri River near Lexington, Missouri, which contains two bends joined by an inflection point. Bathymetric surveys taken from 2019-2021 include weekly surveys (0.87 km^2) of the lower bend during flood conditions [2].

3 Methods

Using multibeam echosounder bathymetry [3], we utilize the Bedform Analysis Method for Bathymetric Information, BAMBI [1] to quantify the spatial variability of bedform morphology in the Sheepnose Bend. Since BAMBI was originally created for straight river sections, we compare results using both curvilinear and cartesian coordinate systems.

To perform the Cartesian to curvilinear coordinate system transformation, we utilize ArcGIS Pro 3.4 and the MATLAB Curve Fitting Toolbox to generate the centerline of the river [3]. We then convert the bathymetric raster data into curvilinear coordinates by orienting the raster cells to the centerline following methods by [3]. Finally, we run BAMBI on both the original cartesian and transformed to curvilinear bathymetric maps following methods by [1]. Results for the transformed to curvilinear maps are converted back to cartesian coordinates for statistical analysis and spatial comparison. Specifically, we compare bedform height, wavelength and leeside angle from maps in both coordinate systems to test the effectiveness of employing BAMBI on data from meandering sections. Finally, we use these bedform morphology measurements, specifically bedform height and leeside angle, and theoretical relationships to predict how flow and bedload transport will occur in the river bend.

4 Results

We show that BAMBI can resolve bedform morphology in bathymetric data transformed to curvilinear coordinates. Both coordinate system results show high spatial variability of bedform morphology, with similar trends of bedform height, wavelength and leeside angle between the original cartesian and transformed to curvilinear maps. Additionally, the spatial variability of bedform morphology is linked to the flow and sediment transport heterogeneity seen in river bends.

5 Conclusions

These results support the use of BAMBI in meandering sections of rivers. The spatial quantification of bedform morphology supports evidence for spatial variability of sediment fluxes and flow within meandering rivers. Understanding the relationship between bedform morphology, flow and sediment transport in meandering sections will offer new insights to meander dynamics.

References

[1] Cisneros, J., Best, J., van Dijk, T., Almeida, R. P. de, Amsler, M., Boldt, J., Freitas, B., Galeazzi, C., Huizinga, R., Ianniruberto, M., Ma, H., Nittrouer, J. A., Oberg, K., Orfeo, O., Parsons, D., Szupiany, R., Wang, P., & Zhang, Y. (2020). Dunes in the world's big rivers are characterized by low-angle lee-side slopes and a complex shape. Nature Geoscience, 13(2), 156–162.

[2] Elliott, C.M., Jacobson, R.B., Call, B., and Roberts, M., Bedform distributions and dynamics in a large, channelized river: Implications for benthic ecological processes, (2023).

[3] Elliott, C.M., Call, B.C., Li, G., and Wang, B., 2022, Field Data and Models of the Missouri River at Sheepnose Bend, near Lexington, Missouri, 2019-2021: U.S. Geological Survey data release.

[4] Güneralp, İ. and Rhoads, B.L. (2008), Continuous Characterization of the Planform Geometry and Curvature of Meandering Rivers. Geographical Analysis, 40: 1-25.

A Hybrid Approach for Morphodynamic Prediction in Estuaries

Mirian Jiménez[1], Beatriz Pérez-Díaz[1] , Pablo Alonso-Aguacil[1], Laura Cagigal[1], Sonia Castanedo[1] and Fernando Méndez[1]

[1] Geomatics and Ocean Engineering Group, University of Cantabria, Spain
Corresponding author: mirian.jimenez@unican.es

Keywords: morphodynamic, estuaries, hybrid methodology.

1 Introduction

Sustainable management of estuarine environments requires a reliable prediction of their morphodynamic evolution. The morphodynamic behavior of these systems is influenced by various spatio-temporal scales: short-term processes (e.g., erosion caused by extreme events), medium-term processes (e.g., seasonal variability of sediment transport), and long-term processes (e.g., the system's evolution towards a dynamic equilibrium state). All these scales interact and must be considered when predicting the morphology of estuaries. In recent decades, significant advances have been made in process-based modeling, which have been combined with morphological acceleration techniques [2] and input reduction strategies [1]. However, the complexity of implementing such models, with their high computational costs, highlights the need for new approaches. To address this challenge, this study takes a step further by presenting a hybrid predictive model to simulate the morphodynamic evolution in estuaries.

2 Methodology

2.1 Data collection

To implement this methodology, two data sources are required: (1) a bathymetry catalog of the study case, and (2) dynamics that influence the estuary's behavior, including astronomical tide, storm surge, wave action, and fluvial discharge.

2.2 Hybrid methodology

Principal Component Analysis (PCA) will be applied to the bathymetry catalog to capture the primary modes of morphodynamic variability within the system. The outcomes of this analysis, combined with the parameterization of continental and marine forcings, will facilitate the implementation of the proposed hybrid methodology, which comprises five key steps: (1) Parameterizing the identified drivers, the potential initial bathymetry through a PCA-EOF analysis, and the main hydrodynamic forcings (2) utilizing the Latin Hypercube Sampling (LHS) method to generate synthetic parameterizations of the most significant dynamics and bathymetries drivers; (3) selecting representative cases through the Maximum Dissimilarity Algorithm (MDA); (4) modeling the selected cases with a morphodynamic model; and (5) applying interpolation via Radial Basis Functions (RBFs) to construct an interpolation surface. A schematic representation of this methodology is provided in Figure 1.

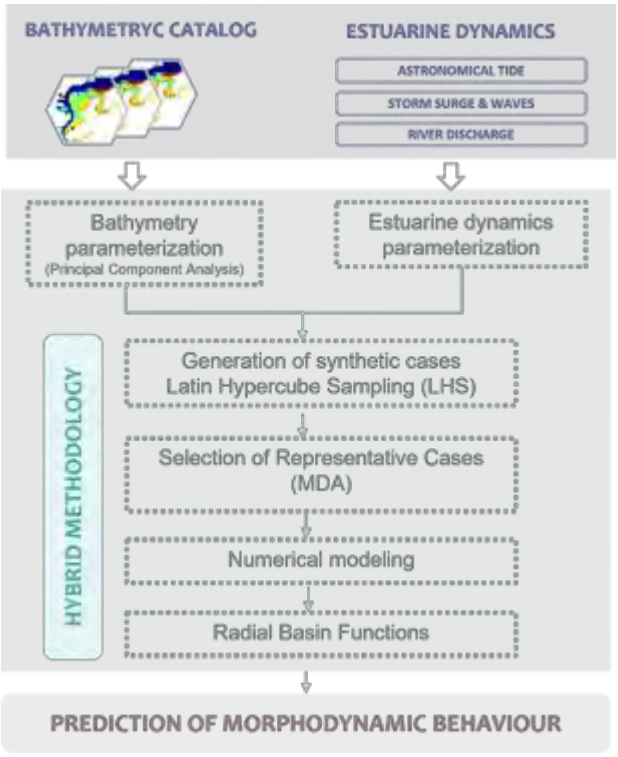

Figure 1: Methodological framework.

3 Results

This methodology aims to provide the morphodynamic evolution of the system, based on the parameterization of its dynamics and its previous morphodynamic conditions. To further enhance its predictive capacity, this methodology would allow the incorporation of climate emulators, enabling a more robust representation of the system's evolution under several environmental scenarios.

Acknowledgments

HyBay (PID2022 – 141181OB I00, MCIN / AEI / 10.13039 / 501100011033 / FEDER, EU) and BahiaLab project (funded by the Autonomous Community of Cantabria and by the European Union Next Generation EU/PRTR).

References

[1] Luijendijk, A. P., de Schipper, M. A., & Ranasinghe, R. Morphodynamic Acceleration Techniques for Multi-Timescale Predictions of Complex Sandy Interventions. *Journal of Marine Science and Engineering*, *7*(3), 78. 2019

[2] Lesser, G.R.; Roelvink, J.A.; van Kester, J.A.T.M.; Stelling, G.S. Development and validation of a three-dimensional morphological model. *Coastal Engineering*, 51, 883–915. 2004

PIV measurements of periodic waves around emerged vertical cylinders

Johann K. Delgado [1], Alejandro Orfila[2,1], Edwin A. Cowen [1]

[1]DeFrees Hydraulics Laboratory. School of Civil and Env. Eng. Cornell University. 14853 Ithaca, NY. USA
[2]IMEDEA(CSIC-UIB). Miquel Marques, 21. 07190 Esporles, Balearic Islands. Spain

e-mail corresponding author: alejandro.orfila@csic.es

Keywords: *mangroves; wave-structure interactions; PIV; canopy flows*

1 Introduction

Mangroves play a crucial role in preventing coastal erosion, acting as natural barriers between land and sea. The dense root systems of mangroves dissipate wave energy, reducing the impact of strong waves and surges on coastlines. In addition, mangroves have high ecosystemic value, as they trap sediments and stabilize coasts, preventing erosion, particularly during extreme weather events. To gain a deep understanding of the hydrodynamic effects around mangroves, we performed a set of laboratory experiments analyzing the velocity field and the free surface elevation measuring the flow around a random array of vertical cylinders under periodic waves from Particle Image Velocimeter (PIV) measurements. Cylinders are allocated at the bottom of the wave flume, simulating the spatial coverage of mangroves. Since the forcing form the waves are 2-D we present spatially and temporally resolved measurements in the plane of the wave, that is the x-z plane.

2 Experimental set-up

Experiments were conducted in a $15 \times 0.8 \times 1$ m wave tank at the DeFrees Hydraulics Laboratory at Cornell University (Figure 1). The flume is equipped with a piston-type wave-maker and a 1:10 dissipative slope at the far end.

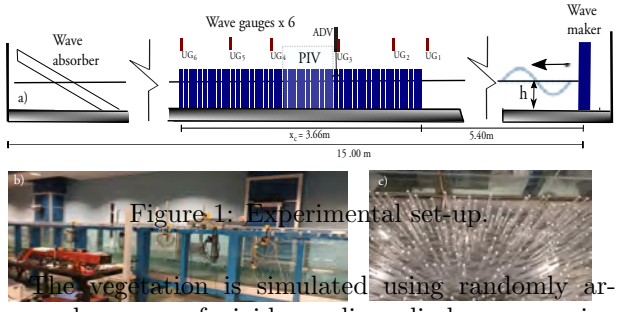

Figure 1: Experimental set-up.

The vegetation is simulated using randomly arranged arrays of rigid acrylic cylinders, spanning 0.60 m in width and 3.66 m in length. The leading edge of the array was located 5.4 m from the wave maker. The cylinder array was configured with a minimum spacing of $S_{\min} = 2d$ and an average spacing of $S_{\text{avg}} = 2.89d = 0.056$ m, where d is the cylinder diameter. The cylinder diameter and height were $d = 0.0126$ m and $h_v = 0.20$ m. The chosen solid fraction was $\phi = 0.04$, resulting in a frontal area per unit volume of $a_v = 4\phi/d\pi = 4.0$ m^{-1} and a spatial density $n = a_v/d$ (number of cylinders per unit area) of 316 m^{-2}.

For velocity measurements, two-dimensional velocity fields were captured in the $x-z$ plane along the full flow depth at the tank's centerline using PIV. The field of view (FOV) was illuminated by an Argon Ion laser. Image pairs were recorded at 15 Hz for a duration of 300 s per experimental condition.

Post-processing for instantaneous velocity applied a dynamic sub-window PIV technique [1]. Each image was divided into 32 × 32 pixel sub-windows with a 75% overlap, producing a 124 × 116 array of velocity vectors within the $x-z$ plane (Figure 2).

3 Results

In this presentation, we show the results from four different wave conditions corresponding to two different water depths with Ursell numbers ranging from 6.5 up to 45 (see Table 1).

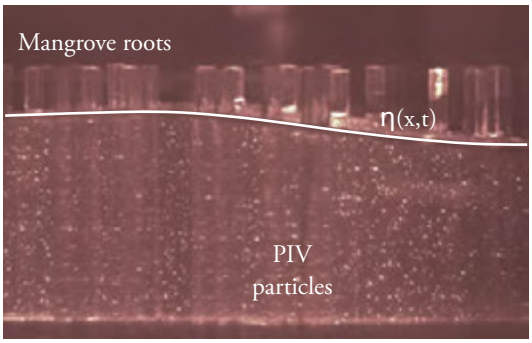

Figure 2: Typical PIV image.

Velocity fields from PIV measurements will be presented and discussed in terms of the energy dissipation induced over the mangrove field.

Depth (m)	f(Hz)	a(m)	$a\,k$	$k\,h$	Ur
0.15	1.25	0.025	0.192	1.152	9.911
	0.60	0.020	1.667	0.484	44.987
0.20	1.25	0.033	0.234	1.415	6.505
	0.60	0.023	0.065	0.566	28.363

Table 1: List of experiments performed.

References

[1] E. Cowen and S. Monismith. A hybrid digital particle tracking velocimetry technique. *Experiments in Fluids*, 22:199–211, 1997.

One-dimensional morphodynamic effects of perpendicular logs as obstacles in rivers

Manuel Faúndez[1], Carles Ferrer-Boix[1], Francisco Nuñez[1], Juan P. Martín Vide[1], Hernán Alcayaga[2]
[1]Universitat Politècnica de Catalunya, Barcelona, Spain
[2]Universidad Diego Portales, Santiago, Chile
Corresponding author: manuel.faundez@upc.edu

Keywords: River morphodynamics, Log obstruction, Bedload transport, 1D morphodynamic model

1 Abstract

The effect of vegetation in rivers is a phenomenon widely studied in the literature, particularly highlighting the crucial role played by large woody debris (LWD) in fluvial dynamics. These elements not only enhance aquatic ecosystems but also significantly influence channel morphology and flow hydraulics. By generating flow resistance, LWD induce backwater effects upstream and sediment deposition [1]. Most studies have focused on longitudinally aligned LWD with the flow [2, 3, 4]. However, when log jams extend across the channel width (i.e. transverse to the flow), they have the potential to trap sediment upstream and modify the channel profile. In addition, these obstructions in rivers reduce the effective cross-sectional flow area, leading to sediment accumulation upstream and localized erosion due to an increase in flow velocity [5]. These changes directly impact sediment transport and bed dynamics in both upstream and downstream directions. Understanding these processes is essential for predicting the morphological evolution of rivers, particularly in low-gradient channels where LWD mobility and jam formation occur at timescales ranging from decades to centuries [1].

This study presents first results of an on-going study with a simple one-dimensional (1D) morphodynamic model, to analyze the evolution of the riverbed profile, under the presence of a log, placed transversely across the riverbed. Through this approach, the study examines the effects of the obstruction on the bed slope, sediment transport rates, and changes in bed elevation. Preliminary results show that there is a strong interaction between the backwater flow induced by the log, local scour around the obstacle and sediment supply downstream of the obstruction, inducing distinct changes on the bed profile both up- and downstream.

The model is an initial base for future developments with more complex factors, such as the long-term impacts of natural obstacles of different sizes, on sediment transport in rivers. The morphodynamic model will provide valuable insights into the interaction between flow and sediment transport in rivers affected by natural obstacles, such as woody debris.

References

[1] J.C. Curran. Mobility of large woody debris (LWD) jams in a low gradient channel. Geomorphology 116 (3–4), 320–329, 2010.
[2] A. Iroumé, A. Paredes, K. Sánchez, L. Martini, L. Picco. Large wood fluctuation and longitudinal connectivity conditions along a segment of the Blanco River (Chilean Patagonia), Geomorphology, Volume 452, 2024.
[3] T. Galia, Z. Poledniková, V. Škarpich. Impact of large wood on sediment (dis)connectivity in a meandering river. Geomorphology, Volume 453, 2024.
[4] T. Galia, M. Horáček, V. Ruiz-Villanueva, Z. Poledniková, V. Škarpich. Large wood retention in a large meandering river: Insights from a 5-year monitoring in the Odra River (Czechia), CATENA, Volume 224, 2023.
[5] H. Patt, R. Jüpner. Hochwasser-Handbuch. Auswirkungen und Schutz. 2., neu bearbeitete Auflage. Berlin: Springer, 2013.

From Physical to Numerical Model: Simulating Laboratory Experiments to Generate Synthetic Data of Shoreline Response to Sea-Level Rise

Maurizio D'Anna[1,2], Francesca Ribas[1], Daniel Calvete[1], Albert Falqués[1], Giovanni Coco[2]
[1]Universitat Politècnica de Catalunya, Barcelona, Spain
[2]University of Auckland, Auckland, New Zealand
Corresponding author: maurizio.d.anna@upc.edu

Keywords: Shoreline change, Sea-Level Rise, Laboratory Data, Synthetic Data

1 Introduction

The accelerating global sea-level rise (SLR) increases the need for long-term shoreline projections to inform adaptation planning. However, the interplay between SLR and waves remains poorly understood, also due to lack of long-term observations. While laboratory studies provide a viable alternative, the limited number of available experiments and their different geometric scales constrain the effectiveness of existing data. This study combines existing laboratory measurements, shoreline modelling and a scaling technique to generate synthetic time-series of shoreline response to SLR and explore the effects of varying wave-SLR combinations in a non-dimensional space.

2 Method

We gathered data from three laboratory studies (1)(2)(3), comprising 17 experiments of different scales and covering a range of wave and step-wise SLR conditions. To complement these datasets with synthetic shoreline data we used the Quasi-2D morphodynamic model (4). The model is calibrated and validated using one (the richest) set of experiments (1). Then, we simulate shoreline responses to new wave-SLR combinations close to those of the experimental data. To compare data of different scales (real and synthetic) on a consistent dimensionless space, we scaled the beach data adapting the (5) approach, originally developed to compare experiments of different geometric scales but similar (erosive) conditions.

3 Results & Discussion

3.1 Model Results

Q2Dmorfo effectively reproduces the shoreline behavior observed during the laboratory tests, achieving RMSE ~2 cm, bias ~1 cm, and R^2 > 95% (Fig.1). Consistently with the laboratory data, the simulations feature the immediate passive flooding followed by the continuous wave-driven shoreline response. Preliminary applications show realistic patterns of the synthetic shoreline data between experimental points (not shown). Ongoing work includes synthetic data generation on a broader range of wave-SLR combinations and comparisons with experimental datasets of different scales.

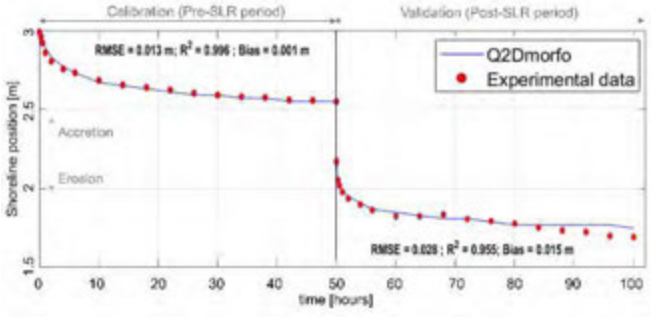

Figure 1: Example of shoreline position time series from the calibrated Q2Dmorfo model (blue line) and experimental data (red dots) before (calibration) and after (validation) the SLR step.

3.2 Dimensionless data

The comparison of scaled beach profiles showed that the proportions of shoreline change between different experiments of the same geometric scale are preserved in the dimensionless space. This is also verified for experiments dominated by accretive processes, suggesting that the validity of the scaling approach can extend to accretive conditions, enabling integrated analyses of dimensionless datasets from tests of different scales.

Acknowledgments

This study is funded by the European Union HORIZON-MSCA-2022-PF, PhySeaCS project (101107336). We thank A. Atkinson, P. Bayle, T. Beuzen, and T. Baldock for providing experimental data.

References

[1] A.L. Atkinson et al.. Laboratory investigation of the Bruun Rule and beach response to sea level rise. *Coast. Eng.*, vol. 136, 2018.
[2] T. Beuzen et al.. Physical model study of beach profile evolution by sea level rise in the presence of seawalls. *Coast. Eng.* vol. 136, pp. 172–182, 2018
[3] P.M. Bayle et al.. Beach Profile Changes under Sea Level Rise in Laboratory Flume Experiments at Different Scale. *J Coast Res*, vol. 95, no. sp1, 2020.
[4] J. Arriaga et al.. Modeling the long-term diffusion and feeding capability of a mega-nourishment. *Coast. Eng.*, vol. 121, pp. 1–13, 2017.
[5] P.M. Bayle et al.. A new approach for scaling beach profile evolution and sediment transport rates in distorted laboratory models. *Coast. Eng.*, vol. 163, p. 103794, 2021.

Fundamental Hydraulic Experiments on Channel Alternation in a Gourd Shaped Channel

Hirokazu Matsui[1] Yasuharu Watanabe[2*]
[1] Kitami Institute of Technology, Master's Program, Graduate School of Engineering, Japan
[2] Kitami Institute of Technology, Professor, Japan
*Corresponding author: y-watanb@mail.kitami-it.ac.jp

Keywords: Channel Alternation, Gourd Shaped Channel, Hydraulic experiment, Braided channels

1 Introduction

In general, rivers in alluvial fan form braided channels. The braided rivers consists of a main channel with a high flow rate and secondary channels with relatively low flow rate. The main and secondary channels may switch when flood occurs, a phenomenon known as channel alternation. When alternation of channels occurs, bank erosion occurs in the channel that changes from the secondary channel to the main channel due to increased discharge and if the main channel moves near embankment it may be a very serious situation for river management. On the other hand, it is also expected to promote a channel disturbance and suppress channelization which has become a problem in recent years. Thus, channel alternation is considered to be a very important phenomenon not only from the viewpoint of channel maintenance, but also from the viewpoint of restoration and conservation of the river environment.

2 Aims

Hydraulic experiments have been conducted by Hasegawa et al. and Tubino et al. on channel alternations in straight flumes. In these researches, it was suggested that the channel alternation was infuenced by the direction of the flow and sediment transport on the alternate bars at just upstream of the channel alternation area. However, these experiments were conducted in the non erodible bank channels. In this study, we consider that cross-sectional channel migration is also an important factor in channel alternation and aim to conduct hydraulic experiments on channel alternation phenomena under conditions where cross-sectional channel migration occurs due to streambank erosion, and to analyze the mechanism of channel alternation occurrence.

3 Materials and Methods

In this study, experiments were conducted using a movable bed channel with a channel width of 1.6 m and a total length of 14.7 m, which was filled with a uniform grain size of 0.765 mm sand in a compound cross-sectional channel. The experimental conditions were selected based on the results of the bed change calculations using iRIC 3.0Nays2DH, so that channel alternations would occur within the channel area. The hydraulic conditions were set to be near the boundary of the formation conditions of alternate bars and double-row bars, which are considered to be prone to the formation of bifurcated channels. That is, the initial straight channel width was set at 0.5 m, the riverbed gradient was set at 1/110, and the flow rate was set at 1250 cm^3/s. The main channel was determined by comparing the channel width and velocity of paint flowing down from the upstream end of the channel.

4 Results

After 4 hours of water flow, several branches and mergers of the channels were formed in longitudinal succession. At the third branch from upstream end of the flume, channel alternation occurred after 6 hours and a half of water flow. The contour map of the measured bed height before and after the channel alternation. are shown in Fig.1. Deep pools were formed at the points where the divergent channels meet and immediately afterwards diverge again. Figure 1 shows that sediment was deposited on the left side of the pool before the channel alternation and on the right side of the pool after the channel alternation at the third branching point of the channel from the upstream end of flume. This indicate that the right bank side channel is the main channel before the alternation, and the left bank side channel is the main channel after the alternation. Focusing on the leading edge of sandbar formed the pool, the development of the bar at the main channel upstream of the pool is remarkable, and that sediment is transported into the main channel downstream of the pool in a concentrated manner. This indicates that one of the two sandbars forming the pool has developed and the area around the pool is temporarily approaching a single row bar. The above results show that even when the river bank is freely eroding, the flow and sediment transport imbalance in the bifurcated channels causes channel alternation, similar to the pseudo formation of alternate bars.

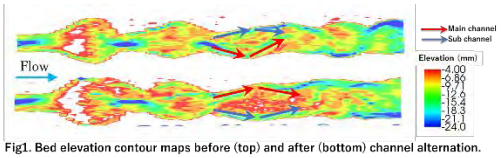

Fig1. Bed elevation contour maps before (top) and after (bottom) channel alternation.

References

[1] Hasegawa K., et al. ; Experiments and Analysis on Alternating Mainstream Change in the Bifurcated Channel in Mountain rivers, JSCE Proceedings of Hydraulic Engineering ,Vol.47, pp.679-684, 2003.

[2] Bolla Pittaluga M., et al. ;Channel Bifurcation in One-dimensional Models: A Physically Based Nodal Point Condition, pp.305-314, 2001.

Natural levees are hotspots for organic carbon sequestration in tidal marshes

Mona Huyzentruyt[1], Maarten Wens[1], Greg Fivash[1], David Walters[2], Glenn Gunterspergen[2], Matthew Kirwan[3], Stijn Temmerman[1]

[1]Department of Biology, ECOPSHERE, University of Antwerp, Antwerp, Belgium

[2]U.S. Geological Survey Eastern Ecological Science Centre, Maryland, USA

[3]Virginia Institute for Marine Science, College of William and Mary, Virginia, USA

Corresponding author: mona.huyzentruyt@uantwerpen.be

Keywords: tidal marshes, carbon sequestration, spatial heterogeneity, microtopography

1 Introduction

Coastal vegetated wetlands, including mangroves and tidal marshes, are considered the most efficient ecosystems in terms of soil organic carbon sequestration rate per surface area [1]. This high carbon sequestration rate is induced by high carbon inputs, both locally derived from vegetation and externally derived from suspended sediments deposited on the marsh during flooding [2]. Besides the high carbon inputs, the decomposition of soil organic carbon (SOC) is limited, because of the frequent waterlogging of the marsh soil [3]. Marsh systems are however heterogeneous systems, with a distinct geomorphic structure consisting of tidal channel networks, natural levees bordering the channels, and interior marsh basins that are 0.1-0.4 m lower than the levees and >10-20 m away from the channels. This levee-basin gradient is induced by a decrease in external sediment deposition rate as the distance to the tidal channel increases [4]. As this gradient is known to induce differences in for example sediment drainage, vegetation productivity and sediment deposition, it can be expected to also induce spatial differences in SOC sequestration rates, however this has been rarely studied.

2 Methods

A fieldwork campaign was carried out in the Blackwater marshes in Maryland, USA. Within this system, three transects perpendicular to the tidal channel were selected and sediment cores and above-ground vegetation biomass were sampled. The sediment was analysed for total organic carbon content, bulk density and sediment accretion rates, which allowed computation of organic carbon accumulation rates (OCAR).

3 Results and Conclusion

Our results show that the organic carbon accumulation rate is up to four times higher in levees compared to basin sites. Our data suggest that this is caused by the combination of three processes: vegetation productivity, sediment accretion and sediment compaction. Since levees experience better drainage towards the channels than basin sites, this allows more oxygen in the soil, creating better conditions for vegetation growth and hence resulting in higher biomass. Sediment accretion rates are higher on levees, partly due to this higher vegetation productivity, but also due to higher deposition rates of suspended sediments closer to the tidal channel. Finally, with deeper soil drainage on the levees, there is a higher degree of compaction of the sediments on the levees. This pattern is confirmed by the trends in bulk density found in our study. Our results highlight the importance of including spatial variability, especially in relation to the typical geomorphic levee-basin structure of tidal marshes, in the quantification of carbon sequestration in tidal marshes.

References

[1] Temmink, R. J. M., Lamers, L. P. M., Angelini, C., Bouma, T. J., Fritz, C., van de Koppel, J., Lexmond, R., Rietkerk, M., Silliman, B. R., Joosten, H., & van der Heide, T. (2022). Recovering wetland biogeomorphic feedbacks to restore the world's biotic carbon hotspots. *Science*: https://doi.org/10.1126/science.abn1479

[2] McLeod, E., Chmura, G. L., Bouillon, S., Salm, R., Björk, M., Duarte, C. M., Lovelock, C. E., Schlesinger, W. H., & Silliman, B. R. (2011). A blueprint for blue carbon: Toward an improved understanding of the role of vegetated coastal habitats in sequestering CO2. *Frontiers in Ecology and the Environment:* https://doi.org/10.1890/110004

[3] Luo, M., Huang, J. F., Zhu, W. F., & Tong, C. (2019). Impacts of increasing salinity and inundation on rates and pathways of organic carbon mineralization in tidal wetlands: a review. *Hydrobiologia:* https://doi.org/10.1007/s10750-017-3416-8

[4] Temmerman, S., Govers, G., Wartel, S., & Meire, P. (2003). Spatial and temporal factors controlling short-term sedimentation in a salt and freshwater tidal marsh, Scheldt estuary, Belgium, SW Netherlands. *Earth Surface Processes and Landforms*, *28*(7): https://doi.org/10.1002/esp.495

Long-Term Numerical Modelling of Sediment Transport Impacts on Sand Nourishments Distribution

Ana Margarida Ferreira[1], Carlos Coelho[1], Paulo A. Silva[2]
[1]RISCO and Civil Engineering Department of the University of Aveiro, Aveiro, Portugal
[2]CESAM & Physics Department of the University of Aveiro, Aveiro, Portugal
Corresponding author: margarida.ferreira@ua.pt

Keywords: longshore, cross-shore, sediment dynamics, shoreline and dune evolution, coastal management

1 Introduction

The sediment distribution after sand nourishment interventions raises questions related with its long-term feasibility in mitigating coastal erosion [1]. The numerical approach presented by Ferreira *et al*. [2] was applied to evaluate the sediment dynamics and the morphological evolution of a coastal domain, considering nourishment interventions under an irregular wave climate. Designed for long-term analyses with low computational effort, the proposed numerical model combines longshore and cross-shore sediment transport processes, including sandbar-berm dynamics, wind-blown sand transport, and dune erosion due to wave impact.

2 Methodology and Assessed Scenarios

The study examined the evolution of a coastal domain after nourishment interventions over a 5-year period, considering the offshore wave climate of the Portuguese West Coast. It was conducted on a generic beach with regular and parallel bathymetry, covering a 5000x1400m^2 area represented by 15 cross-shore profiles spaced 100m apart. The initial scenario (S1) assumed a uniform longshore sandbar volume (Vbar) of 129.46m^3/m and a 50m berm width (BW). Three additional scenarios simulated nourishments in this domain: S2 and S3 simulate nearshore nourishments, increasing Vbar in the centre (P6-P10) to 210m^3/m and 498m^3/m, respectively. S4 simulated dune reinforcement in the centre of the domain with 210m^3/m.

3 Results

The morphological evolution within the numerical domain results from the balance between the longshore sediment transport (LST) and the bar and dune sediment exchanges (Fig.1a). Under a variable wave climate, the sandbar-berm dynamics, in energetic periods, moves sediments from the berm to the bar and produce the opposite effect during lower energy wave conditions. Dune erosion due to wave impact transfers sediment to the berm, resulting in landward dune toe recession. This process is more pronounced during high-energy waves and in profiles with lower berm width. Due to the interactions between processes, the shoreline moves landward and seaward along time (Fig.1b). Nourishments increase sediment availability, leading to seaward shoreline advancement in the early years, compared to the S1 scenario. Within the profiles, sandbar-berm dynamics redistribute nearshore nourishments, while dune nourishment is dispersed by wave impact. Longshore transport spreads sediment to non-nourished areas. At the end of the 5-year period, the shoreline position is similar across all scenarios, indicating that the nourishments considered in the study complete their life cycle in this period (Fig.1b). Comparing similar scenarios in terms of nourishment volume (S2 and S4), the shoreline position exhibits similar evolutions, but dune nourishment (S4) slightly reduces dune retreat compared to S2.

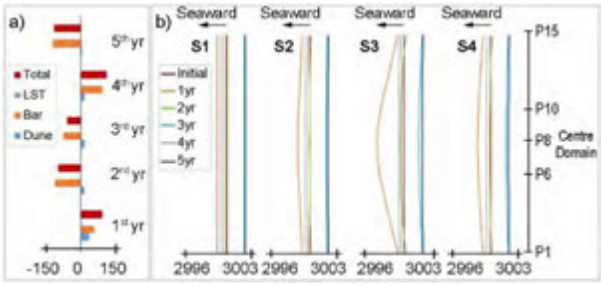

Figure 1: a) Annual sediment balance within the numerical domain for scenario S1 (x10^3 m^3); b) Annual shoreline position of the assessed scenarios (m).

4 Conclusion

The evolution of coastal parameters (shoreline and dune positions, sandbar and dune volume and berm width) depends on the relationship between various components of sediment transport, influenced by nourishment volume, wave climate and beach width. The numerical results highlight the potential of the applied numerical approach to support coastal management over medium to long-term time scales (years), particularly in designing artificial sand nourishments.

Acknowledgments

We would like to thank FCT by the financial support provided to A. M. Ferreira (PhD grant 2021.07269.BD).

References

[1] M. de Schipper, B. Ludka, B. Raubenheimer, A. Luijendijk, T. Schlacher. Beach nourishment has complex implications for the future of sandy shores. *Nat Rev Earth & Environ*, 2, 70–84 (2021).

[2] A. M. Ferreira, C. Coelho, P. A. Silva. Numerical evaluation of the impact of sandbars on cross-shore sediment transport and shoreline evolution. J. Environ. Manage. 370, 15 (2024).

Experimental study on the three-dimensional flow field in a river confluence

Juan Pablo García Rivera[1,2], Carles Ferrer-Boix[1], Juan P. Martín-Vide[1], and Jorge Reyes Salazar[3]
[1]Department of Civil and Environmental Engineering, Universitat Politècnica de Catalunya, Barcelona, Spain
[2] Department of Civil Engineering, Universidad Privada Antenor Orrego, Trujillo, Peru
[3]Institute of Hydraulics, Hydrology and Sanitary Engineering, Universidad de Piura, Piura, Peru
Corresponding author: carles.ferrer@upc.edu

Keywords: river confluences, hydrodynamics, secondary currents, flow oscillations

1 Abstract

This abstract presents the preliminary results of an ongoing research on a river confluence. The hydrodynamics of the confluence of Toltén (main river) and Allipén (tributary river), two large gravel-bed rivers draining the Chilean Andes, is being studied by means of a reduced-scale physical model. Previous to this experimental research, 4 month-long field campaign aiming at measuring bedload transport rates at the confluence was carried out [1]. Flow rates at the confluence during the field campaign varied from 183 m^3/s to 905 m^3/s and flow ratios $Q_{Tributary}/Q_{Main}$ ranged from 0.3 to 1.7. Bedload transport was collected at a relatively narrow section at the confluence labelled 'transect' (Figure 1).

The main goal of the research is to describe the complex three-dimensional flow field at the confluence with the hope that the description can help us understand sediment transport dynamics at the confluence.

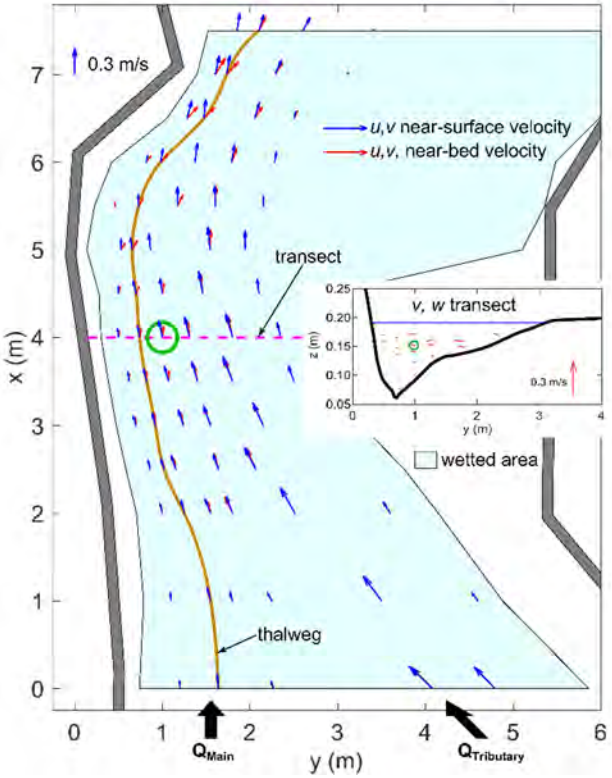

Figure 1: Time-averaged velocities (u, v, w) for an experiment with a flow ratio $Q_{Tributary}/Q_{Main}$ = 1.53. Q_T = Q_{Main} + $Q_{Tributary}$ = 745 m^3/s in the prototype. The green circles point the location where time series of the velocity in Figure 2 was measured.

The experimental setup, located in the Hydraulics Laboratory at the University of Piura (Peru), consists of a fixed-bed experiments at undistorted 57.9 scale using Froude similarity. Bed slope of both rivers at the confluence area is around 0.2%. Flow discharges from both main and tributary rivers were introduced at a constant rate. Sixteen experiments were conducted reproducing flow ratios measured during the field campaign. Detailed three-dimensional instantaneous pointwise velocity measurements were collected using an ADV at 25 Hz for 2 minutes. Figure 1 shows the time-averaged planform velocity components (u, v). The inset panel in Figure 1 includes the vertical and the approximately crosswise time-averaged components of the velocity (w and v, respectively) at the transect.

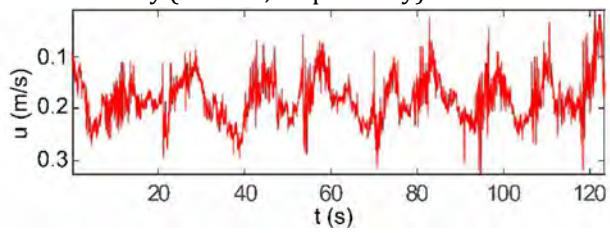

Figure 2: Time series of the instantaneous longitudinal component of the velocity at planform position [x = 4 m, y = 1 m] and at 6 cm above the bed for the same experiment as in Figure 1 (green circles).

Secondary cells near the bed in the deepest areas of the main river were detected (Figure 1). Deviations in (u, v) components of the time-averaged velocity highlight the influence of the bend in the left side of the model (Figure 1). Interestingly, in spite of the well-organized time-averaged velocity flow field (Figure 1), flow oscillations were identified in the instantaneous velocity signals. Time series of instantaneous velocity measurements show flow oscillations, whose period in the order of tens of seconds and with amplitudes of the same order of magnitude as time-averaged flow velocities (Figure 2).

References

[1] J.P. Martín-Vide, A. Plana-Casado, A. Sambola, S. Capapé. 2015. Bedload transport in a river confluence, Geomorphology, 250, 15-28.

Measuring overnight tidal beach overwash events at Cape Cod National Seashore, USA using thermal infrared imagery timestacks

Evan T. Heberlein[1], Katherine Castagno[2], Seth A. Schweitzer[1], Michelle Hummel[3], Kasra Naseri[3], Kevin M. Befus[4], Meagan Eagle[5], Edwin A. Cowen[1]

[1]DeFrees Hydraulics Laboratory, Cornell University, Ithaca, New York USA
[2]Center for Coastal Studies, Provincetown, Massachusetts USA
[3]University of Texas at Arlington, USA
[4]University of Arkansas, Fayetteville, USA
[5]USGS Woods Hole Coastal and Marine Science Center, Woods Hole, Massachusetts USA

e-mail corresponding author: eth47@cornell.edu

Keywords: *overwash; image velocimetry; sea level rise; beaches; sediment transport*

1 Introduction

Spring tide overwashes at Duck Harbor Beach (Massachusetts, USA) have impacted the Herring River Estuary since winter 2021, periodically sending seawater into the upper estuary with severe ecological impacts. These events typically happen overnight near a full moon, and yield very shallow flows (<< 1m) across a 30m breach in the dune system, presenting significant measurement challenges. Accurately measuring the overwash volume entering the estuary will support an ongoing tidal restoration project and reactive transport model development in this system.

2 Methods

During three overnight overwash events (July 31 to August 2, 2023) the flow rate of seawater through the beach breach was measured using thermal infrared imagery, which can detect subtle temperature variations exhibited by flowing water as a trackable signal [1]. Timestacks assembled from rows of infrared pixels in the center of the overwash channel show two distinct slopes: steeper and brighter slopes show waves shoaling and breaking, and flatter more moderate slopes represent the thermal signature of the overwash bulk flow over the beach (Figure 1).

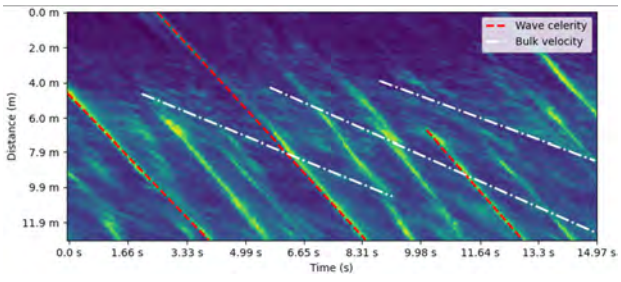

Figure 1: Timestack with slopes, August 1, 2023.

Channel depth can be estimated from these data by subtracting the bulk flow slope u_{bulk} from the wave slope $c_{observed}$ and inverting water depth h from the shallow water approximation for wave celerity $c_{shallow}$, where g is gravitational acceleration:

$$c_{shallow} = c_{observed} - u_{bulk} = \sqrt{gh} \rightarrow h = \frac{c^2}{g} \quad (1)$$

3 Results

Averaging across the georeferenced slopes identified in Figure 1 yields an average depth of 0.19m along this timestack location based on Equation 1.

Centimeter-accuracy GPS measurements of the overwash channel bathymetry were collected before and after each overwash event, and the change in cross-channel bathymetry is shown in Figure 2:

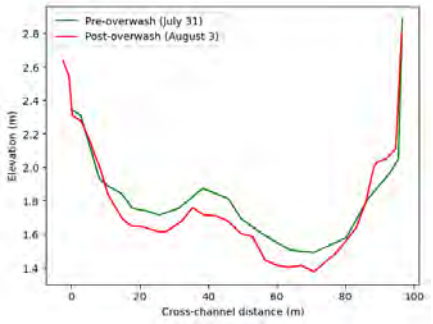

Figure 2: Pre- and post-overwash bathymetry.

Furthermore, current profiler data collected "downstream" of the beach breach (approximately 1.6km inland) shows that these overwashes send significant volumes of seawater into the main channel of the Herring River, elevating near-stagnant side channel flowrates to 1.5 m^3/s in the hours following a spring tide. The presence of increased water level in this "downstream" channel, even during non-overwashing high tides, as well as the phase lag of 3-4.5 hours between the tidal peak and the peak water level in the side channel, present potential insights into the high degree of groundwater connectivity in this system.

4 Conclusion

This project presents a new methodology to measure tidal discharge in wide, shallow tidal overwash channels, with positive implications for estuarine management and adaptation to sea level change.

References

[1] Seth A. Schweitzer and Edwin A. Cowen. Instantaneous River-Wide Water Surface Velocity Field Measurements at Centimeter Scales Using Infrared Quantitative Image Velocimetry. *Water Resources Research*, 57(8), 2021.

River Flow Variability as a Catalyst for Vegetation Growth and Carbon Pumping

Luca Salerno[1], Matteo Bertagni[1], Carlo Camporeale[1]

[1]Politecnico di Torino, Turin, Italy

e-mail corresponding author: luca.salerno@polito.it

Keywords: *carbon cycle, rivers, stochastic processes*

1 Introduction and Background

Rivers constantly reshape their floodplains through interconnected hydrological, sedimentological, and biological processes [1] that drive riverine landscape evolution and influence global carbon fluxes [2]. Riparian zones, transitional areas between aquatic and terrestrial ecosystems, are highly sensitive to river flow variability, which affects vegetation through flooding, sediment deposition, and water table fluctuations. These processes support riparian vegetation by providing moisture, nutrients, and seeds but can also impair it through uprooting during extreme events.

Photosynthetic carbon fixation by riparian vegetation, along with its recruitment, transport, and burial during extreme events, forms an integrated system in which rivers drive a two-step ecomorphodynamic carbon pumping mechanism (ECP) [3]. This mechanism transports carbon from the atmosphere to long-term reservoirs such as river sedimentary deposits and the ocean. The first step, ecomorphodynamic carbon export (eCE), involves the recruitment of large wood biomass through flood-induced uprooting, which may be retained within the riverine system or transported to the ocean. The second step, enhanced net primary production (ENPP), is characterized by carbon fixation via vegetation encroachment and primary production in newly exposed riparian areas. These two steps create compensating carbon fluxes, respectively outgoing and incoming.

To investigate how riparian vegetation reworking under flow fluctuations influences riverine carbon pumping, a stochastic modeling framework was developed.

2 Stochastic modeling

This model analyze intermittent flooding and its effect on riparian vegetation. The water discharge is modeled to reflect sudden flood events, while vegetation biomass follows a logistic growth that includes a stochastic uprooting term when water levels exceed a critical threshold.

This approach makes it possible to quantify the series of vegetation fall events due to uprooting, consequently, the amount of carbon exported by the river. This exported carbon (eCE) is then compared with the average amount of carbon that a plant, under undisturbed conditions (absence of uprooting), can store over its entire life cycle. Based on this comparison, we define an index that captures the capability of riparian environments to catalyze carbon sequestration:

$$\mathcal{I} = \frac{eCE}{K}. \tag{1}$$

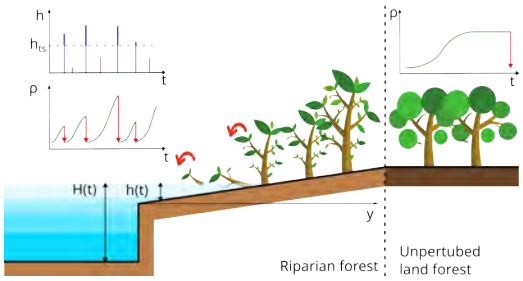

Figure 1: Effect of random hydrological fluctuation on riparian forest

3 Results and Conclusions

Our results show that within the riparian zone there exist areas where periodic uprooting events (eCE) lead to a net primary production (ENPP) surpassing that of an undisturbed forest (K), thus yielding $\mathcal{I} > 1$ and indicating a substantial ecomorphodynamic carbon pumping (ECP). Conversely, in regions strongly affected by river dynamics—where the disturbance regime is more intense—uprooting exerts a negative influence on vegetation development, resulting in $\mathcal{I} < 1$. The final fate of carbon exported by eCE remains uncertain. While some fraction eventually re-enters the atmosphere through processes such as decomposition and respiration, another portion settles in sedimentary compartments, where it can stay locked away for long periods and thus contribute to long-term carbon storage.

References

[1] C. Camporeale, E. Perucca, L. Ridolfi, and A. Gurnell. Modeling the interactions between river morphodynamics and riparian vegetation. *Rev. Geophys.*, 51:379–414, may 2013.

[2] T. W. Drake, P. A. Raymond, and R. G. M. Spencer. Terrestrial carbon inputs to inland waters: A current synthesis of estimates and uncertainty. *Limnol. Oceanogr. Lett.*, 3(3):132–142, 2018.

[3] L. Salerno, F. Giulio Tonolo, and C. Camporeale. Author correction: A global dataset of carbon pumping by the world's largest tropical rivers. *Sci. data*, 11(1):647, 2024.

Improving Flood Forecasting in Estuaries with Satellite-Derived Digital Elevation Models

Ernesto T. Mendoza[1,2], Edward Salameh[3], Nicolas Huybrechts[1], Imen Turki[3], Sophie Le Bot[3], Vanessya Laborie[1], Julien Deloffre[3], Tatiana Goulas[1,3], Andre Hebrard[1,2], Jean-Philippe Lemoine[1,3]
[1]CEREMA REM, Research Team, Margny-lès-Compiègne, France
[2]Univ. Caen Normandie, Univ. Rouen Normandie, CNRS, Normandie Univ, UMR 6143 M2C, 14000 Caen, France
[3]Univ. Rouen Normandie, Univ. Caen Normandie, CNRS,Normandie Univ, M2C UMR 6143, Rouen, France
Corresponding author: ernesto.mendoza-ponce@cerema.fr

Keywords: satellite, estuary, digital elevation models, Bay of Somme

1 Introduction

The Normandy and Hauts de France coasts are particularly sensitive to the risk of submersion and flooding due to the combination of high tidal ranges, storms and continental inputs. The risk is set to increase over the coming decades, with more frequent and more intense storms in coastal areas as a result of climate change. The Somme estuary (Figure 1) is regularly the scene of river-sea flooding events. This study integrates remote sensing, *in-situ* measurements, and numerical modelling to enhance flood forecasting in estuarine environments. As part of the PRISME project, the study proposes an innovative approach that integrates satellite-derived Digital Elevation Models (DEMs) with numerical hydro sedimentary models. By using remote sensing techniques to both generate input data and validate model outputs**,** this method aims to enhance flood forecasting accuracy in estuarine environments.

Figure 1: Location of the Somme Bay in northern France.

2 Methods

2.1. Extreme Storm Identification

Wave time series from historical and real-time datasets will be analysed to identify high-impact storm events affecting the Somme estuary.

2.2. Satellite-Derived DEM

Pre- and post-storm DEMs will be generated using satellite imagery from Sentinel-2, SWOT, and Pleiades, focusing on intertidal areas.

Multi-temporal DEM comparisons will capture morphological changes due to storm impacts, allowing for precise flood zone delineation.

2.3. In-Situ DEM Validation

Ground-truth surveys will be conducted using airborne LiDAR and high-precision GPS to validate the satellite-derived DEMs.

2.4. Numerical Modelling for Flood Forecasting

A hydro sedimentary numerical model (TELEMAC) will be used to simulate flood dynamics based on the validated DEMs. Model calibration will rely on historical flood events and adjusted based on real-time satellite observations.

3 Results

The final contribution will present the high-resolution DEMs of the Somme estuary before and after an extreme storm event with a precise flood impact assessments. Furthermore, preliminary results of the TELEMAC model will be presented. The comparison with the results of the model

Acknowledgments

The authors would like to thank Institut Carnot Clim'adapt for support of the PRISME project.

Morphodynamic Response of River Deltas to Unsteady Discharge and Sediment Supply

Zhenwei Wu[1], and Muriel Z.M. Brückner[1]
[1]Department of Civil and Environmental Engineering, Louisiana State University, USA
Corresponding author: zwu22@lsu.edu

Keywords: Delta morphodynamics; Sediment supply; Unsteady discharge; Delft3D

1 Introduction

The morphology of river deltas plays a crucial role in their resilience against environmental changes, making the study of delta morphological evolution essential. Previous research has demonstrated that in river-dominated deltas, sediment transport, particularly non-cohesive sediment, serves as a primary driver of morphological change (Broaddus et al., 2022). Sediment flux is largely dependent on river discharge, with discharge variability significantly influencing sediment transport patterns (Nittrouer et al., 2011). Using Delft3D, we explore here how unsteady discharge and sediment supply affect long-term deltaic evolution.

2 Methods

Our study area, the Wax Lake Delta (WLD), is a river-dominated, actively growing delta located in coastal Louisiana. Receiving an estimated 25.6 to 38.4 million tons of sediment annually, the delta has reached a current area of about 100 km^2 (Kim et al., 2009). In this study, we utilized Delft3D-Flow to investigate the impact of river discharge variability on the formation of an ideal river-dominated delta inspired by WLD in terms of initial basin geometry, discharge and sediment supply. We modelled delta evolution over a 50-year period using three scenarios: constant discharge, a unimodal flood hydrograph, and monthly flood hydrograph (Fig.1). To ensure comparability, all scenarios maintained the same annual total discharge and we systematically vary sediment supply rates based on well-established power laws, allowing for a controlled analysis of the effects of discharge variability on delta evolution.

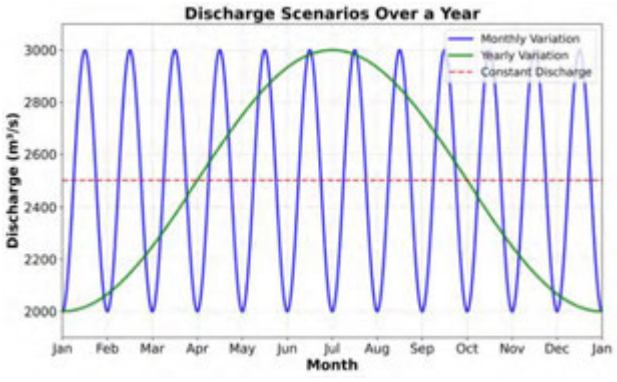

Fig.1. Three discharge scenarios with same annual total discharge

3 Results

Preliminary results indicate that the final delta morphology depends on the discharge scenarios. Compared to the constant discharge scenario, unsteady discharge leads to a more symmetric delta through wider sediment deposition. In contrast, under constant discharge conditions, sediment deposition is more localized with higher deposition close to the river mouth. This results in a more elongated delta morphology driven by the formation of individual delta lobes with fewer channels.

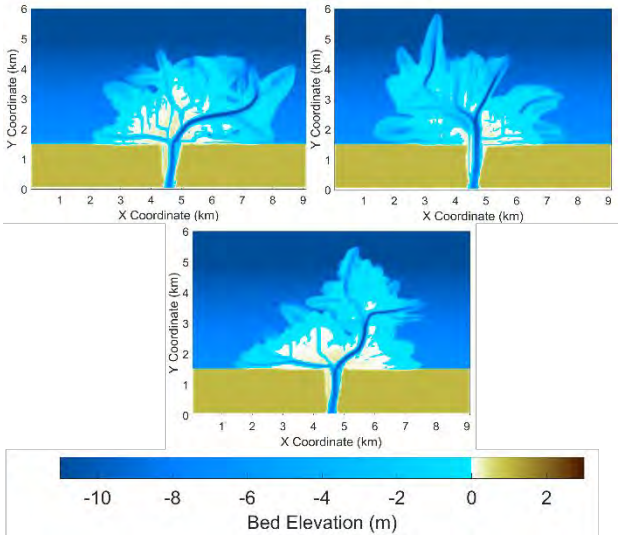

Fig.2. Delta morphology at year 50 for the different discharge scenarios. Bed elevation of 0m is mean sea level.

References

[1] Broaddus, C. M., Vulis, L. M., Nienhuis, J. H., Tejedor, A., Brown, J., Foufoula-Georgiou, E., & Edmonds, D. A. (2022). First-order river delta morphology is explained by the sediment flux balance from rivers, waves, and tides. *Geophysical Research Letters*, 49(22), e2022GL100355.

[2] Kim, W., Mohrig, D., Twilley, R., Paola, C., & Parker, G. (2009). Is it feasible to build new land in the Mississippi River Delta? *Eos, Transactions American Geophysical Union*, 90(42), 373–374.

[3] Nittrouer, J. A., Mohrig, D., & Allison, M. (2011). Punctuated sand transport in the lowermost Mississippi River. *Journal of Geophysical Research: Earth Surface*, 116(F4).

Research on mixed-grain sediment on bed rock channels

Y.Song[1], T.Inoue[1], T.Sumner[1], T.Uchida[1]
[1] Civil and Environmental Engineering, Hiroshima Univercity, Hiroshima, Japan
Corresponding author: inouetakuya@hiroshima-u.ac.jp

Keywords: mixed-grain sediment, mixed alluvial-bedrock channel, alluvial cover

1 Introduction

The sediment transport rate in a mixed bedrock river depends on the areal fraction of alluvial cover on the bedrock. [1]. Parker et al. [2] proposed a model that can calculate the sediment transport rate over the bedrock by defining the alluvial cover ratio as the ratio of the alluvial thickness to the macroscopic bedrock roughness. However, their model has the disadvantage of not being able to handle the transport of mixed-grain sediments. Mixed-grain sediment is subject to complex interactions like hiding effect between particles. In a bedrock-alluvial channel, the hiding effect and the bedrock roughness also comes into play, making the sediment transport pattern even more complex. In this study, we experimentally investigate sediment transport and deposition in a bedrock-alluvial channel and compare the results with existing mixed-grain sediment transport models for alluvial channel.

2 Experimental methods

We used the experimental channel with 5 m long, 0.1 m wide and a bed slope of 1/300. To imitate bedrock with large roughness, we embedded gravels of a particle size of 30 mm on the concrete fixed bed. We created a complete alluvial bed by layering mixed-grain sediments on the bed. The mixed grain-size sediments are composed of four particles sizes (0.77 mm, 1.42 mm, 2.84 mm, 5 mm) with a mixing ratio of 1:1:1:1. These particles were painted in different colors.

We performed a total of 20 runs combining four different flow discharges and five different sediment supply rates. The flow discharges were 4.57 L/s , 5.91 L/s, 7.08 L/s , and 8.37 L/s. The sediment supply rates q_s were set at five levels: 0 %, 25 %, 50 %, 75 %, and 100% of the transport capacity q_c.

We measured the volume and grain-size fraction of sediment transport out of the experimental channel. We calculated the alluvial cover ratio for each grain size from the color pixel counts in the vertical photographs. We measured the water depth and water surface gradient to obtain the shear velocity and shear stress necessary for calculating existing bedload transport models.

3 Experimental results

When the sediment supply rate q_s was equal to the transport capacity q_c, the bedrock was completely covered by sediments, and alluvial cover fraction decreased with decreasing sediment supply rate q_s/q_c. However, the rate of decrease in alluvial cover varied depending on the flow discharge, and the greater the flow discharge, the greater the rate of decrease (Figure 1 [a]). Figure 1 [b] shows comparison between experimental results and existing mixed-grain sediment transport models: the Ashida-Michiue equation[3] and Wilcock and Crowe equation[4]. Due to space limitations, we only show results for the 5 mm particle size here. When $q_s/q_c = 1$ (i.e., completely alluvial bed), the results of existing models are in good agreement with our experimental results. However, when $q_s/q_c = 0.25$ (i.e., mixed bedrock-alluvial bed), the results of existing models overestimated our experimental results. In our experiments, reduced sediment deposition exposed the bedrock, and the protruding bedrock's hiding effect, leading to the reduction of sediment transport. An exciting future challenge will be to incorporate the hiding effect of bedrock roughness into bedload transport models.

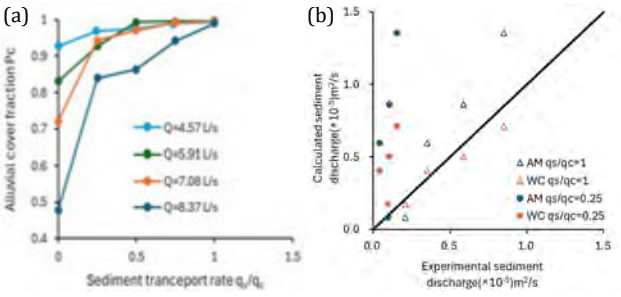

Figure 1 [a]: Variation in alluvial cover fraction with sediment supply
Figure 1 [b]: Comparison of experimental and calculated sediment discharge

References

[1] Sklar et al.: A mechanistic model for river incision into bedrock by saltating bed load, Water Resour. Res., 40, W06301, 2004.
[2] Parker et al.: Interaction between waves of alluvia tion and incision in mixed bedrock-alluvial rivers, Advances in River Sediment Research, Proc. of 12th International Symposium on River Sedimentation, ISRS, 615-622, 2013.
[3] Ashida et al.: STUDY ON HYDRAULIC RESISTANCE AND BED-LOAD TRANSPORT RATE IN ALLUVIAL STREAMS, Proceedings of the Japan Society of Civil Engineers, V1972,59-69,1972.
[4] Wilcock et al.: Surface-based transport model for mixed-sized sediment, Journal of Hydraulic Engineering, ASCE, V129. No.2, pp.120-128, 2003.

Influence of Vegetation-Induced Roughness on the Morphodynamics of River-Dominated Deltas

A. Amaya-Saldarriaga[1], J. H. Nienhuis[2], J. F. Paniagua-Arroyave[3] and M. Z. M. Brückner[1]

[1]Department of Civil and Environmental Engineering, Louisiana State University, USA.
[2]Department of Physical Geography, Utrecht University, The Netherlands.
[3]Area of Natural Systems and Sustainability, Universidad EAFIT, Colombia.

e-mail corresponding author: asalda6@lsu.edu

Keywords: *delta morphology; Delft3D; saltmarshes; roughness*

1 Introduction

First-order delta morphology is primarily governed by the dominant driver of sediment transport (river, waves, or tides), which dictates the overall sediment balance of the delta [1, 2]. Vegetation affects morphology through its influence on hydraulic roughness, introducing flow resistance, altering velocity distributions, and modulating sediment deposition. In turn, morphodynamic changes affect vegetation, creating a biogeomorphic feedback loop that results in a dynamic equilibrium, where the delta's morphology and dynamic vegetation co-evolve over decadal timescales. This study examines how dynamic saltmarsh vegetation influences delta morphology in a river-dominated delta.

2 Methods

We used Delft3D to simulate the feedback-loop between dynamic vegetation and an idealized river-dominated delta, inspired by Wax Lake Delta, Louisiana. The eco-morphodynamic model simulates vegetation establishment, growth, and mortality resulting in dynamic variations of vegetation height and density that produce realistic hydraulic roughness distributions.

The hydraulic resistance due to vegetation is represented by the Chézy Coefficient, C, as:

$$C = C_b + \frac{\sqrt{g}}{\kappa} \ln\left(\frac{h}{h_v}\right) \sqrt{1 + \frac{C_D n h_v C_b^2}{2g}}, \quad (1)$$

where C_b is the bed roughness coefficient, g is the gravitational acceleration, κ is the von Kármán constant, h is the water depth, h_v is the vegetation height, C_D is the drag coefficient, and n is the vegetation density. Note that lower values of C indicate higher roughness

3 Results

Vegetation alters delta morphology by modifying flow patterns, which redistributes sediments and alters deposition and erosion (Figure 1A-B). The difference map (Figure 1C) highlights distinct shifts in depositional and erosional zones due to vegetation-driven changes in flow resistance. The Cumulative Density Function (CDF) of intertidal elevations (Figure 1D) shows an increase in the scenario with vegetation, indicating that vegetation enhances sediment retention and alters the floodplain's elevation. This alteration can be attributed to the variability in Chézy values (Figure 1E), calculated with Equation (1), showing increased roughness in vegetated areas, compared with bare sediments (Bare Sediment Chezy = 65).

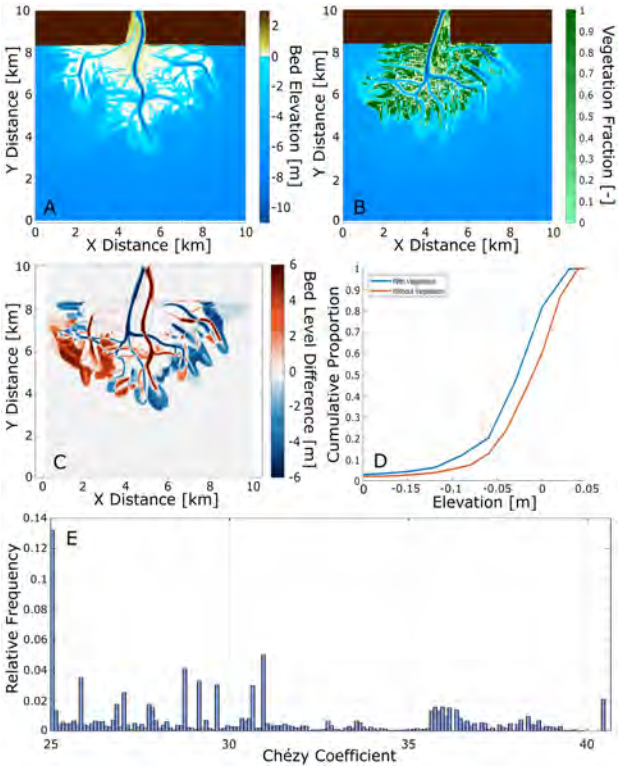

Figure 1: (A) Unvegetated delta and (B) vegetated delta, both simulated with the same parameters in Delft3D. (C) Difference in bed elevation between the unvegetated (A) and vegetated (B) model. (D) CDF of inundation zone elevations for both cases. (E) Relative frequency distribution of Chézy values. Note that a lower Chézy is representative of higher hydraulic roughness.

4 Conclusions

We assessed the influence of vegetation on delta morphodynamics using Delft3D coupled with an eco-morphodynamic model. Our findings demonstrate how vegetation-induced roughness variations can influence sediment redistribution and changes in bed elevation. This research highlights the importance of considering vegetation in morphodynamic studies, improving the understanding of delta systems.

References

[1] C. M. Broaddus, L. M. Vulis, J. H. Nienhuis, A. Tejedor, J. Brown, E. Foufoula-Georgiou, and D. A. Edmonds. First-order river delta morphology is explained by the sediment flux balance from rivers, waves, and tides. *Geophysical Research Letters*, 49(22):1–10, 2022.

[2] W. E. Galloway. Process framework for describing the morphologic and stratigraphic evolution of deltaic depositional systems. In M. L. Broussard, editor, *Deltas: Models for Exploration*, pages 87–98. Houston Geological Society, Houston, TX, 1975.

Recirculation zones in meandering rivers: the Sabine River case study

Bonanomi, R.[1], Konsoer, K.[2], Langendoen, E.[3], Zolezzi, G.[1,4], Tubino, M.[4]

[1]Center Agriculture Food Environment, University of Trento, Trento, Italy
[2]Department of Geography and Anthropology, and Coastal Studies Institute, Louisiana State University, Baton Rouge, LA, USA
[3]USDA National Sedimentation Laboratory, Oxford, MS, USA
[4]Department of Civil, Environmental and Mechanical Engineering, University of Trento, Trento, Italy

e-mail corresponding author: riccardo.bonanomi@unitn.it

Keywords: *meandering rivers; bank erosion; flow field measurements; recirculation zones; satellite data*

1 Introduction

We carried out an extensive field survey along a reach of the Sabine River (Texas, USA), downstream the Bon Wier bridge. Three-dimensional velocities and high resolution bathymetric data were collected during near bankfull condition from May 15-16, 2024. The measurements provided a unique dataset to investigate meandering river flow fields over a series of consecutive bends. Of particular interest, we found the presence of recirculation zones on the outer bank of high curvature bends. Their occurrence, which is often linked to rapid changes in channel curvature and implies a substantial reduction of local bank erosion, is often overlooked in meander evolution models, leading to an overestimation of the migration rates.

2 Methods

The flow field measurements were performed with the TeleDyne WorkHorse Rio Grande 1200 kHz acoustic Doppler current profiler (ADCP). We measured 67 cross-sections, with 4 transects per section, which were then spatially and temporally averaged and analysed with the help of the VMT software [3]. The software PyRIS [2] was used to process Landsat satellite images between 1984 and 2024 to obtain the corresponding river migration.

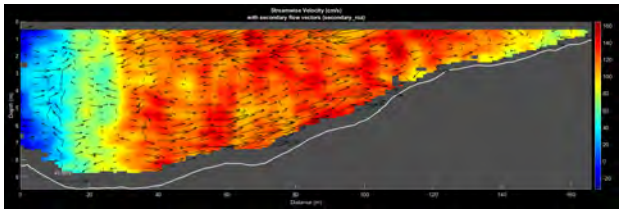

Figure 1: Example of a cross-section with the longitudinal velocity magnitude (colour map) and the secondary circulation (vectors).

3 Results

The presence of vanishing and negative velocities in the outer bank region and of secondary circulations cells is clearly visible in Figure 1. The flow structure is similar to that described by previous works [1], though the recirculation zones seem to be much wider than those measured in laboratory experiments. However, an increase in their width has been linked with the bank roughness, and the high vegetation cover of the bank in Sabine River could justify this behaviour. The role of recirculation zones on bank erosion has been investigated through the analysis of river migration evaluated from satellite data. The analysis reveals that, despite the large value of curvature, nearly no lateral migration is displayed by cross sections where recirculation zones develop, while bank erosion mainly occurs in downstream less-curved segments.

4 Conclusions

Recirculation zones can have a great impact on meandering river dynamics, as they may reduce bank erosion in high-curvature bends. However, their effect has not been considered in most of meander migration models, though its inclusion could lead to a more accurate prediction of bank erosion.

Acknowledgements

The work was partially supported by the Italian Ministry of Universities and Research (MUR) in the framework of the project DIP-ECC18-22 (Departments of Excellence 2018–2022, grant L232/2016). The boats and instruments for the field survey were provided by Louisiana State University and the US Department of Agriculture. We thank Mick Ursic and Jacob Ferguson for their assistance with field measurements.

References

[1] K. Blanckaert. Hydrodynamic processes in sharp meander bends and their morphological implications. *J. Geophys. Res. Earth Surf.*, 2011.

[2] F. Monegaglia, G. Zolezzi, I. Güneralp, A. J. Henshaw, and M. Tubino. Automated extraction of meandering river morphodynamics from multitemporal remotely sensed data. *Environ. Model. Softw.*, 2018.

[3] D. R. Parsons, P. R. Jackson, J. A. Czuba, F. L. Engel, B. L. Rhoads, K. A. Oberg, J. L. Best, D. S. Mueller, K. K. Johnson, and J. D. Riley. Velocity mapping toolbox (vmt): a processing and visualization suite for moving-vessel adcp measurements. *Earth Surf. Process. Landf.*, 2013.

QUANTIFYING MORPHOLOGICAL CHANGES DRIVEN BY OYSTER REEF BREAKWATERS UNDER DIFFERENT TIDAL AND WAVE CONDITIONS

Jacopo Composta[1], Daniele Pinton[1], Alberto Canestrelli[1], Pietro Lazzarini[2]

[1] Department of Civil & Coastal Engineering, University of Florida, Gainesville, USA.
[2] Department of Civil, Environmental and Architectural Engineering, University of Padua, Padua, Italy
Corresponding author: compostajacopo@ufl.edu

Keywords: Oyster reefs, Coastal protection, Sediment transport, Numerical modelling, Physical modelling

1. Introduction

In recent years, the alarming trends associated with climate change, such as extreme weather events and sea level rise, have sparked an interest in shoreline protection in coastal areas, where approximately 80% of the global population is estimated to reside.

Coastal regions, which are ecologically and socioeconomically important, are particularly vulnerable to climate change, with rising sea levels causing more frequent flooding and erosion, threatening both habitats and human settlements. Oyster reefs are gaining attention as a sustainable alternative to traditional "grey" infrastructure. Unlike non-living structures, which often exacerbate erosion and require costly maintenance, oyster reefs adapt to sea level rise and recover autonomously after extreme events. In addition to their ability to protect coastal zones by mitigating wave energy and reducing erosion, oyster reefs also provide critical ecological services, such as water purification and habitat for marine species. This has attracted growing interest in their restoration as a viable solution for coastal protection.

2. Methodology

Previous research has predominantly focused on the morphological changes induced by breakwaters in wave-dominated environments, where tidal currents are minimal. However, the performance of oyster reefs in estuarine environments, characterized by small wave heights (typically around 0.1-0.5 m) and significant tidal currents, remains largely underexplored. These tidal currents play a crucial role in sediment resuspension and transport, and understanding how they interact with oyster reefs is essential for effective coastal protection.

This research aims to address these gaps by investigating the factors influencing sedimentation landward of an oyster reef, with a particular focus on estuarine and reef geometry, as well as local hydrodynamic conditions. Specifically, the study examines the effects of tidal currents, tidal water level variations, initial tidal flat profiles, and the geometry of oyster reefs on morphological changes along marshy coastlines.

To achieve this, a coupled Delft3D FLOW+SWAN numerical model is used to conduct a series of simulations that assessed the short-term morphological effects of various reef configurations and hydrodynamic conditions. This approach enables the identification of reef configurations that results in aggradation, and the ones that instead lead to erosion.

3. Conclusions

This study highlights the potential of oyster reefs as an effective and sustainable solution for coastal protection. The simulations indicate that oyster reefs significantly mitigate erosion, dissipate wave energy, and promote sediment deposition, particularly in shallow waters where tombolos form behind the reefs. The results also show that the orientation of incoming waves plays a crucial role in reef performance: oblique wave results in more sediment accumulation, whereas perpendicular waves lead to less effective protection, especially for narrower barriers. Therefore, wave direction must be considered when designing reef configurations, especially in deeper waters. The study further demonstrates that wider barriers are more efficient than narrower ones, as they attenuate wave energy more effectively and encourage greater sediment retention near the shoreline. While sediment accumulation increases with the distance of reefs from the shore, barriers closer to the coast provide better localized protection. Additionally, wider gaps between barriers are preferred as they allow for effective sediment distribution while minimizing environmental impact and construction costs.

In a subset of the model runs, erosion behind the oyster reef is present. For each analyzed reef geometry, we determine the parameter space for which erosion occurs, in term of tidal level amplitude, tidal currents intensity, wave height and period, and settling velocity.

In conclusion, oyster reefs offer an innovative and nature-based approach to shoreline protection, with their design being key to their effectiveness. These findings are essential for optimizing coastal defense strategies in the face of climate change and rising sea levels.

Acknowledgments

The research is funded by the United States Army Corps of Engineers

Embayed beach morphodynamics under storms and sediment delivery

Candela Marco-Peretó[1], Ruth Durán[1], Gonzalo Simarro[1], Jorge Guillén[1]
[1]Institut de Ciències del Mar (ICM)-CSIC, Barcelona, Spain
Corresponding author: cmarco@icm.csic.es

Keywords: stream dynamics, extreme events, post-storm response, Catalan coast, NW Mediterranean

1 Introduction

Coastal storms are key drivers of short-term morphological change on Mediterranean embayed sandy beaches. These beaches are often influenced by small streams that supply sediment during brief but intense runoff episodes. Although storm-induced beach responses have been widely studied, the combined effects of stream discharge and wave forcing remain largely unexplored. Focusing on Castell Beach (NW Mediterranean), this study examines beach–stream interactions during two energetic storm events (December 2019 and January 2020), both characterised by heavy rainfall and significant stream activity.

2 Study site

Castell Beach is a non-urbanised, stream-fed, embayed beach on the northwestern Mediterranean coast. The beach stretches 320 m and is backed by small, vegetated dunes and a wetland associated with the Aubi stream. The site has a microtidal regime with wave-driven coastal dynamics, primarily influenced by seasonal storms coming from the north and east. Headlands shelter the shore by limiting wave entrance from specific directions, thereby influencing wave exposure and sediment transport patterns. The main sediment source is the material supplied by the Aubi stream during episodic flood events.

3 Methods

Morphological beach evolution was analysed using six GNSS-RTK topographic surveys of the subaerial beach conducted between November 2019 and February 2022, and three echo-sounder bathymetric surveys between November 2019 and July 2020. To examine stream dynamics, these data were complemented by historical LiDAR datasets (2012–2017) and satellite imagery. Altimetric differences between surveys were used to estimate volumetric changes and sediment exchanges in both the subaerial beach and the nearshore.

4 Results and Discussion

The results revealed that the stream mouth location varies along the beach during intense rainfall events, influenced by hydrodynamic conditions. Distinct responses were observed during two high-energy events, reflecting the complex interplay between wave forcing and fluvial input. While the storm in December 2019 led to limited morphological changes, the January 2020 storm (Storm Gloria) resulted in significant sediment loss from the subaerial beach due to both stream activation and wave-induced offshore sediment transport. This material, along with new sediment inputs delivered by Aubi stream, was accumulated in the shallow nearshore, between -1 and -7 m depth (Figure 1a). Over time, the subaerial beach showed signs of natural recovery, gradually returning to its pre-storm configuration by February 2022.

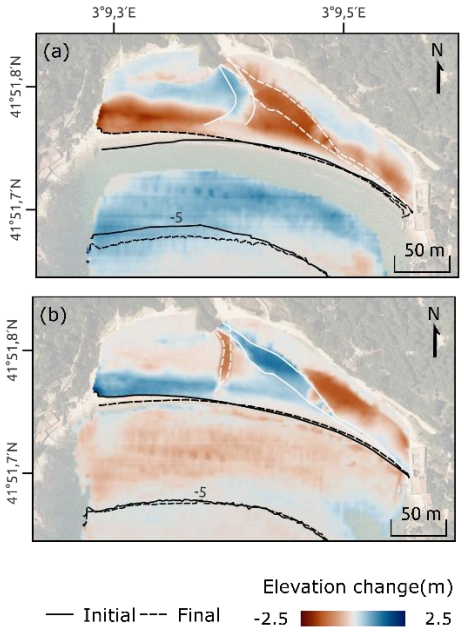

Figure 1. Elevation changes at the subaerial beach and shallow nearshore at Castell Beach: (a) Storm impact: differences between December 2019 and January 2020 at the subaerial beach, and between November 2019 and January 2020 in the nearshore; (b) Beach recovery: differences between July 2020 and January 2020.

5 Conclusion

This study underscores the key role of stream–wave interactions in shaping sediment dynamics and morphology in embayed beaches, which show dynamic resilience to storms.

Acknowledgments

This work has been carried out in the framework of the MOLLY (PID2021-124272) and SOLDEMOR (TED2021-130321B-I00) research projects funded by the Spanish Ministry of Science, Innovation and Universities. This work is contributing to the ICM's Severo Ochoa "Centre of Excellence" *CEX2024-001494-*. C. Marco-Peretó is supported by Spanish FPI grant (PRE2022-101492).

Numerical modelling of bar formation in the Elbe river

Prof. Dr. Nils Reidar B. Olsen[1], Marcel Reiß[2], Dr. Gudrun Hillebrand[2]
[1]Norweigan University of Science and Technology, Trondheim, Norway
[2]Federal Institute of Hydrology, Koblenz, Germany
Corresponding author: Marcel Reiß

Keywords: Elbe river, morphodynamics, alternating bars, bar formation, numerical modelling

1 Study area

The study area is located in the German part of the inland Elbe-river between Elbe-km 508 and 521 (s. Figure *1*). This 13 km long section of the lower part of the Middle-Elbe is considered as a lowland river with an average slope of around 0.12 ‰ and a mean discharge (1991 bis 2015) at the nearest gauge Neu Darchau of 683 m^3/s. The river bed and the bed load transport mainly consist of sand with small amounts of gravel (on average less than 10 %).

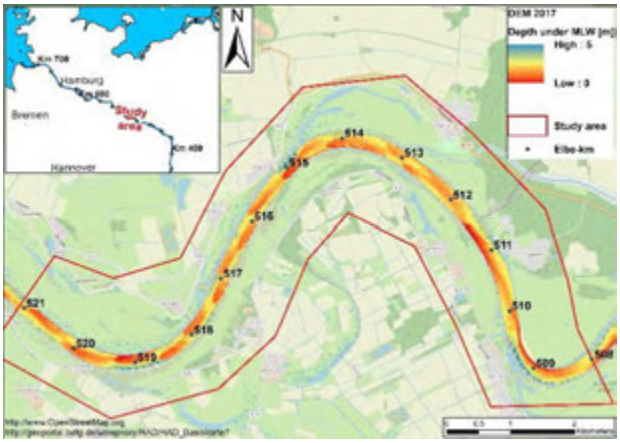

Figure 1: Study area with DEM 2017

The flow below mean discharge in the German part of the Elbe-river is mainly directed by river training works such as groynes or longitudinal training walls to optimize the shipping traffic conditions. The 13 km long survey area is a section with a wider active riverbed (around 40 to 50 m wider) compared to the up- and downstream areas and wider flow cross sections [1]. This favors the formation of free, alternating bars [2]. Based on sounding data, it was observed that these bars migrate about 200 and 600 m per year with wave lengths between 1000 and 1500 m [2]. Due to their high mobility, they present a challenge to the safety and ease of navigation. Figure *1* shows an example of alternating bars.

2 Methods

Besides the ratio of river width to depth, there are more factors influencing the formation of these bars. To get more insight into their genesis, the numerical model SSIIM [3] was applied. The computer program solves the Navier-Stokes equations in three dimensions on an unstructured non-orthogonal grid to find the water velocities and the turbulence. The bed shear tress is also computed. The sediment transport is calculated by the Engelund-Hansen formula. Sediment deposition and erosion are computed from the Exner equation. The changes in the water and bed level over time are taken into account with a wetting-drying algorithm that changes the grid dynamically in all three spatial directions.

3 Results and conclusions

The numerical model was started with a flat bed. A time series of water discharges and water levels from the year 2015-2016 repeated 10 times was given as boundary conditions. A cyclic boundary condition was set for sediment input. Alternating bars that had formed after modelling 6 years are given in Figure 2. The figure shows several bars in the modelled geometry. Migrating bars develop in the same section as observed in the field. The modelled bars seem to migrate at a speed similar to values derived from field measurements. Observations from the field shows bars that are smaller, more numerous and they have a more constant spacing. The results show that the model is able to produce alternating, migrating bars. However, there are still open questions regarding factors influencing bar geometry.

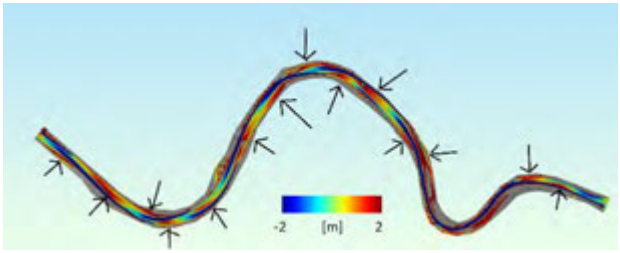

Figure 2: Computed bed elevation changes [meters] after 6 years. The arrows point to bars that have formed.

References

[1] Hillebrand, G., Faulhaber, P., Reiß, M., Backhaus, L.: Vergleich hydraulischer und morphodynamischer Charakteristika in Beispielstrecken der Binnenelbe. In: Korrespondenz Wasserwirtschaft, Heft 9, 2023, S. 573–580.

[2] Branß, T., Aberle, J.: Alternierende Bänke im Bereich der Elbe-Reststrecke. In: Korrespondenz Wasserwirtschaft, Heft 9, 2023, S. 594–599.

[3] Olsen, N. R. B. (2021) 3D numerical modelling of braided channel formation Geomorphology, 375, doi:10.1016/j.geomorph.2020.107528.

Characterising alternate bars facilitating single beam fairway surveys

Till Branß[1], Jochen Aberle[1], Bernd Hentschel[2]
[1]Technische Universität Braunschweig, Braunschweig, Germany
[2]Federal Waterways Engineering and Research Institute (BAW), Karlsruhe, Germany
Corresponding author: t.branss@tu-braunschweig.de

Keywords: alternate bars, bar characteristics, single beam echo-sounding, sand bed rivers

1 Introduction

Free alternate bars are large-scale morphological features that are often associated with river training measures [1]. Due to their high mobility and association with deep scours, bars can pose significant risks to navigation and the integrity of river training structures [2]. Despite their importance, there has been limited research on alternate bars in trained sand bed rivers, particularly regarding the influence of the hydrograph on bar shapes and dynamics. Analysing this interplay necessitates bed elevation data with adequate temporal resolution, which is often unavailable or costly to obtain. In contrast, one-dimensional echo soundings are more widely accessible, particularly in navigable rivers in Germany, where the Federal Waterways and Shipping Administration conducts frequent depth monitoring to ensure safe navigation. Although these surveys typically limit themselves to single beam scans, the high temporal resolution of the data presents a unique opportunity to gain insights into the dynamics of alternate bars. This study therefore aims to explore the potential of single beam echo sounding data in characterizing alternate bars and their dynamics in sand bed rivers.

2 Methodology

The data used for the analyses stem from a section of the Elbe River in Germany (river kilometres 505-530), where the river is trained via groynes and the bed is sandy. This site was selected due to data availability and prior studies on free bars, which utilized annually available spatial echo sounding data [3]. Here, we focus on the analysis of 950 one-dimensional echo soundings along the fairway conducted by the German Waterways and Shipping Administration from 2012 to 2019. The one-dimensional soundings were analysed by projecting them along the river centreline (e.g. [3]) to characterize bar structures and their dynamics.

3 Preliminary results

Our preliminary analysis reveals that alternate bars can be effectively identified using one-dimensional survey data. This is shown in Figure 1, where the x-axis represents time and the y-axis river kilometres. Bed elevations are color-coded, with dark blue denoting negative elevations and bright yellow indicating positive bed elevations.

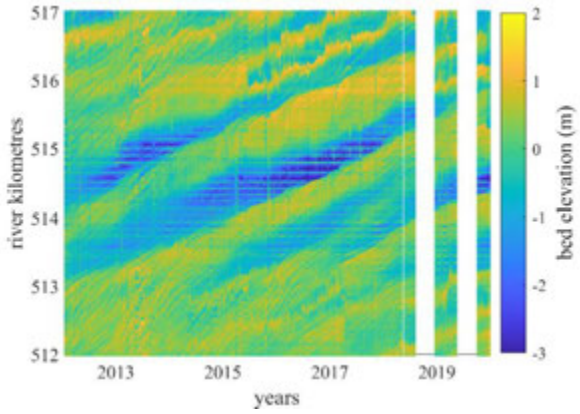

Figure 1: Detrended, one-dimensional bed surveys of Elbe River (river kilometres 512-517) projected on the river axis and plotted over time (white areas are data-gaps).

The figure demonstrates the presence of large-scale (approx. 1 km long) morphological features migrating downstream over time, evident through structures exhibiting positive slopes. These structures are partially overlain by smaller, faster-moving structures, which may correspond to large dunes. Additionally, fine horizontal and stationary structures, likely representing groynes and their associated scours, can also be discerned. This visualization underscores the potential of one-dimensional echo sounding data in advancing our understanding of morphodynamic processes in trained river systems. Ongoing analysis will further benchmark the bar characteristics obtained from this data with those obtained from spatial data [see 3].

Acknowledgments

We would like to thank those who are collaborating voluntarily in the organisation of the RCEM2025.

References

[1] D. Corenblit, F. Vautier, E. González and J. Steiger. Formation and dynamics of vegetated fluvial landforms follow the biogeomorphological succession model in a channelized river. *Earth Surf. Process. Landforms* 45, 2020–2035, 2020.

[2] M. Carlin, M. Redolfi and M. Tubino. The long-term response of alternate bars to the hydrological regime. *Water Resour. Res.* 57, e2020WR029314, 2021.

[3] T. Branß, J. Aberle and B. Hentschel. Impacts on alternate bar geometry and dynamics in a trained sand bed river. *Frontiers in Water* 4, 2023.

Free bars in straight channels: modulation and predictability through the Complex Ginzburg-Landau Equation

F. Weber [1], M.Toffolon[1], H.A. Dijkstra[1,2] and A. Siviglia[1]

[1]Department of Civil Environmental and Mechanical Engineering, via Mesiano 77, Trento, Italy
[2]Institute for Marine and Atmospheric research Utrecht, Princetonplein 5, Utrecht, The Netherlands

e-mail corresponding author: francesco.weber-1@unitn.it

Keywords: *river morphodynamics, free bars, predictability, perturbation theory*

1 Introduction

Effective management strategies of fluvial and estuarine systems require the accurate modelling and predicition of morphological trajectories over long timescales. But is there any predictability horizon? To assess this, we study the simple case of formation and development of free bars in straight channels.

2 Methods

We consider the 2D depth averaged Shallow Water equations coupled with the Exner equation with uniform sediment and Meier-Peter & Müller parametrization of bedload transport. The goal is the study of the behaviour of bar amplitude A on temporal and spatial scales (T, X) much longer than those involved in bar formation. This is done by extending the linear analysis at the weakly nonlinear level, obtaining the Complex Ginzburg-Landau equation:

$$\frac{\partial A}{\partial T} = A + (1 + i\alpha_1)\frac{\partial^2 A}{\partial X^2} - (1 + i\alpha_2)\ A \mid A \mid^2 \quad (1)$$

where α_1 represents diffusion and α_2 the nonlinear saturation of $A(T)$. The CGLE [1] has been studied in the last decades for many other physical processes near critical thresholds. In this work, we extend the derivation of the CGLE for river bars by R. Schielen [2] by relaxing the rigid-lid assumption in the derivation and linking the coefficients (α_1, α_2) to crucial dimensionless parameters of a richer sediment transport model. Eventually mapping the known dynamics of the CGLE (1) in parameter space (Fig. 1) to morphodynamics allows us to assess when free bars exhibit limited predictability due to sensitive dependence on initial conditions.

3 Results

We derive analytical expressions of the coefficients (α_1, α_2) in terms of base flow transport intensity θ_0, aspect ratio β and relative roughness d_s. In our model, the limited predictability behaviour (Fig. 1a) occurs for bedload, provided that sediment transport θ_0 is sufficiently intense. An inverse relationship is found for d_s, in concordance with Schielen [2]. A resulting minimum spatial scale L_c at which a constant amplitude train of bars (Fig. 1b) is unstable to perturbations is found to be approximately $L_c \simeq 6 \div 10$ times the critical wavelength for bar formation.

4 Conclusions

These preliminary results indicate that free bars in straight channels have limited predictability characteristics for some values of fundamental morphodynamic parameters (β, θ_0, d_s). We are currently working on extending the analysis to model total sediment load and to incorporate multiple grainsizes.

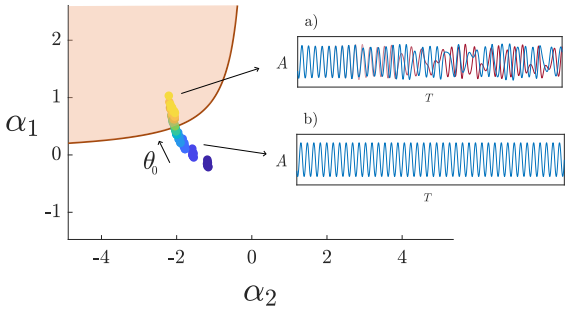

Figure 1: Plot of the CGLE coefficients (1) versus θ_0 for free bars in straight channels. Above the $1 + \alpha_1\alpha_2 = 0$ curve predictability is limited due to sensitive dependence on initial conditions, resulting in temporal chaos for $A(T)$, shown in panel a).

References

[1] I. S. Aranson and L. Kramer. The world of the complex ginzburg-landau equation. *Rev. Mod. Phys.*, 74:99–143, Feb 2002.

[2] R. Schielen, A. Doelman, and H. E. De Swart. On the nonlinear dynamics of free bars in straight channels. *Journal of Fluid Mechanics*, 252:325–356, 1993.

Numerical Modelling of Migrating and Steady Alternate Bar Dynamics during Floods in the Alpine Rhine River

David F. Vetsch[1], Annunziato Siviglia[2]
[1]Laboratory of Hydraulics, Hydrology, and Glaciology (VAW), ETH Zurich, Switzerland
[2]Dept. of Civil, Environmental and Mechanical Engineering, University of Trento, Italy
Corresponding author: dvetsch@ethz.ch

Keywords: Shallow-Water-Exner model, morphodynamics, gravel bed river

1 Introduction

Mathematical models based on the two-dimensional Shallow-Water-Exner (SWE) equations are widely used to predict the formation and propagation of alternate bars in confined rivers characterized by straight reaches, bends, and structures such as ramps. While analytical linear and weakly non-linear solutions can predict the formation and propagation of alternate free bars (e.g., [1]) in straight channels, they cannot capture the interactions between free bars and the steady bars that may develop at river bends or at structures like ramps.

2 Methods

In this work we use a numerical model based on the solution of the SWE equations to study the dynamics of migrating and steady alternate bars in a 10 km long reach of the Alpine Rhine River for hydrographs with different duration and peak discharge. The considered reach is characterized by the presence of both migrating and steady bars as illustrated in Figure 1 and discussed in [2].

For the numerical simulations we used the freely available BASEMENT software (Vetsch et al., 2024) developed at VAW, ETH Zurich. For the present study the submodule BASEMD-2D of was employed. The governing equations for hydrodynamics are the 2-D shallow-water equations incorporating a logarithmic flow resistance law as closure for the friction term in the momentum equations. Bed load transport is modelled using Exner equation with Meyer-Peter Müller transport rate and considering correction of transport direction on laterally sloped beds. For more details see https://basement.ethz.ch [3].

3 Results

The numerical model successfully predicted migrating and steady bar formation in the considered reach, in accordance with aerial images and bed level surveys. However, the absolute magnitude of bar height and scour depth were not reached within the simulation time. Point bars formed at inner side of the bends and with increasing discharge, both bar height and scour depth tended to increase. In contrast, the amplitude of migrating and steady bars in between the bends tend to decrease.

Figure 1: Alpine Rhine River reach with migrating (short) and steady (long) bars, flow direction from bottom to top (aerial image ©swisstopo)

References

[1] M. Colombini, G. Seminara, and M. Tubino. Finite amplitude alternate bars. Journal of Fluid Mechanics, 181:213–232, 1987.

[2] L. Adami, W. Bertoldi, G. Zolezzi. Multidecadal dynamics of alternate bars in the Alpine Rhine River, *Water Resources Research*, 52, 8938–8955, 2016.

[3] D.F. Vetsch, S. Frei S., M.C. Halso., J.C. Schierjott, M. Bürgler, D. Vanzo. Basement V4—A Multipurpose Modelling Environment for Simulation of Flood Hazards and River Morphodynamics Across Scales. *Advances in Hydroinformatics*, Vol. 1, SimHydro 2023. Springer Water, 2024.

Prediction of alternate bar characteristics using a neural network

Victor Chavarrias[1], Guus van Hemert[1]

[1]Deltares, Delft, the Netherlands

e-mail corresponding author: victor.chavarrias@deltares.nl

Keywords: *alternate bars, morphodynamics, sediment transport, neural network*

1 Introduction

Predicting morphodynamic development is key for managing riverbank erosion, planning river training, assessing sedimentation in navigational channels, and predicting avulsions, among many other cases. Predictions are usually done by solving the flow equations (mass and momentum conservation for water) coupled to a mass conservation equation for the sediment phase in combination with a suitable sediment transport relation. This forms a hyperbolic system of partial differential equations (PDE) that is solved by numerically discretizing the equations and march the solution in time starting from an initial condition. While this method has proved its ability to predict morphodynamic changes accurately for decades, it is rather expensive computationally, especially when the interest lays in the long-term evolution. The current fast development in hardware and software suited for artificial intelligence has opened the possibility of accelerating morphodynamic predictions by changing the paradigm. Rather than solving a discretized set of PDE, a neural network trained with the right data-set could be able to provide an acceptable level of accuracy in a fraction of the time. Usually, neural networks are only applicable in the range of conditions in which they have been trained. Yet, what conditions are sufficient is loosely defined. Here, we test the ability of a neural network to predict morphodynamic development at the most fundamental limit for exploring the current challenges of this approach.

2 Case

A straight sloping channel composed of mobile sediment is unstable above a critical width-to-depth ratio [e.g. 1]. For a sufficiently narrow channel, all perturbations to the equilibrium solution decay, returning to normal flow. Above a critical point a pattern of migrating alternate bars of a certain wavelength emerges autonomously. Figure 1 shows the domain of growth and decay of infinitesimal waves (i.e., the linear solution) for a case with a discharge per unit width equal to $1\,\mathrm{m}^2/\mathrm{s}$, flow depth of 1 m, non-dimensional friction coefficient of 0.007, and sediment size of 0.001 m. Sediment transport is computed using Engelund and Hansen [2] and the transverse bed slope effect with a factor of 1 and no power of the bed shear stress. For a width B below approximately 20 m ($L_\mathrm{y} = 2B$ for alternate bars), all waves decay. For a wavelength below approximately 450 m, all waves propagate downstream.

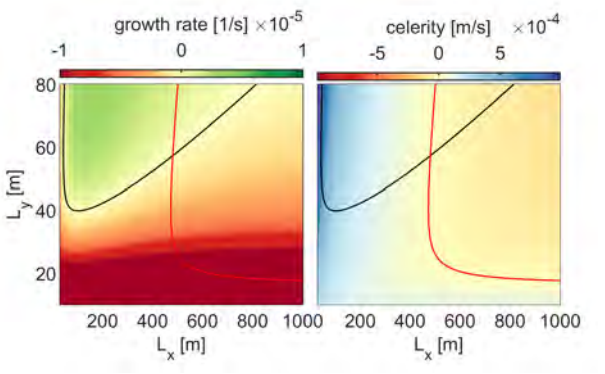

Figure 1: Growth rate (left) and celerity (right) of an infinitesimal alternate bar pattern of wavelength in streamwise direction L_x and transverse direction L_y. The black and red lines divide the domains of positive and negative growth rate and celerity, respectively.

3 Methodology

Solving the linear system of equations, we create synthetic data of the evolution in time of waves with varying streamwise and transverse wavelength. The data concerns the evolution of flow variables and bed level. These data is fed into a neural network model for training, which we use to assess the following question: How good is the model in predicting conditions inside and outside the domain in which it has been trained? First we train the model with data over all the domain and test the ability to predict conditions which are not given for training but are inside the domain. Second we train the model with partial data (e.g., only conditions in which bars decay) and test the ability to predict conditions outside the domain (e.g., in which bars grow).

Acknowledgements

Bert Jagers has contributed through discussion on multiple occasions.

References

[1] M. Colombini, G. Seminara, and M. Tubino. Finite-amplitude alternate bars. *J Fluid Mech*, 181:213–232, 9 1987.

[2] F. Engelund and E. Hansen. Monograph on sediment transport in alluvial streams. Tech. Univ. of Denmark, Copenhagen, 1967.

Experimental and analytical evidence of steady alternate bars forced by a localized asymmetric drag distribution

Mirko Musa[1], Michele Guala[2], Marco Redolfi[3]

[1]Laboratory of Sustainable River Engineering, Energy and Morphodynamics (STREEM), School of Architecture, Civil and Environmental Engineering (ENAC), EPFL, Switzerland
[2]St. Anthony Falls Laboratory, Department of Civil, Environmental, and Geo-Engineering, University of Minnesota, Minneapolis, MN, USA
[3]Dipartimento di Ingegneria "Enzo Ferrari", Università degli Studi di Modena e Reggio Emilia, Italy

e-mail corresponding author: mirko.musa@epfl.ch

Keywords: *river bars, sediment transport, shallow water flows, hydropower, anthropogenic stressors*

1 Introduction and Motivation

Experimental observations by [1] indicate that asymmetric deployments of in-stream fluvial turbines can induce the formation of large-scale, persistent alternate distortions in the bathymetry, resembling steady fluvial bars. These distortions may be perceived as a detrimental non-local impact induced by the technology. River bars are meso-scale bedforms that spontaneously arise from instabilities of the riverbed [3] or can be forced by localized geometric variations, such as channel curvature, bifurcations, or in-stream obstacles, like river turbines. According to linear theories (e.g., [4]), the spatial extent of these features depends not on the specific nature of the forcing but rather on channel characteristics, particularly the width-to-depth ratio (β), the Shields stress, and the relative roughness. However, experiments by [1] suggest that the characteristics of the external forcing, such as those introduced by turbines, may also influence the resulting bed distortion. These observations raised two key questions: (1) Is the observed bathymetric distortion indeed a bar-type phenomenon? (2) How do the characteristics of the external forcing (in this case, turbines) affect the resulting bed deformation? This work addressed these questions by developing a new analytical model and validating it through a new set of experiments (see the associated publication [2]).

2 Methodology

The model formulation builds on the linearized, 2-D, depth-averaged shallow water equations introduced by [4]. The model is then coupled with a novel internal boundary condition that accounts for localized, asymmetrical drag forces. This addition allows us to represent the non-local effects exerted by hydrokinetic turbines, or any permeable perturbation that influences a limited portion of the channel cross-section (e.g., vegetation patches, hydraulic structures). To validate the model, we conducted a new set of experiments using a porous grid to simulate finite perturbations. The grid covers a well-defined section of the cross-section and adheres to the boundary conditions specified in the formulation. By using a porous grid without depth constraints, we can incorporate a spatially impulsive drag force similar to turbines, while exploring a broader range of β values.

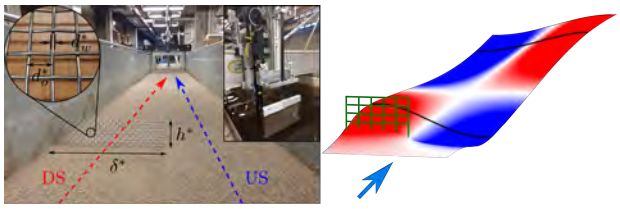

Figure 1: Experimental set-up and analytical solution of the 2D bed distortion.

3 Results

Comparing analytical solutions with experiments, we concluded that: 1) the relatively simple depth-averaged shallow water model, coupled with our novel boundary condition for localized drag forces, can accurately capture key features of non-local bed deformation induced by an obstruction, offering an analytical and computationally efficient solution; 2) the resulting bed deformation depends not only on the magnitude of the drag force but also on the degree of asymmetry of the disturbance within the channel cross-section; and 3) the forced bar solution, along with the direction and extent of its propagation, is primarily governed by the difference between the aspect ratio β and the resonant aspect ratio β_R.

References

[1] M. Musa, C. Hill, and M. Guala. Interaction between hydrokinetic turbine wakes and sediment dynamics: array performance and geomorphic effects under different siting strategies and sediment transport conditions. *Renewable Energy*, 138:738–753, 2019.

[2] M Redolfi, M Musa, and M Guala. On steady alternate bars forced by a localized asymmetric drag distribution in erodible channels. *Journal of Fluid Mechanics*, 916:A13, 2021.

[3] G. Seminara. Fluvial sedimentary patterns. *Annual Review of Fluid Mechanics*, 42(1):43–66, 2010.

[4] G. Zolezzi and G. Seminara. Downstream and upstream influence in river meandering. part 1. general theory and application to overdeepening. *Journal of Fluid Mechanics*, 438(13):183–211, 2001.

Numerical Calculation Method for Bed Height Variation of Two Grain-size Sediment based on the Avairable Porosity and Dynamic Rough Wall Law

R. Mitani[1*], K. Sakagami[1], T. Uchida[1], T. Inoue[1]
[1] Graduate School of Advanced Science and Engineering, Hiroshima University. Hiroshima, Japan,
[*]*e-mail corresponding author:* m240960@hiroshima-u.ac.jp

Keywords: Dynamic Rough Wall Law, mixed grain-sized bed, Numerical calculation of bed elevation

1 Introduction

In Rivers, these is a selective sorting effect with the variation in the porosity structure, which effects significantly on the sediment transport and riverbed topography for the wide grain size distribution. However, no reliable model has been developed to calculate selective sorting in a depth-integrated flow with the Eulerian sediment transport model framework. In this study, we apply the Numerical calculation of two grain-sized bed elevation with the dynamic rough wall law for simulating flow over a rough bed to the experimental data we conducted.

2 Numerical Method

In this study, the GBVC4-DWL (general bottom velocity computation 4 with dynamic wall law) [1] is used for the flow analysis method, which is originally proposed for the roughness layer composed of uniform grain size. In a two grain-sized bed, the grain size of the bed is not uniform as shown in Figure 1, and different size particle has a different deposition height. Therefore, the near-surface layer is divided into a coarse-particle layer and a fine-particle layer, and the coarse-particle layer is treated as the roughness layer in GBVC4-DWL. To evaluate the shear stress $\boldsymbol{\tau_{0i}}$ acting on the fine roughness layer in a sediment transport analysis, the shear stress is derived by transforming the shear stress on the fine roughness layer from the momentum equation in the coarse roughness layer to a form using the mean flow velocity $\boldsymbol{u_{ri}}$. In addition, this shear stress is also composed of the thickness at the coarse roughness layer δz_r and the porosity n_c at coarse roughness laye . These components are required for the flow analysis. Hence, the Eulerian deposition-ero-

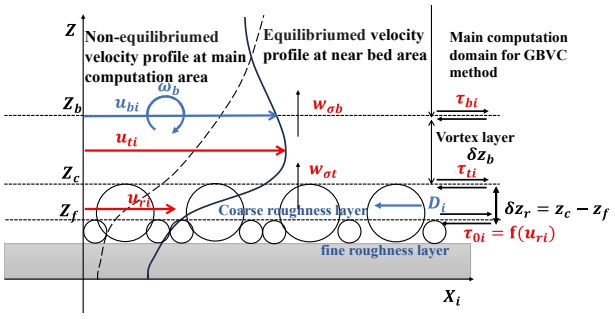

Figure 1 : Enlarged figure of near riverbed

sion formulation [2],[3] was applied as a riverbed continuous equation for the instead of the active layer model to calculate changes in the near-surface riverbed structure based on the available void ratio concept.

3 Experimental setup

The following experimental data were used for validation. We conducted the experiment using the following conditions as shown in Table 1. The initial bed shape was formed as shown in Figure 2, debris flow sediments captured downstream, and water continued to flow until there were no more bedloads. The volumetric ratio of coarse particles to fine in the initial bed was 1:4.

Table 1 : Experimental conditions

Dicharge [m^3/s]	Width [m]	Coarse diameter[mm]	Fine diameter[mm]
0.003	0.2	75.27	1.55

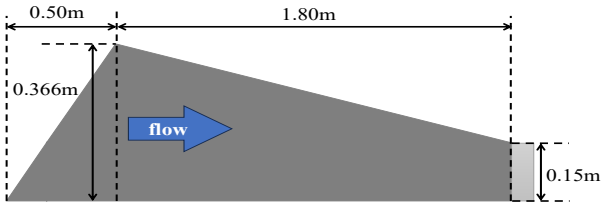

Figure 2: Experimental conditions

4 Result and Discussion

The decrease of the coarse-particle deposition height with time due to the flow of fine-particle was observed in the experiment, which can also be reproduced by the calculations.

References

[1] Uchida, T., Fukuoka, S., Papanicolau, A.N., and Tsakiris, A. G. (2016). "Nonhydrostatic Quasi-3D Model Coupled with the Dynamic Rough Wall Law for Simulating Flow over a Rough Bed with Submerged Boulders." *J. Hydraulic Eng.*, 10.1061/(ASCE)HY.1943-7900.0001198.

[2] Uchida, T., Kawahara, Y., Hayashi, Y., and Tateishi, A. (2020). "Eulerian deposition model for sediment mixture in gravel-bed rivers with broad particle size distributions", Journal of Hydraulic Engineering, Vol 146, Issue 10, 04020071.

[3] Nakashima, N., Uchida, T., and Kawahara, Y. (2020). "A Sediment Transport Model Considering Porosity Variation of Sediment Mixture Coupled with a Eulerian Deposition model." *Proceedings of the 22nd IAHR-APD Congress 2020, Sapporo, Japan*

Investigating flow-morphology interactions in a step-pool unit by combining physical and numerical modeling

Chendi Zhang [1], Marwan Hassan[2], Yuncheng Xu[3]
[1] Key Laboratory of Land Surface Pattern and Simulation, Institute of Geographic Sciences and Natural Resources Research, Chinese Academy of Sciences, Beijing, 100101, China
[2] Department of Geography, University of British Columbia, Vancouver, V6T1Z2, Canada
[3] College of Water Resources and Civil Engineering, China Agricultural University, Beijing, 100081, China
Corresponding author: zhangchendi@igsnrr.ac.cn

Keywords: Step-pool; Structure from Motion (SfM); computational fluid dynamics (CFD); flow-morphology interaction; mountain river

1 Introduction

Step-pools are common bedforms in mountain streams and have been utilized in river restoration or fish passage projects around the world. Step-pool units exhibit highly non-uniform hydraulic characteristics which have been reported to closely interact with the morphological evolution. Further understanding towards these interactions builds the basis for better prediction of channel evolution and more advanced design of artificial step-pool system. However, detailed information on the flow-morphology interactions has been limited due to the difficulty in measuring the flow structures or the flow forces in a step-pool unit [1].

2 Methods

To fill in this knowledge gap, we established an approach combining physical experiment and computational fluid dynamics (CFD) simulation for a step-pool unit made of natural grains at six flow conditions [2]. Structure from motion (SfM) was used to capture the detailed 3D reconstructions of the bed surfaces with various conditions of pool scour. The hydraulic measurement was applied both as input data at the inlet boundary and also in the validation for the CFD model. The high-resolution 3D flow structures for the step-pool unit were visualized, as well as the distributions of flow forces from both pressure and shear stress.

3 Results

The results illustrate the segmentation of flow velocity downstream of the step, i.e., the integral recirculation cell at the water surface, streamwise vortices formed at the step toe, and high-speed flow in between, resulting from the complex morphology of the step-pool unit. Both the recirculation cells at the water surface and the step toe perform as energy dissipaters to the flow with comparable magnitudes. Pool scour development during flow increase leads to the expansion of the recirculation cells until step-pool failure occurs. Significant transverse variability of the flow forces from both the shear stress and pressure has been revealed. The flow forces in both streamwise and transverse directions are closely related to the flow structures and morphology in the unit. The ratios between skin and form drag have large variations at low flows while show a relatively limited range of 0.05-0.1 at high flows, suggesting a small proportion occupied by the skin resistance in the total flow resistance in the step-pool channel. The drag coefficient of the step-pool unit is around 0.3 at high flows. Our results highlight the feasibility of the approach combining physical and numerical modeling in investigating the complex flow-morphology interactions of step-pool features.

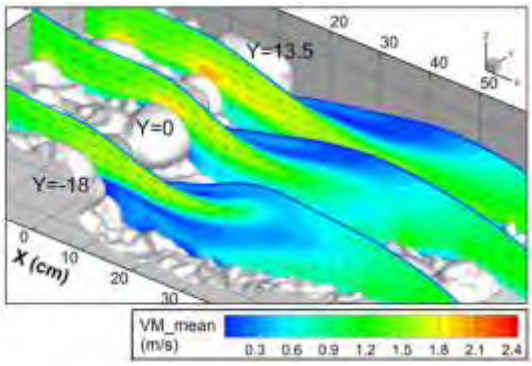

Figure 1: Distribution of time-averaged velocity magnitude (VM_mean) and vectors in three longitudinal sections in a step-pool unit at the discharge of 49.9 L/s, which was the highest flow condition tested in this work.

Acknowledgments

This research was funded by the National Natural Science Foundation of China (42471086), the National Key R & D Program of China (2023YFC3006700), and the international partnership program of the Chinese Academy of Sciences (177GJHZ2022064FN).

References

[1] Zhang, C., Hassan, M.A., Saletti, M., Zimmermann, A.E., Xu, M., Wang, Z., 2023. A unit-scale framework for designing step-pool sequences. *J. Hydraul. Eng.*, 149 (1), 04022033.

[2] Zhang, C., Xu, Y., Hassan, M.A., Xu, M., He, P., 2022b. A combined approach of experimental and numerical modeling for 3D hydraulic features of a step-pool unit. *Earth Surf. Dyn.*, 10 (6), 1253 – 1272.

Acceleration of the Sediment Transport Analysis for Braided Rivers Using the Average Component Acceleration Method

Y. Kitayama[1], D. Matsuo[1], T. Uchida[1], T. Inoue[1]
[1] Civil and Enviromental Engineering, Hiroshima University
Corresponding author: utida@hiroshima-u.ac.jp

Keywords: Sediment Transport Analysis, High-speed calculation, Average Component Acceleration (ACA) Method

1 Introduction

Higher-order analyses that consider vertical flow changes enable the analysis of complex hydraulic phenomena, including riverbed change. In addition, to consider long-term variations and uncertainties, such as the prediction of climate change impacts, it is necessary to consider many patterns over a long period by numerical analysis. Therefore, it is necessary to reduce the computational load and accelerate the analysis. In this study, we accelerate sediment transport analysis using the Average Component Acceleration (ACA) method [1].

2 Method

As a fluid flow model, this study uses the Simplified Bottom Velocity Computation with quadratic velocity distribution (SBVC2) method[2], assuming equilibrium condition of water surface and hydrostatic pressure distribution based on the BVC method[2] that calculate bottom flow velocities within the framework of 2D analysis. In sediment transport analysis, the equilibrium bedload formula is used to the Exner equation for hight variation. To accelerate the analysis stably, the ACA method[1] separates the water depth variation at each location into two components. One is the average component, which changes gradually over time, and the other is the local component, which changes over short time intervals due to local flows. By increasing the time step interval of only the average component, it is possible to accelerate a stable analysis while remaining the micro-oscillations in the water depth. The shortening of the discharge hydrograph at the upstream end means a shortening of the time step of the average component, because it is determined by the discharge hydrograph at the upstream end. The ACA method adds a new term to discretization formula that increases the time step of the average component, as shown in Equation (1). We calculated the average component by the local component being averaged over the channel and weighted by the celerity as in equation (2).

$$h^{n+1} = h^n + \Delta h^n + (\alpha - 1)\overline{\Delta h^n} \tag{1}$$

$$\overline{\Delta h^n} = \frac{\sqrt{h^n}}{\overline{\sqrt{h^n}}} \frac{1}{LB} \int_L \int_B \Delta h^n dy\, dx \tag{2}$$

where h: water depth, L, B: longitudinal and transverse distances, respectively, α: acceleration factor, n: time step, Δh^n: local component, and $\overline{\Delta h^n}$: average component. On the other hand, assuming the bed hight variation is considered gradual compared to water surface variation, the analysis for the temporal variation in the riverbed topography is accelerated by simply applying an acceleration factor to the variations, as

$$Z_b{}^{n+1} = Z_b{}^n + \alpha \Delta Z_b{}^n \tag{3}$$

where Z_b:riverbed height.

3 Result and Discussion

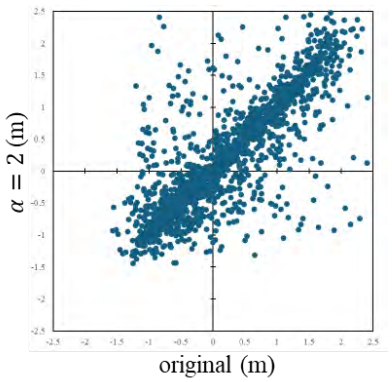

Figure1: Correlation of riverbed variation for original analysis and analysis with $\alpha = 2$

The analysis conditions are channel length 4 km, width 20 m, slope 1/400, and acceleration factor α of 1, 2, 5, and 10. The discharge hydrograph given at the upstream end increased and decreased slowly 10 times, under the condition that result in alternate bars. Fig. 1 shows the correlation plot for original analysis and α=2. The correlation coefficient is 0.82. However, there are some plots that deviate significantly from the Y=X due to the misalignment of bars. For α = 5 and 10, the values are 0.34 and 0.44.
The result suggests that the average component term should be applied to sediment transport analysis as well as to flow analysis.

Reference

[1] Matsuo D. and Uchida T.: Attempt to Accelerate Flood Flow Analysis Using Average Component Acceleration Method Journal of JSCE, Ser. B1(Hydraulic Engineering), Vol.80, No.16, 2024. https://doi.org/10.2208/jscejj.23-16170
[2] Lugina F.P., Uchida T. and Kawahara Y.: Numerical Calculations for Curved Open Channel Flows with Advanced Depth-Integrated Models, KSCE Journal of Civil Engineering, Vol.28, No.3, pp.1026-1040, 2024.

Application of Multi Grid Model for Computing River Morphodynamics

Takeshi Sakai[1], Ichiro Kimura[2]
[1]University of Toyama, Toyama, Japan
Corresponding author: m24c1703.ems@u-toyama.ac.jp

Keywords: Double-grid model, morphodynamic, depth-averaged two-dimensional model

1 Introduction

To improve the accuracy and the efficiency of morphodynamic simulation, many multi grid models are developed. One of multi grid model is the doble-grid model by Volp et al. (2016). The objection of this study is to validate the double-grid model in morphodynamic simulation. We simulated the development of alternate bars by double-grid model. We validated the accuracy by comparing the experimental results with the simulated results and verified the efficiency of the double-grid model by comparing with the single-grid model.

2 Double-grid model

In this study, we employed the double-grid model by Volp et al. (2016) [1]. The double-grid model is characterized by using two types of computational grids, a coarse grid and a fine grid. The coarse grid is used for discretization of the governing equations (a depth-averaged continuity equation and depth-averaged momentum equations). On the other hand, the fine grid is used for discretization of the Exner equation and calculates the changes of bed level. To calculate bedload sediment flux, we used Kovacs-Parker equation.

3 Methodology

3.1 Experiment

We validated the accuracy of Double-grid model by comparing the experimental results by Akahori et al. (2011) [2]. This experiment was conducted in a 0.9 m wide and 50m long water flume. The bottom of the channel was covered with silica sand with an average grain size of 0.76 mm and the discharge was set constant (6.4 l/s).

3.2 Calculation conditions

The Hydraulic conditions of calculation were the same as those of Akahori's [2] experiment. Periodic boundary conditions were set at the upstream and downstream ends, and the computational domain was set at 12.06 m. The calculation time was up to 10000 seconds.

Table1 shows grid conditions. The resolution of the fine grid is same in all cases (1200 × 90 grid cells) though the number of the coarse grids are varied in Cases A and B. The computation with a single-grid model with iRIC software (Nays2DH) was also carried out under two cases with different grid resolution (Cases C and D).

4 Result

Figures 1 and 2 show the simulated bed elevation along the central axis and along the axis 10 cm from the right bank, respectively. In both case A and B, alternate bar was simulated. Regarding the period along the centerline, the Case B shows the better result than the Case A. Case B is as accurate as or more accurate than Case D. Case C is the worst result of four cases.

Table 1 also shows the CPU times. Case B reduced the CPU time by 66% compared to Case D. This result shows efficiency of the double grid model.

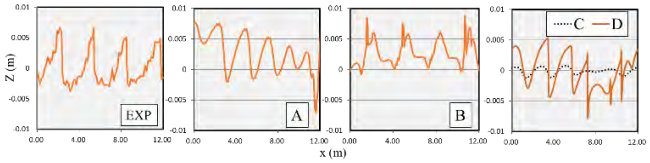

Figure 1: Bed change along the central axis

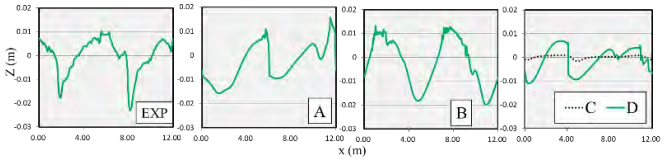

Figure 2: Bed change along the he axis 10 cm from the right bank

Table 1: Grid conditions and CPU time

Case	coarse grid	Relative CPU time(%)
A (W grid)	60×5	17
B (W grid)	120×9	34
C (Nays2DH)	120×10	0.9
D (Nays2DH)	1200×90	100

Acknowledgments

This work was supported by JSPS KAKENHI Grant Number JP24K00985.

References

[1] N.D. Volp. B.C. van Prooijen. J.D. Pietrzak. G.S. Stelling. A subgrid based approach for morphodynamic modelling. Advances in Water Resources. 105-117. 2016

[2] R. Akahori. S. Yamaguchi. I. Kimura. T. Iwasaki. Y. Shimizu and K. Hasegawa. Evolution of channel bed topography in a 50 meter laboratory flume under various hydraulic conditions of bar instability and resonance. RCEM2011. 1998-2009. 2011

Modeling Boundary Shear Stress for River Width Prediction

Artini Giada[1], Francalanci Simona[1], Lanzoni Stefano[2]
[1]Department of Civil and Environmental Engineering, University of Florence (Italy)
[2]Department of Civil, Environmental and Architectural Engineering, University of Padua (Italy)
Corresponding author: giada.artini@unifi.it

Keywords: boundary shear stress distribution, morpho-hydrodynamics, ray-isovel method, numerical modeling

1 Introduction

The morphology of natural river channels is shaped by the interplay between flow, sediment transport and vegetation. Understanding boundary shear stress and velocity distribution is crucial for estimating flow discharge, sediment transport and predicting river morphology changes. Riverbank dynamics control equilibrium cross-sections, impacting flood conveyance. Riverbank erosion and mass failure are the main drivers of cross-sectional adjustment, eventually determining equilibrium river width. Riverbank shear stress is influenced by vegetation and irregular topographic elements or "bumps", resulting from erosion and bank collapse. A reliable tool for accurately predicting boundary shear stress is essential for modeling river evolution to manage river ecosystems efficiently. This study aims to generalize the Cross-Section Evolution Model (CSEM), which predicts the width of rectangular river sections based on bank erosion [1]. The updated model includes an improved bed and bank shear stress estimation for sections of generic shape using the Ray-Isovel Model (RIM) [2]. The new model will be tested on an actively migrating section of the Ombrone River to predict its lateral evolution.

2 Materials and Methods

2.1 Ray-Isovel and CSEM Models

The RIM determines the shear stress distribution along the wetted perimeter using a turbulence closure for eddy viscosity *K*, defined along rays perpendicular to curves of constant velocity (isovels). Given *K* throughout the cross-section, the steady uniform flow momentum equation is solved as:

$$0 = \rho g S + \frac{\partial}{\partial y}\left(\rho K \frac{\partial u}{\partial y}\right) + \frac{\partial}{\partial z}\left(\rho K \frac{\partial u}{\partial z}\right) \qquad (1)$$

Where ρ is the fluid density, g acceleration of gravity, S friction slope, u downstream velocity and y,z the transverse and vertical coordinates, respectively. A no-flux condition $\partial u/\partial z = 0$ is imposed at the free surface, while $u = 0$ at the roughness height. The model includes the effects of vegetation and bumps on shear stress distribution [3].

The CSEM computes the cross-section equilibrium width based on the balance between skin friction and the critical shear stress for bank erosion. Accurate estimation of the skin friction acting on the bank surface is fundamental for the model reliability. The RIM will be integrated into CSEM to enhance bank shear stress estimation and improve model reliability. The updated CSEM will account for vegetation effects on river width prediction and will be expanded beyond rectangular sections to support generic cross-section geometries.

2.2 Case Study

The case study is a reach of the Ombrone Grossetano River (Tuscany, Italy), characterized by cohesive banks with significant vegetation cover and a highly dynamic channel migration. Over the past 20 years, the left bank has shifted approximately 150 m, leading to the loss of agricultural land.

Detailed field surveys were conducted to collect data on bumps geometry using Lidar surveys, vegetation with APR system, channel bathymetry with a single-beam echosounder and sediment size distribution.

3 Expected Results

The updated CSEM model will be applied to assess the consistency between surveyed cross-sections and the predicted equilibrium width. The RIM, currently limited to straight channels, will be extended to include secondary currents by including the information from curved-channel flow models. Incorporating the updated method to estimate boundary shear stress in hydro-morphodynamic simulations will improve flow field characterization across the study reach, enabling a physics-based analysis of inner and outer bank dynamics on channel morphology.

Acknowledgments

This research is part of the SECURE project "Safety Equilibrium Conditions for rivers UndeR changing climatEs", funded by "Next Generation EU" (M4.C2.1.1).

References

[1] Francalanci, S., Lanzoni, S., Solari, L., and Papanicolaou, A. N. Equilibrium cross section of river channels with cohesive erodible banks. *J. Geophys. Res.: Earth Surface,* 125.1, 2020.

[2] Kean, J. W., and J. D. Smith. Flow and boundary shear stress in channels with woody bank vegetation. In *Riparian vegetation and fluvial geomorphology,* 8: 237-252, 2004.

[3] Kean, J. W., and J. D. Smith. Generation and verification of theoretical rating curves in the Whitewater River basin, Kansas, *J. Geophys. Res.,* 110, F04012, 2005.

COUPLING A SLOPE FAILURE MODEL WITH GROUNDWATER EFFECTS AND 2D RIVERBED DEFORMATION MODEL.

Y. KASAGI[1], T. INOUE[1]
[1]Graduate School of Advanced Science and Engineering, Hiroshima University, Hiroshima, Japan
Corresponding author: inouetakuya@hiroshima-u.ac.jp

Keywords: riverbank erosion, groundwater level, 2D riverbed deformation model

1 Introduction

Riverbank erosion occurs as a result of a complex interaction of various factors, including changes in the flow and riverbed within the channel, the groundwater level and cohesion within the banks. Langendoen et al. [1] proposed a slope failure model that considered the effects of groundwater and cohesion in river banks, but their model could not consider flow and bed changes in a channel. On the other hand, Takemura and Fukuoka [2] coupled a slope failure model and 2D flow / bed deformation model, but did not consider the effect of bank cohesion. In this study, we incorporate the simplified model of Langendoen et al. [1], based on the study of Takemura and Fukuoka [2], into a 2D flow/bed deformation model called Nays2DH [3] to analyse the effect of groundwater levels on bank erosion.

2 Method

iRIC Nays2DH [3] is a numerical model that calculates the flow field and riverbed changes in a channel by combining the plane 2D shallow water flow equations, the Meyer-Peter-Muller bedload model, and the Exner bed deformation model. In our model, the riverbank erosion occurs when the bank safety factor F_s is smaller than 1. The safety factor F_s is calculated using the following equation, which is a simplification of the model proposed by Langendoen et al. [1].

$$F_s = \frac{c'L + (W\cos\alpha - Q + F\sin\alpha)\tan\varphi + U\tan\varphi_b}{W\sin\alpha - F\cos\alpha} \quad (1)$$

where c' is effective cohesion, L is length of sliding surface, W is the weight of soil mass, Q is lifting pressure, F is water pressure from the river side, U is pore water pressure, φ is effective angle of internal friction, φ_b is an angle indicating the rate of increase in shear strength for increasing matric suction.

We used the channel shown in Figure 1. The channel length is 560 m, the channel width is 56 m, the bed gradient is 0.005, the bank height is 4 m, and the bank angle is 45°. The riverbed and banks are composed of gravel with an average grain size of 13 mm. The bed is not cohesive, but the banks have a cohesion of c' = 0.25 Kpa. The Manning's roughness coefficient is 0.03. The flow discharge is 100 m^3/s. The downstream water level is 2 m lower than the bank elevation and higher than the uniform flow depth. Therefore, the flow is affected by the backwater of the downstream water level.

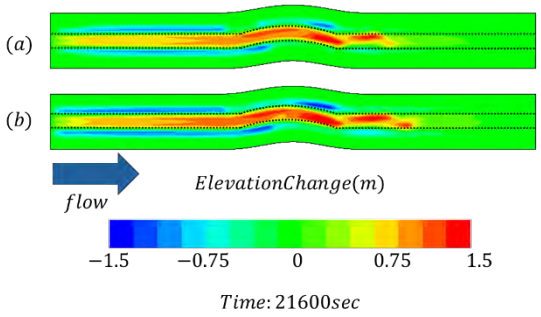

Figure 1: Calculation Results

We calculated two runs with different groundwater levels: run (a) without groundwater level and case (b) with the groundwater level at the same height as the riverbank elevation.

3 Calculation Results

Figure 1 shows the numerical results of the bed and bank changes using our model. Due to the influence of backwater, sediment has accumulated in the channel and the bed elevation has risen. Bank erosion has occurred mainly on the upstream side, where the influence of backwater is less, and on the outer bank of the bends. The results show that case (b) has a higher erosion rate and that the groundwater table has an influence on riverbank erosion.

4 Conclusion

In this study, we introduced a slope failure model considering the groundwater level and bank cohesion into a plane-2D flow / bed deformation model. Our results show that a higher groundwater level leads to greater bank erosion. In the future, we plan to use this model to analyze the effects of groundwater and tide levels on meandering rivers in estuaries.

References

[1] E. J. Langendoen, M. ASCE, and A. Simon.: Modelling the evolution of incised streams. Ⅱ :Streambank erosion. *Journal of hydraulic engineering.*, 2008, 134(7): 905-915.

[2] Y.Takemura and S.Fukuoka. Analysis of riverbank erosion processes in alluvial fans: Application to the field experiment in the Joganji river. *JSCE* Vol.7, No.2, I_799-I_804, 2021.

[3] Y.Shimizu et al.: Advances in computational morphody-namics using the International River Interface Cooperative (iRIC) software. *Earth Surf. Process. Landforms*, Vol. 45, pp. 11–37, 2020.

Effects of an Arrested Avulsion on Long-Term River Channel Stability: Lower Mississippi River

Brandon McElroy[1], Jeff Nittrouer[2], Reuben Heine
[1]University of Wyoming, Laramie, Wyoming, USA
[2]Texas Tech University, Lubbock, Texas, USA
Corresponding author: bmcelroy@uwyo.edu

Keywords: Diversion, Flooding, Sedimentation, Risk

1 Overview

The lower Mississippi River (LMR) is a highly engineered sinuous channel that supports billions of dollars of industry and millions of people. The Old River Control Complex (ORCC) was originally completed in 1964 with the primary purpose to maintain the existing LMR channel by arresting its avulsion into the Atchafalaya basin. Measurements made since that time indicate that the ORCC, including the hydropower structure added in 1991, has allowed approximately 23% of the total LMR water and sediment volumes to pass into the Atchafalaya.

2 Modeling Approach

Here we explore the morphodynamic consequences of the construction and operation of the ORCC through the application of a 1-D numerical model applied to the longitudinal profile of the LMR with the historic splits of sediment and water. We then compare the model outcomes to LMR geomorphic changes as represented in a time-series of Mississippi River bed elevation surveys.

3 Results

To a first order, sediment transport theory predicts that the fixed 1:1 splitting of flow and sediment at the ORCC would create a condition in which the LMR main channel receives a greater sediment load that is greater than its integrated transport capacity. This prediction is observed in the results of the morphodynamic model. Across the suite of boundary conditions that honor the natural range of physical parameters in the LMR, model outcomes show sediment accumulation and commensurate river stage increases throughout the LMR (Figure 1). Confirming the model, repeat surveys indicate that sedimentation has occurred from Arkansas City, AR, just over 200 miles above the ORCC, to near Baton Rouge, LA, located approximately 80 miles below the ORCC. Additionally, specific gage analyses for gaging stations on the LMR near the ORCC also show rising trends of stage for a given discharge consistent with model outcomes (Figure 2). These results are also consistent with recent flooding patterns of the LMR in the vicinity of the ORCC.

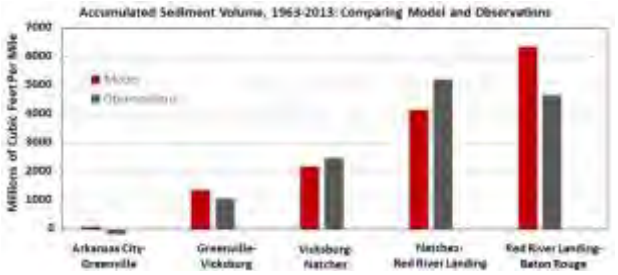

Figure 1: Sediment aggradation values for the Lower Mississippi River due to ORCC operations: predicted (red), and measured

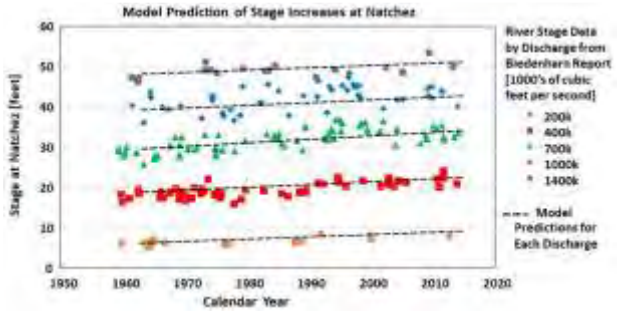

Figure 2: Flow stage data for discharge (points) [1], compared to the model output (lines).

4 Conclusions

The ORCC was conceived to maintain the viability of the LMR main channel through Louisiana. Its operation has preserved the partitioning of flow since mid-20th century. However, it has caused sediment accumulation in the main channel and scouring in the Atchafalaya River. Ultimately, this condition has increased the topographic instability that was the original driver of avulsion, and commensurately, flooding in the LMR has increased. Together, these conditions increase the risk of uncontrolled avulsion of the Mississippi River into the Atchafalaya Basin.

References

[1] Biedenharn, D. S., Allison, M. A., Little, C. D., Thorne, C. R. and Watson, C. C. (2017) *Large-Scale Geomorphic Change in the Mississippi River from St. Louis, MO, to Donaldsonville, LA, as Revealed by Specific Gage Records*. US Army Engineer Research and Development Center, Coastal and Hydraulics Laboratory.

River Avulsion Precursors Encoded in Alluvial Ridge Geometry

J. H. Gearon[1], and D. A. Edmonds[1]

[1]Indiana University, Bloomington, Dept. of Earth & Atmospheric Sciences

e-mail corresponding author: jake.gearon@gmail.com

Keywords: *river avulsion, alluvial ridges, hazard assessment, fluvial geomorphology, flood risk*

1 Introduction

River avulsions generate catastrophic floods that threaten communities worldwide [2], yet predicting their occurrence remains challenging because their precursors are incompletely understood. Alluvial ridges—elevated regions of near-channel topography—form through channel migration and overbank deposition and are thought to precede avulsions, but their spatial patterns and relationship to avulsion impact remain poorly quantified. Here, we test whether alluvial ridge geometry displays systematic patterns that could serve as quantifiable precursors to avulsion.

2 Methods

To quantify avulsion potential (Λ), we analyzed thousands of topographic cross-sections from fourteen rivers with recent avulsion activity. This metric combines ridge height and slope relative to the channel [2]. When $\Lambda \geq 2$, alternative floodplain paths have a higher shear stress than the main channel and avulsion can initiate. For each river, we generated cross-sections every 200 m along the centerline using the SWOT River Database (SWORD) [1] and the Forests and Buildings Removed Copernicus Global DEM (FABDEM) [3]. We calculated avulsion potential (Λ) and employed semivariograms and wavelet power spectra to identify the spatial dependence and structure of Λ downstream.

3 Results

Our analysis reveals systematic downstream variations in Λ (Fig. 1A). From the semivariogram analyses, we identify two characteristic length scales: a longer-wavelength complex ($\overline{L_\lambda} \approx 30$ km) composed of shorter ridge segments ($\overline{L_C} \approx 8$ km). Within these characteristic length scales, values near avulsion sites are 75% larger than at locations randomly distributed beyond L_C. We interpret these segments as alluvial ridge complexes composed of discrete alluvial ridges. These discrete ridges appear to control the spatial extent of avulsion activity. Using the planform extent of avulsion channels and progradational crevasse splays as a measure of avulsion size (L_A), we find that L_A exhibits near 1:1 scaling with L_C (Fig. 1B).

4 Discussion

These findings demonstrate that alluvial ridges serve as quantifiable precursors to avulsion activity. Critically, avulsion length (L_A) scales linearly with L_C ($R^2 = 0.88$), providing the first field-based predictive framework for avulsion extent. Our results pave the way for creating global avulsion risk maps for communities in the Global South, where avulsions occur disproportionately [2].

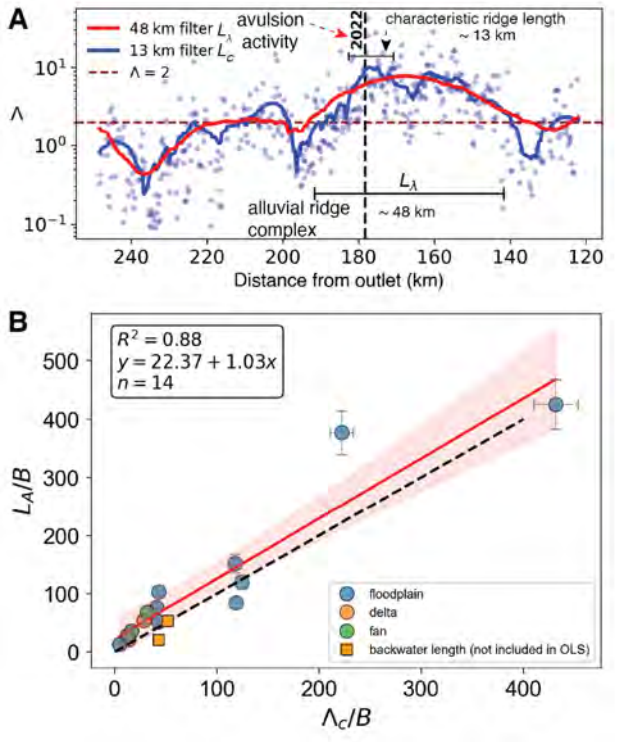

Figure 1: A) Downstream changes in Λ on Río Zulia, Venezuela displays two characteristic scales of alluvial ridge geometry (L_λ and L_C), shown here with Savitzky-Golay filters. B) The planform extent of avulsion, or the avulsion activity length (L_A) exhibits a 1:1 scaling with Λ correlation length (L_C).

References

[1] E. H. Altenau, T. M. Pavelsky, M. T. Durand, X. Yang, R. P. D. M. Frasson, and L. Bendezu. The Surface Water and Ocean Topography (SWOT) Mission River Database (SWORD): A Global River Network for Satellite Data Products. *Water Resources Research*, 57(7), July 2021.

[2] J. H. Gearon, H. K. Martin, C. DeLisle, E. A. Barefoot, D. Mohrig, C. Paola, and D. A. Edmonds. Rules of river avulsion change downstream. *Nature*, pages 1–5, Sept. 2024.

[3] L. Hawker, P. Uhe, L. Paulo, J. Sosa, J. Savage, C. Sampson, and J. Neal. A 30 m global map of elevation with forests and buildings removed. *Environmental Research Letters*, 17(2):024016, Feb. 2022.

Stochastic Dynamics of Morphological Units in Anabranching Rivers

Niccolò Ragno[1], Marco Tubino [1], Carlo Camporeale[2], Luca Ridolfi[2]

[1]Department of Civil, Environmental, and Mechanical Engineering, University of Trento, Trento, Italy
[2]Department of Environment, Land and Infrastructure Engineering, Politecnico di Torino, Torino, Italy

e-mail corresponding author: niccolo.ragno@unitn.it

Keywords: *anabranching rivers; bifurcations; confluences; stochastic modelling*

1 Introduction

When a river divides into two branches that reconnect further downstream, it gives shape to the simplest anabranching pattern: a closed loop. Nested sequences of channel loops characterize anabranching rivers, but these morphological unit can be frequently encountered also in single-thread rivers with transitional planforms between meandering and braiding, being the result of mid-channel bars emergence or of chute cutoffs.

It has been shown [3] that a close relationship exists between the planform characteristics of individual channel loops and the bankfull, geometrical properties of the reach in which they are hosted. Observations indicate that actual channel loops tend to exhibit a mean length of the anabranches proportional to the reach-averaged bankfull depth, regardless of the reach slope and, consequently, the specific river type. This scaling relationship is associated with a modest degree of asymmetry in branches lengths and apparently remains valid even in the case of multithread networks consisting of multiple loop sequences. The theoretical model proposed by [4], which simulates the coupled dynamics of a bifurcation-confluence loop using a one-dimensional equilibrium formulation, suggests that the planform characteristics are intrinsically connected to the partitioning of water and sediment fluxes between the two anabranches.

This previous analyses raise a series of questions to be answered: do channel loops always achieve a planform equilibrium once they form? What are the drivers of their planimetric evolution? This contribution tackles these questions aiming to investigate the long-term evolution of a geometrically simple anabranching system through a one-dimensional stochastic model.

2 The basic ingredients

The stochastic character of the model arises from the variability of the flow regime. Assuming constant and equal sinuosity of the two anabranches, the problem reduces to compute the nodal spacing between the bifurcation and confluence nodes. Two deterministic mechanisms compete to drive the evolution of the loop length: the rate of elongation and the rate of recession, both of which depend on the nodal length. It is further assumed that elongation and shortening alternate stochastically, depending on whether the flow discharge exceeds a certain threshold value: below the threshold, loop elongation occurs; *vice versa*, loop shortening takes place. The definition of this threshold is linked to the nature of the drivers causing the length changes. While elongation is supposed to be a function of the sediment flux distribution at the bifurcation [1], recession may be caused by erosion of previously deposited sediment during floods. This dynamic behaviour can be effectively described using a Langevin equation, where a dichotomous noise allows to switch between the two phases [2].

3 Some preliminary results

The problem can be solved analytically, providing the probability density function of the loop length. The solution exhibits a peculiar negative skewness (due to the different dependencies of the elongation and shortening rates on the nodal distance), and is particularly sensitive to the time spent by the system in each evolution phases with respect to the planform timescale. The average nodal distance is also obtained and shows the key role of the elongation-to-shortening time ratio.

Acknowledgements

This work is part of the project SEDMORNET funded by the European Union Next-GenerationEU - Mission 4 - Component C2 - Investment Fund 1.1 "Fondo per il Programma Nazionale di Ricerca e Progetti di Rilevante Interesse Nazionale (PRIN)".

References

[1] Leif M. Burge. Stability, morphology and surface grain size patterns of channel bifurcation in gravel-cobble bedded anabranching rivers. *Earth Surface Processes and Landforms*, 31(10):1211–1226, 2006. doi: 10.1002/esp.1325.

[2] Carlo Camporeale and Luca Ridolfi. Riparian vegetation distribution induced by river flow variability: A stochastic approach. *Water Resources Research*, 42(10):1–13, 2006. doi: 10.1029/2006WR004933.

[3] Niccolò Ragno and Marco Tubino. Equilibrium of morphological units in anabranching rivers. *Earth Surface Processes and Landforms*, 50, 2025. doi: 10.1002/esp.70004.

[4] Niccolò Ragno, Marco Redolfi, and Marco Tubino. Coupled Morphodynamics of River Bifurcations and Confluences. *Water Resources Research*, 57 (1):1–26, 2021. doi: 10.1029/2020WR028515.

Numerical Testing of Channel Pattern Thresholds

Hannah Schwedhelm[1], Antonia Dallmeier[1], Hannah Schmid[1], Nils Rüther[1]
[1]Chair of Hydraulic Engineering, TUM School of Engineering and Design, Technical University of Munich
Corresponding author: hannah.schwedhelm@tum.de

Keywords: openTELEMAC, hydromorphology, bedforms, braiding, morphodynamics

1 Introduction

Channel pattern classifications have been largely discussed in the literature using observations from rivers and laboratory results [e.g. 1,2]. However, morphodynamic modelling of channel pattern transitions and river responses to hydromorphological changes remains a current field of research [3]. Therefore, we investigate if the formation of these channel patterns can be triggered within morphodynamic simulations by changing hydromorphological parameters, according to thresholds and region plans [1,2]. Instead of replicating bedforms of a specific river, we aim at modelling large-scale channel patterns.

2 Methods

We use the openTELEMAC modeling system and couple the hydrodynamic module TELEMAC-2D with the morphodynamic module GAIA. The mesh dimensions are based on the general hydromorphologic conditions of the At-Bashy River in Kyrgyzstan (Figure 1 a). The model has a width of 500 m and a length of 3.6 km, where the first 600 m represents a stretch for braiding initiation (Figure 1 b). For the hydromorphological simulations, we use the Meyer-Peter and Müller formula [3] as a sediment transport function while suspended load transport is not considered in this study. We simulate different hydromorphological scenarios, to test the model's ability to capture different channel patterns. These scenarios are defined using the anabranching and braiding thresholds developed by [2]. Therefore, we select different values of discharge and mean grain size diameter to account for different dimensionless formative discharges which should theoretically trigger different channel patterns.

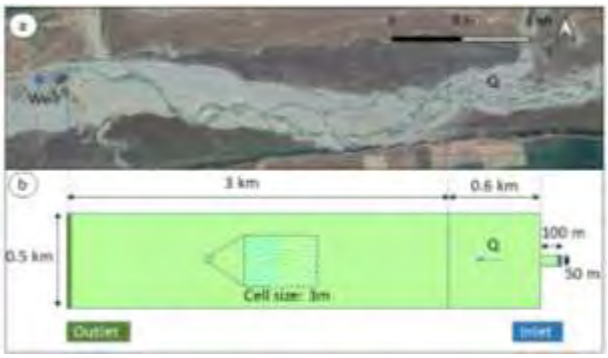

Figure 1: a) Dimensions of At-Bashy River in Kyrgyzstan (Google Earth Images for the 18th August 2019 © 2023 CNES / Airbus), b) dimensions of numerical mesh.

3 Results and Discussion

Different channel patterns develop when changing mean grain size and discharge values, demonstrating the models' ability to react to hydromorphological changes [3]. Further simulations are needed to evaluate how sensitive the formation of these patterns is to changes in the input values, how strongly these patterns differ, and whether they persist over a longer simulation time.

Testing the model's ability to replicate bedforms according to thresholds and region plans [1,2] is, hence, a first step towards tackling current research topics of simulating the riverbed evolution in response to natural or anthropogenic changes [3]. Such an assessment as done in this study is crucial, especially when the objective is to reproduce similar channel patterns as observed in nature rather than accurately simulate the formation of individual river threads.

4 Conclusion

In this study, we test the ability of TELEMAC-2D coupled with GAIA to simulate channel pattern according to thresholds derived from literature [1,2]. However, further investigations are needed to more accurately assess different channel patterns and the sensitivity of the model to changing input parameters.

Acknowledgments

This project has received funding from the European Union's Horizon 2020 research and innovation programme under grant agreement No 101022905.

References

[1] M.S. Yalin and A.M.A.F. Da Silva. Fluvial processes. IAHR Monograph, Delft, 2001

[2] B.C. Eaton, R.G. Millar & S. Davidson. Channel patterns: Braided, anabranching, and single-thread. Geomorphology, 120(3-4), 353–364, 2010.

[3] Y. Hu, H. Yang, H. Zhou & Q. Lv. A Review of Numerical Modelling of Morphodynamics in Braided Rivers: Mechanisms, Insights and Challenges. Water, 15(3), 595, 2023.

[4] E. Meyer-Peter and R. Müller. Formulas for Bed-Load transport. IAHSR 2nd meeting, Stockholm, appendix 2, 1948.

3D complex shapes of river dunes through nonlinear stability analysis

Marco Colombini[1], Costanza Carbonari[2]
[1]Dipartimento di Ingegneria Civile, Chimica e Ambientale, Università degli Studi di Genova, Genoa, Italy
[2] Dipartimento di Ingegneria Civile e Ambientale, Università degli Studi di Firenze, Florence, Italy
Corresponding author: costanza.carbonari@unifi.it

Keywords: lunate and linguoid dunes, interaction of 2D and 3D disturbances, amplitude equations of perturbations

1 Introduction

In rivers with sandy beds, the flow can generate a wide variety of bed forms, which are typically categorized based on their main spatial scales, particularly the longitudinal wavelength. Focusing on river dunes, whose wavelength is proportional to the flow depth, they are observed to have a two-dimensional straight-crested structure under low flow conditions. As flow velocities increase, the dunes develop into three-dimensional linguoid patterns [1]. Colombini and Stocchino's [2] theoretical work supported these findings, demonstrating that, within a linear framework, a transition from 2D to 3D occurs as the flow becomes shallower, eventually leading to the formation of alternate bar patterns. These bars have a longitudinal wavelength that scales with the channel width rather than the flow depth. The clear distinction between different bed forms, such as alternate bars and oblique dunes, has recently been debated, and it is increasingly recognized that bed forms exist along a continuum of sediment patterns that gradually transform into one another as flow and sediment parameters vary.

A similar pattern of behaviour has been observed in coastal morphodynamics, particularly in studies of 2D and 3D ripple formation [3-5]; likewise aeolian dunes whose wide variety of shapes [6] can be obtained through the combination of 2D and 3D modes, with different amplitudes, aspect ratios and phases.

In this work, we explore the formation of linguoid and lunate river dunes by examining how 2D and 3D bed waves interact with one another by means of a weakly nonlinear analysis similar to those on 3D ripples [3-5].

2 Formulation of the problem and linear analysis

The model is composed of the governing equations of hydrodynamics, consisting of the dimensionless Reynolds and continuity equations, and the dimensionless equation for sediment mass-conservation. Hydraulically rough conditions are adopted for the turbulent flow and the quasi-steady approximation is assumed. We considered a well-sorted sediment mixture, characterized by its median diameter and transported as bedload only. At the linear level, the eigenvalue of the bed wave is determined for both 2D and 3D perturbations, revealing that within a specific range of flow and sediment parameters, both 2D and 3D disturbances are unstable and can grow simultaneously.

3 Weakly nonlinear analysis

The competition between 2D and 3D modes of instability is studied through a weakly nonlinear expansion in a neighbourhood of the critical condition (in terms of Froude and wavenumbers) of the 2D perturbation.

We obtained a system of 2nd order amplitude equations which describe the simultaneous evolution of a triad of bottom waves, composed of one 2D disturbance and two 3D disturbances, the latter with longitudinal wavenumber half of that of the 2D perturbation and with opposite transverse wavenumber [7]. The symmetry of the problem in the transverse direction leads to a system of two amplitude equations, whose time evolution include a variety of scenarios depending on the sign of linear and nonlinear coefficients. Among the possible behaviours we have *i)* the predominance of one mode over the other, with one mode vanishing and the other growing exponentially according to its linear growth rate; *ii)* the resonance of the system, with one of the two modes linearly unstable providing energy to the linearly stable mode through nonlinear interaction; *iii)* the existence of stable equilibrium solution. The third scenario is of particular interest since it represents the case of stable, finite amplitude dunes of complex shapes. Ongoing results are providing novel insights on the formation of lunate and linguoid dunes.

References

[1] J.G Venditti, M. Church, and S.J. Bennett. On the transition between 2D and 3D dunes, *Sedimentology*, 52:1343-1359, 2005.

[2] M. Colombini, A. Stocchino. Three-dimensional river bed forms. *J. Fluid Mech.*, 695:63-80, 2012.

[3] P. Blondeaux. Sand ripples under sea waves. Part 1. Ripple formation. *J. Fluid Mech.*, 218:1-17, 1990.

[4] G. Vittori and P. Blondeaux. Sand ripples under sea waves. Part 3. Brick-pattern ripple formation. *J. Fluid Mech.*, 239:23-45, 1992.

[5] P.C. Roos and P. Blondeaux. Sand ripples under sea waves. Part 4. Tile ripple formation. *J. Fluid Mech.*, 447:227-246, 2001.

[6] E. McKee. Structure of dunes at White Sand National Monument, New Mexico (and a comparison with structures of dunes from other selected areas. *Sedimentology,* 7(1):3-69, 1966.

[7] A.D.D. Craik. Non-linear resonant instability in boundary layers. *J. Fluid Mech.*, 50:93-413, 1977.

Experimental observations on a tidal channel bifurcation

Alessia Ruffini[1], Shaahin Nazarpour Tameh[1] , Lorenzo Durante[1] and Nicoletta Tambroni[1]

[1]University of Genoa, Italy

e-mail corresponding author: alessia.ruffini@edu.unige.it

Keywords: *Sediment dynamics, tidal channels, flood regulation, experimental measurement.*

1 Introduction

Tidal networks are characterised by bifurcating channels. While the issue of bifurcation has been extensively studied in the riverine literature (e.g., [1]), the case of tide-influenced bifurcation remains less understood. Some theoretical approaches have addressed river bifurcation under weak tidal influence of small amplitude [3], while numerical simulations have been carried out to investigate the morphological evolution of bifurcations in deltas influenced by tides [2]. The results suggest that river bifurcations often develop asymmetric morphologies, with one downstream channel silting up while the other becomes dominant. However, in tide-influenced systems, bifurcations are typically less asymmetric, with both downstream channels remaining open. Iwantoro et al. (2020) found that downstream channels become less asymmetric as the tidal influence increases over the river. Here, we wish to experimentally investigate the evolution of a fully tidal-influenced bifurcation.

2 Methods

The experiments are carried out in the DICCA laboratory at the University of Genoa. Two different cases are examined: the first is a reference case characterised by a single tidal channel with a converging width, decreasing exponentially landward. In the second case, a partition is introduced in the middle of the landward part of the channel to simulate bifurcation dynamics. This setup allows us to explore how sediments are distributed when the flow is split, revealing information on morphological evolution under controlled settings.

The setup shown in Fig. 1, which opens at one end to a basin subject to tidal oscillations and is closed at the other, allows for a scaled-down replication of natural tidal channels. The investigations use the DICCA hydraulics laboratory's tidal wave-producing equipment. It has a basin and a straight convergent channel that is 22.5 meters long and 0.3 meters wide at the entry before narrowing to 0.1 meters at the end of the channel. The sediments used in the experiments consisted of polycarbonate grains, characterised by a density $\rho = 1.27 \times 10^3$ kg/m^3 and a median grain size $d_s = 0.15$ mm. The tidal wave was generated using a periodically oscillating cylinder in a feeding tank, imposing a sinusoidal free surface elevation $\eta = a_0 \cos(\omega t)$, with amplitude $a_0 = 1.5$ cm and period T = 180 s. This wave was selected to ensure sediment mobilisation both in the bed and in suspension while minimising resonance effects within the channel.

The apparatus includes an electronically controlled wave production system as well as a laser scanner for bottom topography.

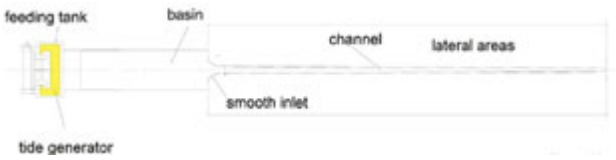

Figure 1: Sketch of the tidal channel at the Dicca laboratory.

CloudCompare software is used to manage the point cloud created by laser scan acquisitions.

3 Conclusion

This study aims to provide valuable insights into sediment dynamics in fully tide-influenced bifurcations. By investigating the complexity of bifurcations characterised by a complete reversal flow in a tidal cycle, the study will contribute to a deeper understanding of how tides influence sediment transport and deposition patterns in bifurcating channels. The experimental results are expected to offer a crucial benchmark for validating and refining both theoretical and numerical models.

Currently, the experiments are ongoing; results will be presented at the Conference.

Acknowledgements

This research has been supported by the Italian Ministerial PRIN 2022 "Prot&Cons" n. 2022FZNH82— CUP D53D23004660006 and by the Italian Ministerial PRIN PNRR 2022 "SECURE" n. P2022KA5CW— CUP D53D23022870001.

References

[1] M. Bolla Pittaluga, R. Repetto, and M. Tubino. Channel bifurcation in braided rivers: Equilibrium configurations and stability. *Water resources research*, 39(3), 2003.

[2] A. P. Iwantoro, M. Van Der Vegt, and M. G. Kleinhans. Morphological evolution of bifurcations in tide-influenced deltas. *Earth Surface Dynamics*, 8(2):413–429, 2020.

[3] N. Ragno, N. Tambroni, and M. Bolla Pittaluga. Effect of small tidal fluctuations on the stability and equilibrium configurations of bifurcations. *Journal of Geophysical Research: Earth Surface*, 125(8):e2020JF005584, 2020.

Quantifying the evolution of channel-floodplain connectivity in a near-natural river widening via a Eulerian-Lagrangian numerical model

F. Caponi[1], M. O. M. Awadallah[1], S. Fink[3], D. Vanzo[2], D. F. Vetsch[1]
[1]Laboratory of Hydraulics, Hydrology and Glaciology (VAW), ETH Zurich, Switzerland
[2]Institute for Water and Environment, Karlsruhe Institute of Technology (KIT), Karlsruhe, Germany
[3]Swiss Federal Institute for Forest, Snow and Landscape Research (WSL), Birmensdorf, Switzerland
Corresponding author: caponi@vaw.baug.ethz.ch

Keywords: channel-floodplain connectivity, river widening, Lagrangian model, river morphology

1 Introduction

Fluxes of water, sediment, and floating matter along rivers are key to several geomorphic and ecological processes. Exchange of surface water between channels and floodplain plays a central role in the transport and deposition of sediments, organic matters, as well as natural and anthropogenic debris [1]. Connectivity frameworks have been increasingly used in geomorphology to conceptualize these exchanges [2]. However, quantifying connectivity remains challenging. Lagrangian (particle tracking) methods offer a way to quantify connectivity metrics at multiple spatial and temporal scales [3]. Here we used a newly developed Eulerian-Lagrangian numerical model to quantify channel-floodplain connectivity in a dynamic, near-natural river widening.

2 Methods

Our study case is a 1 km-long river widening located in the catchment of Moesa, Switzerland. We used topographical surveys conducted before and after major flood events (Figure 1) as input to the numerical model [4]. We setup numerical simulations in each of these morphologies and calibrated the 2D hydrodynamic model (BASEMENT) using aerial images and discharge measurements. We then employed a novel unsteady Lagrangian solver to simulate the transport of floating particles in the water flow. We simulate different hydrological scenarios having floods of different magnitude and short-term discharge fluctuations (e.g. hydropeaking). We quantify (structural) connectivity within the reach using particle residence times, trajectories and water fluxes [1,3].

3 Results

Preliminary results show that particle residence times in the floodplain depends primarily on discharge, with morphological patterns playing a secondary role. We highlight how unsteady flow conditions promote particle trapping in shallow areas and channel shorelines by disconnecting secondary channels from the main one. At low flows, flow paths and channel-floodplain water exchange differ before and after flood events because of the riverbed reworking. As the discharge increases, these differences tend to vanish,

Figure 1: River widening at Cabbiolo, Switzerland, in 2015 and 2024 (©swisstopo).

4 Conclusion

This study aims at quantifying relevant connectivity metrics through the application of a Lagrangian model in a typical alpine river widening. The model allows us to understand the temporal evolution of reach-scale water and matter fluxes and relate them to the morphodynamic evolution of the river.

Acknowledgments

This work is supported by the Federal Office of the Environment FOEN thought the research program "River hydraulics and ecology" (Resilient Rivers, 2022-2026).

References

[1] Czuba, J. A., David, S. R., Edmonds, D. A., & Ward, A. S. (2019). Dynamics of surface-water connectivity in a low-gradient meandering river floodplain. *Water Resources Research*, 55, 1849–1870.

[2] Poeppl, R. E., Polvi, L. E., Turnbull, L., & Ronald Poeppl, C. E. (2023). (Dis)connectivity in hydro-geomorphic systems – emerging concepts and their applications. *Earth Surface Processes and Landforms*, *48*(6), 1089–1094.

[3] Tull, N., Passalacqua, P., Hassenruck-Gudipati, H. J., Rahman, S., Wright, K., Hariharan, J., & Mohrig, D. (2022). Bidirectional River-Floodplain Connectivity During Combined Pluvial-Fluvial Events. *Water Resources Research*, 58(3)

[4] van Rooijen, E., Siviglia, A., Vetsch, D. F., Boes, R. M., & Vanzo, D. (2024). Quantifying fluvial habitat changes due to multiple subsequent floods in a braided alpine reach. *Journal of Ecohydraulics*, 9(1), 1–21

Detecting Compound Meanders Bends via Curvature Energy Spectrum

Sergio Lopez Dubon[1], Alessandro Sgarabotto[2], Stefano Lanzoni[3]
[1]School of Engineering, University of Edinburgh, Edinburgh, United Kingdom
[2]School of Engineering, University of Birmingham, Birmingham, United Kingdom
[3]Department of Civil, Environmental and Architectural Engineering, University of Padova, Padova, Italy
Corresponding author: sergio.ldubon@ed.ac.uk

Keywords: Compound meanders, Autoencoder, Energy Spectrum, Curvature, Pattern recognition

1 Introduction

Meandering rivers are among the most observed natural features in fluvial systems. A meander is characterised by alternating bends connected by short, nearly straight segments at inflexion points. The scientific community has long been captivated by the study of meanders, striving to quantify their structural complexity, model their morphodynamic evolution, and develop classification systems [1]. The detection of single and compound bends has often relied on inflexion points. However, this procedure prevents the unambiguous identification of compound meanders comprising multiple bends [3]. This study aims to detect compound meanders via wavelet-based spectral methods applied to meander curvature.

2 Methods

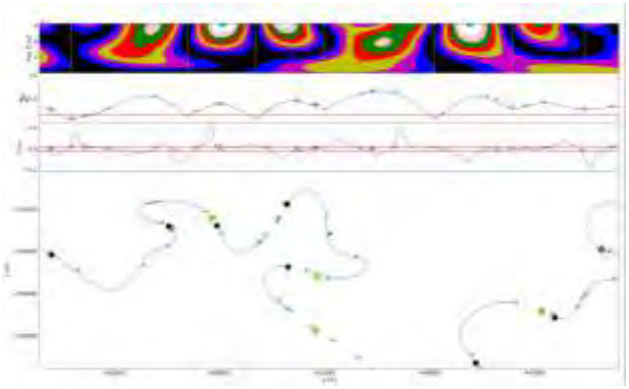

Figure 1: (a) Curvature energy spectrum via continuous wavelet transforms; (b) Energy sum at each channel axis location; (c) Curvature; (d) Meander planform of Jurua River extracted by [4] from 1997 satellite images. This river stretch was analysed by [3] to develop an automated identification and characterisation of compound meander loops.

Satellite-based meander planforms with a pixel resolution of 30 m were retrieved from the online datasets provided by [4]. River centreline and width were used to compute curvature and its energy spectrum via continuous wavelet transform [5]. The energy spectrum was analysed to identify distinctive meander shape patterns along the river course. After extracting the energy spectrum, the range of wavenumbers of interest was determined based on the energy distribution (Fig. 1a). Subsequently, the mean spectrum energy at each location of the channel axis, obtained by integrating over the previously determined range of wavenumbers, was plotted along the river to highlight dominant patterns (Fig. 1b). Finally, meanders were singled out based on the prominence associated with the along channel distribution of the mean spectrum energy represent as yellow dots in Fig. 1d. The final adjustment of the points identifying the various meander shapes was carried out considering the minimum amount of mean energy and minimum curvature for the begging and end of each meander shape unit (either simple or composite). This can be seen in Fig 1d 1d, where a black dot and the end of the meander with a cyan dot represent the begging of a meander.

3 Results and Conclusions

The proposed method does not rely on inflexion points and, thus, can detect meander shape units composed of single or multiple bends. The curvature energy spectrum identifies the single or compound meanders based on the influence of the different bends and their interactions in the space and wavenumber domains, both downstream and upstream. The preliminary results seem promising for identifying multilobed meanders based on their curvature-based spectral interactions. These results will help in understanding the migration potential of meander shapes and possibly classify them within a new data-driven framework.

References

[1] S. Lopez Dubon, and Lanzoni, S., Meandering evolution and width variations: A physics-statistics-based modelling approach. *Water Resources Research*, 55(1):76- 94, 2019.

[2] L. B. Leopold et al., *Fluvial Processes in Geomorphology*. San Francisco, Freeman. 1964.

[3] A.-B. Li et al., Automated identification and characterization of compound meander loops. *Water Resources Management*, 1-23, 2024.

[4] Z. Sylvester et al., High curvatures drive river meandering, *Geology*, 47, 10, 263-266, 2019.

[5] S. Lopez Dubon et al., A curvature-based framework for automated classification of meander bends. *ESS Open Archive*, 1-27, doi: 10.22541/essoar.171172070.03122913/v1, 2024.

Geomorphic Evolution of Peatland Streams: Controls on Sinuosity and Channel Stability

Jeffrey A. Nittrouer[1], John Nelson[1], Gary Parker[2]
[1]Texas Tech University, Lubbock, Texas, USA
[2]University of Illinois, Urbana-Champaign, Illinois, USA
Corresponding author: Jeffrey.Nittrouer@ttu.edu

Keywords: peat streams, channel migration, carbon storage, bankline strength

1 Introduction

Peatland environments cover approximately 3% of Earth's land surface, yet possess ~ 30% of its terrestrial carbon [1]. The hydrology of peat environments is influenced by a combination of surface and groundwater processes, both of which are critical to establishing the carbon storage capabilities of peatlands. The surface hydrological system of peatlands self-organizes into open-channel streams [2] that interact with lakes and bogs. Peat streams are by nature low-sloping and transport minimal amounts of inorganic sediment. Nevertheless, over time, peat streams and adjacent peatlands aggrade due to accumulation of organic matter, and therefore tend to fill their occupied valley [3]. There remain stark morphological contrasts between low-gradient (10^{-5} - 10^{-4}) alluvial and peat streams: the latter is typified by a "zig-zag" pattern and sharp, ninety-degree bends, and the former, by sweeping but gentle bends (Watanabe et al., 2015). Such characteristics for peat streams lead to differing (opposing) flow patterns, whereby the high-velocity core of fluid flow is situated along the inner bankline of bend segments, which is in contrast to alluvial systems. Such a hydrodynamic condition may contribute to the markedly lower lateral migration rates of peat streams compared to their alluvial brethren [3]. Here, we seek to quantify rates of lateral mobility, and evaluate driving mechanisms, by using field-based data to inform a numerical modeling framework evaluating migration habit over time.

2 Methods & Results

The field site of this study is Cedar Creek, a peat stream located in central Minnesota, U.S.A. This system occupies a lowland valley bound by bluffs built during the most recent ice age, recognized as glacial eskers, and composed primarily of sandy deposits. Surveys of Cedar Creek have been conducted during winter and summer seasons, and have collected a variety of data, including: 3-m long vibracore (7.6 cm diameter) of organic and inorganic sediment from the channel and the floodplain; and flow velocity and stage data collected during the spring freshet flood season. Additionally, aerial imagery of Cedar Creek, by way of photographs (dating from 1930's - 1960's) and satellite images (1970's - current).

The cores show spatially varying amounts of peat and inorganic sand. Specifically, in the upstream reaches of Cedar Creek, cores collected from the floodplain show sediment is composed of significantly more (if not entirely) organic matter. In downstream reaches, the proportion of peat relative to sand decreases: cores show a nearly fifty percent split. Interestingly, cores collected from the channel at both the upstream and downstream reaches are nearly entirely composed of sand.

Comparing the channel centerline of Cedar Creek over time, it is evident that, within the resolution of the photographs and satellite images, the upper reaches of Cedar Creek are immobile, and the lower reaches of Cedar Creek are relatively mobile. Even the downstream reaches show that, relative to alluvial streams, which tend to migrate at rates equivalent to a channel width per 1-5 yrs, Cedar Creek is much slower, migrating its mean channel width over multiple centuries.

3 Discussion and Conclusions:

The observations from Cedar Creek are consistent with other peat-stream systems, and suggest that a fundamental control on the migration of Cedar Creek is hydrology of the stream, which provides insufficient stress to overcome the strength of the bankline. Additionally, the morphology of peatland channels is affected by proximity to inorganic sediment supply: where unconsolidated (sandy) sediment is contributed to the system, the bed and floodplain system are subject to alluviation that drives fundamental changes in channel morphology (width/depth) and planform migration habits. For example, migration of sand-bed streams flowing through peatlands is greatly suppressed, but not stopped by, the presence of organic banks, which render migration sporadic and spatially intermittent. The co-evolution of a sand-bed stream in peat and the peatland that surrounds it is governed by the ratio of the rates of streambed aggradation to peatland accumulation. This ratio must be order-one, otherwise the peatland is converted into a clastic alluvial floodplain (high ratio), or the channel is erased by peat encroachment.

References

[1] R. S. Claymo. The limits to peat bog growth. *Phil. Trans. Royal Soc. of London*. Series B, Biological Sciences, 303(1117), 605-654. 1984.

[2] R. A. Nanson *et al.* The hydraulic geometry of narrow and deep channels; evidence for flow optimisation and controlled peatland growth. *Geomorphology*, 117(1), 143-154. 2010

[3] J.H.J Candel *et al*. Oblique aggradation: a novel explanation for sinuosity of low-energy streams in peat-filled valley systems. *Earth Surface Processes and Landforms*, 42(15). 2016

Timescales of River Bifurcations

Gabriele Barile[1], Marco Redolfi[2], Marco Tubino[1]

[1]Department of Civil, Environmental and Mechanical Engineering, University of Trento, Trento, Italy
[2]Department of Engineering "Enzo Ferrari", University of Modena and Reggio Emilia, Modena, Italy

e-mail corresponding author: gabriele.barile@unitn.it

Keywords: *bifurcations,timescales,numerical model,linear stability*

1 Introduction

River bifurcations are the fundamental building blocks of braiding rivers, alluvial fans, and river deltas. Their long-term equilibrium configurations have been widely explored, together with the influence of several external forcing factors, whereas less attention has been devoted to investigate the characteristic timescale with which bifurcations evolve over time. In this work, we address this gap by means of 1-D numerical and linear analyses.

2 Methods

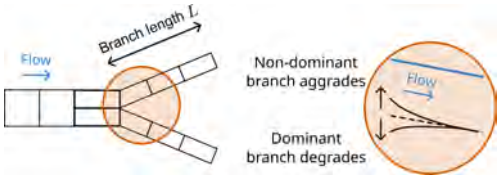

Figure 1: Sketch of the bifurcating domain and the local morphodynamic processes that control the evolutionary timescale of the bifurcation.

We employ the numerical model of a simple bifurcation developed by [1] with a novel linear model, which both solve the 1-D shallow water and Exner equations along the branches and rely on the quasi-2D nodal point relationship proposed by [2]. We consider an initially balanced bifurcation that evolves toward an unbalanced equilibrium configuration.

3 Results and conclusions

A first key result of this analysis is the identification of two distinct timescales. The first quantifies the velocity of the local morphodynamic evolution at the bifurcation node (Figure 1), which mainly controls the flow and sediment partitioning. The second timescale is much longer than the first and is related to the overall adjustment of the bed slope of the downstream branches. Our analysis focuses on the first timescale (T_{BIF}), which decreases with the difference between the upstream width-to-depth ratio β_0 and the critical threshold for the bifurcation stability β_R. The bifurcation evolution is also accelerated by the boundary condition set at the downstream end of the branches, which in the proposed formulation is a constant water level. However, this accelerating effect diminishes with the length of the bifurcates; as a result, the bifurcation timescale increases with the branch length L (Figure 2). When L exceeds a given threshold, which can be derived analytically, the evolution of the bifurcation node no longer depends on the downstream

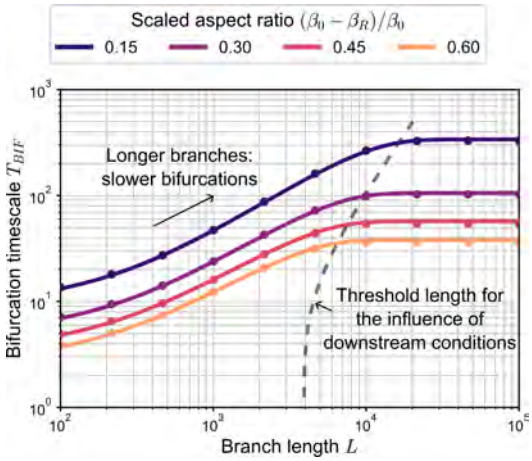

Figure 2: Dependence of the bifurcation timescale, scaled with the reference timescale of sediment transport, on the branch length and upstream aspect ratio. Dots and lines indicate the results of the numerical and linear model, respectively.

condition and the bifurcation timescale stops increasing with the branch length.

The analysis of a large dataset of gravel-bed bifurcations reveals that the evolutionary timescale of most of them, as retrieved from the linear model, is larger than that of natural flow variations. Moreover, the rate at which the water and sediment partitioning at bifurcations changes over time is generally smaller than the fluctuation rate of sediment transport caused by the migration of bars in the upstream channel, especially for bifurcations with long branches.

Acknowledgements

This work has been supported by the Italian Ministry of Universities and Research (MUR) in the framework of the project DICAM-EXC (Departments of Excellence 2023–2027, grant L232/2016).

References

[1] G. Barile, M. Redolfi, and M. Tubino. Analysis of autogenic bifurcation processes resulting in river avulsion. *Earth Surface Dynamics*, 12(1): 87–103, 2024. ISSN 2196-632X. doi: 10.5194/esurf-12-87-2024.

[2] M. Bolla Pittaluga, R. Repetto, and M. Tubino. Channel bifurcation in braided rivers: Equilibrium configurations and stability. *Water Resources Research*, 39(3):1–13, 2003. ISSN 00431397. doi: 10.1029/2001WR001112.

Evolution of mine tailings released in sand-bed rivers

Andrés F. Rojas-Aguirre[1], Marcelo H. García[2]
[1]University of Illinois at Urbana-Champaign, Urbana, United States of America
Corresponding author: afr3@illinois.edu

Keywords: Sediment density, iron tailings, Engelund-Hansen equation, Exner Equation

1 Introduction

In this study, we conduct a long-term numerical simulation to track iron-ore tailings along the Paraopeba River (Brazil) by implementing a proposed mathematical formulation alongside a calibrated SEH transport equation [1]. The simulation assumes a constant dominant discharge and utilizes sediment density as a surrogate to track tailings within both the active layer and substrate.

2 Methods

The study area spans from 10 km upstream of the Ferro Carvão Creek confluence (site of the accidental release) to the headwaters of the Retiro Baixo Reservoir. A 6.0 m high spillway, built to supply water to the Igarapé Thermal Power Station, is situated 47 km downstream of the Ferro Carvão confluence.

Our approach incorporates the rate of change of sediment density and the mean sediment size in the active layer – factors often overlooked, in the Exner Equation,

$$\frac{\partial \eta}{\partial t} = -\frac{1}{\rho_I(1-\lambda)}\frac{\partial q_T}{\partial x} - \left(\frac{\rho_a}{\rho_I} - 1\right)\frac{\partial L_a}{\partial t} - \frac{\partial \rho_a}{\partial t}\frac{L_a}{\rho_I} \quad (1)$$

Where η represents bed elevation, t is time, λ is porosity, and q_T is total mass transport rate per unit width, L_a active layer thickness, ρ_a density in the active layer, ρ_I density in the interface substrate-active layer.

In this study, two representative diameters and densities were considered for both the iron ore tailings and the ambient sand. Under this simplification, the rates of change $\partial L_a/\partial t$ and $\partial \rho_a/\partial t$ can be estimated as a function of the rate of change fraction of the ambient sand F_s, $\partial F_s/\partial t$ [2].

To estimate sediment transport rates, we applied and recalibrated the SEH equation [1] to reflect the conditions in the Paraopeba River, which experiences significant anthropogenic pressures that deviate from its natural sediment regime.

4 Results

The evolution of sediment density and geometric diameter within the active layer indicates that iron ore tailings rapidly interact and mix with natural sediments along the reach from the Ferro Carvão confluence to upstream of the spillway at Igarapé.

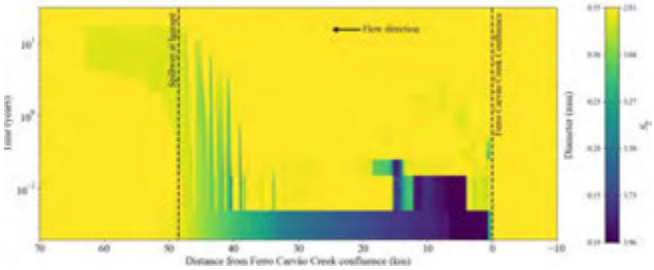

Figure 1: Evolution of sediment density and diameter in the active layer

Upstream of the spillway, the evolution of riverbed grain size suggests a stratigraphic change influenced by the backwater effect caused by the structure. The reduced flow velocities in this area result in lower bed shear stresses, thereby decreasing sediment transport rates compared to other river locations. Stratigraphic simulations indicate that iron tailings are likely to be buried in this reach of the river (Figure 2)

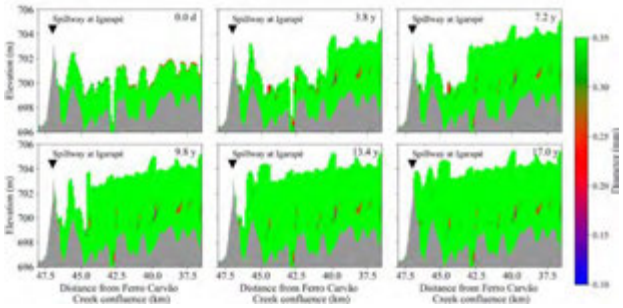

Figure 2: Evolution of diameter in the substrate in the pool upstream of the spillway at Igarapé

Acknowledgments

We thank Joel Cortez, Fernando Verassani Laureano, and Vitor Pimenta from Vale S.A. for their collaboration, as well as Prof. Enrica Viparelli, Dongchen Wang, and Zhi Li for their valuable recommendations that improved our numerical model.

References

[1] An, C., Gong, Z., Naito, K., Parker, G., Hassan, M. A., Ma,H., & Fu, X. Grain size-specific Engelund-Hansen type relation for bed material load in sand-bed rivers, with application to the Mississippi River. *Water Resources Research*, 57, 1–25, 2020.

[2] A.F Rojas-Aguirre and M.H Garcia. Spatiotemporal evolution of mine tailings released in sand-bed rivers. *Journal of Hydraulic Research*, 67(1):64-87, 2025.

Fundamental Study on Sand Storage Function of Sand Retarding Basins during Sediment and Flood Disaster

Mikako Ishikura[1], Ichiro Kimura[1], Norio Harada[2]
[1]University of Toyama, Toyama, Japan
[2] Mitsui Kyodo Construction Consultants, Inc.
Corresponding author: i.kimu2@gmail.com

Keywords: Sediment and flood disaster, sand retarding basins, numerical analysis

1 Introduction

"Sediment and Flood Disaster (SFD)" has been newly defined as a river disaster type. To mitigate SFD, sand retarding basins (SRB) are constructed upstream of the residential area in rivers. In this study, computations on SRB were conducted to clarify its fundamental aspects. SRBs with different aspect ratios (B/b, B: width of SRB, b: width of the channel) are considered, and their effects on the sediment storage function and mitigation effectiveness are discussed.

2 Methods

In the previous study [1], a laboratory test was conducted under four different aspect ratios: B/b=1, 2, 3, 4. In this study, computations are performed under the same conditions in the experiments. The plane two-dimensional solver: Nays2DH on iRIC [2] was used for the computations. In the computations, wider range of the aspect ratios is considered (B/b=1~8). The riverbed slope was set to 1/30, Manning's coefficient to 0.015. The discharge Q is set constant in three cases (0.37, 0.49, and 0.58 L/s). Sediment was initially placed on the bed at upstream region of inflow channel as a trapezoidal shape. The capture performance was evaluated with the temporal change of the amount of sediment deposited inside the SRB and the sediment discharged downstream of the SRB. The experimental results were compared with the simulation results in terms of sediment volume and profile of the deposition.

3 Results and Discussion

Figure 1 shows the deposition pattern at t = 600s in B/b = 4. The deposition area locates mainly on both side of the SRB.

Figure 2 shows the temporal change of sediment amount inside SRB in eight different aspect ratios. It is

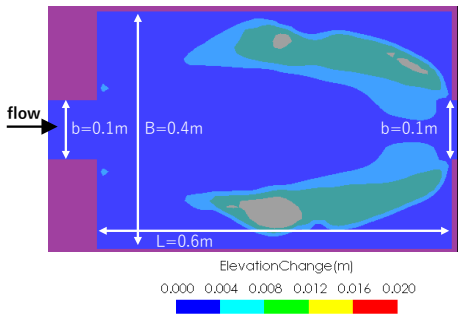

Figure 1 A snapshot of the computational result at t =600s in B/b =4 (deposition pattern).

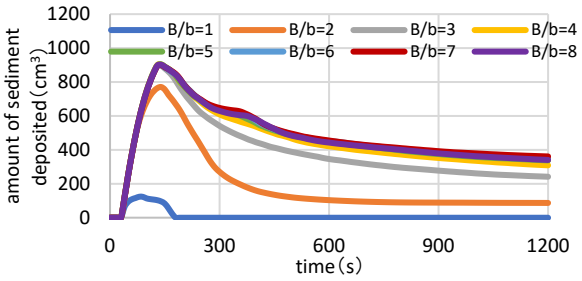

Figure 2 Amount of sediment deposited in the SRB (flow rate 0.49 L/s)

indicated that the amount of deposition increases with increasing B/b in the range of B/b=1~5 but is almost the same in the range of B/b ≥ 5. This means that it becomes uneconomical when B/b is greater than 5. According to the existing guideline [3], it is recommended that the aspect ratio of SRB should be B/b < 5. The present numerical results support the validity of this criteria (B/b < 5) on the design guideline. [3].

The results also confirmed that SRBs have two effects. The SRB of B/b =2 temporally caught the sediment (t < 300 s) though most of the sediment was released after t = 600s (short-term effect). On the other hand, the SRB with B/b ≥ 3 could keep considerable amount of sediment ever after t = 1000s (long-term effect).

4 Conclusion

We conducted the plane two-dimensional computations on sediment transport around SRB. The calculation results showed that B/b > 5 may result in an uneconomical design, which was consistent with the criteria in the existing design guidelines [3]. In addition, SRB has two different effects, and the long-term effect can be achieved only when B/b ≥ 3.

Acknowledgments

This work was supported by JSPS KAKENHI Grant Number JP24K00985.

References

[1] M. Ishikura, I. Kimura, and N. Harada, Study on mitigating sediment and flood disasters with sand retarding basins and the effects of driftwood, J. River Eng., 30, 2024

[2] I. Kimura, River simulation with iRIC, Morikita publishing Co. Ltd., 2021

[3] National Inst. for Land and Infrastructure Management (NILM), Tech. note of NILM, 2016. https://www.nlim.go.jp/lab/bcg/siryou/tnn/tnn0905.htm

Suppressed Morphodynamic Activity in Restored Gravel-Bed Rivers

Paul Demuth[1], David F. Vetsch[1], Robert M. Boes[1], Volker Weitbrecht[1]
[1] Laboratory of Hydraulics, Hydrology, and Glaciology (VAW), ETH Zurich, Switzerland
Corresponding author: demuth@vaw.baug.ethz.ch

Keywords: gravel-bed rivers, reach scale river restoration, sediment supply, floodplain offset

1 Introduction

Rivers are dynamic systems in which water and sediment flows, large wood and morphology interact to create diverse habitats and support ecological complexity. Human interventions, such as channelization and sediment extraction, have disrupted these systems, causing habitat homogenization, reduced connectivity, and declining biodiversity.

River restoration projects, such as channel widening, aim to reintroduce morphodynamic processes and improve ecosystem health locally. This study focuses on understanding how sediment supply and floodplain offset influence the morphodynamic processes of widened gravel-bed rivers.

2 Methods

Laboratory experiments were conducted in a 31.6 m long and 4 m wide flume with an initial longitudinal slope of 0.003. Within the flume, a b_0 = 0.79 m wide trapezoidal channel and a one-sided wider area in the middle with a maximum width of b_{max} = 3.22 m was constructed (Figure 1).

The offset height between the mean river bed elevation and the floodplain varied between high, low, and no offset. The sediment mixture used as bed material and sediment supply (at 100% of the channel transport capacity) corresponded to a well-graded gravel-bed river with a geometric standard deviation of σ_g = 2.49. The morphological evolution due to simulated bed-forming discharges was measured using high-resolution laser scanning, and hydrodynamic conditions were analysed using 2D simulations with the software BASEMENT, version 4 [1].

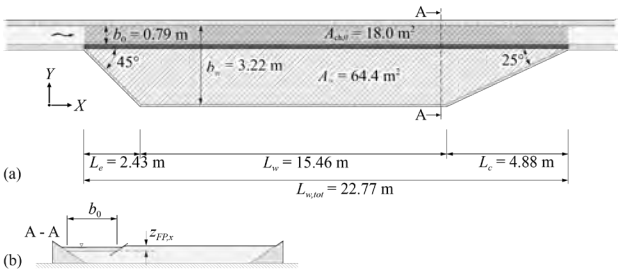

Figure 1: (a) Planform geometry and (b) cross-section of the experimental flume with variable floodplain offset height $z_{FP,x}$.

3 Results and Discussion

Previous research on steeper slopes (0.01) [2] indicated that sufficient sediment supply close to the transport capacity promotes increased heterogeneity. However, under the mild slope used in this setup (0.003), sediment supply alone did not drive morphodynamic activity and heterogeneity. Floodplain offset significantly affected channel behaviour. The resulting topography ended in an almost straight channel with nearly no sediment relocation during the simulated flood events for low and no floodplain offset (Figure 2b & c). For the high offset configuration, the channel shifted into the floodplain and was stabilized by the fixed bank at the end of the wider area and the embankment on the right side (Figure 2a).

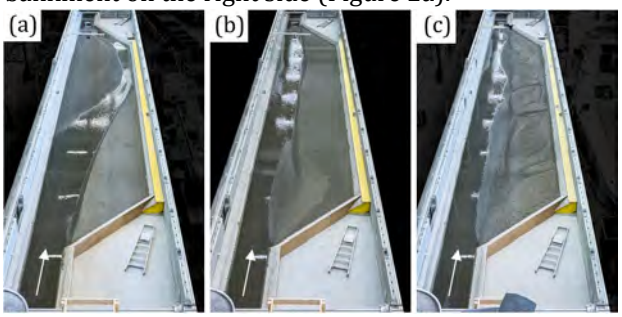

Figure 2: Photographs of the resulting topography at the end of the experimental series for (a) high, (b) low, and (c) no offset with a discharge of 1 l/s.

4 Conclusions

This study provides valuable insights into the role of sediment supply and floodplain offset on the morphodynamic development of widened river reaches. It showed that sediment supply alone cannot drive morphodynamic activity under mild slope conditions. In addition, the floodplain offset's height influenced the resulting topography and channel stability. Further work on the use of initiation measures is needed to foster morphodynamic activity and improve the design of restored river reaches.

References

[1] Vetsch, D. F., Frei, S., Halso, M. C., Schierjott, J. C., Bürgler, M., & Vanzo, D. (2023). Basement V4—A multipurpose modelling environment for simulation of flood hazards and river morphodynamics across scales. *SimHydro*, 125-138. Springer, Singapore. https://doi.org/10.1007/978-981-97-4072-7_8

[2] Rachelly, C.; Vetsch, D.; Boes, R.M.; Weitbrecht, V. (2022). Sediment Supply Control on Morphodynamic Processes in Gravel Bed River Widenings. *Earth Surface Processes and Landforms*, 47(15): 3415-3434. https://doi.org/10.1002/esp.5460.

Effect of engineered logjams on flow and local morphology

Simone Speltoni[1,2], Volker Weitbrecht[1], Robert M. Boes[1], Isabella Schalko[2]
[1] Laboratory of Hydraulics, Hydrology and Glaciology (VAW), ETH Zurich, Zurich, Switzerland,
[2] Swiss Federal Institute for Forest, Snow and Landscape Research (WSL), Birmensdorf, Switzerland,
Corresponding author: speltoni@vaw.baug.ethz.ch

Keywords: deposition, local scour, physical experiments, river restoration, wood

1 Introduction

Engineered logjams (ELJ) are wooden structures that can enhance flow variability [1] and morphological heterogeneity [2] in rivers. As a result, they are increasingly implemented in river restoration projects, with a wide range of shapes and designs. Physical experiments have investigated the effects of the main variables (e.g., widths, porosity, placement) on the local flow field, assessing the increase in backwater rise, the extension of the wake and the turbulence intensity. Nevertheless, questions remain open about the effects of different ELJ designs on the local morphology. For example, partial-spanning ELJ can enhance local flow acceleration and hence shear stresses, causing scours and deposits. Such morphologies may alter flow fields, changing the wake extension and the backwater rise.

2 Materials and methods

Physical experiments were performed in a 0.6 m wide, 13 m long and 0.6 m deep flume at the Laboratory of Hydraulics, Hydrology and Glaciology at VAW, ETH Zurich. Partial-spanning ELJ were built with a scaling factor λ = 30, using wooden dowels with a mean diameter of d_L = 0.012 m. The ELJ were built with different widths B_j = 0.2 – 0.6 m, solid volume fractions (ratio of solid wood volume to total jam volume) Φ = 0.2-0.4, and placed at the flume side or centre. The water depth was measured using Ultrasonic Distance Sensors (UDS), while velocity profiles (streamwise, lateral and vertical) were measured using Acoustic Doppler Velocimetry (ADV). The bed elevation was scanned with a Laser Distance Sensor (LDS). Different sub- and supercritical flow conditions were tested by changing the discharge Q, slope J and unobstructed water depth h_0. The mobile bed had a uniform grain size distribution with d_m = 2.7 mm. Note that the initial conditions for the mobile bed experiments were set so the non-dimensional critical bed shear stress was slightly below incipient motion.

3 Results

The scour developed upstream and next to the ELJ (Fig. 1), as flow was accelerated in the gap between the ELJ and the side wall. The magnitude of the scour depended on the specific discharge, slope and the mean grain size diameter. Additional variables like placement and porosity of the ELJ also affected the scour depth. The resulting scour reduced backwater rise compared to fixed bed conditions by 16%.

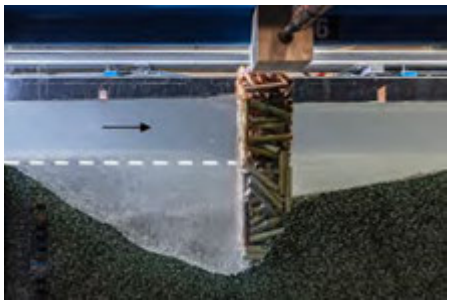

Figure 1: Scour upstream of a side-placed ELJ. Flow from left to right. Dashed line indicates the reference riverbed elevation.

Sediment was transported and deposited downstream of the ELJ, forming a bar with a longitudinal footprint that extended up to 30 times B_j. The bar shape and extension differed between central- and side-placed ELJs. The bar seemed to reduce the wake length, as the flow recovered faster compared to the fixed bed (Fig. 2).

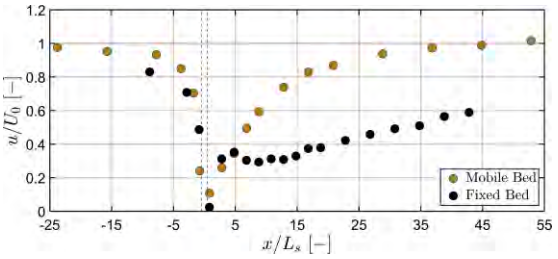

Figure 2: Longitudinal velocity profiles at the centreline of the ELJ for mobile vs. fixed bed experiments with a side placement of the ELJ.

4 Conclusions and outlook

Morphological changes around an ELJ significantly influence backwater rise and the surrounding flow fields. Further research should examine the interaction effects of multiple ELJs.

References

[1] I. Schalko, E. Follett and H. Nepf. Impact of Lateral Gap on Flow Distribution, Backwater Rise, and Turbulence Generated by a Logjam. *Water Resources Research,* Vol. 59, 2023.

[2] H. Ismail, Y. Xu, X. Liu. Flow and scour around idealized porous engineered log jam structures. *Journal of Hydraulic Engineering*, Vol. 147, 2021.

A disaster caused by overmining of sediment: case of Shi-ting River, China

Chenge An[1], Gary Parker[2], Anjun Deng[1], Xudong Fu[3], Ruihua Nie[4], Yee-Meng Chiew[5]
[1] China Institute of Water Resources and Hydropower Research, Beijing, China
[2] University of Illinois Urbana-Champaign, Urbana, USA
[3] Tsinghua University, Beijing, China
[4] Sichuan University, Chengdu, China
[5] Nanyang Technological University, Singapore
Corresponding author: Anjun Deng (denganj@iwhr.com)

Keywords: sediment mining, bed degradation, grade control structure, Shi-ting River

1 Background

In the foreland rivers downstream of the Longmenshan Mountains in China, significant bed degradation has been observed ever since the 2008 Wenchuan (Ms. 8.0) Earthquake. Among these, the Shi-ting River has experienced the largest degradation, in excess of more than 20 m in 7 years (Figure 1). This degradation was driven by massive sediment mining, which was in turn motivated in part by the need for concrete aggregate for reconstruction after the earthquake. Several grade control structures were constructed in the Shi-ting River to diminish bed degradation, but all of them failed within a few years [1].

Previous studies have suggested that intensive mining of bed sediment has been the main driver of the dramatic degradation in the Shi-ting River, although other factors like the existence of grade control structures and the input of fine sediment also have played a role [2]. However, the morphodynamic process of how local sediment mining leads to global bed degradation is still not well understood.

Figure 1: A photo of the Shi-ting River taken in 2021, with the elevation drop between the upstream and downstream sides of the weir being 24 m. There was no elevation drop at this site before 2008.

2 Methodology

A 1D morphodynamic model is applied to study this problem. Flow hydraulics is calculated with the backwater equation. Mass conservation of sediment mixtures is described using the Exner equation with the active layer formulation. Bedload transport is calculated with the Wilcock-Crowe [3] relation. The grade control structure is treated as nonerodable in the model.

3 Results

The foreland reach of Shi-ting River is used as the prototype of the simulation. Various rates of sediment mining are applied. Results show that a larger mining rate leads to larger bed degradation. Bed degradation can happen far (10 km in our simulation) beyond the region of sediment mining, indicating a global effect of local sediment mining. When a grade control structure is also considered, sediment mining can significantly increase the bed degradation at the grade control structure, especially when the grade control structure is within the mining region.

Acknowledgments

This study was supported by the National Natural Science Foundation of China (Grants U2340223 and 52379068).

References

[1] L. Wang, B. W. Melville, Z. Xu, A. Y. Shamseldin, W. Wu, X. Wang, and R. Nie. Massive riverbed erosion induced by inappropriate grade control: a case study in a large-scale compound channel. *Journal of Hydrology*, 612, 128313, 2022.

[2] Y. Lin, C. An, S. Zheng, R. Nie, G. Parker, M. A. Hassan, M. J. Czapiga, and X. Fu. Degradation of a foreland river after the Wenchuan Earthquake, China: a combined effect of weirs, sediment supply, and sediment mining. *Water Resources Research*, 59, e2023WR035345, 2023.

[3] P. R. Wilcock, and J. C. Crowe. Surface-based transport model for mixed-size sediment. *Journal of Hydraulic Engineering*, 129, 120–128, 2003.

Sediment supply effects on fish habitat dynamics in a morphologically active river widening

Mahmoud O. M. Awadallah[1], Francesco Caponi[1], David F. Vetsch[1], Robert M. Boes[1], Davide Vanzo[2]
[1]Laboratory of Hydraulics, Hydrology and Glaciology (VAW), ETH Zurich, Switzerland
[2]Institute for Water and Environment, Karlsruhe Institute of Technology (KIT), Karlsruhe, Germany
Corresponding author: awadallah@vaw.baug.ethz.ch

Keywords: river restoration, sediment supply, aquatic habitat, brown trout, morphodynamics

1 Background

Flow and sediment regimes are key morphodynamic drivers that shape fluvial habitats hosting diverse freshwater species. Natural hydro-morphological processes are vital for creating these habitats and sustaining their ecological functions. However, anthropogenic activities—such as damming and channelization—have disrupted these regimes, causing river narrowing and floodplain disconnection, reducing habitat heterogeneity, and ultimately a decline in freshwater biodiversity. River restoration measures, including river widening, have been proposed to favour morphological processes and restore physical habitat complexity. While some experimental evidences highlight the influence of sediment supply on the morphodynamics of local widenings [1], the further implications on fish habitat dynamics remains poorly understood [2].

2 Data and Methods

Starting from experimental widening morphologies formed under various sediment supply levels and hydraulic conditions (Figure 1a), we delineated the habitat availability of brown trout (*Salmo trutta*) under multiple discharge conditions using 2D hydrodynamic models and habitat suitability curves. We spatially quantified the habitat dynamics during different morphodynamic evolution phases of the local widening (i.e. channelized, one-sided steady-state widening, and after 30-years flood); we then linked the underlying morphodynamic processes with the evaluated habitat metrics [3] (Figure 1b).

3 Results and Conclusions

Our results (Figure 1c) reveal that widening morphologies formed with near-natural sediment supply (100% and 80% of the channel's transport capacity) showed a significant increase in habitat availability at all discharge conditions—especially drought and flood discharges—compared to the initial channelized state. Notably, the flood event further enhanced habitat availability at low discharge conditions in these scenarios. Conversely, widening morphologies with reduced sediment supply (60% and 20% of the channel's transport capacity) did not show an improvement in habitat quantity following the widening formation nor after a flood event. This study shows the direct connection between sediment supply and fish habitat dynamics in gravel-bed river widenings. It highlights the key role of morphodynamic processes in shaping aquatic habitats, helping to guide effective river restorations that promote ecosystem resilience.

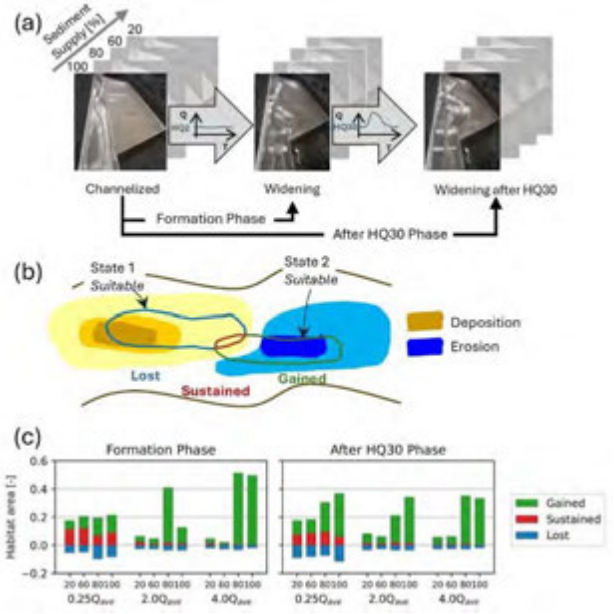

Figure 1: (a) Experimental widening morphologies and program [1]; (b) example of the approaches used to evaluate habitat dynamics; (c) variation of the habitat gained, lost, and sustained for adult brown trout with discharge.

References

[1] Rachelly, C., Vetsch, D.F., Boes, R.M. & Weitbrecht, V. (2022) Sediment supply control on morphodynamic processes in gravel-bed river widenings. *Earth Surface Processes and Landforms*, 47(15), 3415–3434.

[2] Soto Parra, T., Politti, E. & Zolezzi, G. (2024) Morphological and fish mesohabitat dynamics following an experimental flood under different sediment availability. Earth Surface Processes and Landforms, 49(15), 5167–5185.

[3] Moniz, P. J., & Pasternack, G. B. (2021). Chinook salmon rearing habitat–discharge relationships change as a result of morphodynamic processes. River Research and Applications, 37(10), 1386–1399.

Cyclone-Driven Sediment Pulses and River Morphodynamic Response in Tairāwhiti, Aotearoa New Zealand

Jon Tunnicliffe
School of Environment, Faculty of Science, University of Auckland, Auckland, 1010, New Zealand
Corresponding author: j.tunnicliffe@aucklanduni.ac.nz

Keywords: Cyclone Gabrielle, landslide-sediment coupling, LiDAR differencing, aggradation, sediment budget, floodplain storage, morphodynamic response, Tairāwhiti, New Zealand.

1 Introduction

In early 2023, the East Cape region of Aotearoa New Zealand was struck by two intense ex-tropical cyclones, Gabrielle and Hale, triggering widespread geomorphic disturbance. These events mobilized thousands of landslides and prompted unprecedented channel changes along major river corridors. Leveraging a unique four-epoch airborne LiDAR dataset (2019, 2022 pre-storm; 2023, 2024 post-storm), we quantify river sediment budgets and morphodynamic change at catchment scale, capturing a full disturbance-recovery sequence in high spatial and temporal resolution. The Waiapu River is well known for exceptional rates of bedload transfer, even in quiescent periods [1].

2 Data and methods

The LiDAR surveys were carried out using conventional infrared LiDAR (Optech Orion H300) for the topographic capture of the catchment, and green topo-bathymetric LiDAR (Riegl VQ880GII) in subsequent surveys. By evaluating elevation differences across the exposed alluvial surfaces changes in floodplain and channel storage were calculated throughout the drainage network over 5-6 years. While topography is mostly accessible to infrared LiDAR during low summer flows, some interpolation was used to recover the contours of deeper sections in the volumetric analysis. Using the 'morphological method' [2], we traced the mass balance of gains and losses along the major river reaches, revealing sites of transient aggradation and degradation over the survey epochs.

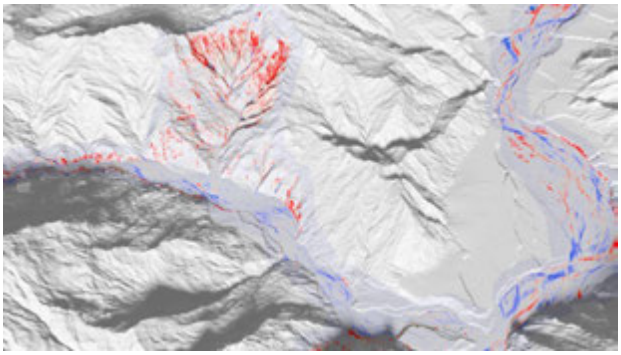

Figure 1. DEM of difference (red is erosion, blue is deposition, +/-2m; scene is approximately 7km across), showing major gully mass wasting and bank erosion contributing to major sediment flux with the Waiapu (Tapuaeroa) River valley. High rates of sediment yield to the channel result in highly dynamic floodplain storage and mobilization in the major reaches downstream.

3 Preliminary Results

Differencing of the LiDAR-derived digital terrain models reveals a marked transition from a pre-storm, supply-limited sediment regime characterized by net channel degradation, to an immediate post-storm state dominated by widespread aggradation across upland and lowland reaches. The subsequent evolution into a re-equilibration phase underscores the contrasting sediment dynamics between steep, landslide-coupled tributaries (Figure 1) and lower-gradient alluvial floodplains, where storage and lateral connectivity govern downstream sediment propagation.

Our analysis demonstrates how extreme climatic events can temporarily shift dominant geomorphic processes and sediment regimes and provides a novel framework linking sediment storage dynamics to bedload transport rates [3]. These insights offer critical implications for modeling landscape response to climatic extremes and inform future river management strategies, including the design of flood hazard mitigation and sustainable, locally appropriate extraction practices.

Acknowledgements

We gratefully acknowledge Gisborne Council's LiDAR surveys and river monitoring programme.

References

[1] Tunnicliffe, J., Brierley, G., Fuller, I. C., Leenman, A., Marden, M., & Peacock, D. 2018. Reaction and relaxation in a coarse-grained fluvial system following catchment-wide disturbance. *Geomorphology*, 307, doi: 10.1016/j.geomorph.2018.12.018.

[2] Vericat, D., Wheaton, J. M., & Brasington, J. (2017). Revisiting the morphological approach: Opportunities and challenges with repeat high-resolution topography. Gravel-bed rivers: Processes and disasters, 121-158.

[2] Hassan MA, Li W, Viparelli E, An C, Mitchell AJ. 2023. Influence of sediment supply timing on bedload transport and bed surface texture during a single experimental hydrograph in gravel bed rivers. Water Resources Research. 59(12):e2023WR035406.

Morphodynamics of hanging ice dams: interaction between flow, sediment, frazil ice and a solid ice roof

Gary Parker[1], Yuntong She[2]
[1]Dept. of Civil & Environmental Engineering and Dept. of Earth Science and Climate Change, University of Illinois Urbana-Champaign USA
[2]Dept. of Civil & Environmental Engineering, University of Alberta, Canada

Corresponding author: parkerg@illinois.edu

Keywords: ice, sediment, frazil, northern rivers, scour

1 Abstract

Cold climates offer river phenomena that are not seen in warmer climates. One such phenomenon is the hanging ice dam. Consider the case of a steep, quasi-bedrock reach of a river that gives way downstream to a purely alluvial sand-bed stream with a significantly lower slope. Under atmospheric conditions that are well below freezing, a solid ice cover forms over the flow in the low-slope reach. In some cases, however, the strong turbulence in the steeper, upstream reach prevents the formation of an ice cover. Instead, the water supercools and generates copious amounts of frazil ice. These ice particles act like suspended sediment, but with a fall velocity directed upward vertically. The open-channel flow upstream of the slope break is thus laden with both suspended sand and suspended frazil ice. As this flow dives under the ice cover at the slope break, frazil ice tends to deposit and accumulate on the bottom side of the ice cover. This forces the flow downward, so creating a scour hole in the sand bed. At the height of winter, such scour holes have been measured to have depths of up to 2 m, and depths of as much as 10 m have been inferred. This scour poses risks to infrastructure such as bridge piers and buried pipelines. As summer approaches, however, the scour hole can disappear without a trace. Here we develop a simple morphodynamic model of hanging ice dams involving a) depth-integrated flow relations with and without an ice cover and b) transport, deposition and erosion of frazil ice. We use this model in order to gain insight into the scour produced by hanging ice dams, and the morphodynamic response after the solid ice cover breaks up in the spring.

2 Formulation

A numerical model of hanging ice dam formation will include:

1. A floating ice cover of specified thickness.
2. 1D open channel flow under this floating cover assuming hydrostatic pressure distribution.
3. Input of frazil ice particles (settle upward) and sediment (settle downward).
4. Resistance from both the river bed and the ice cover.
5. Transport and morphodynamics of frazil ice as both bedload and suspended load.
6. Morphodynamic interaction, including formation of scour hole on the river bed.

3 Information concerning the submission

This submission falls in the “river” category. We would prefer an oral presentation.

Temporal evolution of water residence times throughout the growth of a river dominated delta

Matthew Hiatt[1,2], Md. Muzahidul Islam[1,3], Hemanth Vundavilli[1,4]

[1]Department of Oceanography & Coastal Sciences, Louisiana State University, Baton Rouge, Louisiana, USA
[2]Coastal Studies Institute, Louisiana State University, Baton Rouge, Louisiana, USA
[3]Department of Geography & Anthropology, Louisiana State University, Baton Rouge, Louisiana, USA
[4]Department of Civil & Environmental Engineering, Louisiana State University, Baton Rouge, Louisiana, USA

e-mail corresponding author: mhiatt1@lsu.edu

Keywords: *river delta, water transport timescales, geomorphology*

1 Introduction

Deltas deliver a significant fraction of Earth's water, sediment, and nutrients to oceans and are dynamic, complex landscapes with tremendous ecological and economic value. However, deltas are vulnerable to a myriad of both natural and anthropogenic activities such as sea level rise, wetland erosion and drowning, eutrophication, leveeing, dredging, and hydrocarbon/groundwater extraction. As a result, nature-based restoration options have recently gained popularity as a strategy to restore deltaic systems to a more natural state while maximizing both environmental and human interests. In particular, sediment diversions aimed at returning the flow of water, sediment, and nutrients to drowned deltaic wetlands that have been previously isolated from the river by flood control levees are being used to combat wetland loss. While much study has been devoted to understanding how land might be built by sediment diversions, less attention has been given to the effect diversion will have on water residence times and subsequent nutrient transport/removal [1]. Water residence time is defined as the time required for a water parcel to exit a control volume is a useful parameter for estimating nutrient removal and water quality in surface waters. The reintroduction of water and nutrients to previously-isolated wetlands will dramatically impact system ecology. However, there is no record of how the residence time is influenced by the geomorphological evolution of the delta itself and, thus, there is a limited understanding of how sediment diversions will impact both local and downstream nutrient dynamics. This study aims to quantify residence time distributions throughout the morphological development of a river delta over restoration time scales.

2 Methods

The effects of sea level rise and sand/mud composition on deltaic evolution and subsequent residence time distributions are tested using the reduced-complexity morphodynamic model DeltaRCM [2]. Four sea level rise scenarios are used and the percentage of sediment load that is sand (total = mud + sand) is varied from 25 to 100 for each sea level rise scenario to produce the morphological evolution of the delta through time (e.g., Fig. 1 depicts final topographies for each sand/mud ratio with no sea level rise). Due to the stochastic nature of DeltaRCM's sediment routing schemes, five realizations are performed for each set of parameters. At each time step, the water residence time distribution is calculated for each inundated grid cell by tracking the propagation of a numerical tracer.

3 Results & Discussion

Sea level rise rate and sediment composition (% sand) hold inverse relationships with system-scale residence time. In other words, deltas formed under conditions of increased sea level rise and sand content have lower reaisdence times than muddier deltas formed with lower rates of sea level rise. The temporal trajectory of residence time distribution is generally positive (Fig. 1), as expected, since the delta is growing a flow paths are increasing in length, on average, but the increase in both median and extreme values of the RTD appear to decrease over time or potentially invert, in some cases. This suggests there is a non-linear relationship between system-scale hydrology and delta growth.

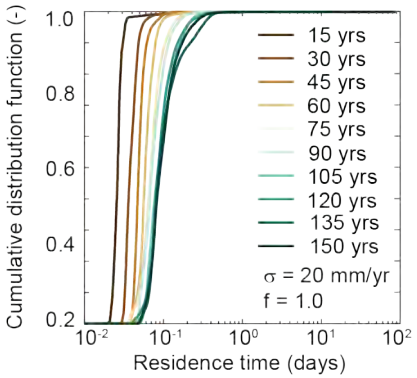

Figure 1: Temporal evolution of the cumulative RTD for one realization with incoming sediment composition (f) of 100% sand and subject to a sea level rise rate (σ) of 20 mm/yr.

References

1. Rivera-Monroy, V. *et al.* Denitrification in coastal Louisiana: A spatial assessment and research needs. *J. Sea Res.* **63,** 157–172 (2010).
2. Liang, M., Van Dyk, C. & Passalacqua, P. Quantifying the patterns and dynamics of river deltas under conditions of steady forcing and relative sea level rise. *Journal of Geophysical Research: Earth Surface* **121,** 465–496 (2016).

Certainty of floodplain flux source as a function of river discharge

Andrew J. Moodie[1], Elena Lundeen[1]
[1]Texas A&M University, College Station, TX, USA
e-mail corresponding author: amoodie@tamu.edu

Keywords: *connectivity, floodplain, oxbow lake, entropy*

1 Introduction

Elements of river-floodplain heterogeneity, such as levees and oxbow lakes, influence water, sediment, and nutrient transport through the fluvial landscape, and therefore impact floodplain ecosystem diversity and function. It is known that river-floodplain connections are activated across a range of river discharges less than "bankfull." Our understanding of this activation is largely binary (i.e., wet or dry), and does not quantify how the magnitude of fluxes through connections shift with increasing discharge, or how these fluxes move through the floodplain to variably connect the river to lakes that support floodplain ecosystems.

2 Linking oxbow lake to flux sources

We use a particle tracking approach to understand material flux in a river-floodplain system (after [1]). We simulated flows from 50 to 1,191 m^3/s on the Mission River (TX, USA), and identified transport pathways traversing from the river to an overbank area and traversing to a selected oxbow lake (Fig. 1a).

We first quantified the fraction of total particles that entered the overbank area (F_o) and the fraction of total particles entering the lake (F_l; Fig. 1b); henceforth subscripts differentiate calculations for the overbank area ($_o$) and the oxbow lake ($_l$). We then separated flux based on overbank-flow spatial continuity to determine the number of unique connections (N_c; Fig. 1b). Finally, we calculated the Shannon Entropy of the connections (H_c) and an effective number of connections (E_c) as $H_c = -\sum_{i=1}^{n} (p_i/P) \log_2 (p_i/P)$ and $E_c = 2^{H_c}$ [2], where p_i is the number of particles through river-floodplain connection i, n is the number of connections, and P is the total number of particles in all connections (Fig. 1b).

As discharge increases, river-floodplain connections become stronger and increase in number, but these discrete connections become integrated above ~400 m^3/s (Fig. 1b). The number of connections to the overbank area and the oxbow lake are correlated (Fig. 1b). The effective number of connections decreases above ~400 m^3/s discharge, though the rate and magnitude of this decrease is markedly different between the overbank area and oxbow lake (Fig. 1b).

3 Discussion and conclusions

The effective number of channels can be qualitatively interpreted as uncertainty in flux source for an area of interest. We find that the uncertainty of flux sources to the oxbow lake is maximized at a moderate ~400 m^3/s discharge.

So while fraction of particles (F_l) measures overall flux connectivity, the effective number of connections captures the variation in sources of that flux from across the river-floodplain boundary, and how specific feature connectivity diverges from the overall overbank area connectivity. In our full work, we apply our analysis to many floodplain features across a coastal backwater transition, as well as quantify floodplain exposure times and integrate measures across decadal hydrographs to understand the temporal component of this variable floodplain activition. Time-integrated effective channel number provides a quantitative target for connectivity restoration projects aiming to support diverse ecosystems.

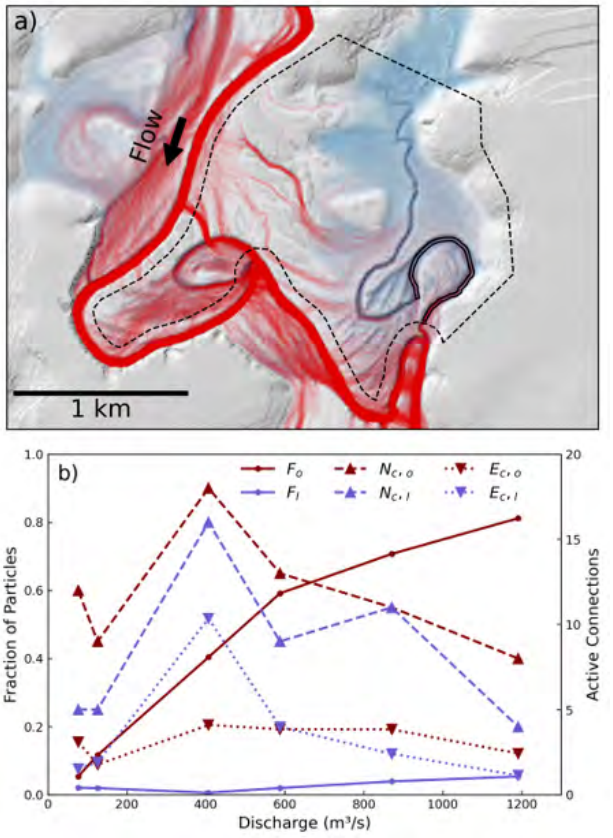

Figure 1: a) Hillshade of overbank area (dashed line) including oxbow lake (solid line) in the Mission River, TX river-floodplain system, overlaid by water depth for 588 m^3/s river discharge (blue intensity indicating depth) and material transport pathways (red intensity indicating transport magnitude). b) Measures of river-floodplain connectivity from the text, as a function of river discharge.

References

[1] N. Tull, A. J. Moodie, P. Passalacqua, *Frontiers in Water* **5**.
[2] A. Tejedor *et al.*, *Geophysical Research Letters* **49**(16) (2022).

The impact of hydrograph shapes on riverbed evolution at a knickpoint

Soichi Tanabe[1], Toshiki Iwasaki[1]
[1]Hokkaido university, Sapporo, Japan
Corresponding author: okushishiku@eis.hokudai.ac.jp

Keywords: knickpoint, hydrograph shape, lateral erosion, channel morphology

1 Introduction

Flood damages are increasing at a knickpoint where riverbed slope and/or channel width change abruptly, because a knickpoint is likely to cause non-equilibrium sediment condition, leading to massive deposition and associated channel changes. Recent climate change may increase this type of flood damage because of significant increase of the magnitude of water runoff and modification of the hydrograph shape. However, the impact of hydrograph shape on riverbed evolution, especially at a knickpoint, has not been deeply investigated. To clarify this, we perform numerical calculations on a morphological change of a river with a knickpoint considering a variety of hydrographs (i.e., peak discharge and overall shapes).

2 Method

We use iRIC-Nays2DH as a morphodynamic model. Our target is the Pekerebetsu River, Japan, which is a typical small-sized river with a knickpoint (upstream slope: 2.1%, downstream slope: 1.5%). The riverbed material is assumed as uniform grain size of 90 mm, and we consider only bedload transport as the sediment transport mode. We set the dynamic equilibrium transport rate as an upstream sediment feed condition.

We analysed the massive hydrograph data calculated from a large ensemble climate and runoff calculations and categorized them into 16 simple hydrographs. These simplified hydrographs contain single-peak and double-peak cases (forward and backward peak) as shown in Figure 1.

3 Results

The knickpoint that we address is upward concave, causing bed aggradation in the entire channel. Upstream reach of the knickpoint remains straight, in contrast, in the downstream reach of the knickpoint, bars and meandering flow are dominant due to a gentle riverbed slope, suppressing deposition [1].

3.1 Single-peak case

In the upstream of the knickpoint, the amount of sediment deposition depends on the total flow volume, namely sediment inflow. This is because sediment deposition fills the pre-existing channel, promoting lateral channel migration. In the downstream of the knickpoint, the channel morphology transitions from meandering toward braided when the discharge exceeds a threshold value (i.e., 300 m³/s in this river, Figure 2). In this case, formation of braided channel with chute cutoff supresses the further bank erosion. However, the lower discharge retains the meandering channel, eventually causing the amplification of meandering channel. This indicates that the lateral erosion and associated flood damages strongly depends on the channel morphology formed before the flood event.

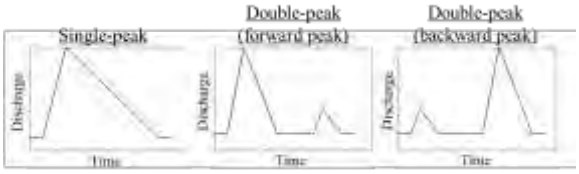

Figure 1: Example of simple hydrograph shapes.

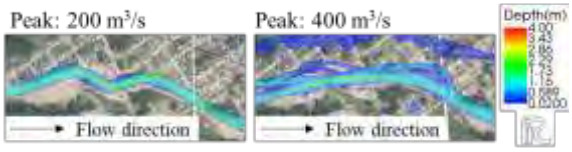

Figure 2: Plane bathymetries at 180 m³/s in falling limb for the single-peak case with peak discharge of 200 m³/s and 400 m³/s, respectively.

3.2 Double-peak case

The results above also mean the importance of the hydrograph sequence to the channel evolution and the flood risk. The result of double-peak hydrograph case show that in the upstream of the knickpoint, the lateral erosion depends on the total flow volume, meaning that the hydrograph shape has little contribution to the lateral erosion. Meanwhile, in the downstream of the knickpoint, the amount of the lateral erosion varies significantly by the order of peaks. In the forward peak case, the channel is braided during the 1st large peak, and then, the lateral erosion does not progress at the 2nd small peak. In the backward peak case, on the other hand, the channel remains meandering during the 1st small peak, so that both the small peak and the large peak contribute to the lateral erosion, resulting in larger lateral erosion.

References

[1] Tanabe, S., Iwasaki, T. and Shimizu, Y. Morphological response of gravel bed rivers near a knickpoint: Effect of bars on dynamic equilibrium river profile. Earth Surface Processes and Landforms, 49(13), 2024.

Effects of Unsteady Flow on Bar Morphology and Dynamics in an Experimental Flume

Atsuko MIZOGUCHI[1, 2]
[1]Meijo University, Aichi, JAPAN
[2]Tohoku University, Miyagi, JAPAN
Corresponding author: atsu@meijo-u.ac.jp

Keywords: alternate bar, unsteady water discharge condition, shape of bars

1 Introduction

In Japan, bank erosion and bridge collapse occur due to heavy rainfall. Recently, we have recognized the possibility that these disasters could be triggered by bar migration during the falling stage of a flood. Sediment transport and bed changes become more active during flooding, but their behaviours differ between the rising and falling stages of the water level. Therefore, this study focuses on bar deformation and migration during flooding, and experiments were conducted to investigate this phenomenon.

2 Experimental Setup

The experiment was conducted in a flume with an adjustable slope, measuring 17.5 m in length and 0.6 m in width, as shown in Fig. 1.

Unsteady discharge was supplied to the experimental flume using a system equipped with an automatic valve and a flow discharge measurement device. Fig.2 presents the experimental setup and the actual water discharge conditions, highlighting their differences. In all cases, water supply was repeated several times, and the formation of sandbars in the channel was measured at each water stop. During water supply, the water surface and bed elevation changes along the sidewall were recorded using multiple cameras.

3 Characteristics of Bar Formation under the unsteady flow discharge

In all cases, alternating sandbars formed steadily after multiple water supply cycles, as illustrated in Fig. 3. However, the number of cycles required for a stable sandbar shape to form varied between cases. Additionally, the characteristics of bar shapes differed, as shown in Fig. 4. For instance, in Cases A and C, where the low-water period was prolonged, the sandbars were longitudinally scoured along the sidewall. Sandbar migration under unsteady flow conditions was observed from the sidewall. The results indicate that sandbars were more active during the rising stage of the water level, but their migration slowed after reaching the peak water level. This process plays a crucial role in the morphological evolution of bars.

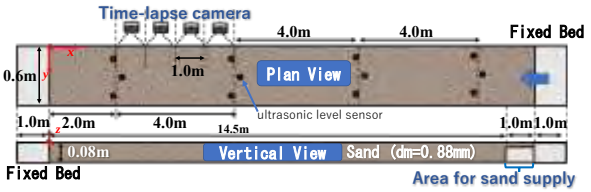

Figure 1: Experimental Set Up

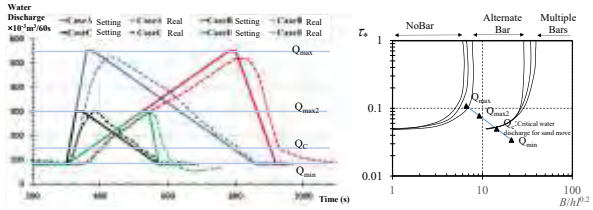

Figure 2: Water discharge condition in each case and regime criteria [1] of sand bars in water discharge

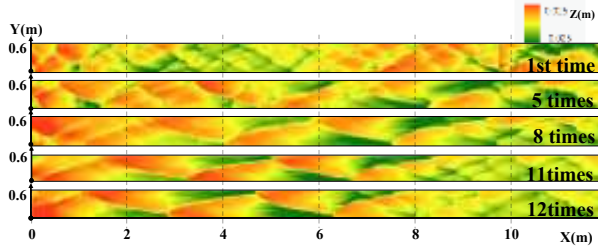

Figure 3: Process of bar formation in CaseA

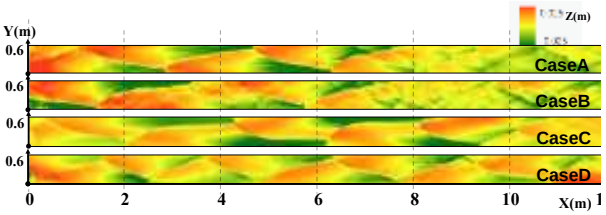

Figure 4: Differences of bar shape in the cases

4 Summary

A series of flume experiments were conducted to clarify the mechanisms of bar migration during flooding. The results indicate that the rising stage of the time-series variation in flow rate plays a crucial role in bar migration, while the falling stage is more influential in bar deformation. The time-series variation in flow rate affects not only bar formation and migration but also the overall bar morphology.

References

[1] Kuroki, M. and T. Kishi, 1984. Theoretical study on regime classification of meso-scale bed forms, *Proc. JSCE*, Vol.342, pp.87-94 (in Japanese).

A simple laboratory test case for suspended load modelling

Benoît Camenen[1], Céline Berni[1], Fabien Thollet[1], Adrien Bonnefoy[1], , Théophile Terraz[1]

[1]INRAE RiverLy, Lyon, France

e-mail corresponding author: benoit.camenen@inrae.fr

Keywords: *laboratory experiments; suspended sediment; deposition; erosion; 1D modelling*

1 Introduction

Modelling sediment transport dynamics in rivers is of utmost interest to conduct flood risk assessment and sediment management. For fine sediment dynamics, advection-dispersion models are usually used with a major issue being the source terms: the Partheniades formula for the erosion rate and Krone formula for the deposition rate are classically implemented[1]. However, such empirical formula, especially for the erosion rate, are very uncertain. To the authors knowledge, there exist very few test cases in the literature based on bed evolution to calibrate such models and equations. In this communication, we present a simple laboratory test case used to calibrate a 1D advection-dispersion model.

2 Material and methods

The laboratory experiment was set in the 1 m-wide tilting flume of the HHLab at INRAE Lyon, France (see Fig. 1a). A slope of 0.5% and an upstream discharge of 10 L/s were fixed. The bed was uniformly covered with artificial grass with dense rigid strands of 5 mm height. Crushed glass beads with a median grain size of 30 μm were first tested with a concentration maintained at 1 g/L approximately using a recirculation system. The downstream gate was first set at 8 cm for 8 hours to induce a general deposition in the system due to the backwater effect, then lowered to 0 cm to create a general erosion. Calibrated turbidity meters were set to measure the sediment concentration continuously.

(a)

(b)

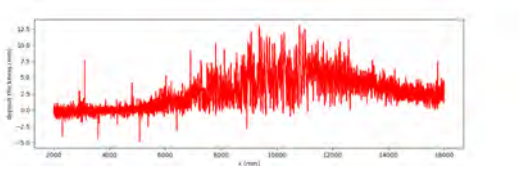

Figure 1: Photography of the tilting flume during the experiment (a) and deposit thickness along the canal after 10 hours (b).

We used the 1D software Mage-AdisTS [1] to simulate the laboratory experiment. In the AdisTS software, the source term were simplified as a single term:

$$(E - D) = a_{PD} W_s (C_{eq} - C) \tag{1}$$

where C is the concentration averaged over the river cros-section, C_{eq} the equilibrium concentration, W_s the settling velocity and a_{PD} the recovery coefficient (set to 1 here). The equilibrium concentration is defined as follows:

$$C_{eq} = C_0 \left(\frac{\tau}{\tau_c} - 1 \right) \tag{2}$$

where τ is the effective section averaged bed shear stress and τ_c its critical value for inception of transport, and C_0 is a calibration parameter. Two parameters can be calibrated here: first the critical bed shear stress even if a first estimation can be obtained using the Shields curve, second the coefficient C_0 that was estimated to 0.5 by Guertault et al. (2016[1]).

3 Results

A first result is presented in Fig. 1b corresponding to the bed elevation after 10 hours in the canal reference frame. A clear deposit due to the backwater effects can be observed despite the scatter due to the formation of ripples (see photo Fig. 1a). Even if the backwater effect leads to a continuously decreasing bed shear stress along the canal, a maximum deposit height is observed at approximately 10 m due to the concentration decrease related to upstream deposition.

A calibration of the model is currently in process to reproduce this result as well as the erosion phase. One issue here is to properly estimate the head loss due to bedforms, which characteristics evolved during the experiment.

4 Conclusion

A simple laboratory test is presented here that can be useful for the calibration of advection-dispersion models. The deposition phase is controlled by the vertical flux $W_s C$ although the presence of ripples enhances the turbulence and affects the calibration of the reference concentration C_0. The erosion phase should allow us to provide a better calibration of the controlling parameters of our model.

References

[1] L. Guertault, B. Camenen, C. Peteuil, A. Paquier, and J.-B. Faure. One dimensional modelling of suspended sediment dynamics in elongated dam reservoirs. *Journal of Hydraulic Engineering*, 142 (10, 10-04016033):1–9, 2016.

Morphological and non-morphological bedload varying river confinement: a laboratory investigation

Pandrin Enrico[1], Bertoldi Walter[1], Bernard Thomas[1]

[1]University of Trento, Trento, Italy

e-mail corresponding author: enrico.pandrin@unitn.it

Keywords: *gravel-bed rivers, bedload, non-morphological bedload*

1 Introduction

Fluvial systems are fundamentally characterized by the interplay between bedforms and processes [1]. Although numerous studies have examined the relationship between sediment transport and morphological changes [2], the link between bedload transport and its morphological imprint remains only partially understood. In this work, laboratory experiments were conducted to investigate both the morphological and non-morphological components of bedload.

2 Material and Methods

Laboratory experiments were conducted in a flume (0.6 m × 25 m) filled with homogeneous sediment. Five discharge rates ($0.7, L/s$ to $2.0, L/s$) produced channel configurations from braiding to wandering. For each discharge, nine flood repetitions were performed, each bracketed by topographic surveys. Morphological variations were quantified using Difference of Digital Elevation Models (DoDs), with survey frequency effects assessed by omitting intermediate DEMs. Continuous bedload monitoring was carried out via photographic surveys [3].

The experiments identified two primary components of bedload transport: (i) morphological bedload, in regions with detectable variations, and (ii) non-morphological bedload, where variations were absent. The latter was further subdivided into areas with compensatory sediment transport, areas where DoD filtering removed variations, and areas of equilibrium bedload, where local equilibrium resulted in zero spatial flux variation 1. The spatial extent of these components was quantitatively assessed across the channel, and their variations were examined as functions of discharge and survey frequency.

3 Results

Figure 1: Example map where bedload (green), compensation (yellow), and filtering (red) area are superimposed to the DoD for the $0.5\,L/s$ discharge. Flow from left to right.

The results indicate that the effects of compensation increase with discharge and, for a given discharge, further intensify as survey frequency decreases. The influence of compensation, which is more pronounced than that of DoD filtering, leads to a substantial underestimation of morphological changes when survey frequency is reduced.

Furthermore, the equilibrium bedload component exhibits an increasing trend with higher discharge rates, while it diminishes as survey frequency decreases. The intensity of bedload flux within equilibrium bedload and compensation areas is comparable to that observed in morphological bedload regions.

4 Discussion and Conclusion

Our findings are significant as this study represents the first direct comparison between bedload transport and its morphological imprint. Compensation effects lead to a substantial underestimation of morphological variations, highlighting the critical role of survey frequency. Moreover, regions influenced by compensation exhibit bedload flux intensities similar to those in morphological bedload areas.

Equilibrium bedload is a significant component in both spatial extent and flux intensity, yet it remains challenging to quantify. It may persist even in areas showing compensation or morphological variations, meaning that a purely morphological approach underestimates overall bedload activity.

Furthermore, in more confined systems, both equilibrium bedload and compensation effects are enhanced, underscoring an increased morphological component in braided configurations. This behavior is likely due to greater lateral variability in bedload transport, which results in net morphological changes rather than simple sediment re-mobilization.

These insights not only advance our understanding of sediment dynamics but also support the calibration of theoretical and numerical models.

References

[1] C. Ancey. Bedload Transport: A Walk between Randomness and Determinism. Part 2. Challenges and Prospects. 58(1):18–33.

[2] W. H. Booker and B. C. Eaton. Morphodynamic Styles: Characterising the Behaviour of Gravel-Bed Rivers Using a Novel, Quantitative Index. 10 (2):247–260.

[3] M. Redolfi, L. Guidorizzi, M. Tubino, and W. Bertoldi. Capturing the Spatiotemporal Variability of Bedload Transport: A Time-Lapse Imagery Technique. 42(7):1140–1147.

Lab experiments on the permeability of a gravelly river bed

Anouk Boon[1], Menno Straatsma[1], Maarten Kleinhans[1]

[1]Department of Physical Geography, Utrecht University, Utrecht, the Netherlands

e-mail corresponding author: a.boon1@uu.nl

Keywords: *fluvial morphodynamics, colmation, gravel, fine sediments*

1 Introduction

Gravel bed rivers are dynamic systems with a wide range of grain sizes. The permeability of gravel beds can be very high, but can also become much lower if it is filled and clogged with finer sediments (colmation) [1]. Reduction of the water flow through the river bed sediment has many implications, among which the degradation of ecological habitat quality due to oxygen depletion and temperature imbalance. This is one of the hypothesised causes for the poor ecological status in the Common Meuse (Netherlands). To test this hypothesis, we need to identify which fine sediment fractions contribute to colmation and to understand the processes underlying silting and resuspension of these sediments into and out of the gravel bed.

2 Methods

We conducted a set of experiments in a transparent cylinder with a diameter of 14.5 cm, partially filled with a layer of sediment of varied grain sizes and water (Figure 1A). Water flowed through the sediment by opening a valve at the bottom of the cylinder. The through-flow was timed and used to calculate the saturated hydraulic conductivity K_{sat} as

$$K_{sat} = v\frac{h_{sed}}{h_{wat}} \tag{1}$$

where v is the flow velocity (m/s), h_{sed} is the thickness of the sediment layer and h_{wat} is total water height.

The median grain size of the Common Meuse is about 32 mm, as determined from field measurements by Rijkswaterstaat. For the experiments, we used a relatively fine sediment sample of the river bed limited to a maximum grain size of 11.2 mm in view of the cylinder diameter (Figure 1B). We defined sand as smaller than 2 mm, fines as smaller than 0.063 mm.

3 Results

Our results show a decline in K_{sat} with the addition of finer sediments (Figure 2). A substantial reduction occurs at the highest fraction (0.4) for the fines, as they wash away with the water until an almost non-permeable layer is formed. For sand, a substantial reduction occurs at a lower fraction (0.2). The combination of sand and fines causes a substantial reduction at very low fractions of (0.03) as the sand prevents the fines from flushing out. We see variation in K_{sat} between experiments due to the difference in compaction, explaining the higher initial values for fines compared to sand.

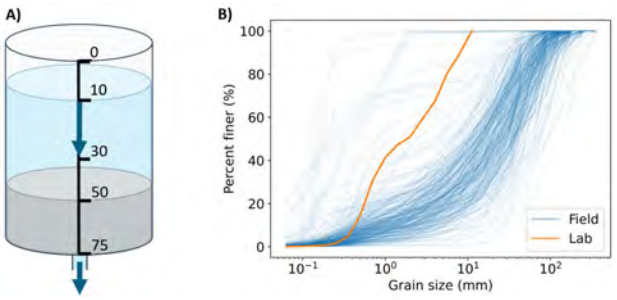

Figure 1: A) The lab set-up with the transparent cylinder, filled with water (blue) and sediment (grey). Through-flow is timed between 10 and 30 cm below the top. B) Sieve curves of 300 field samples by Rijkswaterstaat and of the experimental sediment.

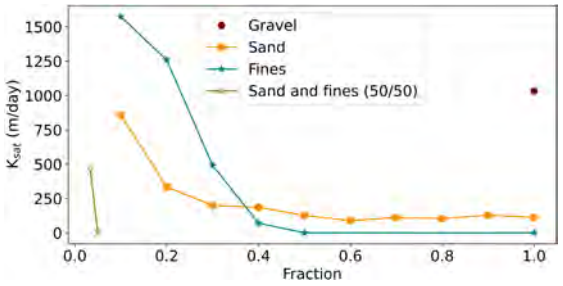

Figure 2: Saturated hydraulic conductivity K_{sat} through our gravel bed, with varying fractions of sand, fines and a combination of sand and fines.

4 Conclusions

The experiments show that a mix of sand and fines causes the most substantial reduction of water flow through our gravel bed at very low fractions. Ongoing lab work will include effects of hyporheic flow through gravel bars and potential of resuspension of finer sediments. This and the presented results will help understand the colmation pattern found in the Common Meuse and aid management.

Acknowledgements

We thank Arjan van Eijk and Henk Markies for their indispensable lab support. This project was funded by Rijkswaterstaat's Rivers2morrow.

References

[1] G. Wharton, S. H. Mohajeri, and M. Righetti. The pernicious problem of streambed colmation: A multi-disciplinary reflection on the mechanisms, causes, impacts, and management challenges. *Wiley Interdisciplinary Reviews: Water*, 4(25), 2017.

Using porosity and submergence ratio to assess particle transport past submersed in-stream structures.

Rafael O. Tinoco[1], Hojung You[2,1]
[1]University of Illinois at Urbana Champaign
[2]Woods Hole Oceanographic Institution
Corresponding author: tinoco@illinois.edu

Keywords: particle transport, in-stream obstructions, turbulence, sediment transport

1 Introduction

Porous obstacles in aquatic environments create intricate flow conditions. Vegetation patches, logjams, and reefs can control erosion and deposition of sediment and drifting matter. Coherent flow structures [1], porosity [2], and submergence ratio have ecological and geomorphic applications at their vicinity. We present results from laboratory experiments using simplified geometries to assess the effect of obstacle and particle properties on particle transport, aimed to improve predictions of drifting matter in natural environments.

2 Methods

Experiments were conducted in an Odell-Kovasznay flume with a test section 2 m long, 0.15 m wide. Rectangular channel-spanning obstacles (Figure 1) with length $L = 0.035\,m$ and height $h = 0.105\,m$ were used to create gaps of length d. Six barriers were tested, with porosities from $\phi_0 = 0.0$-0.36, to cover a wide range of porous structures in nature. Three submergence ratios, $h/H = 2,3,4$ were investigated. Two types of particles were tested to cover a wide range of microplastics, plant seeds, and fish eggs properties, with mean diameters of 1 and 4.8 mm, and specific gravities of 1.00 and 1.0025, respectively. Particle Image Velocimetry (PIV) and Lagrangian Particle Tracking (LPT) were used to obtain velocity fields and particle trajectories.

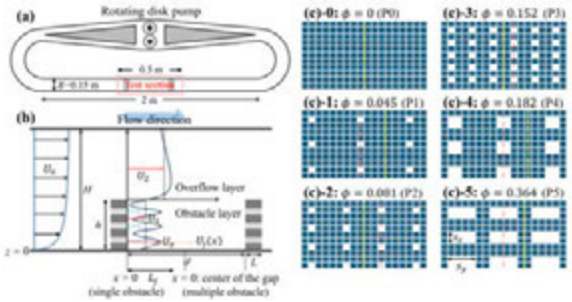

Figure 1: Top (a) and sideview (b) sketches of experimental setup. Configuration of porous barriers (c).

3 Results and Discussion

Porous obstacles created heterogeneous flow conditions (Figure 2). The local flow scales were set by interaction between jets emanating from pores and downstream backward flow motions created by flow blockage of obstacles. Recirculation zones formed downstream of obstacles with small pore sizes, while increasing the pore sizes increased jet velocity and length, creating dominant forward flow. Individual pore size showed to be as relevant as mean porosity to characterize the flow. The study revealed that local suspension of sediment within the gap is more pronounced when obstacles are porous compared to solid, especially at the upstream corner of the gap. Larger vertical pore size also led to an increase of the sediment diameter that can remain suspended, suggesting a higher capacity to keep fine sand in suspension behind porous obstacles, which allows a better identification of deposition-prone zones dictated by coherent flow structures past porous barriers. These findings can inform monitoring, sampling, and management strategies for sediment transport, plastic debris, and invasive species in rivers.

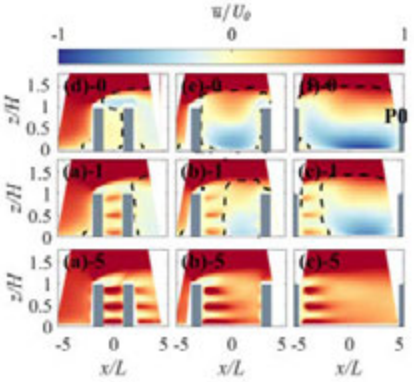

Figure 2: Mean velocity $\bar{u}/U$ for cases ϕ_0 (top), ϕ_1 (middle) and ϕ_5 (bottom), for gaps of d/L=2 (left), 6 (center), 10 (right).

Acknowledgments

We acknowledge support by US Geological Survey (G22AP00022). Comments are those of authors and don't necessarily represent the views of the sponsors.

References

[1] H. You & R.O. Tinoco. Characterization of Porous In-Stream Structures to Assess Their Implications on Flow Dynamics and Sediment Transport. *JGR-Earth Surface*, 2025.

[2] H. You & R.O. Tinoco. Turbulent coherent flow structures to predict the behavior of particles with low to intermediate Stokes number between submerged obstacles in streams. *Water Resources Research*, 59, 2023

Laboratory Study on the Flocculation and Settling Behaviour of Sediment from the Three Gorges Reservoir

Dayu Wang[1], Le Wang[2], Lei Zhang[1]
[1]China Institute of Water Resources and Hydropower Research, Beijing, China
[2]North China Electric Power University, Beijing, China
Corresponding author: wangdy@iwhr.com

Keywords: Three Gorges Reservoir, sediment, floc, density, settling velocity

1 Introduction

The Three Gorges Reservoir (TGR) in China has experienced significant sedimentation of fine particles since its construction, raising concerns about its impact on reservoir capacity, water quality, and overall ecosystem health. While the sedimentation process is complex and influenced by various factors, recent studies have suggested the potential role of fine sediment flocculation in this phenomenon. This study investigates the flocculation and settling behavior of TGR sediments through laboratory experiments and analysis, aiming to provide insights into the mechanisms driving sedimentation and its implications for reservoir management.

2 Methods

The study utilized a custom-designed coaxial double-cylinder rotational flocculation device to simulate the water-sediment conditions of the TGR. Sediment samples were collected from the reservoir bed and processed to ensure the particles were in a single-particle state. Two sets of experiments were conducted using two different sediment mixtures with varying grain size distributions. The first mixture, referred to as LRS (origin-proximal sediment), contained particles with diameters less than 150 μm, including both cohesive and non-cohesive sediments. The second mixture, referred to as SRS (contrasting sediment), contained only cohesive sediments with diameters less than 50 μm. The flocculation and settling process was observed using image technology, allowing for the identification and analysis of settling particles' size and settling velocity.

3 Results

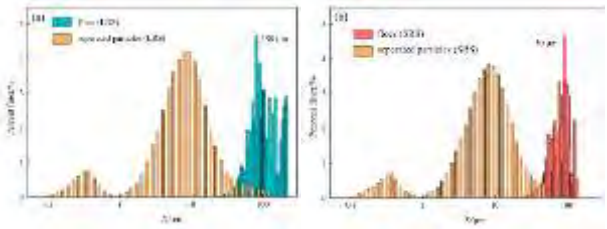

Figure 1: Relative proportions of each size in the input sediment and settling particles within the (a) LRS and (b) SRS series

The experiments confirmed the presence of flocculation in both LRS and SRS sediment mixtures(Figure 1). The settling velocities of observed particles were significantly different from those of single particles of the same size, indicating the formation of flocculated aggregates. The average settling velocities of flocculated particles were lower than those of individual particles, suggesting lower and variable densities of the flocculated aggregates. Additionally, the study employed fractal theory to estimate the density of flocculated particles and established a relationship between flocculated particle size and effective density. Based on these findings, two formulas for calculating the settling velocity of flocculated particles were developed and compared with measured values, demonstrating good agreement.

$$\begin{cases} \omega_s = 1.056 \frac{gD_f^{0.65}}{18\mu} & (LRS) \\ \omega_s = 1.667 \frac{gD_f^{0.65}}{18\mu} & (SRS) \end{cases} \quad (1)$$

4 Conclusions

The study provides strong evidence for the occurrence of fine sediment flocculation in the TGR, highlighting its potential contribution to the observed sedimentation patterns. The developed formulas for calculating flocculated particle settling velocities offer valuable tools for understanding and predicting the settling behavior of fine sediments in reservoir environments. Further research is needed to investigate the specific mechanisms driving flocculation in the TGR and its interactions with other factors influencing sedimentation, such as water dynamics, organic matter content, and clay mineralogy. Understanding these complex interactions is crucial for developing effective strategies to manage and mitigate the impacts of sedimentation on the TGR and other reservoir systems.

References

[1] FAN Y, MAX, DONG X, et al. Characterisation of floc size, effective density and sedimentation under various flocculation mechanisms. *Water Science and Technology*, 82(7): 1261-1271, 2020.

[2] CUTHBERTSON A J S, DONG P, DAVIES P A. Non-equilibrium flocculation characteristics of fine-grained sediments in grid-generated turbulent flow. *Coastal Engineering*, 57(4): 447-460, 2010.

Riverbed and banks coupled evolution

Ludovico Agostini[1], Marco Redolfi[2], Peter Molnar[1], Marco Tubino[3]

[1]Eidgenössische Technische Hochschule Zürich, Switzerland
[2]Università degli studi di Modena e Reggio Emilia, Italy
[3]Università degli Studi di Trento, Italy

e-mail corresponding author: lagostin@ethz.ch

Keywords: *riverbank erosion, cross section, morphodynamic, river trajectory*

1 Introduction

The morphology of a river channel in equilibrium conditions is characterized by regime values of channel width and bed slope. These values are essentially controlled by the upstream hydro-morphological conditions: formative discharge, sediment feed and grain size distribution.
In the present contribution we investigate the river channel non-equilibrium dynamics, in particular the transitory state that follows a perturbation of with respect to the original equilibrium state. The resulting river channel evolutionary trajectory is a product of the mutual influence between the riverbed evolution and the riverbank adjustment. The model is compared with real data from [2],[5].

2 Method

We represent the coupled evolution of riverbed and width through a zero-dimensional mathematical model. We solve the morphodynamic system in response to a stepwise perturbation in the formative discharge or sediment feed. The solution of the ODE system presented is both numerical and analytical, through a small perturbation approach.
In the model, the slope changes are studied in relation to a fixed riverbed point downstream; for the cross section we consider two types of geometry. Specifically, we use a rectangular channel as benchmark model to then test the channel evolution of a trapezoid cross section under two different closures of the riverbank erosion/construction process. In the first closure we assume that the channel top width (W) evolves through excess shear stress [4],[1] conditions, eq.1.
In the second closure width evolves through a combined effect of excess shear stress and toe erosion by channel incision [3], as in eq.1.

$$\begin{aligned} \text{closure A: } & \frac{\mathrm{d}W}{\mathrm{d}t} = E(\tau^* - \tau_r^*) \\ \text{closure B: } & \frac{\mathrm{d}W}{\mathrm{d}t} = E(\tau^* - \tau_r^*) - \frac{2}{\tan\alpha}\frac{\mathrm{d}\eta}{\mathrm{d}t} \end{aligned} \tag{1}$$

where E is the riverbanks erosional rate in $[m/s]$, $\tau^* - \tau_r^*$ is the excess Shields parameter, with respect to a reference value that accounts for the banks cohesivity; η is the bed elevation and α the friction angle of the riverbanks sediment.
When the model is scaled with its regime hydraulic and morphological configuration; it's evolution depends on the parameters of φ_0 and R_t. φ_0 is ratio between the characteristic scales of width and bed elevation, while R_t is the ratio between the riverbanks evolution timescale T_b^* and the riverbed timescale to sediment transport equilibrium T_t^*.

3 Results

The results suggest a wider variability range in the morphodynamic system response when subject to a change of the formative discharge and sediment feed. The solution of the coupled evolution strongly depends on the time scale ratio R_t which controls both the river channel time to reach the new equilibrium and the possible non-monotonic convergence to it. For $R_t = 10^{-1} \sim 10^0$, the banks adjustment interacts in phase with the riverbed morphodynamic response. The mutual influence that arises increases the time to equilibrium and also reproduces a dumped oscillator dynamics. In this region the transient evolution to the new regime is non-monotonic and displays significant overshoots over the new theoretical equilibrium of width and slope.

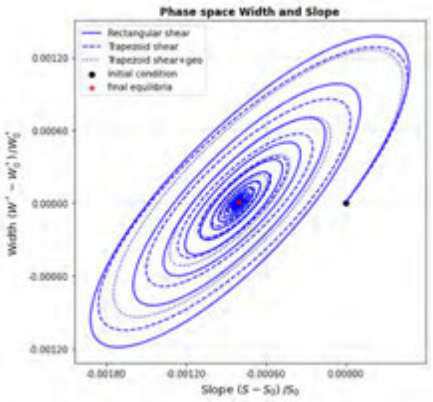

References

[1] A. Cantelli, M. Wong, G. Parker, and C. Paola. 2007.
[2] W. P. Clark, 1984.
[3] Y. Cui, G. Parker, C. Braudrick, W. E. Dietrich, and B. Cluer. 2006.
[4] E. Partheniades and R. Paaswell. 1970.
[5] J. E. Pizzuto. 1994.

Hydro-Environmental Conditions Modulate the Temporal Variability of Streambank Erodibility Parameters

Karol Sanchez[1], MSc.; Celso Castro-Bolinaga[1], Ph.D.; Kristina Hopkins[2], Ph.D.; Sam Holberg[1]
[1] Biological and Agricultural Engineering, North Carolina State University, Raleigh, NC, USA
[2] U.S. Geological Survey (USGS), Washington Water Science Center, Tacoma, WA, USA
Corresponding author: cfcastro@ncsu.edu

Keywords: erosion, Jet Erosion Test, moisture content, streambank, temperature

1 Introduction

Streambank erosion is a ubiquitous morphodynamic process. However, high rates of streambank erosion are detrimental to the stability and function of streams. Over time, such high rates can lead to excessive bed erosion and deposition, increased loading of fine-grained material and nutrients, and poor water quality and habitat conditions. The occurrence of this natural phenomenon has been accelerated in response to climate-change induced fluctuations in the timing and intensity of hydrologic events, highlighting the importance of characterizing the inherent variability that mark drivers of streambank erosion in nature. The objective of this work was to characterize the temporal variability of streambank erodibility parameters in response to rapidly changing hydro-environmental conditions and hydrological fluctuations.

2 Study Area & Overview of Methods

The applied methodology consisted of three main components, namely, site selection, soil physical characterization, and in-situ Jet Erosion Tests (JET) [1]. First, site selection incorporated feedback from collaborators at USGS and City of Raleigh. The main selection criteria included having a nearby USGS stream gage and easy access for data collection. A total of seven streambanks along three reaches of Crabtree Creek and Walnut Creek within the City of Raleigh's planning jurisdiction were selected. Secondly, the physical characterization of streambank material was performed via volumetric core samples collected at the selected sites and analyzed following ASTM standards. Lastly, repeated JET testing was performed in-situ, obtaining measurements of streambank material's critical shear stress (τ_c) and erodibility coefficient (k_d) [1] normalized by instantaneous values of moisture content (MC), electrical conductivity (EC), and soil temperature (T).

3 Results & Concluding Remarks

JET testing results highlight that for a single location characterized by the same soil type/texture, the relationship between τ_c and k_d, as well as their magnitude, is dynamic and dependent on the values of MC, EC, and T. For example, as shown in Fig. 1, selected streambanks along Walnut Creek exhibited a nearly vertical variation in the relationship between τ_c and k_d, indicating that k_d – which describes detachment rates after the onset of erosion – is more sensitive to changing hydro-environmental conditions than τ_c. Nonetheless, despite exhibiting a similar vertical trend in their relationship, the composition of each

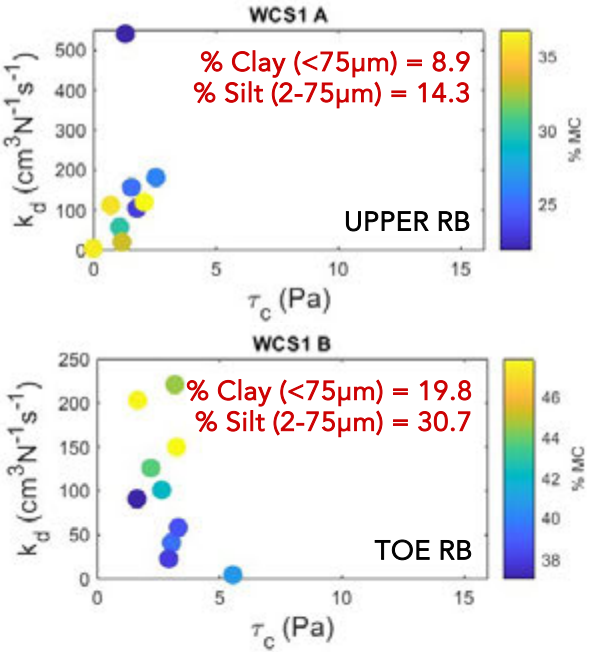

Figure 1: Relationship between τ_c and k_d, as well as their magnitude relative to changes in Moisture Content (MC), for streambanks along a reach of Walnut Creek in Raleigh, NC, USA.

streambank ultimately modulated the magnitude of k_d relative to changes in MC, EC, and T. As shown in Fig. 1, for some streambanks along Walnut Creek, k_d increased with an increasing MC (bottom), whereas for other streambanks along the same reach, lower values of k_d were associated with higher values of MC (top). The main difference between these two streambanks is their composition, with the former streambank material classified as sandy lean clay with a high plasticity index, and the latter material characterized by a higher sand content.

Acknowledgments

The authors acknowledge funding from the North Carolina Water Resources Research Institute (NCWRRI). The authors also acknowledge the support from Charles Stillwell and Laura Gurley from the USGS South Atlantic Water Science Center (SAWSC), as well as from Joyce Gaffney, Courtney Baker, and Megan Walsh from the City of Raleigh.

References

[1] Fox, G.A., Guertault, L., Castro-Bolinaga, C.F., Allen, P., Bigham, K.A., Bonelli, S., Hunt, S.L., Kassa, K., Langendoen, E.J., Porter, E., Shafii, I., Wahl, T., Wynn-Thompson, T., 2022. Perspectives on the Jet Erosion Test (JET): Lessons Learned, Challenges and Opportunities in Quantifying Cohesive Soil Erodibility. *Journal of the ASABE*, 65(2): 197-207, https://doi.org/10.13031/ja.14714.

Hydraulic or seepage erosion: What drives bank collapse in tidal environments?

Kun Zhao[1,2], Stefano Lanzoni[2], Giovanni Coco[3], Alvise Finotello[4], Kaili Zhang[1], and Zheng Gong[1]

[1]*The National Key Laboratory of Water Disaster Prevention, Hohai University, Nanjing 210098, China*

[2]*Department of Civil, Environmental and Architectural Engineering, University of Padua, Padua 35122, Italy*

[3]*School of Environment, University of Auckland, Auckland 1010, New Zealand*

[4]*Department of Geosciences, University of Padova, Padova 35131, Italy*

Corresponding author: kunzhao1357@gmail.com

Keywords: bank collapse, tidal channel, seepage, laboratory experiment

Abstract

Research on bank collapses in tidal environments has traditionally relied on theories from fluvial systems, emphasizing the predominant role of hydraulic (flow-driven) erosion in these failures. However, the presence of residual pore water within tidal channel banks, due to daily fluctuations in tidal levels, leads to persistent seepage that can significantly affect bank stability. This discrepancy prompts a critical yet largely unanswered question: what is the dominant driver of bank collapse in tidal settings? Here, we develop a prototype experiment to model bank collapse under varying conditions of tidal currents and seepage. We observe significant variability in failure patterns, varying from fast, abrupt toppling failures caused by tidal currents to slow, continuous pop-out failures driven by seepage (Figure 1). Numerical simulations further reveal a predominance of seepage on bank collapse as the tidal range increases. Experimental and numerical results are used to derive dimensionless predictive functions that integrate both hydraulic and seepage erosion, providing a unified framework for understanding and predicting the dynamics of bank collapse in tidal environments. Our findings elucidate a long-overlooked mechanism driving bank collapses in tidal settings, with broad implications for the evolution of tidal channels and related coastal wetland ecosystems.

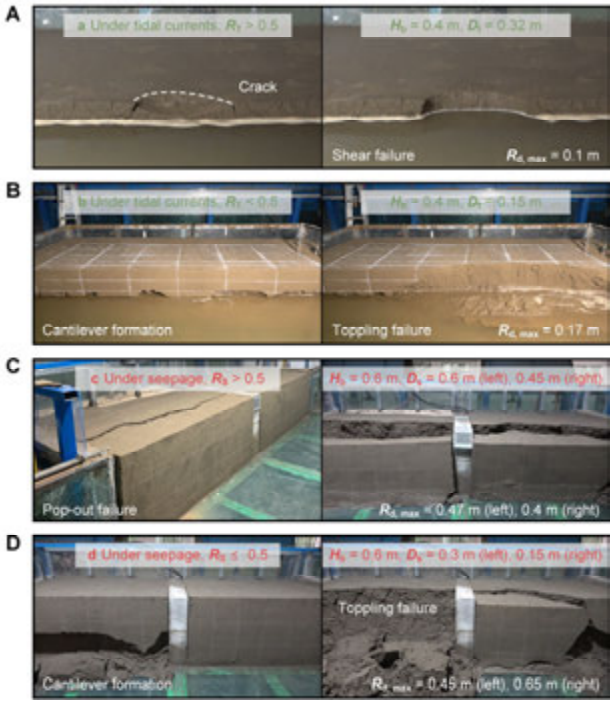

Figure 1: Examples of bank collapse observed from laboratory experiments. Each photograph captures a distinct bank collapse event under either tidal currents (A, B) or seepage flow (C, D), with indicated the corresponding input parameters and the observed maximum retreat distance, $R_{d,max}$ (right panels).

Acknowledgments

The study was supported by the National Key R&D Program of China (2022YFC3106204) and National Natural Science Foundation of China (51925905, 52201318). We thank Keyu Wang and Shuai Tang for their assistance in laboratory experiments.

Numerical Investigation of Alluvial Ridge Development in Meandering Rivers

JeongYeon Han[1], Yuan Li[1], James H. Gearon[1], Douglas A. Edmonds[1]
[1]Department of Earth and Atmospheric Sciences, Indiana University Bloomington, IN, US
Corresponding author: hanjeon@iu.edu

Keywords: River, Floodplain, Sedimentology, Morphodynamics, Levee

1 Introduction

In meandering rivers, the overbank aggradation (e.g., levee growth and crevasse splays) and lateral bank-migration contribute to the formation of alluvial ridges along the channels. Alluvial ridges are crucial elements of the fluvial system that influence river avulsion processes and the stratigraphic stacking patterns of channels, yet few numerical studies have investigated how these ridges form and the relative importance of lateral and vertical accretion in their formation. This study examines the development of alluvial ridges through a one-dimensional morphodynamic model that incorporates both meandering and levee construction in river channels. We then focus on how these factors affect superelevation over time, which reflect bankfull channel depth and local relief of levee crest relative to adjacent flood basins.

2 Field Observations

Based on few observations, we hypothesize that smooth ridges are associated with stable channels exhibiting slow lateral migration (Fig. 1a-b), whereas rough ridges are found along newly avulsed channels that migrate relatively faster over time (Fig. 1c-d).

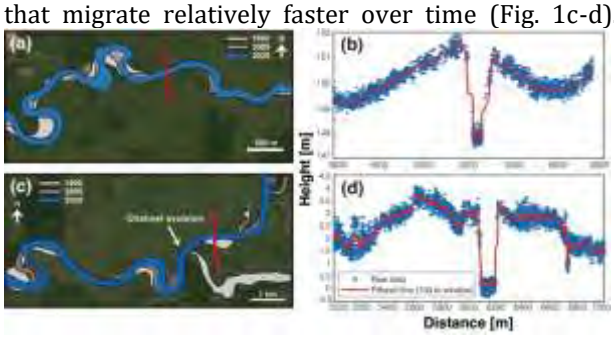

Figure 1: Satellite images and elevation profiles along the red lines, processed using Savitzky-Golay filter shown for (a-b) Rio Ele River in Columbia and (c-d) Motagua River in Guatemala. Channel locations are indicated by different colors.

3 Results

We will measure the morphology of alluvial ridges, including their super-elevation and ridge slopes, and explore the relationship between these morphological features and the channel mobility number. The channel mobility number, defined as the ratio of lateral migration rate to channel bed aggradation rate [1], is given by

$$\frac{H_c}{B} \cdot \frac{M_r}{A_c}, \qquad (1)$$

where H_c denotes channel depth, B is channel width, M_r is lateral bank migration rate, and A_c is in-channel aggradation rate.

Our modelling results show that the overbank deposits on the inner bank side resemble scroll bars while outer bank exhibits natural levees or levee-like features, aligning with typical patterns observed in meandering channels (Fig. 2). The alluvial ridge with a higher channel mobility number produces a lower, gentler, and rougher ridge compared to one formed by a lower channel mobility number, as the main channel shifts before reaching its maximum elevation (Fig. 2b).

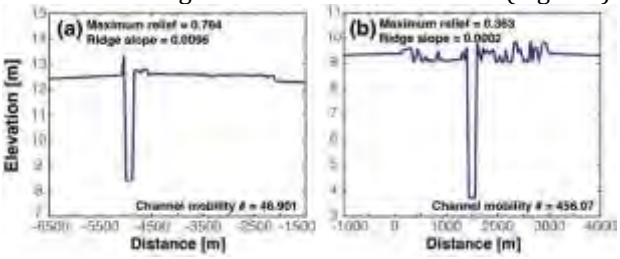

Figure 2: Examples of topographic profiles in our model illustrating (a) relatively steep slope and (b) gentle slope of alluvial ridges.

4 Conclusions

Our results highlight the significant role of both lateral and vertical accretion processes in the formation of alluvial ridge complexes, with channel mobility number serving as a key indicator. By examining the relationship between channel mobility, ridge morphology, and superelevation ratios through a numerical model, we illustrate how channel mobility affects the evolution of alluvial ridges and their avulsion dynamics. These findings suggest that areas with higher channel mobility tend to have gentler and rough ridges, which may take longer time to reach the superelevation threshold as the channel continuously migrates before achieving maximum accretion. Based on this, our study enhances the understanding of avulsion conditions in meandering rivers.

Acknowledgments

This research has been supported by NSF grants 2321056 and 2436929 awarded to DAE.

References

[1] D. J. Jerolmack and D. Mohrig. Conditions for branching in depositional rivers. *Geology*, 35(5):463-466, 2007.

MODELING OF NATURAL LEVEE FORMATION IN AN ENGINEERED COMPOUND CHANNEL OF THE ABIRA RIVER, JAPAN

Kensuke Naito[1], Shinji Egashira[1]
[1]International Centre for Water Hazard and Risk Management, Public Works Research Institute, Japan
Corresponding author: kensuke.g.naito@gmail.com

Keywords: natural levees, 2D morphodynamic model, numerical experiment

1 Introduction

Natural levees form when relatively fine sediment deposits on floodplains adjacent to the channel during overbank events, and floodplain deposition constitutes an important part of the sediment routing.

Although the importance of suspended sediment in the natural levee formation has long been well recognized, its treatment in modelling framework remains as a challenge. This is due primarily to lack of physical understanding at the bottom boundary, where suspended sediment interacts with the bedload layer, and most previous studies assume equilibrium between diffusion and advection at the interface [1].

Recent study has tackled this challenge by employing the concept of entrainment velocity from the bedload layer into suspension, diverging from relying on equilibrium assumption at the bedload - suspended load interface [2]. The presented study aims to reproduce the observed levees including its characteristics in the Abira River, Japan, where natural levee formation was observed along an engineered compound channel, and to discuss some of the key controlling factors, including processes at the bottom boundary.

2 Methodology

A set of depth-averaged 2D flow governing equations coupled with sediment transport and sediment conservation equations are solved. For the sediment entrainment into suspension, we employ the entrainment velocity concept proposed by [2].

The lower channel of the compound cross-section is 4 m-wide and 1.2 m-deep and floodplains are 5 m-wide. The channel is 200 m-long, and longitudinal slope is 0.0025. At the upstream end, hydrograph, sediment concentration and its size distribution, as well as the initial bed configuration were specified.

3 Preliminary result

The numerical simulation successfully reproduced the natural levees as well as the downstream fining trend, which were observed in field. Resulting plot shows the floodplain sedimentation along the lower channel – floodplain boundary (Figure 1). It is shown that the natural levees grow both vertically and horizontally in time, and that no development are observed after approximately t = 13 hr, which corresponds to a lowering stage in the hydrograph. It should also be emphasized no re-entrainment of deposited sediment is observed, and that the lower channel bed shows no apparent bed elevation change.

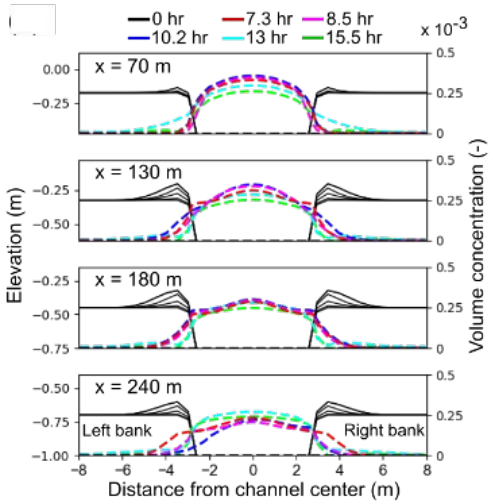

Figure 1: Numerical simulation result in cross-section view. Note that there is no change between t=13hr and t=15.5hr.

4 Discussion and summary

While some features such as downstream fining agree with the observation, the numerical model simulates the finer and longer natural levees. In the simulation, the natural levees are not formed when suspended sediment is not supplied from the upstream, indicating that the sediment that deposited on the floodplain was sourced from far upstream reach, rather than nearby lower channel bed. Further discussions are needed in terms of the treatment of the suspended sediment deposition and erosion at the vegetated surface in modelling framework.

Acknowledgments

This research was supported by the Science and Technology Research Partnership for Sustainable Development (SATREPS) in collaboration between the Japan Science and Technology Agency (JST, JPMJSA1909) and the Japan International Cooperation Agency (JICA).

References

[1] M. Garcia and G. Parker. Entrainment of bed sediment into suspension. *Journal of Hydraulic Engineering*, 117(4), pp. 414-435, 1991.

[2] D. Harada, S. Egashira, T.S. Ahmed, and H. Ito. Entrainment of bed sediment composed of very fine material, *Earth Surface Processes and Landforms*, 47(13), pp. 3051-3061, 2022.

Measuring the abundance and dimensions of natural river levees

E. A. Barefoot[1], J. H. Gearon[2] J. Han[2], and D.A. Edmonds[2]
[1]Department of Earth and Planetary Sciences, University of California, Riverside, USA.
[2]Department of Earth and Atmospheric Sciences, Indiana University, Bloomington, USA.
Corresponding author: ebarefoo@ucr.edu

Keywords: Natural Levees, Flood variability, Observational study

1 Information

Natural levees form at the channel margin during overbank floods as a product of sediment exchange between the river channel and the adjacent floodplain. Despite forming on nearly every kind of channel on Earth as well as other planets, scientific models are consistently unable to predict where or how levees form. This knowledge gap is surprising and impactful because levee formation processes are an important aspect of sediment dispersal and nutrient cycling in alluvial environments, and therefore key to conservation strategies in riparian ecosystems. Since levees are often elevated above the surrounding floodplain, they also represent an important natural flood mitigation structure, and are usually attractive areas for development on river corridors. The most widely employed models of levee formation take a one-dimensional approach, in which sediment suspended in the channel is deposited at the channel margin by one of two mechanisms: (1) eddy diffusion in shear zones along the channel margin, which dissipates kinetic energy and allows sediment to deposit, or (2) advection settling away from the channel, where transport is governed by lateral water surface gradients away from the channel (Adams et al. 2004). The first mechanism has been extensively studied in laboratory settings but has rarely been directly observed in the field. The second mechanism is nearly ubiquitous in field observations of overbank flow, but does not well predict the location, extent, composition, or dimensions of levees in real floodplains.

2 Methodology

In this study, we take a functional approach to classifying levees: any sediment deposit within one channel width of the channel margin that is also higher in elevation than the surrounding floodplains, is labelled as a levee. We also take a reach-averaged approach. We determined levee abundance by inspecting lidar maps and visually identifying levees on river banks, estimating the proportion of the river reach (≥ 10 channel widths long) that has levees. Using lidar data available across the contiguous USA, we evaluated levee abundance at n=561 river reaches. These reaches span a range of environments, climates, and land-use practices. The sample of rivers is evenly spread from the coast to the mountains, and we have accompanying data to quantify the river's lateral migration rate, discharge variability, and average suspended sediment concentration. Using this sample of rivers reaches, we identify the main factors controlling the abundance of channel-margin levees. We then examined rivers with levees, and measured their height above the surrounding floodplain, as well as the levee width orthogonal to the riverbank.

3 Results

We found that all else being equal, there are six factors that make rivers more likely to have levees. 1) Steep rivers have fewer levees. 2) Rivers with coarse bedload sediment have fewer levees. 3) Slowly-migrating rivers have fewer levees. 4) Rivers in narrow valleys have fewer levees. 5) Rivers in arid climates have fewer levees. 6) Rivers with consistent width have fewer levees.

4 Expectations and discussion

Work is ongoing to examine trends in levee dimensions. We expect that levee dimensions will scale with three main parameters: discharge variability, floodplain width, and lateral migration rate. Rivers with highly variable flow (for example, the Indus, with annual monsoons) may generate swift overbank flows that disperse sediment across the floodplain, preventing accumulation close to the channel. Floodplain width also affects overbank flows. Narrow floodplains fill quickly with floodwaters, diminishing flow velocity across the channel margin. Channels that migrate rapidly across their floodplains abandon their levees while the levees are still small, preventing substantial channel-margin deposits from accumulating.

Acknowledgments

E.A. Barefoot acknowledges funding support from NSF Grant #2052844.

References

[1] Adams, P. N., Slingerland, R. L., and Smith, N. D. (2004). *Geomorphology*. 61.1, pp. 127–142. doi: 10.1016/j.geomorph.2003.10.005.

Using Gaussian mixture models and topo-bathymetric LiDAR data to decipher morphology of large rivers

Andréault, A.[1,2], Rodrigues, S.[1,2], Gaudichet, C.[3], Wintenberger, C.L.[4]
[1]: UMR CNRS 7324 CITERES, Tours, France
[2]: Graduate School of Engineering Polytech Tours, University of Tours, Tours, France
[3]: UMR 6553 ECOBIO-University of Rennes CNRS, Rennes, France
[4]: CEREMA, Blois, France
Corresponding author: alex.andreault@univ-tours.fr

Describing river morphology contributes to the study of hydraulics, sediment transport, morphodynamics, habitat organization and for risks assessment. So far, no fully objective tool was available to classify fluvial styles and to decompose river channel network into morphological units [2]. Based on this observation, we propose a workflow designed to analyze river morphology using only the elevation data of the active width of a river reach [1]. Thanks to a topobathymetric LiDAR survey, we were able to capture both emerged and submerged areas simultaneously with high accuracy and extensive coverage. This LiDAR survey was performed over 450 km of the largest river in France: the Loire.

We tested a new segmentation method on four reaches with different morphological styles (*i.e.*: anabranching, meandering, braided, and trained) on which high density LiDAR data were acquired (survey during 2020). Data processing relies on three distinct steps. Firstly, elevation data were cleaned (geospatial extent, detrending) and scaled to make sites and further results comparable between each other. Secondly, elevation data within the active width was summarized into a probability density function (PDF), from which the resulting signal was simplified and decomposed using a Gaussian Mixture Model (GMM). Statistical parameters of the PDF and the Gaussian components were extracted and compared. Thirdly, a validation step is conducted through cross-validation between the morphological units identified by the GMM and the segmentation performed by management services.

The results of the study show that the PDFs of elevation are specific to the reaches they describe (Figure 1). This specificity is further emphasized by differences observed in the PDFs of the same site surveyed over four years. Both the manual decomposition of these PDFs and the GMM analysis revealed groups of morphological units (Figure 1). When compared, the GMM approach identified a greater diversity of groups of morphological units sharing similar elevation ranges. The cross-validation further demonstrated that the GMM was capable of identifying groups of units that are geomorphologically coherent.

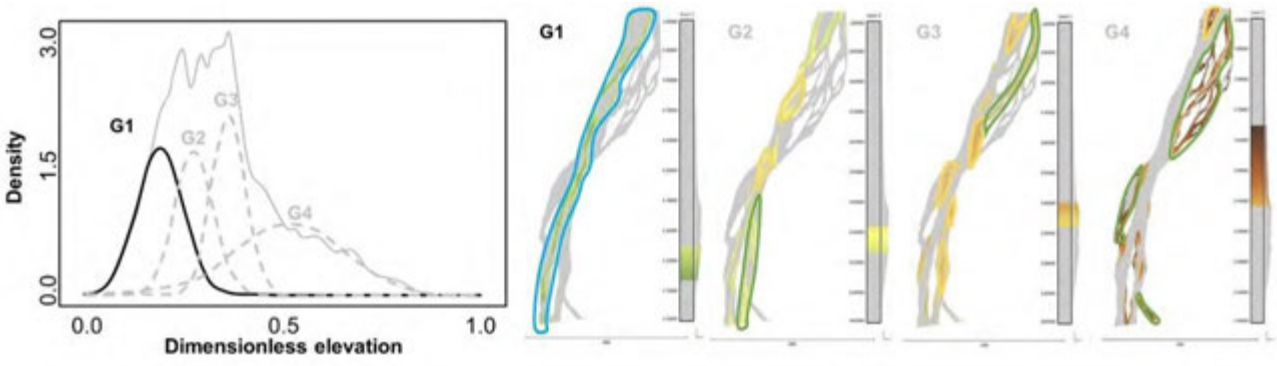

Figure 1: Projection of Gaussians extracted from PDF on corresponding DTM. Blue polygon represents the low flow channel approximated area, yellow represents sandbars and green highlights lateral channels.

At first glance, PDFs appear to be a valuable tool for in-depth analysis of riverine morphology. Moreover, the rarely employed method of PDF decomposition using Gaussian Mixture Models (GMM) seems well-suited for this purpose. We have demonstrated that GMM method is more sensitive than the manual one for detecting morphological units. Finally, the GMM method provides a relatively objective framework for geomorphological analysis in fluvial environments and can be applied across a wide range of spatial scales.

References:

[1] A., Andréault, S., Rodrigues, C., Gaudichet, C.L., Wintenberger. Statistically derived morphological signatures of large river channels extracted from topo-bathymetric LiDAR data., Earth surface Processes and Landforms, vol. 49, issue 2, 2024.

[2] P. Carling, J. Jansen, L. Meshkova. Multichannel rivers: their definition and classification. Earth Surface Processes and Landforms, vol. 39, issue 1, 2014

Climate Change Impacts on a River Bifurcation Region

M. Kifayath Chowdhury[1], Astrid Blom[1], Clàudia Ylla Arbós[2], Ralph Schielen[1,3]

[1]Delft University of Technology, Netherlands
[2]AXA Climate, France
[3]Ministry of Infrastructure and Water Management-Rijkswaterstaat, Netherlands

e-mail corresponding author: m.k.chowdhury@tudelft.nl

Keywords: *river bifurcation, climate change, flow partitioning*

1 Introduction

River bifurcations are critical in regulating water and sediment distribution in delta systems. In engineered river systems, maintaining a stable flow partitioning is essential for managing flood risk, navigation, and freshwater supply. However, climate change may introduce long-term shifts in hydrographs and sediment dynamics, potentially altering flow division at bifurcation points. Following [1, 2], our objective is to enhance insight into the effects of climate change on flow partitioning at two important bifurcations (Pannerdense Kop and IJsselkop) in the Dutch Rhine. A one-dimensional numerical model, informed by sediment partitioning data from a two-dimensional numerical model of the system and field data for water level and bed level change, is used to analyze these effects over a 150-year projection period.

2 Results

In the reference case, which assumes no additional climate change effects beyond the current rate of sea level rise, the relative share of the flow transported through the largest branch, the Waal, continues to increase. The flow in the smallest branch, the IJssel, continues to decrease under low flow conditions. The rate of change slowly decreases as the system approaches equilibrium. This shift in flow partitioning is a continuation of trends observed in recent decades. In addition, the bifurcation region is projected to continue to experience erosion, with sediment flux arriving at the bifurcation significantly declining over time, leading to further channel bed erosion.

Hydrograph change scenarios, which reflect climate-induced shifts in discharge patterns, are projected to affect flow partitioning under low-flow conditions only. The dominance of the Waal branch is further amplified, while the flow in the smallest branch is reduced more strongly than in the reference case. Effects become particularly pronounced after 2060–2080, when the sediment flux reaching the bifurcation region coarsens, triggering intensified erosion across the entire bifurcation region, leading to further adjustments in flow division. The climate-driven increase of medium flows increases the overall mobility of the sediment, which mitigates the severe reduction in sediment flux in the reference case.

Results for sea level rise scenarios indicate an opposing trend to hydrograph change scenarios. As sea level rises, upstream-migrating bed level adjustments increase the relative discharge towards the IJssel branch, partially counteracting the hydrograph-driven increase in Waal dominance. Similar to hydrograph change scenarioss, sea level rise scenarios are expected to affect flow partitioning under low-flow conditions mostly. Effects depend on the rate of sea level rise, with more extreme scenarios exerting a greater influence on flow partitioning. Sea level rise impacts flow distribution progressively over the coming decades, as the associated bed level adjustment takes time to propagate upstream and reach the bifurcation region.

In combined scenarios, where both hydrograph changes and sea level rise are included, the effects of climate-related hydrograph shifts tend to dominate over sea level rise, except in extreme sea level rise cases. The Waal's discharge continues to increase, and flow partitioning trends diverge more strongly from the reference case over time.

3 Conclusions

This study highlights that climate change will play an increasingly dominant role in shaping flow partitioning in engineered river bifurcations over the coming century. Hydrograph changes due to climate change will surpass the effects of historical interventions after 2060–2080. We project a 5–9% increase in Waal discharge and a 17–27% decrease in IJssel discharge under low-flow conditions.

Overall, this study provides a long-term projection of flow and sediment changes in a key river bifurcation system, underscoring the urgency of integrating climate resilience into river management policies and need for adaptive river management strategies. Future work should further explore localized morphodynamic feedbacks, event-driven responses, and potential engineering solutions to mitigate these changes.

References

[1] M.K. Chowdhury, A. Blom, C. Ylla Arbós, M.C. Verbeek, M.H.I. Schropp, and R.M.J. Schielen. Semicentennial response of a bifurcation region in an engineered river to peak flows and human interventions. *Water Resources Research*, 59(4), 2023. doi: 10.1029/2022WR032741.

[2] C. Ylla Arbós, A. Blom, C.J. Sloff, and R.M.J. Schielen. Centennial channel response to climate change in an engineered river. *Geophysical Research Letters*, 50(8), 2023. doi: 10.1029/2023GL103000.

Measuring planimetric features of fluvial bifurcations

Pascal Pirlot[1,2], Marco Redolfi[3], Marco Tubino[1]

[1]Università degli Studi di Trento
[2]Hochschule Karlsruhe, Technik und Wirtschaft
[3]Università degli Studi di Modena e Reggio Emilia

e-mail corresponding author: pascal.pirlot@h-ka.de

Keywords: *fluvial morphology; remote sensing; planimetry; Euclidian Distance Transform*

1 Introduction

Several studies on fluvial bifurcations have analysed the role of planform parameters (e.g., branch length, bifurcation angle) and of geometrical asymmetries (differences in branch widths and lengths, downstream branches alignment) on water and sediment partitioning at the node [1, 2, 3]. This line of investigations sets the need for a method to compute these planform parameters rigorously. With the present contribution, we aim at (1) providing a precise and robust semi-automated planform extraction procedure for natural fluvial bifurcations, and (2) establishing how these computed planform parameters are distributed, by applying this procedure to a large number of real-world bifurcations.

2 Procedure

The procedure is based on RGB pictures derived from satellite or aerial images. The channel banks are first manually extracted to obtain a binary shape of the bifurcation. The channel centerline is then automatically computed from the Euclidean distance transform of the binary image. This allows extracting planimetric characteristics such as the length of centerline, the channel width, orientation and curvature in a unique, non-ambiguous manner.

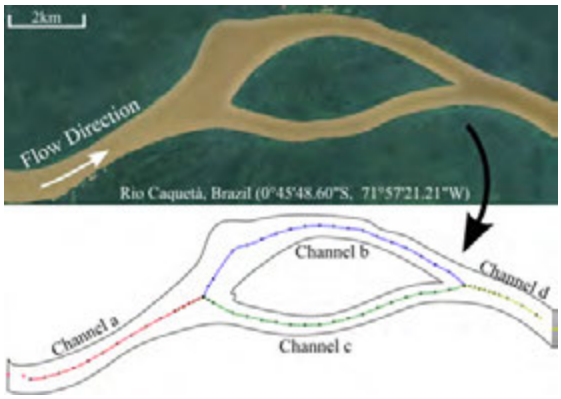

Figure 1: Extraction of the planform binary leading to the skeleton, from which the centerlines and local width of the channels are computed. The channels are defined stream-wise as: a upstream (red), b left (blue), c right (green) and d downstream (yellow).

3 Results

The procedure has been applied to a large number of bifurcations belonging to anabranching units occurring in single-thread reaches of sand-bed and gravel-bed rivers worldwide [2]. Two key parameters have been identified as representative of the degree of the longitudinal and transverse geometrical asymmetry of bifurcations, namely the channel width asymmetry ΔW and the bifurcation enlargement E_W:

$$\Delta W = \frac{W_b - W_c}{W_b + W_c}, \qquad E_W = \frac{W_b + W_c}{W_a}, \qquad (1)$$

where W_a, W_b and W_c denote respectively the average width of channels a, b and c. The figure 2 displays the resulting distributions of ΔW and E_W.

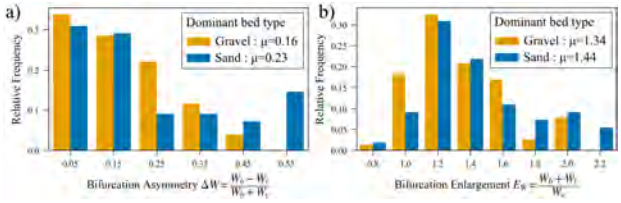

Figure 2: Distribution of the values of the parameters ΔW and E_W for the considered dataset.

A third of these bifurcations appear symmetric, whereas two thirds are decisively asymmetric. Most of them have a net enlargement value bounded within $[1.2 - 1.4]$. These features indicate that fluvial bifurcations obey some sort of regime.

4 Conclusion

The proposed extraction method enables the computation of parameters that characterize the planform properties of bifurcations, such as the degree of width and length asymmetry of the bifurcates and the local change of channel width at the bifurcation node. The resulting distributions provide information on how fluvial bifurcations are found in nature and allow the identification of the suitable ranges of parameters that need to be considered in theoretical models aimed at predicting their influence on the behaviour of fluvial bifurcations.

References

[1] T.Y. Dong et al. (2020). Predicting water and sediment partitioning in a delta channel network under varying discharge conditions. *Water Resources Research*, 56(11).

[2] N. Ragno et al. (2022). Quasi-universal length scale of river anabranches. *Geophysical Research Letters*, 49(16).

[3] G. Barile et al. (2023). Effect of width asymmetry on equilibrium and stability of river bifurcations. *RCEM 2023 Book of Abstracts, p.143.*

Processes of channel formation on meandering river floodplains revealed by repeat lidar

Douglas A. Edmonds[1], Garret D. O'Hara[1], Jonathan A. Czuba[2]
[1]Department of Earth and Atmospheric Sciences, Indiana University-Bloomington
Department of Biological Systems Engineering, Virginia Tech University
Corresponding author: edmondsd@iu.edu

Keywords: floodplain, meandering river, lidar, differencing

1 Introduction

Meandering river floodplains are commonly depicted as relatively flat, featureless deposits adjacent to the river channel. Yet, recent field-based studies have shown that floodplains have a surface morphology etched with channels [1] that influence inundation patterns and timing [2], connectivity [3], and ecological functioning (see example floodplain in Fig. 1). Despite their importance, it is unclear how floodplain channels originate and what controls whether they enlarge or shrink over time.

2 Study Site and Methodology

Our study site is the meandering East Fork of the White River in Indiana, USA. The White River flows through a broad alluvial valley and the floodplain channels flood every ~19 days [1]. To assess the geomorphic evolution of these channel we use lidar differencing from 2013, 2017, and 2025. The 2013 and 2017 surveys were collected by the state of Indiana. Differencing these surveys has been challenging because 2013 flight lines are misaligned and there are horizontal georeferencing errors. We developed a new workflow using CloudCompare to align the point clouds using fiduciary points. Then over regions of geomorphic change, we collected additional drone-based lidar data in 2025. Our drone-based lidar is a Riegl MiniVux that collects 300,000 points per second, from which we can create bare-earth point clouds with density of 400-700 pts m^{-2}. After we aligned all the points clouds, the root mean square error between the clouds was 2-3 cm.

3 Results

Our workflow of point cloud alignment can generate floodplain difference maps that resolve deposition and erosion across the floodplain of the East Fork White River, Indiana, USA (Fig. 1). Unsurprisingly, sediment deposition on the floodplain occurs near the channel in the form of scroll and point bars and seems to be limited to the channel belt. Erosion on the floodplain seems to be restricted to the paths of floodplain channels with magnitudes ranging from 10 to 50 cm over 4 years (Fig. 1). There are examples of erosion across the length of the channel (arrows) and isolated zones of erosion (circles). We hypothesize that floodplain channels form by linking up isolated erosion zones via migrating headcuts.

4 Future Work

Our approach here is to generate topographic difference maps across the entire E. Fork White River and look at the spatial control on erosion and deposition. At targeted sites we will fly drone-based lidar to assess if the observed topographic change is still occurring.

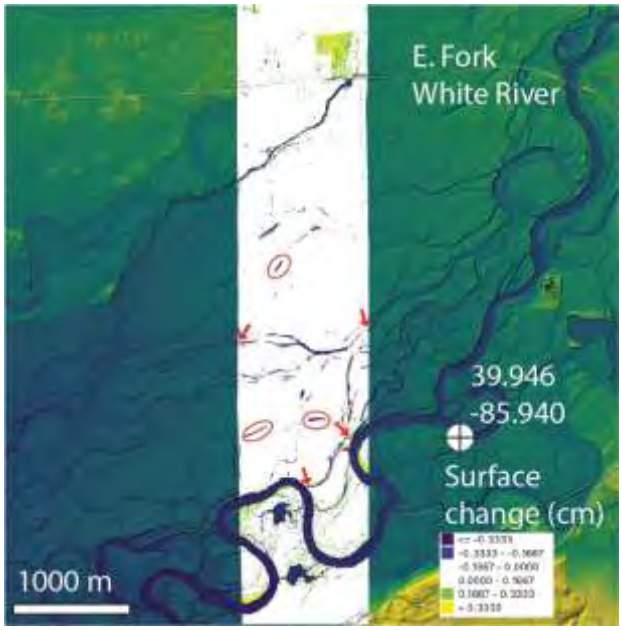

Figure 1: Topographic differencing on E. Fork White River, Indiana, USA. Middle strip shows difference after alignment of 2013 and 2017 lidar surveys. The red arrows point out examples of floodplain channel erosion of ~30 cm. Lat, Lon coordinates shown on image.

Acknowledgments

We would like to thank United States Department of Agriculture grant 2023-67019-39705

References

[1] J. A. Czuba, S. R. David, D. A. Edmonds, and A. S. Ward, "Dynamics of Surface-Water Connectivity in a Low-Gradient Meandering River Floodplain," *Water Resources Research*, 2019.

[2] M. R. Cain, J. L. Hixson, C. N. Jones, B. L. Rhoads, and A. S. Ward, "Empirical Evidence of Dynamic Hydrogeomorphic Feature Inundation in a Lowland Floodplain," *Hydrological Processes*, vol. 39, no. 1, p. e70043, 2025, doi: 10.1002/hyp.70043.

[3] N. Tull *et al.*, "Bidirectional River-Floodplain Connectivity During Combined Pluvial-Fluvial Events," *Water Resources Research*, vol. 58, no. 3, p. e2021WR030492, 2022, doi: 10.1029/2021WR030492.

Creation of Oxbow Lakes Depends on Bifurcation Dynamics

Y. Jing[1],Y. Li[1], D. Shoemaker[2], M.M. Islam[2], J.A. Constantine[3], K.M. Konsoer[2], D.A. Edmonds[1]
[1]Department of Earth and Atmospheric Sciences, Indiana University, Bloomington, IN, United States
[2]Department of Geography and Anthropology, Louisiana State University, Baton Rouge, LA, United States
[3]Department of Geosciences, Williams College, Williamstown, MA, United States
Corresponding author: yejing@iu.edu

Keywords: Cutoff, Oxbow, Bifurcation, Meandering river, Plug formation.

1 Backgrounds

Oxbow lakes are characteristic and environmentally important features of meandering river floodplains. They function as critical habitat for many species and as effective sinks for fine sediment and associated contaminants [1]. However, it is unclear why some oxbow lakes are persistent whereas others get filled in quickly. Oxbow lakes are persistent when plug bars form at each entrance, stopping the flow of sediment into the channel [2]. The controls on plug occurrence and size are not clearly constrained.

We hypothesize that the formation of persistent oxbow lakes depends on the stability of the bifurcation. When the bifurcation is unstable, the plugs form rapidly, sealing off the oxbow and creating a persistent feature that slowly fills with sediment. Further, we test if unstable bifurcations are associated with neck cutoffs because the significant slope advantage created by the cutoff should lead to rapid plug formation.

2 Methodology

We built a one-dimensional numerical model to investigate how bifurcation stability contributes to oxbow lake persistence (Fig. 1). The model consists of a main channel and an abandoned channel. The model solves the Saint-Venant equations for flow, and the Exner and the Engelund and Hansen [3] sediment transport equation for bed-level change. The upstream boundary conditions were set to constant water and sediment discharge, and the downstream condition was set to a constant water elevation. The first and last cells of the abandoned channel were set to the same water elevations from adjacent main channel cells. Water and sediment flux from the main to the abandoned channel is determined by the nodal point relationship from Bolla Pittaluga [4].

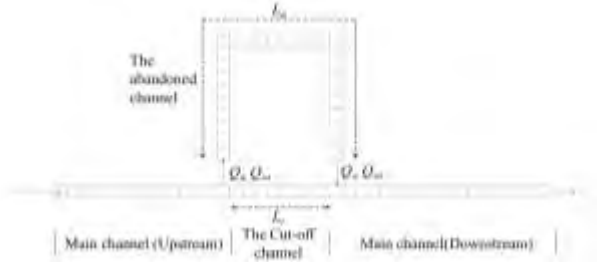

Figure 1: Model definition sketch. The abandoned channel is connected with the main channel at adjacent nodes.

3 Results and Conclusion

We analyzed plugging behavior as a function of the length of the cutoff channel (L_c) relative to the abandoned channel (L_a). Our key result is that as L_a/L_c increases, the relative plug length decreases (Fig. 2a). Neck cutoffs with large L_a/L_c have the shortest plug, which would lead to the biggest oxbow lake (Fig. 2c) compared to the oxbow lake induced by the chute cutoff run (Fig. 2b). These results are consistent with our hypothesis.

Our model shows that the length ratio determines the plug size and thus the surface area of the oxbow lake. For a given filling rate, lakes with larger surface area should persist longer. These results are consistent with field data that show oxbow lakes formed by chute cutoffs fill twice as fast as those formed by neck cutoffs. Our findings highlight the importance of bifurcation dynamics in the creation of persistent oxbow lakes.

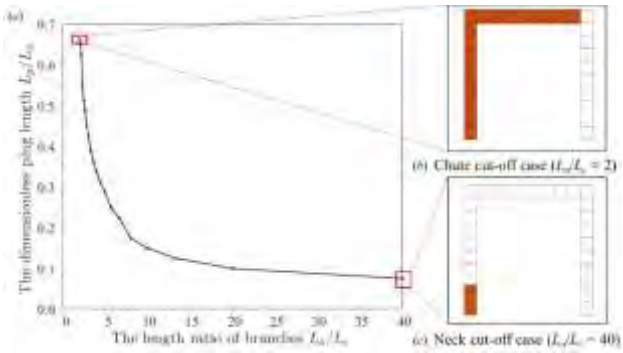

Figure 2: (a) Variation of the dimensionless plug length (L_p/L_a) versus the ratio of channel lengths (L_a/L_c). Visualized plugging processes in the chute and neck cutoffs are sketched in (b) and (c), respectively. Brown cell indicates plug areas and blank cell indicates the remaining water surface.

Acknowledgments

We would like to thank support from the NSF 2321056.

References

[1] Constantine, J. A., Dunne, T., Ahmed, J., Legleiter, C. & Lazarus, E. D. Sediment supply as a driver of river meandering and floodplain evolution in the Amazon Basin. *Nature Geoscience*, 7(899-903), 2014.

[2] Toonen WH, Kleinhans MG, Cohen KM. Sedimentary architecture of abandoned channel fills. *Earth surface processes and landforms*,37(4):459-72, 2012.

[3] Engelund F, Hansen E. A monograph on sediment transport in alluvial streams. Tech. Univ. of Denmark, Technisk Forlag, Copenhagen, Denmark. 1967.

[4] Bolla Pittaluga, M., Repetto, R. & Tubino, M. Channel bifurcation in braided rivers: Equilibrium configurations and stability. *Water Resources Research*, 39, 2003.

Using passive acoustics to map bedload over migrating bars

Jules Le Guern[1], Stéphane Rodrigues[2], Alex Andréault[2], Philippe Jugé[3]
[1]UMR CNRS CITERES, University of Tours, Tours, France
[2]Polytech Tours, University of Tours, Tours, France
[3]CETU ELMIS Ingénieries, University of Tours, Chinon, France
Corresponding author: leguern@univ-tours.fr

Keywords: bedload, bars, acoustics, sandy-gravel bed river

1 Introduction

The recent development of passive acoustic tool enables better quantification of bedload transport [1]. This tool shows strong potential for large lowland river systems [2] where determining solid fluxes by classical techniques remains difficult and inaccurate. Because this methodology is easy to deploy, bedload quantification is now possible at both large (watershed) and local (macroforms) scales. We conducted acoustic mapping measurements over an alluvial bar to monitor its evolution, relate the spatial distribution of bedload fluxes and understand sedimentary processes involved at different migration stages.

2 Materials & methods

We performed acoustic mapping measurements in the downstream reaches of the largest French river: the Loire (S=0.0002 $m.m^{-1}$; W=500 m; D_{50}=1 mm). Acoustic drifts were carried out by boat using a hydrophone paired to an acoustic recorder (Teledyne RESON TC4014 – RESEA320 RTSYS) over an area of approximately 600m long and 450m wide. During each drift, hydrophone position was recorded using a RTK DGPS (Leica GS25). About 30 drifts of 150-200m length, spaced approximately 40m apart, were needed to cover this area. In addition to acoustic measurements, we conducted bathymetric measurements using a single-beam altimeter (Tritech PA500) along longitudinal profiles. We conducted several acoustic mapping surveys between October 2024 and January 2025 for flows varying between 1270 and 1840 $m^3.s^{-1}$.

3 Results & discussion

Acoustic mappings results are in line with some classical traits of bar migration. For instance, we observe the impact of the bar front on bedload sediment transport immediately downstream. The flow separation associated with the lee effect is clearly identified as a low acoustic power zone traducing that almost no sediment is transported as bedload (Figure 1). This dynamic shelter zone increases in size when water depth over the bar decreases. The acoustic measurements also allow the accurate location of the reattachment point. During low flows, bedload sediment accumulation occurs in this zone when bars are exposed. For these water levels, bedload transport occurs in low-flow channels around emerged bars. These sediment accumulations, whose functioning was described in [2], are hardly mobilizable due to their position downstream of the bar front and are captured by the upstream bar during its migration. Flux intensity also appears higher on the bar when water depth is higher, while at lower water depth over the bar, the form roughness induced by the bar limits bedload fluxes on the stoss side of the bar (Figure 1).

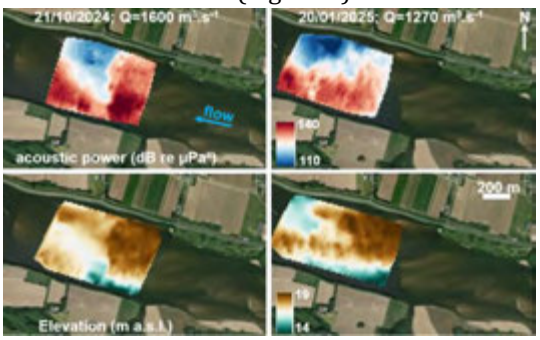

Figure 1: Acoustic mapping (up) and bathymetry map (down) over a migrating bar.

4 Conclusion

These results constitute a promising way to spatialize sediment transport rates over large macroforms using *in-situ* measurements. This is seldom performed in the literature because of technical issues and spatial scales involved. In the future, it would be interesting to compare these measurements to a 2D hydro-sedimentary model to compare flux spatialization and question calibration parameters and sediment transport equations implemented in such numerical models.

Acknowledgments

This work is part of SSESAR project (Sound of Sediments in Sandy Rivers) which is founded by the Region Centre Val-de-Loire, France.

References

[1] Le Guern, J., Rodrigues, S., Geay, T., Zanker, S., Hauet, A., Tassi, P., Claude, N., Jugé, P., Duperray, A. and Vervynck, L.: Relevance of acoustic methods to quantify bedload transport and bedform dynamics in a large sandy-gravel-bed river; Earth Surface Dynamics, 9, 423-444, 2021.

[2] Le Guern, J., Rodrigues, S., Tassi, P., Cordier, F., Wintenberger, C. L., and Jugé, P.: Migrating bars influence the formation and dynamics of their peers in large sandy-gravel bed river, Earth Surface Processes and Landforms, 1-14, 2023.

How to build a 3D probabilistic drainage network by hydraulic geometry

Li Zhang[1], Dnyanesh Borse[2], Arvind Singh[2], James Pizzuto[3], Gary Parker[4]
[1]North China Electric Power University, Beijing, China
[2]University of Central Florida, Orlando, USA
[3]University of Delaware Newark, DE, USA
[4]University of Illinois Urbana-Champaign, Urbana, USA
Corresponding author: 459178283@qq.com

Keywords: hydraulic geometry, drainage network, bankfull, drainage density

Abstract

There are numerous theories describing self-formed drainage networks, and also formulations describing the hydraulic geometry of single self-formed channels. Here we join these together for a complete description of the problem of fluvial drainage networks. Theories predicting 2D networks themselves include purely statistical and topological approaches like random walk models, observational and experimental studies, process-based models, and optimality based models. Natural drainage networks and most simulated drainage networks generated by probabilistic models showing self-similarity in the form of power law rules for characteristic parameters such as basin area A, stream length L and stream slope S as related to stream order. Formulations describing bankfull hydraulic geometry[1], on the other hand, characterize parameters such as bankfull depth H, width W and slope S as power law functions of bankfull water discharge Q and sediment transport rate Q_s for a single channel within certain ranges of bed grain size D_{grain}. We approximate the bankfull water discharge Q of a single channel as a linear function of its basin area A. Our joint modelling of a 2D probabilistic drainage network[2] and the hydraulic geometry of its channels, along with specified length and slope of unchannelized hillslopes allows us to construct a fully 3D field-scale drainage basin within which elevation, slope and channel characteristics are all computed. We can limit the degree of complexity of the network in terms of a threshold drainage density $D_{drainage}$ related to the inverse of hillslope length. We use this method to reverse-engineer 3D landscapes from 2D probabilistically generated river network. The application we report is for a purely alluvial system, but it is generalizable to systems where bedrock also plays a role.

Acknowledgments

We would like to thank Xudong Fu and Tiejian Li of Tsinghua University who help with the drainage network generation and extraction.

References

[1] G. Parker, R. Wilcock, C. Paola, W.E. Dietrich and J. Pitlick. Physical basis for quasi-universal relations describing bankfull hydraulic geometry of single-thread gravel bed rivers. *Journal of Geophysical Research*, 112:F04005, 2007.

[2] B. Dnyanesh and B. Basudev. A novel probabilistic model to explain drainage network evolution. *Advances in Water Resources*, 171:104342, 2022.

Improving and extending a unified model for bedload and suspended sediment transport modes

Kim-Jehanne Lupinski[1,2], Pablo Tassi[1,2], Florian Cordier[1], Magali Jodeau[1,2], Nicolas Claude[3], Alessandra Crosato[4]

[1]Electricity of France EDF R&D, National Laboratory for Hydraulic and Environment, Chatou, France
[2]Saint-Venant Laboratory for Hydraulics, Chatou, France
[3]Electricity of France CIH, La Motte Servolex, France
[4]IHE Delft Institute for Water Education, Delft, the Netherlands

e-mail corresponding author: kim-jehanne.lupinski@edf.fr

Keywords: *Total sediment transport; morphodynamics; numerical modelling; openTelemac; stage modes*

1 Introduction

Sediment transport in rivers encompasses both bedload and suspended load, traditionally modelled separately. This separation can compromise accuracy in scenarios where both transport modes interact. To overcome this limitation, we implemented a unified sediment transport model in the openTelemac system, enabling a more comprehensive representation of sediment transport processes across a wide range of transport stage modes T^*.

2 Unified modelling framework

The model relies on a 2D mass balance equation describing total sediment transport in the water column [2]:

$$\frac{\partial \overline{C_{m,t}}}{\partial t} + \nabla \cdot (\overline{C_{m,t}}\mathbf{u}) = \frac{\dot{e_m} - \dot{d_m}}{h} \tag{1}$$

with $\overline{C_{m,t}}$ the depth-averaged total sediment concentration [kg·m^{-3}], $\mathbf{u}$ the velocity vector [m·s^{-1}], h the water depth [m]. The erosion rate $\dot{e_m} = \frac{\pi}{6}\frac{c_e}{w_s}(\tau - \tau_c)$ and deposition rate $\dot{d_m} = \frac{\overline{C_{m,t}} h \mathbf{u}}{h_s \overline{v_s}} w_s$ represent the sediment fluxes at the bed interface [kg·m^{-2}·s^{-1}], w_s the sediment settling velocity [m·s^{-1}], $c_e = 37.64$ an empirical coefficient, τ and τ_c the total and the critical bed shear stresses [Pa]. The characteristic transport height h_s [m] and the average sediment velocity $\overline{v_s}$ [m·s^{-1}] unify the bedload and suspended transport of sediment particles, ensuring a continuous transition between both transport modes. This continuous transition is further defined by h_s, which is a function of the saltation height h_{slt}. The model has been extended to include morphodynamics processes:

$$(1-\lambda)\rho_s \frac{\partial z_b}{\partial t} = \dot{d_m} - \dot{e_m} \tag{2}$$

with z_b the bed elevation [m], $\lambda \approx 0.4$ the bed porosity and $\rho_s = 2650$ kg·m^{-3} the sediment density.

3 Results

The model was validated using 88 experiments [1] in a 45.7m×2.44m flume with uniform sands (0.19-0.93mm) under equilibrium conditions. Hydrodynamic results showed excellent agreement with the measured water depths and velocities. Sediment transport variables (w_s, $\dot{e_m}$, h_s, $\overline{C_{m,t}}$) matched well the theoretical predictions. Morphodynamic validation was performed using one of the 88 experimental cases, characterized by an equilibrium slope of 0.339%. The initial bed profile was deliberately perturbed with three segments of varying slopes to assess the model's ability to predict the bed evolution. Over time, the bed adjusted dynamically, progressively converging toward the expected equilibrium profile (Fig. 1, top). The results confirm that the implemented morphodynamic framework correctly simulates morphodynamic adjustments leading to equilibrium conditions. However, differences between simulated and measured sediment concentrations were observed, motivating a refinement of the saltation height h_{slt} using supervised polynomial regression. The original relation $h_{slt} = 0.6d + 0.025dT^*$ with $T^* = \tau/\tau_c - 1$ and d the grain diameter [m], was replaced by a 2nd-degree polynomial:

$$\begin{aligned} h_{slt} = {} & c_0 + c_1\overline{d} + c_2\overline{\tau} + c_3\overline{T^*} + c_4(\overline{d})^2 + c_5(\overline{T^*})^2 \\ & + c_6(\overline{\tau})^2 + c_7(\overline{d}\cdot\overline{\tau}) + c_8(\overline{d}\cdot\overline{T^*}) + c_9(\overline{\tau}\cdot\overline{T^*}) \end{aligned} \tag{3}$$

$\overline{X} = (X - \mu_X)/\sigma_X$ with (μ_X, σ_X) standardization parameters. This revision reduced the Mean Absolute Percentage Error (MAPE) from 208% to 184%, improving the precision of sediment concentrations (Fig. 1, bottom).

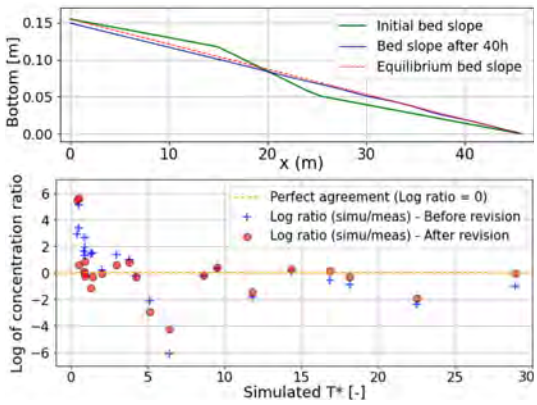

Figure 1: Top: Bed evolution from initial to equilibrium states. Bottom: Concentration ratio (simulated/measured) vs. T^* before and after revision of h_{slt} (only 26 results are shown here).

4 Conclusion

The unified model accurately reproduces hydrodynamics, sediment transport, and bed evolution. Future work will focus on morphodynamic processes involving both bedload and suspended sediment transport, with emphasis on bar formation under various transport stage modes.

References

[1] P. Guy, D. B. Simons, and E. V. Richardson. *Summary of alluvial channel data from flume experiments, 1956-61.* US GPO, 1966.

[2] M. Le Minor, P. Davy, J. Howarth, and D. Lague. Multi grain-size total sediment load model based on the disequilibrium length. *JGR: ES*, 127(11), 2022.

Large scale assessment of the clogging dynamics in gravel-bed river : experimental and numerical approaches.

Dorian Hernandez[1], Benoît Camenen[1], Adrien Bonnefoy[1]

[1]INRAE RiverLy, Lyon, France

e-mail corresponding author: dorian.hernandez@inrae.fr

Keywords: *field experiment; 1D modelling; clogging; suspended sediment; deposition*

1 Introduction

Clogging of riverbeds is an important issue for benthic species, fish habitat and river-groundwater exchanges. Partly caused by the deposition of fine sediments on the surface of the riverbed and their infiltration into the substrate, clogging assessment and evolution at a large-scale still remain challenging [1]. To better understand riverbed clogging dynamics, a potential solution would be to combine experimental clogging tests with an hydro-sedimentary numerical simulation. In particular, numerical modelling could help to locate zones where deposits can easily form. The present work focuses on an experimental and numerical study of a specific reach of the River Rhône upstream of Lyon, France, where different degrees of clogging are observed.

2 Material and methods

Two experimental clogging tests were deployed along a reach of the River Rhône (Figure 1a): an infiltration test, which allows to measure the subsurface hydraulic conductivity and a pumping test, which allows to measure the silt-clay (<100 μm) and sand (>100 μm) interstitial concentrations [1]. In parallel, a 1D hydro-sedimentary numerical model was built using the Mage-AdisTS solver [2] in order to identify areas of fine sediment deposition and mobilization. Five classes of sediments with a diameter d varying between 35 and 560 μm were considered. Based on Deng et al. [1], the riverbed coarse grain size is assumed to equal $d_{84,RK<1} = 5$ cm for the first river kilometer (RK), and $d_{84,RK>1} = 2$ cm for the next RK. A first test was made assuming a constant concentration of 60 mg/l at the upstream boundary condition and a flow discharge varying between 25 and 600 m^3/s. For this specific reach, the downstream condition is mainly controlled by the flow discharge of the Jonage canal imposing a nearly constant water level.

3 Results

Figure 1b presents the average experimental subsurface hydraulic conductivity K along the studied reach together with the section-averaged hydraulic velocity V and the thickness of the deposit E obtained after a 24 hours simulation with $Q = 25$ m^3/s and $d = 70$ μm. These first results highlight an unclogged area upstream, with high hydraulic conductivity values, followed by a heavily clogged area for $1.20 < RK < 2.60$. The simulation shows a decrease of the velocity and a general sediment deposition, which is well correlated to the permeability measurements.

The dynamic response of the model is currently studied to better understand the hydro-sedimentary dynamics on the site including deposition and erosion phases depending on the sediment grain size and flow discharge.

(a)

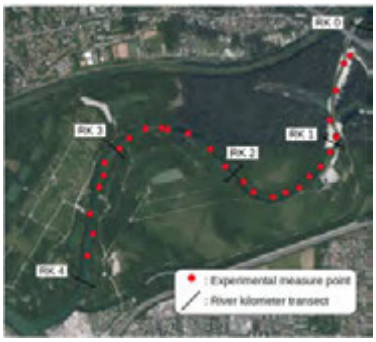

(b)

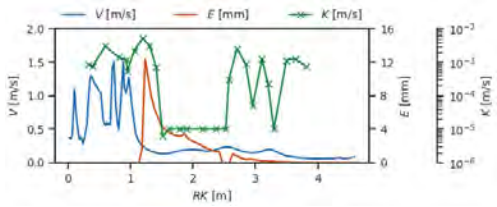

Figure 1: Location of the experimental tests along the studied reach on the River Rhône (a) and comparison between experimental and numerical results (b).

4 Conclusion

An experimental and numerical combined approach is presented here in order to understand riverbed clogging and its dynamics. A good correlation between experimental clogging test and hydraulic behaviour is observed. Also, the deposition and erosion process are well predicted and consistent with the experimental results. This study highlights the interest of 1D numerical modelling in understanding the large-scale hydro-sedimentary dynamics of a river where a heterogeneous clogging is observed.

References

[1] J. Deng, B. Camenen, D. Hernandez, J. Liégeois, and A. Bonnefoy. Methodological evaluation of riverbed clogging - insight from field measurements. *River Research and Applications*, (in revision).

[2] L. Guertault, B. Camenen, C. Peteuil, A. Paquier, and J.-B. Faure. One-Dimensional Modeling of Suspended Sediment Dynamics in Dam Reservoirs. *Journal of Hydraulic Engineering*, 142(10): 04016033, 2016.

Effect of Suspended Sediment on Turbulent Flow Diffusion

LOC-RCEM2025[1], Bateman, A.[2], Sosa, R[2].
Grupo de Investigación en Transporte de Sedimentos GITS-UPC[2]. Departamento de Ingeniería Civil y Ambiental.
[1]Universitat Politècnica de Catalunya, Barcelona, Spain
allen.bateman@upc.edu, raul.sosa@upc.edu

Keywords: sediment transport, turbulence, flow roughness, Karman constant

1 Introduction

After analysing numerous velocity profiles and the associated roughness coefficient in large rivers such as the Magdalena River, it has been observed that the only way to adjust the measured velocities, depths, and energy slopes is by decreasing the Von Karman constant. From this observation, research begins on the effect of suspended sediment on turbulence.

2 State of the Art

Theoretically, an open-channel flow in normal regime has a logarithmic velocity distribution as a function of u_*, K_s and k. The Von Karman constant is considered a universal invariant with a value of $k = 0.41$, while u_* and K_s are associated with the power of flow and bed roughness.

In (Bateman & Sosa, 2019), numerous velocity profiles were measured in the Magdalena River, along with the water surface slope over 40 km. It was observed that the only consistent way to match the measured driving slopes with those calculated from velocity profiles was by modifying k, obtaining a constant of approximately 0.3.

Since 1940, various authors have studied this phenomenon. There seems to be consensus that the Von Karman constant k varies as a function of suspended sediment transport, but existing formulations are highly empirical, and the reason why sediment alters turbulence remains unknown. Guo and Julien (2001) demonstrated through kinetic energy balance that suspended sediment reduces vertical turbulent diffusivity, i.e., a decrease in the Von Karman constant k. However, this reduction is only noticeable at very high sediment concentrations.

3 Methodology

This research aims to study the effect of sediment transport on turbulence, and therefore on the Von Karman constant *k*, near the bed where sediment concentration is highest. The sediment concentration, C, gradient produces the following variation in momentum exchange in the vertical plane:

$$\tau = l_m{}^2 \cdot \frac{du}{dz} \cdot \frac{d}{dz}(\rho u) = l_m{}^2 \cdot \left|\frac{du}{dz}\right| \cdot \left(\rho \cdot \frac{du}{dz} + \frac{\mathbf{d\rho}}{\mathbf{dz}}\mathbf{u}\right)$$

Near the bed, the value of $\frac{d\rho}{dz}u$ can be very large and significantly affect momentum exchange. With mixing length lm, velocity u, density ρ, z axis.

For this study, data collected by Coleman and Vanoni were analysed, and several experimental tests performed in the Morphodynamic LABORATORY flume at AGROPOLIS, UPC. This channel features a loose sand bed with sediment recirculation. Measurements were performed using PTV, capturing an image every 2 ms, allowing analysis of turbulence scales such as the Kolmogorov scale. A relationship between the Kolmogorov scale, grain size, relaxation time (Stokes number, St), and concentration enables determining how, within a range of scales, the Von Karman constant decreases.

$$k = k_0\left(1 - a \cdot e^{-b\left(\frac{\eta}{d_p}\right)^n - \gamma \cdot C \cdot \left(\frac{\lambda}{\eta}\right)} \cdot e^{-\alpha \cdot St}\right)$$

Relaxation time related to the energy transfer capacity from the appropriate scale to the particle and vice versa. If the minimum energy scale, η is much larger than the particle size, *dp*, the particle becomes embedded in the fluid, behaving as part of it. Conversely, if the particle is much larger than the Taylor scales, λ, vortex energy does not alter its dynamics. Only particles with a size similar to the energy transfer capacity between fluid and particle influence each other. This results in a fundamental change in vortex size around the particle and, consequently, in the value Von Karman constant k.

3 Conclusions

The data measured by Coleman and Vanoni show a clear relationship between the Von Karman constant and sediment concentration near the bed.

Furthermore, the PTV measurement analysis shows turbulence attenuation near the bed of the flow.

References

[1] Bateman, A., & Sosa, R. (2019). Flow resistance coefficient measurment in big rivers. *RCEM 2019*.

[2] Coleman, N. L. (1986). Effects of Suspended Sediment on the Open-Channel Velocity Distribution. *Water Resources Research*.

[3] Guo, J., & Julien, P. Y. (2001). Turbulent velocity profiles in sediment-laden flows. *Journal of Hydraulic Research*.

[4] Vanoni, V. A. (1940). *Experiments on the transportation of suspended sediment by water* (p. 80). California Institute of Technology.

Monitoring of megacusp development events from satellite-derived shorelines: a case study of two Mediterranean microtidal beaches

Eduard Angelats[1], Riccardo Angelini[2], Guido Luzi[1], Andrea Masiero[3], Gonzalo Simarro[4], Francesca Ribas[5]
[1]Geomatics Research Unit, Centre Tecnologic de Telecomunicacions de Catalunya (CTTC/CERCA), Spain
[2]Department of Civil and Environmental Engineering, University of Florence, Italy
[3]Interdepartmental Research Center of Geomatics (CIRGEO), University of Padova, Italy
[4]Department of Marine Geosciences, Institut de Ciencies del Mar, Spain
[5]Physics Department, Universitat Politecnica de Catalunya, Spain
Corresponding author: eduard.angelats@cttc.cat

Keywords: coastal morphodynamics, megacusps, shoreline, multispectral imagery

1 Introduction

Coastal zones, especially sandy beaches, are dynamic and influenced by both natural and human factors. Shoreline undulations, such as megacusps, are periodic shoreline perturbations that can affect beach width and usability. Traditionally, video monitoring systems were used to study these phenomena [1], but they offer limited spatial coverage. Instead, multispectral satellite imagery from Sentinel-2 (S2) and PlanetScope (PLN) was explored to monitor megacusp formation and dynamics [2]. This work analyses two megacusp events on Mediterranean microtidal beaches, incorporating wave conditions, and computes beach width reduction to assess the impact on beach usability.

2 Materials and Methods

The two megacusp events on Mediterranean microtidal beaches were located at southern Llobregat Delta (SLD) in Spain and Feniglia (FNG) beach in Italy. The FNG event (Feb–Jun 2022) was tracked using 19 S2 and 16 PLN images, while the SLD event (Mar–Oct 2023) was monitored using 20 S2 and 20 PLN images from two adjacent segments. Shorelines were extracted following the methodology in [2], and wave conditions were obtained from the Barcelona Buoy II (SLD) and Giannutri buoy (FNG). Shoreline oscillations were characterized using sinuosity (s) and standard deviation (σ_s). Then, an algorithm detected peaks and valleys, applying varying amplitude thresholds (2–5 m) to identify significant megacusp features. Amplitude (a) was defined as half the cross-shore distance between horns and bays, while wavelength (λ) represented the alongshore distance between successive horns, with their mean values calculated. Effective beach width was estimated too, every 20 m, using orthogonal transects, measuring width reduction throughout the event.

3 Results and conclusions

Megacusps (8–10 m amplitude, 150–200 m wavelength) persisted throughout the study in SLD. In late May 2023, a two-day event of 1 m SEE-directed waves increased amplitude to 15 m without changing wavelength. Amplitude then decreased with smaller, variable waves. By late June, a similar wave event again raised amplitude to 15 m, this time increasing wavelength to 400 m. The results of 2022 FNG event reveals that megacusps mainly formed in the central beach area (Figure 1). Initially, small amplitude features remained stable ($1.010 < s < 1.020$, $\sigma_s \approx 4–5$ m, $a \approx 10–15$ m, $\lambda \approx 150–250$ m). By late March, minor storms (H_s up to 2 m, S direction) increased amplitude to 20 m with a more regular wavelength (160–220 m). In early April, stronger SW storms (H_s 3–4 m) reduced amplitude to 10 m while maintaining wavelength. This pattern persisted, with a gradual amplitude decline until June. Our findings show that multispectral satellite imagery provides a viable solution for monitoring shoreline megacusp undulations, tracking their evolution during events, and paving the way for an enhanced understanding.

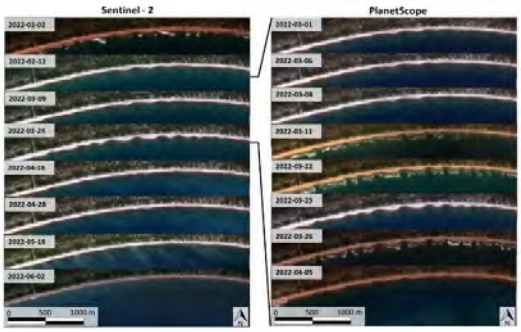

Figure 1: Comparison of the optical images of the FNG beach acquired at different dates through S2 and PLN showing the temporal evolution of the shoreline.

References

[1] R.L. de Swart, R.L., F. Ribas, F, D., Calvete, G., Simarro. J. Guillen. Observations of megacusp dynamics and their coupling with crescentic bars at an open, fetch-limited beach. Earth Surf. Process. Landf. 2022, 47, 3180‑3198.

[2] R. Angelini, E. Angelats, G. Luzi, A. Masiero, g., Simarro, G., F. Ribas. Development of Methods for Satellite Shoreline Detection and Monitoring of Megacusp Undulations. Remote Sens. 2024, 16, 4553.

Predicting Short-term Satellite-Derived Shoreline Positions around New Zealand

Amirmahdi Gohari, Giovanni Coco, Karin R.Bryan
School of Environment, Faculty of Science, University of Auckland, Auckland, 1010, New Zealand
Corresponding author: amgh628@aucklanduni.ac.nz

Keywords: Shoreline Prediction, Numerical Models, Machine Learning, Satellite Data, Morphodynamics

1 Introduction

Accurate predictions of shoreline change are crucial for effective coastal management, and for understanding the impacts of climate change on coastal areas. This study investigates the short-term (up to 3 years) evolution of shorelines around New Zealand using satellite-derived observations and two modelling approaches: a data-driven model "Shoreline Prediction at Different Time-Scales" (SPADS) **[1]**, and an AI-based model XGBoost. The performance of each model was assessed using a loss function that combines correlation coefficient, normalized root mean squared error and normalized standard deviation.

2 Data and methods

Models were trained using shoreline data derived from satellite (www.coastalhub.science/data) for the period 1999 to 2025, with the last three years selected for assessment. To account for limitations in the satellite data and to handle outliers, a smoothing algorithm was applied to the raw shoreline positions extracted from satellite. Wave parameters, including wave height, period, and direction, were used as key inputs for the models. An existing high-resolution partitioned wave hindcast of New Zealand waters, incorporating a SWAN model, was used for input between 1999 and 2019 **[2]**, which was extended to include the last five years using the 2025 WAVERYS global wave analysis **[3]**. The study was conducted at two stations: on the west coast (Muriwai Beach) and east coast (Otama Beach) of New Zealand. Model performance was evaluated based on its ability to predict shoreline changes accurately. A comparison of the wave parameter statistics for the two beaches is presented in Table 1.

Table 1. Comparison of wave parameters of the two beaches

	Hs (m)	Tp (s)	Dir (°)
Otama			
Minimum	0.05	1.94	2.21
Maximum	4.29	19.69	357.29
Mean	0.9	7.44	150.47
Muriwai			
Minimum	0.47	4.19	49.53
Maximum	6.8	21.85	347.5
Mean	2.33	12.76	235.75

3 Preliminary Results

The results highlight the strengths and limitations of the different numerical approaches. At Otama Beach on the east coast, both XGBoost and SPADS were capable of reproducing the overall variability. However, SPADS struggled with extremes in accretion and erosion, while XGBoost performed well in these areas. A similar pattern was observed at Muriwai Beach on the west coast, where XGBoost demonstrated better performance in handling extreme conditions compared to SPADS (results are shown in Figure 1). This superior performance of XGBoost may be attributed to its advanced algorithmic structure, which better captures complex patterns in the data.

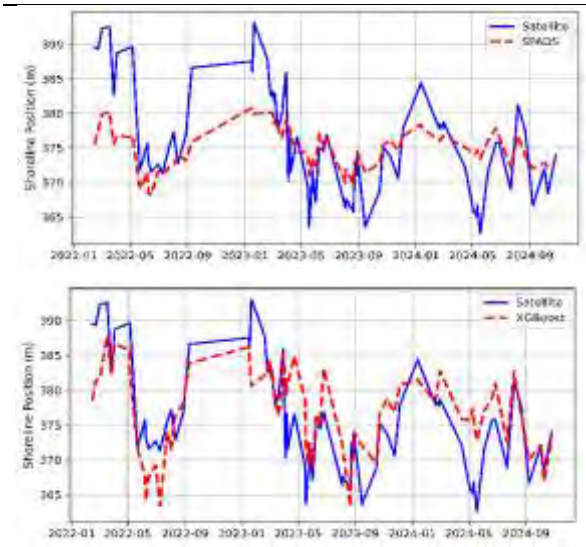

Figure 1. Model performance comparison at Muriwai Beach using SPADS (top panel) and XGBoost (bottom panel).

Acknowledgements

We gratefully acknowledge funding from "Our Changing Coast" (MBIE-6001001).

References

[1] Montaño, J., Coco, G., Cagigal, L., Mendez, F., Rueda, A., Bryan, K.R. and Harley, M.D., 2021. A multiscale approach to shoreline prediction. *Geophysical Research Letters*, *48*(1), p.e2020GL090587.

[2] J. Albuquerque, J. A. A. Antolínez, R. M. Gorman, F. J. Méndez, and G. Coco, "Seas and swells throughout New Zealand: A new partitioned hindcast," *Ocean Modelling*, vol. 168, p. 101897, Dec. 2021, doi: 10.1016/j.ocemod.2021.101897.

[3] S. Law-Chune, L. Aouf, A. Dalphinet, B. Levier, Y. Drillet, and M. Drevillon, "WAVERYS: a CMEMS global wave reanalysis during the altimetry period," *Ocean Dynamics*, vol. 71, no. 3, pp. 357–378, Mar. 2021, doi: 10.1007/s10236-020-01433-w.

Non-Stationary Calibration of Equilibrium Shoreline Evolution Models via Cartesian Genetic Programming

Lucas de Freitas[1], Camilo Jaramillo[1], Mauricio González[1]
[1]IHCantabria – Instituto de Hidráulica Ambiental de la Universidad de Cantabria, Santander, Spain
Corresponding author: lucas.defreitas@unican.es

Keywords: Shoreline modelling, non-stationarity calibration, long-term morphodynamics.

1 Introduction

Coastal evolution models are essential for understanding and predicting shoreline changes under varying wave conditions. In particular, equilibrium-based shoreline evolutions models (EBSEMs) have gained prominence because they capture large-scale morphodynamic adjustments with relatively simple formulations. These models assume that shorelines tend toward a dynamic balance with prevailing wave conditions, with deviations from equilibrium driving accretion or erosion. Although widely used for medium- to long-term evolution and coastal management, their reliability critically depends on accurately calibrating free parameters.

Traditional calibration methods typically assume stationarity, overlooking the inherent temporal variability in sediment supply, storm frequency, and human influences. By contrast, non-stationary calibration techniques allow model parameters to evolve over time in response to changing environmental conditions. This study explores a non-stationary parameter estimation framework for equilibrium shoreline models using Cartesian Genetic Programming (CGP).

2 Methods

The proposed calibration method treats the estimation of EBSEMs' parameters as a regression problem using the Y09 [1] and ShoreFor [2] models. The goal is to evolve mathematical expressions that generate time series for each free parameter. In this approach, non-stationary parameters are encoded as functions of dynamic variables—such as Day of Year, wave energy, wave power, and Dean's parameter.

A CGP algorithm is implemented using the DEAP framework in Python. Each individual in the population comprises four expression trees (one per parameter), built from custom primitive sets that include basic arithmetic, protected functions (e.g., safe division, logarithm, exponential), and bounded functions that use logistic transformations to ensure outputs remain within physically meaningful limits.

The fitness evaluation consists in three steps. First, the expression trees are compiled to obtain time series for the four parameters. After that, the shoreline evolution simulation with these time series is performed. Finally, a performance metric (e.g., a skill score) that quantifies the discrepancy between simulated and observed shoreline positions is calculated.

This methodology was applied to two study sites—Tairua Beach in New Zealand and Porsmillin Beach in France—to compare the evolved expressions and assess site-specific characteristics.

3 Results

The non-stationary calibration framework yielded distinct outcomes for different model parameters. The analysis indicates that the equilibrium parameters of the both models are best represented by near-constant expressions, suggesting that a stationary approach may suffice for these terms. In contrast, the erosion and accretion parameters benefited from dynamic formulations that incorporate relationships with wave power and Dean's parameter.

Overall, the skill scores improved compared to traditional stationary calibrations, demonstrating enhanced model performance in replicating observed shoreline evolution.

4 Conclusions

Integrating non-stationary calibration via CGP to EBSEMs by evolving parameter expressions that adapt to dynamic environmental conditions, improved the simulations for both study cases. While some parameters remain nearly constant, others—particularly those governing erosion and accretion—require dynamic formulations to capture system complexity. These findings support more robust coastal evolution modeling and offer valuable insights for coastal management and climate impact assessments.

Acknowledgments

The authors acknowledge the support of the ThinkInAzul programme, supported by MCIN/Ministerio de Ciencia e Innovación with funding from the European Union NextGeneration EU (PRTR-C17.I1) and by Comunidad de Cantabria.

References

[1] M. L. Yates, R. T. Guza, W. C. O'Reilly. Equilibrium shoreline response: Observations and modeling. *Journal of Geophysical Research*, 114, C09014, 2009.

[2] M. A. Davidson, K. D. Splinter, I. L. Turner. A simple equilibrium model for predicting shoreline change. *Coastal Engineering*, 73, 191-202, 2013.

Shoreline Evolution in a Natural Semi-Embayed Mediterranean Beach

Francisco Fabián Criado-Sudau[1], Elena Sánchez-García[1], Jesús Soriano-González[1], León Gonzalez[1],Francesc Bernat Bieri[1] , Àngels Fernàndez-Mora[1]

[1] Balearic Islands Coastal Observing and Forecasting System, Mallorca, Spain

e-mail corresponding author: ffcriado@socib.es

Keywords: *Shoreline Evolution, Beach-Lagoon Interactions, Microtidal Environment*

1 Introduction

Sandy beaches are critical for coastal protection, acting as the first line of defense against wave energy. These environments are particularly vulnerable to climate change effects, such as sea level rise and storminess. Coastal lagoons, situated behind beaches, play a critical role in sediment transport and storage, influencing beach morphodynamics. Understanding the complex interactions between beaches, waves and coastal lagoons, is essential for effective coastal management and adaptation strategies. However, the integrated monitoring of these areas is challenging, requiring high human and economic resources. Therefore mid to long-term high-frequency morpho-hydrodynamic datasets remain scarce in the literature, particularly for coastal systems with lagoons. This study focuses on the shoreline evolution of a microtidal semi-embayed beach, investigating the impacts of waves and lagoon opening.

2 Study Site

Son Bou beach (SNB), situated on the island of Menorca in the Balearic Islands archipelago (Western Mediterranean Sea), is a 2.4 km long semi-enclosed beach characterised by well-sorted medium to fine biogenic carbonate sand. Classified as a natural beach by [1], SNB is backed by a well-preserved dune system and a coastal lagoon, whose mouth typically opens for several weeks annually, affecting beach morphodynamics.

3 Data and Methods

The in situ data-set used in this study is part of the Modular Beach Integral Monitoring Systems (MOBIMS). Since 2011, the Balearic Islands Coastal Observing and Forecasting System (SOCIB) has been implementing this systme to monitoring SNB. MOBIMS aims to bridge the gap in high-resolution and continuous beach monitoring by integrating data from hybrid field surveys and remote sensing systems. The system includes a low-cost, open-source video monitoring system (SIRENA). This system provides time-exposure images (TIMEX) and snapshots, enabling the generation of plan views for shoreline extraction and tracking the lagoon's opening and closing dates. Additionally, Acoustic Wave and Current Profilers (AWAC) are used to collect hydrodynamic data. Biannual high-resolution bathymetric and topographic surveys offer further morphodynamic information.

4 Preliminary Results

Preliminary results of shoreline analysis at Son Bou beach (2011-2024), utilizing 290 shorelines extracted from SIRENA indicate an overall negative trend of -0.3 m/yr. However, this trend is not linear, exhibiting shorter periods of both shoreline advance and retreat. The most pronounced short-term fluctuation occurred between November 2011 and May 2012, with shoreline shifts exceeding 20 m. This substantial change is particularly notable given the microtidal nature of Son Bou and is likely influenced by the annual sea-level cycle, wave dynamics, and rainfall conditions. These factors are closely linked to the opening of the coastal lagoon, as illustrated in Figure 1. Preliminary analysis suggests that the lagoon's opening process plays a key role in controlling beach morphodynamics.

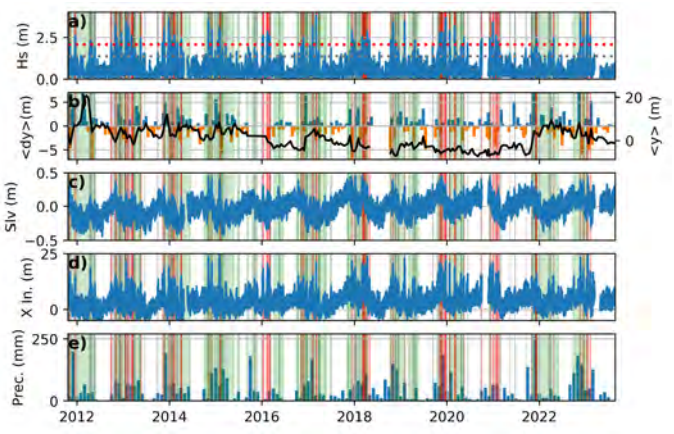

Figure 1: Time series of environmental parameters and shoreline response at Son Bou beach from 22 October 2011 to 23 August 2023. (a) Significant wave height (H_s), with 95th and 99th percentiles indicated. (b) Shoreline change (dy), with positive values indicating accretion (blue bars) and negative values indicating erosion (orange bars), with the black line representing the mean shoreline position. (c) Sea level (η). (d) Inundation distance (X_{In}). (e) Monthly precipitation accumulation. Green shaded areas denote coastal lagoon opening, grey vertical lines mark storm events, and red vertical lines indicate extreme events.

References

[1] Andrew Cooper. "Response of Natural, Modified and Artificial Sandy Beaches to Sea-Level Rise". In: *Geographical Research Letters* 48 (2022).

Coupling littoral and fluvial sediment transport for shoreline morphodynamics modelling: a sensitivity assessment

Marta Crivellaro 1, Francesco De Leo 2, Bestar Cekrezi 1 , Flamur Bajrami 1, Giovanni Besio 2 , Guido Zolezzi 1

1 Department of Civil, Environmental and Mechanical Engineering, DICAM, University of Trento, Italy.
2 Department of Civil, Chemical and Environmental Engineering, DICCA, University of Genova, Italy

Corresponding author: marta.crivellaro@unitn.it

Keywords: one-line model, shoreline evolution, sediment transport, river sediment supply, sensitivity assessment

1 Introduction

Much research attempts to reproduce coastal morphodynamics through models with increasing complexity and multiple parameters. However, most of these models ultimately rely on simplified formulas, which choice can yield huge uncertainties that are ultimately magnified across the modeling chain. For example, using different long-shore transport formulas can induce deviations to a factor up to 10 in the resulting sediment budget [1]. This becomes particularly critical when multiple inputs need to be accounted for, as in the case of waves and river sediments supply, without any knowledge regarding which parameters are the most important to be carefully calibrated. A model coupling littoral transport, river flow and sediment transport rates to the sea, and ensemble techniques is developed to reproduce the shoreline dynamics. The model is tested on a simplified configuration with input data coming from the case of the Lalzit Bay in Albania, which has experienced massive coastal erosion throughout the past ≈30 years [2,3]. A sensitivity analysis is then applied to understand which are the most relevant model parameters to be carefully calibrated.

2 Materials and Methods

3.1 The model

The modeled configuration consists of a straight shoreline with a river mouth that contributes sediments. The numerical model relies on the one-line theory, which assumes that the coastline sections can only rigidly move back and forth (i.e., erode or accrete) with respect to their initial condition while maintaining an equilibrium shape. The displacement of a section depends on the net amount of sand entering or leaving a control volume, defined along the active profile of the beach. The rate of change of each section can be expressed as:

$$\frac{\partial y}{\partial t} = -\frac{1}{D_c+B_h}\left(\frac{\partial Q}{\partial x} + q\right) \qquad (1)$$

Where y and x are the cross-shore and long-shore position of the control point, respectively; D_c is the depth of closure, B_h the berm height, while Q indicates the wave-induced littoral transport and q refers to external sediment inputs (such as those associated with rivers). Q can be parametrized accounting for the grain size distribution of the beach and breaking waves parameters [4]; q can be calibrated by taking advantage of topographic surveys and estimates of river sediment transport rates using classical formulae that are applied using reach-averaged parameters and the grain size distribution of riverine sediments [5,6].

3.2 The Sensitivity Assessment

Integrating historical data on the river flow time series, channel geometry as measured in, fieldwork with wave hindcast downscaling, an average representative year of the shoreline dynamic is defined. For this representative year,a variance-based sensitivity analysis is applied to the model, expressed as follow:

$$\frac{\partial y}{\partial t} = f(D_c, B_h, K, H_{sb}, T_p, \theta_b, W, i_f, \varphi_r) \qquad (2)$$

Where K is the Kamphuis coefficient, H_{sb} is the significant wave height at breaking, T_p is the peak wave period, θ_b is the wave angle at breaking, and W, i_f, φ_r represent the river width, slope and grain size distribution, respectively.

3 Expected Results

This work investigates the sensitivity of the coupled one-line model of littoral transport with riverine sediment transport rates for a simplified shoreline evolution model. The results obtained from the sensitivity analysis allow the proper definition and estimation of the approach's most important parameters to be focused on, enabling the model to be applied to real-world case studies with an enhanced understanding of its sensitivity.

References

[1] Casas-Prat, M., McInnes, K. L., Hemer, M. A., & Sierra, J. P. (2016). *Future wave-driven coastal sediment transport along the Catalan coast (NW Mediterranean).* Regional Environmental Change, 16, 1739-1750, 2016.

[2] Cekrezi, B. *Hydro-morphology, channel change and sediment transport dynamics of major Albanian Rivers,* Ph.D. dissertation, University of Trento, 2023.

[3] De Leo, F., Besio, G., Zolezzi, G., Bezzi, M., Floqi, T., & Lami, I. *Coastal erosion triggered by political and socio-economical abrupt changes: The case of Lalzit Bay, Albania.* Coastal Engineering Proceedings, (35), 13-13, 2017.

[4] Kamphuis, J. W. *Alongshore sediment transport rate.* Journal of Waterway, Port, Coastal, and Ocean Engineering, 117(6), 624-640, 1991.

[5] Van Rijn, L.C., *Sediment transport, part II: suspended load transport.* J. Hydraulic Division 110(11), 1613—1641,1984.

[6] Wilcock, P. R., & Crowe, J. C. (2003). Surface-based transport model for mixed-size sediment. *Journal of hydraulic engineering*, *129*(2), 120-128.

Exploring Future Shoreline and Nearshore Evolution Under Sea-Level Rise Projections: Application of the LX-ST Model to Lacanau

Mohammad Traboulsi[1,2],Déborah Idier[1], Bruno Castelle [2], Arthur Robinet[3], Vincent Marieu[2], Rémi Thieblemont[1], Alexandre Nicolae Lerma[3]

[1]BRGM, 3 Av. Claude Guillemin, Orléans, 45100, France
[2]Univ. Bordeaux, CNRS, Bordeaux INP, EPOC, UMR 5805, Allée Geoffroy Saint-Hilaire, Pessac, 33600, France
[3]BRGM Nouvelle Aquitaine, 24 av. Léonard de Vinci, Pessac, 33600, France

e-mail corresponding author: m.traboulsi@brgm.fr

Keywords: *shoreline change, shoreface translation, sea-level rise, nearshore morphology, climate projections*

1 Introduction

In the context of rising sea levels and increasing coastal vulnerability, understanding the long-term evolution of shorelines under future climate scenarios is critical for effective coastal management. While process-based models can provide detailed insights, their computational demands make them impractical for decadal-to-centennial scales. Instead, reduced-complexity models offer an efficient alternative by simulating dominant processes over large spatial and temporal scales [2]. This study applies LX-ST to explore future shoreline position and associated nearshore-beach-dune morphology at a wave-dominated partially urbanized sea front. Simulations are performed under IPCC sea-level rise projections through 2100, integrating local geomorphological features, and multiple climate scenarios.

2 LX-ST

LX-ST is a reduced-complexity numerical model developed to simulate shoreline and nearshore evolution over medium to long-term timescales. By integrating the one-line shoreline evolution model LX-Shore [2] with the shoreface profile translation tool ShoreTrans [1], LX-ST captures both shoreline and 3D nearshore morphology changes. The model accounts for processes such as sea-level rise (SLR), longshore sediment transport, and the presence of natural and artificial coastal features.

3 Study site

Lacanau-Océan, a seaside resort on the central sandy coast of Gironde, southwest France, has experienced chronic erosion over the last century, with rates reaching up to 1.5 m/year in recent decades. A 1.2-km seawall was built to protect the urbanized coastline; however, it may disrupt sediment transport dynamics under future sea-level rise scenarios, particularly by interfering with longshore drift if erosion persists. This makes Lacanau an ideal test case for assessing the impacts of sea-level rise and sediment dynamics under varying climate scenarios. LX-ST was applied on a 5-km section of the beach, incorporating local topobathymetry from LiDAR and bathymetric data, realistic wave conditions derived from ERA5 data (assuming no significant changes in future wave climate), and considerations of sediment bypassing to assess shoreline and nearshore evolution.

4 Results

Simulations predict a shoreline retreat ranging from O(10 m) to 0(100) m by 2100, depending on the considered IPCC scenario and SLR decile. The most severe erosion occurs downdrift of the seawall due to reduced sediment supply. In the second half of the century, the retreat of the beach-dune system contrasts with the relative stability of the shoreline position along the seawall sector, resulting in partial retention of longshore sediment transport. As a result, updrift erosion is smaller compared to downdrift where the dune can be fully eroded in the most extreme scenarios. The beach in front of the seawall experiences shoreface lowering.

5 Conclusion

This study illustrates the use of LX-ST in projecting long-term shoreline and nearshore evolution under varying climate scenarios, providing valuable insights into the future trajectories of vulnerable urbanized coasts. The findings underscore the combined influence of rising sea levels and artificial structures on coastal morphology.

Acknowledgements

This work was conducted within the framework of the ANR SHORMOSAT project (ANR-21-CE01-0015). OCNA for the LiDAR data.

References

[1] R. Jak McCarroll, Gerd Masselink, Nieves G. Valiente, Timothy Scott, Mark Wiggins, Josie-Alice Kirby, and Mark Davidson. A rules-based shoreface translation and sediment budgeting tool for estimating coastal change: Shoretrans. *Marine Geology*, 435:106466, May 2021. ISSN 0025-3227. doi: 10.1016/j.margeo.2021.106466.

[2] Arthur Robinet, Déborah Idier, Bruno Castelle, and Vincent Marieu. A reduced-complexity shoreline change model combining longshore and cross-shore processes: The lx-shore model. *Environmental Modelling & Software*, 109:1–16, November 2018. ISSN 1364-8152. doi: 10.1016/j.envsoft.2018.08.010.

Breach development during successive hurricanes and impacts on the inner lagoon hydrodynamics

Ella Bear[1], Maitane Olabarrieta[1], Nina Stark[1], Ping Wang[2], John Warner[3], Jon Moskaitis[4], James Doyle[4]

[1]University of Florida, Gainesville, FL, USA
[2]University of South Florida, Tampa, FL, USA
[3]US Geological Survey, Woods Hole, MA, USA
[4]U.S. Naval Research Laboratory, Monterey, CA, USA

e-mail corresponding author: ebear@ufl.edu

Keywords: *Breaching; hurricane; residence time; numerical modeling; COAWST*

1 Introduction

Barrier islands, with their beach and dune systems, protect coastlines from extreme water levels and wave impacts. Climate change has accelerated the increase in sea levels and increased the frequency of extreme storms [4]. As the elevation of the barrier islands decreases relative to the total water levels, they become more vulnerable to storm damage, consistent with Sallenger's storm impact regime [5].

On the west coast of Florida, Hurricanes Helene and Milton (2024) caused a breach in the dune system, creating a new connection between the ocean and the inner lagoon. These two major hurricanes hit Sarasota Bay in two weeks (Figure 1). Hurricane Helene, overtopped and eroded the barrier island, weakening the dune system. During Hurricane Milton, this coastal area transitioned to an inundation regime, drastically altering the coastal dynamics and opening a breach known as Midnight Pass.

The formation of Midnight Pass has potential implications, including changes in sediment transport dynamics, the barrier island's geomorphology, and the lagoon's hydrodynamics. This work's objective is to evaluate the ability of morphodynamic process-based models to simulate openings of breaches, using Midnight Pass as a case study. The breach occurred due to two consecutive storms, offering a valuable opportunity to analyze whether these models can accurately reproduce the breach formation and assess the breach's impact on the inner lagoon's hydrodynamics and residence time.

2 Methods

We integrate pre- and post-storm aerial imagery with numerical modeling to verify the fidelity of the COAWST modeling system [2, 3], driven by COAMPS-TC atmospheric forcing, to accurately reproduce the breaching observed in Sarasota Bay following Hurricanes Helene and Milton. After verifying the model, we utilize in situ measurements from Acoustic Doppler Current Profiler (ADCP) observations to further validate the velocity fields associated with the breach opening. These velocity comparisons allow for a more comprehensive understanding of the hydrodynamic response to breaching events. Additionally, we apply the particle tracking model ROMSPath [1] to analyze changes in the residence time of the inner lagoon before and after the breach. This analysis provides insights into how barrier island breaches influence water retention, circulation, and overall lagoonal flushing, which are critical factors for assessing the ecological and geomorphic stability of the system.

Figure 1: Left: Best-track of Helene and Milton (2024) from the National Hurricane Center and Right: aerial images from NOAA showing barrier island morphology before and after.

3 Results and Conclusions

Through the application of a morphodynamic process-based model, we have been able to reproduce the breach formation and replicate the changes in lagoon dynamics, confirming the model's capacity to capture the effects of such breaches. Furthermore, the residence time of the lagoon has been found to be reduced due to the breach.

Acknowledgments

This research is supported by the NOPP (N00014-21-1-2203). The authors acknowledge funding from NSF (grants 1939275 (NEER), 1826118 (GEER), 2130997 (NHERI RAPID), and 2501467 (Stark)). We acknowledge all NEER/GEER team members who collaborated on the data collection.

References

[1] Hunter et al. Romspath v1.0: offline particle tracking for the regional ocean modeling system. *Geoscientific Model Development*, 15(11), 2022.
[2] Warner et al. Development of a three-dimensional, regional, coupled wave, current, and sediment-transport model. *Computers Geosciences*, 34(10), 2008.
[3] Warner et al. Development of a coupled ocean–atmosphere–wave–sediment transport (coawst) modeling system. *Ocean Modelling*, 35 (3), 2010.
[4] IPCC. Climate change report 2023. 2023.
[5] Jr. Sallenger. Storm impact scale for barrier islands. *J. of Coastal Research*, 16(3), 2000.

The recent asymmetric morphological evolution of the Wadden Sea

Marvin Lorenz[1], Diego Pineda[2], Frank Kösters[1], Christian Winter[3], Robert Lepper[1]

[1]Federal Waterways Engineering and Research Institute (BAW), Hamburg, Germany
[2]smile consult GmbH, Hanover, Germany
[3]Christian-Albrecht-Universität zu Kiel, Kiel, Germany

e-mail corresponding author: marvin.lorenz@baw.de

Keywords: *accretion; erosion; topography; sea-level rise; Wadden Sea*

1 Introduction

Tidal flats are natural components for coastal protection and provide a unique habitat for flora and fauna. Anthropogenic climate change and sea level rise pose major threats to tidal flats in many coastal regions. Tidal flats will disappear in the future if they cannot cope with sea level rise. Therefore, quantifying and understanding their current and projecting their future morphological evolution is of key interest. In this study, we quantified the recent evolution of the world's largest channel-shoal system, the Wadden Sea. We generated new, very high resolution topographic datasets using new observations. These datasets serve as the basis for a sophisticated statistical analysis of the morphodynamics of the Wadden Sea. Preprint: Pineda Leiva et al. [2].

2 Methods and Data

We use annual topographic datasets at 10 m resolution for the entire Wadden Sea for the time period of 1996 to 2022 [1]. We define regional units that include tidal deltas and study the statistical temporal evolution of elevation distributions in these units using *quantile regression*. In contrast to studying the evolution of intertidal and subtidal mean depths, quantile regression allows a statistically robust quantification of the evolution of the entire depth range. Integration of positive and negative trends allow a quantification of accretion and erosion rates that statistically significantly alter the height distributions.

3 Results

Greatest accretion occurs below the low water line in the upper subtidal elevations between -6 mNHN and -3 mNHN (Fig. 1), a previously hidden result. Accretion in this range is consistent in all regions. Erosion is mainly observed in the deep subtidal with regional differences. This asymmetrical accretion-erosion pattern leads to steepening of topographic gradients, especially at the channel-shoal interface, but also system-wide.

Based on the quantile regression results, we could estimate the sediment volume changes. Most net accretion was observed north of the Elbe estuary, the northern Wadden Sea, whereas the Dutch (western) Wadden Sea has eroded. Overall, the Wadden Sea has accumulated $19.7 \cdot 10^6$ m^3 yr^{-1} during the study period.

4 Conclusions

Analysis of bathymetric data has revealed that the intertidal flats of the Wadden Sea have been increasing in size and their accretion rates have exceeded the rate of mean sea level rise in the last decades. If trends continued, the Wadden Sea's intertidal flats would further expand, assuming an abundant supply of sediment and no acceleration of sea level rise.

Quantile regression provides a new, statistically reliable tool for quantifying morphological changes in time. Its results can further be used to extrapolate present morphodynamics into the future to generate better topographies for scenario studies.

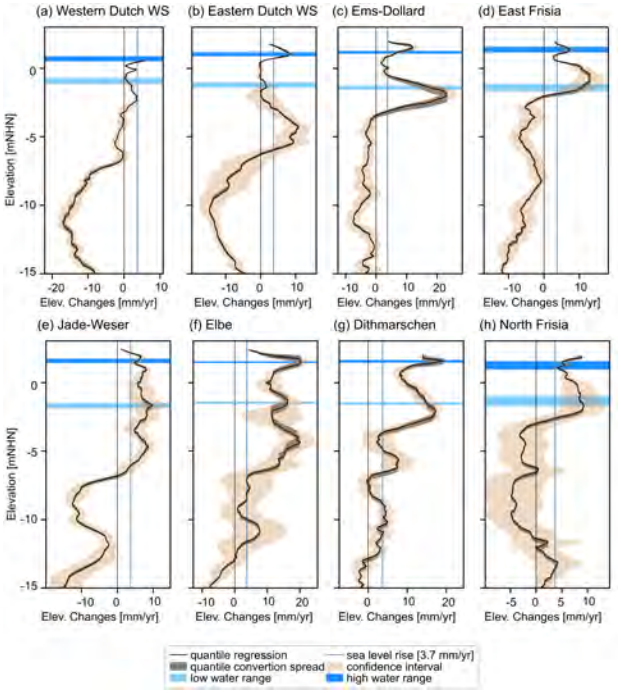

Figure 1: Quantile regression results of the average elevation changes (accretion/erosion rates) for the complete elevation range for each region. Blue lines indicate tidal high and low water lines, shaded areas mark uncertainties of the regression results. Figure taken from Pineda Leiva et al. [2].

References

[1] P. Milbradt and D. Pineda Leiva. Trilawatt: Topographie (2015-2021) [data set]. Technical report, Bundesanstalt für Wasserbau., 2024.

[2] D. Pineda Leiva, M. Lorenz, F. Kösters, C. Winter, and R. Lepper. Asymmetric morphodynamics of the Wadden Sea. *Research Square*, 2025. doi: 10.21203/rs.3.rs-5840833/v1.

Effects of mud availability on suspended sediment concentrations in the Dutch Wadden Sea

Roy van Weerdenburg[1,2], Bas van Maren[1,2], Thijs van Kessel[2], Qilong Bi[2] & Bram van Prooijen[1]
[1]Delft University of Technology, Delft, the Netherlands
[2]Deltares, Delft, the Netherlands
Corresponding author: r.j.a.vanweerdenburg@tudelft.nl

Keywords: sediment dynamics, mud, turbidity, resuspension, Wadden Sea

1 Introduction

The Wadden Sea, the world's largest system of coherent tidal flats, stretches along the North Sea coast of the Netherlands, Germany and Denmark. Key challenges for sustainable development of the Wadden Sea stem from sediment dynamics. High turbidity reduces light availability and leads to filling up of fairways, with consequently extensive maintenance dredging. In contrast, over longer timescales this sediment is needed for intertidal areas to keep pace with relative sea level rise. In the current study, we investigate variations in suspended sediment concentrations (SSC) in the Ameland Basin, located in the Dutch part of the Wadden Sea. In particular, we aim to quantify how SSC is affected by variations in mud availability, through supply from the North Sea and resuspension from the sediment bed.

2 Field data

This study is built upon the combined analysis of multiple datasets. Hydrodynamics (i.e., water levels, flow velocity profiles and wave conditions) and SSC are continuously measured at two permanent measurement stations deployed in tidal channels since July 2022. Hydrodynamics and suspended sediment transport at intertidal flats are measured in two measurement campaigns in the past two winters. We additionally use the SIBES dataset [1] to estimate the mud availability in the seabed since 2008, and the long-term monitoring program (MWTL; monthly to bimonthly sampling) of the Dutch Ministry of Infrastructure and Water Management (Rijkswaterstaat) since 1989 to evaluate variations in SSC over multiple years to decades.

3 Results and conclusions

Over short timescales, ranging from hours to days, SSC variations are primarily driven by tidal currents and wind waves, in line with earlier studies. Local wind conditions significantly impact (residual) sediment transport rates through the channels. Storms mobilize large amounts of fines from the seabed, influencing the local availability of mud. However, our results also reveal that storm events have long lasting effects impacting SSC over successive years.

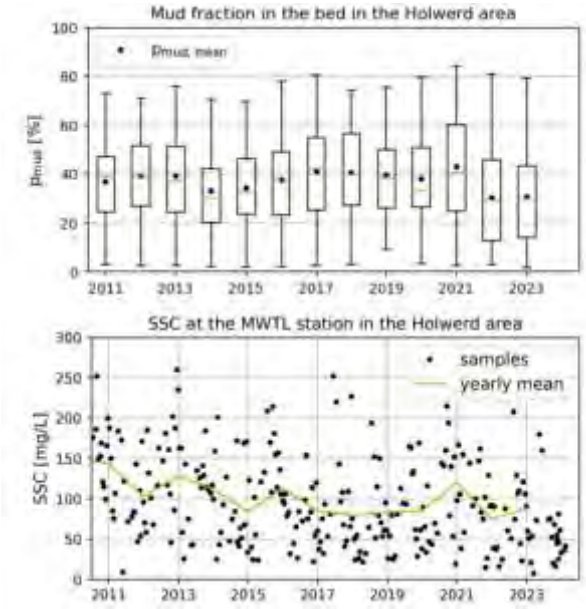

Figure 1: Variation in mud fraction in the seabed (top; boxplots of the SIBES data [1]) and SSC (bottom; samples and yearly mean of MWTL data) since 2011.

For instance, both the mud content in the bed and the SSC were low throughout 2022 (Figure 1), following an extreme storm event with winds from the west-southwest in February. In contrast, periods of exceptionally strong winds from the east in February 2021 and October 2023 initiated periods of elevated SSC. Such long-lasting effects of storms changes our modelling approach and emphasizes the need for long-term and high resolution measurements.

Acknowledgments

This study is part of the WadSED project, which is funded by the Dutch Research Council (NWO), and the BenO Wadden project of Deltares and Rijkswaterstaat, which is financed by the Dutch Ministry of Infrastructure and Water Management. We would like to thank all who contributed to the collection of field data in the Dutch Wadden Sea.

References

[1] Bijleveld, A.I. et al. (2012) Designing a benthic monitoring programme with multiple conflicting objectives. *Methods in Ecology and Evolution,* 3**,** 526-536.

Balancing coastal urban flood protection with ecosystem resilience: insights from the Venice Lagoon, Italy

A. D'Alpaos[1], A. Michielotto[1,2], A. Finotello[1], R. A. Mel[3], D. Tognin[4], L. Carniello[4]
[1]University of Padova, Department of Geosciences, Padova, Italy
[2]Department of Land, Environment, Agriculture and Forestry, University of Padova, Padova, Italy
[3]Italian National Institute for Environmental Protection and Research, ISPRA, Roma, Itlay
[4]University of Padova, Department of Civil, Environmental, and Architectural Engineering, Padova, Italy
Corresponding author: alessandro.michielotto@unipd.it
Keywords: Estuarine ecosystems; Flood defence; Numerical modelling; Hydrodynamics

1 Introduction

Low-lying coastal areas, home to approximately 11% of the global urban population, are increasingly vulnerable to flooding due to sea level rise and extreme weather events. In recent decades, storm-surge barriers and floodgates have been widely adopted to prevent flooding and support the socio-economic functioning of high-value coastal areas. Although effective in protecting human settlements from flooding, storm-surge barriers raise concerns regarding their impact on the ecomorphodynamics of coastal areas.

Focusing on the flood-regulated Venice Lagoon, Italy, where the Mo.S.E. system has been in operation since October 2020 to safeguard Venice and other lagoonal urban settlements from storm-surge-induced flooding, we perform hydrodynamic numerical simulations to compare the impacts of different flood-regulation scenarios on urban protection and ecosystem resilience.

2 Methods

We used a two-dimensional hydrodynamic model [1] to simulate tidal and wind-wave-driven circulations across the entire Venice Lagoon for the years 2020 to 2023, comparing the results obtained from the real-case flood-regulated scenario (hereafter referred to as the "**MoSE** scenario"), with those from a hypothetical non-regulated conditions (the "**OPEN** scenario"). We also considered a third hypothetical flood-regulated scenario to evaluate the effects of a more conservative floodgate management approach, following the Adaptive Threshold Operative Strategy (**AThOS** [2]), which aims to minimize the frequency and duration of closures.

We analysed simulation results in terms of the spatial and temporal extent of flooding in both Venice City and lagoonal wetlands, as sufficient flooding depth and duration are essential for sustaining mineral sediment delivery and ensuring ecosystem resilience in the face of rising relative sea levels.

3 Results and discussions

Our analysis highlights a critical imbalance in the current management of the Venice Lagoon. Although storm-surge barriers effectively mitigate flooding risks for lagoonal settlements, frequent and prolonged activations greatly reduce or even prevent salt marsh flooding. This negatively affects the supply of mineral sediments, essential for the vertical accretion of salt marshes. Retrospective analysis of the hypothetical **OPEN** scenario indicate that 30% of the Mo.S.E. activations to date were unnecessary, as lagoonal settlements would have remained un-flooded without raising the floodgates. Furthermore, the optimized **AThOS** scenario reveals that closures were often excessively long, with yearly cumulative operation durations up to 55% longer than required.

Following the AThOS procedure to minimize floodgate closures ensures water levels remain low enough to prevent urban flooding while still high enough to sustain salt marsh flooding (see Figure 1). These findings highlighs the feasibility of a balanced management strategy that not only effectively safeguards urban areas from flooding but also preserves the ecological resilience of critical estuarine ecosystems, ensuring the long-term sustainability of the Venice Lagoon.

Figure 1: Flooding area for Venice city (left) and for salt marshes (right) according different flood-regulation management scenarios (i.e., OPEN, MoSE, and AThOS).

Acknowledgments

RETURN Extended Partnership and European Union Next-GenerationEU (NRRP, Mission 4, Component 2, Investment 1.3 – D.D. 1243 2/8/2022, PE0000005)

References

[1] Carniello, L., A. D'Alpaos and A. Defina. Modeling wind waves and tidal flows in shallow micro-tidal basins, *Estuarine, Coastal and Shelf Science*.

[2] Mel, R. A., Carniello, L. & D'Alpaos, L. How long the Mo.S.E. barriers will be effective in protecting all urban settlements within the Venice Lagoon? The wind setup constraint. *Coastal Engineering* **168**, (2021).

Leveraging Vestigial Vegetation Imprints in Marsh LiDAR Geomorphometry

T. Blount[1], S. Silvestri[2], M. Marani[3], A. D'Alpaos[1]
[1]Department of Geosciences, University of Padova, Padova, Italy
[2]Department of Biological, Geological and Environmental Sciences, University of Bologna, Ravenna, Italy
[3]Department of Civil, Environmental and Architectural Engineering, University of Padova, Padova, Italy
Corresponding author: teganrose.blount@unipd.it

Keywords: tidal wetlands, biogeomorphology, LiDAR, vegetation, digital terrain model

1 Introduction

Mediterranean salt marshes are biogeomorphically complex ecosystems with low-lying vegetation and notable variability in aboveground biomass. The intertwined vulnerability and multifaceted worth of these ecosystems give rise to an implicit need for cost-effective marsh-scale monitoring approaches [1, 2]. In particular, LiDAR derived terrain and canopy models of relevant precision that can be realistically employed in coastal management frameworks. This research focuses on a Mediterranean salt marsh unmanned aerial vehicle (UAV) LiDAR dataset and addresses (1) how seven halophytic species associations influence spatial patterns in point cloud geometry and elevation error; (2) the derivation of species-specific canopy and terrain model correction factors in Mediterranean environments; and (3) the dialogue between spatial resolution and precision in this context. Insights from our analyses are crucial for improving our understanding of the biomorphodynamic evolution of salt marsh systems and enabling long-term evolution models that account for different climate change scenarios.

2 Materials and Methods

2.1 Study Site and Field Data

The study marsh (Venice Lagoon, Italy) is predominantly colonised by halophyte species associations of *Salicornia veneta*, *Sporobolus anglicus*, *Sporobolus maritimus*, *Limonium narbonense*, *Sarcocornia fruticosa*, *Juncus maritimus* and *Inula crithmoides*. These species occur in densely mosaicked vegetation zonation patterns linked to edaphic features, morphology, tidal regime and competition [3, 4]. In 2023, a UAV LiDAR survey and field measurement campaign addressing aboveground biomass composition was completed. During this vegetation measurements were made at 516 topographic points (Leica Viva GNSS GS15 RTK GPS), geographically dispersed to cover the full range of biogeomorphological associations present.

2.2 Data Processing and Analysis

The LiDAR point cloud was generated in *DJI Terra-Pro*, pre-processed in the *Spatix-Terrascan* suite and post processed in *Terrascan wizard*. DTMs were generated in R using both grid minimum and mean binning techniques. The mean absolute error (MAE) and the root mean square error (RMSE) were used to analyse the LiDAR elevation error associated with the different species associations.

3 Results and Conclusions

The results demonstrated that halophyte distribution strongly drives DTM error and species association-specific corrections are highly effective. In addition, in cases where LiDAR point clouds seemingly fail to capture dense and low-lying vegetation, hardly discernible signals of vegetation canopies can still be obtained from datasets. Overall, high spatial resolution DTMs and vegetation canopy models can be enhanced by leveraging vestigial vegetation imprints in marsh LiDAR geomorphometry. These findings promote the understanding as well as the sustainable management of a crucial ecosystem.

Acknowledgments

This research was supported by the National Science Foundation under Grant No. 2016068, "Coupled Ecological-Geomorphological Response of Coastal Wetlands to Environmental Change"; the University of Padova SID2021 project, "Unraveling Carbon Sequestration Potential by Salt-Marsh Ecosystems" (PI A. D.) and the RETURN Extended Partnership, and received funding from the European Union Next-GenerationEU (National Recovery and Resilience Plan – NRRP, Mission 4, Component 2, Investment 1.3 – D.D. 1243 2/8/2022, PE0000005).

References

[1] E. Barbier, S. Hacker, C. Kennedy, E. Koch, A. Stier, and B. Silliman. The value of estuarine and coastal ecosystem services. *Ecological Monographs*, 81(2):169–193, 2011.

[2] C. Duarte, J. Middelburg, and N. Caraco. Major role of marine vegetation on the oceanic carbon cycle. *Biogeosciences*, 1:1–8. (2005).

[3] M. Marani, T. Zillio, E. Belluco, S. Silvestri and A. Maritan. Non-neutral vegetation dynamics. *PLoS ONE*, 1(1), 2006.

[4] A. Puppin, D. Tognin, M. Ghinassi, E. Franceschinis, N. Realdon, M. Marani, and A. D'Alpaos. Spatial patterns of organic matter content in the surface soil of the salt marshes of the Venice Lagoon (Italy). *Biogeosciences*, 21(12): 2937–2954, 2024.

Machine learning implementation to capture morphological response on the Bay of Biscay

Manuel Viñes[1], Irati Epelde[2], Cesar Mösso[1], Javi Franco[2], Joaquim Sospedra[1], Aritz Abalia[2], Pedro Líria[2], Manel Grifoll[1], Manuel González[2], Agustín Sánchez-Arcilla[1]
[1] Laboratori d'Enginyeria Marítima, UPC, 08034, Barcelona, Spain
[2] AZTI Marine Research Unit, Basque Research and Technology Alliance (BRTA), 20110, Pasaia, Gipuzkoa, Spain
Corresponding author: manuel.vines@upc.edu
Keywords: *Machine learning, Gradient Boosting Regressor, SWAN, hydro- and morphodynamic variables, cross-correlation*

1 Introduction

Understanding morphodynamic drivers across different spatial and temporal scales is essential for the analysis and predictions of the beach morphological evolution on the scope of coastal management strategies. Recent works (e.g., [1]) have emphasized the importance of accurately analysing beach erosion and accretion processes. as these influence their evolution at different scales and the related socioeconomic development of coastal zones. Particularly in regions like the Bay of Biscay (North Atlantic Ocean) where the combination of extreme events and highly urbanized beaches play a key role. In this context, this study aims to enhance the insight on the morphological response by developing an innovative methodology to characterize and predict the response of inter and supratidal areas using machine learning (ML) techniques. The study focuses on four pocked beaches near Bilbao and combines morphodynamic variables obtained from the KOSTASystem videometry and hydrodynamic time-series. To complement that, traditional methods such as polynomial regression are also modeled as an initial step toward a more comprehensive comparison between conventional models and models based on ML.

2 Machine learning treatment versus morphological response

After exploring the relationship between the variables, the Gradient Boosting Regressor (GBR) algorithm is implemented, which operates similarly to decision trees (DA). The main idea is to represent a complex system as a tree structure, thereby simplifying the problem [2]. Once the optimal hyperparameters were determined using the Grid Search technique, the algorithms for each beach were optimized [3].

3 Prediction of the morphological response

The application of the GBR model to the different study cases demonstrated better performance compared to traditional regression methods. For certain beaches, the model produced coefficients of determination (R^2) up to 0.80 and mean absolute percentage error (MAPE) values below 1%. As an example of the application of GBR algorithms across all studied beaches, the results, such as the supratidal area (SA), in Arriatera Beach are shown in Figure 1.

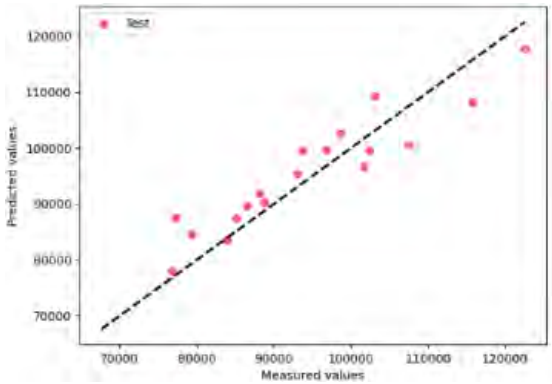

Figure 1: Prediction of the SA of Arriatera Beach.

In this case, the model achieved a MAPE of 0.08 in the training set and 0.07 in the test set, with a Mean Squared Error of 2399 m^2 and 2237 m^2, respectively. Additionally, it obtained R^2 of 0.82 for the training and 0.86 for the test set, suggesting a high ability of the model to explain the variability observed.

3 Conclusions

This study highlights that the temporal scale can be a limiting factor when predicting morphological responses. Moreover, the time series implemented and the substantial impact of external factors can affect the ability of certain models to analyse and interpret morphodynamic conditions accurately. However, in general terms, the GBR approach demonstrates a significant improvement over traditional methods.

Acknowledgments

This work was partially funded by the project "Environmental monitoring of sand extraction in Zone II of the Port of Bilbao (2022-2026) and co-worked with the UPC REST-COAST team.

References

[1] A. Sánchez-Arcilla *et al.*, "Beach Dynamics in the Presence of a Low Crested Structure. The Altafulla case," *J Coast Res*, vol. II. No. 39. Proceedings of the 8th International Coastal Symposium (ICS 2004), 2006.
[2] A. Pourzangbar *et al.*, "Machine learning application in modelling marine and coastal phenomena: a critical review," *Frontiers in Environmental Engineering*, vol. 2, Sep. 2023,
[3] Z. M. Alhakeem *et al.*, "Prediction of Ecofriendly Concrete Compressive Strength Using GBR Tree Combined with GridSearchCV Hyperparameter-Optimization Techniques," *Materials*, vol. 15, no. 21, p. 7432, Oct. 2022

Cohesive sediments alter coastal bar dynamics under waves and currents

Anne Baar[1], Brendan Murphy[2], Stuart McLelland[2], Daniel Parsons[3]
[1]Faculty of Civil Engineering and Geosciences, Delft University of Technology, Delft, NL
[2]Energy and Environment Institute, University of Hull, UK
[3]Geography and Environment, Loughborough University, UK
Corresponding author: a.w.baar-1@tudelft.nl

Keywords: coastal bar dynamics, estuary, cohesive sediment, wave-current interaction, bedform morphology

1 Introduction

Coasts and estuaries are highly dynamic systems where sand and mud are transported under the complex interactions of bathymetry, currents and waves. A better understanding of the natural dynamics at the scale of individual bars is required for a fundamental understanding of the formation of coastal environments and how they will respond to changes in the future. However, current sediment predictors and empirical relations of bar dynamics do not take into account the effect of cohesive sediment, whereas many coastal environments have an abundance of fine-grained deposits and consist of highly spatially varying mixtures of sand and mud [1].

The current research aims to characterize the relative influence of clay on the direction of sediment transport and resulting morphodynamic change of coastal bars, under the combined action of waves and currents.

2 Methodology

Experiments were conducted in the Total Environment Simulator, a large-scale wave-current flume facility at the University of Hull (6m x 11m, 0.4m deep)(Figure 1). The experimental setup was based on [2] and consisted of a circular mound (0.2m high, diameter of 1.5m), placed on top of a flat sand bed in the centre of the flume. The mound consisted of a mixture of sand and clay. The experimental conditions were systematically varied between runs, with 4 different clay percentages of the mound, and 5 different combinations of wave height and current velocity. The total bed shear stress generated by the waves and currents remained constant between runs, but their relative contributions varied. Clay content varied between 3 and 11%, based on the transition between non-cohesive and cohesive behaviour of the sand-clay mixture [1].

Experiments were run for 50 minutes, and the bed was scanned before and after each run. Flow velocity, water level and bed levels were monitored during each run, providing well-controlled bed development data over time. At the end of each run, bed samples were taken to analyse the spatial variation in clay content.

3 Results and implications

Observations of the mound morphology show lateral diffusion due to sediment transport perpendicular to the wave direction under the influence of gravity, and streamwise migration due to sediment transport in the direction of the flow. Increasing the cohesivity altered the relative influence of the waves and currents on the direction of sediment transport and therefore the final shape of the mound. With higher clay content, there was relatively more lateral than streamwise transport under the same wave and current conditions. Furthermore, wave height had a greater control on the morphology with increasing clay content, since higher waves were more effective in winnowing out the clay into suspension and thereby mobilizing the sand fraction.

Cohesive sediments therefore alter the direction and rate of morphodynamic change of coastal bars. Coastal and estuarine environments with spatially varying clay content will adapt differently to changing hydrodynamic conditions. In systems with a relatively high clay content, wave energy will have an important control on the dynamics as it is needed to mobilize the sediment.

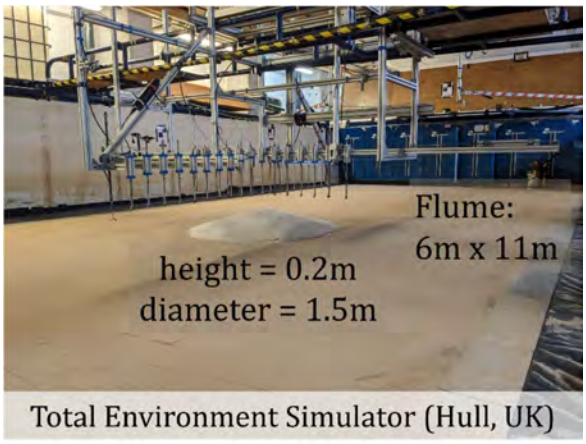

Figure 1: flume setup

References

[1] Van Ledden, M. 2003. Sand-Mud Segregation in Estuaries and Tidal Basins. *University of Technology Sydney.*

[2] De Schipper, M., et al. (2019). Modex: Laboratory experiment exploring sediment spreading of a mound under waves and currents. *Coastal Sediments 2019: Proceedings of the 9th International Conference* (pp. 511-524).

Numerical modelling of breaker bar morphodynamics and the role of longwave presence

Buckle Subbiah Elavazhagan[1], Maria Maza[1], Javier Lara[1]

[1]Instituto de Hidráulica Ambiental Cantabria, Calle Isabel Torres 15, Santander 39011, Spain

e-mail corresponding author: subbiahb@unican.es

Keywords: *Beach profile morphodynamics; Beach erosion; Breaker bar; CFD; IH2VOF-SED*

1 Introduction

Beaches and their immediate nearshore are highly dynamic under storm conditions with breaker bar formation being an important morphodynamic response. Numerical models help in understanding relationship between these complex morphodynamic processes and the governing hydrodynamics. Excessive calibration and computational time can be limiting when using these models as predictive tools. IH2VOF-SED model was developed [1] to be efficient by enabling accurate morphodynamic predictions with reduced computational time and calibration efforts. The model was previously validated for regular wave conditions, but it is necessary to extend the capabilities of the model for random sea state modelling to increase its applicability. This work focus on breaker bar formation in bi-chromatic wave condition and including the analysis of the influence of presence of long waves in the morphodynamic processes.

2 Methods

IH2VOF-SED is a 2DV RANS based depth-resolving one-phase sediment transport model. Experiments [2] using bichromatic waves, carried out in Large scale wave flume located in LIM, UPC, Barcelona were used for this study. Bichromatic waves with two primary frequencies of 0.3041 Hz and 0.2365 Hz are considered. Due to the unavailability of motion signals at the wave maker, wave data measured at a distance of 54.69m from the wave paddle is used as the input boundary condition. The experiment was run using 1st order wave generation with no active wave absorption, while the numerical model has capabilities of generating 1st and 2nd order waves together with active wave absorption. Two cases with different boundary conditions will be discussed one utilizing 1st order wave generation with original wave data and the second utilizing 2nd order wave generation after filtering out sub harmonics and super harmonics from the measured data.

3 Results

In both the cases the primary breaker bar was predicted, while in the 1st case there is an over prediction of erosion and bar development, the 2nd case produced a more accurate primary breaker bar (Figure 1). There is a considerable difference in phase lag of the long and short waves between the 1st case and measured, leading to a different breaking condition. This is due to driving the model from wave gauge data with long wave presence and length of the numerical flume being different. But the 2nd wave is driven with a longwave of phase closer to the laboratory conditions especially in the breaking zone which led to a more desirable breaking and more accurate breaker bar formation.

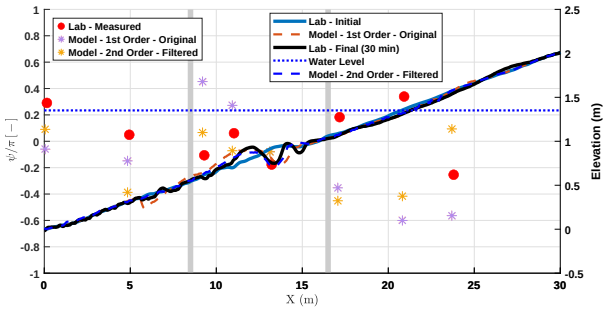

Figure 1: Right y-axis represents the elevation of beach profiles(lines), and Left y-axis represents the Phase lag between the long and short wave components(points). Grey lines are the two breaking points.

4 Conclusion

The model has predicted the morphodynamic evolution of the breaker bar very well with a reduced computational time and with no morphological calibration. Improvement in the long wave and the introduction of them closer to laboratory conditions, especially in the breaking zone, have been shown to increase the accuracy of morphodynamic prediction.

Acknowledgements

Financial support has been provided by European Union's (EU) Horizon Europe Framework Programme (HORIZON) via SEDIMARE (Grant Agreement No. 101072443), an MSCA Doctoral Network (HORIZON-MSCA-2021-DN-01) and Grant TED2021-130804B-I00 of the project funded by MCIN/AEI/10.13039/501100011033 and by the "European Union NextGenerationEU/PRTR".

References

[1] García-Maribona J. et.al. An efficient RANS numerical model for cross-shore beach processes under erosive conditions. *Coastal Engineering*, 170, December 2021.

[2] Grossmann F. et.al. Near-Bed Sediment Transport During Offshore Bar Migration in Large-Scale Experiments. *Journal of Geophysical Research: Oceans*, 127(5), May 2022.

Integrating Physical and Numerical Models to Assess Wave Dissipation and Sediment Accumulation at Restored Oyster Reefs

Alberto Canestrelli[1], Jacopo Composta[1], William Nardin[2], Rafael O. Tinoco[3], Salman Fahad Alkhidhr[3], Kamil Czaplinski[3], Luca Martinelli[4], Savanna Barry[1], Anthony Priestas[5], Duncan Bryant[5]
[1]University of Florida,
[2]University of Maryland,
[3]University of Illinois Urbana-Champaign,
[4]University of Padova,
[5]US Army Corps of Engineers
Corresponding author: alberto.canestrelli@essie.ufl.edu

1. Introduction

Oyster reef ecosystems are increasingly recognized for their resilience and self-maintenance properties, making them attractive nature-based alternatives to traditional "gray" infrastructures. These reefs provide critical benefits to adjacent habitats, such as salt marshes, by mitigating erosion and promoting sediment deposition. However, a knowledge gap remains regarding the physical processes driving sediment transport around oyster reefs under varying wave and tidal conditions, as well as for different reef locations and geometries. Addressing this gap is essential for understanding how and when oyster reefs retain sediments and support shoreline progradation.

2. Methodology

To tackle this challenge, we quantify sediment retention and shore stabilization mechanisms of oyster reefs under controlled hydrodynamic and geometric conditions. Our methodology combines physical and 3D numerical modeling to evaluate the influence of tidal and wave dynamics, longshore currents, reef geometries, and distances from the coast. We conducted small-scale experiments using scaled-down (1:7) 3D printed oyster reefs in a wave flume at the Ven Te Chow Hydrosystems Lab at the University of Illinois Urbana-Champaign (UIUC), which measures 40 meters in length and 1.80 meters in width. Concurrently, we run numerical simulations using OpenFOAM, specifically using Waves2Foam and SedInterFoam toolboxes, on the HiPerGator high-performance computing cluster at the University of Florida. These simulations incorporate orthogonal waves of varying heights and periods and examine oyster reefs with different geometries.

3. Conclusions

Small-scale (SS) and mid-scale (MS) experiments revealed distinct patterns of erosion and deposition influenced by reef gap sizes, reef width, and wave regimes. Smaller gaps in SS experiments increased local speeds, enhancing erosion within reefs and shifting sediment deposition to the beach away from reefs. Reef width affected wake generation, with thinner structures causing increased scour. Wave excursions significantly influenced bed morphology, altering both slope and length past the reefs, while finer materials were more mobilized through gaps, and larger grains settled in lower stress areas. MS experiments, despite differing sediment types and conditions, showed similar erosion and deposition patterns within gaps and past reefs, with sediment accumulating on the onshore side and increased scouring where waves broke. Ripple patterns indicated the effects of wave dissipation and flow structures from wave-reef interactions.

The outcome of this research includes (i) A comprehensive dataset of sediment concentrations, velocity profiles, surface elevations, flow velocities, and morphological changes, providing a benchmark for future models; (ii) Numerical model inputs, outputs, and source code to ensure reproducibility and accessibility; (iii) Practical guidelines for stakeholders to optimize net sediment deposition in oyster reef restoration projects. This work enhances understanding of oyster reef dynamics and support the development of effective, sustainable restoration strategies. Finally, the insights from these initial studies guide the selection of critical test cases for large-scale physical experiments at the Large-scale Sediment Transport Facility (LSTF) at the Coastal Hydraulic Lab (CHL) in Vicksburg, MI. At this facility, physical experiments at a larger model-to-prototype scale (1:2) will be conducted. These tests will include regular and irregular waves (i.e., wave spectra in both frequency and direction), wind-driven and tidal longshore currents, and tidal variations in water level. Four distinct reef geometries will be tested under these hydrodynamic conditions.

Acknowledgments

The research is funded by the United States Army Corps of Engineers.

Predicting Tombolo and Salient formations in complex coastal settings

Arnau Garcia[1] , Albert Gallego[1] , Erica Pellón[1] & Mauricio González[1]
[1]IHCantabria - Instituto de Hidráulica Ambiental de la Universidad de Cantabria, Santander, Spain.
Corresponding author: arnau.garcia@unican.es

Keywords: *Detached breakwaters, Tombolo and Salient formations.*

1. Introduction

Detached breakwaters play a crucial role in coastal protection, but traditional emerged designs often have substantial environmental and aesthetic drawbacks. Submerged and low-crested breakwaters suppose viable alternatives; however, their impact on shoreline morphodynamics, particularly in forming tombolos and salients, remains inadequately understood [1]. Current approaches to defining these sedimentary features often rely on numerical approximations and dimensionless ratio analyses [2], which can yield inconsistent results depending on the methodology applied. While most research has focused on the morphodynamics of fully emerged structures, this study targets the prediction challenges mainly associated with low-crested, and submerged designs. By employing Machine Learning (ML) classification techniques, this work introduces an innovative framework aimed at enhancing prediction reliability and reducing uncertainty in defining the formation limits of tombolo and salient features.

2. Methods

To predict the morphodynamic response of beaches protected by detached structures, we developed an ML-based methodology using a dataset of over 250 beaches across six countries. A total of 254 structures were analysed—85 emerged, 57 low-crested and 112 submerged—. The 3 key attributes considered, include: the distance from the original shoreline to the structure (S), the length of the breakwater (B) and the wavelength (L) at this depth, combined as the following 5 input parameters: B, S, B/S, S/L, and B/2L . Three models— Random Forest, XGBoost and KNN —were optimized through cross-validation to ensure robust performance. These base models were then combined in a stacking ensemble, leveraging their strengths to enhance prediction accuracy. While applicable to all breakwater types, this methodology primarily focuses on submerged ones, addressing the key knowledge gap in predicting their type of response.

3. Results

The stacking ensemble model showed significant improvements in prediction accuracy and reliability, outperforming the individual base models. It achieved consistent performance across training and test sets, with 157 observations used for training and 86 for testing. Four metrics—accuracy, precision, recall, and F1-score—were employed to assess the model's performance comprehensively. The confusion matrix (Fig. 1) highlights the model's reliability, showing correct predictions on the major diagonal, and misclassified on the minor diagonal.

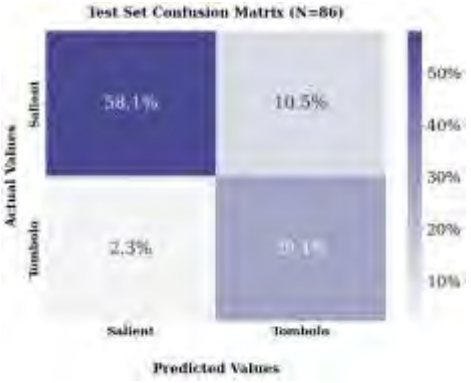

Fig 1. Confusion matrix result obtained for the Test set.

4. Conclusions

This study effectively predicted beach responses to a wide range of detached breakwater types, demonstrating particular effectiveness in handling complex structures like low-crested and submerged designs. These results underscores the potential of ML as a powerful complement to traditional empirical models, dimensionless analysis, providing a robust framework to reduce uncertainty in predicting tombolo and salient formations across diverse coastal settings.

Acknowledgments

This study is part of the ThinkInAzul programme and was supported by the Ministerio de Ciencia, Innovación y Universidades (PRTR-C17.I1) with funding from the NextGeneration EU and the Comunidad de Cantabria, as well as by the research project PID2023-153343OA-I00, funded by MICIU/AEI (10.13039/501100011033) and co-financed by FEDER, EU.

References

[1] R. Ranasinghe and I. Turner, 'Shoreline response to submerged structures: A review', *Coastal Engineering*, vol. 53, pp. 65–79, Jan. 2006, doi: 10.1016/j.coastaleng.2005.08.003.

[2] R. Macêdo, V.A.V. Manso, and A.E.F Klein, 'The geometric relationships of salients and tombolos along a mesotidal tropical coast', *Geomorphology*. https://doi.org/10.1016/j.geomorph.2022.108311.

River sand inputs, headland bypassing, and the infilling of a pocket beach

Ruth Durán[1], Jorge Guillén[1], David Amblas[2], Candela Marco-Peretó[1], Antoni Calafat[2], Susana Costas[3]
[1]Institut de Ciències del Mar (ICM)-CSIC, Barcelona, Spain
[2]GRGM, Dept. DTO, Facultat de Ciències de la Terra, Universitat de Barcelona, Barcelona, Spain
[3]CIMA/ARNET, Universidade do Algarve Faro, Portugal
Corresponding author: rduran@icm.csic.es

Keywords: Catalan coast, NW Mediterranean, ephemeral streams, longshore sediment transport, coastal headlands.

1 Introduction

Embayed beaches are often considered as isolated systems with limited sediment exchange across their boundaries. However, under specific conditions, sand can bypass rocky headlands. Understanding this sediment transport is essential to assessing the evolution of these beaches, especially when influenced by fluvial inputs and longshore drift. This study focuses on the Sa Riera pocket beach, located south of the Pals beach, on the Catalan coast (NW Mediterranean).

2 Study site

The Catalan coast is a microtidal environment with a predominant sediment transport towards the SW (25,000-100,000 m^3/year). Pals Beach is a large embayed beach (6.8 km) fed by the Ter and Daró rivers. Sa Riera, a smaller pocket beach (186 m long), is bounded by 45 m high cliffs and fed by a small stream. From 1945 to 2020, Pals Beach remained relatively stable, while Sa Riera tripled its emerged beach area.

3 Methods

Data used in this study consist of repeated high-resolution bathymetric surveys conducted in 2004, 2022, 2023 and 2024, along with surficial sediment samples collected in 2023. Comparisons of bathymetric datasets over the last two decades were used to identify sediment accumulation and erosion patterns.

4 Results and Discussion

The submerged morphological evolution of the Pals and Sa Riera beaches over the last two decades shows significant changes linked to the dynamics of cuspate morphologies down to 10 m depth, and to localized sediment accumulation off Sa Riera, down to 14 m depth. The dynamics of these cuspate features appear to be the main mechanisms of sand bypassing between the headland-bounded beaches. This connectivity is supported by backscatter data and sediment samples indicating a continuous coarse sediment domain extending around the headland. Additionally, cross-shore sediment alignments at 22 m depth suggest offshore sediment escape during storms, while grain size analysis indicates local fluvial inputs from an ephemeral stream supplying fine-medium sand to the shoreface of Sa Riera during floods.

5 Conclusions

The decadal morphological evolution of the Sa Riera pocket beach highlights a transition from a system influenced by sediment inputs from a small local stream to one dominated by sediment contributions from the up-drift embayed beach, which bypass the headland. This shift occurs when fluvial sediment input at Pals Beach accumulates near the headland and eventually bypass it, leading to the continuous progradation of Sa Riera. The apparent mechanism of sediment bypassing is associated with the dynamics of crescentic bars in the Pals beach.

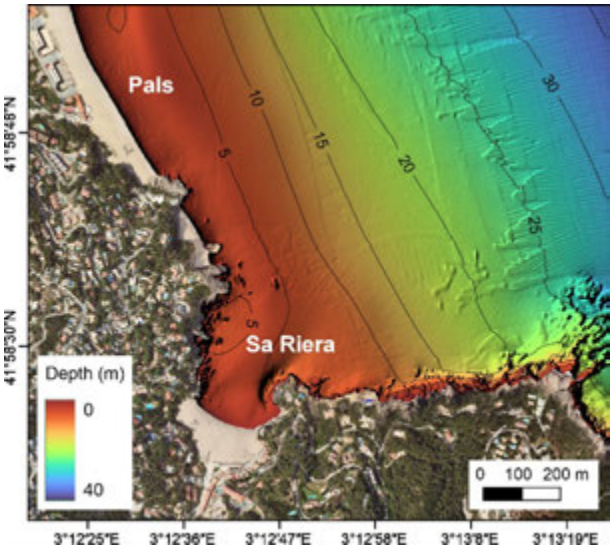

Figure 1: Shaded relief coloured bathymetric map of Pals and Sa Riera beaches. Ortophotos and bathymetric data provided by ICGC.

Acknowledgments

This work was supported by the MOLLY (PID2021-124272OB-C21) and SOLDEMOR (TED2021-130321B-I00) projects funded by MICINN and the Catalan Government Excellent Research Groups grant no. 2021-SGR-01195. It contributes to the Severo Ochoa "Centre of Excellence" of the ICM (CEX2019-000928-S). We thank the DGPMPS (*Generalitat de Catalunya*) for the access to R/V Lluerna, the SGP of the Spanish MAPA and TRAGSA for the 2004 ESPACE Project bathymetric dataset and the ICGC for the 2024 bathymetric dataset. C. Marco-Peretó is supported by an FPI grant (PRE2022-101492) and S. Costas by FCT (CEECINSTLA/00018/2022).

Effects of a Sloping Shelf on Tidal Sand Wave Formation: A Linear Stability Analysis

L. Portos-Amill[1], P.C. Roos[1], H.M. Schuttelaars[2], S.J.M.H. Hulscher[1]

[1]Water Engineering and Management, University of Twente, Enschede, The Netherlands
[2]Delft Institute of Applied Mathematics, Delft University of Technology, Delft, The Netherlands

e-mail corresponding author: l.portosamill@utwente.nl

Keywords: *tidal sand waves; linear stability analysis; sloping shelf; tide-topography interactions*

1 Introduction

Tidal sand waves are rhythmic bed features often found in tide-dominated sandy shelf seas. They usually have wavelengths of $100 - 1000$ m, heights of $1 - 10$ m, and migration rates of $1 - 10$ m/yr.

Sand waves have been explained as free instabilities of a flat seabed subject to tidal motion using a linear stability analysis [2]. Recently, observations have indicated that their shape depends on the underlying topography, resulting in e.g., sand waves on top of sand banks being more two-dimensional than those on the slopes [3]. However, these shelf effects on sand wave characteristics have not been studied in detail.

Therefore, the main aim of this contribution is to systematically study the effects of a sloping shelf on sand wave formation. Inspired by previous work on the formation of shoreface-connected sand ridges [1], we make use of a linear stability analysis.

2 Methods

Consider an offshore part of a shallow shelf sea with a background topography that is alongshore uniform and sloping in the cross-shore direction y, $H(\gamma y)$. We assume a weak cross-shore dependence, hence γ is a small parameter. The background topography is in morphodynamic equilibrium, on top of which sand waves may develop (Figure 1).

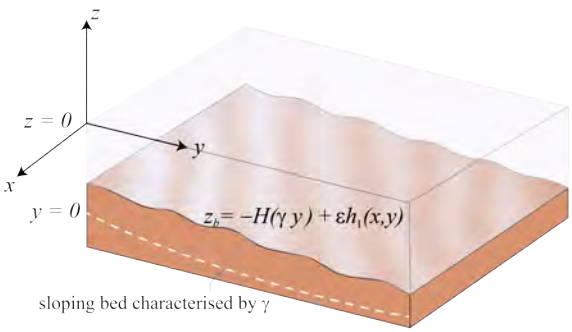

Figure 1: Sketch of the model geometry, with alongshore, cross-shore and vertical coordinates (x, y, z).

Our model is governed by the 3D shallow water equations, and bed evolution is modelled with the Exner equation considering bed load sediment transport. The model is forced with an M2 tidal flow in the alongshore direction. We assume periodicity in the alongshore direction.

By performing a linear stability analysis, we study the growth or decay of perturbations on a basic state (the shelf without sand waves). Thus, the solution is decomposed into

$$\phi(x, y, z, t) = \phi_0(y, z, t) + \epsilon\phi_1(x, y, z, t) \ , \qquad (1)$$

where ϕ_0 and ϕ_1 represent the basic and perturbed states, and $\epsilon = h/H \ll 1$ is the ratio of sand wave height and mean water depth. Since $\epsilon \ll 1$, our model is only representative of the initial growth stage.

We solve for the alongshore-uniform basic state $\phi_0(y, z, t)$ semi-analytically by expanding the equations in terms of the small parameter γ.

We obtain the first-order equations by collecting the terms linear in ϵ. We consider the first-order state to be of the form

$$\phi_1(x, y, z, t) = \hat{\phi}_1(y, z, t) \exp(ikx) + \text{c.c.} \ , \qquad (2)$$

where k is the topographic wavenumber. The linear stability analysis yields, for each possible k, all modes (sand wave shape and flow structure) and their respective growth and migration rates. The mode with the highest (and positive) growth rate is considered to dominate the dynamics of the system.

3 Results and Further Work

The basic flow shows tide-topography interactions leading to upslope residual currents at the seabed similar to those over sandbanks.

Our first-order model reproduces the perturbed state flow over an imposed sand wave topography. It is also able to compute the fastest growing mode for the flatbed case ($\gamma = 0$), reproducing the results of [2]. Results on the stability analysis with a non-zero shelf slope ($\gamma > 0$) will be presented at the conference.

References

[1] D. Calvete, A. Falqués, H.E. de Swart, and M. Walgreen. Modelling the formation of shoreface-connected sand ridges on storm-dominated inner shelves. *Journal of Fluid Mechanics*, 441:169–193, 2001.

[2] S.J.M.H. Hulscher. Tidal-induced large-scale regular bed form patterns in a three-dimensional shallow water model. *Journal of Geophysical Research: Oceans*, 101(C9):20727–20744, 1996.

[3] J. Krabbendam, A. Nnafie, B.W. Borsje, and H.E. de Swart. Background topography affects the degree of three-dimensionality of tidal sand waves. *Journal of Geophysical Research: Earth Surface*, 128(11):e2023JF007153, 2023.

The Role of Cohesive Sediment in Sand Wave Formation

Wout Ploeg[1], Pieter C. Roos[1], Bas W. Borsje[1], Suzanne J.M.H. Hulscher[1]

[1]University of Twente, Enschede, The Netherlands

e-mail corresponding author: w.ploeg@utwente.nl

Keywords: *cohesive sediment; sand wave dynamics; sediment sorting; bed forms; linear stability analysis*

1 Introduction

Effective planning of sediment extraction from coastal shelves requires a detailed understanding of bed form dynamics in relation to sediment properties. Sand waves are most relevant, as their wavelength (hundreds of meters) is comparable to typical extraction pit lengths. Thus far, sand wave dynamics has mainly been researched for non-cohesive sediment mixtures. However, the role of cohesive sediment has never been explored, whilst the impact of cohesive sediment on sand wave occurrence might be profound [2]. In this study, we specifically focus on the interaction between cohesive sediment and sand waves.

2 Methods

We have developed a new idealized 2DV-model, extending Campmans et al. [1] to accomodate multiple sediment fraction. For the non-cohesive fraction, a critical bed shear stress is included. Cohesive sediment locally increases the critical bed shear stress and is transported via suspended load only. It is brought in suspension by erosion along with the non-cohesive sediment based on the local sediment composition [3].

The model is analysed by means of a linear stability analysis [1], yielding the system

$$\frac{\partial}{\partial t}\begin{bmatrix} h \\ f_{\text{mud}} \end{bmatrix} = \underbrace{\begin{bmatrix} c_{11} & c_{12} \\ c_{21} & c_{22} \end{bmatrix}}_{\Gamma} \begin{bmatrix} h \\ f_{\text{mud}} \end{bmatrix}. \tag{1}$$

The growth matrix Γ is quantifies the initial response of bed elevation h and mud content f_{mud} for features of varying wavelength $L = 2\pi/k$. The maximum real part of the eigenvalues of Γ is termed the growth rate γ, revealing whether bed feature of this wavelength grows ($\gamma > 0$) or decays ($\gamma < 0$). The bed feature with the largest growth rate is termed the 'Fastest Growing Mode' (FGM). The eigenvectors of Γ also reveal the sorting of the mud over the topography.

3 Results & Conclusion

Depending on the initial mud content of the bed, three regimes are distinguished (see Fig. 1): low mud content ($0 < f_{\text{mud}} < f_1$), permitting the generation of sand-crested sand waves; intermediate mud content ($f_1 < f_{\text{mud}} < f_2$), where mud-crested sand waves form; and high mud content $f_{\text{mud}} > f_2$, for which no sand waves form. The transition behaviour is explained by the increase of the critical shear stress following increases in mud content. In the low mud content regime, standard sand wave behaviour in non-cohesive sediment dominates. In the intermediate mud content regime, the impact of the critical shear stress is strong enough to initiate a positive feedback loop: mud patches locally reduce the erosion rates, whereas erosion increases at sandier patches. This yields an effective transport of mud towards the muddier locations, reinforcing this cycle. When increasing the mud content beyond f_2, the critical shear stress exceeds the tide-maximum bed shear stress, preventing any sediment transport and sand wave formation.

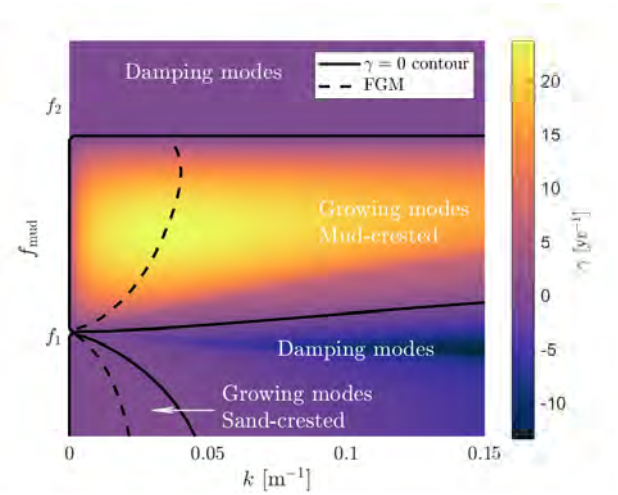

Figure 1: Growth rate γ as function of the topographic wavenumber $k = 2\pi/L$ and mud content f_{mud}

In future work, we further explore this interaction and the underlying mechanisms. Furthermore, we extend the analysis into the nonlinear regime, allowing to analyse the further development of the topography and equilibrium configurations.

Acknowledgements

This project is funded by the Dutch Research Council (NWO; no. NWA.1389.20.097) and part of the project 'OR ELSE: Operational Recommendations for Ecosystem-based Large-scale Sand Extraction'.

References

[1] G. H. P. Campmans, P. C. Roos, H. J. de Vriend, and S. J. M. H. Hulscher. Modeling the influence of storms on sand wave formation: A linear stability approach. *Cont Shelf Res*, 137:103–116, 2017.

[2] S. J. M. H. Hulscher and G. M. Van Den Brink. Comparison between predicted and observed sand waves and sand banks in the North Sea. *J Geophys Res: Oceans*, 106(C5):9327–9338, 2001.

[3] M. Van Ledden. *Sand-Mud Segregation in Estuaries and Tidal Basins*. PhD thesis, Delft University of Technology, Delft, 2003.

Assessing Offshore Wind Farm Impacts on Marine Dune Migration: A Case Study in the Southern North Sea

Noémie Durand[1,2], Pablo Tassi[2], Olivier Blanpain[1] & Alice Lefebvre[3]

[1]France Energies Marines, Plouzané, France
[2]Saint-Venant Laboratory LHSV, ENPC, Institut Polytechnique de Paris, EDF R&D, Chatou, France
[3]MARUM, University of Bremen, Bremen, Germany

e-mail corresponding author: pablo.tassi@edf.fr

Keywords: *marine dunes, meteorological forcing, tidal forcing, opentelemac, offshore wind farm*

1 Introduction

By the end of 2020, Europe had around 5,400 offshore wind turbines installed or under construction. As offshore wind farms grow to meet climate goals, understanding how their fixed foundations interact with marine dunes (sand waves) is crucial. These dunes, found in shallow seas, are large and mobile, migrating up to tens of meters annually. Studies show that dunes generally regenerate after the engineering work involved in installing wind turbine foundations. However, monopiles are likely to locally affect dune migration, which may affect dune plan shape in the long term. A 3D numerical model is used to study the interactions between dunes and monopiles.

2 Materials and methods

A 3D coastal area model using the openTELEMAC system was created to study marine dune migration over time. This model combines the TELEMAC-3D hydrodynamic module with the GAIA sediment transport module, focusing on tidal flows, weather, and bedload transport, while omitting wave influence and suspended sediment transport. The model covers the area from Calais to Ostend, using a detailed unstructured mesh, and is driven by tidal and meteorological data. It has been calibrated and validated with field data, effectively replicating marine dune migration and offering valuable insights into coastal dynamics [1].

3 Results

To evaluate the impact of turbine foundations on marine dune migration, a baseline simulation modelled natural hydrodynamic and sediment transport processes offshore Dunkirk without monopiles for two years. This simulation was then repeated with 46 monopiles within the Dunkirk offshore wind farm footprint, located at least 10 km from the coast and spaced about 1 km apart. Additional scenarios with half the number of turbines were also simulated.

3.1 Baseline simulation

The baseline simulation shows natural variations in sediment transport across the offshore wind farm area due to differences in tidal currents and wind conditions, where dunes are not uniformly distributed. Two zones of distinct morphological behaviour are analysed in detail: 1) a gully between sandbanks with southwest-migrating dunes, and 2) the slopes of the sandbanks.

3.2 Influence of the fixed foundations

Numerical results showed that in a tidally dominated environment, fixed foundation turbines (monopiles) act as morphodynamic magnets, causing dune sections on the tidal axis to converge towards them. This is due to a velocity and sediment transport deficit downcurrent for each tidal phase, known as the 'wake effect'. A wider tidal ellipse results in a more diffuse monopile impact, which becomes less pronounced with increased distance from the monopile. This effect is illustrated in Figure 1, showing the predicted seabed changes two years after installing the array of turbines.

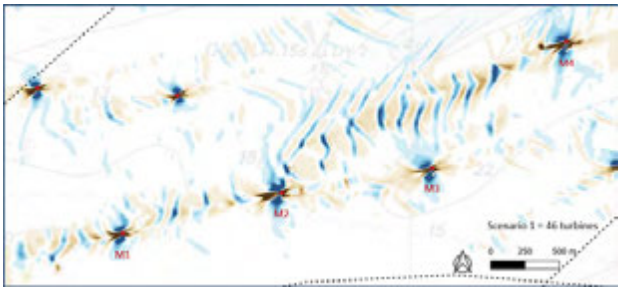

Figure 1: Bathymetric changes two years after the implementation of wind turbines (filled red circles), calculated as the difference between predicted seabed levels and baseline levels (without monopiles).

4 Conclusions

The placement of turbines has been identified as an important factor influencing seabed dune movement. This insight is valuable for the design phase of offshore wind projects, as it highlights a crucial factor for sustainable development.

Acknowledgements

This work was supported by France Energies Marines, through the MODULLES project, co-funded by the French National Research Agency as part of France 2030 Investment Plan ANR-10-IEED-0006-34.

References

[1] Noémie Durand, Pablo Tassi, Olivier Blanpain, and Alice Lefebvre. Meteorological conditions influence the migration of a marine dune field in the southern North Sea. *Journal of Geophysical Research: Earth Surface*, 130(1), 2025.

Long-Term Interaction Between Offshore Sand Banks and the Active Beach

Sebastian Dan[1], Toon Verwaest[1], Rik Houthuys[2], Arvid Dujardin[2], Abdel Nnafie[3], Björn Röbke[4], Anouk de Bakker[4], Bart De Maerschalck[1]
[1]Flanders Hydraulics, Government of Flanders, Antwerp, Belgium
[2] Antea Group, Belgium
[3] Institute for Marine and Atmospheric research Utrecht (IMAU), Utrecht University, The Netherlands
[4]Department of Applied Morphodynamics, Deltares, The Netherlands

Corresponding author: sebastian.dan@mow.vlaanderen.be

Keywords: sand banks, century scale, active beach, morphological evolution, numerical modelling

1 Introduction

For most sandy coastlines around the world, the offshore limit of the active beach function as a sink for sediments. The Belgian coast differs due to a unique system of sandbanks, primarily located offshore, that continuously interacts with the active beach. Over the last millennium, this system supplied the beach with significant volumes of sand. However, especially in the last century, this source of sand has diminished due to the strong influence of human activities. Project MOZES (MOrfolgische interactie kustnabije ZEebodem en Strand) [1] was setup to investigate and quantify the evolution of two types of sand banks in relation with the nearshore area: shoreface-connected sand ridges (SFCR) and tidal sand ridges (TSR) (Fig. 1).

2 Methods

Firstly, a detailed morphological analysis of the inner shelf and nearshore areas was performed using maps from 1804, 1866, 1908, 1938, 1970s, and 1980s and 1990s, 2010s and 2022. Secondly, idealized numerical modelling was developed to simulate the evolution of SFCR and TSR on the shelf. Thirdly, process-based numerical modelling (using Delft3D Flexible-Mesh FlemCo and TELEMAC Scaldis-Coast) was employed to investigate the hypothesis of natural sand feeding of the active beach from the sandbanks.
Lastly, the nearshore area was analysed, accounting for volumes extracted or deposited, based on yearly topo-bathymetric maps from the past 30 years. Additionally, for some parts of the coast, a 1D numerical model (ShorelineS) was applied.

3 Results

In the offshore inner shelf, no systematic movement of TSR has been observed, although some sediment loss has occurred. In the nearshore zone (7 km wide), SFCR migration towards the shoreline and general shallowing are evident, with a gradual 4 km-wide transition zone between the nearshore and offshore areas. The attachment points of the SFCR to the coast have not shifted, but the shoreface migrates landward at rates similar to SFCR migration, resulting in coastal squeeze. The nearshore zone is restricted from migrating inland, leading to a loss of accommodation space. Combined with the long-term shoreward movement of sandbanks, this could result in channel deepening.
The large-scale morphological changes observed between 1804 and 2022 are most probably the result of natural processes, driven by hydrodynamics and ongoing sea-level rise. A generalized response to sea-level rise seems to be the accumulation of sand towards the coast.
The cutting of navigation channels across the nearshore sandbanks has depleted the downdrift (eastward) part of the affected sandbanks, which likely also deprives the downdrift beach of sand supply. Due to flow constriction, scour channels have developed at the seaward side of the new harbor dams that protrude into the nearshore area. Simultaneously, sedimentation occurs at both sides of the new harbor dams.

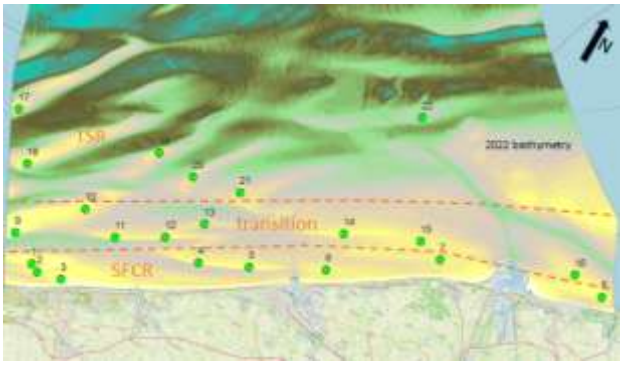

Figure 1: Belgian shelf and distribution of the sand banks. The green dots are locations where in depth morphological analysis was performed.

4 Future developments

The idealized numerical model successfully reproduces a realistic ridge configuration, and ongoing developments aim to enhance the coupling between the shelf and shoreline areas. In general, the process-based models accurately replicate the observed morphological changes, with further improvements focusing on erosion and accretion around harbour dams, as well as cross-shore transport.

Modelling the Morphodynamic Response to Sand Extraction from Tidal Sandbanks in Sediment-Scarce Environments

Sem J. Geerts[1], Pieter C. Roos [1], Suzanne J.M.H. Hulscher[1]

[1]University of Twente, Enschede, Netherlands

e-mail corresponding author: s.j.geerts@utwente.nl

Keywords: *marine sand extraction; tidal sandbanks; idealised modelling; sediment scarcity; continental shelf*

1 Introduction

Tidal sandbanks are large-scale bedforms with heights of 5-30 m, lengths of 5-60 km and crest spacing of 2-15 km [1] and tend to exist in sandy continental shelf seas throughout the world, e.g., the North Sea, East China Sea and Irish Sea. They can form when tidal flow velocities are sufficiently large, and evolve on a centennial timescale. Tidal sandbanks have been explained as free instabilities of a flat, sandy seabed subject to tidal flow [3].

Marine sand is needed for coastal nourishments, land reclamation and the construction industry. However, in some marine systems, the total amount of sand is limited and depleting. This includes the Belgian Continental Shelf (BCS), located in the Southern Bight of the North Sea, where most of the sand that is available is located in tidal sandbanks [2]. The underlying clay layer is exposed in the troughs between the banks, often together with gravel. In turn, sandbanks form attractive locations for sand extraction and a significant portion of mined sand is extracted from sandbanks. However, these extractions may threaten the morphological balance of the environment with adverse impacts on future sand stocks, sediment quality, foundations of wind farms and protected Natura 2000 areas. Here we present an idealised process-based modelling study that aims to understand the morphodynamic response to sand extractions from tidal sandbanks, in sediment-scarce systems such as the BCS.

2 Methodology

Our model, based on Van Veelen et al. [4], focuses on the cross-sectional dynamics of a tidal sandbank, assuming no variation in the along-crest direction of the bank. The flow is modelled by the depth-averaged shallow water equations. The model formulation allows for a residual current and an asymmetric tide, and the hydrodynamics are solved using a spectral method. The model employs periodic boundary conditions, and the domain length and bank orientation are equal to the fastest-growing mode that results from linear stability analysis.

Sediment transport is modelled as bedload only, as it is considered the dominant transport mode for sandbank formation. Contrary to Van Veelen et al. [4], the bedload transport is solved in physical space using a finite volume approach.

Our approach consists of two stages. First, the system starts from a flat bed, with a sediment layer on top of a non-erodible layer, and is run until a dynamic equilibrium is attained. Second, sand is extracted from the sandbank, creating a sandpit, and the morphodynamic response is examined (see Figure 1).

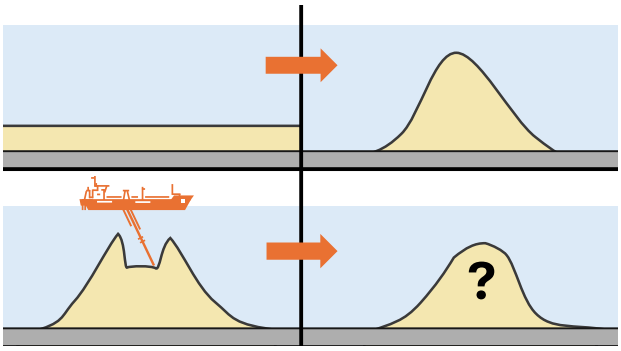

Figure 1: Schematisation of the model approach and results. Top: tidal sandbank forming as free instability from a flat bed, and then evolving to an equilibrium in a sand-scarce environment. Bottom: Morphodynamic response to sand extraction from the crest.

3 Results

First model results show how tidal sandbanks develop on non-erodible layers and results are compared to earlier results obtained with suspended load only [4]. Furthermore, we investigate the influence of tidal ellipticity on the cross-sectional shape. Lastly, we show how - after extraction - the system evolves to a new equilibrium shape. If the extracted sand is taken out of the system, this new equilibrium differs from the initial equilibrium.

References

[1] K.R. Dyer and D.A. Huntley. The origin, classification and modelling of sand banks and ridges. *Cont. Shelf. Res.*, 19(10):1285–1330, 1999.

[2] V. Hademenos, J. Stafleu, T. Missiaen, L. Kint, and V.R.M. Van Lancker. 3D subsurface characterisation of the Belgian Continental Shelf: a new voxel modelling approach. *Neth. J. Geosci.*, 98: e1, 2019.

[3] J.M. Huthnance. On one mechanism forming linear sand banks. *Estuar. Coast. Shelf. S.*, 14(1): 79–99, 1982.

[4] T.J. van Veelen, P.C. Roos, and S.J.M.H. Hulscher. Modeling the cross-sectional dynamics of tidal sandbanks in sediment-scarce conditions. *J. Geophys. Res.: Earth Surf.*, 129(4), 2024.

Predicting decadal evolution of coastal morphodynamics: A case study on the Belgian Continental Shelf

Yagiz Arda Cicek[1], Jaak Monbaliu[1], Erik Toorman[1], Víctor Cartelle[2], Ruth Plets[2], Tine Missiaen[2], Zoë Vanbiervliet[3], Soetkin Vervust[3], Christian Schwarz[1]
[1]KU Leuven, Belgium – [2]Flanders Marine Institute (VLIZ), Belgium – [3]Vrije Universiteit Brussel, Belgium
Corresponding author: yagizarda.cicek@kuleuven.be

Keywords: coastal modelling, coastal morphodynamics, morphological acceleration

1 Introduction

Predictions of long-term coastal morphological changes remain a major challenge. The modelling may not only be computationally demanding but it also raises questions about uncertainties in future forcing. Incorporating the impacts of intermittent extreme events, such as storms, remains particularly difficult. In this study, we further develop the combination of input reduction for waves, storm surges and tides with the online morphological acceleration method (MORFAC) [1], and assess their impacts on the predictive capability of a state-of-the-art hydro-morphodynamic model using the Belgian Coast as a case study.

2 Methodology

In the present study, the online coupling of TELEMAC2D (tides and wind-induced currents), TOMAWAC (waves) and GAIA (sediment transport and morphology) is used to predict coastal morphodynamics. The wave breaking term is modified following [2]. The new implementation provides better wave height estimations, especially during storm conditions. To determine the most robust MORFAC approach, a comparison was made between a 10-year-long "real-time" validated simulation (with non-schematized boundary conditions) and a parameter study on morphological upscaling. Subsequently, 28 MORFAC scenarios were tested, each representing different configurations of historical wave climate, storm surge conditions [3], astronomical tides, and MORFAC value. The morphological evolution from these 28 scenarios is compared to the 10-year reference run by means of a Brier Skill Score (BSS) and matching erosion-deposition points (except for the intertidal zones). The best MORFAC model obtained from this comparison was used to hindcast 38 years of coastal evolution of the Belgian Coast between 1984 and 2022 [4].

3 Results

Preliminary results indicate that the choice of the MORFAC value (during calm and storm conditions) and the way the schematized random wave time-series is constructed are the most influential, while the inclusion of parameterized directional storm surges has a secondary role outside the nearshore. The best model prediction with a BSS of 0.96 consisted of a MORFAC of 30 which was constant during 6 storm and 12 calm conditions and a schematized storm surge. The optimized MORFAC model was then used to assess the coastal evolution of Belgium between 1984 – 2022. This model can correctly reproduce the main patterns and magnitude of 38 years of morphological change, except for the migration of a nearshore shore-parallel sand ridge, the Stroombank. After a careful analysis, the mismatch in the Stroombank's migration has been linked to cross-shore wave-induced sediment transport being intensified during storms. The issue was solved by adjusting the sediment advection velocity following [5], and the bedload transport vector direction. This approach was validated by comparing the measured and modelled long-term morphological evolution data.

4 Conclusion

The MORFAC implementation appears robust but morphological results show sensitivity mainly to wave schematization and MORFAC values under the current GAIA formulations, while storm-surge schematization has minimal impact. Although a proper schematization improves the accuracy, missing processes such as the cross-shore sediment transport may limit the predictive performance in shallow areas.

Acknowledgments

The project 'TESTEREP" is part of the Strategic Basic Research (SBO) program of the Research Foundation - Flanders (FWO). The resources and services used in this work were provided by the VSC (Flemish Supercomputer Center), funded by the FWO.

References

[1] J. A. Roelvink, "Coastal morphodynamic evolution techniques," *Coast. Eng.*, vol. 53, no. 2–3, pp. 277–287, 2006, doi: 10.1016/j.coastaleng.2005.10.015.

[2] M. Pezerat, X. Bertin, K. Martins, B. Mengual, and L. Hamm, "Simulating storm waves in the nearshore area using spectral model: Current issues and a pragmatic solution," *Ocean Model.*, vol. 158, no. December 2020, p. 101737, 2021, doi: 10.1016/j.ocemod.2020.101737.

[3] L. Pineau-Guillou, J. M. Delouis, and B. Chapron, "Characteristics of Storm Surge Events Along the North-East Atlantic Coasts," *J. Geophys. Res. Ocean.*, vol. 128, no. 4, pp. 1–16, 2023, doi: 10.1029/2022JC019493.

[4] A. Dujardin *et al.*, "MOZES – Research on the Morphological Interaction between the Sea bottom and the Belgian Coastline: Working year 1. Version 4.0. FH Reports, 20_079_1. Flanders Hydraulics: Antwerp," 2023.

[5] E. Fonias *et al.*, "Implementation of cross-shore processes in GAIA," *Proc. Pap. Submitt. to 2020 TELEMAC-MASCARET user Conf. - Oct. 2021*, pp. 138–143, 2021, [Online]. Available: http://0.5.78.221

High-resolution morphodynamic evolution of a dune field in the macro-tidal bay of Somme (France)

Tatiana Goulas[1,2], Julien Deloffre[2], Nicolas Huybrechts[1, 3], Sophie Le Bot[2], Romain Levaillant[2], Jérémy Mahieu[2]
[1]Cerema REM, RHITME Research Team, Margny Les Compiègne, France
[2]Univ Rouen Normandie, Université Caen Normandie, CNRS, Normandie Univ, M2C UMR6143, Rouen, France
[3]Univ Rouen Normandie, Université Caen Normandie, CNRS, Normandie Univ, M2C UMR6143, Margny Les Compiègne, France
Corresponding author: tatiana.goulas@cerema.fr

Keywords: high-resolution morphodynamics, coastal sediment transfers, macrotidal bay, Somme bay

1 Introduction

Bays in the English Channel face ebb-tide delta erosion and intertidal sand infilling, intensified by climate change-driven shifts in hydro-meteorological and marine dynamics [1]. This work studies the temporal variability of coastal sediment transfers by analyzing hydro-sedimentary dynamics in the Somme bay's intertidal area through in situ measurements over a year, focusing on dune field dynamics.

2 Study site

The Somme Bay is continuously shaped by strong tidal currents and prevailing wave conditions, with limited human impact. It is infilling with marine sands (D50 of 230µm) from the subtidal supply, though some sectors are eroding over periods shorter than two years [2]. The study site is in the southern intertidal area, covered with small dunes (20-60cm high, 6-22m wavelength) [2], at elevations about 3.30m (Chart Datum).

3 Methods

Two cross-shore aligned moorings, 360 m apart, have been deployed at the study site since October 2024.

3.1 Deployed sensors on moorings

Each mooring includes five sensors set up to acquire high-frequency measurements for one year: pressure (RBR), bed elevation (ALTUS echosounder), turbidity (OBS) and currents velocities (ADCP and ADV).

3.2 Topographic and sediment measurements

LiDAR data provide topographic information at monthly intervals of the study site. The flight-covered area is 340m wide and 750m long, centred on the moorings. Simultaneously, sediment samples are collected along transects near each mooring.

4 Objectives and preliminary data

All collected data are compared over time and between the two study sites. Local-scale interactions between waves, currents, morphodynamic structures, and sediment fluxes will be analyzed, along with variations in sediment fluxes over storm events, tidal cycles, spring-neap cycles, and seasonal cycles. Preliminary data already provide insights into sediment dynamics at the study site (Figure 1).

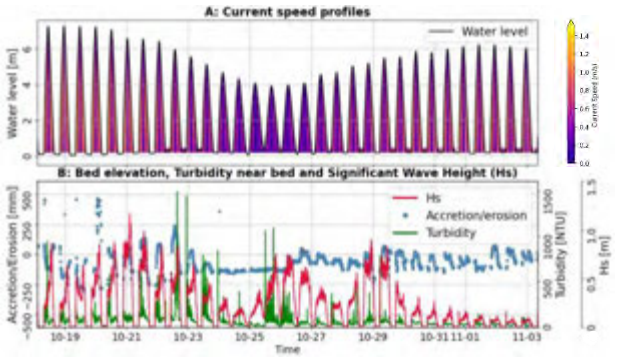

Figure 1: Hydrosedimentary dynamics evolution over a fortnight at the study site, Oct.-Nov. 2024.

5 Conclusion

A year-long high-frequency monitoring captures tidal, wave, and seasonal variations, identifying key drivers of sediment fluxes under diverse hydro-meteo-marine conditions. Characterizing these conditions and their influence on sediment transfer scenarios will provide valuable insights into sediment budget evolution, quantified at the bay scale over the past decade [2, 3].

Acknowledgments

We thank all contributors to data collection. This work is partly funded by the Clim-Adapt PRISME project.

References

[1] B. Van Vliet-Lanoë, A. Penaud, A. Hénaff, C. Delacourt, A. Fernane, J. Goslin, B. Hallégouët and E. Le Cornec. Middleto late-Holocene storminess in Brittany (NW France): Part II – The chronology of events and climate forcing. The Holocene 24, 434-453, 2014

[2] C. Michel. Morphodynamique et transferts sédimentaires au sein d'une baie mégatidale en comblement (Baie de Somme, Manche Est). Stratégie multi-échelles spatio-temporelles. Thèse de doctorat, Université de Rouen, 325 p., 2016

[3] T. Goulas, S. Le Bot, J. Deloffre, N. Huybrechts, I. Turki, L. Froideval, C. Conessa, O. Monfort and E. Salameh. Morphodynamic variability of the Somme Bay from seasonal to pluriannual scale in response to hydrodynamic forcings, 21st Physics of Estuaries and Coastal Seas Conference, Bordeaux, 2024

The role of outwash on barrier evolution: how shoreface-dune couplings influence barrier recovery

Katherine Anarde[1], Alexis Van Blunk[1], A. Brad Murray[2], Laura J. Moore[3], Christopher Sherwood[4]
[1]North Carolina State University, Raleigh, NC, USA, [2]Duke University, Durham, NC, USA
[3]University of North Carolina at Chapel Hill, Chapel Hill, NC, USA, [4]U.S. Geological Survey, Woods Hole, MA, USA
Corresponding author: kanarde@ncsu.edu

Keywords: barrier islands, outwash, overwash, dunes

1 Introduction

Outwash is the process by which elevated bay-side water levels overtop low-lying dunes, resulting in a seaward directed flow of water and sediment. While infrequent, outwash is an erosive process that scours the interior of barrier islands as flow is channelled through dune gaps. The occurrence of outwash has been well documented in the aftermath of storms, particularly along barrier systems backed by large estuaries [1]. However, the fate of outwashed sediment on the shoreface and in the nearshore environment is unknown, as is the role of outwash in barrier evolution.

2 Model

Here we modify an existing barrier evolution model, the CoAStal Community lAndscape Evolution Model (CASCADE)[2], to assess the evolutionary impact of outwash on barrier dynamics. Outwash is simulated in CASCADE using a cellular flow routing algorithm where slope drives the amount of flow and sediment distributed to downstream cells [3]. The model is tuned to best match real-world examples of outwash features from North Core Banks, North Carolina, USA following Hurricane Dorian in 2019 (Figure 1). We use the model to examine how barrier recovery following outwash events is influenced by subaqueous and subaerial factors, including 1) the degree to which outwashed sediment is incorporated in the shoreface, and 2) how quickly dunes recover following an outwash event.

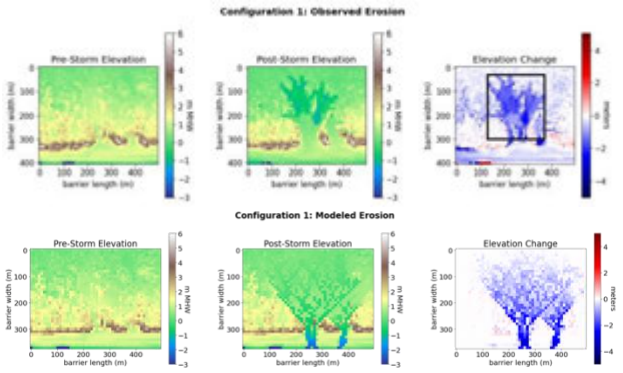

Figure 1: Sediment transport parameters were tuned to best match observed erosion volumes from outwash features following Hurriane Dorian (2019).

3 Results and Conclusions

We tested three scenarios for washout placement on the shoreface – 100% (i.e., all sediment remains in the cross-shore barrier system), 50% (i.e., some sediment is lost from the cross-shore barrier system), and 0% (i.e., all sediment is lost) – and two scenarios for dune recovery (a high and low dune growth rate) for a single initial barrier configuration. Stochasticity in dune-storm interactions was accounted for by running each outwash scenario for 100 overwash storm sequences.

Model simulations show that the more outwash that stays in the cross-shore barrier system (via integration into the shoreface), the less likely the barrier is to drown or be incised by subsequent outwash events (here, spaced every 20 years) as the beach/upper shoreface provides a buffer for dunes to recover. Similarly, higher dune growth rates enhance recovery in dune gaps and therefore promote resilience to the erosional effects of subsequent outwash events. Importantly, there is a tradeoff between dune growth and overwash. While barriers with higher dune growth rates are less vulnerable to subsequent outwashing events, they receive less overwash due to faster dune recovery and are therefore lower and narrower than the barriers with lower dune growth rates.

References

[1] Over, J.-S. R., Brown, J. A., Sherwood, C. R., Hegermiller, C. A., Wernette, P. A., Ritchie, A. C., & Warrick, J. A. (2021). A survey of storm-induced seaward-transport features observed during the 2019 and 2020 hurricane seasons. *Shore and Beach*, *89*(2), 31–40.

[2] Anarde, K. A., Moore, L. J., Murray, A. B., & Reeves, I. R. B. (2024). The future of developed barrier systems: 1. Pathways toward uninhabitability, drowning, and rebound. Earth's Future, 12, e2023EF003672. https://doi.org/10.1029/2023EF003672

[3] Murray, A. B., & Paola, C. (1994). A cellular model of braided rivers. *Nature*, *371*(6492), 54–57. https://doi.org/10.1038/371054a0.

Spit Responses to a Severe Storm

Drude F. Christensen[1,2], Anna Adell[2,3], Aart Kroon[2]
[1]DHI A/S, Hørsholm, Denmark
[2]University of Copenhagen, Denmark
[3]Lund University, Sweden
Corresponding author: dc@ign.ku.dk

Keywords: sand spits, storm event, morphodynamics, structure-from-motion (SfM)

1 Introduction

Coastal spits are narrow, elongated landforms of low elevations. Spits are highly dynamic and during storm events of elevated water levels and high waves, they are vulnerable to erosion, overwash, breaching, and inundation [1]. On undisturbed coastlines, overwash makes an important sediment input to the system which is key for spits ability to keep up with predicted future sea level rises. Contrary, breaches often act as sediment sinks. Being able to predict overwash and breach occurrence is thus of great importance for coastal management. Based on the storm surge Babet (2023), we assess the predictive capability of two storm impact models [2,3], and the cross-shore sediment exchange associated with washover fans at two Danish spits (Figure 1).

2 Babet storm event

During the storm surge Babet on October 19-21, 2023, strong easterly winds with mean speeds of up to 20 m/s resulted in offshore wave heights of up to 3 m at the field sites (Figure 1). At the same time, surge levels of up to 2 m occurred as a result of seiching in the Baltic Sea. The event resulted in numerous cases of extreme beach erosion, damaged houses and infrastructure, and a number of overwashes in southeastern Denmark.

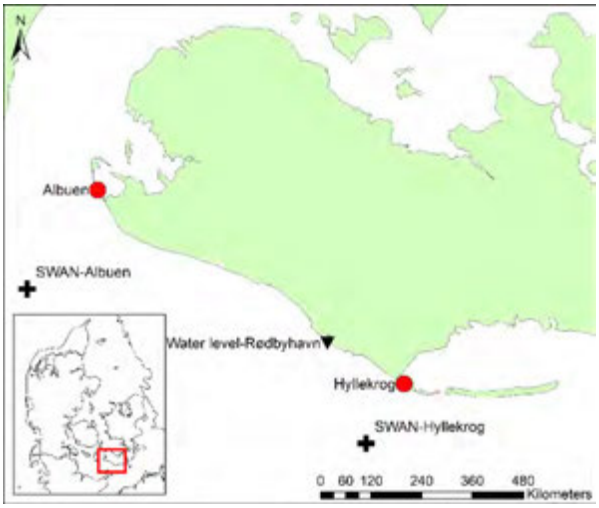

Figure 1: Map of Denmark and Lolland (in red square). Red dots showing field sites. Tide gauge and wave data points marked by black triangle and crosses.

3 Overwash fans and breaches

Storm impact predictions [2,3] are assessed based on pre-storm beach morphology using a lidar-derived digital elevation model (DEM) from 2022 together with measured water levels, and modeled nearshore wave heights using a calibrated and validated SWAN wave model [4]. Predicted washover fan volumes [3] are compared to quantified sediment budgets. These are calculated based on elevation changes between the 2022 DEM and post-storm elevations found from SfM image processing on drone images [5]. Figure 2 shows an example of pre- and post-storm images including estimated volume changes.

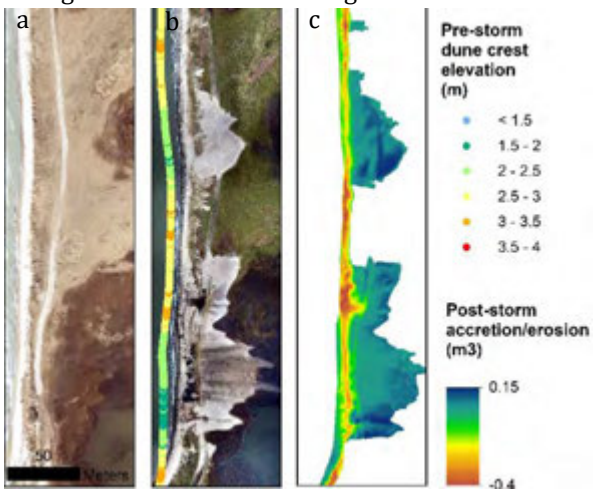

Figure 2: Pre- (a) and post-storm (b) images from Albuen and estimated volume changes (c).

References

[1] C. Donelly, N. Kraus and M. Larson. State of Knowledge on Measurement and Modeling of Coastal Overwash. *Journal of Coastal Research*, 22, 2006.

[2] A.H. Jr. Sallenger. Storm Impact Scale for Barrier Islands, *Journal of Coastal Research*, 16, 2000.

[3] J.H. Nienhuis, L.G.H. Heijkers and G. Ruessink. Barrier Breaching Versus Overwash Deposition: Predicting the Morphological Impact of Storm on Coastal Barriers, *JGR: Earth Surface*, 2021.

[4] A. Adell, B. Almström, A. Kroon, M. Larson, C.B. Uvo and C. Hallin. Spatial and temporal wave climate variability along the south coast of Sweden during 1959-2021, *Regional Studies in Marine Science*, 63, 2023.

[5] L.Ø. Hansen, V.B. Ernstsen, L.B. Clemmensen, Z. Al-Hamdani and A. Kroon. A method for estimating sediment budgets of washover deposits using digital terrain models. *Earth Surface Processes and Landforms*, 41, 2021.

Assessment of the intermittency of river mouths using cloud-enabled Earth observation analysis

Marcus Silva-Santana[1], Juan Del-Rosal-Salido[1], María Bermúdez[1], Miguel Ortega-Sánchez[1]
[1]Andalusian Institute for Earth System Research, University of Granada.
Corresponding author: marcussanta@ugr.es

Keywords: Intermittently open/closed rivers, remote sensing, coastal morphodynamics

1 Introduction

Intermittently open/closed river mouths are found at river systems where the simultaneous action of marine and riverine drivers leads to the formation of intermittent sedimentary bars. These bars can generate issues related to the services the river provide (ecological, economical, navigation, etc) and their study normally rely on locally driven and high-cost techniques such as numerical models or in-situ measurements.

This paper presents a satellite-based methodology for detecting the state of river mouths (open/closed). In contrast to current satellite-based tools for similar purposes [1], the workflow presented was developed on a cloud computation environment (Google Earth Engine) which allowed its application to the entire Spanish mediterranean coast (approx. 1500 km) where more than 40 intermittently open/closed river mouths were detected. Results show a good agreement with observations. Open/closed states were compared to hydro-oceanic drivers and morphological features, enhancing current understanding of intermittent river bar dynamics.

2 Data and Methods

Intermittently open/closed rivers were detected through open access high resolution satellite imagery from Google Earth. Once these rivers were detected, the river channel was digitalized. An index-based workflow was applied to each river using Sentinel-2 catalogue. The workflow is based on NDWI index for water pixel classification and subsequent detection of the hydraulic connection between the maritime zone and the river channel. The time cover ranges from 2017-2023 with a temporal resolution of 15 days and image pixel dimension of $10m^2$.

Rainfall is used as a proxy of river discharge at the study zone. Rainfall information was gathered from AEMET stations. Marine levels (wave height and surge) are obtained at 10km resolution from a hindcast model database [2]. Geomorphic information such as river width, basin area, river mouth slope and elevation nearshore were directly obtained or derived from the Ministry for the Ecological Transition and the Demographic Challenge (MITECO) and National Geographic Institute (IGN) databases.

3 Results

Figure 1 show an example of the correlation between closure mean times and hydro-oceanic drivers (Fig 1a) and geomorphic features (Fig 1b).Result shows that less intense rainfall regimes are linked to river systems more often closed. Additionally, river systems with higher river mouth slope are prone to be open more time. These preliminary results shows that the applied methodology is capable of detecting bar breaching at analysed river systems as a result of river discharge action. Additional and complementary results will be presented at the Conference.

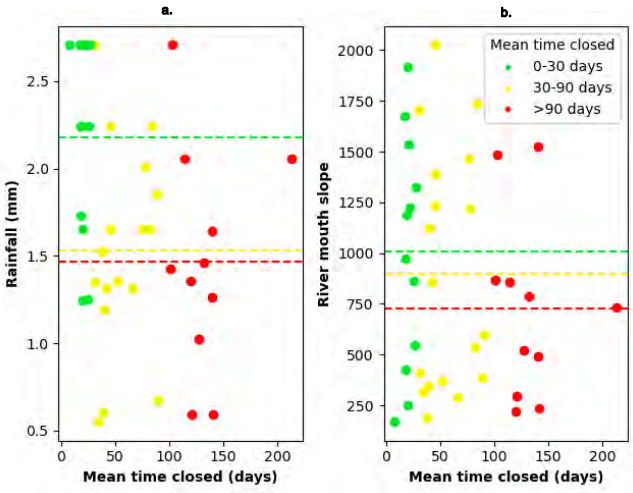

Figure 1: Correlation between rainfall and river mouth slope with mean river time close. Mean times are grouped into three categories. Horizontal dashed lines represent averaged values.

Acknowledgments

This publication is part of the R&D project PLEC2022-009362, funded by MCIN/ AEI/10.13039/51100011033/ and by the European Union NextGenerationEU/PRTR.

References

[1] Heimhuber, V., Vos, K., Fu, W., & Glamore, W. (2021). InletTracker: An open-source Python toolkit for historic and near real-time monitoring of coastal inlets from Landsat and Sentinel-2. Geomorphology, 389.

[2] Toomey, T., Amores, A., Marcos, M., & Orfila, A. (2022). Coastal sea levels and wind-waves in the Mediterranean Sea since 1950 from a high-resolution ocean reanalysis. Frontiers in Marine Science, 9.

Assessing the impact of sand fences on foredune development in high urban beach: A four-year study of Calafell Beach (Costa Daurada, Spain)

Carla Garcia-Lozano[1], Francesc Xavier Roig-Munar[1,2], Aron Marcos[3], Josep Pintó[1]
[1]Universitat de Girona, Girona, Spain
[2]Coastal manager
[3]Councilor for Urban Ecology in Calafell City Council

Corresponding author: carla.garcia@udg.edu

Keywords: 1. Dune restoration, nature-based solutions, coastal resilience, sediment retention, urban beach management.

1 Introduction

Coastal dunes are dynamic ecosystems shaped by wind-transported sediments and human interventions. Historically, they have been managed to protect coastlines from erosion, but they have suffered significant degradation due to tourism and urbanization [1]. In this context, the study analyses geomorphological changes and management practices at Calafell beach (Costa Daurada, NE Spain) over four years. The beach stretches approximately 6 kilometers and is divided into two sections: Llevant Beach, located east of the port, and Ponent Beach, situated to the west. Calafell's economy is highly dependent on beach tourism, with its 27,000 permanent residents seeing their numbers triple during the summer, weekends, and holidays, reflecting the town's strong seasonal tourism influx.

2 Methodology

This study investigated the geomorphological changes of the foredune between 2020 and 2024 following the implementation of recovery-oriented management measures. The sand traps constructed in 2020 have dimensions of 10-15 meters in length, with a 50-60% porosity and a height of 70 cm, a width between 10 and 15 meters each, and orientated SSE. The study used digital elevation models (DEM) obtained from unmanned aerial vehicles (UAVs). UAV flights occurred in 2020 and in 2024, before and after the implementation of management measures. Analyses focused on sediment accumulation, including variations in dune height (Average height (AH), maximum height (maxH), and minimum height (minH)) and volume development (Vol).

3 Results and discussion

Llevant Beach has been the most positively impacted by the sand fences, with over 1,000 m^3 of sediment accumulated (Figure 1), particularly in the wind retainer test field, which alone retained nearly 500 m^3 over three years. This significant accumulation is mainly attributed to the presence of the test field and the protection provided by the port during Storm Nelson on March 27, 2024, which approached from the SSW direction.

Figure 1: Sediment gain in the foredune of Llevant Beach from 2020 to 2024.

In contrast, Ponent Beach (Figure 2) was directly exposed to the storm, leading to sediment deficits of approximately 500 m^3 in some areas with sand fences. These same areas had shown positive sediment balances of 400 m^3 the previous year, indicating that without the implementation of nature-based solutions, sediment loss in Llevant Beach would have been significantly higher.

Figure 2: Sediment loss in the foredune of Ponent Beach from 2020 to 2024.

References

[1] Garcia-Lozano, C., Pintó, J., & Daunis-i-Estadella, P. (2018). Changes in coastal dune systems on the Catalan shoreline (Spain, NW Mediterranean Sea). Comparing dune landscapes between 1890 and 1960 with their current status. *Estuarine, Coastal and Shelf Science*, 208, 235-247. https://doi.org/10.1016/j.ecss.2018.05.004

On the role of ripple secondary crest on nearbed hydrodynamics

Chuang Jin[1,2,6], Zheng Gong[3], Jorge E. San Juan[4], Tinoco O. Rafael[5], Giovanni Coco[6]
[1] Jiangsu Key Laboratory of Coast Ocean Resources Development and Environment Security, Hohai University, Nanjing, China
[2] Key Laboratory of Coastal Zone Exploitation and Protection, Ministry of Natural Resources, Nanjing, China
[3] State Key Laboratory of Hydrology-Water Resources and Hydraulic Engineering, Hohai University, Nanjing, China
[4] Department of Civil Construction and Environmental Engineering, North Carolina State University, Raleigh, North Carolina, US
[5] Department of Civil and Environmental Engineering, University of Illinois at Urbana-Champaign, Urbana, IL, US
[6] School of Environment, Faculty of Science, University of Auckland, Auckland, New Zealand
Corresponding author: c.jin@hhu.edu.cn

Keywords: Sand Ripples, Defects, Vortex, Turbulent, Wave friction factor

1 Introduction

The critical role of ripples in shaping bedform roughness and influencing the near-bottom flow structure has been extensively documented (e.g., Trowbridge and Lentz, 2018). The presence of ripples increases the turbulence and sediment resuspension within the bottom boundary layer.

Under naturally dynamic wave forcing conditions, ripples usually exhibit three-dimensional (3D) bedform features characterized by bedform defects, such as terminations, bifurcations, and secondary crests, reflecting their complex response to varying hydrodynamic conditions (Perron et al., 2018; Jin et al., 2022).

While considerable research has focused on the dynamic of ripple defects (Werner and Kocurek, 1999; Huntley et al., 2008), the intricate hydrodynamics associated with these defects remain poorly understood.

2 Method

Laboratory experiments were conducted in a U-shaped oscillatory tunnel at the Ecohydraulics and Ecomorphodynamics Laboratory, University of Illinois at Urbana-Champaign (USA). Two distinct fixed 3D-printed ripple morphologies were examined: uniform ripples and ripples with superimposed secondary crests. To replicate natural roughness, sand grains of sizes matching the ripple scale were adhered to the ripple surfaces.

Flow measurements were performed using Particle Image Velocimetry (PIV) in the central span of the oscillatory tunnel. Key flow parameters, including vorticity, turbulent kinetic energy (TKE), shear stress, and the wave friction factor, were calculated and compared across the two ripple geometries. These measurements allowed us to quantify the hydrodynamic impacts of secondary crest features on ripple-induced flow.

3 Results

The introduction of secondary crests significantly altered flow dynamics, not only over the modified ripple but also over adjacent ripples. Secondary crests generated a thicker boundary layer compared to uniform ripples. On the upstream side of the secondary crest, velocity profiles deviated substantially from the baseline uniform ripple case, while downstream effects were less pronounced.

Shear velocity at the crest of ripples with secondary features was notably higher, indicating an enhanced capacity for sediment transport and bedform evolution. Turbulent kinetic energy over ripples with secondary crests was approximately twice as high as that observed over uniform ripples. These findings demonstrate that hydraulic roughness is influenced not only by ripple height and wavelength but also by specific morphological structures, such as secondary crests.

References

[1] Huntley, D. A., Coco, G., Bryan, K. R., & Murray, A. B. (2008). Influence of "defects" on sorted bedform dynamics. *Geophysical Research Letters*, 35(2), L02601.

[2] Jin, C., Coco, G., Tinoco, R. O., Ranjan, P., Gong, Z., Dutta, S., San Juan, J. E., & Friedrich, H. (2022). High-Resolution Large Eddy Simulations of Vortex Dynamics Over Ripple Defects Under Oscillatory Flow. *Journal of Geophysical Research: Earth Surface*, 127(3), 1–24.

[3] Perron, J. T., Myrow, P. M., Huppert, K. L., Koss, A. R., & Wickert, A. D. (2018). Ancient record of changing flows from wave ripple defects. *Geology*, 46(10), 875–878.

[4] Trowbridge, J. H., & Lentz, S. J. (2018). The Bottom Boundary Layer. *Annual Review of Marine Science*, 10(1), 397–420.

[5] Werner, B. T., & Kocurek, G. (1999). Bedform spacing from defect dynamics. Geology, 27(8), 727–730.

Unraveling sediment transport by shallow waves over rippled beds: insights from particle-resolved Direct Numerical Simulation

Marco Mazzuoli[1]

[1]University of Genoa, Genoa, Italy

e-mail corresponding author: marco.mazzuoli@unige.it

Keywords: *wave turbulence; two-phase flow; vortex ripples*

1 Introduction

The sediment dynamics in the coastal shallow waters is significantly affected by the flow associated with non-breaking wind waves. Let us consider the problem of sediment transport caused by monochromatic wind waves propagating over a horizontal rippled bottom. While far from the bottom the flow is practically irrotational, most of the sediment is transported in the wave boundary layer (WBL) developing close to the bottom. Providing reliable predictions of the WBL flow is a formidable problem because (*a*) sediment and fluid dynamics are strongly coupled, (*b*) turbulence may appear in certain phases of the wave cycle with properties that depend on the sediment (concentration, size, density, shape) and wave characteristics (period, amplitude), (*c*) ripples can form and strongly affect the flow structure. Moreover, the wave surface can be also significantly affected by the WBL (e.g. wave attenuation). Indeed, the spatial and temporal scales of the coupled problem of wave propagation and sediment transport approximately range six orders of magnitude without any clear separation, which makes the numerical approach extremely challenging. Hence, for practical purposes, the WBL is often approximated by an oscillatory boundary layer (OBL), namely the flow close to the bottom driven by horizontal pressure gradient oscillations in the direction of wave propagation. In the present contribution, (*i*) the validity of the OBL approximation is first discussed in the light of an extreme direct numerical simulations (DNS) of the WBL. Finally, (*ii*) the wave sediment transport is characterised on the basis of a particle-resolved (PR) DNS of the OBL over a rippled bed of spherical sediments [1].

2 Methods

Two DNSs were carried out to achieve the objectives (*i*) and (*ii*), which are hereinafter referred to as DNS1 and DNS2, respectively. DNS1 consists of the free-surface simulation of wave propagation over a fixed wavy bottom. Waves characterised by length, height and period equal to 5.6 m, 0.3 m and 2.3 s, respectively, with mean flow depth equal to 0.7 m are considered. In DNS1, the Navier-Stokes equations in strong-conservation form are solved in a time-dependent domain by mapping the physical space into a rectangular parallelepiped via a non-orthogonal algebraic transformation. DNS2 is the simulation of the OBL approximating the WBL of DNS1 and developing over vortex ripples of spherical quartz particles of diameter equal to 0.25 mm. The incompressible Navier-Stokes equations are solved numerically using the semi-implicit second-order fractional-step method, based on the finite difference approximation of time- and space-derivatives. Periodic boundary conditions are enforced along the streamwise and spanwise directions, while no-slip and free-slip conditions are imposed at the bottom and top of the domain, respectively. In DNS2, the flow field is resolved around the individual sediment particles using the immersed boundary approach. The inter-particle contact forces are simulated with the discrete element method using a linear spring-dashpot contact law.

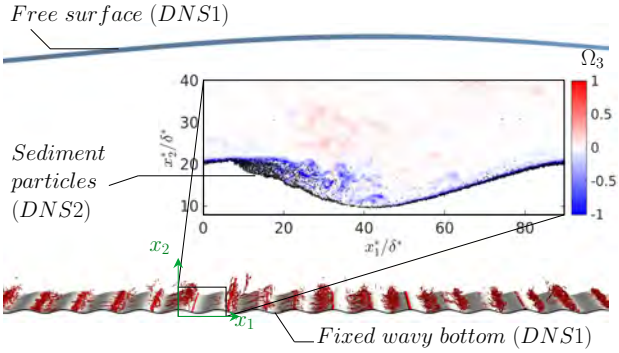

Figure 1: In the main panel, turbulent vortices developing underneath the wave crests, are visualised by isosurfaces of Q (DNS1). In the inset, the side view of the domain about a single ripple is shown: black sediment particles are set into motion by the vortices shed from the ripple crest. Dimensionless spanwise vorticity component Ω_3 is also shaded (DNS2).

3 Results and Conclusions

The main results of the present contribution are (*I*) the distribution of the stresses over a rippled bottom for values of the wave parameters such that the turbulence appeared at the bottom, (*II*) the fair comparison of the bottom shear stress obtained from the DNS either of the WBL (DNS1) or of the corresponding OBL, (*III*) the evaluation of the mass transport associated with the currents developing in the WBL, (*IV*) the interaction between the turbulent vortices shed by the ripple crests and the sediment particles, (*V*) the evaluation of the sediment transport and the ripple evolution during the wave cycle [1].

References

[1] Marco Mazzuoli, Paolo Blondeaux, and Giovanna Vittori. Particle-resolved direct numerical simulation of the oscillatory flow and sediment motion over a rippled bed. *International Journal of Multiphase Flow*, 172:104707, 2024.

Biofilms as the "ecosystem engineers": the microbiological mediation of intertidal sediment behavior

Xindi Chen[1]
[1]Hohai University, Nanjing, China
Corresponding author: chenxindi1991@hhu.edu.cn

Keywords: Sediment behavior, erosion, biofilms, bed stability, bio-physical interaction

The term “ecosystem engineering” emerged in the 1990s, which commonly refers to the activities of larger organisms like mangroves. However, while people think that bigger organisms generate bigger potential engineering effects, there may be microscale organisms who can result in significant impacts on the ecosystems through their number rather than their size. Currently, cohesive extracellular polymeric substances (EPS) generated by microorganisms have been widely reported to increase the threshold for sediment erosion by flowing water, which is known as “biostabilization”. However, most observations of this phenomenon have been taken under steady flow conditions. In contrast, we present how EPS affect the bed movement under wave action, showing a destabilization of the system. We demonstrate a complex behavior of the biosedimentary deposits, which encompasses liquefaction, mass motion, varying bed formations and erosion, depending on the amount of EPS present. Small quantities of EPS induce higher mobility of the sediments, liquefying an otherwise stable bed. Bed with larger quantities of EPS undergoes a synchronized mechanical oscillation. Our analysis clarifies how neglecting even low content of EPS can result in inaccurate prediction of the bed stability and coastal safety under wave action. The risk of bed liquefaction is expected to pose potential threats to wetlands where microbial communities occupy habitats while the production of EPS is much higher. The misinterpretation of the vulnerability of wetlands when exposed to waves could put the existing ecosystems at risk, considering that these ecosystem services are valued at about US$10,000 per hectare.

Figure 1: The examples of biofilm distribution on intertidal sediments. a) Awase intertidal, Okinawa, Japan, b) New Zealand, post-earthquake (the moment magnitude (Mw) 7.8 November 2016 Kaikōura earthquake) seafloor in the head of the Kaikōura Canyon, where bacterial mat (gray patch on the top right) on sediment surface, c) Green algal mat from Brays Bay, Australia. Note the bright green colour and how the mat is raised up compared with areas without a mat, where water pools. Small holes are crab burrows, d) Regular bedforms with ridges covered by Vaucheria algal mats and runnels without algal cover. Picture taken on 26 August 2016 at Ketenisse (around 51.284836°N, 4.312567°E), e) Wadden Sea, the Netherlands. The dark areas are mats of diatoms forming on sands, who create bubbles by photosynthesizing and producing oxygen, f) & g) Observation profile S4 & S5, Jiangsu Coast, China, h) Regularly patterned landscape of diatom-covered hummocks alternating with water-filled hummocks at the Intertidal flat Kapellebank, The Netherlands. i) Evidence of abundant microorganisms on tidal channel banks (Jiangsu coast, China; image taken by K. Zhao on July 2021).

References

[1] Chen, X., Kang, Y., Zhang, Q., Jin, C. & Zhao, K. Biophysical contexture of coastal biofilm-sediments varies heterogeneously and seasonally at the centimeter scale across the bed-water interface. *Front. Mar. Sci.* **10**, 1131543 (2023).

[2] Chen, X. et al. The Resilience of Biofilm-Bound Sandy Systems to Cyclic Changes in Shear Stress. *Water Resour. Res.* **58**, e2021W-e31098W (2022).

[3] Chen, X. et al. Biological Cohesion as the Architect of Bed Movement Under Wave Action. *Geophys. Res. Lett.* **48**, e2020G-e92137G (2021).

[4] Chen, X. et al. Hindered erosion: The biological mediation of noncohesive sediment behavior. *Water Resour. Res.* **53**, 4787-4801 (2017).

Sediment Dynamics in Coral Rubble Flats

Ana Vila-Concejo[1,2], Tristan Salles[1,2], Ana Paula da Silva[1,2], Maria Byrne[2,3]
[1] Geocoastal Research Group, School of Geosciences, The University of Sydney, Sydney, Australia
[2] Marine Studies Institute, Faculty of Science, The University of Sydney, Sydney, Australia
[3] School Life & Environmental Sciences, The University Sydney, Sydney, Australia
Corresponding author: ana.vilaconcejo@sydney.edu.au

Keywords: coral rubble, tropical storms, sediment transport, climate change

1 Introduction

Coral reef platforms are primarily composed of sedimentary deposits, including coral, sand, and rubble. Coral rubble refers to fragments of dead coral and other organisms and often represents evidence of coral destruction. However, coral rubble is a fundamental sedimentary component of coral reefs systems, formed through the constructive processes associated with tropical cyclones (TC) [1]. Climate change effects on coral reefs promote rubble formation [2] and decline of coral reef environments [2,3]. Despite its significance, the dynamics of coral rubble remain poorly understood and are the focus of this paper.

2 Coral Rubble at One Tree Reef

One Tree Reef (OTR), southern Great Barrier Reef, is located approximately 100 km offshore from NE Australia and only 20 km from the edge of the continental shelf. The reef is directly exposed to swells from the Pacific Ocean, with average significant wave height of 1.7 m and average peak period of 5.8 s; mean maximum wave heights during TCs reach 4-5 m [4].

Rubble-dominated environments are ubiquitous at OTR (Fig. 1). Coral rubble originating from the reef front is transported towards the lagoon by wave action [5]. Rubble changes are correlated with the frequency and/or intensity of TCs and with their proximity. For example, a Category 3 TC passing within 100 km of OTR caused greater changes than a Category 5 TC that remained several hundreds of kms away [6].

3 Rubble Dynamics

Coral rubble flats consist of sediment particles of heterogeneous shapes and sizes typically larger than sand. These particles often imbricate and interlock, hindering entrainment and transport. Previous research at OTR has found that rubble transport primarily occurs under high wave conditions and high tides, leading rubble deposits forming during TCs [7].

Here, we present the results from RFID tags on rubble clasts, deployed in November 2024 as a pilot study and in February 2025. Preliminary results show transport towards the island at the center of the reef tract, even under low-energy conditions. Ongoing hydrodynamic analysis includes in-situ wave data from pressure sensors and a Spotter wave buoy deployed in the nearshore environment.

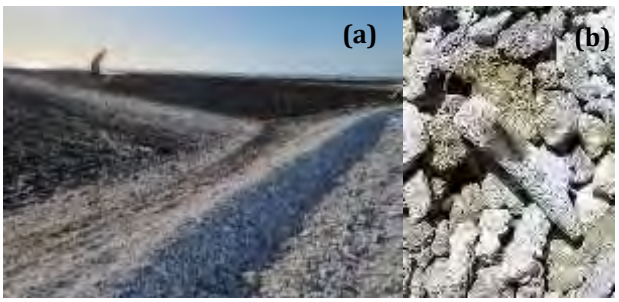

Figure 1: (a) A rubble flat in One Tree Reef. Rubble is white while subject to transport and turns brown once it settles. (b) Rubble clasts with RFID tags were deployed over the active rubble tracks.

Acknowledgments

Funding by ARC Discovery DP220101125 & Geoscience Australia. Much of the fieldwork was undertaken by students and volunteers. One Tree Island Research Station is a facility of the University of Sydney.

References

[1] A. Vila-Concejo and P.S. Kench, *Storms in coral reefs*, in *Coastal Storms: Processes and Impacts*, P. Ciavola and G. Coco, eds., John Wiley and Sons, 2017, pp. 127–144.

[2] T.M. Kenyon, C. Doropoulos, K. Wolfe, G.E. Webb, S. Dove, D. Harris et al., Coral rubble dynamics in the Anthropocene and implications for reef recovery, *Limnology and Oceanography* 68 (2023), pp. 110–147.

[3] M. Byrne, A. Waller, M. Clements, A.S. Kelly, M.J. Kingsford, B. Liu et al., Catastrophic bleaching in protected reefs of the Southern Great Barrier Reef, *Limnology and Oceanography Letters* n/a .

[4] C. Smith, A. Vila-Concejo and T. Salles, Offshore wave climate of the Great Barrier Reef, *Coral Reefs* 42 (2023), pp. 661–676.

[5] K.J. Thornborough and P.J. Davies, *Reef flats*, in *Encyclopedia of Modern Coral Reefs*, D. Hopley, ed., Springer, Netherlands, 2011, pp. 869–876.

[6] L. Talavera, A. Vila-Concejo, J.M. Webster, C. Smith, S. Duce, T.E. Fellowes et al., Morphodynamic controls for growth and evolution of a rubble coral island, *Remote Sensing* 13 (2021), .

[7] E. Woolsey, S. Bainbridge, M. Kingsford and M. Byrne, Impacts of cyclone Hamish at One Tree Reef: integrating environmental and benthic habitat data, *Marine Biology* 159 (2012), pp. 793–803.

3D evolution of the Millars River and shoreline changes on the surrounding beaches. Case of study in Castelló (E Spain)

Josep E. Pardo-Pascual[1], Carlos Cabezas-Rabadán[2,3], Jesús Palomar-Vázquez[2]
[1]CGAT research group, Dept. Cartographic Eng., Universitat Politècnica de València, Spain
[2]Univ. Bordeaux, CNRS, Bordeaux INP, EPOC, UMR 5805, F-33600 Pessac, France
Corresponding author: jepardo@cgf.upv.es

Keywords: fluvial sediment supply, aerial digital photogrammetry, satellite-derived shorelines, coastal erosion.

1 Introduction

The mouth of the Millars River is located 7 km south of the Port of Castelló, which begun its construction in 1893. This coast presents a strong dowdrift toward the south, which in combination with the artificial structures quickly started to lead to strong erosion [1]. This disequilibrium resulted in the implementation of coastal engineering actions. The last significant change (2003) came with the construction of a long (partly submerged) groin just to the north. The Millars River's final stretch forms a large prograding alluvial fan, mainly composed by coarse materials. This river is a classic braided Mediterranean intermittent riverbed, carrying mainly pebbles and gravel, and underwent gravel and aggregate extraction during the second half of the 20th century, which altered its natural fluvial bottom morphology. Sustained on remote methods, the present works jointly analyses the morphological evolution of the river final stretch and the evolution of the surrounding beaches over the last 40 years.

2 Methodology

The work is based on: (a) the 3D information of the river's last 4km stretch, for which the Digital Surface Models (DSMs) were obtained [2] from historical aerial photography from 1976, 2018, 2019, 2020, 2021 and 2022; and (b) the annual mean shoreline positions from 1984 based on more than 1000 satellite-derived waterlines (SDWs) from Landsat (5,7,8,9) and Sentinel-2 cloud-free imagery using SHOREX [3].

3 Results and conclusions

The sequence of average annual shorelines reveals a progressive accretion from 2003, reaching widths over 50 meters in some segments. This accumulation is unexpected given the location south (downstream) of the new breakwater, a cross-shore obstacle that typically disrupts the alongshore sediment transport, and that led to significant sediment accumulation at its northern part. In the final stretch of the Millars River, a notable excavation of the riverbed has occurred, deepening some areas by more than 5 m when compared to 1976 (Figure 1). This has resulted in the re-emergence of the river's dynamic braided morphology, characterised by fluvial bars and multiple channels. The low erosion rates observed on the southern beaches could be attributed to the extension of the breakwater, which provides protection against ENE swells. Additionally, the release of fluvial sediments during flood events supplies new material to the coastal system. However, the breakwater's presence weakens the southward sediment transport, causing much of this material to be retained near the river mouth, which can explain the significant beach accretion. Here, the morphological dynamism of the lower course of the river appears closely related with the sediment supply and the evolution of the surrounding beaches. This demonstrates the complementarity of both datasets for assessing the sedimentary state of the coast from a holistic perspective.

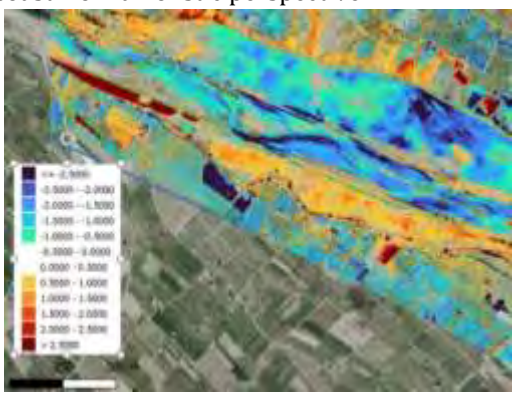

Figure 1: 3D evolution (DSM 2019-1976) of the river morphology 1.5 km upstream of the mouth.

Acknowledgments

SIMONPLA project from Thinkinazul programme supported by the MCIN with European Union Next GenerationEU (PRTR-C17.I1) and Generalitat Valenciana (GVA) funds; contract CIAPOS/2023/394 funded by the GVA and European Social Fund Plus.

References

[1] Mateu, J. F. El norte del País Valenciano: Geomorfología litoral y prelitoral. *València: Universitat de València*, 1982.

[2] Almonacid-Caballer, J. et al. Re-Using Historical Aerial Imagery for Obtaining 3D Data of Beach-Dune Systems: A Novel Refinement Method for Producing Precise and Comparable DSMs. *Remote Sensing*, 17(4), 594, 2025.

[3] Cabezas-Rabadán, C., Pardo-Pascual, J. E., Palomar-Vázquez, J., & Cooper, A. (2025). A remote monitoring approach for coastal engineering projects. Scientific Reports, 15(1), 2955.

Transition to turbulence close to a rough sea bottom

Giovanna Vittori [1], Paolo Blondeaux[1]

[1]DICCA, University o Genoa, Genoa, Italy

e-mail corresponding author: giovanna.vittori@unige.it

Keywords: *transition to turbulence, linear Stokes waves, viscous boundary layer, rough bottom.*

1 Introduction

As pointed out by [2], there are phenomena of great importance to coastal engineers that are affected by the flow regime within the boundary layer generated at the sea bottom by the propagation of surface waves. The sediment transport, the wave damping and the steady drift currents are just a few examples.

Since laboratory experiments by [2] showed that a laminar flow over a rough bottom made up of medium sand can be observed up to values of the Reynolds number equal to about 250, real situations exist such that the flow regime is laminar and the bottom can be considered hydrodynamically rough.

In the present contribution, using a simplified model for the oscillating boundary layer close to a rough bottom [1], the transition from the laminar regime to the turbulent regime is investigated by means of a linear stability analysis.

2 The problem and the results

The flow generated close to the sea bottom by the propagation of a surface wave can be approximated as the oscillatory flow close to a fixed wall. Hence, we consider the flow generated close to a rough horizontal wall by a uniform pressure gradient that oscillates in time. The continuity and two-dimensional momentum equations are written in dimensionless form using $1/\omega$ as time scale, $\delta = \sqrt{\frac{2\nu}{\omega}}$ as length scale and U_0 as velocity scale. In the definitions above, U_0 and ω are the amplitude of the velocity oscillations outside the bottom boundary layer and the angular frequency, δ is the thickness of the boundary layer and ν is the kinematic viscosity. . The vortices that are generated close to the bottom by the sediment grains are accounted for by introducing an eddy viscosity that vanishes far from the bottom. Moreover, the no-slip condition at the bottom is replaced by a partial-slip condition, to account for the presence of the bottom roughness. To investigate the stability of this basic flow, we determine the time development of a perturbation of small amplitude ϵ, superimposed to the basic flow. The momentum equation is written in terms of the streamfunction ψ that is expanded as a power series of ϵ:

$$\psi(x,y,t) = \psi_0(x,y,t) + \epsilon\psi_1(x,y,t) + \text{terms of order}\epsilon^2 \tag{1}$$

The problem at order ϵ suggests that ψ_1 should have the form:

$$\psi_1(x,y,t) = f(y)\exp\left[i\alpha\left(x - \frac{R_\delta}{2}\int c(\tau)d\tau\right)\right] + c.c. \tag{2}$$

where α is the wavenumber of the generic Fourier component of the perturbation and R_δ,the Reynolds number ($R_\delta = \frac{U_0\delta}{\nu}$), The complex-valued quantity c appearing in 2, describes the evolution of the perturbation. In particular, the real part c_r of c is the wave speed of the perturbation, while the imaginary part c_i describes its growth/decay. Figure 1 shows the time development of c_r and c_i for different values of the sediment diameter d. As expected, the bottom roughness favours transition to turbulence and the results allow to quantify the critical value of the Reynolds number as function of the roughness size.

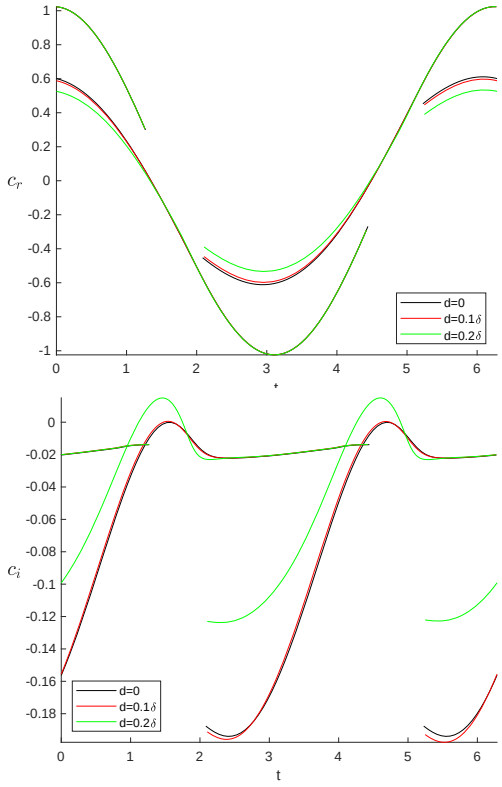

Figure 1: Time development of the real and immaginary part of c for $\alpha = 0.5$, $Re = 85$ and different values of sediment diameter d

References

[1] P. Blondeaux and G. Vittori. Wave boundary layer over a rough bottom at moderate Reynolds numbers. *Journal of Hydraulic Engineering*, 149 (6):04023013, 2023.

[2] J.F.A. Sleath. Transition in oscillatory flow over rough beds. *Journal of waterway, port, coastal, and ocean engineering*, 114(1):18–33, 1988.

Impacts of Extreme Storms on Urban Beaches: A Comprehensive Study of the Gloria Storm in Cala Millor, Balearic Islands

Àngels Fernàndez-Mora[1], Francisco Criado-Sudau[1], Elena Sánchez-García[1], Daniel Calvete[2]

[1]Balearic Islands Coastal Observing and Forecasting System (ICTS SOCIB), Palma, Spain
[2]Universitat Politècnica de Catalunya, Barcelona, Spain

e-mail corresponding author: mafernandez@socib.es

Keywords: *extreme wave storm, storm Gloria, coastal flooding, beach recovery*

1 Introduction

Rising sea levels and extreme storms intensify coastal erosion, flooding, and infrastructure damage, particularly on urban beaches with rigid defenses that restrict sediment movement (1). The 2020 Gloria storm caused severe shoreline retreat in Spain and France. This study integrates observational and numerical analysis to assess its impact on a semi-enclosed urban beach, focusing on shoreline evolution, hydrodynamics, and sediment dynamics. Findings are crucial for improving coastal resilience to extreme events and mitigating climate change-related hazards.

2 Data and Methods

Cala Millor, a 2 km semi-embayed urban beach on Mallorca's northeastern coast, features crescentic bars, rip channels, and a seagrass meadow. After Storm Gloria in February 2020, a field campaign was conducted to assess its impact. SOCIB beach monitoring facility, including a weather station, video cameras, and an AWAC profiler, facilitated high-resolution topobathymetric surveys. Shoreline data were extracted from video images, and the campaign focused on analyzing wave and currents dynamics, sediment exchanges, and beach evolution. The XBeach model was used to simulate beach morphodynamics during the storm. The model incorporated effects from the seagrass meadow and non-erodible cells for realistic simulations. It was forced with in-situ wave data from January 19-23, 2020, and initialized with pre-storm bathymetry.

3 Beach flooding and morphodynamic response

Storm Gloria caused significant flooding, damaging beach infrastructure and extending into urban areas. Storm surges were the primary contributor to the flooding, surpassing the impact of run-up. Flood depth was a crucial factor in analyzing beach inundation, as it directly influenced sediment transport in the inner surf zone and swash processes. The flood depths were substantial enough to transform the swash zone into an inner-surf zone, promoting onshore sediment transport, which was deposited both against the seawall and in areas near the mean shoreline. Additionally, the storm triggered the offshore migration of the existing crescentic sandbar (Figure 1). However, the presence of the *P. oceanica* meadow acted as a barrier, preventing the sandbar from migrating further offshore into less active areas. Despite the storm energy and shoreline erosion, the beach recovered quickly within 15 days. This rapid recovery was attributed to the sediment transported to the regular inner-surf zone, which was rapidly returned to the dry beach.

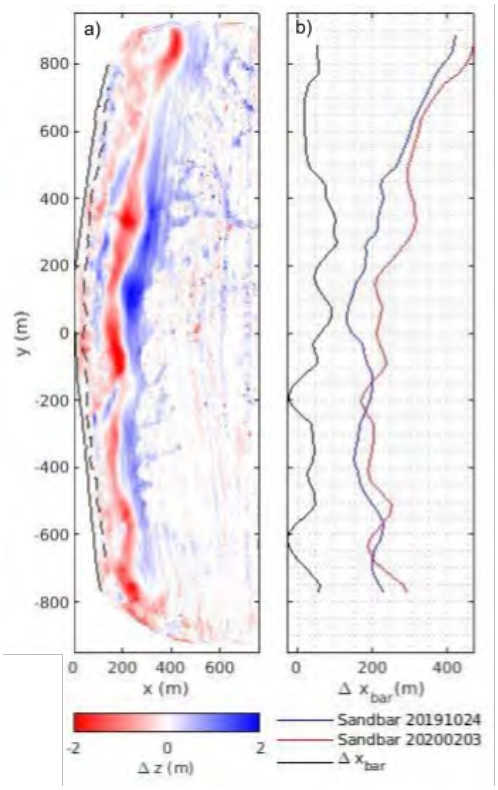

Figure 1: a) Bottom changes from Oct. 24th, 2019 to Feb. 2nd, 2020; b) Sandbar position at the study dates and sandbar cross-shore movement.

Acknowledgements

Authors acknowledge financial support from Project LIFE AdaptCalaMillor – LIFE21 GIC/ES/101074227 funded by UE, and from SOLDEMOR (TED2021-130321B-I00) and MOLLY (PID2021-124272OB-C22) projects funded by the Spanish Ministry of Science, Innovation and Universities.

References

[1] Cooper, J. A. G. et al. Sandy beaches can survive sea-level rise. *Nature Climate Change*, 10(11): 993–995, 2020. URL https://EconPapers.repec.org/RePEc:nat:natcli:v:10:y:2020:i:11:d:10.1038_s41558-020-00934-2.

Assessment of the risks of flooding in Andalusia (Spain) for the XXI century

Manuel Cobos, Marcus Silva-Santana, Pedro Otiñar, Asunción Baquerizo
Universidad de Granada (Spain)
Andalusian Institute for Earth System Research (IISTA)
Corresponding author: mcobosb@ugr.es

Keywords: flood hazards, flood risk, coastal zones, climate change

1 Introduction

We present a methodology for flood risk characterization in coastal areas in line with the Flood Risk Management Plans (FRMPs) required in the European Union Directive 2007/60/EC transposed into Spanish law by Royal Decree 903/2010. The FRMPs are elaborated for flood scenarios associated to different return periods (T_R) and follow Spanish guidelines to evaluate the impact on (1) the population, (2) the economic activities, (3) the environment and (4) points of special importance. The methodology has been applied to the Andalusian coast (Spain) using the results of ICCOAST project [1] along that coast with RCP 8.5 climate projections.

2 Methodology

The methodology consists of the following steps and uses the information obtained from a large number of simulations of hydro and morphodynamic processes at a particular study site from ICCOAST.

2.1 Calculation of levels and affected areas

We follow two approximations to obtain the return period levels. One is based on non-homogeneous Poisson processes and another based on a non-stationary generalized extreme distribution. The extension of flooded areas is then estimated from the samples of the curves that delimit the areas affected by flooding.

2.2 Flood hazards characterization

The hazard associated to every flood scenario is studied by means of the following variables: (1) the relative loss of dry beach area and (2) the area of estimated flooded zones. The classification of obtained values into different hazard levels ranging from very low to very high is done by considering the benefit per m^2 of a beach, the percentage of low permeability uses, and the data provided by [2] related to flood damage for Andalusian urban zones.

2.3 Flood risks characterization

The flood risk characterization involves (1) the identification for every scenario of the goods and uses flooded, (2) the estimation of the population directly affected and (3) the identification of key points and areas of special importance, including the zones that deserve an especial protection due to their environmental value.

The risk to the economy is estimated by means of a database of elementary flood-depth damage curves and updated unitary values that include, among other, those developed by [3].

The risk to key points and areas of special importance included the identification of Pollutant Release and Transfer Register facilities and the Wastewater Treatment Plants that are used themselves to estimate the risk to the environment by considering the distance of these potentially polluting facilities to protected areas and their degree of affection determined by the percentage of affected area and flood water depth.

The analysis also includes the classification of the risks values into categories ranging from very low risk to very high risks.

3 Results

In the conference we will illustrate the methodology along with the results for a particular study site. In addition, a statistical analysis of the aggregated results will be presented.

Acknowledgments

This work was carried out within the framework of a contract (Exped. Contr. 2020 194906), competitively bid by the Junta de Andalucía (with funds of the Fondo Europeo de Desarrollo Regional) and awarded to the University of Granada.

References

[1] P. Otiñar, M. Santana, M. Cobos, A. Millares, D. Gutiérrez, J. Martín, A. Lira-Loarca and A. Baquerizo. Projections of flooding and erosion in coastal zones of Andalucía (Spain) for the XXI century: a probabilistic approach. Proc. of the 38th Conf. on Coastal Engineering. Rome. 2024.

[2] B. F. Prahl, M. Boettle, L. Costa, J.P. Kropp and D. Rybski. Damage and protection cost curves for coastal floods within the 600 largest European cities. *Scientific Data* 5 180034, 2018.

[3] E. Martínez-Gomariz, E. Forero-Ortiz, M. Guerrero-Hidalga, S. Castán and M. Gómez. Flood Depth–Damage Curves for Spanish Urban Areas. *Sustainability*, 12, 2666, 2020.

Automatic shoreline detection in time-exposure images by using bi-LSTM networks: Input channel selection for high accuracy

Miquel Caballeria[1], Moises Serra-Serra[1], Pere Marti-Puig[1], Gonzalo Simarro[2], Francesca Ribas[3]
[1]Universitat de Vic – Universitat Central de Catalunya, Vic, Spain
[2]Institut de Ciències del Mar, Barcelona, Spain
[3]Uniersitat Politècnica de Catalunya, Barcelona, Spain
Corresponding author: miquel.caballeria@uvic.cat

Keywords: Remote sensing, Timex images, Automatic shoreline detection, Bi-LSTM neural network

1 Introduction

To analyse shoreline variability and evolution from digital coastal images, shoreline detection techniques has been developed using different shoreline indicators and water indexes [1]. Bidirectional Long Short-Term Memory (bi-LSTM) neural network have provided very good results for automatic shoreline detection from time-exposure video images (timex images) with a method that processes images by columns [2]. Applying this methodology to planviews from Castelldefels (south of Barcelona, Spain), obtained shorelines accuracy was of 1.4 m per column.

In the present work, many single channels of different colour spaces and various water indices of the main detection techniques, as well as sets of two or three individual channels, have been tested as input data to improve the performance of the bi-LSTM network.

2 Methods

The images are decomposed into individual columns, which are processed independently by a bi-LSTM network. The bi-LSTM network is a sequencial processing model consisting in two LSTM layers: one stars processing the data forward (from land to sea) and the other in the opposite direction (backward, from water to land). The designed bi_LSTM network takes as input one or more channels per column.

The individual channels *R*, *G*, *B* of RGB; *H*, *S*, *V* of HSV; *L*, *a*, *b* of Lab; and *Y*, *Cb*, *Cr* of YCbCr colour spaces have been tested as single input channels. Other channels corresponding to water indexes related to different shoreline detection techniques have also been considered: *B-R*, *G-R* and *G-B*, related to the sensitivity to the colour dominance; a gray-scaled channel, *GRAY*, related to the luminance; and a variance channel, *VAR*, which is sensitive to the contrast between the fixed/changing luminosity over the land/sea. Sets of two or three channels have been also tested as input.

3 Results

The same images of Catelldefels used in [2] have been employed. The best single channels (with the mean error per column, in meters, in the parenthesis) are: *b* (1.1), *B-R* (1.3), *G-R* (1.4), *G-B* (1.5), *Cr* (1.8), *B* (2.2), *VAR* (2.5), *V* (2.5) and *L* (2.6).

The best results for sets of three channels are: Lab (1.1), *b*/*B-R*/*G-R* (1.3), YCbCr (1.4). For sets of two channels: *Cr*/*L* (0.85), *Y*/*Cr* (0.90), *G-R*/*L* (1.07).

The best result corresponds to the set *Cr*/*L*, that practically equals the error of the shoreline detection by the experts, which according to [2] is 0.60 m (by filtering out spurious undulations it would even fall below the expert error). The major errors occur in burn parts (backlights), in the contour of objects/people that partially cover the shoreline, and in 'spurious' undulations of the planview shoreline introduced by the planview generation from the video images.

Although the best single channels are *b*, *B-R* and *G-R*, the best set of three channels is Lab, which is given by the 9th, 12th and 1st. In fact, the single channels more sensitive to the colour dominance (i.e. *b*, *B-R*, *Cr*) are also the most sensitive to the 'spurious' undulations, whereas the single channels related to luminance (i.e. *L*, *V*, *Y*, *GRAY*) practically do not detect them. Channel pairs or trios that contain one channel of each type are the ones that achieve the best results (i.e. *Cr*/*L*, *b*/*L*, Lab).

4 Conclusions

The bi-LSTM network achieves the best accuracy for shoreline detection by taking couples of complementary channels as imputs, one sensitive to the colour dominance and the other sensitive to luminance.

Such a wise selection of the input channels in neural networks for shoreline detection in video-camera images can therefore significantly decrease the errors to human levels.

Acknowledgments

This work has been funded by the Spanish government through the research projects PID2021-124272OB-C21/C22 (MINECO/FEDER).

References

[1] E.H. Boak and I. L. Turner. Shoreline Definition and Detection: A Review. *Journal of Coastal Research*, 21(4):688-703, 2005.

[2] P. Marti-Puig, M. Serra-Serra, F. Ribas, G. Simarro and M. Caballeria. Automatic shoreline detection by processing planview timex images using bi-LSTM networks. *Expert Systems With Applications*, 240 122566, 2024.

Morphological evolution of a channel-shoal complex in the mouth of the Ems estuary (Dutch Wadden Sea)

Rinse de Swart[1], Meike Traas[1], Nathanaël Geleynse[1]
[1] WaterProof Marine Consultancy & Services BV, 8221 RC Lelystad, The Netherlands
Corresponding author: rinse.deswart@waterproofbv.nl

Keywords: channel-shoal complex, morphological evolution, cyclicity, Ems estuary, Wadden Sea

1 Introduction

The Dutch Wadden Sea consists of several tidal inlet systems that typically feature one or several channel-shoal complexes. One example is the Huibertgat-Horsborngat channel-shoal complex, which is located in the mouth of the Ems estuary between the islands of Borkum and Schiermonnikoog (Figure 1). Recent bathymetric surveys have indicated that progressive erosion is taking place in the area, which is threatening the sediment coverage of some assets (cables, pipelines) in the area. In this work, the historic morphological evolution of the Huibertgat-Horsborngat area has been analysed and the resulting findings have been used to provide an outlook for the expected developments in the near future.

2 Methods

Large-scale bathymetric surveys with a resolution of 20 m (availability every 1 to 4 years) were obtained from Rijkswaterstaat (Ministry of Infrastructure and Water Management) for the period 1970-2023. These surveys were examined through establishing morphological trends in transects and erosion-sedimentation maps, and paired to cross-sectional flow area developments through time. Based on the findings of these analyses, a hypothesis was formulated on the morphodynamics of the study area.

3 Results

The analyses of the historic bathymetric surveys indicate that sedimentation/erosion rates within the area of interest can be over 15 m within a 10-year period. Two dominant morphological processes are responsible for the morphological evolution of the Huibertgat-Horsborngat area: 1) north-westerly migration of channels and shoals as a result of ebb tidal currents flowing through the Westereems channel and 2) southeasterly migration of channels and shoals as a result of flood tidal currents flowing through the Horsborngat/Huibertgat. In the period 1995-2007, the southern flank of the Huibertgat-Horsborngat area was located several hundreds of metres farther to the north than its present location and the cross-sectional flow areas were large. From 2010 onward, the southern flank of the Huibertgat-Horsborngat area migrated approximately 200 m towards the south, while at the same time the cross-sectional flow area decreased substantially (similar to the configuration in 1980s).

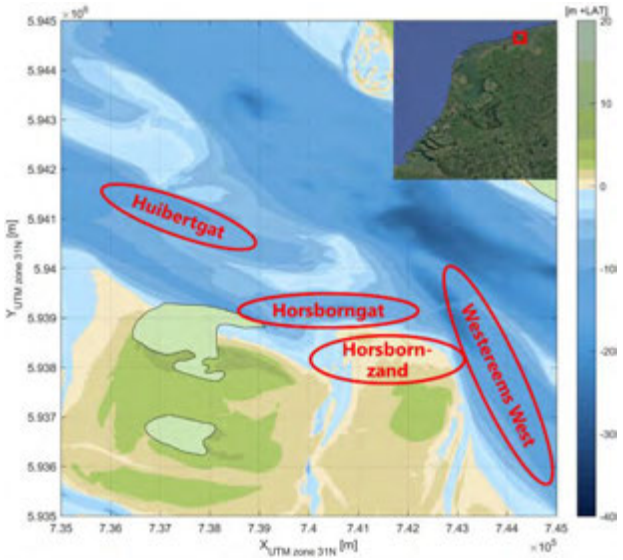

Figure 1: Overview of the study area.

3 Discussion and outlook

Based on the analysis of the historic bathymetric surveys, it is hypothesized that the Huibertgat-Horsborngat area shifts between two distinct configurations in a cyclic pattern with a duration of about 25-40 years. One configuration ('Ebb-dominant' morphology) corresponds to a single channel system with no distinct Horsborngat and large cross-sectional flow areas (present during 1995-2007), whilst the other endmember ('Flood-dominant' morphology) corresponds to a system with multiple flood-dominant channels, including a pronounced Horsborngat and featuring smaller cross-sectional flow areas (present in the 1980s and from 2010 onward). In the 'Ebb-dominant' configuration, the southern flank of the channel area is typically located several hundreds of metres farther to the north compared to the 'Flood-dominant' configuration. Currently, the southern flank of the Horsborngat continues to migrate southward, accompanied by severe erosion of the Horsbornzand. This trend will likely continue in the near future (~5 years). Based on the hypothesised cyclic trend, it is possible that in the distant future the migration reverses and the system will move towards a more 'Ebb-dominant' configuration. Future large-scale bathymetric surveys are required to underline or falsify this hypothesis.

Acknowledgments

We would like to thank Rijkswaterstaat for providing the large-scale bathymetric surveys.

Investigating the stability of hoa channels bisecting reef islands

Andrew Ashton[1]

[1]Woods Hole Oceanographic Institution, Woods Hole, Massachussets, United States of America
Corresponding author: aashton@whoi.edu

Keywords: coral reef islands, channel, reef flat, motu

1 Introduction

Significant progress has been made in our understanding of coastal environments by analysis of pattern-forming mechanisms and morphodynamic stability, particularly for sandy and barrier-lined coasts. Coral reef and reef-associated coastal landforms, however, have been less thoroughly studied. A typical annular atoll consists of a reef flat with a depth of 1-2 m (sometimes even exposed at low tide) surrounding a deeper (10's of m) inner lagoon. Islands can often be found on top of this flat, and between these reef islands, or motu, are often found shallow channels, or hoa. Morphologically active, hoa are formed as reef islands expand—much like tidal inlets, sometimes hoa fill in and in other cases they remain open for significant periods of time.

What remains unknown, however, are what wave-setup-driven flows are sufficient to keep these channels open by attaining a critical velocity for sediment transport (e.g. Escoffier [1]). Unlike inlets, tidal flows in hoa tend to be minimal as atolls typically contain one or more deep channels (order 10m), or ava. Instead, flows through hoa are wave-driven, caused by set-up as waves break at the edge of the reef, modulated by the reef flat depth and tidal range [2] Here, we present a preliminary model of hoa stability to determine what environmental variables control whether or not a hoa will remain open or whether adjacent motu islands will merge.

2 Quantifying Hoa Stability

Reef islands are formed from detrital sediment and are reworked by wave and currents, thereby exhibiting some similarities with barrier islands. Barrier island length and dynamics are often considered using theories for inlet stability [1] with barrier length generally decreasing for increasing tidal range and increasing basin area, a phenomenon that has been explained by competition between inlet friction and pressure gradients across shallow landwards lagoons [3]. However, in contrast with tidal inlets, hoa are shallow and typically do not extend much deeper than the shallow reef flat itself. Typical currents in hoa are driven lagoonwards by set-up of waves breaking at the reef edge or at reef island shores [2]. Although this set-up is modulated by tides, it is not a tidally driven flow.

Here, similar to inlet and ideal bank-full fluvial channel studies, we use models and measurements of wave-set-up and reef flat/hoa flow to quantitatively examine the key controls (wave height, island spacing, island width, reef flat width) to allow us to better quantify the broader question of whether hoa are stable features or are ephemeral—i.e. for what conditions is hoa closure inevitable as carbonate sediment accumulates on reef islands.

3 Conclusions

Geometric constraints can significantly affect the ability of hoa to remain open, with island width (and thus hoa channel length) and reef flat depth providing first-order controls. The influence of waves is less clear, as large waves cause more set-up, and therefore flow through hoa whilst also having the potential to drive significant quantities of sediment alongshore that can infill the channels, a phenomenon affected by island length, or hoa spacing. This theoretical framework is then be tested across larger datasets of remotely sensed island and reef flat geometry, although direct application is difficult due the complex nature and variability of reef environments, including varied sediment size and ubiquitous hard basement, including corals and other carbonate conglomeration. Particularly useful are comparisons where hoa have closed over geologic or observational timescales.

References

[1] Escoffier, F. F. (1940), The stability of tidal inlets, Shore Beach, 8(4), 114–115.

[2] Ortiz, A.C., and Ashton, A.D., 2019. Exploring carbonate reef flat hydrodynamics and potential formation and growth mechanisms for motu. Marine Geology 412, 173-186. https://doi.org/10.1016/j.margeo.2019.03.005

[3] Roos, P.C., Schuttelaars, H.M., Brouwer, R.L., 2013. Observations of barrier island length explained using an exploratory morphodynamic model. Geophys. Res. Lett. 40, 4338–4343. doi:10.1002/grl.50843.

Numerical Modelling of Long Transverse Finger Bars at El Trabucador Beach, Spain.

Jing Zheng[1], Fangfang Zhu[1], Nicholas Dodd[2], Albert Falques[3], Meili Feng[4]

[1]Department of Civil Engineering, University of Nottingham, Taikang East Road, Ningbo, 315100, China
[2]Faculty of Engineering, University of Nottingham, Nottingham NG7 2RD, UK
[3]Universitat Politècnica de Catalunya, Barcelona, Spain
[4]School of Geographical Sciences, University of Nottingham, Taikang East Road, Ningbo, 315100, China

e-mail corresponding author: Nicholas.Dodd@Nottingham.ac.uk

Keywords: *coastal morphodynamics; numerical modelling; wave-driven processes; transverse bars*

1 Background

Long transverse finger bars (LTFBs) are a quasi-rhythmic morphological feature that can sometimes be observed along low-energy coasts, typically where $H_s < 1$ m, and $T_p < 5$ s. LTFBs are characterized by their long, thin, and elongated crests, oriented perpendicularly or off-normal to the coastline, with cross-shore extents from $10 - 1000$ m, and spacings $\sim 5 - 500$ m. Notably, LTFBs form at El Trabucador Beach, at which site their scales are toward the lower end of the above scales. Observations there have been described with some success using a phase-averaged model of morphodynamic self-organisation [2], in which the beach state without LTFBs is assumed to be in equilibrium. However, the prevailing cross-shore currents and wave refraction there, and the abundance of fine sand, seem to point to another viable mechanism, which motivated [1] to propose that LTFBs form as the beach slope steepens as sediments are transported shoreward, and thus form as a result of an adjustment in a dis-equilibrium. Here, we present some work in which this hypothesis is tested more rigorously, for El Trabucador Beach, using a wave-resolving model, which should allow the same prevailing dynamics to be seen, but includes a much larger degree of realism.

2 Approach

We use the numerical model FUNWAVE-TVD [3]. We include bed-load sediment transport, which is the prevailing mode of sediment transport at the site, and modify it to include downslope sediment transport. We also consider the case of normal wave incidence, with wave heights in the range $5-15$ cm, periods $1-3$ s, and beach slopes $0.01-0.035$, which are typical for El Trabucador Beach. Our experiments have an initially alongshore uniform beach, on which a very small bed perturbation is imposed. Both the perturbations and the initial beach are then allowed to evolve as dictated by the simulated sediment dynamics.

3 Results

In Figure 1 we show the evolution of bed level during one simulation. Over the course of 80,000 s (40,000 wave periods; ~ 22 hours) the beach exhibits a cross-shore adjustment, and the development of features that resemble the observed LTFBs. The observed spacing is similar to that at El Trabucador Beach.

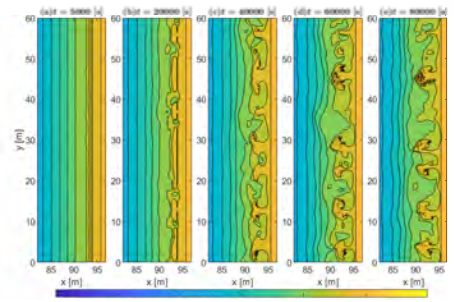

Figure 1: Contour plot of bed level at a series of regular intervals during a simulation. Waves approach the beach from the left side of the domain at normal incidence.

4 Conclusions

Our tentative conclusions are that we do observe LTFBs in our numerical experiments. They are a robust feature of the system we simulate, and their scales are similar to those observed at El Trabucador beach. Numerical experiments are ongoing.

Acknowledgements

This work is supported by the University of Nottingham Ningbo China (Faculty of Science and Engineering PhD Scholarship), the Ningbo Natural Science Foundation of China (project code 2023J190), the Zhejiang Natural Science Foundation of China (Grant NO.: ZJWY23E090024), and the Spanish Ministry of Science, Innovation and Universities within the MOLLY (PID2021-124272OB-C21/C22) project.

References

[1] Falqués A., F. Ribas, A. Mujal-Colilles, and C Puig-Polo. A new morphody-namic instability associated with cross-shore transport in the nearshore. *Geophys. Res. Letters*, 48(13), 2021.

[2] A. Mujal-Colilles, M. Grifoll, and A. Falqués. Rhythmic morphology in a microtidal low-energy beach. *Geomorphology*, 334:151–164, 2019.

[3] F. Shi, J. T. Kirby, J. C. Harris, J. D. Geiman, and S. T. Grilli. A high-order adaptive time-stepping tvd solver for boussinesq modeling of breaking waves and coastal inundation. *Ocean Modelling*, 43-44:36–51, 2012.

History of km-scale shoreline sandwave research and perspectives

Déborah Idier[1]
[1]BRGM, Orléans, France
Corresponding author: d.idier@brgm.fr

Keywords: wave, morphology, feedback, mechanisms, instability

1 Introduction

Rhythmic shorelines with plan-view undulations and relatively regular spacing are common on sandy coasts. We focus here on undulations with wavelengths (L) of approximately 1–10 km, not externally forced but generated by positive feedbacks between waves and morphology via sediment transport. These are referred to as kilometer-scale shoreline sandwaves. This paper revisits past work on the topic.

2 Mechanisms

Km-scale shoreline sandwaves are hypothesized to result from a feedback between coastal morphology and wave dynamics, involving (1) wave-driven longshore sediment transport and (2) cross-shore sediment exchanges governing the equilibrium profile. This mechanism, introduced first in [1] and refined later on (e.g.: [2]), shows that instabilities arise when the deep-water wave angle relative to shore normal exceeds a critical threshold $\theta_c \geq \theta_{c0} \approx 42°$.

Subsequent studies demonstrated that under specific bathymetric configurations and wave conditions, similar feedbacks can occur for lower angles [3], leading to the concepts of High-Angle Wave Instability (HAWI) and Low-Angle Wave Instability (LAWI). While HAWI produces longer wavelengths and timescales, LAWI generates smaller-scale features (O(10^2–10^3 m), O(1–10 days)). LAWI is driven by (1) wave refraction over shoreline-attached shoals, (2) convergence of longshore sediment flux near the shoal, and (3) cross-shore sediment supply from the surf to shoaling zones. A linear stability analysis [4] examined the influence of wave parameters, cross-shore profiles, closure depth, and two types of perturbations (P1: bathymetric profile shift; P2: offshore-decreasing bed perturbation). LAWI emerges only when offshore depth contour curvature exceeds that of the shoreline, which occurs for P2 but not P1. Instability is enhanced by large wave angles, small periods, and deep closure depths; P2-type instabilities are further amplified by steep surf zone slopes and gentle shorefaces.

As shown in [5], under curvilinear bathymetry and P2-type perturbations, θ_c can indeed vary between 0° and 90°, depending on background morphology and closure depth (Dc). Two instability drivers are identified: alongshore gradients in wave angle (wave angle mechanism) and in wave energy (wave energy mechanism, due to crest stretching). While the latter is inherently destabilizing, the former requires sufficiently steep foreshores and deep Dc. When both are destabilizing, θ_c=0°.

3 How it compares with observations

Modeling application to real sites has mainly focused on shoreline sandwaves driven by the wave angle mechanism. Falqués et al. [5], unlike earlier studies, predicted instability at Holmslands Tange, indicating these sandwaves may result from LAWI or mixed-HAWI types. At a larger scale, a global study [6] found 61% of undisturbed coasts exhibit 1–10 km undulations, strongly linked to wave incidence angle. Higher angles increase their likelihood, supporting HAWI as a dominant process, with potential LAWI influence. The study used [6] a single shoreline. However, free satellite imagery now allows global, long-term monitoring, advancing data-driven research on shoreline sandwave dynamics.

Acknowledgments

This participation to RCEM is funded by Agence Nationale de la Recherche (grant n°: ANR-21-CE01-0015).

References

[1] A. Ashton, B. Murray and O. Arnoult. Formation of Coastline Features by Large-Scale Instabilities Induced by High-Angle Waves. *Nature*, 414(6861), 2001.

[2] A. Falqués and D. Calvete. Large-Scale Dynamics of Sandy Coastlines: Diffusivity and Instability. *Journal of Geophysical Research: Oceans*, 110(C3), 2005.

[3] D. Idier, A. Falqués, B. G. Ruessink and R. Garnier. Shoreline Instability under Low-Angle Wave Incidence. *Journal of Geophysical Research: Earth Surface* 116(F4), 2011.

[4] D. Idier, A. Falqués, J. Rohmer and J. Arriaga. Self-Organized Kilometer-Scale Shoreline Sand Wave Generation: Sensitivity to Model and Physical Parameters. *Journal of Geophysical Research: Earth Surface*, 122(9), 2017.

[5] A. Falqués, F. Ribas, D. Idier and J. Arriaga. Formation Mechanisms for Self-Organized Kilometer-Scale Shoreline Sand Waves. *Journal of Geophysical Research: Earth Surface*, 122(5), 2017.

[6] D. Idier, A. Falqués, M. Garcin and J. Rohmer. How observed kilometric sandy shoreline undulations depend on wave climate. *Journal of Coastal Research*, (SI85), 2018.

Effects of shelf sand ridges on decadal shoreline evolution under sea level rise: An idealized modelling approach

Abdel Nnafie[1], Huib de Swart[1], Toon Verwaest[2]

[1]Institute for Marine and Atmospheric Research Utrecht, Utrecht University, The Netherlands
[2]Flanders Hydraulics Research, Antwerp, Belgium

e-mail corresponding author: a.nnafie@uu.nl/abnnafie@gmail.com

Keywords: *Sfcr, tsr, sea level rise, shoreline evolution*

1 Introduction

Shoreline erosion threatens many coastal areas. Addressing this issue requires a thorough understanding of the underlying processes for effective mitigation [9].

Previous modelling studies [7, 5] have demonstrated that large-scale sand ridges on the adjacent continental shelves play a significant role in shaping shoreline evolution over decadal timescales. These ridges, known as shoreface-connected sand ridges (sfcr) and tidal sand ridges (tsr), typically evolve on centennial time scales, are spaced 2–15 km apart, with lengths of 10–50 km, widths of 1–10 km, and heights ranging from 5 to 25 m [4].

A key limitation of those modelling studies is their assumption of a constant mean sea level, albeit that other studies [8, 3] have highlighted the importance of sea level rise in shelf ridge evolution and consequently shoreline dynamics. The objective of this study is to quantify the effects of shelf sand ridges on decadal shoreline evolution under sea level rise (SLR).

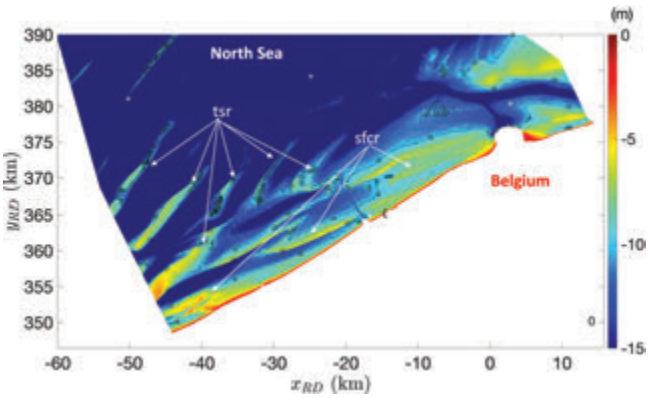

Figure 1: Bathymetric map of the Belgian shelf, showing sfcr and tsr.

2 Material and Methods

The coupled non-linear shelf-nearshore numerical model of [5] is used, which combines a shelf model (Delft3D+SWAN) to a nearshore model, Q2Dmorfo [2]. The model parameters, forcing and configuration, representing and idealized setting of the Belgian shelf (Figs. 1 and 2a), serve as first-order approximations of reality. A series of numerical experiments is conducted for a duration of 100 years, considering present-day (1.6 mm/yr) and projected future SLR rates (5-8.5 mm/y) [6], as well as variations in shelf and nearshore geometry.

3 Results and discussion

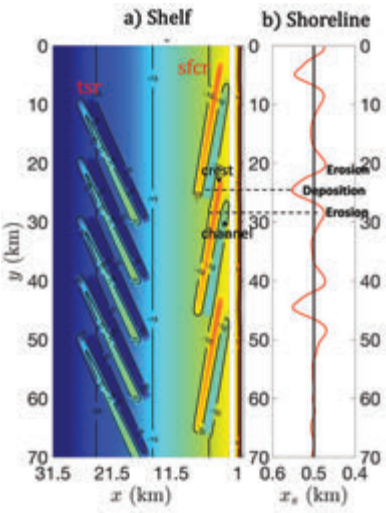

Figure 2: a) Bathymetric shelf configuration used in the experiments. b) Simulated shoreline x_s at $t = 30$ yr (red) without SLR; black shows initial shoreline ($t = 0$ yr). Shoreline deposition and erosion are highlighted.

Model results (Fig. 2b) indicate that, in the absence of SLR, shoreline progradation near the crests of the sfcr and retreat near the channels, consistent with observations. Preliminary results suggest that these shoreline changes are somewhat weaker under the present-day SLR rate. Scenarios with future SLR rates and varying shelf and nearshore geometry are still under investigation, with results to be presented at the conference.

4 Conclusion

Preliminary model results show shoreline progradation near SFCR crests and retreat near channels without SLR, with these changes weakening under present-day SLR.

Acknowledgements

This research is part of Morphological Interaction between the Sea bottom and the Belgian Coastline (MOZES) project, funded by the Flemish government, policy area mobility and public works (MOZES-WL_2021_18).

References

References are available upon request.

Self-organized patterns in Coastal Morphodynamics

A. Falqués[1], D. Calvete[1], F. Ribas[1], M. Caballeria[2], R. Garnier[1], N. van den Berg[1], R.L. de Swart[1], J.Arriaga[1], N. Kakeh[1], A. Fernández-Mora[1]

[1]Universitat Politècnica de Catalunya, Catalonia, Spain
[2]Universitat de Vic, Vic, Catalonia, Spain

e-mail corresponding author: albert.falques@upc.edu

Keywords: *pattern formation, nearshore sand bars, shoreline sandwaves, sand banks*

1 Self-organization

Observed patterns in nature can result from the external forcing or emerge internally as self-organized structures. Coastal systems can exhibit amazing and intriguing self-organized morphological patterns [1]. This presentation revisits their characteristics and possible formation mechanisms.

2 Crescentic bars

Crescentic bars (CB) are sandbars in the breaker zone of sandy beaches, roughly parallel to the coastline but with an undulating shape (see Fig. 1). The alongshore wavelength range is $\lambda = O(100 - 1000)$ m. The shoreward sections are called horns, while the seaward sections are rip channels. CBs are linked to rip current circulation, with offshore flow at channels and onshore flow at horns, driven by stronger wave breaking at horns. They can form from a straight bar when small bathymetric variations induce this circulation, redistributing sand accordingly [1].

3 Transverse bar systems

Transverse bars (TB) are sandbars oriented perpendicular or obliquely to the shoreline, forming alongshore rhythmic patterns (see Fig. 1). Three types have been identified [1]:
1) TBR (transverse bars and rips). They form when a crescentic bar migrates shoreward or its horns attach to the shoreline. They are relatively wide, with $L/\lambda \sim 1$, where L is their length.
2) CTFB (current transverse finger bars). Thinner bars with smaller $\lambda = O(10 - 100)$ m and a larger $L/\lambda > 1$. They are found in the breaker zone, coexisting with one or more longshore bars. They form due to a positive feedback between the developing morphology and the meandering of the longshore current and alongshore gradients in wave breaking.
3) LTFB (long transverse finger bars). Elongated and thin bars ($L/\lambda > 1$) occurring in shallow areas with gentle slopes with $\lambda = O(10-1000)$ m. Unlike CTFB, they are not associated with shore-parallel bars or longshore currents. Essential to their formation is the wave energy focusing by the topographic refraction and the dominant onshore sediment transport.

4 Shoreline undulations

Sandy shorelines can exhibit rhythmic alongshore undulations with a wide range of wavelengths from few m up to tens of Km. An example are megacusps, associated to a crescentic bar or to the shore-attachment of TB. At an even larger scale there are shoreline sand waves [2] which are related to the feedback between bathymetric undulations in both the surf and shoaling zones and the induced gradients in the wave-driven longshore sediment transport (see Fig. 2).

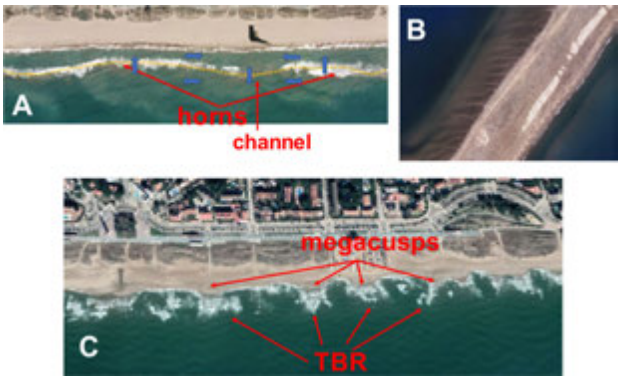

Figure 1: A: crescentic bar at Castelldefels. The rip current circulation is indicated by blue arrows. B: LTFB at the back-barrier Trabucador beach, Ebro delta. C: TBR bars and megacusps at Castelldefels.

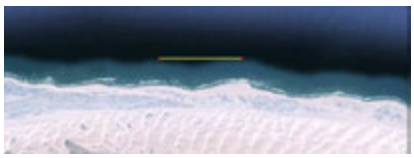

Figure 2: Shoreline sandwaves at Namibia, $\lambda \approx 5$ Km.

5 Shoreface-connected sand ridges

They are sand banks on the gently sloping bed of the continental shelf in depths of 10−20 m [1]. They occur as alongshore rhythmic systems with $\lambda \sim L \sim 4 - 10$ Km and an oblique orientation relative to the shore, opening an accute angle against the dominant storm-induced alongshore current. They emerge from a positive feedback based on the deflection of the current by the developing morphology.

Acknowledgements

Funding by the Spanish Government and the EU (PID2021- 124272OB-C22) is acknowledged.

References

[1] F. Ribas, A. Falqués, H. E. de Swart, N. Dodd, R. Garnier, and D. Calvete. *Rev. Geophys.*, 2015. doi: 10.1002/2014RG000457.

[2] N. van den Berg, A. Falqués, and F. Ribas. *J. Geophys. Res.*, 2012. doi: 10.1029/2011JF002177.

A model-based reference state for suspended sediment concentration in the Wadden Sea

Jannek Gundlach[1], Markus Reinert[1], Robert Lepper[1], Frank Kösters[1]

[1]Federal Waterway Engineering and Research Institute, Hamburg, Germany

e-mail corresponding author: jannek.gundlach@baw.de

Keywords: *Process-based modeling; Suspended sediment concentration; Wadden Sea; Cross-border sediment transport*

1 Introduction

The Wadden Sea, a UNESCO World Heritage Site, is a highly dynamic, morphologically interconnected ecosystem that supports a unique diversity of flora and fauna and is an important food source for migratory birds. Adequate sediment availability and sea level rise have allowed the Wadden Sea's intertidal zone to grow, locally exceeding the rate of sea level rise. However, with accelerated sea level rise and the resulting increased sediment demand, transport pathways of suspended sediments will become a key factor for the future development of the Wadden Sea. In order to assess any changes in sediment transport, one needs to define a valid reference state. One step in this direction and the aim of this study is to define a reference state of the current suspended sediment concentration (SSC) in the Wadden Sea based on hindcast simulations with a large-scale numerical model.

2 Methods

We analyze hindcast simulations, the hydronumerical modeling framework Untrim^2 [1], which has been previously validated [2]. The model domain covers the North Sea from Scotland to the English Channel and the Baltic Sea. The entire Wadden Sea is covered at about 250 m resolution with additional high-resolution subgrid bathymetry. For the simulation of suspended sediment concentration, the model is driven by key processes including tidal motion, meteorological forcing and waves. For suspended sediment transport, three different sediment fractions are defined, representing the behavior of very fine sand, flocs/aggregates, and wash load/primary particles. The simulation results of the SSC are validated against measurements of multiple sources including the Federal Maritime and Hydrographic Agency of Germany (BSH, Kirchgeorg pers. com., given in Figure 1a) in the North Sea. Since the highest SSC is expected near the coast and in estuaries, the measurements are compared within the 12 nautical mile zone.

3 Preliminary Results

The aggregated and averaged simulation results for SSC in the Wadden Sea based on the year 2020 are shown in Figure 1a. SSC values range from close to zero to local peaks of 500 mg/l. High values of SSC are found in the estuarine channels and the backbarrier tidal flats. When comparing simulated and measured SSC for values mainly from 0.5 to 100 mg/l in Figure 1b, the majority is in agreement, but some concentrations are underpredicted by the model. Beyond the validity of the SSC results, seasonal and interannual variations are determined and related to the mean of the last 20 years. In this way, representative SSC conditions and variations are defined.

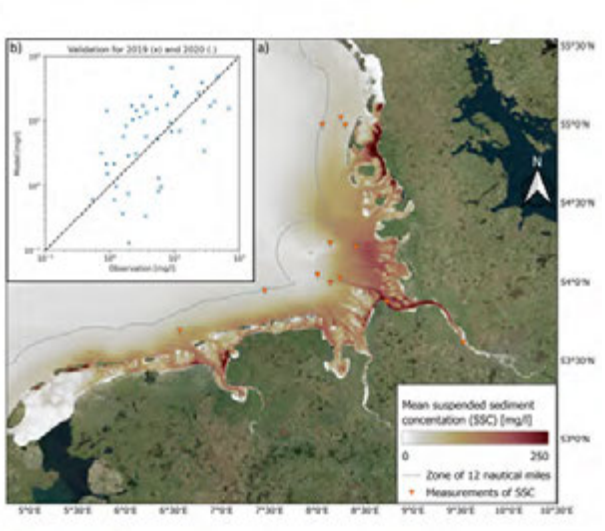

Figure 1: Model-based mean SSC of all sediment fractions in 2020 in the Wadden Sea with a background map from MS Bing is shown in (a), with validation for 2019 and 2020 in (b)

Acknowledgements

The research was conducted as part of the PaRCA project, funded by the German Federal Ministry of Education and Research (BMBF) under the grant number 03F0957B.

References

[1] V. Casulli. A high–resolution wetting and drying algorithm for free–surface hydrodynamics. *International Journal for Numerical Methods in Fluids*, 60(4):391–408, 2009. ISSN 0271-2091. doi: 10.1002/fld.1896.

[2] R. Hagen, A. Plüß, R. Ihde, J. Freund, N. Dreier, E. Nehlsen, N. Schrage, P. Fröhle, and F. Kösters. An integrated marine data collection for the german bight – part 2: Tides, salinity, and waves (1996–2015). *Earth System Science Data*, 13(6): 2573–2594, 2021. doi: 10.5194/essd-13-2573-2021.

Sediment transport in the microtidal Misa River estuary

Agnese Baldoni[1], Carlo Lorenzoni[1], Matteo Postacchini[1], Maurizio Brocchini[1]
[1] Dipartimento di Ingegneria Civile, Edile e Architettura, Università Politecnica delle Marche, Ancona, Italy
Corresponding author: m.brocchini@univpm.it

Keywords: sediment transport, estuary

1 Introduction

The sediment transport of a microtidal estuary is investigated within the MARCUS (Mitigation and Adaptation in Resilient Coastal and estUarine integrated unitS) project, aimed at providing coastal stakeholders with strategies for the safeguard of coastal and estuarine areas. Sediment transport is evaluated through field measurements carried out in the most energetic season, when river floods and sea storms are expected.

2 Study site

The study site is the Misa River estuary of Senigallia, on the Adriatic coast of Italy, characterized by a large sediment transport despite its small dimension [1].
The final river stretch is characterized by lateral masonry embankments, and highly heterogeneous bottom sediments. A layer of fine-grained sediments (silt and clay, mainly montmorillonite) and organic material forms a persistent protective top layer of the riverbed. Approaching the river mouth, fine sand characterizes the riverbed and the nearshore area [2]. Surficial deposits of gravel also form during periods of low river flow, generating a large inner mouth bar [3].

3 Methodology

Two different techniques are used to analyse the sediment transport in the final stretch of the river. A sediment trap made of two non-woven fabric traps, one oriented toward the river mouth and one oriented upriver (Figure 1a), was built to estimate the bedload from the two stream directions. To measure the turbidity and water depth, two multiparametric sondes have been deployed (Figure 1b). A calibration will be performed to convert turbidity measurements in suspended solid concentrations. The instruments were placed in the sites shown in Figure 1c.

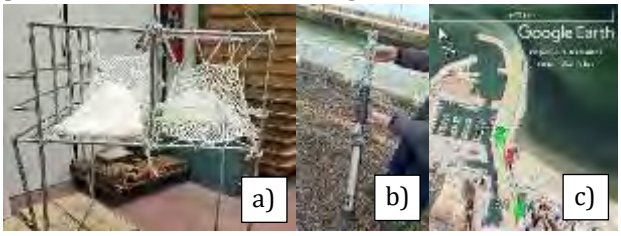

Figure 1: a) Sediment trap; b) multiparametric sonde; c) sites of sediment trap (red pin) and sondes (green pins).

4 Results

Figure 2 shows the sediment collected in a period of low-flow events (Dec 6th - 19th) by the trap's nets: the sediment coming from upriver, more abundant, is denser and seems to be composed of mud and organic matter (a), while the sediment coming from downriver is less abundant and more liquid, likely a mixture of clay and water (b). Future analyses will allow us to better characterize the sediment.
Figure 3 shows the water depth and the turbidity data acquired by the S2 sonde every 6 minutes. An increase of turbidity was observed when higher oscillations occurred, these suggesting an important amount of seawater penetrating the estuary.

Figure 2. Sediment collected by the nets oriented upriver (a) and downriver (b).

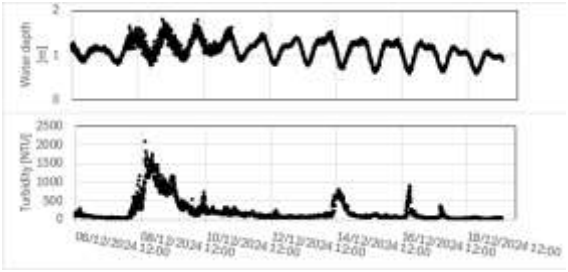

Figure 3: Water depth (from the bottom of the sonde to the water surface) and turbidity measurements at location S2.

4 Conclusions

Further results will be presented at the conference.

References

[1] M. Frignani, L. Langone, M. Ravaioli, D. Sorgente, F. Alvisi & S. Albertazzi. Fine-sediment mass balance in the western Adriatic continental shelf over a century time scale. *Marine Geology*, 222, 113-133, 2005.
[2] M. Brocchini, J. Calantoni, M. Postacchini, A. Sheremet, T. Staples, J. Smith, ... & L. Soldini. Comparison between the wintertime and summertime dynamics of the Misa River estuary. *Marine Geology*, 385, 27-40, 2017.
[3] A. Baldoni, E. Perugini, L. Soldini, J. Calantoni, & M. Brocchini. Long-term evolution of an inner bar at the mouth of a microtidal river. *Estuarine, Coastal and Shelf Science*, 262, 107573, 2021.

Flow Velocities on Fringing Intertidal Flats

B.C. van Prooijen[1], P.L.M. de Vet[2], J.L.J. Hanssen[1,2], M. Schrijver[3], M. van der Wegen[2,4]
[1]TU Delft, Delft, the Netherlands; [2]Deltares, Delft, the Netherlands; [3]Rijkswaterstaat, Middelburg, the Netherlands; [4]IHE, Delft, the Netherlands
Corresponding author: B.C. van Prooijen@TUDelft.nl

Keywords: Flow Velocities; Intertidal Flats; Field Campaign; Western Scheldt; ADCP

1 Aim

We present results of an extensive field campaign in the Western Scheldt (Netherlands) with the aim to quantify the spatial and temporal variations of the velocities on intertidal flats. A better quantification and understanding of flow velocities is needed to improve the habitat mapping of benthic species, as well as the prediction of the morphological evolution of these areas. Results of the campaign are complemented with a predictor of flow velocities on tidal flats, based on water level measurements.

2 Field Campaign

Flow velocity profiles are measured on the Zuidgors tidal flat in the Western Scheldt. 14 ADCPs (Nortek Aquadopps) are distributed over 4 cross-shore transects, covering the longshore and cross-shore variability of the flow, see Figure 1. We measured 28 days, spanning two spring-neap tidal cycles.

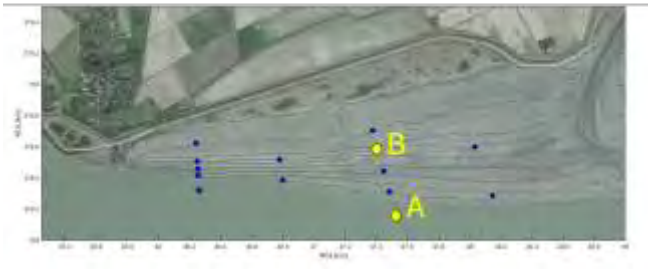

Figure 1: Intertidal flat Zuidgors as part of the Western Scheldt. The markers indicate the locations of the ADCPs. Results at the yellow markers are shown in Figure 2.

3 Measurement Results

We found that flow velocities are generally following the depth contours. Flow velocities decrease towards the dike (for higher bed levels). Variations in longshore direction are limited. The timeseries (Figure 2) show the asymmetry of the tidal flow, especially during spring tides. These seem to be related to the flooding of the shoal. High peaks in flood flow are found just before high water, with magnitudes exceeding 1m/s. Contrarily, the peak velocities in ebb direction hardly vary along the spring-neap tidal cycle and generally do not exceed the 0.6m/s.

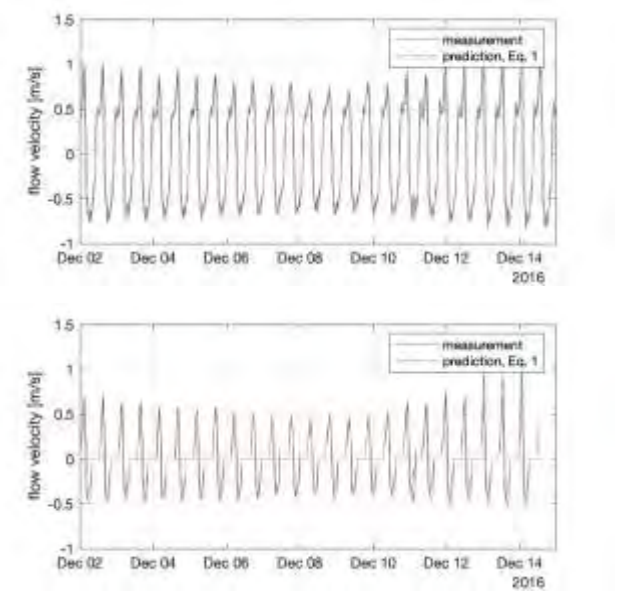

Figure 2: Timeseries of the measured and predicted (Eq 1) velocity in the channel. Upper panel: Location A (channel), z=-5.9m MSL, Lower panel: Location B (tidal flat), z=+1m MSL.

4 Pressure Gradient and Friction

The magnitude of the flow velocities on these shallow areas is dictated by the pressure gradient and the bed friction in longshore direction. By representing the water level gradient by the temporal variability divided by the tidal wave celerity, $\frac{d\zeta}{dx} = \frac{d\zeta/dt}{\sqrt{g d_{channel}}}$, with water level ζ; and depth in the channel $d_{channel}$, we can express the local flow velocity at (x, y) by

$$u_{x,y} = C_{x,y} \sqrt{d_{x,y} \frac{|\mathrm{d}\zeta/\mathrm{d}t|}{\sqrt{g d_{channel}}}}\ \mathrm{sgn}(-\mathrm{d}\zeta/\mathrm{d}t) \qquad (1)$$

with local Chezy's friction coefficient $C_{x,y}$ and local depth $d_{x,y}$ Figure 2 shows the surprisingly good representation of the estimation. The assumption of a progressive wave seems reasonable here, although not all time lags are captured.

5 Conclusions

The extensive field campaign provides a rich data set for in-depth analyses. A clear distortion of the tide was found. A simple estimate can be made for the flow velocities, based on the local depth variations and roughness, as well as by the large-scale tidal motion. The validity of such a prediction at other tidal flats needs to be determined in future studies.

How does the spatial organization of roughness elements alter fine sediment erodibility and transport – an experimental study on cockles

Maxime Laukens[1,2], Christian Schwarz[1,2]
[1] Hydraulics and Geotechnics, Department of Civil Engineering, KU Leuven, Leuven, Belgium
[2] Department of Earth and Environmental Sciences, KU Leuven, Leuven, Belgium
Corresponding author: maxime.laukens@kuleuven.be

Keywords: benthic organisms, bed roughness, spatial configuration, mudflat erodibility, hydrodynamics

1 Introduction

Abrupt step changes in bed roughness frequently occur in natural wall-bounded flows, such as when high river flow velocities deposit gravels/boulders that can no longer be transported, or when biogenic roughness elements like mussel shells settle in coastal intertidal zones [1]. It was found that a large proportion of bed shear stress adjustment occurs rapidly after the interface between different bed surfaces [2]. This underlines not only the importance of the magnitude of roughness change (i.e. the difference in roughness height) but also the spatial configuration of roughness elements.

This study examines how roughness-altering effects of the cockle *Cerastoderma edule*, widespread in temperate estuaries and mudflats, alter sediment transport. Cockles form spatial patterns ranging from cm to hundreds of meters, yet small-scale patterns (<1m) remain underexplored [3]. We focus on how flow interactions with different cockle configurations influence sediment stability, manipulating variables such as cockle density, spacing, and clustering through controlled flume experiments on natural mudflat sediments. Scale dependency is assessed by comparing homogeneous conditions, which create a uniform shear layer, with heterogeneous clusters, where elements extend into the water column and alter near-bed turbulence. The objective is to examine how different cluster configurations and densities influence sediment erosion thresholds and rates.

2 Methods

Experiments are conducted in a straight flume channel by incrementally increasing incoming flow velocities, while continuously measuring suspended and bed load transport. To isolate roughness effects, cockles are immobilized and arranged in various configurations for a particular density. Velocity and turbulence profiles are measured using the UB-Lab 2C acoustic Doppler velocity profiler (UBERTONE®) across multiple transects above the cockles. The critical bed shear stress for erosion (τ_{crit}, N m^{-2}) and erosion rate parameter (M, kg m^{-2} s^{-1}) are calculated for suspended and bed load transport. The impact of spatial configurations on sediment erodibility is assessed by analysing the spatially varying τ_{crit} exceedance for different incoming flow velocities. Near-bed turbulence and flow accelerations/decelerations are compared to a no-cockle reference to identify variations within and around the clusters. Finally, the eroded sediment volume is quantified using photogrammetry.

3 Results

Preliminary results suggest a maximum eroded volume related to cluster configuration (Figure 1). Certain configurations limit sediment erodibility and the erosion threshold more than others. However, findings also reveal added complexity, particularly when distinguishing between suspended load and bed load transport. Observed changes in flow dynamics, with local exceedance of τ_{crit} provide insights into optimal organism configuration. Eroded volume patterns provide insights into the potential impact of *C. edule* on sediment transport on mudflats.

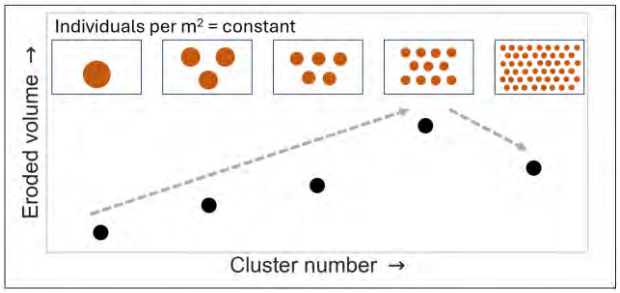

Figure 1: Dependency of eroded suspended sediment volume for different cockle cluster configurations.

4 Conclusion

Preliminary results indicate a context-dependent, nonlinear relationship between cockle density, spatial organization, and sediment erodibility. Transitions in roughness occurring at cluster edges have an important impact on the flow regime and initiation of suspended and bedload transport. Identifying optimal configurations that minimize sediment erosion rates can offer insights into the forces governing the spatial distribution of macrobenthic organisms in natural environments and how favourable arrangements help reduce sediment erodibility.

References

[1] Sansom, B. J., Bennett, S. J., Atkinson, J. F., & Vaughn, C. C. (2020). Emergent hydrodynamics and skimming flow over mussel covered beds in rivers. *Water Resources Research*, 56(8).

[2] Curran, J. C., & Tan, L. (2014). The effect of cluster morphology on the turbulent flows over an armored gravel bed surface. *Journal of Hydro-Environment Research*, 8(2), 129–142.

[3] Boldina, I., & Beninger, P. G. (2013). Fine-scale spatial structure of the exploited infaunal bivalve *Cerastoderma edule* on the French Atlantic coast. *Journal of Sea Research*, 76, 193–200.

Changes in estuarine SSC: long-term trends and variability

Bas van Maren[1,2], Bob Smits[2]
[1]Delft University of Technology, Delft, the Netherlands
[2]Deltares, Delft, the Netherlands
Corresponding author: d.s.vanmaren@tudelft.nl

Keywords: sediment dynamics, trends, anomalies, Wadden Sea

1 Introduction

The Suspended Sediment Concentration (SSC) in estuaries and coastal seas typically varies over tidal, spring-neap and annual cycles. Within a coastal system SSC may display pronounced spatial variation in especially the peak sediment concentration. This large variation reflects the heterogenous composition of the sediment bed and large variation of sediment availability on the bed and the hydrodynamics. Superimposed on these cyclic variations SSC may gradually change over time due to natural processes but more often as a result of human interventions, introducing a trend. Especially this trend is an important parameter, providing a means to quantify to what extent a system is responding to human interventions. However, our recent analyses of a large SSC dataset covering the Dutch Coastal waters since the 1970s reveal that anomalies exist, introducing variabilities with a periodicity of typically several years. This variability is important for determining trends and provides novel insights into the functioning of estuarine systems.

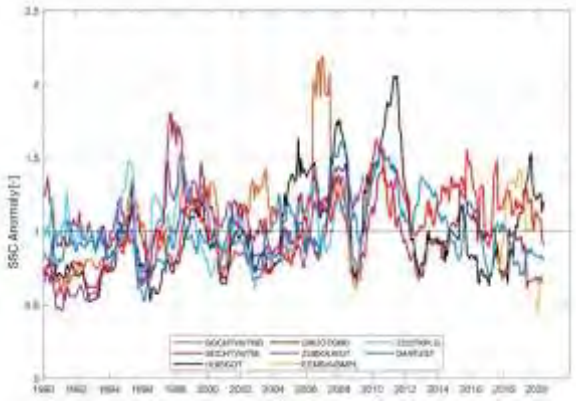

Figure 1: SSC anomaly of eight observation stations in the tidal inlets of the Wadden Sea over the period 1990 – 2020.

2 Field data

This study covers the Dutch part of the Wadden Sea and the Dutch-German Ems Estuary. In the Dutch section we make use of the long-term monitoring program (MWTL; monthly to bimonthly sampling of a.o. SSC) operated by the Dutch Ministry of Infrastructure and Water Management (Rijkswaterstaat) since the 1970s. In the German section of the Ems Estuary we use permanent observation stations measuring SSC continuously, operated by the German NLWKN since around 2010.

3 Results

The SSC values in the Wadden Sea reveal a pronounced spatial variability, with relatively low SSC in the channel inlets and higher SSC at the landward limit of the tidal channels. However, when converting these observations into anomalies (in which these observations are divided by their long term mean) temporal patterns with striking spatial uniformity appear (Fig. 1). These stations are spaced more than 100 km apart, implying that the mechanisms driving their temporal elevation are large-scale as well (such as extremes in fresh water supply, wind patterns and storms, and temperature). However these anomalies do not appear to be related to known physical or biological fluctuations. Understanding such relationships is key to knowing whether fine sediment is indeed supply-limited (as suggested by [1]) which has great implications for the way the Wadden Sea is able to adapt to sea levels rise. Another consequence of the anomalies is that they may suggest trends which are not actually present. Of particular interest herein is the elevation in SSC from 2010 to 2012, observed in all stations. Trend analyses over the period 1990 – 2011 [2], suggested a significant increase in turbidity in several parts of the Wadden Sea and especially of the Ems Estuary. However, as demonstrated by Fig. 1, the end of the period on which they based their trend corresponded with a pronounced peak in SSC. Extending the trend analyses period with more recent data reveals that the temporal increase in SSC is much weaker and may no longer be significant.

Acknowledgments

This study is executed as part of Deltares project 11206835 funded by the Dutch Ministry of Public Works.

References

[1] Colina Alonso, A., van Maren, D. S., Oost, A. P., *et al.* (2024). A mud budget of the Wadden Sea and its implications for sediment management. Communications Earth & Environment, 5(1), 153.

[2] Vroom, J., H.F.P. van den Boogaard, D.S. van Maren, (2012). Mud Dynamics in the Ems-Dollard, research phase 2: analysis existing data. Deltares report 1205711.001, 97 p.

Transport pathways of microbial sediment aggregates with distinct fine-scale morphologies

Naiyu Zhang[1], Jian Shen[2], Fan Xu[1], Haochen Li[3], Charlotte E.L. Thompson[4,5], Ian H. Townend[4] Qing He[1]

[1] State Key Laboratory of Estuarine and Coastal Research, East China Normal University, Shanghai, 200241, China

[2] Virginia Institute of Marine Science, College of William & Mary, Gloucester Point, VA 23062, USA

[3] Water Infrastructure Laboratory, Department of Civil and Environmental Engineering, University of Tennessee, Knoxville, TN 37996, USA

[4] School of Ocean and Earth Science, National Oceanography Centre, University of Southampton, Southampton, SO14 3ZH, UK

[5] Channel Coastal Observatory, National Oceanography Centre, Southampton, SO14 3ZH, UK

Abstract

The interfaces between sediment particles and water provide hotspots for microbial colonization. With the secretion of copious amounts of organic matter (i.e., extracellular polymeric substances (EPS)), the microbial colonization facilitates the adhesion of sediment particles, cells, organic matter and pollutants into aggregates. These aggregates play a crucial role in the fluxes of particulate matter from continental land to the ocean and shaping river, estuary, and coastal morphologies. To precisely predict the transport of microbially-colonized sediment particles, studies have focused on microbial alteration of aggregate size, density and/or gross shape variations. However, discrepancies remain in predicting key sediment transport processes, such as settling velocity, critical shear stress for resuspension, and bedform dynamics, in the presence of microbial colonization.

Our prior research has demonstrated that microbial colonization, in addition to alter size and density, introduces significant complexities in aggregate morphologies, creating micro-scale microbial colonies and meso-scale angularities on aggregate surfaces (Zhang & Xu et al., 2025). Despite this, most studies assume that the drag acting on these aggregates is equal to that on smooth spheres or ellipsoids. This assumption suggests that aggregates and smooth spheres/ellipsoids of equal size, density and gross shape should follow the same transport pathways.

We recently applied an X-ray microcomputed tomography method combined with computational fluid dynamics simulations to analyse aggregate morphology at high spatial resolution and determine the relationship with drag (Zhang & Xu et al., 2025). This method was applied to a variety of microbial sediment aggregates collected from rivers, mudflats and estuaries in China and UK. Our results show that the fine-scale morphologies (micro-scale microbial colonies and meso-scale angularities) critically increase drag compared to that on smooth surfaces. A morphology-corrected drag was proposed to characterize the morphological influences (Zhang & Xu et al., 2025). By incorporating this drag correction, we predicted the transport pathways of aggregates with different morphologies under identical flow conditions. Our results reveal that even when aggregates share the same gross shape (elongation and flatness), small-scale morphological differences can lead to distinct transport behaviours. This result highlights the importance of incorporating fine-scale morphological features into sediment transport predictions, marking a shift from a focus solely on gross particle properties to a more detailed consideration of micro-scale morphology.

References

Zhang, N., Thompson, C. E. L., Townend, I. H., Rankin, K. E., Paterson, D. M., & Manning, A. J. (2018). Nondestructive 3D Imaging and Quantification of Hydrated Biofilm-Sediment Aggregates Using X-ray Microcomputed Tomography. *Environmental Science and Technology*, *52*(22)

Zhang, N., Li, H., Xu, F*., Thompson, C. E. L., Townend, I. H., He, Q. (2025) Microbial colonization effects on drag in suspended sediment transport. *Nature Geoscience, Accepted.*

Identifying small-scale gradients in sediment stability as early indicators of saltmarsh cliff initiation

Victoria G. Mason[1,2*], Pim W.J.M. Willemsen[3,4], Jos R.M Muller[5], Bas W. Borsje[5], Johan van de Koppel[1,6], Tjeerd J. Bouma[1,2]

[1] Royal Netherlands Institute for Sea Research (NIOZ), Yerseke, the Netherlands
[2] Utrecht University, Utrecht, the Netherlands
[3] Wageningen University & Research, Wageningen, the Netherlands
[4] Deltares, Delft, the Netherlands
[5] University of Twente, Enschede, the Netherlands
[6] University of Groningen, Groningen, the Netherlands

Corresponding author: victoria.mason@nioz.nl

Keywords: Cliff formation; erodibility; coastal defence; Nature-based Solutions; cliff erosion

1 Introduction

Saltmarsh cross-shore width is a critical determinant of the ecosystem services it can provide, particularly to what extent waves can be attenuated across its surface. Cliff initiation at the seaward saltmarsh edge is typically the key trigger of marsh retreat, causing the cross-shore marsh width and ecosystem service provisioning to be reduced. Unfortunately, the processes and conditions under which cliffs form remain unknown, making the moment of cliff initiation unpredictable.

2 Methods

We took field measurements of sediment properties (such as grain size distribution and compaction) and sediment stability at comparable cliffed and non-cliffed saltmarsh edges (Fig 1A) and combined them with flume measurements of sediment erodibility (Fig 1B) and experimental wave mesocosm measurements to trigger saltmarsh cliff initiation (Fig 1C).

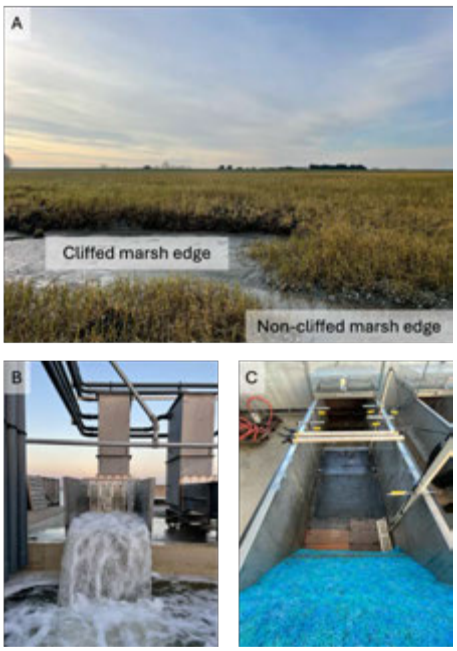

Figure 1: A saltmarsh edge at Hellegat, W.Scheldt with and without a cliff (A) and a fast flow flume (B) and wave mesocosm flume (C) used to conduct erosion measurements.

3 Results & Discussion

We identified that for a cliff to form under raised hydrodynamic conditions, three conditions must be present: 1) a substantial offset in sediment erodibility at the saltmarsh-mudflat interface, governed by small-scale gradients in sediment characteristics such as grain size distribution; 2) a marsh edge with near-negligible erodibility and 3) site-wide sediment characteristics resulting in an erodible mudflat. Without these conditions, increased wind-wave activity is unlikely to initiate cliff formation; instead, a more gently sloping marsh edge will occur as erosion is more evenly distributed. Overall, we provide insight into the role of small-scale gradients in sediment stability for driving the long-term dynamics of biogeomorphic saltmarshes, which can be used as early indicators to identify cliff-initiation prone saltmarsh areas.

Acknowledgments

We would like to thank Marte Stoorvogel, Job Cohen, Jente van Leeuwe, Alex Ji and Cas van der Kaaden for their help conducting field and flume measurements, as well as Lennart van IJzerloo for his valuable practical guidance. The input from VGM, TB, JvdK, JM, BWB and PWJMW was supported by the 'LIVING DIKES – Realising Resilient and Climate-Proof Coastal Protection' project (with project number NWA.1292.19.257) of the NWA research program 'Research on Routes by Consortia (ORC)', which is funded by the Netherlands Organization for Scientific Research (NWO). Pim Willemsen was also supported by the Dutch Research Council in research project: "Salt marshes: where climate change adaptation meets climate change mitigation" (NWO-AES-VENI 2023; 21063).

What controls the height of marsh edge cliffs?

Xiaotian Zhang[1]

[1]Hohai University, Nanjing, China

e-mail corresponding author: zhangxiaotian@hhu.edu.cn

Keywords:

1 Abstract

Marsh edge cliff represents an erosive morphology widely-observed across the globe. This unique configuration exacerbates the erosive forces acting on marsh edge, thus increasing the risk of marsh erosion and wetland loss. Height is the most distinctive characteristic of marsh edge cliffs, and understanding the key factors influencing cliff height is of significant importance. Despite extensive pioneering researches, the explicit relationship between cliff height and key environmental factors has yet to be established. To address this gap, we investigate the height of marsh edge cliffs on the global scale and collect series of parameters charactering the sedimentary environments of each site. Employing a novel segmentation method, we divide cliff into above MSL and below MSL sections and explored their height correlation. The results from both global data and numerical model consistently indicate that the height of above MSL cliff is primarily determined by depositional processes, exhibiting a positive correlation with tidal range. Meanwhile, the below MSL height is mainly influenced by erosional forces and positively correlated with significant wave height. Potential contribution of sediment supply and sea level rise are further explored through numerical experiment. Our study elucidates the correlations between cliff height and multiple factors, providing valuable insights into the evolution of coastal wetlands and further, informing the assessments of and sediment budget and coastal resilience under global climate change.

Storm Surge Impacts on Sediment Dynamics and Habitat Resilience in a Mangrove-Marsh Ecotone

Sanne M. VAASSEN[1], Karin R. BRYAN[1], Andrew SWALES[2], Joel A. CARR[3], Conrad A. PILDITCH[1]
[1]University of Auckland, New Zealand
[2]National Institute of Water and Atmospheric Research, Hamilton, New Zealand
[3]US Geological Survey, Eastern Ecological Science Center, USA
Corresponding author: sanne.vaassen@auckland.ac.nz

Keywords: estuaries, coastal wetlands, sediment dynamics, hydrodynamics

1 Introduction

Estuaries are increasingly impacted by climate change, with rising sea levels, higher temperatures, and more frequent storm events. In estuaries, these long-term changes are altering hydrodynamics and sediment transport, thereby reshaping habitats, including eco-engineering species like mangroves and saltmarshes [1, 2]. Understanding how vegetation-environment interactions respond to climate-driven pressures is crucial for projecting the future of estuarine wetlands. Here we present the results of a study examining storm-surge hydrodynamics and sediment transport and potential effects of this episodic, extreme, event on a mangrove-marsh ecotone in Whangateau Harbour, New Zealand (Figure 1a&b).

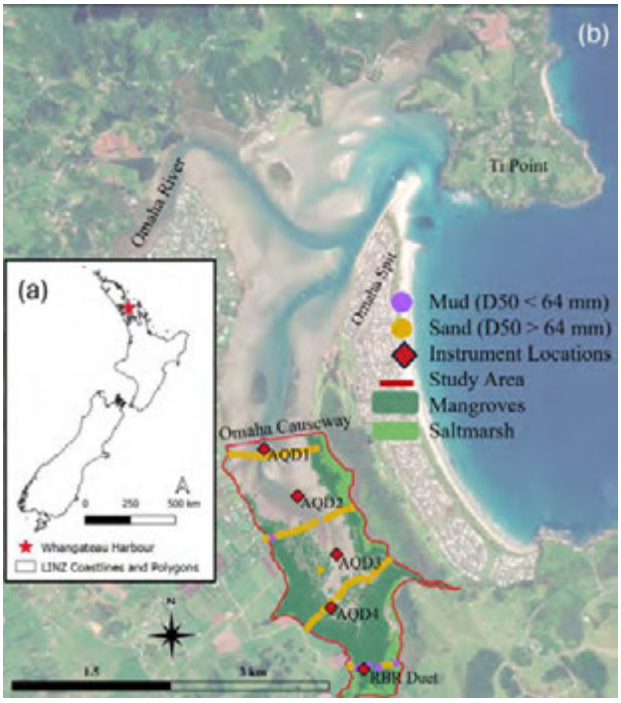

Figure 1: (a) Location of Whangateau Harbour on the North Island of New Zealand. (b) Sediment sampling transects, instrument locations, and mangrove and saltmarsh habitats in the study area south of the Omaha causeway.

2 Methodology

Field data were collected over a 3-week period in October 2023, that included a 99th percentile high water level (storm surge + spring tide). Flow velocities and suspended sediment concentrations (SSC) were gathered using Nortek Aquadopps and optical backscatter sensors (OBS) placed at multiple sites along the main channel (Figure 1b). These observations are integrated into a coupled hydrodynamic-vegetation (Delft3D) numerical model to explore mangrove-marsh ecotone responses to the storm surge.

3 Results

Flood-tide velocities increased substantially at all sites during the storm, with SSC peaking at 70 mg/l, at the causeway inlet (AQD1, Figure 1b) and 50 mg/l in the upper estuary (AQD4, Figure 1b). Sediment fluxes were found to increase 6-fold at the inlet and 600-fold in the upper estuary. Preliminary results suggest that storm-driven sediment delivery, promoting tidal-flat accretion and higher water levels promoting propagule dispersion, may enhance mangrove establishment.

4 Conclusion

This study underscores how storm surges and climate-driven changes shape estuarine sediment dynamics, and in turn, mangrove and saltmarsh habitat evolution. Ultimately, this research will inform strategies for conservation and management of coastal wetland ecosystems under a changing climate.

Acknowledgments

This work is funded by NIWA's [2] Future Coasts Aotearoa Programme (Contract CO1X2107).

References

[1] Fagherazzi, S., Mariotti, G., Leonardi, N., Canestrelli, A., Nardin, W., & Kearney, W. S. Salt marsh dynamics in a period of accelerated sea level rise. *Journal of Geophysical Research: Earth Surface,* 125(8), 2020.

[2] Ward, R. D., Friess, D. A., Day, R. H., & Mackenzie, R. A. Impacts of climate change on mangrove ecosystems: a region by region overview. *Ecosystem Health and sustainability,* 2(4), 2016.

Wave attenuation versus progressive damage during extreme storm conditions: a salt marsh vegetation trade-off

Pim. W.J.M. Willemsen[1,2], Victoria G. Mason[3,4], Vera M. van Bergeijk[2], Mark Klein Breteler[2], Jos. R.M. Muller[5], Dimitrios Dementzoglou[6], Akis Vouziouris[6], Thomas J. van Veelen[5], Kathelijne M. Wijnberg[5], Ton A.J.F. Hoitink[1], Paul Buring[7], Maike Paul[8], Vincent van Zelst[2,6], Bas Hofland[6], Alessandro Antonini[6], Tjeerd J. Bouma[3,4], Bas W. Borsje[5]
[1] Wageningen University & Research, Wageningen, the Netherlands
[2] Deltares, Delft, the Netherlands
[3] Royal Netherlands Institute for Sea Research (NIOZ), Yerseke, the Netherlands
[4] Utrecht University, Utrecht, the Netherlands
[5] University of Twente, Enschede, the Netherlands
[6] Delft University of Technology, Delft, the Netherlands
[7] Wetterskip Fryslân, Leeuwarden, the Netherlands
[8] Leibniz University Hannover, Hannover, Germany
Corresponding author: pim.willemsen@wur.nl

Keywords: Salt marsh, Extreme storms, Wave attenuation, Vegetation breakage, Large-scale flume experiment

1 Introduction

Salt marshes at the border of land and sea are well-known for their ability to attenuate wind waves. Field observations and large-scale lab experiments prove a significant attenuation of wave height and energy due to the elevated bed and vegetation roughness of the salt marsh. However, these results only include waves up to approximately 1.0 m. The efficacy of marsh vegetation to wave attenuation during extreme wave events, with waves exceeding 1.0 m, is largely uncertain as vegetation is progressively damaged. This study quantifies the trade-off between wave attenuation and progressive vegetation damage under extreme waves from 0.7 m up to 2.0 m and water depths from 1.5 m up to 4.0 m. Wave heights and water levels are comparable to design conditions for Dutch dikes.

2 Field-scale Delta Flume experiment

4.4 x 70 m^2 of high salt marsh was transplanted from the Dutch mainland Wadden Sea coast to the Delta Flume at Deltares in Delft, the Netherlands (Figure 1). *Elymus athericus* was dominantly present with an average initial stem height of 0.57 m (range between 0.2 and 0.9 m). The marsh was exposed to +/- 20 hours of extreme waves distributed over three incoming significant wave heights (0.7, 1.2, 2.0 m) and water depths (1.5, 2.5 and 4.0 m). Wave and vegetation characteristics were monitored at multiple locations resp. during and in between experimental runs.

3 Results, Discussion & Conclusions

Vegetation damage was strongly related to exposure duration and not the magnitude of wave height exposure. Wave attenuation decreased over exposure time, due to increasingly damaged vegetation. We can conclude that salt marsh vegetation remains present during extreme wave events and consistently contributes to wave attenuation of nearshore waves up to 2.0 m. However, the contribution of vegetation to wave attenuation decreases during an event due to biomass loss and a decreasing stem height. During the RCEM conference we will present the results of this study, including relations between progressive vegetation damage through biomass loss and vegetation height reduction related to extreme exposure duration; And the trade-off between vegetation damage and wave attenuation towards the peak of an extreme storm. On a global scale these results give confidence in the use of salt marshes for coastal protection during extreme events that have not been observed before, as the salt marsh with its vegetation is still present when it is needed.

Figure 1: Obtaining marsh blocks from the field (left) and Delta Flume filled with marsh blocks (right).

Acknowledgements

This research was supported by the 'LIVING DIKES – Realising Resilient and Climate-Proof Coastal Protection' project (with project number NWA.1292.19.257) of the NWA research program 'Research on Routes by Consortia (ORC)', which is funded by the Netherlands Organization for Scientific Research (NWO). The Delta Flume experiment was commissioned by Wetterskip Fryslân and funded by the Dutch Flood Protection Program (HWBP). Pim Willemsen was supported by the Dutch Research Council in research project: "Salt marshes: where climate change adaptation meets climate change mitigation" (NWO-AES-VENI 2023; 21063).

A Reduced-Complexity Model for Morphodynamic Evolution and Equilibrium Creek Spacing in Salt Marsh Systems

C.C. Chu[1], A. Canestrelli[1], D. Pinton[1], and S. Fagherazzi[2]
[1] Department of Civil & Coastal Engineering, University of Florida, Gainesville, USA.
chuchiachu@ufl.edu, daniele.pinton@ufl.edu, alberto.canestrelli@essie.ufl.edu
[2] Department of Earth and Environment, Boston University, Boston, USA., sergio@bu.edu

Keywords: salt marshes, tidal creeks, sea level rise (SLR), watershed divide, equilibrium spacing

1 Introduction

Salt marshes play a crucial role in coastal protection by reducing storm surges and flood risks. They also support diverse plant and animal species while improving water quality through pollutant filtration. Tidal creeks carve through these marshes, regulating nutrient cycling, water flow, and sediment transport, which in turn drive morphological changes that dynamically alter marsh functions (Donatelli et al., 2018).

Our research seeks to unravel the complexities of salt marsh dynamics by first developing an analytical model to determine the position of watershed divides. This model is then coupled with a simplified numerical morphological model to simulate the evolution of marsh systems dissected by multiple creeks. Finally, we derive an analytical solution for the equilibrium spacing of tidal creeks under different conditions, considering sea level rise (SLR) and wind wave effects, biomass, and the size of marsh. The watershed divide position, which governs the tidal prism, is influenced by factors such as marsh and creek geometry, bed friction (dependent on vegetation biomass), and SLR rate. These factors collectively determine the morphodynamic equilibrium, as sediment transport is closely tied to watershed extension.

2 Methodology

In this study, we analyse the hydrodynamics of a rectangular salt marsh system dissected by multiple creeks using the Poisson equation (Rinaldo et al., 1999). By assuming quasi-two-dimensional flow, we simplify the problem into a linear system of ordinary differential equations (ODEs), which we solve analytically using the Laplace transform method to obtain explicit solutions for the watershed divide positions.

The watershed divide helps quantify the water exchange between tidal creeks and marsh platforms. By integrating Mariotti and Fagherazzi's (2013) morphodynamic model with our analytical formula for divider positions, we develop a fast and efficient model that simulates the coupled evolution of marsh platform elevation, creek width, depth, and spacing. Key input parameters include marsh size, SLR rate, tidal amplitude, wind waves, maximum vegetation biomass, critical shear stress, and sediment availability, all of which influence salt marsh morphology.

Additionally, we derive an explicit algebraic formulation that predicts whether a small bed perturbation evolves into a creek or whether a pre-existing creek fills in, transforming into an intertidal flat. This leads to a simplified equation for creek spacing, which has an analytical equilibrium solution.

Finally, we compare our model results with both Delft3D numerical simulations and creek spacing across the east coast of the United States. There is a good agreement between our reduced complexity model, Delf3D, and the real world.

3 Conclusions

We present a simplified approach to estimating tidal watersheds and equilibrium creek spacing in marsh systems without relying on computationally intensive numerical models. Our models provide a rapid assessment tool for hydrodynamic and morphological impacts, aiding decision-making in marsh restoration and conservation. They can be used to evaluate restoration strategies such as ditch infilling, thin layer placement on marsh platforms and vegetation planting in newly restored areas. Additionally, our models assess the effects of SLR on watershed divider positions and creek spacing, which influence nutrient and sediment distribution and, consequently, marsh resilience to SLR. Ultimately, this framework can guide restoration strategies that enhance the long-term sustainability of salt marshes and the ecosystem services they provide.

Acknowledgments

The authors appreciate the Ministration of Education of the Republic of China (Taiwan) and the Water Institute at the University of Florida for the funding.

References

Donatelli, C., Ganju, N. K., Zhang, X., Fagherazzi, S., & Leonardi, N. (2018). Salt marsh loss affects tides and the sediment budget in shallow bays. *Journal of Geophysical Research: Earth Surface*, 123(10), 2647-2662.

Mariotti, G., & Fagherazzi, S. (2013). A two-point dynamic model for the coupled evolution of channels and tidal flats. *Journal of Geophysical Research: Earth Surface*, 118(3), 1387-1.

Rinaldo, A., Fagherazzi, S., Lanzoni, S., Marani, M., & Dietrich, W. E. (1999). Tidal networks: 2. Watershed delineation and comparative network morphology. *Water Resources Research*, 35(12), 3905-3917.

Morphodynamic feedbacks induced by water level regulation in the Venice Lagoon (Italy)

A. Michielotto[1,2], A. Finotello[1], D. Tognin[3], L. Carniello[3], A. D'Alpaos[1]
[1]University of Padova, Department of Geosciences, Padova, Italy
[2]Department of Land, Environment, Agriculture and Forestry, University of Padova, Padova, Italy
[3]University of Padova, Department of Civil, Environmental, and Architectural Engineering, Padova, Italy
Corresponding author: alessandro.michielotto@unipd.it
Keywords: Numerical modelling; Storm surges; Flood defence; Morphodynamics

1 Introduction

Engineering structures designed to promote safety against flooding of estuarine urban areas, such as storm-surge barriers, have been shown to significantly alter hydrodynamic and morphodynamic processes, thereby disrupting the natural dynamics of coastal ecosystems. Despite their sporadic activations and the limited operational duration, floodgate operations can have profound and long-lasting effects on estuarine evolution, particularly when closures coincide with morphologically significant surge events.

Focusing on the microtidal Venice Lagoon, where a mobile barrier system (i.e., the Mo.S.E. system) has been operative since October 2020, we aim to assess the consequences of repeated floodgate operations on lagoon morphodynamics. Particular attention is paid to floodgate-induced variations in tidal water levels, wind-wave height, and the related bottom-shear stresses and sediment transport processes. The net morphological effects of floodgate operations are finally quantified.

2 Methods

Using a custom-built, two-dimensional numerical morphodynamic model [1,2], we reconstruct four years of morphodynamic evolution of the lagoon (2020–2023), comparing the real-case, flood-regulated conditions (i.e., MoSE) with a non-regulated scenario representing the absence of floodgate closures (i.e., OPEN).

3 Results and discussions

Our comparative analyses demonstrated that reduced water levels within the lagoon dampen wind waves generated during storm surges, but concomitantly increase the wind-wave-induced bottom shear stresses across tidal flats, intensifying sediment resuspension events(Figure 1).

In terms of sediment balance, a more nuanced pattern emerges, as higher concentrations of suspended sediment during floodgate closures are unevenly distributed and deposited across the three fundamental estuarine morphological units (i.e., salt marshes, tidal flats, and tidal channels). Particularly, since the artificially lowered water levels reduce both the depth and duration of salt-marsh flooding [3], marsh vertical accretion via deposition of minerogenic sediments is restricted. In contrast, sediment resuspended by wind waves from the lagoonal tidal flats preferentially settles within the tidal flats or in the nearby tidal channels, causing channel infill at rates twice as fast as those reconstructed in the absence of flood regulation (OPEN scenario).

Altogether, our analyses previous findings that, over time, repeated floodgate activations will lead to a generalized loss of ecogeomorphologic diversity and emphasize the need to balance coastal wetland preservation with efforts to enhance the resilience of coastal communities against flooding.

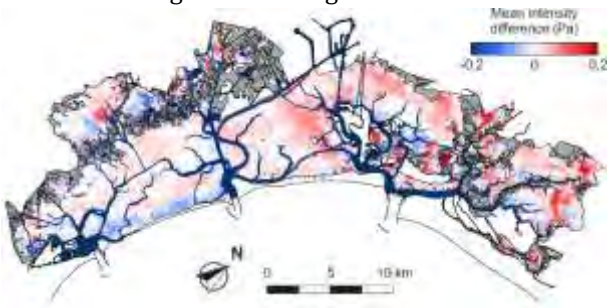

Figure 1: Flood regulation-induced variations in the mean intensity difference for sediment resuspension events in the flood-regulated MoSE scenario against the non-regulated OPEN scenario.

Acknowledgments

RETURN Extended Partnership and European Union Next-GenerationEU (NRRP, Mission 4, Component 2, Investment 1.3 – D.D. 1243 2/8/2022, PE0000005)

References

[1] Carniello, L., A. D'Alpaos and A. Defina. Modeling wind waves and tidal flows in shallow microtidal basins, *Estuarine, Coastal and Shelf Science*, doi:10.1016/j.ecss.2011.01.001, 2011.

[2] Carniello, L., A. Defina and L. D'Alpaos. Modeling sand-mud transport induced by tidal currents and wind waves in shallow microtidal basins: Application to the Venice Lagoon (Italy), *Estuarine, Coastal and Shelf Science*, doi:10.1016/j.ecss.2012.03.016, 2012.

[3] Tognin, D., Finotello, A., D'alpaos, A., Viero, D. P., Pivato, M., Mel, R. A., Defina, A., Bertuzzo, E., Marani, M., & Carniello, L. (2022). Loss of geomorphic diversity in shallow tidal embayments promoted by storm-surge barriers. *Science Advance* (Vol. 8). https://doi.org/10.1126/sciadv.abm8446

Long-Term Impacts of Sediment Disposal Strategies in the Western Scheldt

Jeroen Stark[1], Bart De Maerschalck[1], George Schramkowski[1]
[1]Flanders Hydraulics, Antwerp, Belgium
Corresponding author: jeroen.stark@mow.vlaanderen.be

Keywords: Sediment Management, Morphological Modelling, Dumping Strategies, Western Scheldt

1 Introduction

The Western Scheldt plays a crucial role in regional navigation towards the port of Antwerp. Effective sediment management is essential to maintain navigability and protect the estuarine environment. This study utilizes idealized morphological modelling to analyse the long-term morphological impacts of various disposal strategies, with a focus on sediment disposal in deep pits along the navigation channel itself. Ultimately, the study provides recommendations for sustainable sediment management in view of future permit applications for maintenance dredging.

2 Methods

An existing highly schematized Delft3D model of the Western Scheldt estuary is applied in this study [1]. The model self-forms a bottom layout over hundreds of years based on the most relevant physical processes, estuary geometry, simplified hydrodynamic boundary conditions and parameterization of sediment transport. This methodology minimizes imbalances between the morphology and hydrodynamic boundary conditions, while the model is still capable of producing a recognizable pattern of channels and shoals. A comprehensive scenario analysis is then conducted to investigate the long-term morphological impact of channel maintenance and various disposal strategies, including sediment disposal in deep pits of the main channel, disposal in secondary channels and variation between disposal locations in upstream and downstream parts of the estuary. These model scenarios consist of follow-up runs in which the self-formed morphology is used as initial condition.

3 Results and Discussion

3.1 Fairway maintenance

The model results indicate that fixing the navigation channel limits the natural dynamics of channels and shoals, leading to a more rigid and less adaptable morphology. An alternative strategy could be to apply adaptive fairway maintenance, where the fairway polygon moves with the morphological development of the channels. However, such scenario calculations were not performed in this study.

3.1 Disposal strategy

The scenario analysis shows that long-term disposal in the deep parts of the main channel leads to the silting of the main channel and a relative deepening of the side channels. Although silting of the main channel was not found in shorter-term morphological modelling, it does align with previous expert assessments conducted for the present maintenance dredging permit application [2]. The decrease in depth of the main channel reduces the tidal range and enhances a flood-dominant tidal asymmetry.

Additional scenarios show that disposal in secondary channels leads to silting of the side channels and deepening of the main navigation channel. This strategy may have contrasting effects on tidal range, depending on where the deepening occurs. In particular, the effect on tidal range is opposite in the eastern and western part of the Western Scheldt, highlighting the importance of the ratio between main and secondary channel volumes as well as their orientation for tidal propagation.

The impact of the disposal strategy on dredging requirements depends on the exact dumping location, the direction of residual sediment transport, and the available dumping space. For example, upstream dumping leads to higher dredging volumes in the scenario analysis as the residual transport is directed downstream.

4 Conclusion

This research provides valuable insights into effective sediment management strategies for the Western Scheldt. The findings underscore that morphological changes induced by specific disposal strategies, such as disposal in deep pits, can affect tidal dynamics, which in turn influence sediment transport, deposition patterns, dredging requirements and ecological habitats. Understanding these hydro-morphological feedbacks is crucial for optimizing sediment management strategies. Finally, continuous monitoring and timely adjustments of the applied strategy are essential for their long-term sustainability.

References

[1] A. Nnafie, T. Van Oyen, B. De Maerschalck,; M. van der Vegt and M. van der Wegen, Estuarine channel evolution in response to closure of secondary basins: An observational and morphodynamic modeling study of the Western Scheldt Estuary. *J. Geophys. Res. Surf.*, 123: 167–186, 2018.

[2] B. Huisman, Y. Huismans and J. Vroom, Effecten van storten in diepe putten van de Westerschelde: Synthese van proefstortingen en modelanalyses. Deltares, Delft, The Netherlands. 2020.

Lessons from the circular use of dredged sediment for tidal habitat restoration along the Access Channel to the Port of Rotterdam

Kees Sloff[1,2], Sander Broeders[3]
[1]Deltares, Delft, The Netherlands
[2]Delft University of Technology, The Netherlands
[3]WSP, The Netherlands
Corresponding author: kees.sloff@deltares.nl

Keywords: Beneficial use of dredged sediment, tidal nature, ship waves, Proeftuin Sediment Rijnmond

1 Introduction

Rather than disposing of dredged sediment from the harbours and entrance channel of Port of Rotterdam offshore in the North Sea, we are exploring beneficial use of these sediments to create new nature areas (project 'Proeftuin Sediment Rijnmond'). In December 2022, we placed 10,000 m^3 dredged sand in a groyne section to create shallow areas and smooth land-water transitions. A longitudinal dam was constructed to shield the groyne field from currents and waves from passing sea-ships. However, tidal currents and ship waves still impact the sediment, as tidal flows can pass the groynes, and through three openings that are created in the dam for fish passage. The project can be considered as a nature-based solution, and is being scaled up to neighbouring groyne fields as part of the European Framework Directive. As the pilot aims to enhance conditions for nature development, we investigate the impact of currents and waves on bed dynamics. Biologists from WMR, RAVON, and SOVON monitor impacts on biodiversity (benthos, fish and birds).

Figure 1: Layout of pilot site

2 Methods

We measured flow velocities, ship waves and salinity using a set-up of 6 Acoustic Doppler Velocimeters (ADVs) and Conductivity, Temperature, and Depth sensors (CTDs) in the groyne field, followed by Acoustic Doppler Current Profiler (ADCP) flow velocity measurements at transects over multiple tidal periods [1]. We analysed the grain-size distribution of the bed using laser-diffraction. Rijkswaterstaat surveyed bed topography. To analyse ship waves, we used vessel parameters derived from Automatic Identification System (AIS) data. The ADV signals were analysed using wavelets and combined with the AIS data to establish the causality between draw down and ships passage. The collected data were used to develop a hydrodynamic model using Delft3D-FM software, which simulates passings ships and their impacts within the groyne section [2]. It applies a moving atmospheric pressure method.

3 Results and conclusion

The strongest impacts on sediments result from water-level draw down (primary waves) of passing ships, which interact with tidal flows. The larger and faster the ship, the stronger the draw down in the groyne field. The wavelets analysis also reveal 'natural' oscillations of waves in the semi-closed basin, independent of ship passages. The model successfully predicts the currents and waves in the groyne field. Near-bed velocities increase by approximately 0.2 m/s during ship passage, particularly near the openings. Simulations with different dam- and groyne-opening layouts show that the number and size of the openings, as well as the height of the groynes, significantly impact the hydrodynamic conditions. Currently, shear stress often exceeds the critical values for sediment transport, causing bed dynamics at several zones to be too large for benthos. Simulations also suggest that the planned extension to neighbouring groyne fields will improve conditions in the existing groyne section. Follow-up monitoring will assess how these changes affect the ecosystem. Additionally, the method to place the dredged sediment (either rainbowing or mechanical methods) place a crucial role in shaping the deposits and therefore influences the ecology impact.

Acknowledgments

Partners of the Proeftuin Sediment Rijnmond project (www.proeftuinsediment.nl) are highly acknowledged for their contribution.

References

[1] T. Kouwenhoven. The effect of modifications to a groyne area in the Nieuwe Waterweg. MSc thesis Delft University. 2023.
[2] S. Broeders. Hydrodynamic effects primary vessel waves in a semi-closed groyne fields. MSc thesis Delft University 2023.

Morphodynamic evolution of estuarine intertidal flats under sea level rise and dredging strategies

Mick van der Wegen[1,2], Hesham El Milady[1], Mónica Aguilera Chaves[2], Bjoern Roebke[2]
[1]IHE Delft, Netherlands
[2]Deltares, Netherlands
Corresponding author: m.vanderwegen@un-ihe.org

Keywords: estuarine morphodynamics, intertidal flats, sea level rise

1 Introduction

The estuarine intertidal zone forms an important ecosystem that plays a vital role as habitat, but also serves as a natural coastal protection against flooding by wave attenuation and as a morphodynamic basis for vegetated zones like salt marshes and mangroves, see Figure 1. Accelerating sea level rise (SLR) has the potential of drowning the system while human activities like dredging and disposal strategies may mitigate impact. Sea level rise is historically unprecedented so that detailed understanding of the impact on estuarine morphodynamic development is lacking. Thus, modeling efforts plays an import role in assessment studies. High-resolution models like Delft3D allow detailed physical processes and output heterogeneity, but require extensive computation time and validation efforts, e.g. [1,2,3,4,.

2 Aim

This study aims to assess the morphodynamic evolution of intertidal flats under SLR and dredging strategies using high-resolution modeling (Delft3D) for the Western Scheldt estuary, Netherlands.

3 Method

By applying a process-based approach, validated in a 30-year hindcast, the current research investigates the behaviour of tidal flats under different SLR scenarios and dredging scenarios.

4 Results

Model results show that the morphodynamic behaviour of the intertidal area lags behind SLR while area closer to the sediment source adapts faster to SLR. Partial drowning of intertidal area occurs, when the intertidal area can no longer keep up with SLR. More drowning occurs for larger (extremer) SLR. Applying different dredging and disposal scenarios, shows that in particular disposal strategies may help intertidal area to survive SLR even under extreme (3m SLR/century) scenarios. Model results systematically show the impact of including wind waves, 3D vs 2D and including different sediment types (like sand and mud) on intertidal area and hypsometry.

Closer analysis of modelling results shows that a drowning system with reducing intertidal flat area and intertidal water storage volume significantly alters tidal wave propagation and nett sediment transport direction, with feedback on morphodynamic development.

Figure 1 Intertidal flats in the Western Scheldt estuary, Netherlands. Source: Rijkswaterstaat Beeldbank

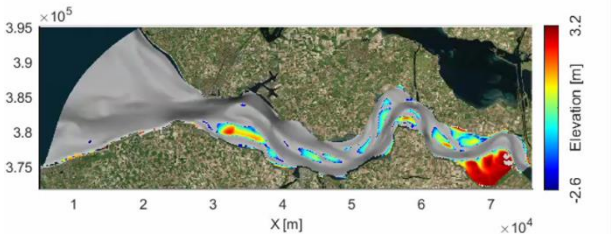

Figure 2 Model results after 80 years SLR (3m/century).

References

[1] Elmilady, Van der Wegen, Roelvink, & Jaffe. (2019). Intertidal area disappears under sea level rise: 250 years of morphodynamic modeling in San Pablo Bay, California. *Journal of Geophysical Research: Earth Surface*, *124*(1), 38-59.

[2] Elmilady van der Wegen Roelvink van der Spek (2022) Modeling the Morphodynamic Response of Estuarine Intertidal Shoals to Sea-Level Rise. Journal of Geophysical Research: Earth Surface 127: e2021JF006152, https://doi.org/10.1029/2021JF006152

[3] Röbke, Elmilady, Van der Wegen, Taal (2020) The long-term morphological response to sea level rise and different sediment strategies in the Western Scheldt estuary (The Netherlands). Deltares, Delft, The Netherlands, pp. 98.

[4] Zheng, Elmilady, Röbke, Taal, Wang, van Prooijen, ... & Van der Wegen. (2021). The impact of wind-waves and sea level rise on the morphodynamics of a sandy estuarine shoal. *Earth Surface Processes and Landforms*, *46*(15), 3045-3062.

Nature-based mitigation of shoreline erosion risks in restored and created tidal marshes

M.M. Stoorvogel[1,2,3], P.W.J.M. Willemsen[4,5], J. van Belzen[1,6], S. Temmerman[7], J.M. de Jonge[8], J. van de Koppel[1,9], B.W. Borsje[3], S.J.M.H. Hulscher[3], T.J. Bouma[1,2]

[1] NIOZ Royal Netherlands Institute for Sea Research, Yerseke, The Netherlands
[2] Utrecht University, Utrecht, The Netherlands
[3] University of Twente, Enschede, The Netherlands
[4] Wageningen University & Research, Wageningen, The Netherlands
[5] Deltares, Delft, The Netherlands
[6] Wageningen Marine Research, Yerseke, The Netherlands
[7] University of Antwerp, Antwerp, Belgium
[8] TU Delft, Delft, The Netherlands
[9] University of Groningen, Groningen, The Netherlands
Corresponding author: marte.stoorvogel@nioz.nl

Keywords: nature-based flood defence, sediment stability, vegetation establishment, sediment grain size, tidal inundation

1 Introduction

Tidal marshes provide many valuable ecosystem services and can play an important role in nature-based flood risk mitigation along low-lying coasts and estuaries, by attenuating waves and increasing erosion resistance. It was previously shown that interacting physical and ecological factors drive the development rate of erosion resistance in tidal marshes. Despite a global effort to restore or create tidal marshes, it remains unknown how different marsh restoration and creation techniques affect the development of erosion resistant sediment beds, which is essential for coastal managers to provide a long-term contribution to flood risk mitigation.

2 Methods

We quantified the erosion resistance of a landward marsh restoration technique (managed realignment) versus a seaward creation technique (sediment nourishment, Figure 1) using a 'fast flow flume' and assessed the effects of tidal inundation, sediment characteristics, and vegetation. This enabled us to determine drivers of the development rate of erosion resistance under different marsh restoration and creation techniques.

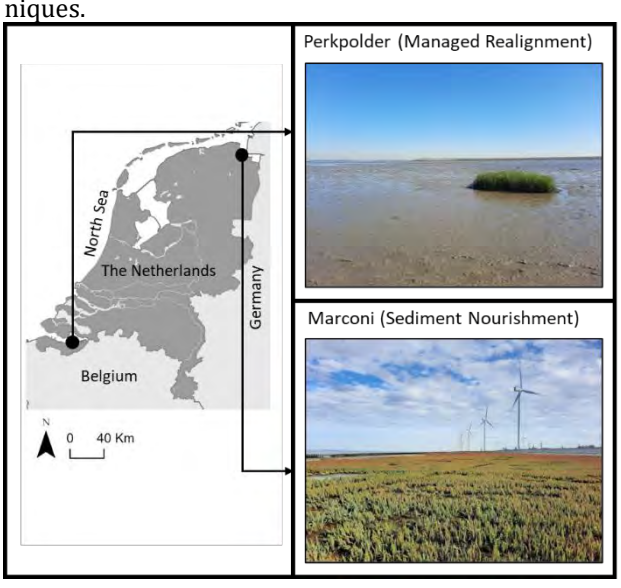

Figure 1: Locations and photos of Perkpolder (the managed realignment site) and Marconi (the sediment nourishment site) in the Netherlands.

3 Results and discussion

Results showed that sediment erosion resistance increased with increasing vegetation density and decreased with increasing sediment grain size at both the managed realignment and sediment nourishment site. Both techniques have advantages and disadvantages for the fast development of erosion resistant sediment beds. Managed realignment will likely lead to fine-grained, cohesive sediment beds, which are colonised by dense, but slowly establishing and patchy vegetation (Figure 1), resulting in spatially heterogeneous erosion resistance. In contrast, sediment nourishments, typically executed with more coarse-grained, non-cohesive sediments for practical reasons, are colonised by initially sparse, but fast establishing vegetation (Figure 1). This results in a spatially homogeneous erosion resistance. A suitable marsh restoration or creation technique should be chosen depending on the available space (landward or seaward), (a)biotic conditions at the planned location, and the amount of time until enhanced flood risk mitigation is necessary. If we plan well ahead of time, restored or created marshes have time to become erosion resistant, thereby enabling a long-term contribution of marshes to nature-based flood risk mitigation.

Acknowledgments

This study is part of the project 'The Hedwige-Prosper Polder as a future-oriented experiment in managed realignment: integrating saltmarshes in water safety' (17589) and the VIDI project 'LIVING ON THE EDGE: Using soft solutions to buffer coasts against extreme hydro-meteorological events' (18924), which are both financed by NWO. Pim Willemsen is supported by NWO (NWO-AES VENI: 21063). We would like to thank NIOZ colleagues and students, Peter Herman, Lennart van IJzerloo, and Zhenchang Zhu for their help with and input on this study. We are grateful for permission of Rijkswaterstaat, Gemeente Eemsdelta, and Groningen Seaports to perform the measurements in the field.

Biodiverse and spatially self-organized tidal marshes are most effective for nature-based shoreline protection

Schoutens K.[1], Fivash G.[1], Schoelynck J.[1], Borsje B.W.[2], Temmerman S.[1]
[1]University of Antwerp, Department of Biology, ECOSPHERE, Belgium
[2]University of Twente, Department of Civil Engineering, the Netherlands
Corresponding author: ken.schoutens@uantwerpen.be

Keywords: Wave attenuation, vegetation, zonation, plant-wave interaction

1 Introduction

Coastal flood protection faces growing challenges due to sea level rise and intensifying storms driven by climate change. Conservation or creation of tidal marshes offers a promising nature-based adaptation for protection of muddy estuarine shorelines against erosion and flood risks, as they attenuate wave impacts while providing ecological benefits [1], [2], [3]. However, limited knowledge exists on how much the efficiency of nature-based wave attenuation depends on (a) biodiversity, i.e. the presence of multiple plant species with species-specific plant-wave interactions, and (b) resulting self-organization of spatial zonation of plant species. This study investigates this question, focusing on tidal marsh species commonly found in NW European estuaries.

2 Methods

We model how species-specific plant-wave interactions lead to cross-shore species zonation and wave attenuation rates using a conceptual 1D cellular automaton (1 km of cross-shore tidal flat, discretized in 10 m cells). The model is parameterized with (a) geospatial analysis of species growth probabilities based on wave exposure and (b) field measurements of wave attenuation rates in function of plant species traits, using the Elbe estuary, Germany, as a case study.
We started an iterative simulation from a bare tidal flat, with vegetation presence determined by bed shear stress and interspecies competition.

3 Results & discussion

Our findings highlight that (a) the species-specific plant-wave feedbacks lead to spatial self-organization of plant species zonation, i.e. small, flexible species cope well with wave exposure and hence thrive in the most seaward, wave-exposed zone, but are less effective in attenuating waves; while taller, stiffer species dominate in more landward wave-protected zones, where they offer higher wave attenuation. Further, our results show that (b) species diversity enlarges the overall width of the marsh vegetation and enhances the overall wave attenuation over the cross-shore profile, as a result of the different complementing plant traits explained in previous sentence. Hence, the self-organized spatial distribution of multiple species, formed through mutual plant-wave interactions, supports the formation of wider marshes with higher wave attenuation capacity and underscores the ecosystem-scale benefits of biodiverse, spatially self-organized plant communities in nature-based shoreline protection.

References

[1] S. Temmerman, E. M. Horstman, K. W. Krauss, J. C. Mullarney, I. Pelckmans, and K. Schoutens, "Marshes and Mangroves as Nature-Based Coastal Storm Buffers," *Annual Reviews in Marine Sciences*, vol. 13, no. 33, 2023, doi: 10.1146/annurev-marine-040422.

[2] E. B. Barbier, S. D. Hacker, C. Kennedy, E. W. Koch, A. C. Stier, and B. R. Silliman, "The value of estuarine and coastal ecosystem services," *Ecol Monogr*, vol. 81, no. 2, pp. 169–193, May 2011, doi: 10.1890/10-1510.1.

[3] K. Schoutens *et al.*, "How effective are tidal marshes as nature-based shoreline protection throughout seasons?," *Limnol Oceanogr*, vol. 64, pp. 1750–1762, 2019, doi: 10.1002/lno.11149.

Sensitivity of Morphodynamic Equilibria of Double-Inlet Systems to Basin Width

H.M. Schuttelaars[1], X.Deng[1,2],T. De Mulder[3]

[1]Delft Institute of Applied Mathematics, Delft University of Technology, Delft, The Netherlands
[2]Now at Zhejiang Lab, Hangzhou, Zhejiang, China
[3]Hydraulics Laboratory, Dep. Civil Engineering, Ghent University, Ghent, Belgium

e-mail corresponding author: h.m.schuttelaars@tudelft.nl

Keywords: *morphodynamic equilibria; double inlet systems; width dependence*

1 Introduction

Double inlet systems consist of a tidal basin that is connected to the outer sea by two connecting channels. A typical example is the Marsdiep-Vlie system, located in the Dutch Wadden Sea. In this presentation, we aim to investigate the existence of morphodynamic equilibria of double–inlet systems, both the number and their stability. Furthermore, the sensitivity of these findings to variations of basin width will be systematically explored. To this end, an idealized morphodynamic model is developed that allows for a direct identification of morphodynamic equilibria of double inlet systems.

2 Methods

The morphodynamic evolution of the double inlet system is modeled using the depth-averaged shallow water equations, the suspended sediment transport equation, and the bed evolution equation. These equations are studied through asymptotic analysis involving a small parameter, which is the ratio of tidal amplitude to the undisturbed water depth. Because water motion and sediment transport occur on a much shorter timescale than bed evolution, the bed is treated as fixed during the fast hydrodynamic processes, with its profile changing only on the longer timescale. After spatially discretizing in the harmonic domain, the equations using the finite element method, morphodynamic equilibria are determined through a continuation method. This approach directly identifies solutions where the tidally averaged sediment transport remains constant within the tidal inlet system. For more details, see [1].

3 Results

To investigate the number and stability of morphodynamic equilibria, we consider a rectangular double inlet system with a length of 30 km, a default width of 1 km, and a drag coefficient $c_d = 0.002$. The system is driven solely by an M2 tidal constituent at both sea connections, with a prescribed M2 amplitude of 0.62 m at both sides and a phase difference of 1 deg between the inlets (with the righthand side inlet a larger phase). Sediment transport is predominantly driven by suspension through diffusive processes.

The governing equations permit a width-averaged morphodynamic equilibrium, characterized by a tidal high located approximately at the center of the basin, as shown in Fig. 1(a). This morphodynamic equilibrium is unstable against small perturbations, as illustrated in Fig.1(b).

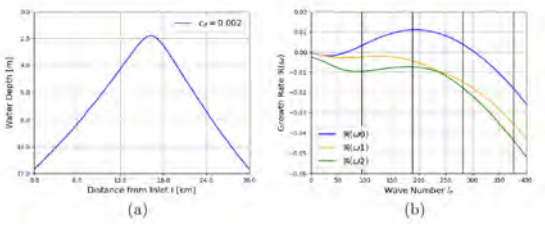

Figure 1: Width–averaged equilibrium bed profile (a) and its associated linear stability (b).

The sensitivity of the underlying morphodynamic equilibria will be systematically investigated for varying embayment widths. The associated equilibrium bed profiles and underlying mechanisms will be discussed in detail, for an example see Fig.2.

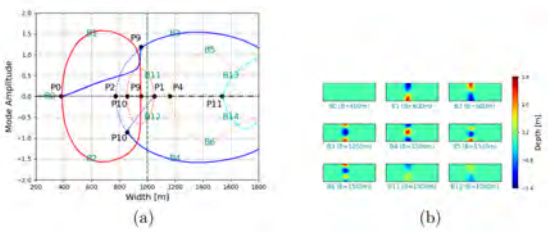

Figure 2: Bifurcation diagram (a) and associated equilibrium bed profiles (b).

4 Conclusions

By applying a continuation method, finite-amplitude morphodynamic equilibria are identified, revealing that the wave number of the fastest-growing mode predicted by linear stability analysis does not always manifest in the finite-amplitude patterns. Moreover, this method provides a systematic framework for exploring the physical mechanisms that give rise to these equilibria.

References

[1] X. Deng. *Morphodynamic equilibria in double–inlet systems, their existence, multiplicity and stability.* PhD thesis, Delft University of Technology, Delft, The Netherlands, 2023. URL https://doi.org/10.4233/uuid:afad2560-3e7b-4b43-9997-17b4e24e9e02.

Using an equilibrium model to explore the influence of climate variations on estuarine evolution

Edouard Basquin[1], Karin R. Bryan[1], Giovanni Coco[1], Ian H. Townend[2]

[1]The University of Auckland, New Zealand
[2]University of Southampton, United Kingdom

e-mail corresponding author: ebas390@aucklanduni.ac.nz

Keywords: *Estuary; Morphological Response; Equilibrium; ASMITA*

1 Introduction

Climate change is a key factor in estuarine morphodynamics evolution; indeed these complex systems at the land-ocean-river interface, undergo numerous forcings that evolve with changing climate. New Zealand; 350 estuaries vary spatially in forcing mechanisms, morphologies, and tidal prisms. Research [1] has shown that sea-level rise (SLR) responses differ between estuary types, complicating predictions of climate-induced changes. SLR depends on the location and can even be negative in some areas due to vertical land movement. Rainfall patterns are also expected to change with some regions, becoming either more or less intense, inducing changes in river discharge and sediment supply. These changes highlight the importance of estuary-scale modeling to consider regional variability in long-term responses over decades to centuries.

2 Methods

In this study, we used the numerical model ASMITA (Aggregated Scale Morphological Interaction between Tidal basin and Adjacent coast), which is a scale-aggregated numerical model [2] based on an equilibrium approach. The estuary is subdivided into different elements that are assumed to be in an equilibrium state under constant hydrodynamic conditions. We first assessed how model settings (e.g horizontal and vertical transport coefficients) influence the morphological responses. Next, a sensitivity analysis was conducted on a cyclical pattern in river discharge and sediment concentration, reproducing the increase in extreme dry and rainy events. This was applied to an artificial estuary to examine the role of river-driven morphological responses to SLR. This sensitivity analysis led us to select Tairua Harbour, New Zealand, as the estuary to study the role of various forcing mechanisms, including sea-level rise (SLR) and rainfall projections. After reconstructing historical bathymetry and applying a calibration framework, the morphological responses of the estuary were simulated for the next century, using the corresponding SLR and rainfall projections.

3 Results

The sensitivity analysis shows different estuarine behaviors under constant and cyclic river inflow conditions in the context of steady SLR. When constant (Figure 1a), the estuary gradually becomes deeper in response to SLR and eventually reaches a new steady

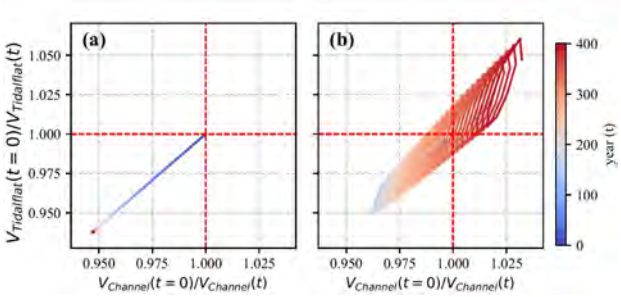

Figure 1: Estuarine morphological response to SLR (1.7 mm/y) under constant (panel a) or linearly amplified cyclical variations in river discharge and concentration (panel b). $V_{Elements}(t)$ represents the water volume for each estuarine element at year = t

state. However, when including a cyclic behavior for the river inflow (Figure 1b), after the estuary becomes deeper, both elements of the estuary become shallower. However, changes in response can still be observed on a yearly or decadal scale, corresponding to the oscillation period of river input changes. Given the range of SLR and rainfall projections for Tairua Harbor, the studied estuary showed varying responses and behaviors highlighting the importance of simulating multiple projections.

4 Conclusion

This study highlights the key role of river discharge and suspended sediment concentration in estuarine morphological responses to SLR. By examining Tairua Harbour responses to multiple projections, we show the variability in long-term morphological responses to climate change.

References

[1] Jasper RFW Leuven, Harm Jan Pierik, Maarten van der Vegt, Tjeerd J Bouma, and Maarten G Kleinhans. Sea-level-rise-induced threats depend on the size of tide-influenced estuaries worldwide. *Nature climate change*, 9(12):986–992, 2019.

[2] Ian Townend, Zheng Bing Wang, Marcel Stive, and Zeng Zhou. Development and extension of an aggregated scale model: Part 1–background to asmita. *China Ocean Engineering*, 30:483–504, 2016.

Tidal inlet and estuary equilibrium relationships

Ian Townend, Zheng Bing Wang[2],Quirijn Lodder[2,3]
[1] School of Ocean and Earth Science, University of Southampton, UK
[2] Faculty of Civil Engineering and Geosciences, Delft University of Technology, Delft, the Netherlands
[3] Rijkswaterstaat, 3500, GE, Utrecht, the Netherlands
Corresponding author: i.townend@soton.ac.uk

Keywords: Morphodynamics, Wadden Sea Inlets, UK Estuaries

1 Introduction

Our focus is on the large scale, or gross properties, of estuaries and inlets, such as surface area, volume and cross-sectional area at different states of the tide. Such properties are typically related to the tidal prism, or basin surface area, as a way of expressing how they scale with basin size. This links closely to the concept of regime theory, which, whilst extensively explored for rivers has also been applied to estuaries and inlets. Such relationships are so ubiquitous that they have been taken to imply an indicative equilibrium state for this type of system [1].

2 Approach

We have explored the differences in the large scale properties of both inlets and estuaries in order to assess the adequacy of volume and area relationships for such systems. We pay particular attention to the nature of the variation of the gross dimensions with tidal prism and basin area and the extent to which individual systems should be characterised by a linear or power law relationship with these properties.

Having reviewed several theoretical formulations, we examine the resulting relationships using data for UK estuaries and Wadden Sea inlets. The results enable a review of the relative merits of the different relationships, the gaps in our current understanding and, hence, where further research could usefully be focussed.

3 Initial results

The observations for inlets of the Wadden Sea and UK estuaries suggests that there is a marked difference. For example, Figure 1 shows how the surface area at mean tide level is strongly correlated with the tidal prism divided by the tidal range in both cases. However, for the UK estuaries this is an almost 1:1 relationship, whereas for the Wadden Sea inlets this is a power relationship, at least for inlets with areas less than $5x10^7$ m^2. The UK estuaries are predominantly single, or branched main channels, with flanking tidal flats. The Wadden Sea is a set of inter-connected inlets, with a network of channels and extensive areas of tidal flats and marshes. Thus, the differing aspect ratios, interconnected nature of the inlets, and the extent of the marsh-flats area may account for the very different morphologies. However, many relationships for the collective data sets, which cover size variations of 3-4 orders of magnitude, also exhibit power law relationships. Notable amongst these is the relationship of volumes at mean tide and low water to the tidal prism. For the Wadden sea inlets this is also the case for the surface area at these elevations. In the presentation we will explore these differences and a possible explanation.

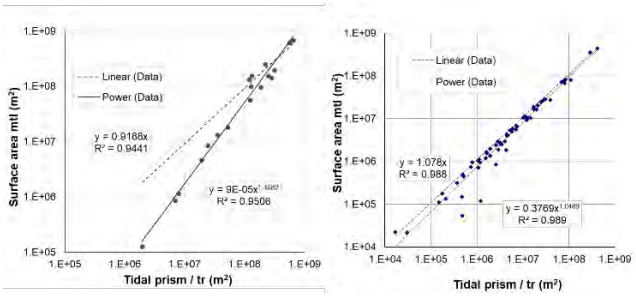

Figure 1: Mean tide surface area as a function of prism/tidal range for (a) the North and West Frisian Wadden Sea inlets and (b) UK estuaries data from [2,3,4].

4 Conclusion

In conclusion, whilst many variables in the natural environment exhibit some form of non-linear behaviour, assuming that this depends on just one parameter may obscure the real dependencies. In the case examined, power law relationships have been used to describe how the gross properties of inlets and estuaries vary with tidal prism (or other governing properties). However, it is not axiomatic that these are valid descriptions of the behaviour of individual systems. In this case, the implicit dependence on some measure of channel length, as well as tidal prism, can lead to the impression of a power law, whilst obscuring the true dependencies. Whereas linear analytical solutions compare well will with the observed data and point to a linear rather than power law relationship.

References

[1] NE. Healthy Estuaries 2020: An Assessment of Estuary Morphological Equilibrium. Report No. NECR250, 107 (Royal Haskoning DHV, Peterborough, 2018).

[2] Yu, Q., Wang, Y., Flemming, B. & Gao, S. Scale-dependent characteristics of equilibrium morphology of tidal basins along the Dutch–German North Sea Coast. *Marine Geology* **348**, 63-72 (2014). https://doi.org/10.1016/j.margeo.2013.12.005

[3] Townend, I. H. An examination of empirical stability relationships for UK estuaries. *Journal of Coastal Research* **21**, 1042-1053 (2005).

[4] Wang, Z. B., Elias, E. P. L., van der Spek, A. J. F. & Lodder, Q. J. Sediment budget and morphological development of the Dutch Wadden Sea: impact of accelerated sea-level rise and subsidence until 2100. *Netherlands Journal of Geosciences* **97**, 183-214 (2018). https://doi.org/https://doi.org/10.1017/njg.2018.8

The Role of Estuarine Processes in River Width Equilibrium

Lorenzo Durante[1], Nicoletta Tambroni[1]

[1]University of Genoa, Genoa, Italy

e-mail corresponding author: lorenzo.durante@edu.unige.it

Keywords: *estuaries; equilibrium; width; profiles;*

1 Introduction

The equilibrium cross-section of natural rivers has been extensively studied in the field of fluvial morphology. Various approaches have been developed to investigate this concept, with one of the most common methodologies relying on regression analysis of comprehensive datasets to derive quasi-universal relationships as functions of bankfull discharge.

More recently, [1] proposed a unified framework for predicting river flow depth and cross-sectional width. They introduced the Cross-Section Evolution Model (CSEM), which accounts for the influence of bank macro-roughness (bumps) on the flow field. This model evaluates friction along the banks and compares it to the critical resistance to erosion of cohesive bank material, thereby determining the equilibrium cross-section of the river.

Despite these advancements, the application of such relationships to estuarine environments remains limited, particularly in contexts where tidal currents significantly influence river morphology. This study develops an iterative approach to address the effects of tidal modulation on equilibrium river width.

2 Methods

In this study, the CSEM model proposed by [1] is extended to incorporate the influence of tidal modulation on the flow field. It is assumed that the most vulnerable circumstances for bank stability occur under ebb conditions, when tidal currents enhance the main river flow. [2] have shown that although tidal influences decrease with distance from the inlet, even small tidal oscillations at the mouth may affect the uniform river flow, in an extent that increases as the forcing tidal amplitude grows. To estimate the flow depth and velocity at each river cross-section, the analytical equilibrium solution of estuaries developed by [2] is employed.

The methodology follows an iterative procedure. Initially, equilibrium bottom profiles are computed for an idealized straight, rectangular channel. The CSEM model is then applied at each cross-section to determine the local equilibrium width. Once a new width distribution is obtained, the equilibrium bottom profiles are thus recalculated, correcting the initial prevision. This iterative process continues until the bottom profile and width distribution reach equilibrium. Note that in order to set up this procedure, the analytical model by [2], which was originally proposed only for exponentially converging estuaries, has been preliminary reformulated to accommodate a generalized width distribution, as predicted by the CSEM model.

3 Results and Conclusions

The iterative procedure enables the determination of the equilibrium width distribution in natural estuaries. As commonly observed in such environments, a funnel-shaped profile emerges, even when only a small-amplitude tide (ϵ) is introduced, as illustrated in Figure 1.

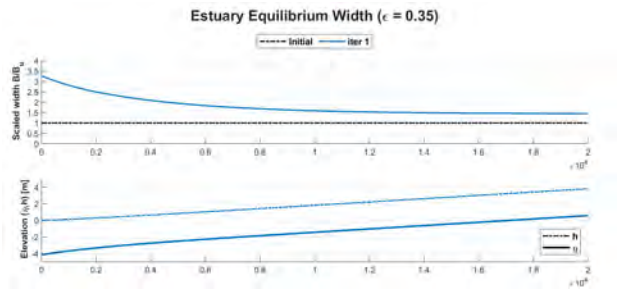

Figure 1: Width and elevation profiles of an estuary for $\epsilon = 0.35$. The top panel shows the initial and first iteration width distribution. The bottom panel illustrates the initial equilibrium bed (η) and free-surface (h) according to [2].

Notably, the widening of the channel at the estuary mouth is closely linked to the velocity increase during ebb conditions with respect to normal uniform flow. This acceleration increases the stresses on the wetted perimeter, thereby driving local widening of the estuary.

Acknowledgements

This research has been supported by the Italian Ministerial PRIN PNRR 2022: "Safety Equilibrium Conditions for rivers UndeR changing climatEs (SECURE)" n. P2022KA5CW— CUP D53D23022870001. The authors would like to thank S. Francalanci, S. Lanzoni, G. Artini, and E. Moresco for their valuable contributions to this project.

References

[1] S Francalanci, S Lanzoni, L Solari, and AN Papanicolaou. Equilibrium cross section of river channels with cohesive erodible banks. *Journal of Geophysical Research: Earth Surface*, 125(1): e2019JF005286, 2020.

[2] G Seminara, M Bolla Pittaluga, and N Tambroni. Morphodynamic equilibrium of tidal channels. *Environmental Fluid Mechanics-Memorial Volume in Honour of Prof. Gerhard Jirka (ed. W. Rodi & M. Uhlmann)*.

Tidal influence over river- width distribution, an analytical approach.

Enrico Moresco[1], Lorenzo Durante[1], Nicoletta Tambroni[1]
[1]Università degli studi di Genova, Genoa, Italy
Corresponding author: enrico.moresco@edu.unige.it

Keywords: estuarine morphodynamics, tides, perturbation methods

1 Introduction

Coastal channel morphology is closely governed by tidal influences. It is well known that a river's cross-sectional width typically increases downstream toward the sea. As a result, estuarine width distribution is often represented by an exponentially converging function from the seaward boundary upstream, characterized by a convergence length. In previous studies on estuarine equilibrium profiles, this width distribution has generally been specified as a given input parameter [1]. However, no analytical formulation currently exists that links width distribution with tidal amplitude in estuarine environments. Here, we address this gap by removing the need to prescribe a width distribution and instead propose a dynamic framework that reveals how estuary equilibrium bed, free-surface, and width profiles interrelate under the hypothesis of fairly small tidal oscillations at the inlet.

2 Methods

Building upon the analytical framework established by [1] for the long-term equilibrium of a river-dominated estuary, we introduce width distribution as a variable within the system. To achieve this, an additional constraint is incorporated alongside the continuity, momentum, and tidally averaged Exner equations to determine the equilibrium width. Specifically, a threshold condition on shear stresses is imposed, assuming that the most critical condition for bank stability occurs during ebb tide, when tidal currents intensify the primary river flow.

The system is conceptualized as a uniform river flow perturbed by a small-amplitude tide at its downstream boundary. The governing equations are made dimensionless by normalizing each variable using the unperturbed upstream uniform flow dimensions, with the perturbation parameter ϵ representing the dimensionless tidal amplitude.

A perturbative approach is thus employed to solve at different orders of ϵ, the problem of the long-term morphodynamic equilibrium of the estuary, according to which the absolute bed elevation does not experience any net variation in a tidal cycle.

3 Results

Solutions up to the first order were derived for the dimensionless river width (B), depth (D), free-surface elevation (h), and fluid discharge (q). As expected, the leading order solution corresponds to the unperturbed uniform flow profile of a cylindrical channel. At the first order, a perturbation in width emerges, leading to the well-known exponential width profile (Figure 1).

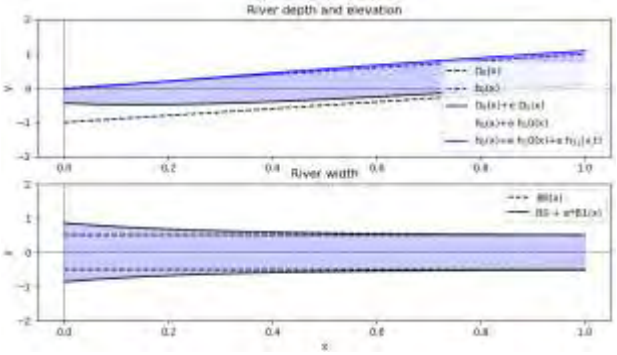

Figure 1: Comparison in terms of bed profiles (upper plot) and width diistributions (lower plot) -between uniform flow (dashed lines) and 1-st order perturbed solution (solid lines)- for ϵ=0.1.

Even under weak tidal forcing, significant variations in width and depth are observed near the river mouth.

This shallowing-widening process aligns well with empirical observations and highlights the dominant role of tidal dynamics in estuarine morphodynamics, even under small amplitude forcings. To further refine our understanding, second-order contributions are currently being evaluated. Additionally, future research will focus on comparing these analytical findings with field observations from the Ombrone River, Tuscany, Italy.

Acknowledgments

This research has been supported by the Italian Ministerial PRIN PNRR 2022: "Safety Equilibrium Conditions for rivers UndeR changing climatEs (SECURE)" n. P2022KA5CW— CUP D53D23022870001. The authors would like to thank ~~S.~~S. -Francalanci, S. Lanzoni and G. Artini for their valuable contributions to this project.

References

[1] Seminara, G., M. Bolla Pittaluga, and N. Tambroni (2012), Morphodynamic equilibrium of tidal channels, in Environmental Fluid Meechanics- Memorial Volume in Honour of Prof. Gerhard Jirka, Karslrhue (Gemany), ed. by W. Rodi and M. Uhlmann, Taylor and Francis.

Interface with sedimentary grains favors biofilm retention and anti-erosion under shear stress

Guotao Tang[1,2]
[1]State Key Laboratory of Hydrology-Water Resources and Hydraulic Engineering, Hohai University, Nanjing, China
[2]Jiangsu Key Laboratory of Coast Ocean Resources Development and Environment Security, Hohai University, Nanjing, China
Corresponding author: Guotao Tang, email: 240403020001@hhu.edu.cn

Keywords: sediments, biofilm retention, anti-erosion, shear stress, interface

Abstract

The biofilm-sediment coupled system plays a pivotal role in the functioning of various aquatic ecosystems, including riverine, coastal, and reservoir environments. Biofilm formation on sediment particles exerts a substantial influence on the Erosion-Transportation-Deposition-Consolidation (ETDC) cycles, which are critical for sediment transport dynamics. The presence of biofilms often mitigates sediment erosion through biostabilization, wherein biofilms induce bio-cohesion between particles, primarily mediated by the secretion of extracellular polymeric substances (EPS). While this process enhances the stability of sediment beds, it can also contribute to siltation in reservoirs through the aggregation of fine particles.

However, sediments may also influence the erodibility of biofilms in a reciprocal manner. In field studies, biofouling on marine instruments often involves not only biofilms but also associated sediments. The coupled structure-consisting of biofilm slime with sedimentary grains as a framework-demonstrates significant resistance to shear erosion, making it difficult to remove even after exposure to storms. This raises a research question: does interface with sands or silts enhance biofilm retention?

Herein, fine sandy beds (D_{50}=147 μm), silty beds (D_{50}=64.5 μm), and glass slides (as control) were used as different substrates for biofilm colonization (*Chlorella* algae). The formation of biofilms on these substrates was monitored using an optical microscope and a hyperspectral camera at intervals of 1, 3, 6, 12, 18, and 24 days of cultivation. The EPS composition, particularly polysaccharides and proteins, was quantitatively analyzed. At 3, 6, 12, 20, and 24 days of cultivation, a stepwise increment of shear force (0, 0.12, 0.18, 0.26, 0.31, 0.40, 0.52, 0.70 Pa) was assess the biofilm's resistance to erosion on each substrate. Hyperspectral data were collected and analyzed using the kNDVI index[1], enabling a quantitative evaluation of biofilm erosion resistance by calculating spatial variations in biofilm retention across different substrates.

The results indicate that the kNDVI index effectively reflects the actual condition of the biofilm (Figure 1a). When using the kNDVI index to monitor biofilm growth on different substrates, it was observed that biofilms grew most rapidly on glass slides, while their development on fine sandy and silty beds was relatively similar. Analysis of optical microscope images revealed that biofilm growth initially occurred within the pores between sediment grains (Figure 1b). After 12 days, the biofilm on silty beds began forming continuous layers, whereas on fine sand, the biofilm predominantly continued to grow within the interstitial gaps. In contrast, the biofilm on glass slides exhibited the fastest and most uniform growth. Following shear treatment and erosion, the biofilm on the blank glass slide was rapidly fragmented into smaller pieces (Figure 2). Conversely, the biofilm on fine sandy and silty beds remained relatively intact, demonstrating better structural integrity and uniformity.

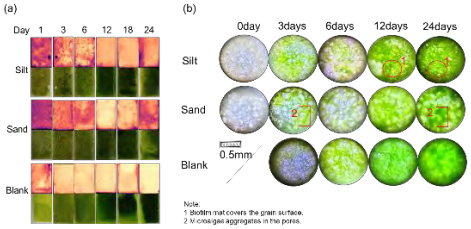

Figure 1. (a)Biofilm and hyperspectral images on different substrates, the top row presents kNDVI-index-processed images, while the bottom row displays photographs captured using a mobile phone; (b) Optical micrographs of biofilms on different substrates at different cultivation times.

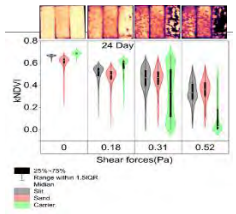

Figure 2. Heat maps and violin plots of kNDVI data remaining after a 24-day cultivation period under shear forces of 0, 0.18, 0.31, and 0.52 Pa.

There are three key findings: (1) Microalgal biofilms colonize more rapidly on smooth surfaces compared to sedimentary ones but are more susceptible to erosion. (2) Sedimentary structures and pores provide shelter for bio-aggregates, with the protective effect varying based on grain size. (3) Sediment supply plays a critical role in biofilm retention by influencing erosion patterns, resulting in gradual removal rather than sudden collapse. These findings contribute to refining the research framework for understanding bio-sediment resistance to erosion.

References

[1] Camps-Valls, G., Campos-Taberner, M., Moreno-Martínez, A., Walther, S., Duveiller, G., Cescatti, A., Mahecha, M.D., Muñoz-Marí, J., García-Haro, F.J., Guanter, L., Jung, M., Gamon, J.A., Reichstein, M. and Running, S.W. 2021. A unified vegetation index for quantifying the terrestrial biosphere. Science Advances 7(9).

Vegetation impacts on crevasse splay dynamics and channel-floodplain connectivity in a river delta

Sarah M Brannum[1,2], Kory Konsoer[2,3], Matthew Hiatt[1,2]

[1]Department of Oceanography & Coastal Sciences, Louisiana State University, Baton Rouge, Louisiana, USA
[2]Coastal Studies Institute, Louisiana State University, Baton Rouge, Louisiana, USA
[3]Department of Geography and Anthropology, Louisiana State University, Baton Rouge, Louisiana, USA

e-mail corresponding author: sbrann5@lsu.edu

Keywords: *Nature-based Solutions, Ecomorphodynamics, Coastal Restoration, Delft3D-FM*

1 General Information

Channel-floodplain connectivity in river deltas describes water mass and momentum transfer from channels to the floodplain through either overbank flow, secondary channels, or crevasses [1]. The presence, density, and seasonality of vegetation affect channel-floodplain connectivity throughout the year. Engineered crevasses target locations to transport sediment-rich water to build splays that create subaerial land. The efficiency and fate of an engineered crevasse is a function of many hydrodynamic and morphodynamic factors, as well as vegetation characteristics [2]. In this study, we explore how vegetation parameters influence the balance of discharge and momentum partitioning between overbank flow and crevasses to assess the viability of engineered crevasses on crevasse splay formation. A hydro- and eco-geomorphic model is used to evaluate crevasse implementation guided by hydrographic surveys.

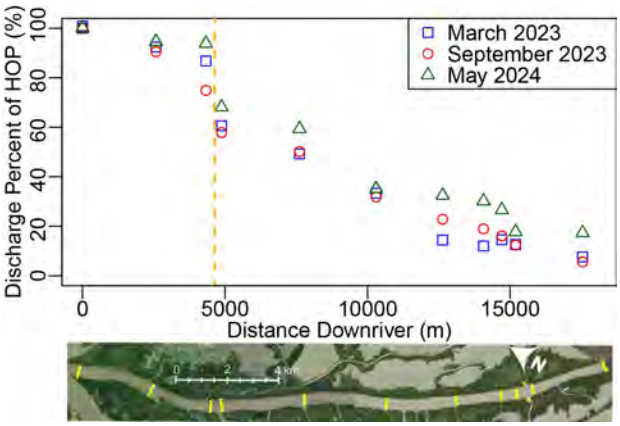

Figure 1: Discharge measurements from an acoustic Doppler current profiler (ADCP) down South Pass. Dashed line shows location of an engineered crevasse.

2 Methods

Hydrographic surveys along South Pass, a major distributary channel on the Mississippi River Delta (MRD) with existing natural and engineered crevasses, show decreasing discharge downstream as flow is redirected into the floodplain via crevasses and overbank flow (Fig.1). A schematized Delft3D-FM model of South Pass, consisting of a straight channel and periphery wetland floodplains, is used to explore geomorphic changes resulting from the flow partitioning between overbank and distributary channels. The model is run over short geomorphic time scales to track patterns of erosion and deposition resulting from crevasse placement and number, alongside variability in vegetative conditions.

3 Expected Results

Based on field surveys, when annual vegetation is present and perennial vegetation is most active (May), a higher fraction of river discharge stays within the main channel, which we attribute to decreased overbank flow due to increased vegetation density along the banks (Fig.1). Discharge loss is also attributed to crevasses, with the fraction of discharge loss depending on the season measured, size of crevasse, and location along main channel (Fig.1). Model results will show the variable impact of the number and arrangement of engineered crevasses on splay formation, elevation capital gain/loss, and erosion and deposition patterns. We will test the hypothesis that splay formation is modulated by lateral and in-channel momentum flux. Field measurements show how vegetation patterns and dynamics control lateral outflow of water (Fig.1), and model results will test vegetation impacts on sediment transport patterns.

4 Implications

The MRD is heavily managed to maintain shipping and commerce, protect communities from major storm events, and provide valuable ecosystem services. This study examines fundamental processes controlling splay dynamics that coastal managers can use to implement cost-effective coastal restoration through engineered crevasses.

Acknowledgments

This project was funded by the US National Academies of Sciences, Engineering, and Medicine Gulf Research Program Grant Number SCON-10000883.

References

[1] Matthew Hiatt and Paola Passalacqua. Hydrological connectivity in river deltas: The first-order importance of channel-island exchange. *Water Resources Research*, 51(4):2264–2282, 2015.

[2] Jaap H Nienhuis, Torbjörn E Törnqvist, and Christopher R Esposito. Crevasse splays versus avulsions: A recipe for land building with levee breaches. *Geophysical Research Letters*, 45(9): 4058–4067, 2018.

A hydrological switch drives the transition from saltmarsh to reedland ecosystem

A. Valsamidou[1,2], M. Bastiaanse[3], D. van der Wal[1,4], M.G. Kleinhans[2], G.K. Keller[2], M. Rietkerk[2], J. van de Koppel[1,5]

[1]Royal Netherlands Institute of Sea Research, Yerseke, The Netherlands
[2]Utrecht University, Utrecht, The Netherlands
[3]University of Cambridge, Cambridge, UK
[4]University of Twente, Enschede, The Netherlands
[5]University of Groningen, Groningen, The Netherlands

e-mail corresponding author: archontoula.valsamidou@nioz.nl

Keywords: *landscape hydrology; drainage; ecosystem states*

1 Introduction

Coastal peatlands are vital freshwater biogeomorphic ecosystems that accumulate organic material and store carbon over millennia. Despite their crucial role in carbon accumulation, peatland initiation under brackish or even saltwater conditions is still poorly understood. Geology highlights that transitional reed-marsh phases often precede the hydrologically isolated ombrotrophic peatlands [2] suggesting biogeomorphological shifts in the saltmarsh feedbacks. This study investigates how *Phragmites australis* (reed), a precursor species for coastal peatlands, establishes on saltmarshes causing new interactions at the local scale that generate a hydrological switch that alters the landscape.

2 Methods

First, based on a saltmarsh development numerical model (SFERE) [1] we simulated the interactions between vegetation, hydrology, and sedimentation processes during the reed establishment and expansion. Model results were analyzed calculating hydrological metrics (topographic wetness index, residence time) to assess the new system state drainage conditions. Our simulations were compared with field observations from reed-established and saltmarsh areas of Saeftinghe. Field data included vegetation as well as elevation remotely sensed time series to assess the clogging influence of reed vegetation on the tidal creek system and salinity measurements to identify the reduction of tidal influence within reed patches.

3 Results and conclusions

Our combined theoretical and empirical results highlight that a hydrological switch triggered by the positive feedback between reed invasion, reduced creek network complexity, and reduced saltwater incursion, drives the transition from saltmarsh to reed-land ecosystems. This process could be a key factor for the establishment of peatlands in the past, as well as for carbon accumulation in reed-based peatlands in the future.

Model results (Figure 1) show that accumulation of roots and organic matter by the reed vegetation reduces the complexity of the creek network, and leads to a higher, more homogeneous freshwater landscape that further facilitates reed growth. The flattened topography and reduced drainage density of the landscape eventually increase the residence time of flow and the surface wetness propensity.

These findings align with the field observations and sequential airborne laser altimetry from Saeftinghe. There is persistent reed expansion, and within the reed patches the significant creek elevation increase leads to altered hydrological conditions and reduced surface soil salt content.

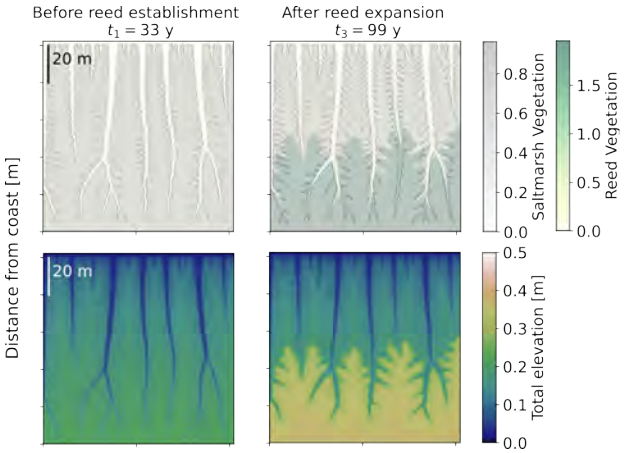

Figure 1: Model results of the saltmarsh and the reed-marsh phase, for the vegetation and sediment (inorganic and organic) variables.

References

[1] R. C. Van de Vijsel, J. van Belzen, T. J. Bouma, D. van der Wal, B. W. Borsje, S. Temmerman, L. Cornacchia, O. Gourgue, and J. van de Koppel. Vegetation controls on channel network complexity in coastal wetlands. *Nature communications*, 14(1):7158, 2023.

[2] M. Waller and J. Kirby. Coastal peat-beds and peatlands of the southern north sea: their past, present and future. *Biological Reviews*, 96(2):408–432, 2021.

Stream Meandering in Tidal Wetlands: Unveiling Patterns, Drivers, and Ecomorphodynamic Impacts

Alvise Finotello[1]
[1]Dept. of Geosciences, University of Padua, Padua, Italy

Corresponding author: alvise.finotello@unipd.it

Keywords: Coastal Wetlands, Ecomorphodynamics, Meandering, Blue carbon

1 Introduction

Sinuous channels found in tidal coastal wetlands are often compared to meandering rivers due to their similar dynamics. However, unlike alluvial plains shaped by meandering rivers, tidal wetlands have long been perceived as lacking clear morphological evidence of active meandering, such as meander cutoffs and oxbow lakes. For much of the past century, geomorphologists have interpreted tidal meanders as differing morphodynamically from their fluvial counterparts, attributing this distinction to the unique ecomorphodynamics of coastal environments, where bidirectional flow plays a key role. More recently, however, studies have suggested that tidal meanders exhibit migration rates and dynamics comparable to those of rivers, challenging the long-standing assumption that tidal and fluvial meanders differ fundamentally in their morphological evolution[1–3]

2 Research questions

Building on these recent advancements in research, we seek to understand why sinuous channels in tidal wetlands appear to lack the morphological footprints of active meandering, such as meander cutoffs and scrolls, despite exhibiting migration rates relative to channel size that are similar to those of meandering rivers. Moreover, we aim to shed light on the broader implications of active channel migration in coastal wetlands, particularly the ecological and geomorphological consequences of such dynamics in these environments. Finally, we explore how stream meandering in tidal wetlands can be reliably modeled numerically, a critical step to advancing current research and practical investigations of coastal wetland ecomorphodynamic evolution.

3 Results

Our findings reveal that meander cutoffs are widespread in tidal coastal wetlands, though often hidden by rapid siltation or changes in the drainage network during the post-cutoff phase[2]. The geometric properties of tidal cutoffs are remarkably similar to those of rivers, suggesting the same physical mechanisms drive meander evolution in both environments. The rarity of tidal cutoffs in literature is mainly due to the high density of channels, hydrological connectivity, and dense vegetation in coastal wetlands, which obscure typical meander features. Additionally, tidal cutoffs often reconnect with their parent original channels, preventing the formation of crescent-shaped oxbow lakes and making cutoffs ephemeral and harder to detect. We also find that the rapid infill of abandoned tidal channels, with vertical accretion rates much higher than in surrounding wetlands, makes these areas hotspots for blue carbon sequestration[4].

Vegetation plays a key role in mediating the lateral migration of meandering streams in tidal wetlands. Channels in unvegetated mudflats are significantly faster than in vegetated marshes and mangroves, though the fluvial-like, curvature-driven migration process remains consistent across all tidal wetlands. The recognized morphodynamic similarities between tidal and fluvial meanders allow the application of river modeling techniques to tidal wetlands, offering more accurate predictions of meandering dynamics and enhancing our understanding of coastal wetland evolution[5].

Altogether, our results challenge the traditional view that tidal and fluvial meanders are fundamentally different, highlighting the shared mechanisms driving meander evolution in both environments. This opens the door to the development of a new generation of ecomorphodynamic models, where tidal streams are properly treated as dynamic geomorphic features. Our findings have broad implications for understanding tidal wetlands' eco-geomorphological and biogeochemical dynamics.

References

[1] Finotello et al. (2018), Field migration rates of tidal meanders recapitulate fluvial morphodynamics. *Proc. Nat. Academy Sci.* 15(7):1463-1468

[2] Gao et al. (2024), Morphometry of Tidal Meander Cutoffs Indicates Similarity to Fluvial Morphodynamics. *Geophys Res Lett.* 51(1):1-12.

[3] Gao et al. (2022), Predominant landward skewing of tidal meanders. *Earth Surf Process Landforms.*

[4] Puppin et al. (2024), Rapid Infill of Abandoned Tidal Channels Creates Hotspots for Blue-Carbon Accumulation in Coastal Wetlands. Published online 2024. doi:10.22541/essoar.173203125.57913538/v1

[5] Mariotti and Finotello (2024), A Flow-Curvature-Based Model for Channel Meandering in Tidal Marshes. *Water Resour Res.* 60(6).

Geometry and morphology of channels around estuarine islands

M. van der Vegt[1] and H. Flikweert[1]
[1]Department of Physical Geography, Faculty of Geosciences, Utrecht University, the Netherlands
Corresponding author: m.vandervegt@uu.nl

Keywords: islands, estuarine channels, geometry, morphology, bifurcation – confluence loop

1 Introduction

Many estuaries have mid-channel vegetated islands, sometimes intersected by smaller channels (Fig. 1). The islands cause the main channel to split and merge and the channels have different length and width. Here we identify the geometrical properties of these islands and their associated channels and study whether these configurations are morphologically stable.

Figure 1. Example of vegetated islands in the Bassac river, Mekong Delta, Vietnam

2 Methods

First a systematic study was performed on the geometric properties of vegetated islands in estuarine channels using Google Earth images. The length and width of the surrounding channels was measured, as well as the length and width of the island. Furthermore, the tidal range and river discharge regime was determined based on public datasets. In total 41 islands from 15 different estuaries/deltas were analysed. Based on the geometric analysis, a series of simulations was performed with a 1D-morphodynamic model [1,2] in which the channel bed evolution of the channels was simulated. The simulations were ran till morphodynamic equilibrium was found.

3 Results

3.1 geometric analysis

The geometric analysis revealed that the length of the channels surrounding the island is approximately six times their width and two times the estuary width (measured from bank to bank). The results suggest there is typically one island in the estuary and that summed width of the islands and summed width of the channel is about the same. The width asymmetry As, calculated as As=(W2-W1)/(W2+W1), where W2 is the width the widest channel and W1 the of the narrowest one, can take any value between 0 and 0.75. The two surrounding channels have the same length with length asymmetry typically smaller than 0.1.

3.2 modelling results

Based on the geometric analysis, channels 2 and 3 had default values of 2 km wide and 12 km long, while channels 1 and 4 were 4 km wide and 40 and 10 km long, respectively (Fig. 2). Initial depth of channel 2 and 3 was slightly different and it was studied whether the equilibrium bed level was asymmetric or symmetric. The simulations were repeated for a wide range of values for the width asymmetry, discharge, tidal amplitude and for small length differences. The results show that for most cases the narrowest channels also is the shallowest one. The depth asymmetry is smaller for larger tidal influence and smaller river influence. A small length asymmetry can overcome the effect of the width asymmetry. When the narrowest channel is also shorter, it can become the deepest one.

Figure 2. Set-up of model simulations.

4 Discussion

The observed geometrical properties of the islands are similar to the properties of compound bars [3]. The island's length scales as twice the estuary width and is approximately twice as long as the typical bar length. This suggests that islands are the result of merging of two bars. The modelled bed levels are asymmetric, but this is difficult to compare with observations, because these are scarce. When assumed that channels keep their width-to-depth ratio, the observed width asymmetry seem to suggest a depth asymmetry as well.

References

[1] A. Iwantoro, M. van der Vegt and M.G. Kleinhans. Effects of sediment grain size and channel slope on the stability of river bifurcations. *ESPL*, 46, 2021.

[2] A. Iwantoro, M. van der Vegt and M.G. Kleinhans. Stability and Asymmetry of Tide-Influenced River Bifurcations. *Journal of Geophysical Research: Earth Surface*, 127(6), 2022.

[3] J. R. F. W. Leuven, M. G. Kleinhans, S. A. H. Weischer and M. van der Vegt. Tidal sand bar dimensions and shapes in estuaries. *Earth-Science Reviews*, 161, 2016.

Dynamics, Mixing, and Sediment Transport in Freshwater Plumes

Cristián Escauriaza[1], Oliver Fringer[2], Megan E. Williams[1,3]

[1]Departamento de Ing. Hidráulica y Ambiental. Pontificia Universidad Católica de Chile, Santiago, Chile.
[2]Department of Civil and Environmental Engineering, Stanford University, CA, USA.
[3]Facultad de Ciencias Biológicas. Pontificia Universidad Católica de Chile, Santiago, Chile.

e-mail corresponding author: cescauri@uc.cl

Keywords: *River plume, mixing, turbulence, numerical model*

1 Introduction

The discharge of small river plumes into the ocean drives horizontal advection of freshwater along the coast and promotes vertical entrainment and mixing at the surface. However, the complex turbulence interactions governing near-field dynamics, close to the river mouth and in the water column across multiple scales have not been fully characterized. To understand the transport and mixing processes of the near field, in this work we simulate the experiments of Yuan & Horner-Devine[2], to resolve the dynamics in supercritical and subcritical conditions, focusing on the characteristics of the plume front and the internal structures that develop near the outlet. Since suspended sediments can also increase the turbidity of coastal water and affect ecological processes by reducing the availability of light or increasing nutrients, we also incorporate the effects of sediments to provide new insights on their interactions with turbulent coherent structures generated by the plume.

2 Methods

We solve the Navier-Stokes equations with the Boussinesq approximation using finite-volume second-order accurate discretizations in space to perform direct numerical simulations (DNS). The equations are advanced in time using a dual-time stepping second-order artificial compressibility solver [1]. The computational domain contains 30 million nodes, and the inlet boundary condition is a fully-developed converged channel flow.

3 Results

The model captures the dynamics of transport and mixing in the plume, showing that the vertical structure and the horizontal spreading These differences evidence that the subcritical and supercritical conditions of the plume as shown in Figure 1 The instantaneous dynamics of the flow shows different mechanisms arising for different Froude numbers, showing that for the $Fr_d = 2.14$ mixing in enhanced by Kelvin-Helmholz instability and secondary streamwise structures that are continuously generated near the surface. We also perform a global energy balance of a freshwater plume in a basin with denser fluid, computing the evolution of turbulent dissipation and background potential energy to quantify the mixing, and evaluate the effects of sediments on the observed dynamics.

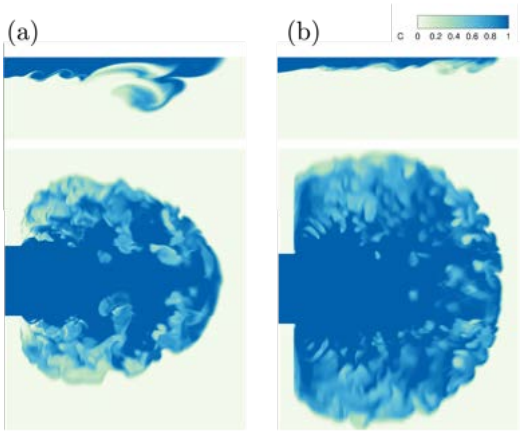

Figure 1: Instantaneous vertical and free-surface volumetric concentration of freshwater. (a) $Fr_d = 2.14$; (b) $Fr_d = 0.50$.

4 Conclusions

The model can capture the near-field dynamics of the plume, resolving the fundamental scales transporting mass and momentum. In the presentation we will discuss the non-dimensional parameters that define the plume structure and study the development and evolution of turbulent coherent structures, quantifying vertical density fluxes, entrainment, and dissipation. This quantitative description helps identify the fundamental mechanisms of mixing and transport, and the role of coherent structures in the predominant time and length scales of the near-field. We will also discuss the effects of suspended sediments in the river, discussing the changes on entrainment and mixing of the plume, driven by the dynamics of vortical structures affected by sediment concentration.

Acknowledgements

This work has been supported by ONR-Global grant N62909-23-1-2004 and computational resources provided by infrastructure of the NLHPC (ECM-02).

References

[1] M Barros and C Escauriaza. Lagrangian and eulerian perspectives of turbulent transport mechanisms in a lateral cavity. *Journal of Fluid Mechanics*, 984:A1, 2024.

[2] Y Yuan and AR Horner-Devine. Experimental investigation of large-scale vortices in a freely spreading gravity current. *Physics of Fluids*, 29 (10), 2017.

Automated Characterisation of Tidal Course Morphology for Intertidal Mudflat Study

Chitrachandika Bhoobun[1], Florent Grasso[2], Romaric Verney[2,3]
[1,2,3]IFREMER – DYNECO/DHYSED, Centre de Bretagne, F-29280 Plouzané, France
Corresponding author: cbhoobun@ifremer.fr

Keywords: intertidal mudflats, tidal courses, DEMs, estuaries, morphological features

1 Introduction

In the context of climate change and increasing anthropogenic pressures, coastal systems are experiencing shifts in the frequency and intensity of hazards. These areas are often densely populated and economically important, making them more vulnerable to changes. Intertidal mudflats, which are vital but fragile coastal habitats, play an essential role in both ecological functionalities and geomorphological processes. Tidal courses within these mudflats, including channels and creeks, are crucial for water and sediment exchange and hence to mudflat stability. Due to their dynamic nature, understanding how the morphology of these courses relates to physical mudflat characteristics is essential. To address this, we developed an automated toolbox for quantifying the morphology of tidal courses using LiDAR-based DEMs, focusing on key dimensions such as width, depth, and rhythmicity. By correlating these features with the mudflat characteristics, we aim to identify the relationship between tidal courses and mudflat dynamics.

2 Study sites

The tidal course characterisation method was applied to several mudflats in three tidal estuaries: (i) the Seine Estuary (NW France), a dynamic environment with a tidal range reaching 8 m; (ii) the Western Scheldt Estuary (the Netherlands), with a tidal range up to 5 m; and (iii) the Ems Estuary (the Netherlands-Germany), experiencing tidal ranges lower than 4 m. These systems combine anthropogenic influences, such as embankments and dredging, and protected areas, such as natural reserves (Grasso and Le Hir, 2019; Hanssen et al., 2022).

3 Methods

To analyse the morphological characteristics of the tidal courses, we developed a specialised toolbox that processes elevation data from DEMs. This toolbox automatically detects and measures key features, such as the depth and width of the tidal courses. It starts by extracting cross-sectional profiles along both the x-axis and y-axis from the DEMs and identifying changes in elevation to determine the edges and calculate the width and depth of the tidal courses. The data from both directions are then integrated to provide a comprehensive distribution of the courses' morphological features.

4 Results and perspectives

The toolbox provided results on the tidal course locations, depths and widths associated with the mudflat slope (e.g., for a Seine Estuary mudflat in Figure 1). Further application to other intertidal areas revealed significant variability in tidal course distributions. Tidal course depths were notably lower within constrained intertidal areas (e.g., elevated mudflats with embankments), whereas the tidal courses were deeper in wider mudflats (e.g., at the mouth of the Seine Estuary). Moreover, tidal course dimensions were related to the mudflat morphology, with the largest courses (i.e., deeper and wider) occurring near the tidal flat slope break. Hence, the developed toolbox provides a generic method to investigate the interaction between tidal courses and mudflat morphologies.

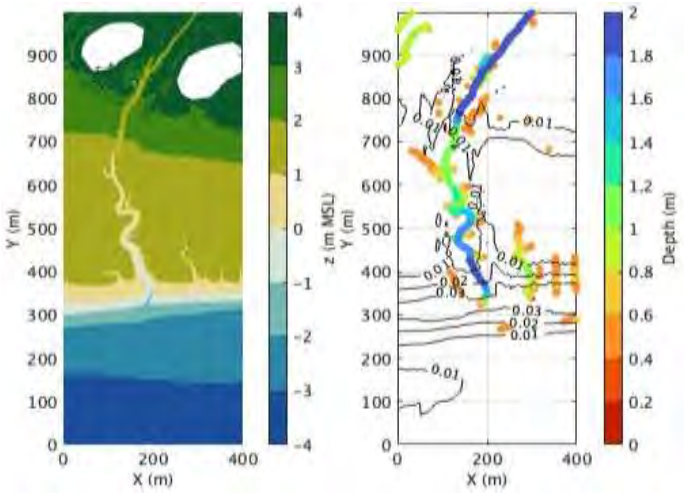

Figure 1: (Right) Mudflat elevation *z*, relative to mean sea level MSL, and (left) tidal course depth (> 0.4 m, colour dots) and mudflat slope (black isolines), at the mouth of the Seine Estuary.

References

[1] F. Grasso and P. Le Hir. Influence of morphological changes on suspended sediment dynamics in a macrotidal estuary: Diachronic analysis in the Seine Estuary (France) from 1960 to 2010. *Ocean Dynamics*, 69(1), pp. 83–100, 2019.

[2] J.L.J. Hanssen, B.C. van Prooijen, N.D. Volp, P.L.M. de Vet, and P.M.J. Herman. Where and why do creeks evolve on fringing and bare tidal flats? *Geomorphology*, 403, p. 108182, 2022.

Machine Learning for Nearshore Satellite-Derived Bathymetry in regions with different tidal regimes and high optical complexity.

Mario Luiz Mascagni[12], Antonio Henrique da Fontoura Klein[12], Anita Maria da Rocha Fernandes[3], Andrigo Borba dos Santos[3], Dennis Kerr Coelho[3], Lais Pool[12], Sonia Castanedo[4], Mirian Jiménez[4], Manuel Zornoza[4]
[1]Federal University of Rio Grande do Sul (UFRGS), Porto Alegre - RS, Brazil.
[2]Federal University of Santa Catarina (UFSC), Florianópolis - SC, Brazil.
[3]University of Vale do Itajaí (UNIVALI), São José - SC, Brazil.
[4]University of Cantabria (UC), Santander - CA, Spain.
Corresponding author: mario.mascagni@ufrgs.br

Keywords: Remote Sensing, Sentinel-2, Convolutional Neural Network, Bathymetric Inversion, Turbid Waters.

1 Introduction

Estimating nearshore depths is extremely important to understand the evolution of the coastal systems. Hydrographic surveys are very expensive and therefore, shallow water bathymetry data is rare and generally, restricted to waterways in port regions. On the other hand, remote sensing applied with publicly available satellite images are a promising source of geospatial information that can contribute to estimating depths in shallow waters from bathymetric inversion approaches for any coastal region of the world.

The present study investigates some satellite-derived bathymetry approaches using the Sentinel-2 collections available in the Google Earth Engine (GEE) platform, with Convolutional Neural Network (CNN) models.

2 Methods

The testing area in this study were (1) the Babitonga Bay, in Santa Catarina - Brazil, an estuary with high optical complexity due to presence of Suspended Particulate Matter (SPM) and Colored Dissolved Organic Matter (CDOM); and (2) The lower Santoña estuary with Laredo beach, in eastern Cantabria - Spain, a fairly shallow estuary with emerged sandbanks and a dominant mesotidal regime. The validation data were acquired from traditional hydrographic surveys. For Babitonga Bay the surveys were carried out in May 2018 and February 2020. For Santoña y Laredo the hydrographic surveys were carried out in September 2019 and September 2020. The surveyed bathymetric data were interpolated using IDW method with anisotropy of 1.2X to generate a regular 10 m grid for the CNN kernels analysis, aiming to give greater weights to depth values along the channel flow orientation, while the original bathymetry values from the hydrographic surveys were preserved.

The satellite images were pre-processed to mask clouds and land pixels; resharpen the B5, B6, B7, B8A, B11 and B12 bands to 10 m scale; correct atmospheric noise using the SIAC GEE tools functions and generate geometric median composed images pixel-by-pixel, aiming to reduce the influence of MPS and CDOM on the analysed scenes.

The CNN model was built using 12, 36 and 72 input channels respectively, where each input channel in the 12-channel version corresponds to the reflectance values of each of the "B" band from Sentinel-2 TOA image found in the closest dates to the bathymetric surveys for both study sites. The CNN versions with 36 and 72 layers were built from multiple Sentinel-2 TOA images in the time interval of 2 months before and 2 months after the bathymetric surveys dates, using geometric median for pixel image composition. The hidden layers were configured using 2D Convolutional Filters and Average Pooling (2X2) for 10X10-pixel kernels. The output channel was divided into 70% for training and 30% for validation where 5 K-Fold interactions were applied to reduce overfitting.

3 Results

The results achieved by the CNN presented a perfect Spearman correlation of 1.0, a RMSE of 0.2 m and a MAE of 0.1 m for the validation data in Babitonga Bay and 0.8 Spearman correlations, 0.9 m MAE and 1.2 RMSE for Santoña region.

4 Conclusions

The integration between remote sensing and machine learning techniques has proven important to improve satellite-derived bathymetry results in optically complex regions, since the representation of nonlinear processes of the interaction of light penetrating the water column with the influence of MPS and CDOM can be well captured by deep learning models, such as CNN.

Acknowledgments

The authors would like to thank the Brazilian National Council for Scientific Development (CNPQ) process: 140717/2022-6; the CASSIE-CORE CNPQ process: 406603/2022-7; the Productive Scholarship 1D - CNPQ process: 302238/2022-0, the Geomatics and Ocean Engineering Group (GeoOcean) for the support and CEDEX (Centro de Estudios y Experimentación de Obras Públicas) for providing field bathymetry data for Spain.

On The Joint Action of Flood-Tidal and Wave-Driven Longshore Currents On an Erosion Hotspot Near the Sado River Mouth

Alphonse Nahon, Paula Freire, André Fortunato, Filipa Oliveira,
Francisco Sancho and Luís Portela
LNEC – National Laboratory for Civil Engineering, Lisbon, Portugal
Corresponding author: anahon@lnec.pt

Keywords: tidal inlet, sandspit, sandwave, longshore drift, Tróia

1 Introduction

Near tidal inlets, surface ocean waves propagate and refract over complex shoals and channels. Waves may also superimpose onto tidal currents with increasing intensities towards inlet entrances, creating gradients of longshore sediment transport (LST) otherwise inexistent in the absence of the inlet [1].

Here, we investigate such remote effects the inlet of the Sado Estuary may have on an erosion hotspot along the Tróia Peninsula (Figure 1). The peninsula is a sandy spit located on the south-western coast of Portugal. It has a concave-seaward shape and the LST is directed (northward) towards the inlet. As Cape Espichel blocks the dominant northwesterly swells, the wave-driven LST slightly decreases along the bend of the spit towards the inlet. Near the inlet, the shoreline has been accreting for decades [2], despite shoreline sandwaves can locally lead to erosion hotspots.

2 A Migrating Erosion Hotspot

The CASSIE shoreline detection tool [3], with satellite LANDSAT images from 1984 to 2024, was used to quantified the largest active erosion hotspot.

Located about 4.5 km southward/updrift from the inlet, the 40 years of Landsat derived shorelines (LDS) revealed a kilometre scale eroding front, migrating alongshore at about 30 m.y^{-1}. The front is bounded on both sides by stable and accreting beaches. Surveys from 2011 and 2024 confirmed the magnitude of the beach retreat, in area and shape, derived from the LDS data, further indicating the loss of at least 220 x 10^3 m^3 of sand and a retreat of 30 m of the dune slope in 13 years.

3 Underlying Physical Mechanism

The examination of the offshore wave data since 1940 [4] suggests the erosion was detected prior to a significant increase of the incoming wave energy from the dominant wave quadrant. Moreover, no other climate driver was detected that could explain the observed shoreline behaviour. Still, a remarkably stable secondary flood-tidal channel is present on bathymetric charts just in front of the study area since at least 1983. Therefore, a numerical sediment transport model was setup with SCHISM [5]. The model aims at disentangling the contribution of waves and flood-tidal currents, as well as their combined effect, on the sediment budget of the spit. It should tell if their nonlinear superposition can trigger shoreline oscillations with the observed magnitude.

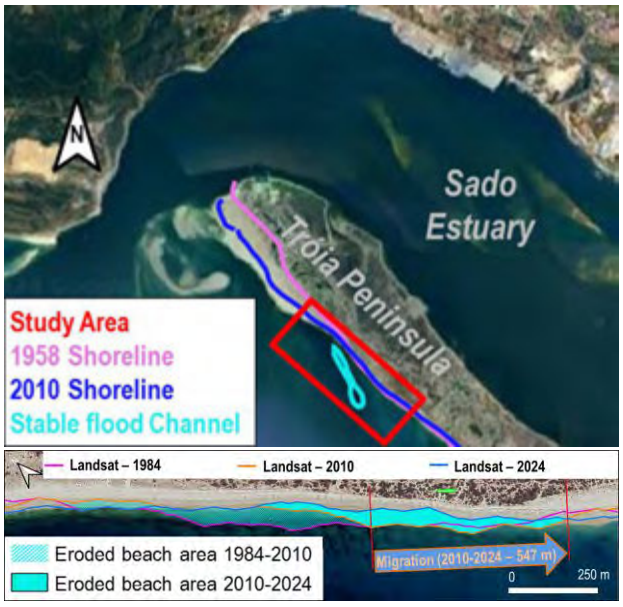

Figure 1: Top: Google Earth view of the study area, and shorelines from 1958 and 2010 [1], and the contour of a secondary flood-tidal; – Bottom: Length and migration of the erosion hotspot between 2010 and 2024.

Acknowledgments

We acknowledge the Pestana Troia Eco Resort for their support during beach surveys.

References

[1] A. Nahon *et al.*, Modelling the contribution of wind waves to Cap Ferret's updrift erosion. *Coast. Eng*. 172, 104063, 2022.

[2] C. Ponte Lira *et al.*, Coastline evolution of Portuguese low-lying sandy coast in the last 50 years: an integrated approach. *Earth Syst. Sci. Data* 8: 265–278, 2016.

[3] L.P. Almeida *et al.*, Coastal Analyst System from Space Imagery Engine (CASSIE): Shoreline management module. *Environ. Model. Softw*. 140, 105033, 2021.

[4] H. Hersbach *et al.*, ERA5 hourly data on single levels from 1940 to present. *Copernicus Climate Change Service, Climate Data Store*, 2023.

[5] Y.J. Zhang *et al.*, Seamless cross-scale modeling with SCHISM. *Ocean Model.* 102, 64–81, 2016.

Modeling salt-wedge dynamics and suspended sediment transport in the microtidal Rhône estuary

Anh, T.K. DO[1,2], Nicolas Huybrecht[1,2], Manu John[1,2], Coraline L. Wintenberger[3], François Sabatier[4]
[1]Cerema Risques, Eaux et Mer (CEREMA REM), RHITME Research Team, Margny-lès-Compiègne, France
[2]Université Rouen Normandie, Université Caen Normandie, CNRS, Normandie Université, M2C, UMR 6143, Margny-lès-Compiègne, France
[3]Cerema Normandie-Centre, Unité Risques Hydrauliques et Surveillance des Ouvrages et des Milieux, Blois, France
[4]Aix-Marseille Université CNRS, IRD, Coll France, CEREGE, Aix-en-Provence, France

Corresponding author: thi-kim-anh.do@cerema.fr

Keywords: Salt-wedge, 3D modeling, OpenTelemac3D, Rhone river delta, Sediment transport

1. Introduction

The Rhône River delta, a major freshwater and sediment source to the Mediterranean, is shaped by river flow and waves due to its low tidal range (25–30 cm). While past studies focused on morphological changes and short-term sediment transport, salinity intrusion and seasonal sediment transport remain understudied. Most numerical models target the river mouth or the Gulf of Lion, neglecting the estuarine zone. Ibáñez et al.[1] found the salt wedge is expelled when discharge exceeds 1,449 m³/s, while Radakovitch et al. [2] observed intrusion below 1,200–1,500 m³/s, intensifying at lower flows. However, no precise salt wedge position criterion exists, posing challenges for agricultural water management. This study develops a 3D numerical model to examine salinity intrusion and sediment transport over a full year, validated with water level data from three stations, salinity and velocity from ADCP surveys in 2023.

2.Methods

Flow and sediment transport simulations were conducted using the openTELEMAC system, which solves the three-dimensional Navier-Stokes equations on an unstructured triangular mesh. The computational domain extends arround 50 km upstream from the river mouth, covering the upper Arles station and the divergence point where the Rhône splits into the Petit Rhône and Grand Rhône. Seaward, the model encompasses adjacent coastal waters, extending 38 km alongshore and 12 km offshore, reaching depths of approximate of 100 m. The model is forced by sea level, river discharge (Tarascon station), and wind from ERA5. Salinity is prescribed from global datasets at the sea boundary, while sediment concentration input comes from Arles station. The simulation runs for 352 days, from January 1 to December 19, 2023, based on available sediment data.

3.Results

Modeled and observed longitudinal salinity distributions are shown in Figure 1. Both profiles depict a well-developed salt wedge with a sharp halocline, where dense seawater intrudes beneath lighter freshwater. However, the model underestimates surface salinity, suggesting weaker vertical mixing.

The results show that the salt wedge develops strongly during low river flow periods, particularly when discharge falls below 1,600 m³/s, allowing salinity to intrude up to 26 km upstream from the river mouth. However, salt intrusion can also occur at higher discharges, such as on day 292 (average flow: 2,321 m³/s), likely due to the preceding five-day period (days 288–291) of significantly lower discharge (average: 801 m³/s).

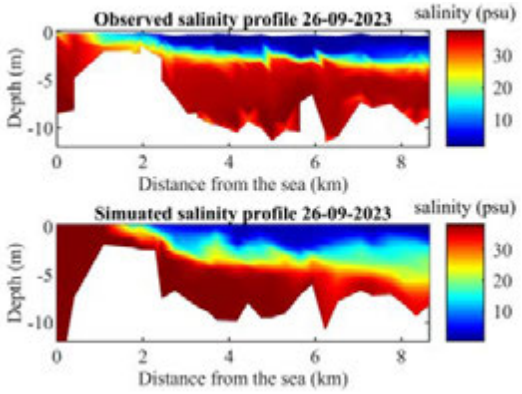

Figure1. Observed and modeled longitudinal salinity distribution at september 26th, 2023.

The primary results indicate a significant flush of suspended sediment as a river plume during high discharge events. The next step involves further validation of the sediment transport model and assessing the impact of waves on sediment dynamics.

Acknowledgments

The authors thank the Compagnie Nationale du Rhône for providing bathymetric data, water level, and salinity measurements in the river. We also acknowledge the OSR for supplying SPM data and Ifremer for offshore bathymetric data (*https://sextant.ifremer.fr/record/baa6e9dc-f479-427d-a2a3-672153e72502/*). Additionally, we extend our gratitude to Salins du Midi for supporting this work through human resource funding.

References

1] Ibañez, Carles, Didier Pont, and Narcís Prat. "Characterization of the Ebre and Rhone estuaries: A basis for defining and classifying salt-wedge estuaries." *Limnology and Oceanography* 42.1 (1997): 89-101.

[2] Radakovitch, O., Verney, R., Camenen, B., Dramais, G., Bonnefoy, A., Le Coz, J., ... & Giner, F. (2024). *Dynamique du coin salé et dynamique sédimentaire à l'embouchure du Rhône* (Rapport de recherche), pp 1-34

Bathymetric Evaluation by Remote Sensing Tools at an Energetic Estuary

Muhammed Said Parlak[1], Agnese Baldoni[1], Luciano Soldini[1],Matteo Postacchini[1], Maurizio Brocchini[1]
[1]Università Politecnica delle Marche, DICEA, Ancona, Italy
Corresponding author: m.s.parlak@univpm.it

Keywords: estuarine dynamics, remote sensing, bathymetry inversion, hydro-morphodynamics

1 Introduction

The water depth has a great influence on physical processes in the relatively shallow waters. Therefore, the collection of bathymetry data is essential to investigate hydro-morphodynamic interactions. Remote sensing tools (RSTs) are tempting alternatives for bathymetric evaluation due to continuous data collection and low operational costs. Two RSTs were exploited to obtain bathymetry at an energetic estuary and compared to surveys. It has been found that RSTs are not only a good alternative to evaluate bathymetry but also hydrodynamic assessments.

2 Methodology

A multi-camera monitoring system (SGS) and an X-Band RADAR (XBR) were deployed at the study site, Misa River Estuary (MSE), at the Adriatic coast of central Italy. The MSE has a complex dynamic environment, e.g., strong sea-river interactions and severe flooding events [1].

The XBR signals were processed and converted to greyscale images [2]. The images from the SGS were orthorectified based on a field survey. Then, both datasets were analysed on the cBathy toolbox to obtain bathymetry results [3]. The performance of the approach was determined by comparing it to in-situ surveys. After obtaining a reliable performance, wave characteristics were extracted to resolve sea state.

3 Results

The SGS and the XBR collected suitable data on 16th April 2024. After preprocessing datasets, the bathymetry results were obtained by analysing with cBathy (Figure 1-a, b). The bathymetry survey, done in December 2024, was selected for comparison (Figure 1-c). Although the survey is from a different time instance, our primary aim is to observe the trends of the results regarding the fact that the morphodynamic evolution time scale is relatively large.

The statistical analyses have been conducted to evaluate the performance of the approach and are demonstrated in Figure 1 (d, e, f). The SGS gave better performance than XBR, although they showed similar trends. Promising results were obtained when the XBR-derived wave characteristics were compared to validated SWAN model. The peak parameters were successfully resolved, such as direction, period, and wavelength. The performance on the significant wave height was relatively moderate, and it is aimed to improve it.

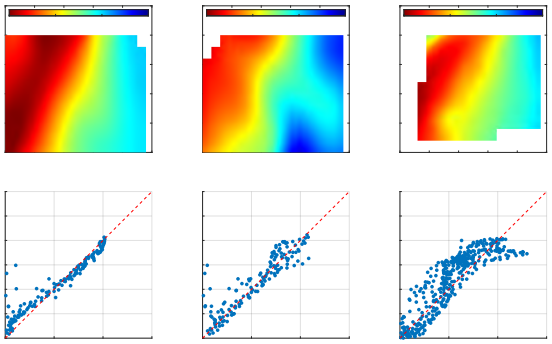

Figure 1: Upper panels: The bathymetry maps from the SGS (a), the XBR (b), and the survey (c). Lower panels: The statistical comparison between SGS-Survey (d), XBR-Survey (e), and SGS-XBR (f).

4 Conclusion and Ongoing Work

The preliminary results showed that the RSTs can be exploited to collect morphodynamic and hydrodynamic information at a chosen location. Due to dense data sampling from a relatively large spatial area, it allows for further investigation on the estuarine dynamics.

Ongoing work is focused on coupling information between the RSTs, numerical models and field observations to create a framework for estuarine and nearshore dynamics.

Acknowledgments

This project has received funding from the European Union's (EU) Horizon Europe Framework Programme (HORIZON) under Grant Agreement No 101072443 as a MSCA Doctoral Network (HORIZON-MSCA-2021-DN-01) of SEDIMARE.

References

[1] Brocchini, M., Calantoni, J., Postacchini, M., Sheremet, A., Staples, T., Smith, J., ... & Soldini, L. (2017). Comparison between the wintertime and summertime dynamics of the Misa River estuary. *Marine Geology*, *385*, 27-40.

[2] Honegger, D. A., Haller, M. C., & Holman, R. A. (2019). High-resolution bathymetry estimates via X-band marine radar: 1. beaches. *Coastal Engineering*, *149*, 39-48.

[3] Holman, R., Plant, N., & Holland, T. (2013). cBathy: A robust algorithm for estimating nearshore bathymetry. *Journal of geophysical research: Oceans*, *118*(5), 2595-2609.

AUTHORS INDEX

AUTHORS INDEX

AUTHORS INDEX

AUTHORS INDEX

SYMPOSIUM WEBSITE

Organized by

UNIVERSITAT POLITÈCNICA DE CATALUNYA BARCELONATECH

Sponsors

UBERTONE

Ajuntament de Barcelona

Collaborators

IEC Institut d'Estudis Catalans

Societat Catalana de Física

AMB

Agència Catalana de l'Aigua

Espais Naturals del Delta del Llobregat

IAHR AIRH International Association for Hydro-Environment Engineering and Research

Hosted by Spain Water and IWHR, China

Technical Secretariat

Activa Congresos
+34 933 238 573
www.activacongresos.com